Lightweight Concrete: Shear Performance

PUBLICATION NO. FHWA-HRT-15-022

MARCH 2019

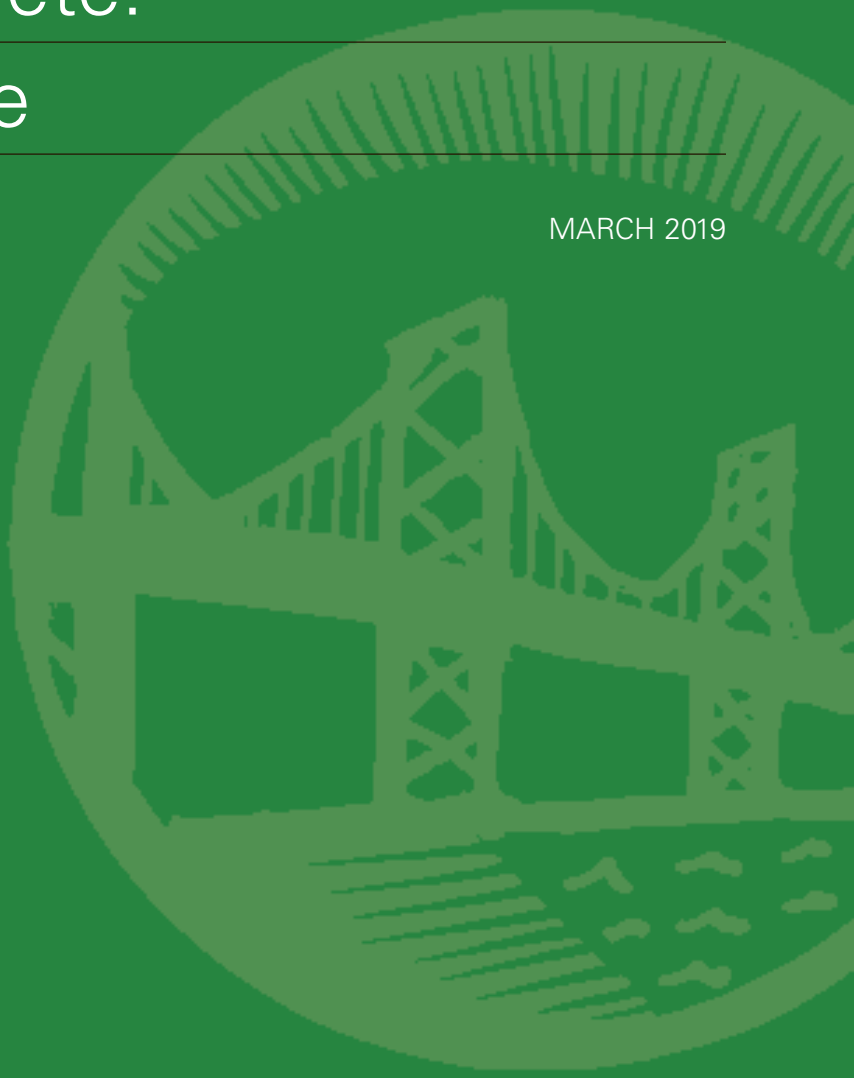

U.S. Department of Transportation
Federal Highway Administration

Research, Development, and Technology
Turner-Fairbank Highway Research Center
6300 Georgetown Pike
McLean, VA 22101-2296

FOREWORD

Broad-based advancements in concrete materials have led to significant enhancements in the performance of lightweight concrete (LWC). Although the value of using LWC within the constructed infrastructure is clear, decades-old performance perceptions continue to hinder wider use of the concrete. Additionally, the lack of modern updates to structural design provisions for LWC has perpetuated additional barriers to the use of LWC. In 2007, the Federal Highway Administration (FHWA) began an investigation of the structural performance of modern LWCs.[1,2] The study described in this report engaged the academic as well as the public- and private-sector communities to compile the body of knowledge on LWC while also conducting nearly 100 full-scale structural tests on LWCs.

This report presents the results of shear tests on high-strength LWC prestressed girders as well as a compilation of data available from the literature. It also provides potential revisions to the *American Association of State Highway and Transportation Officials Load and Resistance Factor Design Bridge Design Specifications* with a focus on nominal shear resistance and the resistance factor for LWC in shear.[3] This report corresponds to the TechBrief, *Lightweight Concrete: Shear Performance*.[4] This report will provide valuable information for researchers interested in the shear performance and reliability of LWC.

Cheryl Allen Richter, P.E., Ph.D.
Director, Office of Infrastructure
Research and Development

TECHNICAL REPORT DOCUMENTATION PAGE

1. Report No. FHWA-HRT-15-022	2. Government Accession No.	3. Recipient's Catalog No.
4. Title and Subtitle Lightweight Concrete: Shear Performance		5. Report Date March 2019
		6. Performing Organization Code:
7. Author(s) Gary G. Greene and Benjamin A. Graybeal		8. Performing Organization Report No.
9. Performing Organization Name and Address Office of Infrastructure Research and Development Federal Highway Administration 6300 Georgetown Pike McLean, VA 22101-2296		10. Work Unit No.
		11. Contract or Grant No.
12. Sponsoring Agency Name and Address Office of Infrastructure Research and Development Federal Highway Administration 6300 Georgetown Pike McLean, VA 22101-2296		13. Type of Report and Period Covered Final Report; 2010–2012
		14. Sponsoring Agency Code HRDI-40

15. Supplementary Notes

This document was developed by research staff at the Turner-Fairbank Highway Research Center. Portions of the work were completed by PSI, Inc. under contract DTFH61-10-D-00017. Gary Greene formerly of PSI, Inc., who was the lead contract researcher on FHWA's lightweight concrete research efforts, and Ben Graybeal of FHWA, who manages the FHWA Structural Concrete Research Program, developed this document.

16. Abstract

Much of the fundamental basis for the current lightweight concrete (LWC) provisions in the *American Association of State Highway and Transportation Officials (AASHTO) Load and Resistance Factor Design (LRFD) Bridge Design Specifications* is based on research of LWC from the 1960s.[3] The LWC that was part of this research used traditional mixes of coarse aggregate, fine aggregate, portland cement, and water. Broad-based advancement in concrete technology over the past 50 yr has given rise to significant advancements in concrete mechanical and durability performance.

This document describes the results of shear tests on high-strength LWC prestressed girders that were conducted as part of an overall Federal Highway Administration (FHWA) research project on LWC. The FHWA test results are included in an internal database of shear tests with over 400 tests on LWC specimens available in the literature. (For sources, see Bibliography section NWC Sources for ACI-DafStb Database.) An analysis of the database was used to develop potential revisions to provisions related to LWC within section 5 of the *AASHTO LRFD Bridge Design Specifications*.[3] The framework for addressing LWC in the specifications that was proposed previously as a part of this research effort is applied to the design expression for nominal shear resistance.[1] The framework includes a proposed revision to the definition of LWC, a proposed modification factor relevant to LWC structural performance, and a proposed revision to the resistance factor for LWC in shear.

17. Key Words	18. Distribution Statement
LWC, Lightweight concrete, Bridge design, LRFD design specifications, Shear strength, Shear resistance, Resistance factor, Reliability analysis	No restrictions. This document is available to the public through the National Technical Information Service, Springfield, VA 22161. http://www.ntis.gov

19. Security Classif. (of this report)	20. Security Classif. (of this page)	21. No. of Pages	22. Price
Unclassified	Unclassified	326	N/A

Form DOT F 1700.7 (8-72) Reproduction of completed page authorized.

SI* (MODERN METRIC) CONVERSION FACTORS

APPROXIMATE CONVERSIONS TO SI UNITS

Symbol	When You Know	Multiply By	To Find	Symbol
		LENGTH		
in	inches	25.4	millimeters	mm
ft	feet	0.305	meters	m
yd	yards	0.914	meters	m
mi	miles	1.61	kilometers	km
		AREA		
in^2	square inches	645.2	square millimeters	mm^2
ft^2	square feet	0.093	square meters	m^2
yd^2	square yard	0.836	square meters	m^2
ac	acres	0.405	hectares	ha
mi^2	square miles	2.59	square kilometers	km^2
		VOLUME		
fl oz	fluid ounces	29.57	milliliters	mL
gal	gallons	3.785	liters	L
ft^3	cubic feet	0.028	cubic meters	m^3
yd^3	cubic yards	0.765	cubic meters	m^3
		NOTE: volumes greater than 1000 L shall be shown in m^3		
		MASS		
oz	ounces	28.35	grams	g
lb	pounds	0.454	kilograms	kg
T	short tons (2000 lb)	0.907	megagrams (or "metric ton")	Mg (or "t")
		TEMPERATURE (exact degrees)		
^oF	Fahrenheit	5 (F-32)/9 or (F-32)/1.8	Celsius	^oC
		ILLUMINATION		
fc	foot-candles	10.76	lux	lx
fl	foot-Lamberts	3.426	$candela/m^2$	cd/m^2
		FORCE and PRESSURE or STRESS		
lbf	poundforce	4.45	newtons	N
lbf/in^2	poundforce per square inch	6.89	kilopascals	kPa

APPROXIMATE CONVERSIONS FROM SI UNITS

Symbol	When You Know	Multiply By	To Find	Symbol
		LENGTH		
mm	millimeters	0.039	inches	in
m	meters	3.28	feet	ft
m	meters	1.09	yards	yd
km	kilometers	0.621	miles	mi
		AREA		
mm^2	square millimeters	0.0016	square inches	in^2
m^2	square meters	10.764	square feet	ft^2
m^2	square meters	1.195	square yards	yd^2
ha	hectares	2.47	acres	ac
km^2	square kilometers	0.386	square miles	mi^2
		VOLUME		
mL	milliliters	0.034	fluid ounces	fl oz
L	liters	0.264	gallons	gal
m^3	cubic meters	35.314	cubic feet	ft^3
m^3	cubic meters	1.307	cubic yards	yd^3
		MASS		
g	grams	0.035	ounces	oz
kg	kilograms	2.202	pounds	lb
Mg (or "t")	megagrams (or "metric ton")	1.103	short tons (2000 lb)	T
		TEMPERATURE (exact degrees)		
^oC	Celsius	1.8C+32	Fahrenheit	^oF
		ILLUMINATION		
lx	lux	0.0929	foot-candles	fc
cd/m^2	$candela/m^2$	0.2919	foot-Lamberts	fl
		FORCE and PRESSURE or STRESS		
N	newtons	0.225	poundforce	lbf
kPa	kilopascals	0.145	poundforce per square inch	lbf/in^2

*SI is the symbol for the International System of Units. Appropriate rounding should be made to comply with Section 4 of ASTM E380.
(Revised March 2003)

TABLE OF CONTENTS

LIST OF FIGURES

LIST OF TABLES

LIST OF ABBREVIATIONS AND SYMBOLS

Abbreviations

AASHTO	American Association of State Highway and Transportation Officials
ACI	American Concrete Institute
BT	bulb tee
CDF	cumulative distribution function
CIP	cast-in-place
C.L.	centerline
COV	coefficient of variation
DafStb	Deutscher Ausschuss für Stahlbeton (German Committee for Structural Concrete)
ERS	electric resistance strain gauge
FHWA	Federal Highway Administration
GFRP	glass fiber reinforced polymer
HG	haydite girder
kcf	kip per cubic foot
LRFD	Load and Resistance Factor Design
LVDT	linear variable differential transformer
LWC	lightweight concrete
MCFT	modified compression field theory
NCHRP	National Cooperative Highway Research Program
NWC	normal-weight concrete
PC	prestressed concrete
RC	reinforced concrete
SCOBS	Subcomsmittee on Bridges and Structures
SDC	specified density concrete
SG	stalite girder
SMR	triple-mirror prism in a spherical steel ball followed by FARO®
SP	string potentiometer
TDL	taut-line deflection
TFHRC	Turner-Fairbank Highway Research Center
UG	utelite girder

Symbols

a	shear span or depth of equivalent rectangular stress block
A_{beam}	beam cross-sectional area
A_{ct}	area of concrete on the flexural tension side of the member
a_g	maximum aggregate size
A_{ps}	area of the longitudinal prestressing steel
A_s	area of the longitudinal tension reinforcement
A'_s	area of the longitudinal compression reinforcement
A_v	area of the shear reinforcement within the spacing
b	width of the compression face of a rectangular member
b_{deck}	deck width of the simulated cross section
$b_{flange,btm}$	beam bottom flange width of the simulated cross section
$b_{flange,top}$	beam top flange width of the simulated cross section
b_v	effective web width
b_w	width of member's web
c	depth from the compression face to the neutral axis
d	distance from the compression face to the centroid of the tension reinforcement
d_p	distance from the compression face to the centroid of the prestressing steel
d_s	distance from the compression face to the centroid of the nonprestressed tension reinforcement
d'_s	distance from the compression face to the centroid of the nonprestressed compression reinforcement
d_v	effective shear depth
E_c	modulus of elasticity of concrete
E_p	modulus of elasticity of prestressing steel
E_s	modulus of elasticity of reinforcing bars
f'_c	concrete compressive strength in reference to material test values and specified compressive strength
f'_{ci}	concrete compressive strength at the time of prestressing in reference to material test values and specified compressive strength at the time of prestressing
f_{cpe}	compressive stress in the concrete at the extreme tensile fiber after all prestress losses have occurred

f_{ct}	concrete-splitting tensile strength
f_{pc}	compressive stress at the centroid of the concrete after all prestress losses have occurred
f_{pe}	effective stress in the prestressing steel after losses
f_{po}	parameter taken as the modulus of elasticity of prestressing steel multiplied by the locked-in difference in strain between the prestresing steel and the surrounding concrete
f_{ps}	average stress in prestressing steel at the time for which the nominal resistance of member is required
f_{pu}	tensile strength of prestressing steel in reference to material test values and specified tensile strength of prestressing steel
f_r	modulus of rupture of concrete
f_s	stress in mild tension reinforcement at nominal flexural resistance
f'_s	stress in the mild steel compression reinforcement at nominal flexural resistance
f_t	concrete tensile strength
f_y	yield strength of reinforcing bars in reference to material test values and specified minimum yield strength
f_{yt}	specified yield strength of the shear reinforcement
h	member height
h_f	compression flange depth
h_{web}	height of the beam below the top flange of the simulated reinforced concrete section and height of the beam below the deck of the simulated prestressed concrete section
IM	nominal dynamic load allowance
k	prestresssing factor
L	span length
$L1$	distance from the end of the girder to the rolling support
$L2$	distance to the first deck concrete anchor
$L3$	anchor spacing
$L4$	distance from the rolling support to the first anchor of the linear variable differential transformer average strain rosette
M	applied moment
M_{cr}	flexural cracking moment
M_{cre}	moment causing flexural cracking at the section due to externally applied loads

M_{dnc}	total unfactored dead load moment acting on the noncomposite section
m_i	mean load effect of an individual load
M_{max}	maximum factored moment at the section due to externally applied loads
M_n	nominal flexural resistance
m_Q	total mean load effect
m_{Qi}	mean of the individual load effects
m_R	mean resistance
M_u	factored moment at the section
n	smallest ratio of test-to-predicted shear resistance
N	total number of ratios of test-to-predicted shear resistance
$N2$	total number of anchors
N_u	factored axial force of the section (positive if tensile)
p_n	cumulative probability
Q	total factored load effects
Q_{DC}	load effects due to dead load of structural components
Q_{DW}	load effects due to dead load of the wearing surface
Q_i	unfactored load effects
Q_{IM}	load effects due to vehicular dynamic load allowance
Q_{LL}	load effects due to vehicular live load
Q_{LL+IM}	load effects due to combined vehicular live load and dynamic load allowance
R	radius of Mohr's circle
r_{DW}	ratio of the load effects due to the dead load of the wearing surface to the load effects due to the dead load of structural components
R_n	nominal resistance
r_Q	ratio of unfactored permanent loads to the total unfactored force effect
s	spacing of the shear reinforcement
s_{beam}	beam spacing
S_c	section modulus for the extreme fiber of the composite section where tensile stress is caused by externally applied loads
s_{max}	maximum permitted spacing of the shear reinforcement
S_{nc}	section modulus for the extreme fiber of the noncomposite section where tensile stress is caused by externally applied loads

s_x	lesser of effective shear depth or the maximum distance between layers of longitudinal crack-control reinforcement
s_{xe}	crack-spacing parameter
t_{deck}	deck thickness of the simulated cross section
$t_{flange,btm}$	beam bottom flange thickness of the simulated cross section
$t_{flange,top}$	beam top flange thickness of the simulated cross section
t_{slab}	concrete slab thickness
t_{ws}	wearing surface thickness
V	applied shear force
V_c	nominal shear resistance provided by tensile stresses in the concrete
V_{ci}	nominal shear resistance provided by concrete when inclined cracking results from combined shear and moment
V_{cr}	applied shear force at web cracking
v_{cw}	average shear stress at inclined cracking
V_{cw}	nominal shear resistance provided by concrete when inclined cracking results from excessive principal tensions in the web
V_d	shear force at the section due to unfactored dead load
V_{DC}	coefficient of variation for the dead load of structural components
V_{DW}	coefficient of variation for the dead load of the wearing surface
V_F	coefficient of variation for the uncertainty in the fabrication
V_{FM}	coefficient of variation for the combined uncertainty in the fabrication and materials
V_i	factored shear force at the section due to externally applied loads occurring simultaneously with the maximum factored moment at the section due to externally applied loads
V_{IM}	coefficient of variation for the vehicular dynamic load allowance
V_{LL}	coefficient of variation for the vehicular live load
V_M	coefficient of variation for the uncertainty in the materials
V_n	nominal shear resistance of the section
V_{n1}	calculated nominal shear resistance of the section (V_n) corresponding to first assumed value of the factored shear force at the section (V_u)
V_{n2}	calculated nominal shear resistance of the section (V_n) corresponding to second assumed value of the factored shear force at the section (V_u)
V_p	component of the effective presstressing force in the direction of the applied shear

V_P	coefficient of variation for the uncertainty in the analysis
V_{Qi}	coefficient of variation of the unfactored load effect
V_R	coefficient of variation for resistance
V_s	nominal shear resistance provided by the shear reinforcement
V_{test}	maximum applied shear force
v_u	average shear stress
V_u	factored shear force at the section
$V_{u,\ assumed}$	assumed value of factored shear force at the section (V_u) equals the nominal shear resistance of the section (V_n)
$V_{u1,\ assumed}$	first assumed value of factored shear force at the section (V_u)
$V_{u2,\ assumed}$	second assumed value of factored shear force at the section (V_u)
w_{beam}	beam unit weight
w_c	concrete unit weight
w_{slab}	slab unit weight
w_{ws}	wearing surface unit weight
β	factor indicating ability of diagonally cracked concrete to transmit tension and shear
β_1	ratio of the depth of the equivalent uniformly stressed compression zone assumed in the strength limit state to the depth of the actual compression zone
β_{LWC}	reliability index for lightweight concrete
$\beta_{LWC,\ \phi\ = 0.90}$	reliability index for lightweight concrete using a resistance factor of 0.90
β_{NWC}	reliability index for normal-weight concrete
β_{RQ}	reliability index
β_{target}	target reliability index
γ_{DC}	load factor for load effects due to dead load of structural components
γ_{DW}	load factor for load effects due to dead load of the wearing surface
γ_i	load factors
γ_{LL+IM}	load factor for load effects due to combined vehicular live load and dynamic load allowance
δ	factor multiplied by the internal shear force and internal moment as part of the iterative procedure to determine nominal shear resistance
ε_s	net longitudinal tensile strain in the section at the centroid of the tension reinforcement
ε_t	strain measured in the stirrups by electronic resistance strain gauges

ε_{ty}	stirrup yield strain
ε_x	longitudinal strain at the middepth of the beam
θ	angle of inclination of diagonal compressive stresses
λ	lightweight concrete modification factor
λ_{DC}	bias factor for the load effects due to dead load of structural components
λ_{DW}	bias factor for the load effects due to dead load of the wearing surface
λ_F	bias factor for the uncertainty in the fabrication
λ_{FM}	bias factor for the combined uncertainty in the fabrication and materials
λ_{IM}	bias factor for the load effects due to vehicular dynamic load allowance
λ_{LL}	bias factor for the load effects due to vehicular live load
λ_M	bias factor for the uncertainty in the materials
λ_P	bias factor for the uncertainty in the analysis
λ_{Qi}	bias factor for the load effects
λ_R	bias factor for resistance
ρ	reinforcement ratio
ρ_ℓ	nonprestressed longitudinal reinforcement ratio (A_s/bd_s)
ρ_p	prestressed longitudinal reinforcement ratio (A_{ps}/bd_p)
ρ_v	shear reinforcement ratio (A_v/b_vs)
σ_Q	standard deviation of the total load effects
σ_Q^2	variance of the mean unfactored load effects
σ_{Qi}	standard deviation of the individual load effects
σ_R	standard deviation of resistance
σ_R^2	variance of the resistance
ΣQ_i	total nominal unfactored load effects
ϕ	resistance factor
ϕR_n	factored nominal resistance

CHAPTER 1. REPORT INTRODUCTION

INTRODUCTION

Much of the fundamental basis for the current lightweight concrete (LWC) provisions in the *American Association of State Highway and Transportation Officials (AASHTO) Load and Resistance Factor Design (LRFD) Bridge Design Specifications* is based on research of LWC from the 1960s.[3,5–8] The LWC that was part of this research used traditional mixes of coarse aggregate, fine aggregate, portland cement, and water. Broad-based advancements in concrete technology over the past 50 yr have given rise to significant advancements in concrete mechanical and durability performance. Research during the past 30 yr, including the recent National Cooperative Highway Research Program (NCHRP) studies on different aspects of high-strength concrete, has resulted in revisions to the *AASHTO LRFD Bridge Design Specifications* to capitalize on the benefits of high-strength normal-weight concrete (NWC).[9–11.3] However, as described by Russell, many of the design equations in the *AASHTO LRFD Bridge Design Specifications* are based on data that do not include tests of LWC specimens, particularly with regard to structural members with compressive strengths in excess of 6 ksi (41 MPa).[12]

The Federal Highway Administration's (FHWA) Turner-Fairbank Highway Research Center (TFHRC) has executed a research program to investigate the performance of LWC with concrete compressive strengths in the range of 6 to 10 ksi (41 to 69 MPa) and equilibrium densities between 0.125 and 0.135 kip per cupid foot (kcf) (2,000 and 2,160 kg/m^3). The research program used LWC with three different lightweight aggregates that are intended to be representative of those available in North America. The program included tests from 27 precast/prestressed LWC girders to investigate topics including transfer length and development length of prestressing strand, the time-dependent prestress losses, and shear strength of LWC. The development and splice length of mild steel reinforcement used in girders and decks made with LWC was also investigated using 40 reinforced concrete (RC) beams. While much of the research program focused on structural behavior, it also included a material characterization component wherein the compressive strength, elastic modulus, and splitting tensile strength of the concrete mixtures used in the structural testing program were assessed. One key outcome of the research program is to recommend changes to the *AASHTO LRFD Bridge Design Specifications* relevant to LWC.[3]

This report describes the results of 30 shear tests on 15 prestressed girders used to evaluate the shear resistance of high-strength LWC. The LWC prestressed girders tested in this study are included in an internal database of shear tests on LWC and NWC specimens that were collected from test results available in the literature.[1] This document describes the database and the analysis of the database. Design expressions in the current edition of the *AASHTO LRFD Bridge Design Specifications* are compared to the database.[3] This report also presents potential revisions to the *AASHTO LRFD Bridge Design Specifications* relating to LWC.

[1]The ACI-DAfStb database is not publicly available. For a list of available sources, see Bibliography section NWC Sources for ACI-DafStb Database.

REPORT OBJECTIVES

This report has four main objectives. First, it provides the results of 30 shear tests on LWC prestressed girders conducted at TFHRC. Second, it describes the internal database, including the TFHRC test results and the analysis of the database. Third, the report presents the reliability analysis performed to evaluate the reduction factor for LWC in shear. Finally, it develops and presents potential revisions to the *AASHTO LRFD Bridge Design Specifications* relating to the nominal shear resistance with a focus on the performance of LWC.[3]

REPORT ORGANIZATION

This report is organized as follows:

- Chapter 2 presents introductory material that summarizes the properties of LWC, the treatment of LWC in the *AASHTO LRFD Bridge Design Specifications*, the mechanism of shear transfer, the factors affecting shear resistance, and the design expressions for nominal shear resistance in the *AASHTO LRFD Bridge Design Specifications*.[3]

- Chapter 3 describes the shear tests of LWC prestressed girders, summarizes the test results, and provides a discussion of the results.

- Chapter 4 includes a description of the shear resistance database as well as statistical information about the database.

- Chapter 5 provides an analysis of the database and comparisons of the shear resistance predicted by design expressions to the shear resistance determined from the tests in the database.

- Chapter 6 describes a reliability analysis to evaluate the resistance factor for LWC in shear.

- Chapter 7 includes potential revisions to the *AASHTO LRFD Bridge Design Specifications*.[3]

- Chapter 8 provides concluding remarks.

- Appendix A provides the material properties for the reinforcing bars.

- Appendix B provides a list of all of the LWC specimen names in the TFHRC shear database.

- Appendix C provides a list of all of the NWC specimen names in the ACI-DafStb database.

- Appendix D provides derivations for selected equations used in the reliability analysis.

- Appendix E provides statistical parameters for LWC tests excluded from the reliability analysis.

- Appendix F provides the drawings for the prestressed concrete (PC) girders tested at TFHRC.

- Appendix G provides details for obtaining the draft version of the research data contained therein.

- The References provides a list of sources found throughout the report, while the Bibliography includes all available source information for the two databases (i.e., TFHRC shear database and ACI-DafStb database).

Note that throughout the report, stress and elastic modulus are shown in kilopounds per square inch (ksi), and unit weight is shown in kcf for all expressions unless stated otherwise. SI units are provided in parentheses for values in the text, and conversion factors are provided for values in the tables. In some equations, U.S. customary units are intentional. If working in metric units, readers should convert variables to U.S. customary units first, apply the equation, and then convert it back to SI units.

SUMMARY OF PRELIMINARY RECOMMENDATIONS

Several revisions to the *AASHTO LRFD Bridge Design Specifications* related to shear resistance of LWC in shear are proposed in this report.[3] The revisions involve the expressions for nominal resistance of LWC in shear, the expression for minimum shear reinforcement, and the resistance factor for LWC in shear. The proposed revisions are based on the recommendations made in previous documents that are a part of this research effort.[1,2] The previous recommendations relate to the definition of LWC and a modification factor for LWC. The definition of LWC was proposed to include concrete with lightweight aggregates up to a unit weight of 0.135 kcf (2,160 kg/m^3), which is considered the lower limit for NWC. Also, the terms "sand-lightweight concrete" and "all-lightweight concrete" were removed in the proposed definition to allow other types of LWC mixtures. An LWC modification factor was proposed to potentially allow a more unified approach of accounting for the mechanical properties of LWC in the *AASHTO LRFD Bridge Design Specifications*.[3]

The proposed LWC modification factor is included in the proposed expressions for nominal resistance of LWC in shear and the proposed expression for minimum shear reinforcement. The validation of the proposed revisions is described in chapters 5 and 6. The proposed code language is presented in chapter 7.

CHAPTER 2. BACKGROUND

INTRODUCTION

This chapter provides background information relevant to the focus of the research effort. It begins with a description of the mechanical properties of LWC, the gap of equilibrium densities on the *AASHTO LRFD Bridge Design Specifications*, and the LWC modification factor.[3] The rest of the chapter covers the shear strength of LWC, including the mechanism of shear transfer, factors that affect shear resistance, and design expressions for nominal shear resistance in the *AASHTO LRFD Bridge Design Specifications*.[3]

MECHANICAL PROPERTIES OF LWC

The aggregate in LWC can either be manufactured or natural with a cellular pore system providing for a lower density particle. The density of lightweight aggregate is approximately half that of normal-weight rock. The reduced dead weight of the LWC has many benefits in building and bridge construction such as smaller, lighter members; longer spans; and reduced substructure and foundation requirements.[13]

As compared to NWC, LWC tends to exhibit a reduction in tensile strength. This difference is generally attributed to the characteristics of the lightweight aggregate. The performance of concrete structures is affected by the tensile strength of concrete in several significant ways. The reduced tensile strength of LWC can affect the shear strength, cracking strength at the release of prestress, and bond strength of prestressed and nonprestressed reinforcement.[13]

EQUILIBRIUM DENSITY GAP IN *AASHTO LRFD BRIDGE DESIGN SPECIFICATIONS*[3]

According to the *AASHTO LRFD Bridge Design Specifications*, *LWC* is defined as concrete having lightweight aggregate and an air-dry unit weight less than or equal to 0.120 kcf (1,920 kg/m^3), while *NWC* is defined as having a unit weight of 0.135 to 0.155 kcf (2,160 to 2,480 kg/m^3).[3] Concretes in the gap of densities between 0.120 and 0.135 kcf (1,920 to 2,160 kg/m^3) are commonly referred to as "specified density concrete" (SDC) and are not directly addressed by the *AASHTO LRFD Bridge Design Specifications*.[3] SDC typically contains a mixture of normal-weight and lightweight coarse aggregate.

Modifications to the *AASHTO LRFD Bridge Design Specifications* are needed to remove the SDC-related ambiguity, give the designer the freedom of specifying a slightly lower density than NWC, and allow for appropriate design with SDC.[3] The inclusion of SDC into the *AASHTO LRFD Bridge Design Specifications* could take many forms but would likely require modifications to both terminology and design expressions.

MECHANISM OF SHEAR TRANSFER IN RC BEAMS

The mechanism of shear transfer depends on whether the beam is cracked or uncracked and whether it is reinforced or unreinforced in the transverse direction. In concrete beams without shear reinforcement, the shear is transferred by developing shear stresses in the uncracked

concrete, through interface shear transfer across a crack, and by dowel action of the longitudinal reinforcement. If the load is applied near the support, arching action may also develop. In concrete beams with reinforcement in the transverse direction, a portion of the shear is transferred by the shear reinforcement. The shear reinforcement also increases the shear transferred through interface shear and dowel action.

Shear Stress in Uncracked Concrete

Uncracked beams or the uncracked portions of beams transfer the shear by developing shear stresses in combination with compressive stresses due to bending. Before cracking, the entire vertical shear force is transferred through a parabolic shear stress distribution. Experimental work has shown that after cracking, between 20 and 40 percent of the total shear was transferred in the uncracked compression zone.[14]

Interface Shear Transfer

Sometimes referred to as "aggregate interlock," interface shear transfer is the transfer of a portion of the total shear across a crack due to surface roughness. Interface shear transfer resists slippage or relative movement along the crack. Experimental work has shown that after cracking, between 33 and 50 percent of the total shear was transferred through interface shear.[14]

Walraven performed a study on the fundamental behavior of interface shear transfer.[15] The study showed that the mechanism of interface shear transfer is dependent on the crack width and shear displacement. Other important variables are the aggregate size, concrete strength, friction coefficient between aggregate and cement paste, and fraction and grading of the aggregate. The shear that can be transferred across a crack is reduced as the crack width increases, the aggregate size decreases, and the shear displacement increases. The shear resistance of specimens with a higher compressive strength or a larger fraction of coarse aggregate was greater for a given crack width or shear deformation. Walraven concluded that the concrete stress is the most important factor in determining the resistance of the crack faces to shear deformation, even more so than the aggregate size.[15] He also concluded that a considerable part of the shear transfer occurs due to friction between the crack faces.

Dowel Action

Some of the shear is resisted by doweling force in the longitudinal reinforcement. The doweling force can result in longitudinal splitting cracks running along the length of the bar. These splitting cracks reduce the stiffness of the concrete around the bar and, as a result, the portion of the shear force transferred by dowel action. Splitting cracks resulting from dowel action can reduce the interface shear transfer. In beams, the dowel shear force is not typically dominant, and experimental work has shown that, after cracking, only 15 to 25 percent of the total shear was transferred through dowel action.[14]

Arching Action

In beams with a concentrated load near the support, a portion of the vertical shear is transferred directly to the support by what is known as "arching action." Arching action produces a strut of

compressive stress from the applied load to the support and is kept in equilibrium by a tensile force developed in the longitudinal reinforcement.[14]

Shear Reinforcement

Transverse shear reinforcement in a beam, or stirrups, carries a portion of the total shear by acting as part of a truss. The concrete between the diagonal cracks carries compression, and the stirrups and longitudinal reinforcement carry the tension. The stirrups also resist the widening of the diagonal cracks, which has the effect of increasing the shear transferred by interface shear transfer and holds the longitudinal bars, which increases the shear transferred by dowel action.[14]

MODES OF SHEAR FAILURE

An inclined diagonal crack forms as the principle stress exceeds the concrete tensile strength.[16] Shear failure modes are characterized by the occurrence of inclined cracking. Inclined cracking that occurs independently of a flexural crack is known as a "web-shear crack," while inclined cracking that occurs as an extension of a flexural crack is known as a "flexure-shear crack." After the occurrence of the primary shear or flexural crack, secondary cracks can occur due to dowel action or slip between the concrete and longitudinal reinforcement.[17]

For beams under concentrated loads, failure modes are strongly influenced by the ratio of the shear span (a) to the effective shear depth (d_v). The ratio of the web thickness to the width of the tension flange and the presence of prestressing will also influence the failure mode.

Deep Beams

Beams with a rectangular cross section and $a/d_v < 1$ can be considered deep beams. After inclined cracking, arching action becomes the dominant shear transfer mechanism. Failure can occur by loss of anchorage of the longitudinal reinforcement, concrete crushing above the support reaction, or compression or tension failure of the concrete arch above the inclined crack.[14,17]

Short Beams

Beams with a rectangular cross section and $1 < a/d_v < 2.5$ generally develop an inclined crack as an extension of a flexural crack. As the load increases, the inclined crack progresses toward the point of concentrated applied load application. A secondary crack can form from the inclined crack downward to the longitudinal reinforcement and then extend horizontally toward the support. The horizontal crack can be due to dowel action and can contribute to loss of anchorage.[14,17]

Failure of short beams may occur as a loss of anchorage and is termed a "shear-tension failure." Failure may also occur by concrete crushing over the upper end of the inclined crack and is termed a "shear-compression failure."[14,17]

Long Beams

Beams with a rectangular cross section and $a/d_v > 2.5$ form several flexural cracks first. An inclined crack will form as an extension of the flexural cracks. Beams without stirrups tend to fail immediately after the first inclined crack in a diagonal tension failure. Beams with stirrups tend to fail in shear-compression or flexure.[14,17]

I-Beams

Beams with an I-shaped cross section have increased shear stress due to thinner webs. The inclined cracks tend to be straighter than in beams with rectangular cross sections. In I-beams with very thin webs or in prestressed I-beams, inclined cracks may occur before flexural cracking. In I-shaped beams with stirrups, the shear force may crush the concrete struts after inclined cracking. This is termed "web-crushing failure."[14]

SHEAR CRACKING STRENGTH OF REINFORCED AND PRESTRESSED BEAMS

This section describes the mechanism causing the formation of web-shear and flexure-shear cracks. The empirical expressions developed to predict web-shear and flexure-shear cracking are presented.

Web Shear Cracks

Web shear cracks typically only occur in prestressed I-beams. They form near the neutral axis of the beam after the principle tensile stress has been exceeded. The approximate expression used in American Concrete Institute (ACI) 318-63 for the web-shear cracking strength is given by equation 1.[18] This expression assumes the concrete tensile strength is $3.5\sqrt{f'_c}$, where f'_c is the concrete compressive strength in reference to material test values and specified compressive strength (ksi), and is given in the form presented by ACI-ASCE Committee 426.[14]

$$v_{cw} = 3.5\sqrt{f'_c} + 0.3f_{pc} + \frac{V_p}{b_w d_p} \quad (1)$$

Where:

v_{cw} = average shear stress at inclined cracking (psi).
f_{pc} = compressive stress at the centroid of the concrete after all prestress losses have occurred (psi).
V_p = component of the effective presstressing force in the direction of the applied shear (lb).
b_w = width of member's web (inches).
d_p = distance from compression face to the centroid of the prestressing steel (inches).

Flexure-Shear Cracks

Before the formation of the inclined crack, the concrete between the flexural cracks or "teeth" experience bending and shearing. These forces are due to the variations in steel stress on either side of the tooth. Shear is transferred by dowel action and interfacial shear stress between the teeth. The inclined cracks that develop at the end of the flexural crack are dependent on the a/d_v

ratio, the height of the flexural crack, and the amount of shear transferred by dowel action and interfacial shear stress.

Several expressions have been traditionally used to predict flexure-shear cracking in RC beams. The first expression, proposed by Viest and ACI-ASCE Committee 326, is given by equation 2.[19,20] A second expression, given by equation 3, was proposed by Bresler and Scordelis as a simplification of equation 2.[21]

$$V_c = bd\left(1.9\sqrt{f'_c} + 2{,}500\frac{\rho V_d}{M}\right) \le 3.5\sqrt{f'_c}bd \tag{2}$$

Where:

V_c = nominal shear resistance provided by tensile stresses in the concrete (lb).
b = width of the compression face of a rectangular member (inches).
d = distance from the compression face to the centroid of the tension reinforcement.
ρ = reinforcement ratio.
V_d = shear force at the section due to unfactored dead load (lb).
M = applied moment (lb-inch).

$$V_c = bd\left(2.0\sqrt{f'_c}\right) \tag{3}$$

For prestressed beams, an expression for the inclined cracking load was proposed by MacGregor and is given by equation 4.[17,22] The first term in equation 4 represents the load to cause flexural cracking at a point along the shear span. The second term represents an additional increment of shear required to cause the inclined crack.

$$V_{ci} = \frac{M_{cr}}{\frac{M}{V} - \frac{d}{2}} + 0.6b_w d\sqrt{f'_c} \le 1.7\sqrt{f'_c}b_w d \tag{4}$$

Where:

V_{ci} = nominal shear resistance provided by concrete when inclined cracking results from combined shear and moment (lb).
M_{cr} = flexural cracking moment (lb-inch).
V = applied shear force (lb).

FACTORS AFFECTING SHEAR STRENGTH

This section describes three factors that affect shear strength: the ratio of shear span to beam depth, the depth of the beam, and lightweight aggregate. The effect that other factors, such as concrete strength and aggregate size, have on the shear transfer mechanism were described previously in the Interface Shear Transfer section of this chapter.

Shear Span to Beam Depth Ratio

As described previously in the Modes of Shear Failure section of this chapter, the a/d_v ratio has considerable effect on the shear resistance of a beam. For beams with an a/d_v ratio greater than 2.5 or 3, inclined cracking occurs as an extension of flexural cracks. As the a/d_v ratio decreases below 2.5, some of the vertical applied load is transferred directly to the support through arching action. As the a/d_v ratio becomes smaller, a larger fraction of the vertical load is transferred to the support, which has the effect of increasing the average shear stress at failure. The failure mode also changes from diagonal tension failures at large a/d_v ratios, shear-compression and shear-tension failures (i.e., anchorage failures) at intermediate a/d_v ratios, and failures related to the compression arch for short a/d_v ratios.[14]

Beam Depth

Since the 1960s, there has been much research on the effect that beam size has on shear strength. Many studies have shown that for beams without stirrups, the shear stress at failure reduces as the beam depth increases.[14] This is commonly referred to as "size effect." Size effect in beams without shear reinforcement is not considered in the provisions of the ACI 318-11 building code.[23] In the *AASHTO LRFD Bridge Design Specifications*, some of the methods to predict shear resistance include the effect of depth for members without shear reinforcement.[3] Size effect in beams with shear reinforcement is usually considered to be minimal. Neither the *AASHTO LRFD Bridge Design Specifications* nor the ACI-318-11 building code includes the effect of beam depth in members with shear reinforcement.[3,23]

Lightweight Aggregate

This subsection provides a summary of some of the research on shear strength of LWC beams. Most of the studies saw a reduction in the average shear stress at failure for LWC beams when compared to similar NWC beams.[5]

A study by Hanson showed that the average shear stress at failure of LWC RC beams without stirrups was between 60 and 100 percent of the stress of comparable NWC beams.[6] The results of the study also showed a good correlation between the splitting tensile strength of cylinders and the shear strength of the LWC beams.

Research by Ivey and Buth proposed factors of 0.75 for all-lightweight concrete and 0.85 for sand-lightweight concrete as a conservative method to account for the shear strength of the RC beams without stirrups considered in their study.[24]

LWC T-beams tested by Hamadi and Regan failed at a lower average shear stress than similar NWC beams in their study.[25] Also, increases in the amount of stirrups in their LWC beams did not result in similar increase in shear stress at failure as similar NWC beams.

Large RC I-beams without stirrups were tested by Walraven and Al-Zubi. The study compared LWC and NWC beams with different amounts of longitudinal reinforcement.[26] The LWC beams had similar shear strengths as the NWC beams in their study. Walraven and Al-Zubi concluded that, although the shear cracks went through the aggregate, the irregular shape of the

crack faces was still able to transfer shear stress. The resulting measured shear displacements along the inclined cracks in the LWC beams was approximately twice that of the NWC beams.

HISTORICAL DESIGN METHODOLOGIES FOR SHEAR

It is common for design codes to ignore the interaction of shear and flexure and design for the worst case of flexure and shear separately.[27] This is the case for the ACI 318-95 building code, where the interaction is accounted for by extending the cut-off locations of the longitudinal reinforcement.[28]

A truss model has been used for the design of RC beams with stirrups. The model (commonly referred to as the "45-degree truss model") consists of two parallel chords with inclined compression diagonal inclined at 45 degrees with respect to the beam's longitudinal axis. The upper chord is under compression, and the lower chord is under tension. Vertical or slightly inclined stirrups carry tension to maintain equilibrium. The truss model has historically neglected concrete acting in tension, interface shear transfer, and dowel action.

The shear strength of beams without stirrups is typically limited to the load to cause the first inclined crack. For beams with stirrups, the truss model was used to estimate the additional shear that could be carried by the stirrups. The shear at first inclined cracking has been considered the concrete contribution to the nominal shear resistance provided by tensile stresses in the concrete (V_c), and the additional shear carried by the stirrups has been considered the nominal shear resistance provided by the shear reinforcement (V_s).

Design for shear then involves predicting the shear to cause inclined cracking. Beams with an applied shear less than the predicted shear to cause inclined cracking were considered adequate for shear. Shear reinforcement was provided for any excess shear (i.e., the difference between the applied shear and shear load at cracking). The basic form of this methodology is still used in the ACI-318-11 building code and in the *AASHTO LRFD Bridge Design Specifications*.[23,3]

DESIGN METHODOLOGIES FOR SHEAR USED IN THE *AASHTO LRFD BRIDGE DESIGN SPECIFICATIONS*[3]

This section describes the critical section for shear and the requirements for minimum area of shear reinforcement and maximum spacing in the *AASHTO LRFD Bridge Design Specifications*.[3] The three design methodologies for determining nominal shear resistance in the *AASHTO LRFD Bridge Design Specifications* are then presented. Last, the modification of the design expressions for LWC is described.

Critical Section for Shear

In beams where the vertical load causes compression in the end region of a member, the critical section for shear is taken as the effective shear depth (d_v) from the internal face of the support as given by Article 5.8.3.2 of the *AASHTO LRFD Bridge Design Specifications*.[3] This occurs in the common case of the bottom surface of a beam resting on its supports with a downward vertical applied load on the top surface of the beam. The effective depth (see equation 5) is determined using the calculated nominal flexural resistance (M_n), which is determined by first

calculating the depth from the compression face to the neutral axis (c) for T-section behavior or rectangular section behavior given by equation 6 and equation 7, respectively.

$$d_v = \frac{M_n}{A_s f_y + A_{ps} f_{ps}} \tag{5}$$

Where:

A_s = area of the longitudinal tension reinforcement (inches^2).
f_y = yield strength of reinforcing bars in reference to material test values and specified minimum yield strength (ksi).
A_{ps} = area of the longitudinal prestressing steel (inches^2).
f_{ps} = Average stress in prestressing steel at the time for which the nominal resistance of member is required (ksi).

$$c = \frac{A_{ps} f_{pu} + A_s f_s - A'_s f'_s - 0.85 f'_c (b - b_w) h_f}{0.85 f'_c \beta_1 b_w + k A_{ps} \frac{f_{pu}}{d_p}} \tag{6}$$

Where:

f_{pu} = tensile strength of prestressing steel in reference to material test values and specified tensile strength (ksi).
f_s = stress in mild tension reinforcement at nominal flexural resistance (ksi).
A'_s = area of the longitudinal compression reinforcement (inches^2).
f'_s = stress in the mild steel compression reinforcement at nominal flexural resistance (ksi).
h_f = compression flange depth (inches).
β_1 = ratio of the depth of the equivalent uniformly stressed compression zone assumed in the strength limit state to the depth of the actual compression zone.
k = prestresssing factor.

$$c = \frac{A_{ps} f_{pu} + A_s f_s - A'_s f'_s}{0.85 f'_c \beta_1 b + k A_{ps} \frac{f_{pu}}{d_p}} \tag{7}$$

The average stress in the prestressing steel at nominal moment capacity is given by equation 8, where the parameter k has a value of 0.28 for low relaxation strand. The expression for the nominal moment capacity in the *AASHTO LRFD Bridge Design Specifications* is then determined using equation 9.[3] Rectangular section behavior can be assumed to occur when the depth of the assumed uniform concrete stress distribution ($a = \beta_1 c$) is less than the compression flange depth (h_f). In the case of rectangular section behavior, b_w is taken as b in equation 9.

$$f_{ps} = f_{pu}\left(1 - k\frac{c}{d_p}\right) \tag{8}$$

$$M_n = A_{ps} f_{ps}\left(d_p - \frac{a}{2}\right) + A_s f_s\left(d_s - \frac{a}{2}\right) - A'_s f'_s\left(d'_s - \frac{a}{2}\right) + 0.85 f'_c (b - b_w) h_f \left(\frac{a}{2} - \frac{h_f}{2}\right) \tag{9}$$

Where:

d_s = distance from the compression face to the centroid of the nonprestressed tension reinforcement (inches).
d'_s = distance from compression face to the centroid of the nonprestressed compression reinforcement (inches).

The stress in the mild steel acting in tension (f_s) is assumed to be yielding if the ratio c/d_s does not exceed 0.6. If this limit is not met, a strain compatibility analysis is necessary to determine f_s. The stress in the mild steel acting in compression (f'_s) is assumed to be yielding if the ratio c/d'_s is greater than or equal to 3.0. If this limit is not met, the compression steel can be conservatively ignored according to Article 5.7.2.1 of the *AASHTO LRFD Bridge Design Specifications*.[3]

Minimum Amount of Shear Reinforcement

The minimum amount of shear reinforcement required by Article 5.8.2.5 of the *AASHTO LRFD Bridge Design Specifications* is given by equation 10.[3] This minimum amount of shear reinforcement is intended to prevent failure after inclined cracking, restrain the growth of the inclined cracking, and increase the ductility in the section.

$$A_v \geq 0.0316\sqrt{f'_c}\frac{b_v s}{f_y} \tag{10}$$

Where:

A_v = area of the shear reinforcement within the spacing (inches^2).
b_v = effective web width (inches).
s = spacing of the shear reinforcement (inches).

Maximum Spacing of Shear Reinforcement

In order to provide adequate crack control, the maximum spacing of the shear reinforcement is limited. The maximum spacing is dependent on the average shear stress with higher levels of shear stress requiring a closer spacing of shear reinforcement. The maximum spacing is given by Article 5.8.2.7 of the *AASHTO LRFD Bridge Design Specifications*.[3] For an average shear stress (v_u) less than $0.125f'_c$, the maximum permitted spacing of the shear reinforcement (s_{max}) is given by equation 11. For v_u greater than or equal to $0.125f'_c$, s_{max} is given by equation 12.

$$\text{For } v_u < 0.125f'_c,\ s_{max} = 0.8d_v \leq 24.0 \text{ inches (609.6 mm)} \tag{11}$$

$$\text{For } v_u \geq 0.125f'_c,\ s_{max} = 0.4d_v \leq 12.0 \text{ inches (304.8 mm)} \tag{12}$$

Nominal Shear Resistance

The sectional design approach is used in the *AASHTO LRFD Bridge Design Specifications* to evaluate the shear resistance of beams away from the supports, points of concentrated loads, or geometric discontinuities.[3] In the sectional design approach, the factored shear force is compared to the factored shear resistance at multiple locations along the length of the beam.

The *AASHTO LRFD Bridge Design Specifications* includes a design method of considering the nominal shear resistance to be the sum of the individual nominal shear resistance provided by tensile stresses in the concrete (V_c), nominal shear resistance provided by the shear reinforcement (V_s), and component of the effective presstressing force in the direction of the applied shear (V_p). The expression for nominal shear resistance of the section (V_n) is given by equation 13. V_c and V_s are limited to 25 percent of the concrete compressive strength multiplied by the section shear area. The expression for V_n including this limit is given by equation 14. The sectional design approach has an additional limit of $0.18f'_c$ placed on the shear stress using equation 15.

$$V_n = V_c + V_s + V_p \tag{13}$$

$$V_n = 0.25f'_c b_v d_v + V_p \tag{14}$$

$$v_u = \frac{\left|V_u - \phi V_p\right|}{\phi b_v d_v} \tag{15}$$

Where ϕ is the resistance factor. There are four different methods in the *AASHTO LRFD Bridge Design Specifications* to determine V_c in equation 13. The first three methods given in Articles 5.8.3.4.1 and 5.8.3.4.2 and appendix B5 use equation 16 to determine V_c. These methods each provide a methodology to determine the factor indicating ability of diagonally cracked concrete to transmit tension and shear (β) in equation 16. The fourth method given in Article 5.8.3.4.3 calculates two terms: nominal shear resistance provided by concrete when inclined cracking results from combined shear and moment (V_{ci}) and nominal shear resistance provided by concrete when inclined cracking results from excessive principal tensions in the web (V_{cw}). The lesser of the two terms is used for V_c. All four methods include the determination of the angle of inclination of diagonal compressive stresses (θ), which is used to determine V_s in equation 17.

$$V_c = 0.0316\beta\sqrt{f'_c}\, b_v d_v \tag{16}$$

$$V_s = \frac{A_v f_y d_v \cot\theta}{s} \tag{17}$$

Simplified Procedure for Nonprestressed Sections

The method in Article 5.8.3.4.1 of the *AASHTO LRFD Bridge Design Specifications* is titled "Simplified Procedure for Nonprestressed Sections" and is applicable only to RC slabs with or without stirrups and to RC beams with stirrups.[3] Throughout this report, it is referred to as "Simplified-RC." The overall member depth is limited to 16 inches (406 mm). This method is based on the simple expression for the average shear stress at inclined cracking (see equation 3) proposed by Bresler and Scordelis and the 45-degree truss model.[21] For this method, β is taken as 2.0, and θ is taken as 45 degrees.

General Procedure Methods

Two methods of the *AASHTO LRFD Bridge Design Specifications* are based on the modified compression field theory (MCFT).[3,29,30] MCFT was developed by Vecchio and Collins to describe the strength and load–deformation behavior of RC membrane elements.[29] Such elements are subjected only to in-plane normal and shear stresses. When the model is applied to the web of RC or PC beams, the only mechanism for shear transfer assumed by the model is that due to interface shear transfer. The contributions of the uncracked concrete in the compression zone and dowel action are not considered.

The method given in appendix B5 of the *AASHTO LRFD Bridge Design Specifications* is an iterative design procedure that is similar to the method originally proposed by Vecchio and Collins and described for prestressed structures by Mitchell and Collins.[3,29,3031] The method is based on MCFT and involves the use of tables B5.2-1 and B5.2-2 in appendix B to iteratively determine β and θ. In this report, it is referred to as the "general procedure with tables" (i.e., GP-table). The method in appendix B5 was simplified by Bentz et al. and validated for the design of reinforced and prestressed beams as part of NCHRP Project 12-61.[30,32] The simplified method uses equations to directly solve for β and θ without iteration and is presented in Article 5.8.3.4.2 of the *AASHTO LRFD Bridge Design Specifications*.[3] In this report, this simplified method is referred to as "general procedure with equations" (i.e., GP-equation).

The two general procedure methods (i.e., GP-table and GP-equation) determine the average strain at a section due to the combined effects of applied bending moment, shear force, axial force, and internal prestressing force. This is a different approach than the historical method for determining shear resistance where the interaction of shear, bending, and axial force is ignored.

In the GP-equation method, the net longitudinal tensile strain in the section at the centroid of the tension reinforcement (ε_s) is determined using equation 18. The axial stiffness terms in the denominator of the equation are applicable when ε_s is positive, indicating a net tensile strain. When ε_s is negative, such as in the case of some prestressed beams, the expression in equation 19 is used and includes an additional stiffness term for the concrete in the lower half of the section acting in compression. The absolute value for the factored moment at the section ($|M_u|$) shall not be taken less than $|V_u - V_p|d_v$, where V_u is the factored shear force at the section, V_p is the coefficient of variation (COV) for the uncertainty in the analysis, and A_s and A_{ps} are adjusted for development length.

$$\varepsilon_s = \frac{\left(\frac{|M_u|}{d_v} + 0.5N_u + |V_u - V_p| - A_{ps}f_{po}\right)}{E_sA_s + E_pA_{ps}} \leq 0.0060 \qquad (18)$$

Where:

N_u = factored axial force the section (kip).
f_{po} = parameter taken as the modulus of elasticity of prestressing steel multiplied by the locked-in difference in strain between the prestresing steel and the surrounding concrete (ksi).
E_s = modulus of elasticity of reinforcing bars (ksi).
E_p = modulus of elasticity of prestressing steel (ksi).

$$\varepsilon_s = \frac{\left(\frac{|M_u|}{d_v} + 0.5N_u + |V_u - V_p| - A_{ps}f_{po}\right)}{E_sA_s + E_pA_{ps} + E_cA_{ct}} \geq -0.00040 \quad (19)$$

Where:

E_c = modulus of elasticity of concrete (ksi).
A_{ct} = area of concrete on the flexural tension side of the member (inches^2).

In equation 18 and equation 19, $V_u - V_p$ is a simplification of tensile force in each flange due to the applied shear. The longitudinal demand due to shear determined by equilibrium is given by the left-hand term in equation 20. By assuming a value of 26.6 degrees for θ, the simplification shown by the right-hand term in equation 20 can be made. The result of this simplification is that equation 18 and equation 19 are not a function of θ, and the design procedure is not iterative.

$$0.5(V_u - V_p)\cot\theta \approx V_u - V_p \quad (20)$$

For beams with the minimum amount of stirrups given in Article 5.8.2.5 of the *AASHTO LRFD Bridge Design Specifications* (see equation 10), β is determined using equation 21.[3] The factor β for beams without the specified minimum amount of stirrups (see equation 22) also includes a term with a crack-spacing parameter (s_{xe}). The expression for s_{xe} is given by equation 23 and accounts for the effect of maximum aggregate size (a_g) on interface shear transfer and for size effect in beams without stirrups. For beams with the concentrated longitudinal reinforcement (i.e., not distributed along the depth of the beam), the lesser of effective shear depth (d_v) or the maximum distance between layers of longitudinal crack-control reinforcement (s_x) is taken as equal to d_v. Combinations of d_v and a_g that result in s_{xe} being greater than 12 inches (305 mm) have the effect of reducing the factor β and, as a result, V_c of the nominal shear resistance (see equation 13). The value of θ (degrees) is determined using the expression in equation 24 or the value of the beams with or without the minimum amount of stirrups specified in Article 5.8.2.5 of the *AASHTO LRFD Bridge Design Specifications*.[3]

$$\beta = \frac{4.8}{(1 + 750\varepsilon_s)} \quad (21)$$

$$\beta = \frac{4.8}{(1 + 750\varepsilon_s)}\frac{51}{(39 + s_{xe})} \quad (22)$$

$$12 \text{ inches (305 mm)} \leq s_{xe} = s_x\frac{1.38}{(a_g + 0.63)} \leq 80 \text{ inches (2,030 mm)} \quad (23)$$

$$\theta = 29 \text{ degrees} + 3{,}500\varepsilon_s \quad (24)$$

The GP-table method (see appendix B5 of the *AASHTO LRFD Bridge Design Specifications*) differs from the GP-equation method in Article 5.8.3.4.2 of the *AASHTO LRFD Bridge Design Specifications* in several ways.[3] Instead of calculating the strain at the level of the tensile reinforcement, the strain is calculated at the middepth of the beam. When the calculated strain is tensile, different expressions are used depending on whether the specified minimum amount of

stirrups is provided. The simplification given by equation 20 is not made. As a result, the method is iterative in that a value of θ must be assumed for the first set of calculations. The values of β and θ are determined from tables instead of directly from an expression. For members with stirrups, β and θ are functions of both the average shear stress and the concrete compressive strength instead of only the calculated strain.

In the GP-table method, the longitudinal strain at the middepth of the beam (ε_x) is determined using equation 25 for a member with at least the minimum amount of stirrups as specified in Article 5.8.2.5 of the *AASHTO LRFD Bridge Design Specifications* (see equation 10) and determined using equation 26 for beams with less than the minimum amount of stirrups.[3] The difference between equation 25 and equation 26 is a factor of 2 in the denominator that doubles the calculated strain for beams with less than the minimum specified amount of stirrups. When ε_x is negative, the expression in equation 27 is used. These expressions for ε_x assume that the strain at the centroid of the compressive flange is 0, which is conservative unless the combination of M_u, V_u, and N_u produces net tension in both flanges.

$$\varepsilon_x = \frac{\left(\frac{|M_u|}{d_v} + 0.5N_u + 0.5\left|V_u - V_p\right| cot\,\theta - A_{ps}f_{po}\right)}{2\left(E_sA_s + E_pA_{ps}\right)} \leq 0.0030 \tag{25}$$

$$\varepsilon_x = \frac{\left(\frac{|M_u|}{d_v} + 0.5N_u + 0.5\left|V_u - V_p\right| cot\,\theta - A_{ps}f_{po}\right)}{E_sA_s + E_pA_{ps}} \leq 0.0030 \tag{26}$$

$$\varepsilon_x = \frac{\left(\frac{|M_u|}{d_v} + 0.5N_u + 0.5\left|V_u - V_p\right| cot\,\theta - A_{ps}f_{po}\right)}{2\left(E_sA_s + E_pA_{ps} + E_cA_{ct}\right)} \geq -0.00020 \tag{27}$$

In beams with at least the minimum specified amount of stirrups, the values of β and θ are determined from table B5.2-1 in the *AASHTO LRFD Bridge Design Specifications*, which is reproduced in this report as table 1.[3] The normalized shear stress (v_u/f'_c) and ε_x are needed for the table. The commentary of appendix B5 allows the values of β and θ determined from the tables to be applied over a range of values. The values of β and θ in a particular cell are applicable for a pair of v_u/f'_c and ε_x values that are less than or equal to the limiting v_u/f'_c and ε_x values given for each row and column. By using this method, a lower value of β and a higher value of θ can be conservatively selected for design. Alternatively, three-way interpolation between the table cells that bound the pair of v_u/f'_c and ε_x values can be used to determine a more exact value of β and θ.

Table 1. Values of β and θ for sections with shear reinforcement.[3]

v_u/f'_c	β or θ	$\varepsilon_x \times 1{,}000$								
		≤–0.20	≤–0.10	≤–0.05	≤0.00	≤0.125	≤0.25	≤0.50	≤0.75	≤1.00
≤0.075	θ	22.3	20.4	21.0	21.8	24.3	26.6	30.5	33.7	36.4
0.075	β	6.32	4.75	4.10	3.75	3.24	2.94	2.59	2.38	2.23
≤0.100	θ	18.1	20.4	21.4	22.5	24.9	27.1	30.8	34.0	36.7
≤0.100	β	3.79	3.38	3.24	3.14	2.91	2.75	2.50	2.32	2.18
≤0.125	θ	19.9	21.9	22.8	23.7	25.9	27.9	31.4	34.4	37.0
≤0.125	β	3.18	2.99	2.94	2.87	2.74	2.62	2.42	2.26	2.13
≤0.150	θ	21.6	23.3	24.2	25.0	26.9	28.8	32.1	34.9	37.3
≤0.150	β	2.88	2.79	2.78	2.72	2.60	2.52	2.36	2.21	2.08
≤0.175	θ	23.2	24.7	25.5	26.2	28.0	29.7	32.7	35.2	36.8
≤0.175	β	2.73	2.66	2.65	2.60	2.52	2.44	2.28	2.14	1.96
≤0.200	θ	24.7	26.1	26.7	27.4	29.0	30.6	32.8	34.5	36.1
≤0.200	β	2.63	2.59	2.52	2.51	2.43	2.37	2.14	1.94	1.79
≤0.225	θ	26.1	27.3	27.9	28.5	30.0	30.8	32.3	34.0	35.7
≤0.225	β	2.53	2.45	2.42	2.40	2.34	2.14	1.86	1.73	1.64
≤0.250	θ	27.5	28.6	29.1	29.7	30.6	31.3	32.8	34.3	35.8
≤0.250	β	2.39	2.39	2.33	2.33	2.12	1.93	1.70	1.58	1.50

In beams without the minimum specified amount of stirrups, the values of β and θ are determined from table B5.2-2, which is reproduced in this report as table 2.[3] In this table, s_{xe} and ε_x are used to determine the values of β and θ. The expression for s_{xe} in the GP-table method is the same as the expression in the GP-equation method (see equation 24) except that the lower limit of 12 inches (305 mm) is effectively reduced to 5 inches (127 mm). Similar to table 1, values of β and θ in a particular cell of table 2 can be applied to a pair of s_{xe} and ε_x values that are less than or equal to the limiting s_{xe} and ε_x values given for each row and column. Alternatively, three-way interpolation between the table cells can be used.

Table 2. Values of β and θ for sections with less than minimum shear reinforcement.[3]

s_{xe}	β or θ	$\varepsilon_x \times 1{,}000$										
		≤–0.20	≤–0.10	≤–0.05	≤0.00	≤0.125	≤0.25	≤0.50	≤0.75	≤1.00	≤1.50	≤2.00
≤5	θ	25.4	25.5	25.9	26.4	27.7	28.9	30.9	32.4	33.7	35.6	37.2
≤5	β	6.36	6.06	5.56	5.15	4.41	3.91	3.26	2.86	2.58	2.21	1.96
≤10	θ	27.6	27.6	28.3	29.3	31.6	33.5	36.3	38.4	40.1	42.7	44.7
≤10	β	5.78	5.78	5.38	4.89	4.05	3.52	2.88	2.50	2.23	1.88	1.65
≤15	θ	29.5	29.5	29.7	31.1	34.1	36.5	39.9	42.4	44.4	47.4	49.7
≤15	β	5.34	5.34	5.27	4.73	3.82	3.28	2.64	2.26	2.01	1.68	1.46
≤20	θ	31.2	31.2	31.2	32.3	36.0	38.8	42.7	45.5	47.6	50.9	53.4
≤20	β	4.99	4.99	4.99	4.61	3.65	3.09	2.46	2.09	1.85	1.52	1.31
≤30	θ	34.1	34.1	34.1	34.2	38.9	42.3	46.9	50.1	52.6	56.3	59.0
≤30	β	4.46	4.46	4.46	4.43	3.39	2.82	2.19	1.84	1.60	1.30	1.10
≤40	θ	36.6	36.6	36.6	36.6	41.2	45.0	50.2	53.7	56.3	60.2	63.0
≤40	β	4.06	4.06	4.06	4.06	3.20	2.62	2.00	1.66	1.43	1.14	0.95

s_{xe}	β or θ	$\varepsilon_x \times 1{,}000$										
		≤–0.20	**≤–0.10**	**≤–0.05**	**≤0.00**	**≤0.125**	**≤0.25**	**≤0.50**	**≤0.75**	**≤1.00**	**≤1.50**	**≤2.00**
≤60	θ	40.8	40.8	40.8	40.8	44.5	49.2	55.1	58.9	61.8	65.8	68.6
≤60	β	3.50	3.50	3.50	3.50	2.92	2.32	1.72	1.40	1.18	0.92	0.75
≤80	θ	44.3	44.3	44.3	44.3	47.1	52.3	58.7	62.8	65.7	69.7	72.4
≤80	β	3.10	3.10	3.10	3.10	2.71	2.11	1.52	1.21	1.01	0.76	0.62

Simplified Procedure for Prestressed and Nonprestressed Sections

The simplified procedure for prestressed and nonprestressed sections (referred to as "Simplified-PC/RC" throughout this report) is based on a model that uses V_{cw} and V_{ci} for web-shear cracks and flexural shear cracks in prestressed beams. This is the model that was introduced into the ACI 318-63 building code, and the expressions are given by equation 1 and equation 4.[18] The method in the *AASHTO LRFD Bridge Design Specifications* was proposed by NCRHP Project 12-61 and is based on the V_{cw}-V_{ci} approach.[3,32] The V_{cw}-V_{ci} approach had already been included in the AASHTO *Standard Specifications for Highway Bridges* and the ACI 318-02 building code.[33,34] The average shear stress at failure included in the *AASHTO LRFD Bridge Design Specifications* version of the V_{cw}-V_{ci} approach has been reduced from the other design documents in order to make the approach applicable to RC beams and PC beams with smaller amounts of longitudinal reinforcement.[32]

The expression for web-shear cracking in the *AASHTO LRFD Bridge Design Specifications* is given by equation 28. The term $0.06\sqrt{f'_c}$ (ksi) corresponds to $1.9\sqrt{f'_c}$ (psi). As described previously in this report, a concrete tensile strength of $3.5\sqrt{f'_c}$ was assumed in the traditional expression for V_{cw} given by equation 1. The term $0.06\sqrt{f'_c}$ represents a lower-bound estimate of the concrete tensile strength applicable to RC beams.

$$V_{cw} = \left(0.06\sqrt{f'_c} + 0.3f_{pc}\right) b_v d_v + V_p \tag{28}$$

The expression for flexural shear cracking in the *AASHTO LRFD Bridge Design Specifications* is given by equation 29.[3] In comparison to the more traditional version of V_{ci} given by equation 4, the term $0.02\sqrt{f'_c}$ (ksi) in equation 29 corresponds to $0.63\sqrt{f'_c}$ (psi). The term $d/2$ was dropped for simplification. The term $0.06\sqrt{f'_c}d_v$ (ksi and inches) corresponds to $1.9\sqrt{f'_c}d_v$ (psi and inches). This is similar to the term $1.7\sqrt{f'_c}d$ (psi and inches) if the depth is assumed equal to $0.9d_v$. The use of $0.06\sqrt{f'_c}$ as the minimum average shear stress in equation 29 makes this value the uniform minimum shear stress regardless of location along the beam as $0.06\sqrt{f'_c}$ is also in equation 28.[32] The moment causing flexural cracking at the section due to externally applied loads (M_{cre}) in equation 29 is given by equation 30.

$$V_{ci} = 0.02\sqrt{f'_c} b_v d_v + V_d + \frac{V_i M_{cre}}{M_{max}} \geq 0.06\sqrt{f'_c} b_v d_v \tag{29}$$

Where:

V_i = factored shear force at the section due to externally applied loads occurring simultaneously with the maximum factored moment at the section due to externally applied loads.
M_{max} = maximum factored moment at the section due to externally applied loads.

$$M_{cre} = S_c \left(f_r + f_{cpe} - \frac{M_{dnc}}{S_{nc}} \right) \tag{30}$$

Where:

S_c = section modulus for the extreme fiber of the composite section where tensile stress is caused by externally applied loads (inches^3).
f_r = modulus of rupture of concrete (psi).
f_{cpe} = compressive stress in the concrete at the extreme tensile fiber after all prestress losses have occurred (psi).
M_{dnc} = total unfactored dead load moment acting on the noncomposite section (lb-inch).
S_{nc} = section modulus for the extreme fiber of the noncomposite section where tensile stress is caused by externally applied loads (inches^3).

The inclination angle of a crack (θ) of diagonal compressive stresses can be predicted using Mohr's circle for an element subjected to combined shear and compression, as shown in figure 1. The radius of Mohr's circle (R) can be used to write an expression that relates the compressive stress at the centroid of the concrete after all prestress losses have occurred (f_{pc}), the shear stress (v_u), and the tensile strength of concrete (f_t), as given by equation 31. Both sides of the expression are squared as given by equation 32. The expression is simplified and solved for v_u as given by equation 33. The expression for v_u from equation 33 is substituted into the expression for cot θ to give equation 34. An expression for cot θ can be determined from the shaded triangle shown on the Mohr's circle (see figure 1).

$$\sqrt{\left(\frac{f_{pc}}{2}\right)^2 + (v_u)^2} = R = \frac{f_{pc}}{2} + f_t \tag{31}$$

$$\left(\frac{f_{pc}}{2}\right)^2 + (v_u)^2 = \left(\frac{f_{pc}}{2}\right)^2 + 2f_t\frac{f_{pc}}{2} + (f_t)^2 \tag{32}$$

$$v_u = \sqrt{f_t f_{pc} + (f_t)^2} = f_t\sqrt{1.0 + \frac{f_{pc}}{f_t}} \tag{33}$$

$$\cot\theta = \frac{v_u}{f_t} = \sqrt{1.0 + \frac{f_{pc}}{f_t}} \tag{34}$$

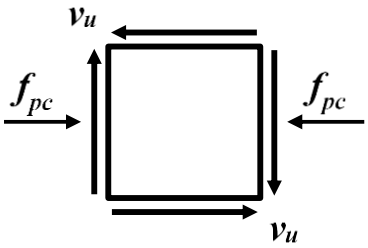

Source: FHWA.

A. Element subjected to shear and compression.

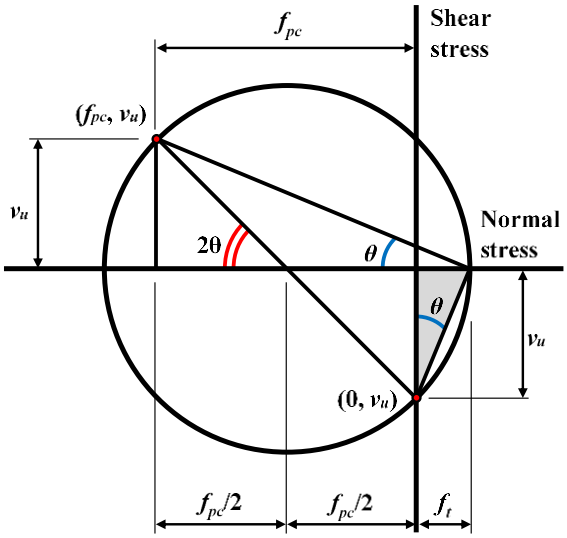

Source: FHWA.

B. Mohr's circle for stress state of element.

Figure 1. Illustrations. Stress condition on an element subjected to shear and compression and Mohr's circle for stress state of an element.

The expression for cot θ in the *AASHTO LRFD Bridge Design Specifications* is given by equation 35 and is the first two terms of a Taylor Series expansion of equation 34.[32] A lower limit of 29 degrees on θ is used for design purposes, which corresponds to the upper limit of 1.8 on cot θ in equation 35. The cot θ is used directly in the expression for V_s in equation 17.

$$\cot\theta = 1.0 + 3\left(\frac{f_{pc}}{\sqrt{f'_c}}\right) \leq 1.8 \tag{35}$$

Modification of Shear Resistance for LWC in *AASHTO LRFD Bridge Design Specifications*[3]

Modification for LWC is explicitly stated in the *AASHTO LRFD Bridge Design Specifications* regarding shear.[3] Specifically, Article 5.8.2.2 states that all expressions in Articles 5.8.2 and 5.8.3, which are the provisions covering design for shear and torsion, shall be modified for the effects of LWC. The modification consists of replacing $\sqrt{f'_c}$ with $4.7f_{ct}$, where f_{ct} is the concrete-splitting tensile strength, when the splitting tensile strength is specified. When f_{ct} is not specified, $\sqrt{f'_c}$ is replaced with $0.75\sqrt{f'_c}$ when all-lightweight concrete is used or $0.85\sqrt{f'_c}$ when sand-lightweight concrete is used.

The modification for LWC described by Article 5.8.2.2 applies to many of the design expression described previously in this chapter.[3] For example, it applies to equation 10 for the minimum amount of shear reinforcement. It also applies to the expression for V_c given by equation 16 that is part of the Simplified-RC method and both methods of the general procedure. The modification affects V_{cw} and V_{ci} (equation 28 and equation 29) of the Simplified-PC/RC method. The modification also applies to the expression for cot θ given by equation 35. The modification

of $\sqrt{f'_c}$ in equation 35 affects the shear resistance of prestressed beams with stirrups. The modification for LWC reduces the value of the denominator in the second term and results in a larger overall value of cot θ. The increase in cot θ directly increases V_s and could result in a calculated V_n for prestressed LWC beams with stirrups that is larger than the calculated V_n for a similar NWC beam. The effect of including a modification for LWC in the expression for cot θ, and the resulting effect on the calculated shear resistance of prestressed LWC beams is described quantitatively in chapter 5 of this report.

FACTOR FOR LWC TENSILE STRENGTH

The tendency for LWC to have a reduced tensile strength is not treated consistently in the *AASHTO LRFD Bridge Design Specifications*.[3] There are many articles where $\sqrt{f'_c}$ is used to represent concrete tensile strength. The provisions for shear- and tension-development length of mild reinforcement currently include a modification for LWC. However, the tensile stress limits in PC do not include a modification for LWC. A potential option to provide a more uniform treatment of LWC tensile strength would be to add the definition of a modification factor for LWC, such as the LWC modification factor (λ), to section 5.4 of the *AASHTO LRFD Bridge Design Specifications*, which could then be referenced in other articles.[3] Then the factor could be added to design expressions where the $\sqrt{f'_c}$ is used to represent concrete tensile strength.

A modification factor for LWC was previously developed from tests on LWC and applied to the prediction of bar stress developed in lap splices of mild steel reinforcement.[1,2] The modification factor is based on the splitting tensile strength when available and the concrete unit weight (w_c) otherwise. An expression for the modification factor for LWC that is based on w_c is convenient to designers because this is a quantity, like compressive strength, that is determined during the design phase. The expression for the modification factor for LWC (λ) based on w_c is given by equation 36 through equation 38. The expression for λ based on splitting tensile strength (f_{ct}) is given by equation 39.

$$\text{For } w_c \leq 0.100 \text{ kcf: } \lambda = 0.75 \tag{36}$$

$$\text{For } 0.100 < w_c < 0.135 \text{ kcf: } \lambda = 7.5 w_c \leq 1.00 \tag{37}$$

$$\text{For } w_c \geq 0.135 \text{ kcf: } \lambda = 1.00 \tag{38}$$

$$\lambda = 4.7 \frac{f_{ct}}{\sqrt{f'_c}} \leq 1.00 \tag{39}$$

CHAPTER 3. RESEARCH ON SHEAR RESISTANCE OF LWC

INTRODUCTION

This research program focused on LWC with compressive strengths from 6 to 10 ksi (41 to 69 MPa) and equilibrium densities between 0.125 and 0.135 kcf (2,000 and 2,160 kg/m^3). LWC used in this research program can be considered high-strength SDC. The program used LWC with three different lightweight aggregates to produce 27 precast/prestressed LWC girders and 40 RC splice beam specimens. Russell recognized the lack of mild steel bond test data and shear test data for LWC.[12] While this research program focused on structural behavior, it also had a material characterization component, as described in *Lightweight Concrete: Mechanical Properties*, and included mechanical property tests on the concrete mixtures used in the structural testing program.[1] Mechanical tests included the compressive strength, elastic modulus, and splitting tensile strength. w_c was determined using several methods (see *Lightweight Concrete: Mechanical Properties* for more information).[1] The 40 splice beam specimens tested by FHWA and used to evaluate the development length of mild steel reinforcement are also described in *Lightweight Concrete: Development of Mild Steel in Tension*.[2]

The details of the FHWA research program involving the shear resistance of precast/prestressed LWC girders are provided in this chapter. It also summarizes the selection process of LWC mix design, the specimen fabrication at the precaster's facility, and the material property testing. The girder design, test setup, and test results for the 30 shear tests on 15 LWC girders are discussed in detail. The results include observations of girder behavior such as failure mode, peak shear force, web cracking shear force, and web cracking angle. The peak shear force, web cracking shear force, and web cracking angle are compared to several design procedures in the *AASHTO LRFD Bridge Design Specifications*.[3]

RESEARCH SIGNIFICANCE

There is a limited amount of test data on the shear resistance of high-strength LWC. This research project included 30 girder tests on this type of concrete. These tests on shear resistance were combined with the results of other tests on LWC to determine the effect of lightweight aggregates. Design expressions for shear resistance that include a proposed modification factor for LWC (λ) were validated using the tests on LWC.

LWC MIX DESIGNS

The Expanded Shale, Clay, and Slate Institute assisted FHWA in obtaining SDC mixes that had been used in production. One of the criteria for this research project was to use lightweight aggregate sources that were geographically distributed across the United States. Additional selection criteria included mixes using a large percentage of the coarse aggregate as lightweight coarse aggregate, mixes using natural sand as the fine aggregate, and mixes with a target equilibrium density between 0.125 and 0.135 kcf (2,000 and 2,160 kg/m^3). In order to make sure that the behavior of the concrete would be controlled by the lightweight aggregate, only mixes with greater than 50 percent of the coarse aggregate as lightweight aggregate were considered. The concrete density needed to be in the range of densities not currently covered by the *AASHTO*

LRFD Bridge Design Specifications because of the limited amount of test data in this density range.[3] Literature has shown that silica fume can increase LWC compressive strength and has also been revealed to improve bond of mild steel reinforcement and prestressing strand.[35–38] As a result, mixes that included silica fume were not selected for this experimental study so that the results would be representative of mechanical properties for SDC without silica fume and most likely conservative for SDC with silica fume.

Three mix designs were selected with a design compressive strength greater than 6.0 ksi (41.3 MPa) to represent concrete that could be used for bridge girders. A fourth mix design was selected that had a design compressive strength less than 6.0 ksi (41.3 MPa) to represent concrete that could be used for a bridge deck.

The selected mix designs are shown in table 3. Each uses partial replacement of the coarse aggregate with lightweight aggregate to achieve its reduced unit weight. The lightweight aggregates in the mixes were haydite, an expanded shale from Ohio; stalite, an expanded slate from North Carolina; and utelite, an expanded shale from Utah. The normal-weight coarse aggregate was No. 67 Nova Scotia granite. Natural river sand was used as the fine aggregate. Type III portland cement was used to obtain the high early strengths typically required in high-strength precast girders. Admixtures included a water reducer, an air entrainer, and a high-range water reducer.

Table 3. Selected concrete-mixture designs.

Design Values and Component Materials	Haydite Girder (HG)	Stalite Girder (SG)	Utelite Girder (UG)
Design 28-day strength (ksi)	6.0	10.0	7.0
Design release strength (ksi)	3.50	7.50	4.20
Target unit weight (kcf)	0.130	0.126	0.126
Lightweight coarse aggregate (kip)	0.80	0.88	0.74
Normal-weight coarse aggregate (kip)	0.52	0.25	0.39
Normal-weight sand (kip)	1.19	1.22	1.27
Class F fly ash (kip)	0.00	0.00	0.15
Type III portland cement (kip)	0.75	0.80	0.60
Water (kip)	0.27	0.25	0.26
Water reducer (oz)	19	19	19
Air entrainer (oz)	2	2	2
High-range water reducer (oz)	34	34	34
Water/cementitious materials ratio	0.36	0.31	0.34

1 ksi = 6.89 MPa.
1 kcf = 16,020 kg/m^3.
1 kip = 4.45 kN.
1 oz = 29.6 mL.

EXPERIMENTAL PROGRAM

The experimental program consisted of 30 tests on 15 PC girders made using three different LWC mixes. Key test parameters included the lightweight aggregate, the amount of shear reinforcement, girder depth, and the use of straight or draped strands. Five girder designs were developed to evaluate the effect of the key parameters. The end of each girder had different amounts of shear reinforcement. A set of five girders was cast for each of three different concrete mixtures intended to represent typical LWC for girders. Table 4 gives the nominal details for the six girder end designs that were AASHTO type II girders (i.e., type II). Table 5 provides similar details for the four girder end designs that were AASHTO/Precast/Prestressed Concrete Institute bulb tee girders with a 54-inch (1.37-m) height (i.e., BT-54).

A naming scheme was developed for the 30 girder tests that included the concrete mixture, girder design, and girder end. The concrete mixtures were designated A through C and were UG, HG, or SG, respectively. The girder design number was used in the naming scheme, as seen in the girder test columns. An "L" or a "D" was used to denote a test near the live or dead end of the girder, respectively. The end of the girder closer to the prestressing bed bulkhead where the strands were jacked is known as the live end, and the end towards the bulkhead with the stationary anchorage is known as the dead end.

Table 4. Design details of type II girders.

Girder Test	d_v (Inches)	v_u/f'_c*	Number of Strands		Stirrups		Design Amount of Stirrups, $\rho_v f_y$ (ksi)
			Bottom	Top	Bar Size	Spacing (Inches)	
5D	35.0	0.068	10 straight	2	No. 3	22	0.12
5L	35.0	0.075	10 straight	2	No. 3	15	0.18
6D	31.7	0.088	10 straight and 4 drape	2	No. 4	15	0.32
6L	31.7	0.096	10 straight and 4 drape	2	No. 4	12	0.40
7D	32.8	0.150	18 straight	4	No. 4	8	0.60
7L	32.8	0.120	18 straight	4	No. 4	12	0.40

1 inch = 25.4 mm.
1 ksi = 6.89 MPa.
*Assumed f'_c for design was 10 ksi (68.9 MPa).

Table 5. Design details of BT-54 girders.

Girder Test	d_v (Inches)	v_u/f'_c*	Number of Strands		Stirrups		$\rho_v f_y$ (ksi)
			Bottom	Top	Bar Size	Spacing (Inches)	
8D	51.6	0.068	16 straight	2	No. 3	22	0.12
8L	51.6	0.076	16 straight	2	No. 3	14	0.19
9D	47.5	0.150	28 straight	4	No. 4	8	0.60
9L	47.5	0.140	28 straight	4	No. 4	10	0.48

1 inch = 25.4 mm.
1 ksi = 6.89 MPa.
*Assumed f'_c for design was 10 ksi (68.9 MPa).

The shear test girders were designed as part of a larger study that included the transfer and development length of prestressing strands in high-strength LWC. A total of nine different girder designs were used in the overall research program. The first four designs were type II girders that were tested to failure to evaluate development length of prestressing strand. Girder designs 5–9 were for the evaluation of shear performance.

Test Specimens

Girder designs 5–7 were type II girders. The amount of shear reinforcement (stirrups) in the test regions near the live and dead ends of the girder varied. The design details for each girder end were shown previously in table 4. A sketch of each girder design showing the cross section, strand pattern, and mild steel reinforcement is shown in figure 2 through figure 4 for girder designs 5–7, respectively. The dead end of girder design 5 (5D) was designed to have the minimum amount of shear reinforcement allowed by the *AASHTO LRFD Bridge Design Specifications* (see Article 5.8.2.5) at nearly the maximum spacing (see Article 5.8.2.7).[(3)] The dead end of girder design 7 (7D) was designed to have a ratio of shear stress to concrete compressive stress (v_u/f'_c) near the limit of 0.18 given in the *AASHTO LRFD Bridge Design Specifications* for the applicability of the sectional design method (see Article 5.8.3.2).[(3)] Girder design 6 had draped strands and an amount of shear reinforcement between the amounts used in girder designs 5 and 7.

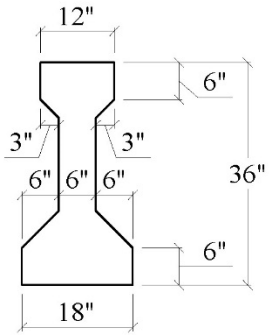

Source: FHWA.

A. Cross-section dimensions.

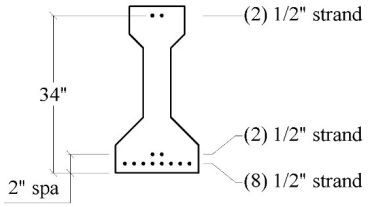

Source: FHWA.

B. Prestressing strand location.

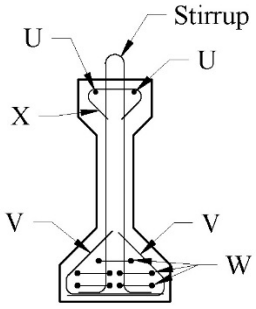

Source: FHWA.

C. Mild steel reinforcement.

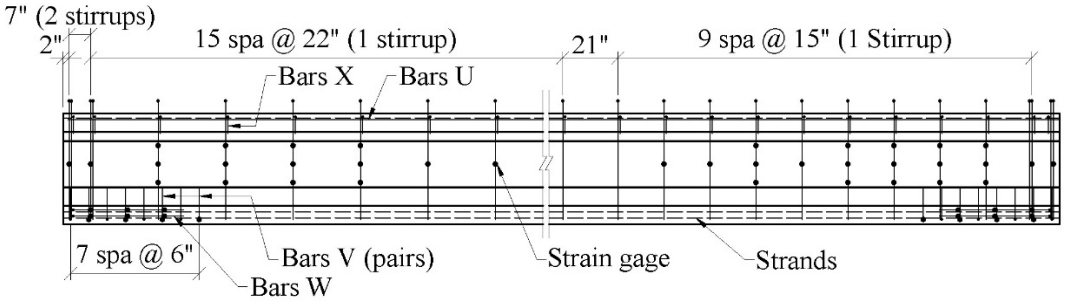

Source: FHWA.

D. Type II girder with 42-ft (12.81-m) girder length.

1 inch = 25.4 mm.
1 ft = 0.305 m.
Note: The following reinforcement is symmetric about the girder centerline: confinement (bars V), splitting (stirrups at 7-inch (177.8-mm) spa), and additional longitudinal for shear (bars W).

Figure 2. Illustrations. Beam girder design 5 showing cross-section dimensions, prestressing strand location, mild steel reinforcement, and elevation view.

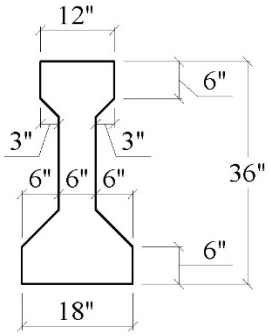

Source: FHWA.

A. Cross-section dimensions.

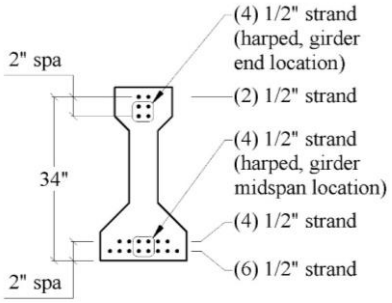

Source: FHWA.

B. Prestressing strand location.

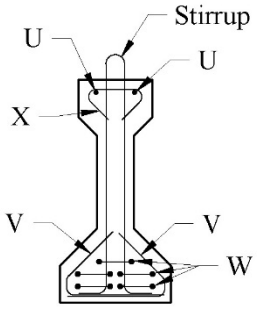

Source: FHWA.

C. Mild steel reinforcement.

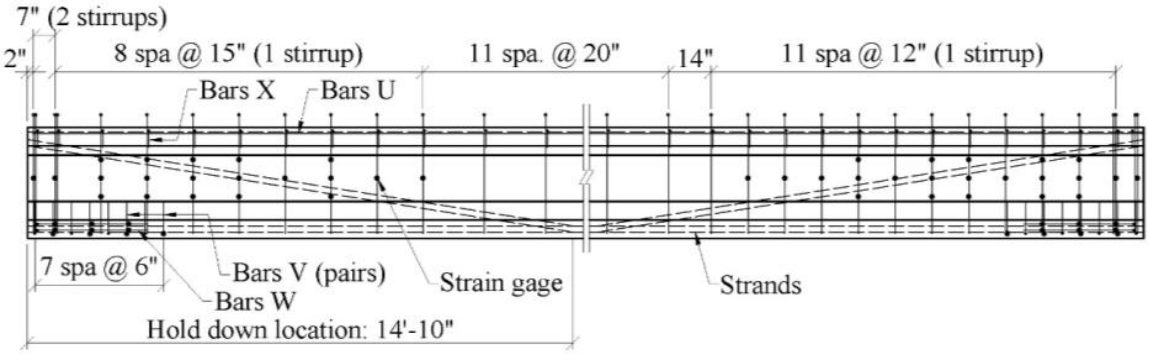

Source: FHWA.

D. Type II girder with 42-ft (12.81-m) girder length.

1 ft = 0.305 m.
1 inch = 25.4 mm.
Note: The following reinforcement is symmetric about the girder centerline: confinement (bars V), splitting (stirrups at 7-inch 177.8-mm) spa), and additional longitudinal for shear (bars W).

Figure 3. Illustration. Beam girder design 6 showing cross-section dimensions, prestressing strand location, mild steel reinforcement, and elevation view.

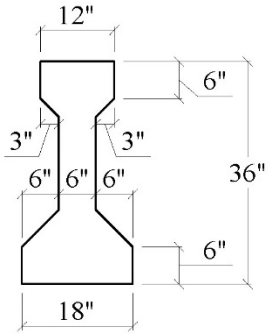

Source: FHWA.

A. Cross-section dimensions.

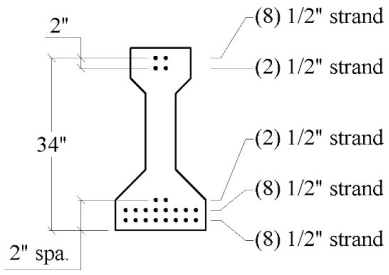

Source: FHWA.

B. Prestressing strand location.

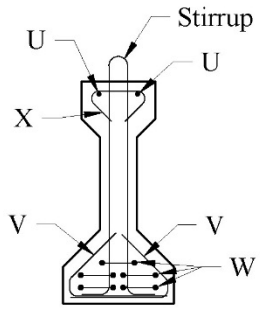

Source: FHWA.

C. Mild steel reinforcement.

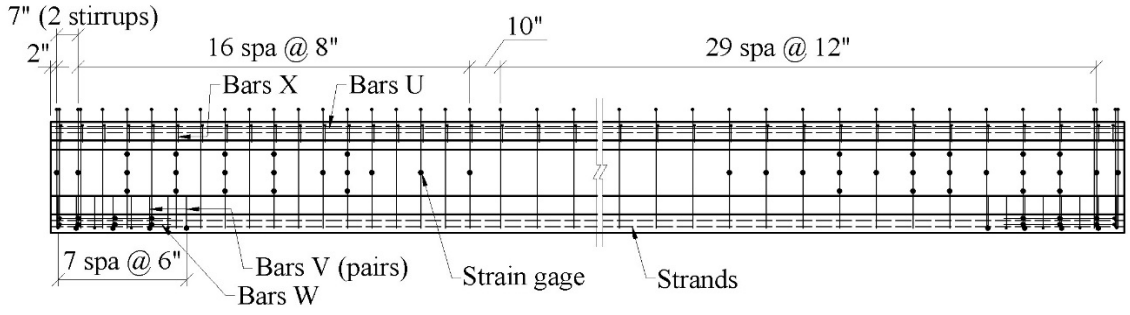

Source: FHWA.

D. Type II girder with 42-ft (12.81-m) girder length.

1 inch = 25.4 mm.
1 ft = 0.305 m.
Note: The following reinforcement is symmetric about the girder centerline: confinement (bars V), splitting (stirrups at 7-inch (177.8-mm) spa), and additional longitudinal for shear (bars W).

Figure 4. Illustrations. Beam girder design 7 showing cross-section dimensions, prestressing strand location, mild steel reinforcement, and elevation view.

The last two designs (i.e., girder designs 8 and 9) were BT-54 girders. The design details for the live and dead ends of the girders were shown previously in table 5, and sketches of the cross sections, strand patterns, and mild steel reinforcement arrangements are shown in figure 5 and figure 6. The amount of shear reinforcement in girder designs 8 and 9 was designed to give similar v_u/f'_c ratios as girder designs 5 and 7, respectively. This was done to investigate the size effect.

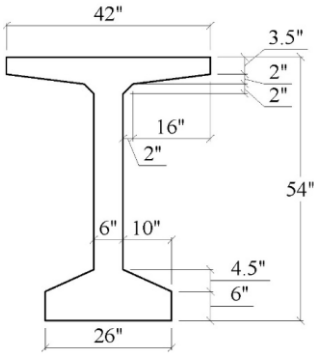

Source: FHWA.

A. Cross-section dimensions (symmetric about centerline).

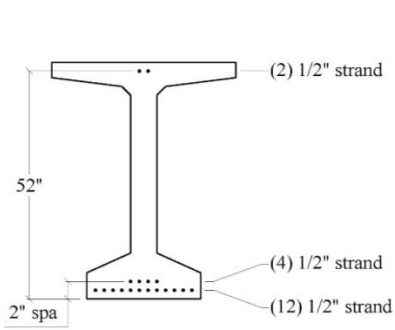

Source: FHWA.

B. Prestressing strand location.

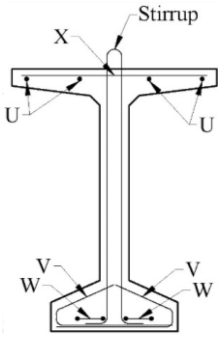

Source: FHWA.

C. Mild steel reinforcement.

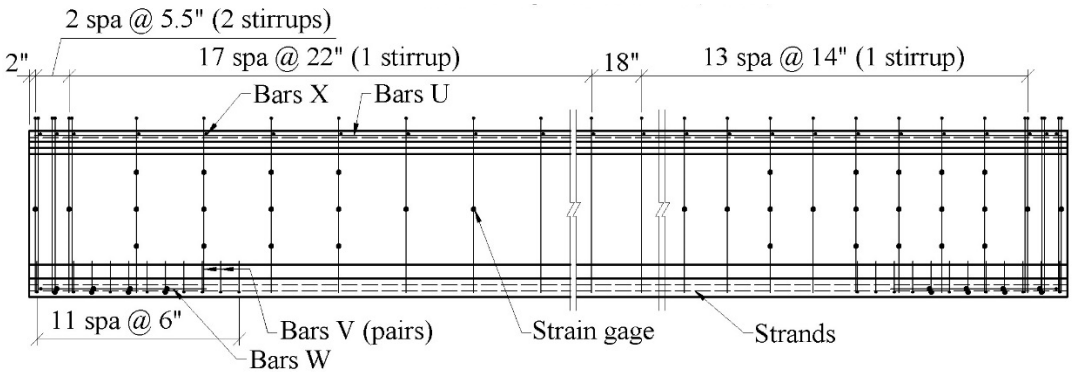

Source: FHWA.

D. BT-54 girder with 50-ft (15.25-m) girder length.

1 inch = 25.4 mm.
1 ft = 0.305 m.
Note: The following reinforcement is symmetric about the girder centerline: confinement (bars V), splitting (stirrups at 7-inch (177.8-mm) spa), and additional longitudinal for shear (bars W).

Figure 5. Illustrations. Beam girder design 8 showing cross-section dimensions, prestressing strand location, mild steel reinforcement, and elevation view.

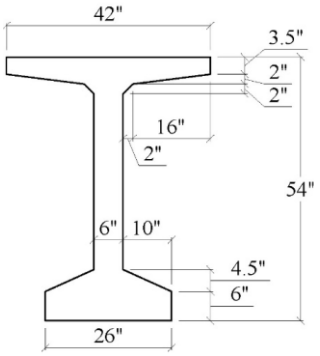

Source: FHWA.

A. Cross-section dimensions (symmetric about centerline).

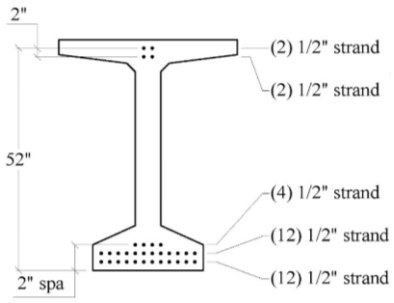

Source: FHWA.

B. Prestressing strand location.

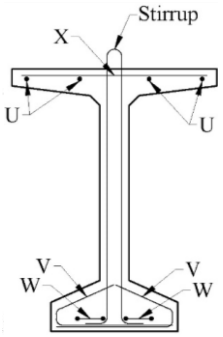

Source: FHWA.

C. Mild steel reinforcement.

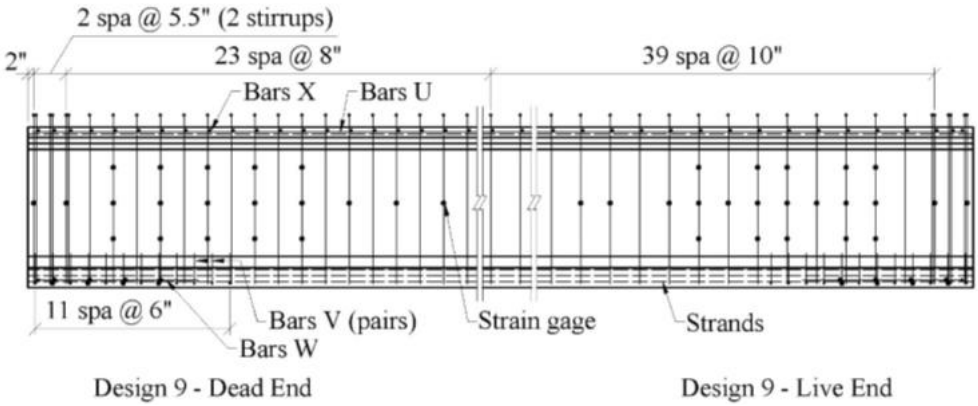

Source: FHWA.

D. BT-54 girder with 50-ft (15.25-m) girder length.

1 inch = 25.4 mm.
1 ft = 0.305 m.
Note: The following reinforcement is symmetric about the girder centerline: confinement (bars V), splitting (stirrups at 7-inch (177.8-mm) spa), and additional longitudinal for shear (bars W).

Figure 6. Illustrations. Beam girder design 9 showing cross-section dimensions, prestressing strand location, mild steel reinforcement, and elevation view.

The end of each girder had additional reinforcement as required by the *AASHTO LRFD Bridge Design Specifications*.[3] No. 6 rebar was added between the strands in the bottom flange to satisfy the requirements of Article 5.8.3.5 for additional longitudinal reinforcement.[3] Additional shear reinforcement (as stirrups) was provided as splitting resistance in the pretensioned anchorage zone per Article 5.10.10.1, and confinement reinforcement was provided around the strands to satisfy Article 5.10.10.2.[3]

The girders were designed with an amount of flexural reinforcement that was intended to ensure that a shear failure would occur prior to a flexural failure. For the design of the girders, a concrete compressive strength (f'_c) of 10 ksi (68.9 MPa) was assumed for all girders, and no modification of the shear resistance for LWC was used.

Specimen Fabrication

The girders were fabricated at a plant in Mobile, AL. The fabricator was asked to prescriptively produce the concrete mixtures without trying to adjust them for target strengths or unit weight. This was intended to remove batch-to-batch variations as a variable in the study. The lightweight aggregates were stored in three piles at the plant and watered continuously using a sprinkler on each pile, as shown in figure 7.

Source: FHWA.

Figure 7. Photo. Lightweight aggregate stockpiles at precaster's facility with continuous sprinklers.

Concrete Properties

Concrete for the three girder mixes was supplied by the precaster. After mixing, the precaster's personnel performed testing of the fresh concrete properties and produced 4- by 8-inch (102- by 203-mm) cylinders for quality-control purposes. The fresh concrete properties, concrete batch weights, and compressive strength tests performed by the precaster's personnel can be found in *Lightweight Concrete: Mechanical Properties*, which covers material properties of the LWC tested within this research program.[(1)]

Independently, research personnel made 4- by 8-inch (102- by 203-mm) cylinders following ASTM C31 for mechanical property testing and density measurements.[(39)] Compression tests were performed according to ASTM C39 to determine the compressive strength at the release of prestressing, at 28 days, and at girder testing.[(40)] Neoprene pads were used inside steel caps at each end of the cylinders. The indirect tensile strength was measured using the splitting tensile test described in ASTM C 496.[(41)] The elastic modulus was determined following ASTM C469 using one of the cylinders intended for compressive strength testing.[(42)] Typically, one cylinder was tested first for compressive strength to determine the proper load level for determining the elastic modulus. The air-dry density was calculated using the measured cylinder weight and measured cylinder lengths and diameters to calculate an average volume. The mechanical properties of the LWC used in the prestressed girders are given in table 6, and the measured unit weights are given in table 7. The compressive strengths, splitting tensile strengths, modulus of elasticity, and air-dry densities shown are based on the average of three cylinders.

Table 6. Mean girder concrete properties by mix design.

Mix Design	Compressive Strength (ksi)			Splitting Tensile Strength (ksi)			Modulus of Elasticity (ksi)		
	Release	28-Day	Test Day	Release	28-Day	Test Day	Release	28-Day	Test Day
HG	7.0	9.5	10.4	0.600	0.720	0.770	3,850	4,420	4,320
SG	7.4	9.7	10.6	0.600	0.680	0.720	3,710	4,140	4,360
UG	6.1	8.6	10.1	0.580	0.680	0.760	3,520	4,080	4,150

1 ksi = 6.89 MPa.

Table 7. Girder w_c by mix design.

Mix Design	w_c (kcf)		
	Release	28-Day	Test Day
HG	0.134	0.132	0.130
SG	0.125	0.125	0.123
UG	0.131	0.130	0.127

1 kcf = 16,020 kg/m^3.

Reinforcing Bar Properties

The reinforcing bars were ASTM A615 grade 60.[43] The mechanical properties were tested under displacement control in a 100-kip (445-kN) testing machine. Two bars were tested for each nominal size used in the prestressed girders. Strain was measured with an 8-inch (203-mm) extensometer. When the extensometer reached a measured strain of 2 percent at the beginning of the assumed strain-hardening regime, the test was paused to remove the extensometer. The test was then continued until the bar fractured. The yield strength was determined using the 0.2 percent offset method. The average yield strength and the ultimate strength of two bars used as stirrups, confinement reinforcement, and girder end longitudinal reinforcement are given in table 8. Test data and stress–strain relationships from individual bars are provided in appendix A.

Table 8. Reinforcing bar properties.

Property	Stirrup Girder Design				Girder End Longitudinal Reinforcement	Confinement Reinforcement
	5	6 and 7	8	9		
Bar size (unitless)	No. 3	No. 4	No. 3	No. 4	No. 6	No. 4
Nominal diameter (inches)	0.375	0.500	0.375	0.500	0.625	0.500
Nominal area (inches^2)	0.11	0.20	0.11	0.20	0.44	0.44
Yield strength (ksi)	70.8	68.0	65.1	65.3	65.8	65.8
Ultimate strength (ksi)	112.2	97.8	101.9	104.8	107.1	107.5

1 inch = 25.4 mm.
1 inch^2 = 645 mm^2.
1 ksi = 6.89 MPa.

NWC Concrete Deck

An 8-inch (200-mm)-thick composite NWC deck was cast onto each LWC girder at TFHRC in order to move the neutral axis above the web and top flange. The concrete used in the decks had a specified compressive strength of 4 ksi (28 MPa). The mean mechanical properties at 28 days and test day for the NWC decks are provided in table 9. As a reminder, type II girders include girder designs 5–7, while BT-54 girders include girder designs 8–9.The decks had two orthogonal mats of reinforcing, as specified in Article 9.7.3 of the *AASHTO LRFD Bridge Design Specifications* for bridge decks.[3] The deck reinforcement is shown in typical cross sections in figure 8.

Table 9. Mean NWC deck properties by girder size.

Girder Type	Compressive Strength (ksi)		Test Day Modulus of Elasticity (ksi)
	28 Day	Test Day	
Type II	3.15	4.72	4,970
BT-54	3.88	6.06	4,700

1 ksi = 6.89 MPa.

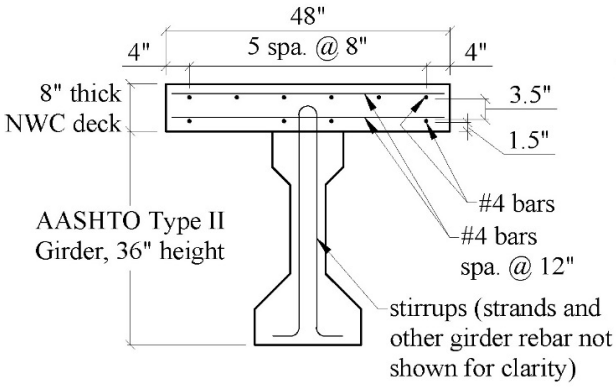

Source: FHWA.
1 inch = 25.4 mm.

A. Deck dimensions and reinforcement of NWC deck cast onto LWC girders for type II girders.

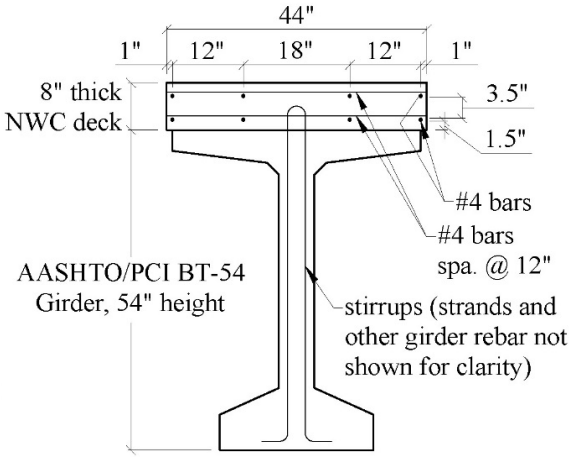

Source: FHWA.
1 inch = 25.4 mm.

B. Deck dimensions and reinforcement of NWC deck cast onto LWC girders for BT-54 girders.

Figure 8. Illustrations. NWC deck cast onto LWC girders for type II and BT-54 girders.

After the first test failed in horizontal shear, the decks of all subsequent tests on type II girders were strengthened to resist horizontal shear throughout the test region by installing concrete wedge anchors through the deck. The holes for the anchors were drilled through the deck so the anchor could be mounted into the top flange of the girders. The concrete anchors were 12 inches (305 mm) long with a 0.75-inch (19.1-mm) nominal diameter. A 1.5-inch (38.1-mm)-thick square bearing plate was placed on the concrete deck. The nuts on the concrete anchors were torqued to 1.5 kip-inch (170 N-m) to provide a small compressive force to the deck.

Flexural Strengthening Using Glass Fiber Reinforced Polymer (GFRP)

The first three shear tests (i.e., A7L, B7L, and C7L) reached a much higher applied shear force than expected, and there was concern that subsequent tests would not experience shear failures unless the flexural resistance of the girders was increased. GFRP was bonded to the lower surface and sides of the bottom flange on many of the remaining shear tests in order to increase the girder flexural capacity. For the tests that included GFRP, the distance from the support centerline to the start of each bottom and side layer is given in table 10. The GFRP layers were kept as far from the critical section for shear as possible in order to avoid increasing the girder's shear resistance due to the increased longitudinal restraint provided by the GFRP. The effect that longitudinal strain has on shear resistance was described previously in this report.

Table 10. GFRP used on the shear girders for flexural strengthening.

Test Number	Girder Design	Distance from Support Centerline to Start of Layer (Inches)					
		Bottom Layer 1	Bottom Layer 2	Bottom Layer 3	Bottom Layer 4	Side Layer 1	Side Layer 2
4	7	48	54	60	66	60	66
5–6	7	30	42	54	66	54	66
8–9	5	42	60	78	—	72	—
10–12	5	42	60	78	96	72	90
16–18	6	42	66	78	—	72	—
19–30	8, 9	84	108	—	—	120	—

1 inch = 25.4 mm.
—Layer not used.

GFRP used for flexural strengthening of the shear girders consisted of a unidirectional fiber fabric (SikaWrap Hex 107G) with impregnating resin (Sikadur 300) over a substrate primer (Sikadur 330). The datasheet for the fiber fabric stated that average tensile strength for the cured laminate was 87.6 ksi (604.0 MPa) and the elastic modulus was 3,700 ksi (25.5 GPa).

The surface was prepared using a concrete grinder to remove the surface paste and was then roughened using an abrasive coal-slag blasting media (grit 20-40). The substrate primer was applied using a roller immediately prior to applying the GFRP layers. The resin and hardener were blended with an electric paddle mixer. A roller was used to saturate both faces of fiber fabric. The saturated fabric was unrolled onto the bottom surface of the girder. A hard rubber roller was used to press the fabric layer in to the substrate primer and remove air bubbles. Additional layers of GFRP were installed in the same manner.

Test Setup

A sketch of the test setup is shown in figure 9. Figure 10 shows a photograph of the setup for test C8D after the completion of the test. Before a test, the girder was supported by a roller at the end being subjected to high shear and by a hydraulic jack at the other end of the span. These supports are referred to as the "roller support" and the "loading jack," respectively. The roller support consisted of a 6-inch (152-mm)-diameter steel roller and a 2-inch (51-mm)-thick steel bearing plate. The bearing plate had a width of 12 inches (305 mm) and was long enough to fully support

the width of the girder's bottom flange. Grout was placed between the girder and bearing plate to uniformly support the girder.

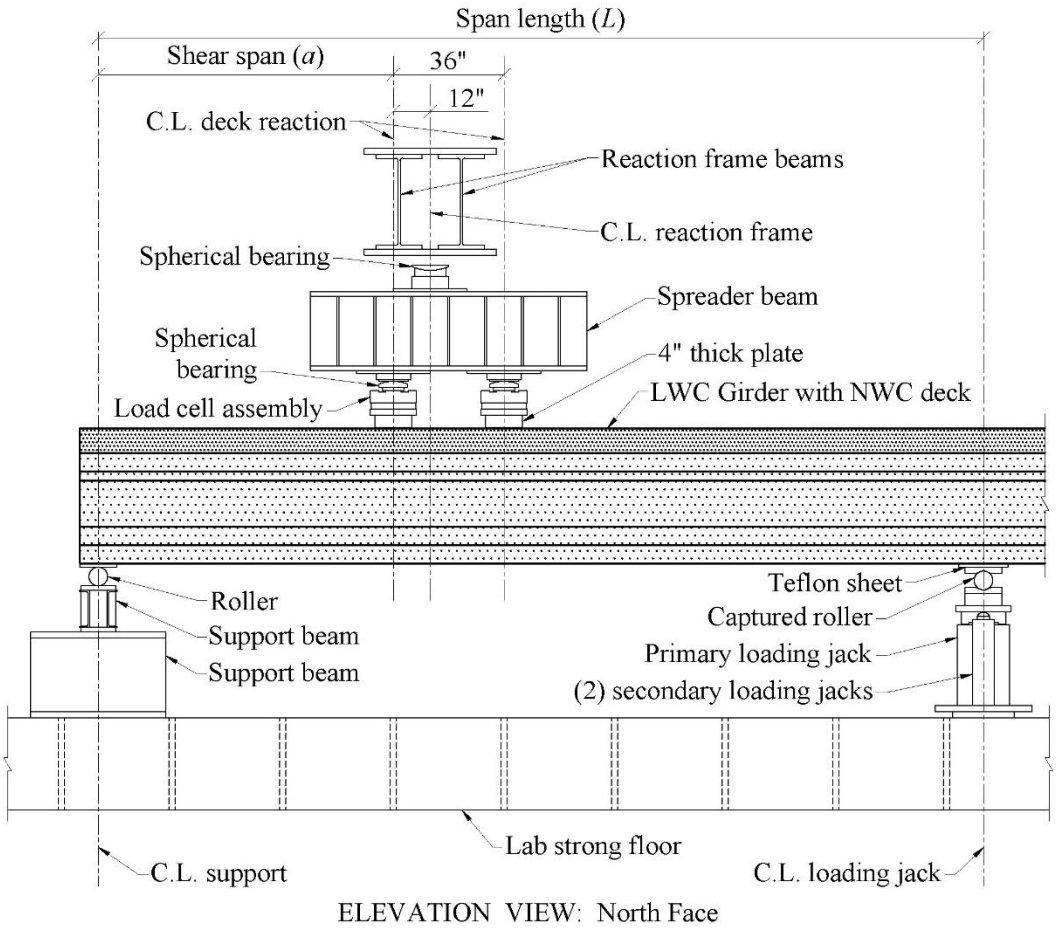

Source: FHWA.
1 inch = 25.4 mm.
C.L. = centerline.

Figure 9. Illustration. Elevation view of the setup for girder shear tests.

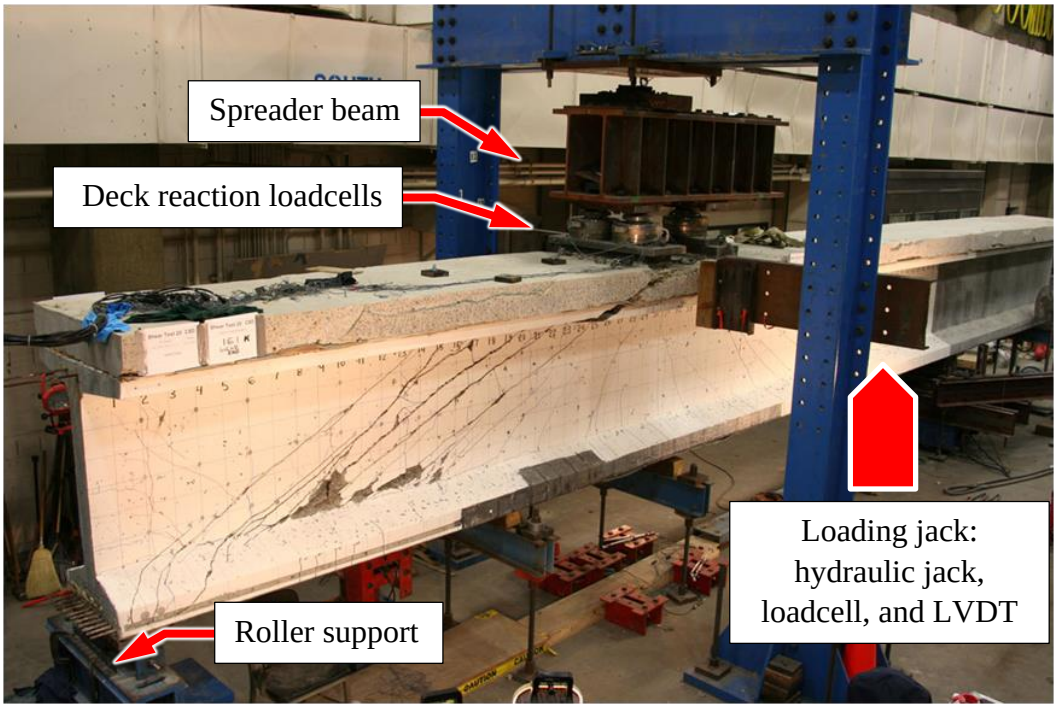

Source: FHWA.

Figure 10. Photo. Test setup on girder test C8D with concrete crushing along the web.

The loading jack is shown in figure 11. The girder rested directly on another 2-inch (51-mm)-thick and 12-inch (305-mm)-wide steel bearing plate. A greased Teflon™ sheet was placed between the bearing plate and a roller assembly. The roller assembly consisted of a 6-inch (152-mm)-diameter roller between two grooved plates. Below the roller assembly was a loadcell with a 300-kip (1,340-kN) capacity and then a hydraulic jack with a 1,000-kip (4,450-kN) capacity. If the full 10-inch (254-mm) stroke of the 1,000-kip (4,450-kN) primary actuator was inadequate to complete a test, two smaller auxiliary hydraulic actuators were used to temporarily support the girder while spacer plates were installed.

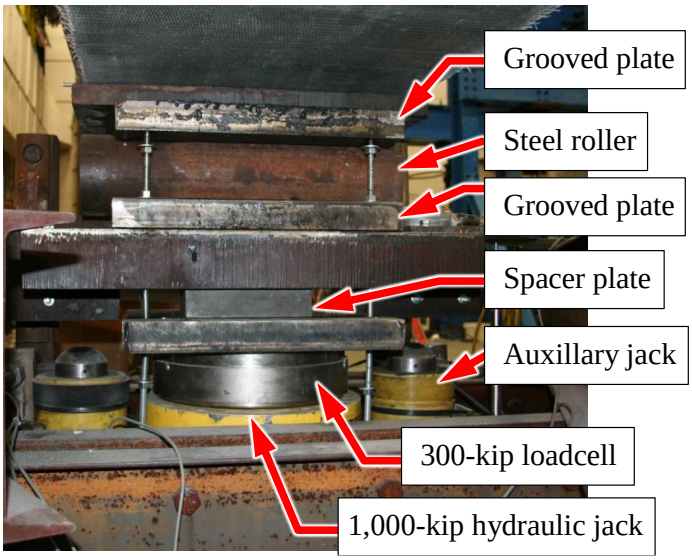

Source: FHWA.
1 kip = 6.89 MPa.

A. End view.

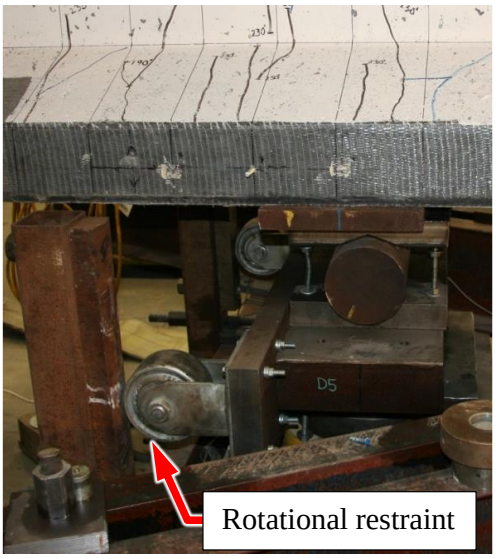

Source: FHWA.

B. Side view.

Figure 11. Photos. Loading jack end and side views.

The load in the jack was controlled by a closed-loop servo-value system. The feedback for the closed-loop system was provided by the loadcell and by a linear variable differential transformer (LVDT) with a 10-inch (254-mm) stroke. The loading was applied by specifying the jack force in load control or by specifying the jack travel in displacement control.

When the jack applied load to the girder, it was reacted by a heavy load frame through a spreader beam, spherical bearing plates, and two pairs of 300-kip (1,340-kN) loadcells on the deck that applied the reaction force into the girder. The loadcells were mounted to 4-inch (102-mm)-thick bearing plates that were grouted to the top of the deck. Figure 9, figure 10, and figure 12 show the bearing plates, loadcells, and spreader beams. The locations of the loadcell pairs on the deck are referred to as “deck reaction points” in this report.

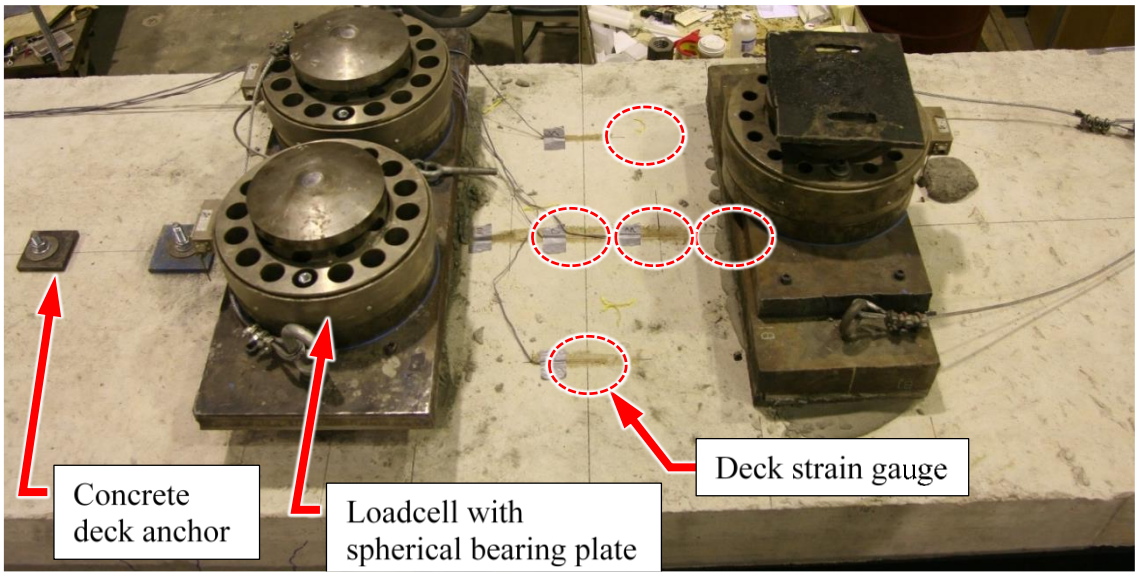

Source: FHWA.

Figure 12. Photo. Concrete deck anchors, loadcells at deck reaction points, and deck strain gauges.

The distance from the roller support to the deck reaction points and the loading jack is shown in table 11 for the tests on the type II girders and in table 12 for the tests on the BT-54 girders. The distance between the centerline of the roller support and the closest deck reaction point is the shear span (a). The test region for each girder end is defined as the portion of the girder along the shear span. The distance from the roller support to the loading jack is the span length (L). The distance from the end of the girder to the rolling support ($L1$) and the distance from the rolling support to the first anchor of the LVDT average strain rosette ($L4$) are shown in table 11 and table 12. The variable dimensions a, L, $L1$, and $L4$ are shown in figure 13 for the type II girders. These four dimensions were held constant for the tests on the BT-54 girders, as shown in figure 14, but for comparison purposes, the dimensions are shown in table 12. The distance to the first deck concrete anchor ($L2$), the total number of anchors ($N2$), and the ($L3$) are found in table 11 and figure 13 for the type II girders.

Table 11. Variable dimensions in figure 13 for type II girders.

Test No.	Girder Test	*a* (Inches)	*L* (Inches)	*L*1 (Inches)	Deck Anchors			*L*4 (Inches)
					*L*2 (Inches)	*N*2	*L*3 (Inches)	
1	A7L	96	288	6.0	—	0	—	33
2	B7L	84	258	6.0	10.0	6	10.0	33
3	C7L	84	258	6.0	10.0	6	10.0	19
4	A7D	84	258	6.0	7.0	9	8.0	20
5	C7D	84	258	6.0	7.0	9	8.0	20
6	B7D	84	258	6.0	7.0	9	8.0	20
7	A5D	90	264	6.0	20.0	4	22.0	16
8	B5D	108	306	6.0	20.0	4	22.0	16
9	C5D	108	306	6.0	20.0	4	22.0	16
10	A5L	108	306	6.0	16.0	6	15.0	19
11	B5L	108	306	30.0	31.0	6	15.0	25
12	C5L	108	306	30.0	46.0	5	15.0	25
13	A6D	108	306	6.0	16.0	4	15.0	19
14	B6D	108	306	6.0	16.0	4	15.0	19
15	C6D	108	306	6.0	16.0	4	15.0	19
16	A6L	108	306	30.0	46.0	5	15.0	25
17	B6L	108	306	30.0	46.0	5	15.0	25
18	C6L	108	306	30.0	46.0	5	15.0	25

1 inch = 25.4 mm.
Note: The concrete deck anchors were 0.75 inch (19.04 mm) in diameter and 12 inches (305 mm) long.
—Dimensions were not applicable.

Table 12. Variable dimensions in figure 14 for BT-54 girders.

Test No.	Girder Test	*a* (Inches)	*L* (Inches)	*L*1 (Inches)	*N*2	*L*4 (Inches)
19	C8D	156	420	6	0	39
20	A9L	156	420	6	0	38
21	C8L	156	420	6	0	43
22	A9D	156	420	6	0	35
23	B8D	156	420	6	0	38
24	A8D	156	420	6	0	38
25	B8L	156	420	6	0	32
26	A8L	156	420	6	0	32
27	B9L	156	420	6	0	43
28	C9L	156	420	6	0	43
29	B9D	156	420	6	0	35
30	C9D	156	420	6	0	35

1 inch = 25.4 mm.

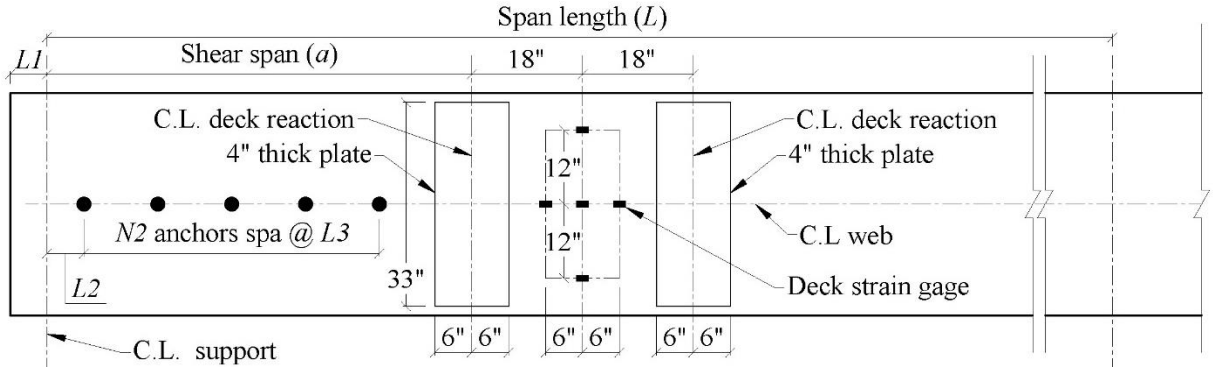

Source: FHWA.
1 inch = 25.4 mm.

A. Plan view—top of deck.

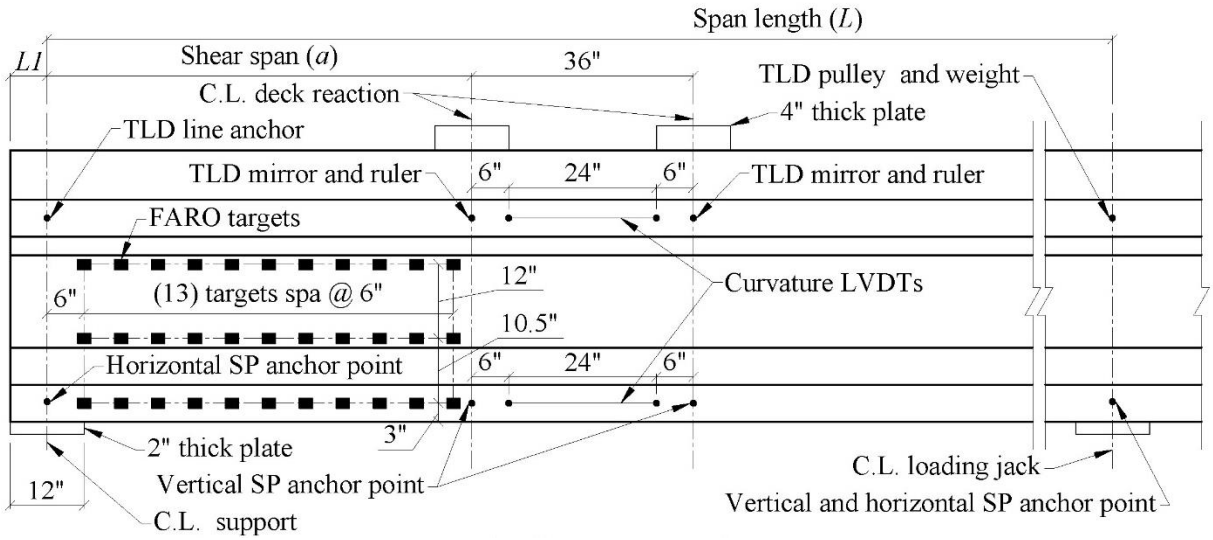

Source: FHWA.
1 inch = 25.4 mm.
SP = string potentiometer.
TDL = taut-line deflection.

B. Elevation view—north face.

Figure 13. Illustrations. External instrumentation for type II girders.

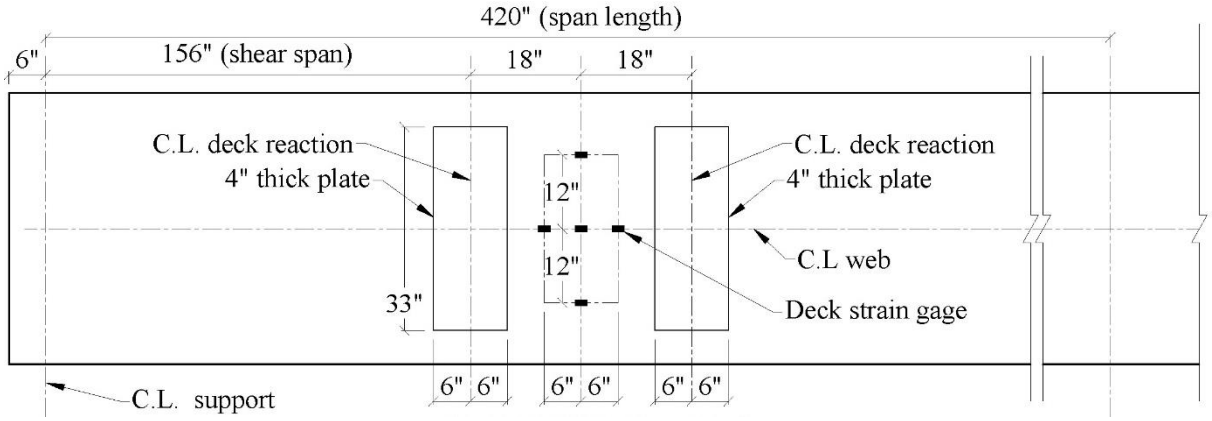

Source: FHWA.
1 inch = 25.4 mm.

A. Plan view—top of deck.

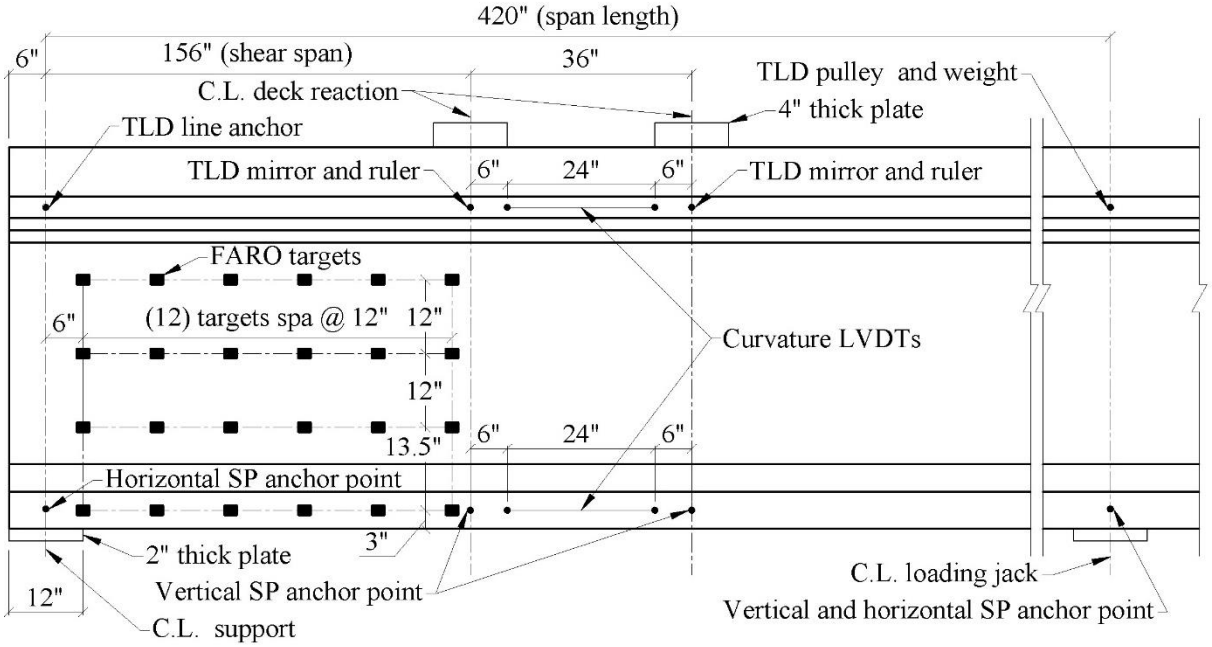

Source: FHWA.
1 inch = 25.4 mm.

B. Elevation view—north face.

Figure 14. Illustrations. External instrumentation for BT-54 girders.

Instrumentation

The shear tests were extensively instrumented to measure applied jack force, deck reaction forces, girder deformations, girder curvature, reinforcement strain, average concrete strain in the web, strand end slip, and concrete deck strain. The electronic instruments were connected to a data acquisition system that recorded data at a rate of 0.1 Hz.

Horizontal and vertical deflections were measured using SPs. The locations of the anchor points for the SPs on the exterior of the type II and BT-54 girders are shown in figure 13 and figure 14,

respectively. Vertical deflections were measured using SPs attached to the bottom flange directly below the deck reaction points. Vertical and horizontal deflections were measured using SPs attached to the bottom flange directly over the loading jack. Horizontal deflections were measured using SPs attached to the bottom flange directly over the roller support. These SPs indirectly measured the deflection of the girder at the deck reaction points. The deflection at the deck reaction points was calculated as the measured change in vertical distance between the deck reaction anchor points and a straight line between the SP anchor points at the roller support and loading support. Girder deflection was directly measured at the deck reaction points using a taut-line system consisting of a weighted wire passing by pairs of rulers and mirrors attached to the top flange directly below the deck reaction points. The mirrors were used to correct for parallax before reading the deflection to the nearest $^{1}/_{128}$ inch (0.20 mm) on the rulers. Photographs showing the components of the taut-line system are in figure 15.

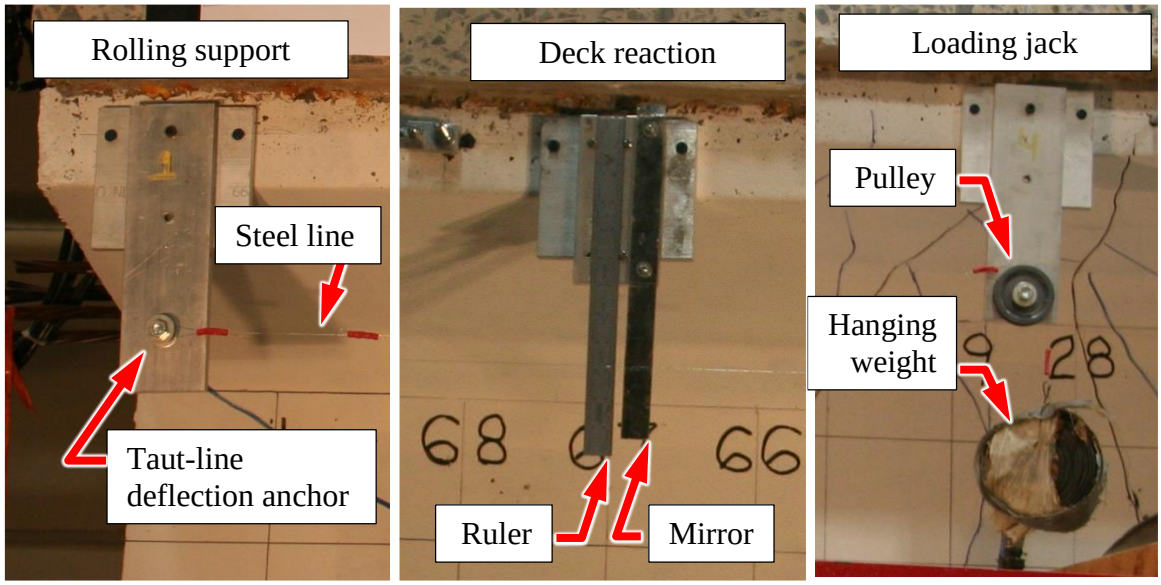

Source: FHWA. Source: FHWA. Source: FHWA.

A. Anchor. B. Measuring point. C. Loading point.

Figure 15. Photos. The anchor, measuring point, and loading point of the TLD measurement system.

Four LVDTs mounted to the top and bottom flanges were used to measured girder curvature between the deck reaction points. At the girder ends, LVDTs were attached to four strands on the bottom row to measure any slip between the strands and the end of the girder. Figure 16 shows an LVDT mounted to an exterior strand to measure strand slip.

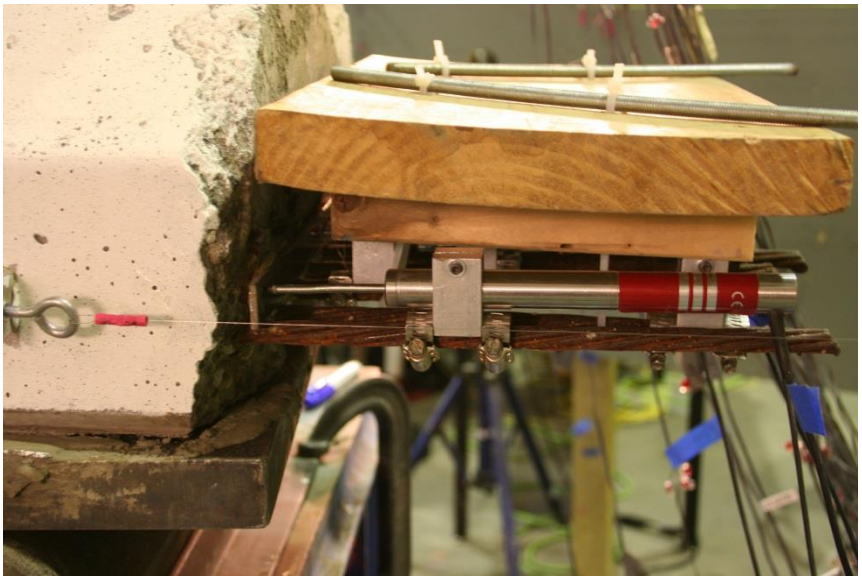

Source: FHWA.

Figure 16. Photo. LVDTs used to measure strand slip.

Strain in the shear reinforcement and strain in the end region reinforcement was measured using electric resistance strain gauges (ERSs). Figure 2 through figure 6 show the locations of ERSs for the five girder designs. ERSs were also used to measure the strain on the top surface of the deck between the deck loading points and the strain near the ends of the GFRP layers bonded to the bottom flange. Figure 12 shows the ERSs on the concrete deck.

Average concrete strain over several cracks was measured using two LVDT rosettes mounted to the web near the critical section for shear. A rosette consisted of three LVDTs oriented to measure the displacement in the horizontal, vertical, and diagonal (45 degrees) directions. ERSs only measure the local strain on a stirrup and will measure much larger strains when a crack opens near the gauge. An LVDT measuring the displacement across several cracks measures an average strain and can be used to calculate the angle of inclination of the diagonal compressive stresses. Figure 17 shows a photograph of the two LVDT rosettes.

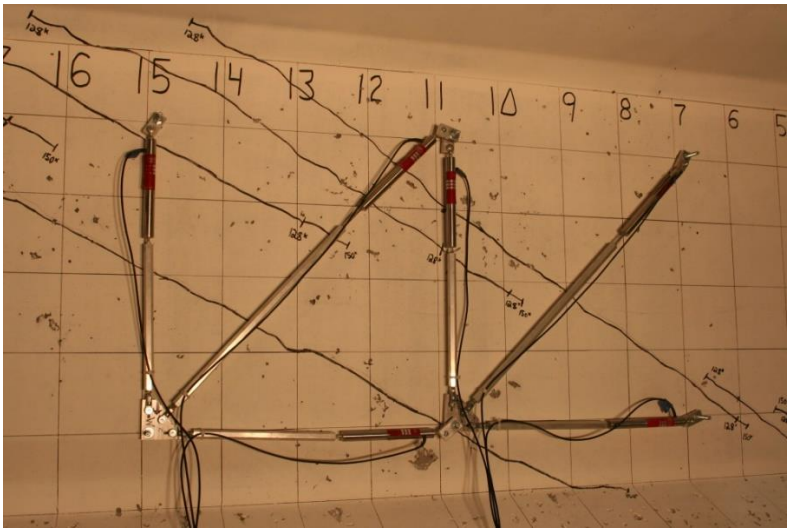

Source: FHWA.

Figure 17. Photo. LVDTs used to measure the average concrete strain in a rosette.

A noncontact laser tracking system, FARO®, was also used to measure average concrete strain. A laser from the FARO® tracker followed the triple-mirror prism in a spherical steel ball (SMR). The FARO® tracker and SMR are shown in figure 18. The ball was then placed in multiple targets mounted to the surface of the girder web and bottom flange. FARO® target locations are shown in figure 13 and figure 14. The FARO® tracker was used to record the three-dimensional position of all the targets at various loading increments. The change in position of adjacent targets was used to calculate the average strain. The FARO® measurements were repeatable to around 0.0010 inch (0.025 mm), which corresponds to less than 100 microstrain when the targets are spaced 12 inches (305 mm) apart.

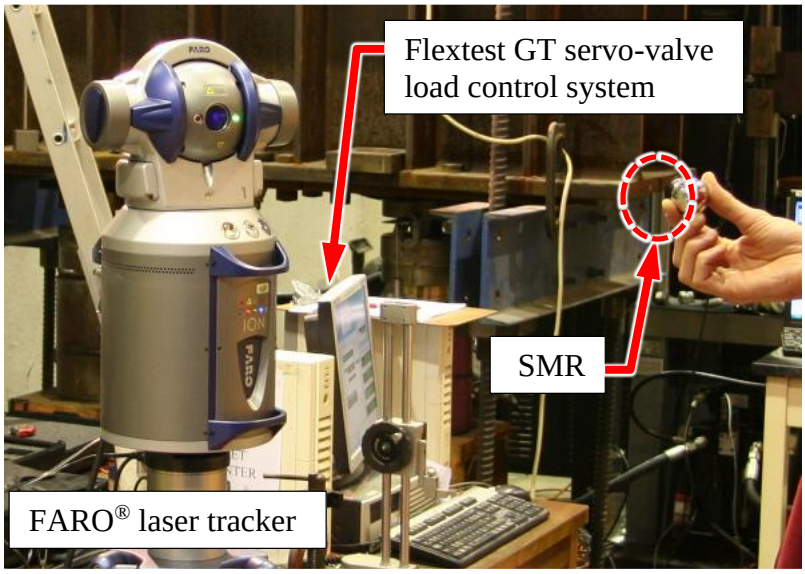

Source: FHWA.

Figure 18. Photo. FARO® laser tracker and load control system.

The angle of the web-shear cracks was measured at the midheight of the web using the crack protractor shown in figure 19. A pencil line was drawn to estimate the path of the crack near the midheight of the web. A horizontal line on the protractor was aligned over the black horizontal line drawn at the midheight of the web. The axis of the protractor was centered over the intersection of the pencil line and the horizontal line. The protractor arm was rotated so that its tip aligned with the pencil line. The angle indicated by the tip of the protractor arm was read to the nearest 1.0-degree angle. The widths of the cracks crossing the midheight of the web were measured using a hand-held optical microscope. The microscope had 0.001-inch (0.025-mm) divisions. The location of the crack width reading was marked so that subsequent readings would be made at the same location.

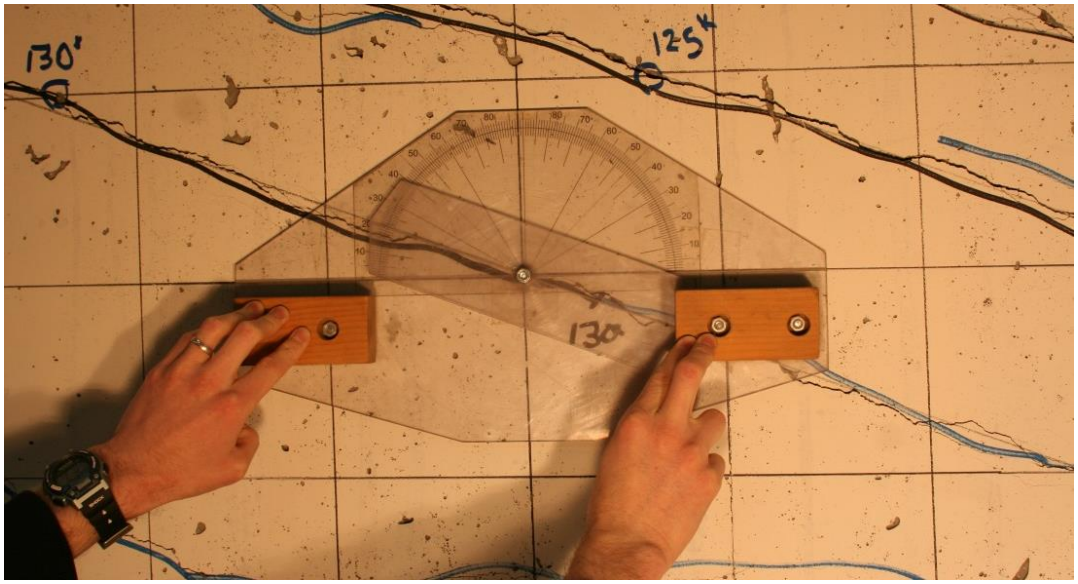

Source: FHWA.

Figure 19. Photo. Crack angle measurement using a crack protractor.

Test Procedure

Each test began in load control with the jack force increased in 5-kip (22-kN) increments up to about 80 percent of the load expected to cause web-shear cracking. Then the load increment was reduced to 2 kip (9 kN) until web-shear cracking occurred. The loading was paused at web-shear cracking in order to mark cracks, take photographs, measure deflections using the TLD system, measure crack widths and angles at the midheight of the web, and take FARO® measurements. After web-shear cracking, the loading was continued in 5-kip (22-kN) increments. The loading was paused four or five times to take measurements and photographs. The load increment after flexural cracking occurred was also recorded. At 80 percent of the expected failure load, the loading was switched to displacement control, and the girder was ramped to failure in increments of 0.25 to 0.45 inch (6.4 to 11.4 mm) corresponding to a load rate of 2 to 3 kip (9 to 13 kN) per 20 s. Flexural shear cracking typically occurred at higher load levels, commonly during the ramp to failure, so the test was not stopped to record these values.

ANALYSIS OF TEST RESULTS

A summary of the girder tests is given in table 13 and table 14 for the type II and BT-54 girders, respectively. The summary includes the effective shear depth (d_v), ratio of the shear span to effective shear depth (a/d_v), concrete compressive strength (f'_c) and splitting tensile strength (f_{ct}) at age of testing, the total area of prestressing strands (A_{ps}), the calculated effective stress in the prestressing steel after losses (f_{pe}), the stirrup strength ($\rho_v f_{yt}$) (which is the product of the shear reinforcement ratio given by equation 40 and the measured yield strength of the stirrups given in table 8), and whether the girder test was flexurally strengthened using GFRP. The effective shear depth was calculated using Article 5.8.2.9 in the *AASHTO LRFD Bridge Design Specifications*.[3] The effective prestress was calculated using the approximate estimate of time-dependent losses in Article 5.9.5.3.

Table 13. Summary of effective depth, concrete strength, prestressing steel, stirrup strength, and GFRP usage for type II girders.

Test No.	Girder Test	d_v (Inches)	a/d_v	f'_c (ksi)	f_{ct} (ksi)	A_{ps} (Inches^2)	f_{pe} (ksi)	$\rho_v f_{yt}$ (ksi)	GFRP Usage (Yes/No)
1	A7L	31.75	3.02	9.2	0.82	3.366	159.6	0.397	No
2	B7L	31.75	2.65	10.4	0.79	3.366	160.8	0.397	No
3	C7L	31.75	2.65	10.3	0.72	3.366	161.6	0.397	No
4	A7D	31.75	2.65	9.2	0.82	3.366	159.6	0.596	Yes
5	C7D	31.75	2.65	10.3	0.72	3.366	161.6	0.596	Yes
6	B7D	31.75	2.65	10.4	0.79	3.366	160.8	0.596	Yes
7	A5D	32.70	2.75	10.6	0.76	1.836	174.1	0.115	No
8	B5D	32.70	3.30	10.4	0.74	1.836	172.3	0.115	Yes
9	C5D	32.70	3.30	11.2	0.75	1.836	173.0	0.115	Yes
10	A5L	32.70	3.30	10.6	0.76	1.836	174.1	0.169	Yes
11	B5L	32.70	3.30	10.4	0.74	1.836	172.3	0.169	Yes
12	C5L	32.70	3.30	11.2	0.75	1.836	173.0	0.169	Yes
13	A6D	33.53	3.22	8.8	0.72	2.448	160.4	0.287	No
14	B6D	33.53	3.22	9.6	0.74	2.448	169.3	0.287	No
15	C6D	33.53	3.22	9.9	0.72	2.448	169.0	0.287	No
16	A6L	33.53	3.22	8.8	0.72	2.448	160.4	0.359	Yes
17	B6L	33.53	3.22	9.6	0.74	2.448	169.3	0.359	Yes
18	C6L	33.53	3.22	9.9	0.72	2.448	169.0	0.359	Yes

1 inch = 25.4 mm.
1 ksi = 6.89 MPa.

Table 14. Summary of effective depth, concrete strength, prestressing steel, stirrup strength, and GFRP usage for BT-54 girders.

Test No.	Girder Test	d_v (Inches)	a/d_v	f'_c (ksi)	f_{ct} (ksi)	A_{ps} (Inches^2)	f_{pe} (ksi)	$\rho_v f_{yt}$ (ksi)	GFRP Usage (Yes/No)
19	C8D	48.60	3.21	11.6	0.73	2.754	177.0	0.118	Yes
20	A9L	47.36	3.29	10.8	0.72	4.896	158.7	0.435	Yes
21	C8L	48.60	3.21	11.6	0.73	2.754	177.0	0.185	Yes
22	A9D	47.36	3.29	10.8	0.72	4.896	158.7	0.544	Yes
23	B8D	48.60	3.21	11.9	0.78	2.754	160.3	0.118	Yes
24	A8D	48.60	3.21	11.2	0.76	2.754	172.5	0.118	Yes
25	B8L	48.60	3.21	11.9	0.78	2.754	160.3	0.185	Yes
26	A8L	48.60	3.21	11.2	0.76	2.754	172.5	0.185	Yes
27	B9L	47.36	3.29	11.0	0.80	4.896	165.5	0.435	Yes
28	C9L	47.36	3.29	10.4	0.66	4.896	163.6	0.435	Yes
29	B9D	47.36	3.29	11.0	0.80	4.896	165.5	0.544	Yes
30	C9D	47.36	3.29	10.4	0.66	4.896	163.6	0.544	Yes

1 inch = 25.4 mm.
1 ksi = 6.89 MPa.

$$\rho_v = \frac{A_v}{b_v s} \tag{40}$$

The a/d_v ratios for the girder tests are given in table 13 and table 14. An a/d_v ratio of less than between 2.5 to 3.0 has been shown to increase the shear strength of a girder.[17,24] The target a/d_v ratio was 3.0; however, the girders were tested over a range of a/d_v ratios between 2.65 to 3.3. The shear span was adjusted from test to test during the first seven tests on type II girders in order to force a shear failure. However, starting with the seventh test, the shear span was left constant so variations in the a/d_v ratio in subsequent tests can be attributed to the differences in the calculated d_v for different girder designs.

A summary of the applied shear force and failure mode for the tested girders is given in table 15 and table 16 for the type II and BT-54 girders, respectively. The summary of shear forces includes the applied shear force at web cracking (V_{cr}), the maximum applied shear force (V_{test}), the average shear stress on the concrete (v_u), and the ratio of the average shear stress on the concrete to the concrete compressive strength (v_u/f'_c). The average shear stress was calculated from V_{test} using Article 5.8.2.9 of the *AASHTO LRFD Bridge Design Specifications*.[3] The effect of girder self-weight was included in the determination of V_{test}. A flexural failure was observed by concrete deck crushing. A flexural failure mode was indicated by the measured deck strain reaching its peak at V_{test} or slightly before V_{test}. The failure mode of GFRP debonding was indicated by the measured GFRP strain reaching its peak before V_{test}. The failure mode of strand slip was indicated by the maximum measured strand slip from four LVDTs reaching a value of 0.010 inch (0.25 mm) before V_{test}.

Table 15. Shear force at web cracking and ultimate, average shear stress, and failure mode for type II girders.

Test No.	Girder Test	V_{cr} (ksi)	V_{test} (ksi)	v_u (ksi)	v_u/f'_c	Failure Mode
1	A7L	—	301.5	1.57	0.170	Shear horizontal
2	B7L	174.8	365.0	1.90	0.184	Shear compression at support
3	C7L	165.5	350.5	1.83	0.177	Shear compression at support
4	A7D	175.5	369.8	1.93	0.209	Shear web compression
5	C7D	187.0	414.4	2.16	0.209	Flexural, GFRP debonding
6	B7D	197.4	416.3	2.17	0.210	Shear web compression
7	A5D	136.4	209.2	1.05	0.100	Flexural, deck crushing
8	B5D	138.8	200.3	1.01	0.097	Flexural, GFRP debonding
9	C5D	131.3	206.1	1.04	0.092	Flexural, GFRP debonding
10	A5L	123.6	211.2	1.06	0.101	Flexural, GFRP debonding
11	B5L	129.1	200.9	1.01	0.097	Flexural, GFRP debonding
12	C5L	136.5	210.7	1.06	0.094	Flexural, GFRP debonding
13	A6D	158.1	204.8	0.93	0.106	Flexural, deck crushing
14	B6D	188.3	205.5	0.93	0.097	Flexural, deck crushing
15	C6D	168.6	210.4	0.95	0.097	Flexural, deck crushing
16	A6L	160.9	241.6	1.11	0.127	Flexural, GFRP debonding
17	B6L	138.9	243.5	1.12	0.117	Flexural, GFRP debonding
18	C6L	164.7	236.9	1.09	0.110	Flexural, deck crushing

1 inch = 25.4 mm.
1 ksi = 6.89 MPa.
—Shear force at the web cracking was not measured.

Table 16. Shear force at web cracking and ultimate, average shear stress, and failure mode for BT-54 girders.

Test No.	Girder Test	V_{cr} (ksi)	V_{test} (ksi)	v_u (ksi)	v_u/f'_c	Failure Mode
19	C8D	152.7	248.1	0.84	0.072	Shear web compression
20	A9L	175.4	457.7	1.60	0.148	Shear compression at support
21	C8L	165.4	287.5	0.97	0.084	Shear web compression
22	A9D	198.7	461.9	1.61	0.149	Flexural, GFRP debonding
23	B8D	175.2	276.5	0.93	0.078	Shear, bar rupture
24	A8D	141.8	274.1	0.92	0.082	Shear, bar rupture
25	B8L	183.4	289.2	0.98	0.082	Flexural, GFRP debonding
26	A8L	147.7	295.7	1.00	0.089	Shear, bar rupture
27	B9L	222.1	458.4	1.60	0.146	Flexural, deck crushing
28	C9L	206.0	439.6	1.53	0.148	Flexural, GFRP debonding
29	B9D	231.6	458.0	1.60	0.146	Flexural, deck crushing
30	C9D	197.8	447.7	1.56	0.151	Flexural, deck crushing

1 inch = 25.4 mm.
1 ksi = 6.89 MPa.

A summary of the level of yielding in the stirrups at V_{test}, the strand slip at V_{test}, and the peak strain in the concrete deck and GFRP at V_{test} is given in table 17 and table 18 for the type II and BT-54 girders, respectively. The level of yielding at V_{test} is given by the number of stirrups with a strain measured by ERSs (ε_t) greater than the yield strain (ε_{ty}), the number of stirrups with ε_t greater than $3\varepsilon_{ty}$, and the ratio of ε_t to ε_{ty}. In some tests, the failure modes of flexure (i.e., concrete deck crushing), GFRP debonding, and strand slip occurred prior to reaching V_{test}. Three columns in table 17 and table 18 indicate whether any of these three events (deck crushing, GFRP disbond, or strand slip) occurred prior to the applied shear force reaching V_{test}. In tests where these events occurred prior to V_{test}, the ratio of the applied shear at the event to V_{test} is given. A ratio of 1.000 indicates that the events (deck crushing, GFRP disbond, or strand slip) occurred at V_{test}. The columns state "No" if deck crushing, GFRP disbond, or strand slip occurred after the applied shear force reached V_{test}.

Table 17. Stirrup strain, strand slip, and occurrence of deck crushing, GFRP debonding, or strand slip prior to ultimate for type II girders.

Test No.	Girder Test	Number of Stirrups with $\varepsilon_t \geq \varepsilon_{ty}$ at Maximum Shear Force	Number of Stirrups with $\varepsilon_t \geq 3\varepsilon_{ty}$ at Maximum Shear Force	Ratio of Maximum ε_t to ε_{ty} at Maximum Shear Force	Strand Slip at Maximum Shear Force	Peak Deck Strain Occurred Prior to Maximum Shear Force[a]	Peak GFRP Strain Occurred Prior to Maximum Shear Force[a]	Strand Slip ≥0.010 inch (0.254 mm) Occurred Prior to Maximum Shear Force[a]
1	A7L	8	8	9.17	0.001	No	N/A	No
2	B7L	7	5	10.10	0.002	0.993	N/A	No
3	C7L	5	3	6.49	0.000	1.000	N/A	No
4	A7D	8	6	7.46	0.010	0.999	1.000[b]	0.999
5	C7D	8	5	7.50	0.017	No	1.000	1.000
6	B7D	11	9	10.46	0.004	0.993	0.993	No
7	A5D	3	1	5.15	0.002	1.000	N/A	No
8	B5D	4	1	3.57	0.001	0.974	1.000	No
9	C5D	6	4	7.03	0.001	1.000	0.977	No
10	A5L	10	8	9.20	0.000	No	1.000	No
11	B5L	8	7	10.18	0.000	No	0.981	No
12	C5L	5	3	9.77	0.001	1.000	0.980	No
13	A6D	1	0	1.11	0.000	1.000	N/A	No
14	B6D	0	0	1.00	0.007	0.992	N/A	No
15	C6D	3	1	5.38	0.001	0.995	N/A	No
16	A6L	7	2	4.98	0.002	1.000	1.000	No
17	B6L	4	0	2.72	0.002	1.000	1.000	No
18	C6L	7	2	6.58	0.001	0.957	1.000	No

1 inch = 25.4 mm.

N/A = GFRP not used on this specimen.

[a]For occurrence with maximum shear force or prior to maximum shear force, value is the ratio of shear force at occurrence to maximum shear force; otherwise "No" is given.

[b]Strain in the GFRP was not measured, value based on the applied shear at observed GFRP debonding.

Table 18. Stirrup strain, strand slip, and occurrence of deck crushing, GFRP debonding, or strand slip prior to ultimate for BT-54 girders.

Test No.	Girder Test	Number of Stirrups with $\varepsilon_t \geq \varepsilon_{ty}$ at Maximum Shear Force	Number of Stirrups with $\varepsilon_t \geq 3\varepsilon_{ty}$ at Maximum Shear Force	Ratio of Maximum ε_t to ε_{ty} at Maximum Shear Force	Strand Slip at Maximum Shear Force	Peak Deck Strain Occurred Prior to Maximum Shear Force*	Peak GFRP Strain Occurred Prior to Maximum Shear Force*	Strand Slip ≥0.010 inch (0.254 mm) Occurred Prior to Maximum Shear Force*
19	C8D	4	1	4.32	0.024	1.000	1.000	0.943
20	A9L	12	7	8.30	0.002	1.000	1.000	No
21	C8L	5	2	8.11	0.010	1.000	1.000	1.000
22	A9D	11	6	5.66	0.010	0.983	1.000	No
23	B8D	4	3	6.00	0.051	1.000	1.000	0.866
24	A8D	2	2	7.07	0.038	1.000	0.967	0.772
25	B8L	6	6	10.04	0.035	0.999	0.987	0.936
26	A8L	5	3	9.97	0.037	1.000	0.983	0.499
27	B9L	7	3	6.80	0.000	0.978	1.000	No
28	C9L	14	12	6.81	0.019	0.991	0.949	0.949
29	B9D	5	0	3.18	0.001	0.994	No	No
30	C9D	6	2	4.20	0.002	0.980	0.995	No

1 inch = 25.4 mm.

*For occurrence with maximum shear force or prior to maximum shear force, value is the ratio of shear force at occurrence to maximum shear force, otherwise "No" is given.

The average shear stress on the concrete (v_u) is shown graphically versus concrete compressive strength (f'_c) in figure 20, versus concrete unit weight (w_c) in figure 21, and versus concrete-splitting tensile strength (f_{ct}) in figure 22. The number of specimens is shown in parentheses in the legends.

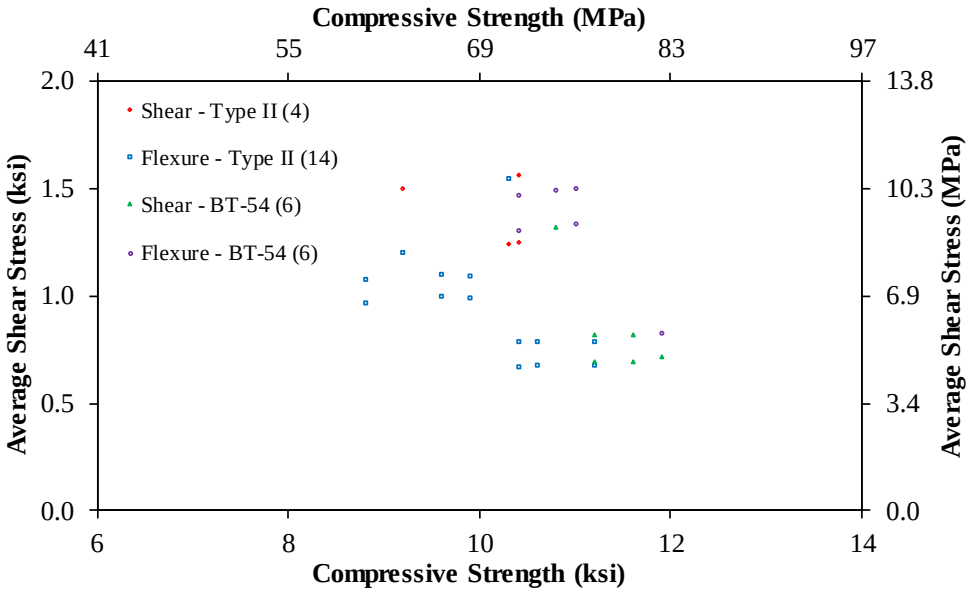

Source: FHWA.
1 ksi = 6.89 MPa.

Figure 20. Graph. Average shear stress compared to compressive strength by girder and failure types.

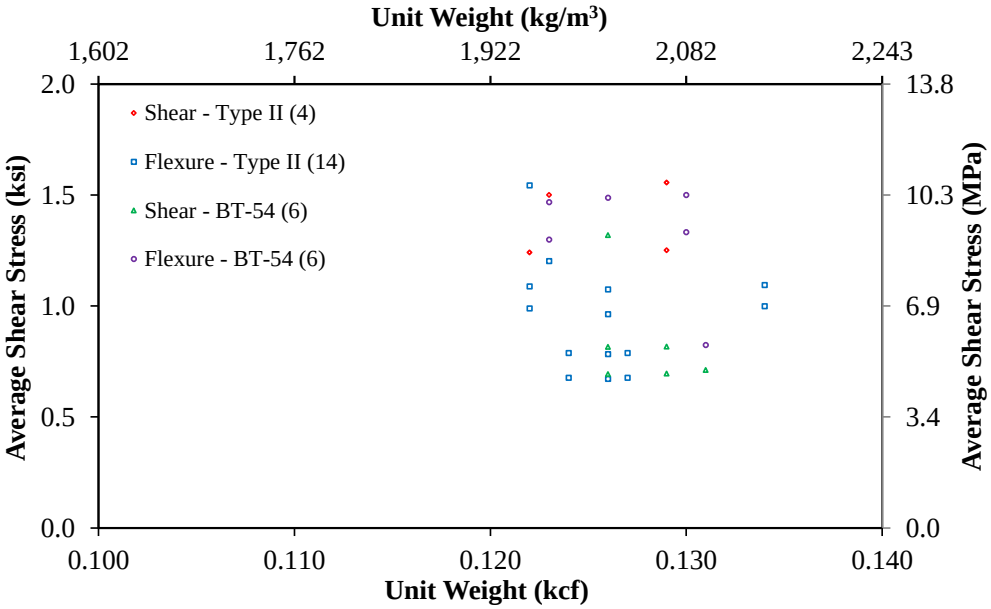

Source: FHWA.
1 ksi = 6.89 MPa.

Figure 21. Graph. Average shear stress compared to unit weight by girder and failure types.

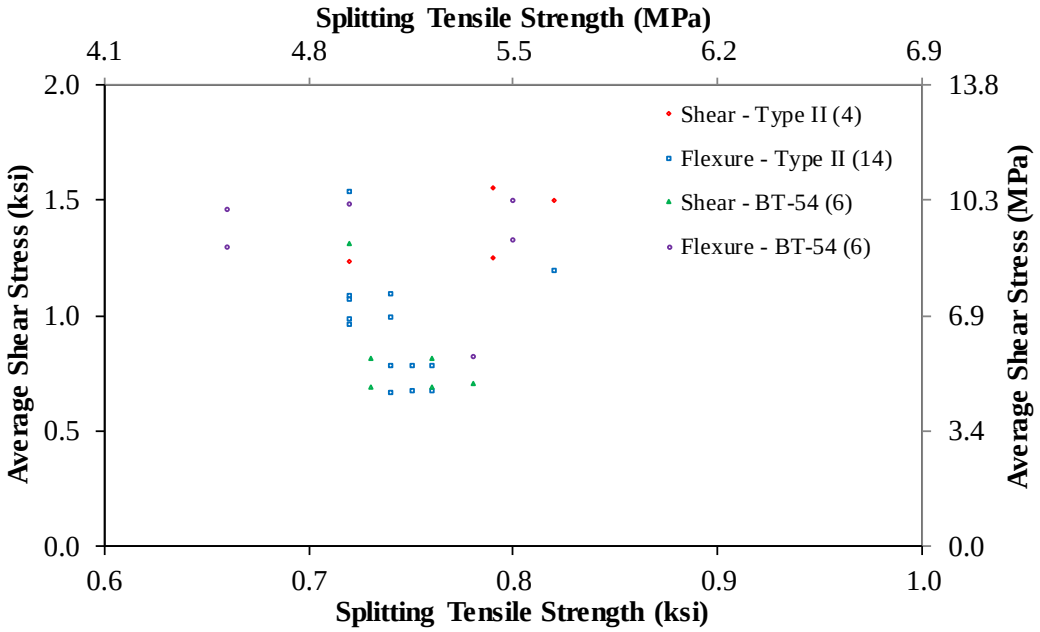

Source: FHWA.
1 ksi = 6.89 MPa.

Figure 22. Graph. Average shear stress compared to splitting tensile strength by girder and failure types.

Figure 23 shows v_u versus d_v, and figure 24 shows v_u versus a/d_v. The normalized average shear stress (v_u/f'_c) is shown versus stirrup strength ($\rho_v f_{yt}$) in figure 25 and versus the normalized stirrup spacing (s/d_v) in figure 26. The maximum stirrup spacing requirements are given in Article 5.8.2.7 in the *AASHTO LRFD Bridge Design Specifications*.[3] The maximum spacing of $0.8d_v$ for average shear stresses less than $0.125v_u/f'_c$ are shown in figure 26 as vertical and horizontal lines, respectively. Vertical and horizontal lines indicating the maximum spacing of $0.4d_v$ for average shear stresses greater than $0.125v_u/f'_c$ are also shown in the figure. As shown in figure 26, the maximum normalized shear stress at failure for each test was within the maximum stirrup spacing requirements specified by the *AASHTO LRFD Bridge Design Specifications*.[3] The number of specimens is shown in parentheses in the legends.

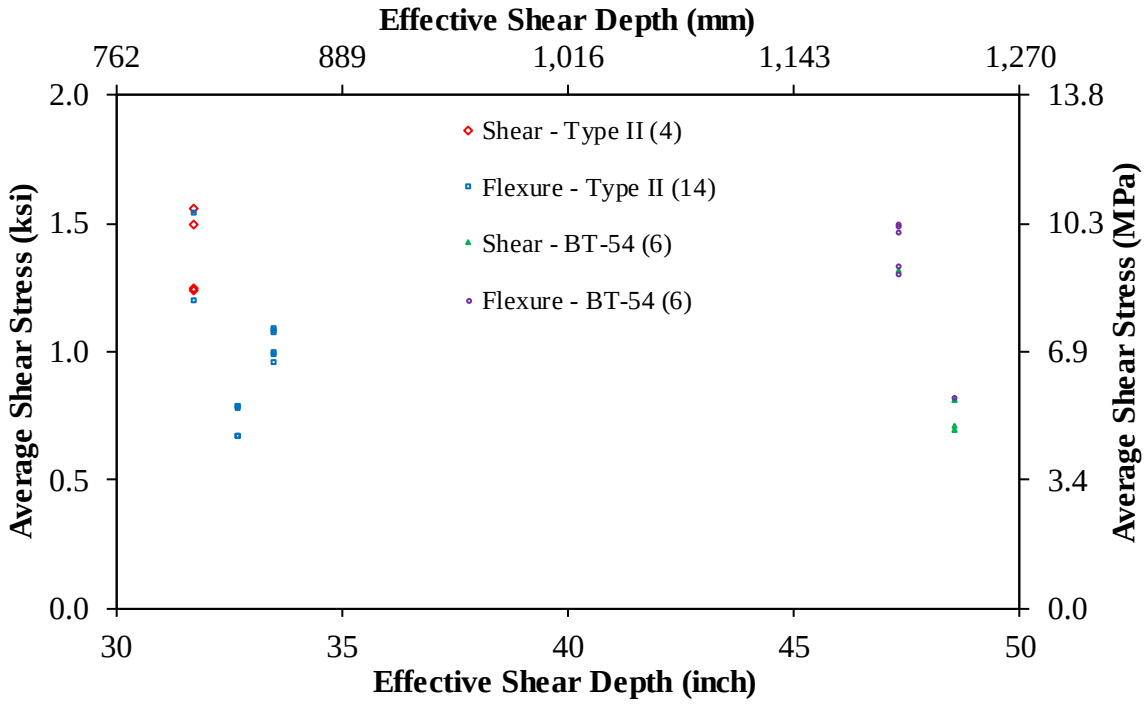

Source: FHWA.
1 ksi = 6.89 MPa.
1 inch = 25.4 mm.

Figure 23. Graph. Average shear stress compared to effective shear depth by girder and failure types.

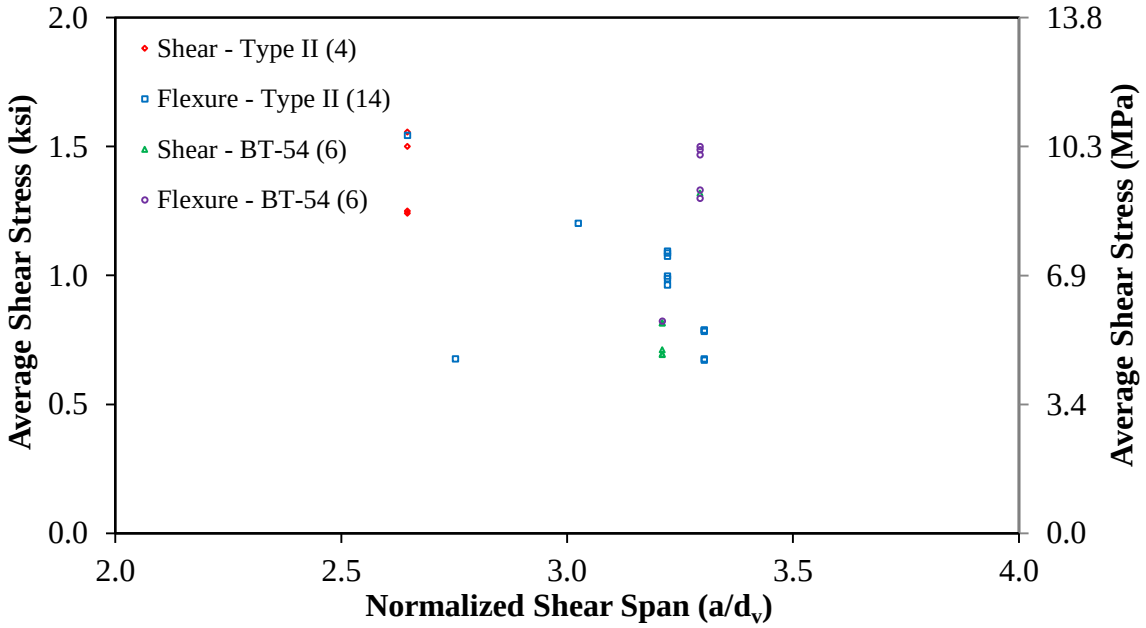

Source: FHWA.
1 ksi = 6.89 MPa.

Figure 24. Graph. Average shear stress compared to normalized shear span by girder and failure types.

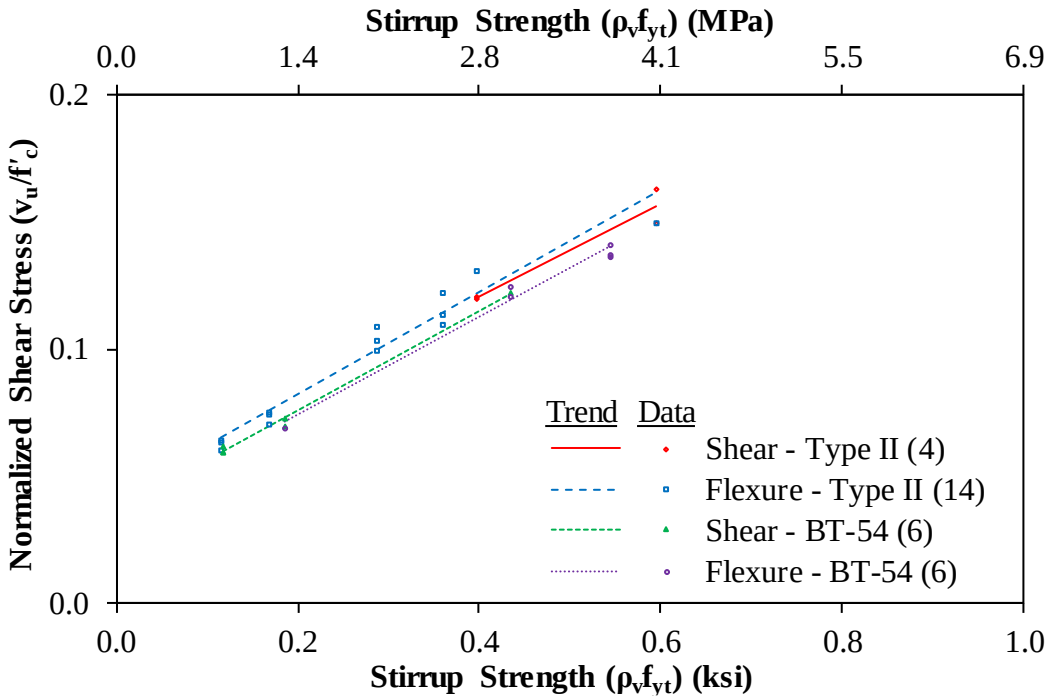

Source: FHWA.
1 ksi = 6.89 MPa.

Figure 25. Graph. Average shear stress compared to stirrup strength by girder and failure types.

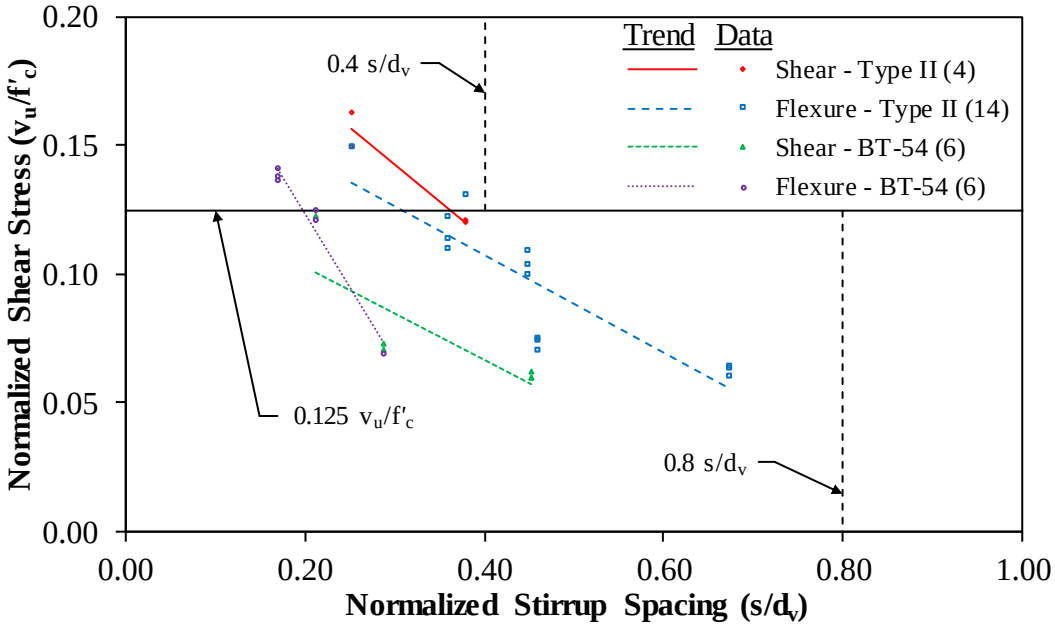

Source: FHWA.
1 ksi = 6.89 MPa.

Figure 26. Graph. Normalized shear stress compared to normalized stirrup spacing by girder and failure types.

Failure Modes

The first girder tested, A7D, failed in horizontal shear through the concrete deck. Of the remaining tests on the type II girders, 4 girders failed in shear, and 13 girders failed in flexure. Six of the tests on the BT-54 girders failed in shear, and the remaining six girders failed in flexure.

As shown in table 15 and table 16, three different types of shear failures were experienced in the tests: concrete crushing over a large region of the web (i.e., shear web compression), concrete crushing near the support (i.e., shear compression at support), and rupture of the stirrups (i.e., shear bar rupture). In each test resulting in a shear failure, there was significant yielding in several of the stirrups as indicated by measured strains greater than three times the yield strain. Two of the type II girder tests that failed in shear experienced concrete crushing in the web over much of the test region. The other two type II girder tests failing in shear had concrete crushing as the diagonal compression was funneled to the support. An example of this kind of failure is shown in figure 27 for the test on C7L. Three of the BT-54 girders tests failed in shear after multiple stirrups ruptured. Two of the tests on BT-54 girders failed in shear after experiencing general yielding in the stirrups followed by local crushing in the web. This kind of failure is shown in figure 10 and figure 28 for the tests on C8D and C8L. The failure of test A9L is shown in figure 29 and was due to concrete crushing as the diagonal compression was funneled to the support.

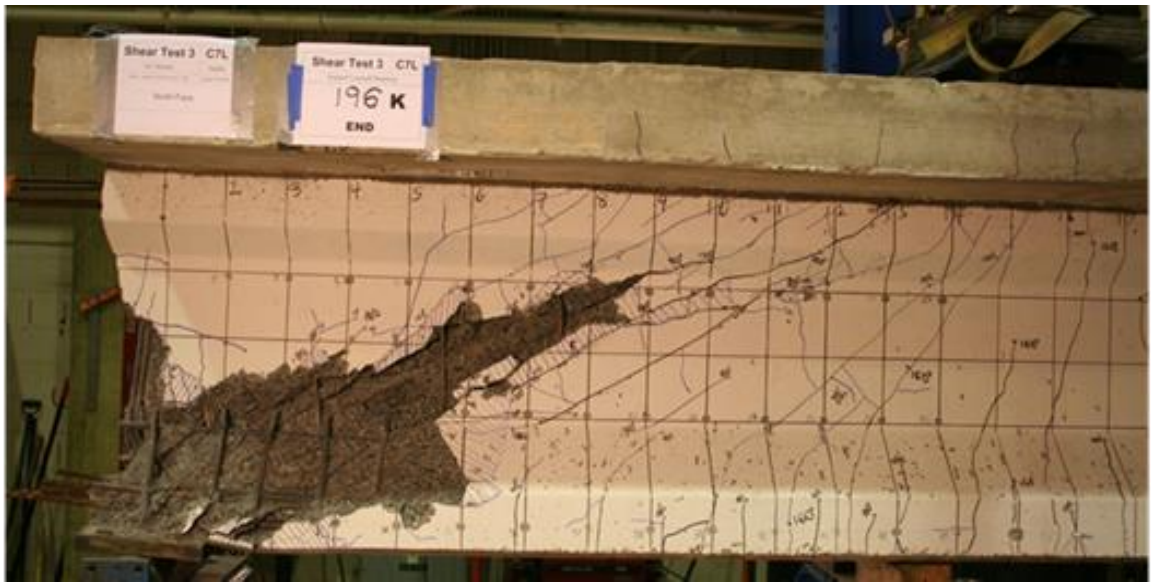

Source: FHWA.

Figure 27. Photo. Shear failure of girder test C7L showing concrete crushing near support.

Source: FHWA.

Figure 28. Photo. Shear failure of girder test C8L showing concrete crushing along web.

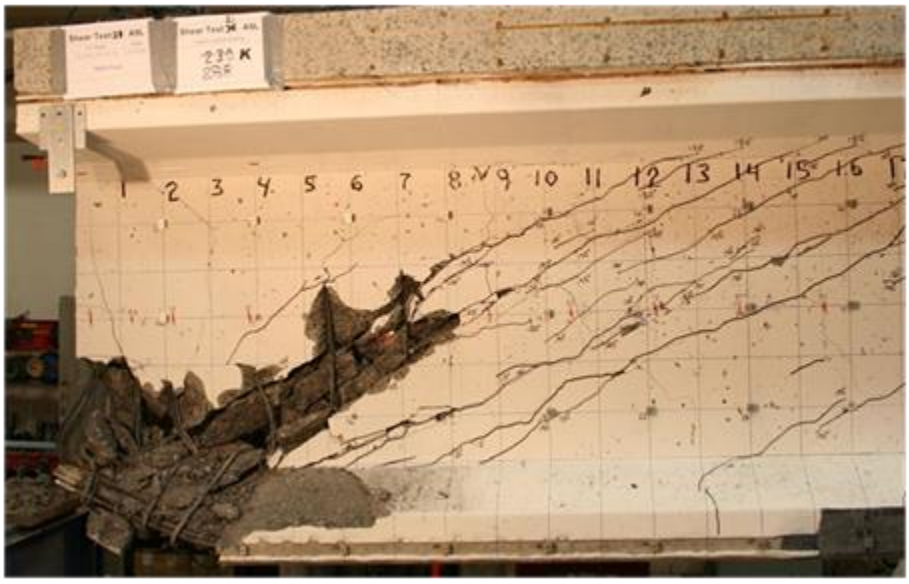

Source: FHWA.

Figure 29. Photo. Shear failure of girder test A9L showing concrete crushing near support.

The tests resulting in flexural failures (see table 15 and table 16) were caused by crushing of the deck (i.e., flexural deck crushing) or by loss of resistance in the GFRP (i.e., flexural GFRP debonding). The loss of resistance in the GFRP was due to the GFRP at the end of a layer debonding from the concrete substrate or the GFRP, causing the concrete substrate to peel away from the bottom layer of strands. Five of the tests on type II girders and three of the tests on BT-54 girders failed after the deck concrete crushed. The flexural failure was initiated by loss of resistance in the GFRP in eight of the tests on type II girders and three of the tests on BT-54 girders.

Test Observations

The first girder tested, A7D, was unintentionally loaded rapidly to an applied shear of 193 kip (858.9 kN) and then immediately unloaded. This shear was 64 percent of the maximum applied shear and below the shear that caused yielding of the stirrups. As a result of the rapid loading, the applied shear at web cracking was not determined. Girder test A7D ended after an arc-shaped crack formed through the thickness the deck, as shown in figure 30, resulting in a horizontal shear failure. Concrete anchors were installed through the decks along the test region in all subsequent tests of type II girders to prevent additional horizontal shear failures.

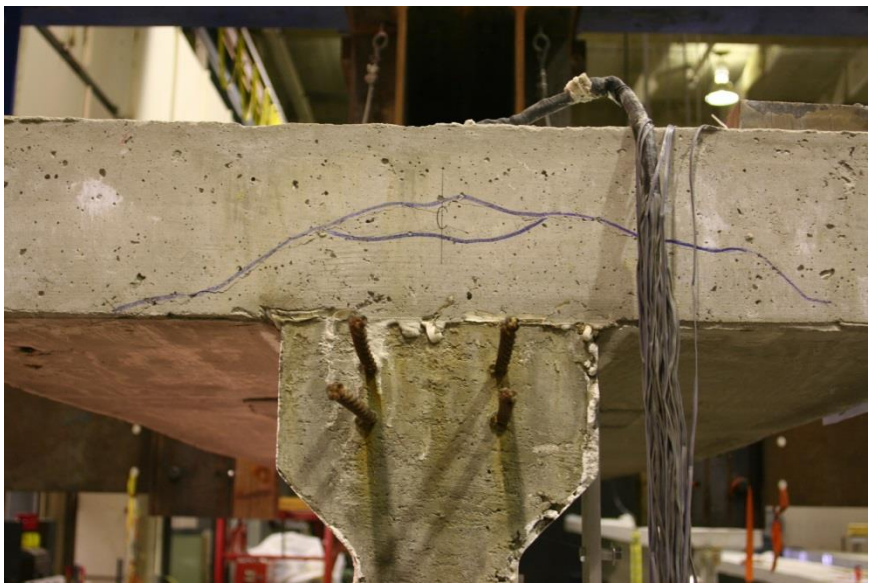

Source: FHWA.

Figure 30. Photo. Horizontal shear failure of girder test A7L.

Before test A7L failed in horizontal shear, there were eight stirrups that had reached a measured strain greater than three times the yield strain. The other two tests on girder design 7L (i.e., test 2 on girder B7L and test 3 on girder C7L) had fewer stirrups that had reached yielding and resulted shear-compression failures at the support. Almost no measurable strand slip was observed in these three tests.

Test 4 on A7D was the first girder test that was flexurally strengthened with GFRP. During the test, the end layer of GFRP removed some of the cover from the bottom face of the bottom flange. The test was continued and resulted in a web compression failure throughout the web. Evaluation of a video taken of the test region using a digital video camera showed that the failure initiated in the web between the support and the end of the GFRP. This observation supports the conclusion that the failure was due to shear and was not limited by the GFRP debonding.

The remaining six tests on type II girders resulted in flexural failures. All of the failures on specimens that were flexurally strengthened with GFRP were due to the debonding of the GFRP except for the test on girder C6L.

All three tests on girder design 8D failed in shear. This girder end had the lower amount of prestressing strands (when compared to girder design 9) and an amount of stirrups nearly equal to the minimum amount specified in the *AASHTO LRFD Bridge Design Specifications*.[3] The test on B8L resulted in a flexural failure, but the other two tests on girder design 8L resulted in shear failures. The tests on girder design 8, except test C8L, had a maximum strand slip that exceeded 0.010 inch (0.25 mm) at V_{test}. The strand slip of test A8L had a maximum strand slip that exceeded 0.010 inch (0.25 mm) at an applied shear force of 50 percent of V_{test}.

Of the six texts on girder design 9, only test A9L resulted in a shear failure. Girder design 9 had a larger amount of prestressing strands and had a larger amount of shear reinforcement when compared to girder design 8.

Web Shear Cracking Angles

The measured angles of the web-shear cracks are given in table 19 and table 20 for the type II and BT-54 girders, respectively. The crack angle was measured directly using a crack protractor. The FARO® and LVDT measurements were determined from smeared strain in the horizontal, vertical, and diagonal directions to calculate the direction of the principle compression strain. The minimum angle, maximum angle, and average angle of the cracks that crossed the midheight of the web between the centerline of the support and a distance of two times the effective depth (d_v) from the centerline of the support are given in table 19 and table 20.

Table 19. Web-shear–cracking angles for type II girders.

Test No.	Girder Test	Direct Measurement of Crack Angle Using Crack Protractor (Degrees)			FARO® Measurement of Crack Angle (Degrees)			Average LVDT Measurement of Crack Angle (Degrees)
		Minimum	Maximum	Average	Minimum	Maximum	Average	
1	A7L	22.0	31.0	27.3	27.5	39.8	30.4	29.1
2	B7L	26.0	37.0	30.8	13.1	37.3	26.1	36.4
3	C7L	32.0	39.0	35.2	24.3	43.4	32.4	18.0
4	A7D	34.0	40.0	36.5	32.1	39.8	36.9	23.9
5	C7D	34.0	38.0	36.6	24.2	42.3	32.8	28.7
6	B7D	27.0	31.0	29.8	25.7	44.2	34.6	26.9
7	A5D	34.0	39.0	36.5	15.6	30.2	22.9	41.2
8	B5D	21.0	41.0	31.8	12.7	35.0	22.8	13.2
9	C5D	20.0	25.0	23.3	16.6	31.5	21.3	14.8
10	A5L	30.0	47.0	36.0	19.9	30.7	25.3	16.2
11	B5L	28.0	35.0	30.4	21.5	43.2	31.6	15.8
12	C5L	26.0	30.0	27.7	14.6	32.5	24.2	19.8
13	A6D	29.0	34.0	31.4	23.1	33.1	29.5	29.0
14	B6D	29.0	45.0	36.0	24.1	41.3	33.3	28.7
15	C6D	30.0	31.0	30.5	23.1	30.8	26.8	28.9
16	A6L	28.0	38.0	33.3	27.3	38.0	32.2	25.7
17	B6L	31.0	34.0	32.8	25.1	41.3	34.7	26.4
18	C6L	27.0	35.0	30.5	27.4	38.5	31.7	22.0

Table 20. Web-shear–cracking angles for BT-54 girders.

Test No.	Girder Test	Direct Measurement of Crack Angle (Degrees)			FARO® Measurement of Crack Angle (Degrees)			Average LVDT Measurement of Crack Angle (Degrees)
		Minimum	Maximum	Average	Minimum	Maximum	Average	
19	C8D	25.0	28.0	27.0	13.9	34.0	21.0	17.1
20	A9L	21.0	31.0	27.8	21.4	24.8	23.8	31.5
21	C8L	26.0	30.0	27.8	23.1	35.9	28.8	24.7
22	A9D	—	—	—	30.6	41.5	37.2	28.4
23	B8D	24.0	32.0	28.7	13.8	20.3	17.4	14.6
24	A8D	25.0	30.0	26.6	13.7	30.7	21.6	17.5
25	B8L	25.0	36.0	29.0	15.6	26.4	19.8	20.1
26	A8L	26.0	30.8	28.0	18.9	30.5	22.9	17.0
27	B9L	27.0	30.0	28.6	25.3	38.5	33.2	21.8
28	C9L	28.0	34.0	30.3	30.9	40.3	36.6	26.7
29	B9D	28.0	31.5	29.5	18.9	38.4	31.5	30.6
30	C9D	28.0	31.5	29.5	18.9	38.4	31.5	30.6

—Direct measurements were not made.

Web shear crack angles were determined using the FARO® noncontact laser tracking system. The change in the distance between measurement targets was used to determine the average concrete strain in the horizontal, vertical, and diagonal directions. The locations of the targets are shown in figure 13 and figure 14 for the type II and BT-54 girders, respectively. The measurements between four targets were used to determine the crack angle. The horizontal strain was taken as the average of the strain determined from the two upper targets and the two lower targets. The vertical strain was taken as the average strain of two sets of targets spaced 12 inches (305 mm) apart. The diagonal strain was measured between the upper-left and lower-right targets. A diagonal average strain measured in this orientation crossed the cracks to give a tensile strain (i.e., not in the direction of the cracks to give a compressive strain). The horizontal, vertical, and diagonal average strains were used to determine the angle of the principle compressive strain (i.e., in the direction of the cracks). The minimum, maximum, and average angles determined from four targets centered between a distance of $0.5d_v$ and $1.5d_v$ from the centerline of the support are shown in table 19 and table 20.

The crack angles were also determined using the LVDT rosettes. The change in displacement measured by the LVDT was used to determine the average concrete strain in the horizontal, vertical, and diagonal directions. The locations of the LVDT anchors are shown in figure 13 and figure 14 for the type II and BT-54 girders, respectively, while figure 17 shows a photograph of the two LVDT rosettes. The horizontal, vertical, and diagonal average strains were used to determine the angle of the principle compressive strain (i.e., in the direction of the cracks). The angles given in table 19 and table 20 were the mean of the angles determined from the three LVDTs shown in figure 17 forming the rosette on the left-hand side with the angle determined from the three LVDTs forming the rosette on the right-hand side.

There was considerable variation in the web cracking angles determined from the crack protractor, FARO® measurements, and LVDT measurements. A comparison of individual crack measurements for each girder test is shown in the draft version of the research data; see appendix G for further details. Most of the individual crack measurements from the crack protractor ranged from 20 to 40 degrees with the mean crack measurements ranging from 23 to 37 degrees. Many of the crack angles determined using the FARO® and LVDT measurements were much smaller than the angles measured using the crack protractor. This is because the FARO® and LVDT measurements are sensitive to the location and number of cracks between the FARO® targets and LVDT anchors. For example, when a web-shear crack did not pass between two vertical measurement points (i.e., FARO® targets and LVDT anchors), the resulting principle angle was much smaller than if web-shear cracks had passed between vertical, horizontal, and diagonal measurement points.

EFFECT OF TEST PARAMETERS ON MAXIMUM SHEAR STRESS

Three major variables in this study were the girder mix design, the amount of stirrups, and the girder depth. This section compares the test results for each of these variables.

Girder Mix Design

The girder tests that resulted in a shear failure are provided in table 21. The tests are grouped by girder end design to compare the average shear stress (v_u) of different mix designs, which was

based on V_{test} and determined using Article 5.8.2.9 in the *AASHTO LRFD Bridge Design Specifications*.[3] v_u normalized by concrete compressive strength and the splitting tensile strength is also shown in table 21. A comparison of the normalized v_u shows that there was very little difference between the different concrete mixtures.

Table 21. Comparison of girder concrete mixture on the normalized shear stress at failure for girder tests resulting in shear failure.

Girder Test	v_u (ksi)	v_u/f'_c	v_u/f_{ct}	Failure Mode
B7L	1.90	0.184	2.41	Shear compression at support
C7L	1.83	0.177	2.52	Shear compression at support
A7D	1.93	0.209	2.37	Shear web compression
B7D	2.17	0.210	2.75	Shear web compression
A8D	0.92	0.082	1.21	Shear bar rupture
B8D	0.93	0.078	1.20	Shear bar rupture
C8D	0.84	0.072	1.14	Shear web compression
A8L	1.00	0.089	1.31	Shear bar rupture
C8L	0.97	0.084	1.33	Shear web compression

1 inch = 25.4 mm.
1 ksi = 6.89 MPa.

Amount of Stirrups

v_u is compared to the shear reinforcement ratio in figure 25. v_u is normalized by the concrete compressive strength and is compared to stirrup strength ($\rho_v f_{yt}$), where the shear reinforcement ratio (ρ_v or also referred to as $A_v/b_v s$) is given by equation 40. The test results are grouped by girder type (i.e., type II or BT-54 girders) and by failure type (i.e., shear failure or flexural failure). Regression lines are shown for the test results in each group. As expected, the regression lines in the figure showed a trend of v_u increasing as the amount of shear reinforcement increased. The regression lines shown in the figure are all nearly parallel, even the lines for tests ending in a shear failure and flexural failure.

Girder Depth

The effect that girder depth had on the v_u is also shown in figure 25. The regression lines for the type II girders resulting in shear and flexural failures are parallel and nearly overlapping. Similarly, the regression lines for the BT-54 girders are parallel and overlapping. The regression lines for the type II girders are clearly above the regression lines for the BT-54 girders, indicating that, on average, the type II girders had larger v_u for a given amount of shear reinforcement.

v_u is shown in table 22 for the two different girder depths. The table provides the results for three pairs of girder tests with similar amounts of longitudinal and shear reinforcement. Girder design 5D is compared to 8D, 5L is compared to 8L, and 7D is compared to 9D. Effective shear depth (d_v), stirrup strength ($\rho_v f_{yt}$), and prestressed longitudinal reinforcement ratio (A_{ps}/bd_v or also referred to as ρ_p) are shown for each pair. For each pair, d_v of the BT-54 girders were approximately 50 percent greater than d_v of the type II girders, but $\rho_v f_{yt}$ and A_{ps}/bd_v were nearly

equal. The mean normalized v_u for girder design 5D was 25 percent larger than the mean normalized v_u for girder design 8D. For girder design 5L, the mean normalized v_u was 16 percent larger than the mean normalized v_u for girder design 8L. Similarly, the mean normalized v_u for girder design 7D was 42 percent larger than the mean normalized v_u for girder design 9D. Except for girder design 8D, some or all of the tests in each of the groups failed in flexure, so the exact magnitude was not as important as the observation that for each girder test compared, the normalized v_u for the type II girders was noticeably higher.

Table 22. Comparison of girder end design on the normalized shear stress at failure for girder tests resulting in shear failure.

Girder Test	d_v (Inches)	$\rho_v f_{yt}$ (ksi)	A_{ps}/bd_v (Percent)	v_u (ksi)	v_u/f'_c	Failure Mode
A5D	32.7	0.115	0.11	1.05	0.100	Flexural, deck crushing
B5D	32.7	0.115	0.11	1.01	0.097	Flexural, GFRP debonding
C5D	32.7	0.115	0.11	1.04	0.092	Flexural, GFRP debonding
A8D	48.6	0.118	0.12	0.92	0.082	Shear, bar rupture
B8D	48.6	0.118	0.12	0.93	0.078	Shear, bar rupture
C8D	48.6	0.118	0.12	0.84	0.072	Shear web compression
A5L	32.7	0.169	0.11	1.06	0.101	Flexural, GFRP debonding
B5L	32.7	0.169	0.11	1.01	0.097	Flexural, GFRP debonding
C5L	32.7	0.169	0.11	1.06	0.094	Flexural, GFRP debonding
A8L	48.6	0.185	0.12	1.00	0.089	Shear, bar rupture
B8L	48.6	0.185	0.12	0.98	0.082	Flexural, GFRP debonding
C8L	48.6	0.185	0.12	0.97	0.084	Shear web compression
A7D	31.7	0.596	0.20	1.93	0.209	Shear web compression
B7D	31.7	0.596	0.20	2.17	0.210	Shear web compression
C7D	31.7	0.596	0.20	2.16	0.209	Flexural, GFRP debonding
A9D	47.4	0.544	0.21	1.61	0.149	Flexural, GFRP debonding
B9D	47.4	0.544	0.21	1.60	0.146	Flexural, deck crushing
C9D	47.4	0.544	0.21	1.56	0.151	Flexural, deck crushing

1 inch = 25.4 mm.
1 ksi = 6.89 MPa.

COMPARISON OF TEST RESULTS TO PREDICTED SHEAR RESISTANCE

The shear resistances predicted by the design expressions in the *AASHTO LRFD Bridge Design Specifications* were compared to V_{test}.[3] The design expressions include the two general procedure methods (GP-table and GP-equation) and the Simplified-PC/RC method.[3] The comparisons are given as test-to-prediction ratios for each design expression. Two parameters, β and θ, were calculated to determine the shear resistance using the GP-table and GP-equation methods. The *AASHTO LRFD Bridge Design Specifications* allows parameters β and θ to be determined using equations in Article 5.8.3.4.2 (i.e., GP-table), or the parameters can be determined using table B5.2-1 and table B5.2-2 in appendix B5 (i.e., GP-equation).[3] Test-to-prediction ratios were determined for β and θ using the GP-table, GT-equation, and Simplified-PC/RC methods.

Procedure for Determining Shear Resistance

For the GP-equation method, β and θ are a function of the net longitudinal tensile strain in the section at the centroid of the tension reinforcement (ε_s) and are solved for in equation 21 and equation 24, respectively. ε_s is also given by equation 18 and equation 19. Specifically, when the calculated ε_s is positive, indicating a net tensile strain at the centroid of the reinforcement, equation 18 is used. When the calculated ε_s is negative, indicating a net compressive strain, equation 19 is used.

For the GP-table method, β and θ depend on the longitudinal strain at the middepth of the beam (ε_x) and the normalized shear stress in the section (v_u/f'_c). ε_x is determined using equation 26 when its value is positive, and it is determined using equation 27 when ε_x is negative. Both equation 26 and equation 27 are a function of θ, which makes the GP-table method iterative. v_u is determined using equation 15. The commentary of appendix B5 allows the values of β and θ determined from table B5.2-1 and table B5.2-2 in the *AASHTO LRFD Bridge Design Specifications* to be applied over a range of values.(3) For this analysis, three-way interpolation between the table cells that bound the pair of v_u/f'_c and ε_x values were used to determine a more exact value of β and θ.

The parameters β and θ are determined using either the GP-equation or GP-table methods. They are used to determine the nominal shear resistance provided by tensile stresses in the concrete (V_c) and the nominal shear resistance provided by the shear reinforcement (V_s) to the nominal shear resistance (V_n). The expressions for V_c and V_s are provided in equation 16 and equation 17, respectively. V_n is the smaller of the values determined using equation 13 and equation 14.

The Simplified-PC/RC uses the smaller of V_{cw} determined using equation 28 and V_{ci} determined using equation 29 as the contribution of V_c. V_s is a function of cot θ, which is taken as 1.0 when V_{ci} is less than V_{cw} and is shown in equation 35 when V_{ci} is greater than V_{cw}. Similar to the two general procedure methods, the nominal shear resistance is the smaller of the values determined using equation 13 and equation 14.

The nominal shear resistance was calculated for each girder test at the critical section for shear. The critical section for shear is given by Article 5.8.3.2 of the *AASHTO LRFD Bridge Design Specifications* as d_v from the internal face of the support.(3) For the girder tests, the critical section was taken as the distance from the centerline of the rolling support equal to half the width of the 12-inch (305-mm)-wide bearing plate plus d_v calculated using equation 5.

Iterative Process for the General Procedure

The expressions for ε_s used in the GP-equation method and ε_x used in the GP-table method are functions of the applied shear. As the applied shear increases, the calculated longitudinal strain as ε_s or ε_x also increases. The values of β, and, as a result, V_c and V_n, decrease as the applied shear and the longitudinal strain increase. V_n calculated directly from V_{test} would result in V_n that is too small when V_{test} is greater than V_n and too large when V_{test} is less than V_n. This concept is illustrated by figure 31 for the case of V_{test} greater than V_n (i.e., $V_{test}/V_n > 1$). The figure shows that for the first calculation of V_n, V_u was taken equal to V_{test}. Because the calculated V_n was less than the assumed V_u, the calculation of V_n was repeated (i.e., iteration 2) with a smaller assumed

value of V_u. The iterations were continued until the calculated V_n equaled the assumed V_u. The resulting test-to-prediction ratios for each successive iteration decreased because the calculated V_n increased. This procedure of iteratively determining for V_n was performed independently for both the GP-equation and GP-table methods. The actual process of varying V_u was handled numerically by multiplying the calculated support reaction due to the applied load by a factor (i.e., δ). δ is a factor multiplied by the internal shear force and internal moment as part of the iterative procedure to determine nominal shear resistance. As a result, both V_u and M_u in equation 18 and equation 19 for ε_s and equation 25 through equation 27 for ε_x were affected by the δ-factor. Iterations to determine V_n using Simplified-PC/RC are not required. This is because the δ-factor in the V_i and M_{max} terms of the expression for V_{ci} cancel out.

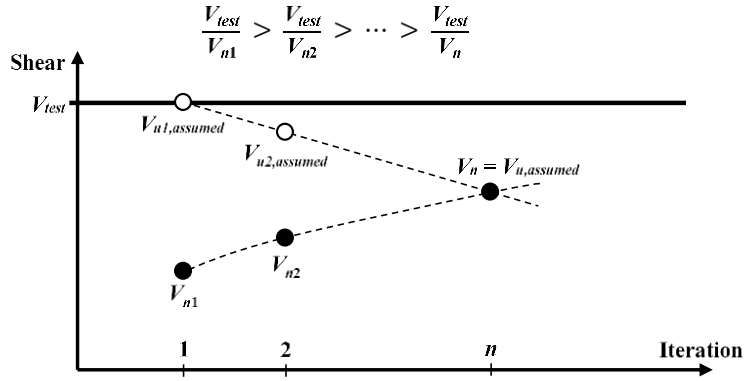

Source: FHWA.

Figure 31. Graph. Iteration procedure to determine shear resistance for a test-to-prediction ratio greater than 1.

Where:

V_{n1} = calculated nominal shear resistance of the section (V_n) corresponding to first assumed value of the factored shear force at the section (V_u).
V_{n2} = calculated V_n corresponding to second assumed value of V_u.
$V_{u,\,assumed}$ = assumed value of V_u equals V_n.
$V_{u1,\,assumed}$ = first assumed value of V_u.
$V_{u2,\,assumed}$ = second assumed value of V_u.

Analysis of Predicted Results

This section discusses the test-to-prediction ratios for the LWC girder tests determined using the GP-equation method, the GP-table method, and the Simplified-PC/RC method.

Test-to-prediction ratios for the three procedures are given in table 23 with no modification for LWC (i.e., λ taken as 1). The ratios are grouped by girder type and failure type. The ratios are shown graphically in figure 32 through figure 40 versus compressive strength (f'_c), effective shear depth (d_v), and stirrup strength ($\rho_v f_{yt}$) for each procedure. The shear reinforcement ratio (ρ_v) is given by equation 40. The ratios are shown in four groups: tests on type II girders resulting in shear failures, tests on type II girders resulting in flexural failures, tests on BT-54 girders resulting in shear failures, and tests on BT-54 girders resulting in flexural failures. A regression line is shown for the data in each group.

Table 23. Test-to-prediction ratio of shear resistance for design expressions with no modification for LWC.

Girder and Failure Types*	Design Expression	Mean	COV (Percent)	Maximum	Minimum	Percent Test-to-Prediction Ratio	
						<1.0	<0.8
Type II shear failure (4)	GP-equation	1.39	7.9	1.50	1.24	0.0	0.0
Type II shear failure (4)	GP-table	1.41	7.3	1.52	1.28	0.0	0.0
Type II shear failure (4)	Simplified-PC/RC	1.26	8.8	1.37	1.11	0.0	0.0
Type II flexure failure (14)	GP-equation	1.18	17.2	1.45	0.92	35.7	0.0
Type II flexure failure (14)	GP-table	1.21	18.2	1.52	0.94	28.6	0.0
Type II flexure failure (14)	Simplified-PC/RC	1.17	21.6	1.53	0.88	42.9	0.0
BT-54 shear failure (6)	GP-equation	1.18	4.4	1.25	1.11	0.0	0.0
BT-54 shear failure (6)	GP-table	1.23	4.9	1.31	1.17	0.0	0.0
BT-54 shear failure (6)	Simplified-PC/RC	1.36	9.5	1.53	1.18	0.0	0.0
BT-54 flexure failure (6)	GP-equation	1.11	5.3	1.19	1.04	0.0	0.0
BT-54 flexure failure (6)	GP-table	1.12	5.8	1.19	1.05	0.0	0.0
BT-54 flexure failure (6)	Simplified-PC/RC	1.12	12.1	1.36	1.00	0.0	0.0
Type II and BT-54 shear failure (10)	GP-equation	1.26	10.1	1.50	1.11	0.0	0.0
Type II and BT-54 shear failure (10)	GP-table	1.30	9.1	1.52	1.17	0.0	0.0
Type II and BT-54 shear failure (10)	Simplified-PC/RC	1.32	9.6	1.53	1.11	0.0	0.0
Type II and BT-54 flexure failure (20)	GP-equation	1.16	15.0	1.45	0.92	25.0	0.0
Type II and BT-54 flexure failure (20)	GP-table	1.18	16.0	1.52	0.94	20.0	0.0
Type II and BT-54 flexure failure (20)	Simplified-PC/RC	1.15	19.2	1.53	0.88	30.0	0.0

*The number of specimens is shown in parentheses.

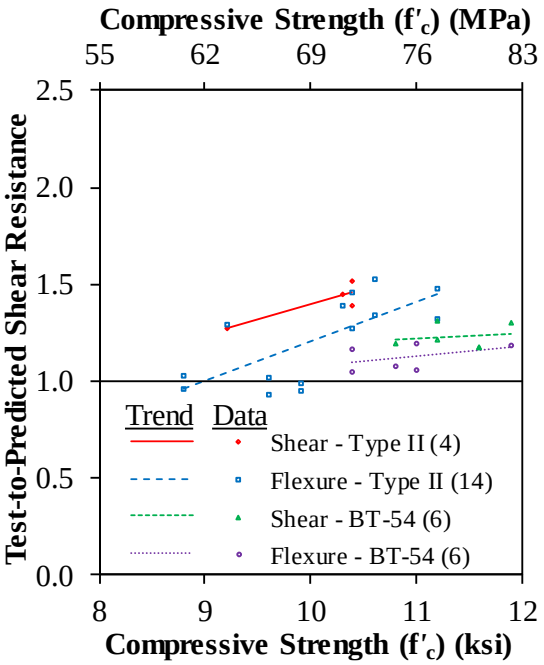

Source: FHWA.
1 ksi = 6.89 MPa.

Figure 32. Graph. Test-to-predicted shear resistance for GP-equation method with no LWC modification (λ-factor = 1) compared to compressive strength.

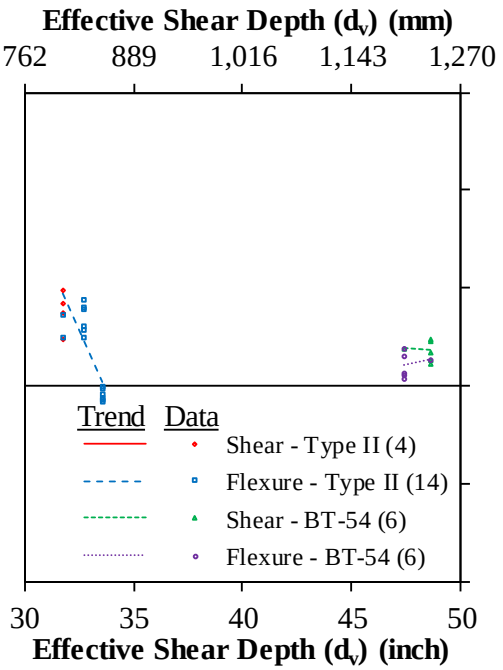

Source: FHWA.
1 inch = 25.4 mm.

Figure 33. Graph. Test-to-predicted shear resistance for GP-equation method with no LWC modification (λ-factor = 1) compared to effective shear depth.

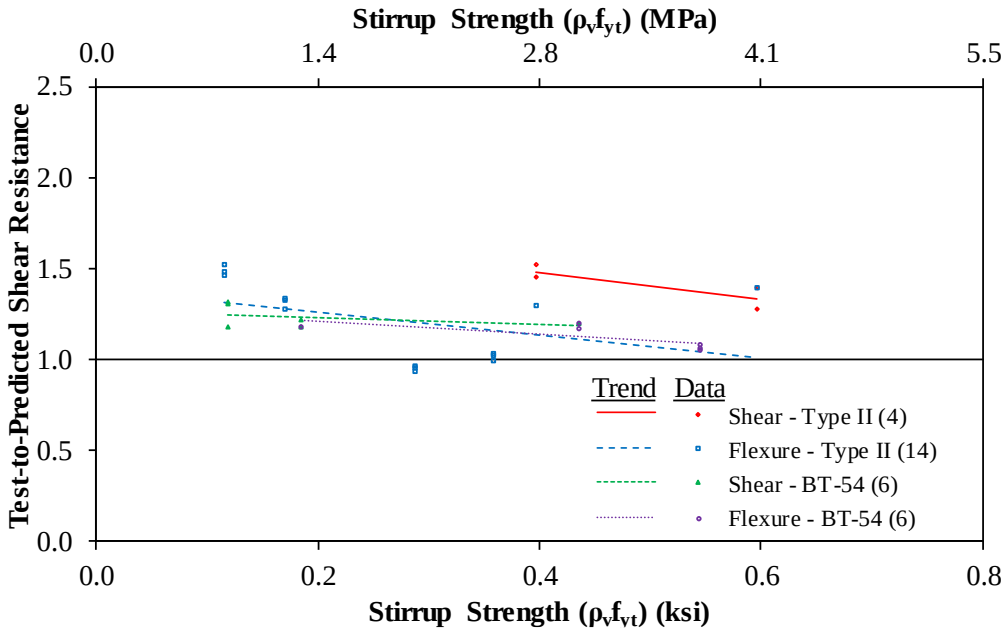

Source: FHWA.
1 ksi = 6.89 MPa.

Figure 34. Graph. Test-to-predicted shear resistance for GP-equation method with no LWC modification (λ-factor = 1) compared to stirrup strength.

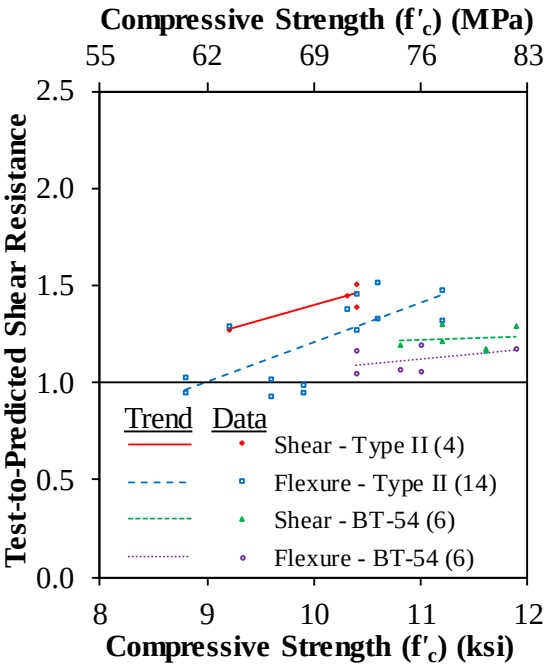

Source: FHWA.
1 ksi = 6.89 MPa.

Figure 35. Graph. Test-to-predicted shear resistance for GP-table method with no LWC modification (λ-factor = 1) compared to compressive strength.

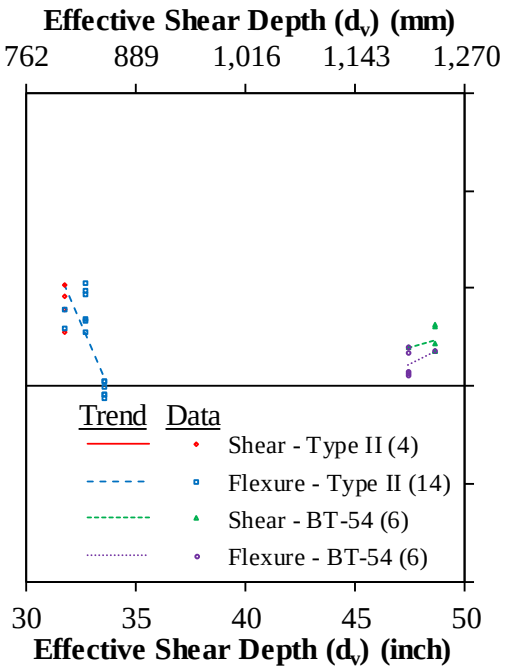

Source: FHWA.
1 inch = 25.4 mm.

Figure 36. Graph. Test-to-predicted shear resistance for GP-table method with no LWC modification (λ-factor = 1) compared to effective shear depth.

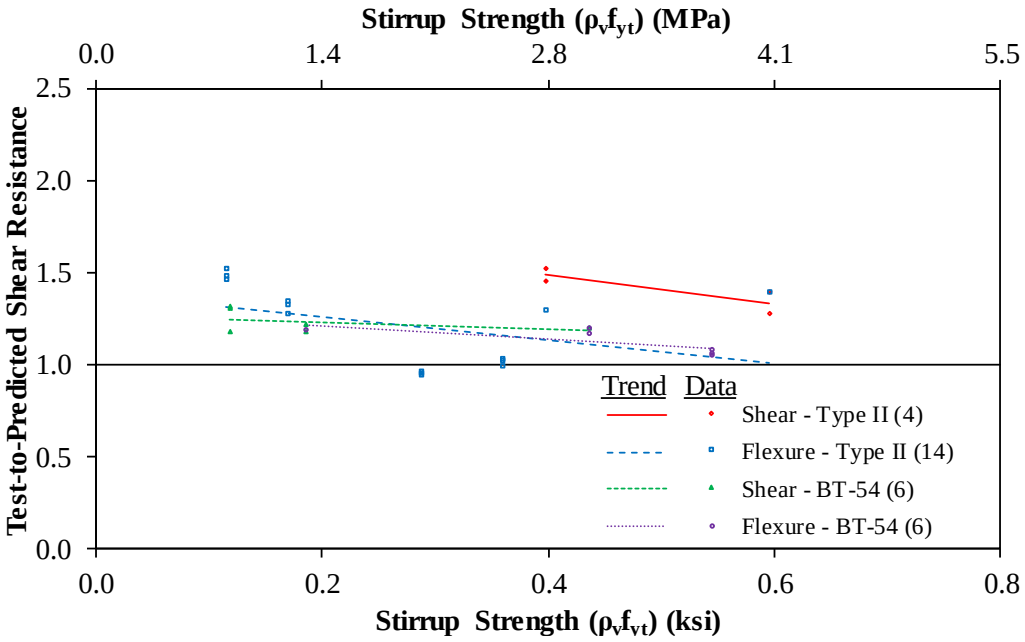

Source: FHWA.
1 ksi = 6.89 MPa.

Figure 37. Graph. Test-to-predicted shear resistance for GP-table method with no LWC modification (λ-factor = 1) compared to stirrup strength.

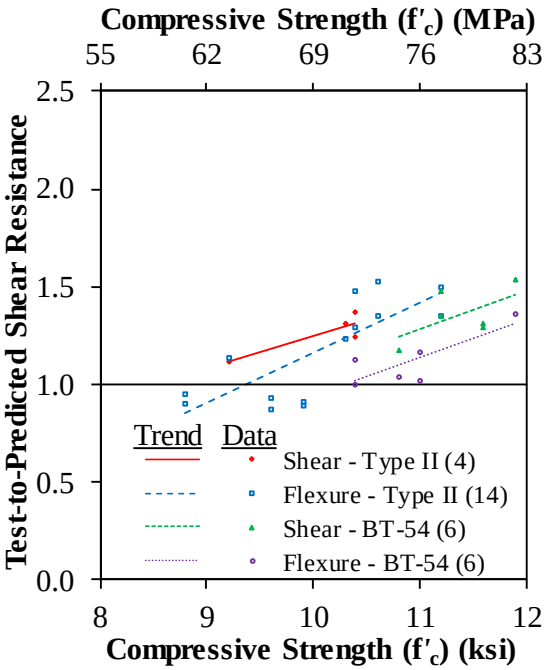

Source: FHWA.
1 ksi = 6.89 MPa.

Figure 38. Graph. Test-to-predicted shear resistance for Simplified-PC/RC with no LWC modification (λ-factor = 1) compared to compressive strength.

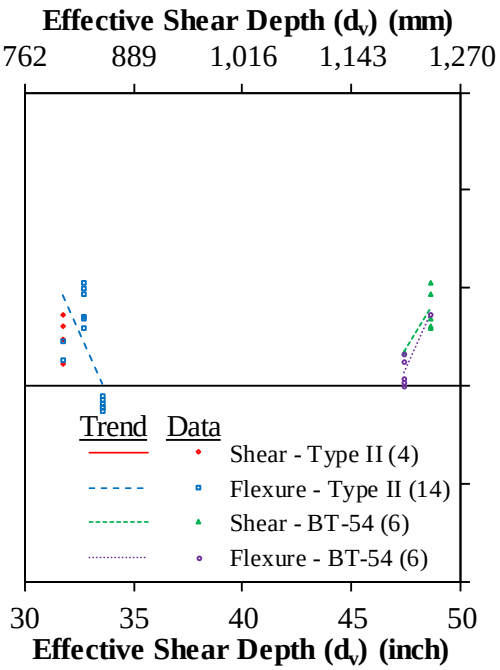

Source: FHWA.
1 inch = 25.4 mm.

Figure 39. Graph. Test-to-predicted shear resistance for Simplified-PC/RC with no LWC modification (λ-factor = 1) compared to effective shear depth.

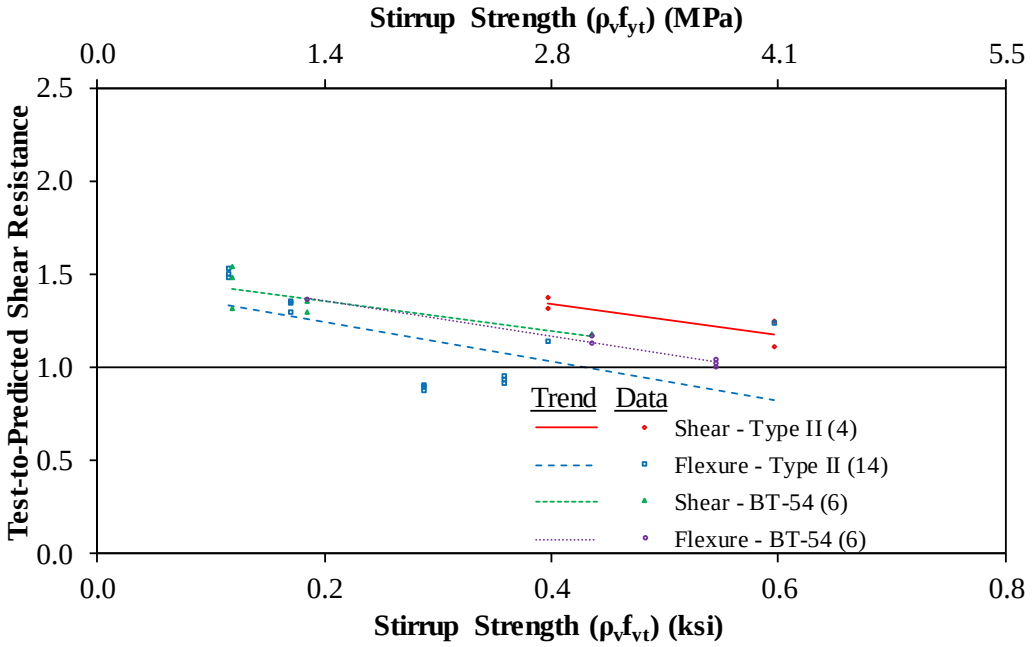

Source: FHWA.
1 ksi = 6.89 MPa.

Figure 40. Graph. Test-to-predicted shear resistance for Simplified-PC/RC with no LWC modification (λ-factor = 1) compared to stirrup strength.

The test-to-prediction ratios in table 23 show that all three procedures gave conservative predictions (i.e., $V_{test}/V_n > 1$) for all of the tests failing in shear. The Simplified-PC/RC procedure had the smallest mean ratio for the type II girders and the largest mean ratio for the BT-54 girders. The mean ratios for GP-equation and GP-table were similar to each other for both girder sizes. The COV was between 4.4 and 9.5 percent for all three methods. The COV is an indication of how close the ratios are to the mean value, with a smaller COV value indicating that there is less scatter. The ratios for tests ending in a flexural failure are shown for informational purposes only. Table 23 also shows that the ratios for the both the GP-equation and the GP-table procedures are larger for the type II girders than the BT-54 girders. The opposite is shown for the Simplified-PC/RC procedure with the ratios for the BT-54 girders larger than the type II girders.

The ratios shown in figure 32 through figure 34 for the GP-equation procedure and in figure 35 through figure 37 for the GP-table procedure show similar trends. The main difference is the slight upward shift in the ratios for the GP-table procedure. The ratios shown in figure 38 through figure 40 for the Simplified-PC/RC procedure are comparable to those of either general procedure method. The most noticeable difference is the increase in test-to-prediction ratio given by the Simplified-PC/RC procedure for the BT-54 girders with compressive strengths near 12 ksi (82.7 MPa).

Analysis of Predicted Results Including Modification for LWC

The test-to-prediction ratios for the LWC girder tests that did not include modification for LWC were compared to the ratios that do include modification for LWC (see table 24). The modification for LWC is based on the inclusion of a λ-factor in the expressions for determining the nominal shear resistance. The proposed expressions that include the λ-factor are described in chapter 5 of this report. Table 24 includes test-to-prediction ratios determined using a λ-factor based on w_c given by equation 36 through equation 38 and based on splitting tensile strength given by equation 39.

The ratios in table 24 are for tests that ended in a shear failure. The LWC girder tests used high-strength SDC. The λ-factor based on w_c was slightly less than 1.0 for the LWC girder tests and resulted in test-to-prediction ratios slightly higher than the ratios with a λ-factor of 1.0. The high-strength concrete also had a relatively high splitting tensile strength, and the λ-factor based on f_{ct} was equal to 1.0, resulting in identical ratios to those without modification for LWC.

Table 24. Test-to-prediction ratio of shear resistance for design expressions with no modification for LWC, proposed expression for the λ-factor and modification for LWC based on splitting tensile strength.[3]

Modification for LWC and Girder Type*	Design Expression	Mean	COV (Percent)	Maximum	Minimum	Percent Test-to-Prediction Ratio	
						<1.0	<0.8
No modification for LWC; type II shear failure (4)	GP-equation	1.39	7.9	1.50	1.24	0.0	0.0
No modification for LWC; type II shear failure (4)	GP-table	1.41	7.3	1.52	1.28	0.0	0.0
No modification for LWC; type II shear failure (4)	Simplified-PC/RC	1.26	8.8	1.37	1.11	0.0	0.0
No modification for LWC; BT-54 shear failure (6)	GP-equation	1.18	4.4	1.25	1.11	0.0	0.0
No modification for LWC; BT-54 shear failure (6)	GP-table	1.23	4.9	1.31	1.17	0.0	0.0
No modification for LWC; BT-54 shear failure (6)	Simplified-PC/RC	1.36	9.5	1.53	1.18	0.0	0.0
Proposed λ-factor based on w_c; type II shear failure (4)	GP-equation	1.41	7.8	1.52	1.26	0.0	0.0
Proposed λ-factor based on w_c; type II shear failure (4)	GP-table	1.42	7.2	1.52	1.29	0.0	0.0
Proposed λ-factor based on w_c; type II shear failure (4)	Simplified-PC/RC	1.27	8.7	1.37	1.12	0.0	0.0
Proposed λ-factor based on w_c; BT-54 shear failure (6)	GP-equation	1.21	3.7	1.27	1.15	0.0	0.0
Proposed λ-factor based on w_c; BT-54 shear failure (6)	GP-table	1.25	4.8	1.33	1.19	0.0	0.0
Proposed λ-factor based on w_c; BT-54 shear failure (6)	Simplified-PC/RC	1.37	9.3	1.54	1.19	0.0	0.0
Proposed λ-factor based on f_{ct}; type II shear failure (4)	GP-equation	1.39	7.9	1.50	1.24	0.0	0.0

Modification for LWC and Girder Type*	Design Expression	Mean	COV (Percent)	Maximum	Minimum	Percent Test-to-Prediction Ratio	
						<1.0	<0.8
Proposed λ-factor based on f_{ct}; type II shear failure (4)	GP-table	1.41	7.3	1.52	1.28	0.0	0.0
Proposed λ-factor based on f_{ct}; type II shear failure (4)	Simplified-PC/RC	1.26	8.8	1.37	1.11	0.0	0.0
Proposed λ-factor based on f_{ct}; BT-54 shear failure (6)	GP-equation	1.18	4.4	1.25	1.11	0.0	0.0
Proposed λ-factor based on f_{ct}; BT-54 shear failure (6)	GP-table	1.23	4.9	1.31	1.17	0.0	0.0
Proposed λ-factor based on f_{ct}; BT-54 shear failure (6)	Simplified-PC/RC	1.36	9.5	1.53	1.18	0.0	0.0

*The number of specimens is shown in parentheses.

COMPARISON OF TEST RESULTS TO PREDICTED WEB-SHEAR CRACKING

The measured shear force at web-shear cracking and the web-shear crack inclination angle from the girder tests were compared to the shear force and angle predicted by the *AASHTO LRFD Bridge Design Specifications*.[3] The crack angles were measured directly using a crack protractor to determine the angle of the web cracks that crossed the midheight of the web. The measured crack angle values are given in table 19 and table 20.

The measured shear force at web cracking and inclination angle were compared to the predictions given by the GP-equation method, the GP-table method, and the Simplified-PC/RC procedure. The prediction of the shear force and inclination angle by GP-equation was taken as V_c and θ, respectively. For the purpose of predicting the shear force at web-shear cracking, the value of β was calculated assuming that there were no stirrups because web-shear cracking is essentially the limiting shear resistance for members without shear reinforcement. The value of β was determined using equation 22 with the factor s_x taken as the effective d_v according to Article 5.8.3.4.2 in the *AASHTO LRFD Bridge Design Specifications*.[3] The prediction by GP-table was also taken as V_c and θ for the shear force and inclination angle, and the value of β was calculated assuming that there were no stirrups. The shear force and inclination angle predicted by the Simplified-PC/RC procedure was taken as V_{cw} and θ determined from equation 35.

The test-to-prediction ratios for the shear force at web-shear cracking for the three procedures are given in table 25 with no modification for LWC (i.e., the λ-factor taken as 1). The ratios are grouped by girder type and failure type for comparison with the test-to-prediction ratios shown in previous tables. The ratios are also shown for all type II and all BT-54 girders. The table shows that the shear force at web-shear cracking for all of the LWC girder tests was conservatively predicted (i.e., test-to-prediction ratios greater than 1.0) by all three procedures.

Table 25. Test-to-prediction ratio of the shear force at web-shear cracking for design expressions with no modification for LWC.[3]

Girder Type and Failure Type*	Design Expression	Mean	COV (Percent)	Maximum	Minimum	Percent Test-to-Prediction Ratio	
						<1.0	<0.8
Type II shear failure (4)	GP-equation	2.62	11.7	2.92	2.32	0.0	0.0
Type II shear failure (4)	GP-table	2.17	6.9	2.31	2.02	0.0	0.0
Type II shear failure (4)	Simplified-PC/RC	1.37	7.6	1.51	1.26	0.0	0.0
Type II flexure failure (13)	GP-equation	2.29	17.5	2.96	1.81	0.0	0.0
Type II flexure failure (13)	GP-table	1.81	17.0	2.33	1.46	0.0	0.0
Type II flexure failure (13)	Simplified-PC/RC	1.34	8.0	1.46	1.07	0.0	0.0
BT-54 shear failure (6)	GP-equation	1.90	7.8	2.11	1.72	0.0	0.0
BT-54 shear failure (6)	GP-table	1.40	9.2	1.63	1.27	0.0	0.0
BT-54 shear failure (6)	Simplified-PC/RC	1.19	10.4	1.40	1.06	0.0	0.0
BT-54 flexure failure (6)	GP-equation	2.43	9.3	2.60	2.00	0.0	0.0
BT-54 flexure failure (6)	GP-table	1.84	10.1	1.98	1.47	0.0	0.0
BT-54 flexure failure (6)	Simplified-PC/RC	1.29	8.4	1.47	1.18	0.0	0.0
Type II (17)	GP-equation	2.37	16.8	2.96	1.81	0.0	0.0
Type II (17)	GP-table	1.90	16.6	2.33	1.46	0.0	0.0
Type II (17)	Simplified-PC/RC	1.35	7.7	1.51	1.07	0.0	0.0
BT-54 (12)	GP-equation	2.16	15.4	2.60	1.72	0.0	0.0
BT-54 (12)	GP-table	1.62	16.9	1.98	1.27	0.0	0.0
BT-54 (12)	Simplified-PC/RC	1.24	10.0	1.47	1.06	0.0	0.0

*The number of specimens is shown in parentheses.

Note: Test A7L failing in horizontal shear was included with type II flexural failures; however, shear force at web-shear cracking was not recorded for test A7L, and the test is not included in this table.

COV for the Simplified-PC/RC procedure was the lowest at 7.7 percent for the type II girders and 10 percent for the BT-54 girders. The variation in ratios was similar for both general procedure methods at a mean of 16.7 percent for the type II girders and 16.2 percent for the BT-54 girders. The Simplified-PC/RC procedure gave the lowest mean ratios at 1.35 for the type II girders and 1.24 for the BT-54 girders. The mean ratios given by the GP-equation procedure at 2.37 and 2.16 for the type II and BT-54 girders, respectively, were the highest.

All three procedures underestimated how much lower the shear force at web-shear cracking would be in the tests of the larger girders. The mean ratios for the BT-54 girders using the GP-equation, GP-table, and Simplified-PC/RC procedure were 21, 28, and 11 percent lower, respectively, than the mean ratios for the type II girders.

The test-to-prediction ratios for the angle of inclined web-shear cracking for the three procedures are given in table 26 with no modification for LWC (i.e., the λ-factor taken as 1). The ratios were grouped by girder type and failure type for comparison with the ratios shown in previous tables. The ratios are also shown for all type II girders and all BT-54 girders. A range of crack angles was measured along the girder web between the centerline of the support and a distance of two times the effective depth ($2d_v$) from the centerline of the support. The mean of the measured crack angles in each test was used to determine the test-to-prediction ratios for each test. The mean of test-to-prediction ratios for all of the girder tests was based on the average measured crack angle. The average measured crack angle was also the basis for the COV, maximum value, and minimum value of the ratios for all of the girder tests. The predicted values were also compared to the largest and smallest measured crack angles in the range of angles measured along the girder web. The percent of predicted crack angles less than the range of measured angles and the percent of predicted crack angles greater than the range of measured angles are shown in table 26.

Table 26. Test-to-prediction ratio of angle of inclination for web-shear cracks for design expressions with no modification for LWC.[3]

Girder Type and Failure Type[a]	Design Expression	Mean	COV (Percent)	Maximum	Minimum	Percent of Predicted Angles	
						Less than Minimum Range[b]	Greater than Maximum Range[c]
Type II shear failure (4)	GP-equation	1.13	12.3	1.26	0.96	50.0	0.0
Type II shear failure (4)	GP-table	0.92	13.0	1.06	0.79	0.0	25.0
Type II shear failure (4)	Simplified-PC/RC	1.12	12.9	1.26	0.94	50.0	0.0
Type II flexure failure (14)	GP-equation	1.11	11.9	1.29	0.81	50.0	7.1
Type II flexure failure (14)	GP-table	0.88	12.2	1.03	0.64	0.0	50.0
Type II flexure failure (14)	Simplified-PC/RC	1.10	11.7	1.26	0.80	35.7	7.1
BT-54 shear failure (5)	GP-equation	0.96	3.0	0.99	0.92	0.0	20.0
BT-54 shear failure (5)	GP-table	0.68	2.9	0.70	0.65	0.0	100.0
BT-54 shear failure (5)	Simplified-PC/RC	0.91	4.1	0.96	0.87	0.0	60.0
BT-54 flexure failure (6)	GP-equation	1.01	3.0	1.06	0.97	0.0	0.0
BT-54 flexure failure (6)	GP-table	0.74	2.7	0.77	0.72	0.0	100.0
BT-54 flexure failure (6)	Simplified-PC/RC	0.99	5.8	1.04	0.88	0.0	16.7
Type II (18)	GP-equation	1.11	11.6	1.29	0.81	50.0	5.6
Type II (18)	GP-table	0.89	12.1	1.06	0.64	0.0	44.4
Type II (18)	Simplified-PC/RC	1.10	11.6	1.26	0.80	38.9	5.6
BT-54 (11)	GP-equation	0.99	4.1	1.06	0.92	0.0	9.1
BT-54 (11)	GP-table	0.71	5.3	0.77	0.65	0.0	100.0
BT-54 (11)	Simplified-PC/RC	0.95	6.7	1.04	0.87	0.0	36.4

[a]The number of specimens is shown in parentheses.
[b]The percent of predicted angles is less than the minimum value of the range of measured web cracking angles.
[c]The percent of predicted angles is greater than the maximum value of the range of measured web cracking angles.
Note: Test A7L failing in horizontal shear is included with type II flexural failures; however, crack angles were not recorded for test A9D, and the test is not included in this table.

The web crack–inclination angles predicted by the three procedures were close to the measured values for many of the tests. A test-to-prediction ratio greater than 1.0 indicates that the predicted angle was smaller than the measured angle (i.e., the crack predicted to be closer to horizontal). A smaller predicted angle will result in an increase in the predicted contribution of the stirrups to the nominal shear resistance (larger V_s) and, for the GP-table procedure, a slight decrease in the predicted V_c (through the larger calculated ε_s).

The mean ratios closest to 1.0 were given by the Simplified-PC/RC procedure for the type II girders at 1.10 and by the GP-equation procedure for the BT-54 girders at 0.99. The GP-equation procedure had a mean ratio greater than 1.0 for the type II girders and underestimated the smallest measured inclination angle for 50 percent of the type II girder tests. An underestimation of the inclination angle will result in an increase in the predicted contribution of the stirrups to the nominal shear resistance (i.e., a larger V_s). The GP-table procedure predicted inclination angles greater than the range of measured angles for all of the BT-54 girders. The mean COV for the predictions was low for the type II girders at 11.8 percent and even lower for the BT-54 girders at 5.4 percent. All three procedures had lower mean ratios for the BT-54 girders than for the type II girders, indicating that the procedures predicted larger cracking angles than the measured angles for the larger-sized BT-54 girders.

SUMMARY OF EXPERIMENTAL RESULTS AND CONCLUDING REMARKS

The performance of 15 prestressed girders was evaluated in 30 tests to investigate the shear resistance of high-strength LWC. Key test parameters included the lightweight aggregate, the amount of shear reinforcement, the girder depth, and the use of straight or draped strands. Five girders designs were developed to evaluate the effect of the key parameters. The end of each girder had different amounts of shear reinforcement. Three different concrete-mixture designs using three different lightweight aggregates were used. The mix designs included two expanded shales and one expanded slate. The concrete mixtures used a blend of lightweight and normal-weight coarse aggregate and normal-weight sand. These mixes were prescriptively produced at the precaster's facility and used to produce the 15 prestressed girders. The design compressive strength ranged from 6 to 10 ksi (41 to 69 MPa), and the target unit weight ranged from 0.126 to 0.130 kcf (2,020 to 2,080 kg/m^3). The resulting concrete had a range in 28-day compressive strength of 8.6 to 9.7 ksi (59.3 to 66.9 MPa) and an air-dry density range of 0.125 to 0.132 kcf (2,000 to 2,110 kg/m^3).

The maximum applied shear force was compared to the shear resistance predicted by three design procedures in the *AASHTO LRFD Bridge Design Specifications*: the GP-equation method (see Article 5.8.3.4.1), the GP-table method (see appendix B5), and the Simplified-PC/RC method (see Article 5.8.3.4.2).[(3)] The measured shear force at web-shear cracking and the inclination angle of the web-shear cracks was also compared to the values predicted by the same three design procedures in the *AASHTO LRFD Bridge Design Specifications*.[(3)]

One girder test failed in horizontal shear through the concrete deck. Four of the remaining tests on the type II girders failed in shear, and 13 girders failed in flexure. Six of the tests on the BT-54 girders failed in shear, and the remaining six girders failed in flexure.

As expected, the average shear stress at failure increased as the amount of transverse reinforcement increased. The mean shear stress at failure for the type II girders was larger than for the BT-54 girders. The effect of reduced shear strength with increased girder depth was observed for three separate groups of tests. Each group of tests had similar percentages of longitudinal and transverse reinforcement. The mean test-day compressive strength was near 10 ksi (68.9 MPa) for all three girder mixes. No dependency on aggregate was observed in the average shear stress at failure.

All three design procedures in the *AASHTO LRFD Bridge Design Specifications* gave conservative predictions of shear resistance for the tests failing in shear.[3] The two general procedure methods gave less conservative predictions of shear resistance for the BT-54 girders than the type II girders. The opposite was observed with the Simplified-PC/RC procedure, which gave more conservative predictions of shear resistance for the BT-54 girders than the type II girders. All of these predictions were made without modification for LWC. The high splitting tensile strength of most of the girders did not require modification for LWC according to Article 5.8.2.2 of the *AASHTO LRFD Bridge Design Specifications*.[3]

The shear force at web-shear cracking was conservatively predicted by all three design procedures in the *AASHTO LRFD Bridge Design Specifications* for all of the tests.[3] The GP-equation procedure and the Simplified-PC/RC procedure gave the most conservative and least conservative predictions of web-shear cracking for both the type II and BT-54 girders, respectively. All three design procedures gave less conservative predictions of web-shear cracking for the BT-54 girders than for the type II girders.

On average, the three design procedures in the *AASHTO LRFD Bridge Design Specifications* tended to underestimate the web-shear-crack–inclination angle of the type II girders (i.e., the observed crack angle was greater than the predicted angle) and overestimate the web-shear crack inclination angle of the BT-54 girders (i.e., observed crack angle was less than the predicted angle).[3] An underestimation of the inclination angle results in an increase in the predicted contribution of the stirrups to the nominal shear resistance (i.e., a larger V_s).

CHAPTER 4. TFHRC SHEAR DATABASE

INTRODUCTION

This chapter describes the information available in the TFHRC shear database.[1] The type of information included in the database for each specimen is described. The number of each type of specimen and the types of concrete mixtures found for each specimen type is described. A large number of NWC specimens are available in a database collected by a joint ACI Committee 445 and Deutscher Ausschuss für Stahlbeton (i.e., the German Committee for Structural Concrete; DafStb).[44–47] The method used to select specimens from the ACI-DafStb database for comparison with LWC specimens in the TFHRC shear database is described.[44] This chapter also includes statistical information by concrete-mixture type and specimen type for the tests in the internal TFHRC shear database.

TFHRC SHEAR DATABASE SUMMARY

A thorough literature review was performed to find published journal papers, conference papers, technical reports, and university dissertations that included tests, analysis, or discussions of LWC. Over 500 references were found in the literature that mentioned LWC. These references were reviewed for data from tests on beam and girder specimens. Tests included in the database were limited to data from RC and PC beams that culminated in a shear failure. (For sources, see Bibliography section LWC Sources for TFHRC Shear Database.) The details of the specimens in each reference are described in the following section. Only test data from published reports were included in the database.

There were 40 references with shear tests on LWC specimens that resulted in a shear failure. Table 27 shows the number of references per specimen type. The specimen types include tests on RC beams with and without shear reinforcement (i.e., specimens with and without A_v) and PC beams with and without shear reinforcement. The tests on beams and girders with shear reinforcement included specimens that did not meet the requirements for minimum shear reinforcement in Article 5.8.2.5 or the requirements for maximum spacing of shear reinforcement in Article 5.8.2.7 of the *AASHTO LRFD Bridge Design Specifications*.[3]

Table 27 shows that the tests for each specimen type came from several different references. While some references had many more shear tests than other references, the mean number of tests from a reference was greater than or equal to five. This indicates that the test results from one reference are not likely to improperly bias the analysis of the test data.

[1]The TFHRC shear database is not publicly available. For a list of available sources, see Bibliography section LWC Sources for TFHRC Shear Database.

Table 27. Summary of the source information for tests on LWC in the TFHRC shear database by specimen type.

Specimen Type	Total Number of Sources	Source*	Number of Tests per Source		
			Maximum	Minimum	Mean
RC without A_v	26	Ahmad, Xie, and Yu (1994); Alrousan et al. (2011); Clarke (1987); Funahashi et al. (2002), Hamadi and Regan (1980a); Hanson (1958), Hanson (1961), Hoff (1993); Ivey and Buth (1967); Jindal (1966); Kang et al. (2011); Kawaguchi et al. (2000); Murayama and Iwabuchi (1986); Nishibayashi, Kobayashi, and Yoshioka (1968); Richart and Jensen (1930); Ritthichauy et al. (2001); Salandra and Ahmad (1989); Swamy and Bandyopadhyay (1979); Swamy and Lambert (1983); Swamy, Jones, and Chiam (1993); Tang, Yen, and Chen (2009); Taylor and Brewer (1963); Thorenfeldt and Drangsholt (1990); Thorenfeldt and Stemland (1995); Thorenfeldt and Stemland (2000); and Yang et al. (2011)	27	3	11.8
RC with A_v	11	Ahmad, Xie, and Yu (1994); Clarke (1987); Hamadi and Regan (1980b); Kawaguchi et al. (2000); Nishibayashi, Kobayashi, and Yoshioka (1968); Ramirez et al. (2000); Richart and Jensen (1930); Salandra and Ahmad (1989); Thorenfeldt, Stemland, and Tomaszewicz (1995); Walraven and Al-Zubi (1995); and Watanabe et al. (2003)	15	2	6.4
PC without A_v	6	Brettle (1962); EuroLightCon (2000); Holste, Peterman, and Esmaeily (2011); Nishibayashi, Kobayashi, and Yoshioka (1968); Peterman, Ramirez, and Okel (1999); and Ramirez et al. (2000)	12	1	5.0
PC with A_v	7	Dymond, Roberts-Wollmann, and Cousins (2009); Greene and Graybeal (2015); Hegger et al. (2005) ; Kassner (2012); Meyer et al. (2002) ; Ramirez et al. (2000); and Watanabe et al. (2003)	14	1	5.9

*Source information can be found in the LWC Sources for TFHRC Shear Database section in the Bibliography.

The information collected for each test included its concrete mixture, associated concrete mechanical property tests, test specimen dimensions, and test results. The recorded concrete mechanical tests included compressive strength, modulus of elasticity, splitting tensile test, modulus of rupture, and Poisson's ratio. Up to two measures of concrete density were also recorded. Concrete-mixture information was recorded, including the type of coarse and fine aggregate, the use of chemical admixtures, and the use of supplementary cementitious materials. Information about the mechanical tests was recorded, including the specimen size, duration and type of curing, and specimen age.

Measured concrete and steel material properties were used when reported. When material properties were not reported, nominal values were used as appropriate (e.g., reinforcement yield strength) and predictions using expressions in the *AASHTO LRFD Bridge Design Specifications* were used as appropriate (e.g., for concrete modulus of elasticity).[3] The effective prestress was calculated using the approximate estimate of time-dependent losses in Article 5.9.5.3.

In addition to data from tests on LWC, a select number of tests on NWC were also included in the database for comparison. The ACI-DafStb database has data from 928 specimens. (For sources, see Bibliography section NWC Sources for ACI-DafStb Database.) A subset of the ACI-DafStb database was selected for comparison to the LWC specimens and included in the TFHRC shear database. The criteria used to select the NWC specimen from the ACI-DafStb database is described later in this chapter. A list of references for the tests of LWC in the TFHRC shear database and the selected NWC specimens in the ACI-DafStb Database is included in the Bibliography section.

Test Specimens

This section describes the types of specimens included in the TFHRC shear database and the type of information collected for each specimen type. The data were limited to specimens that were determined to have failed in shear. If a failure mode was recorded in the literature, only specimens indicated as having failed in shear without bond failure were included. The moment caused by the ultimate force applied to the specimen was also compared to the nominal moment capacity determined using the *AASHTO LRFD Bridge Design Specifications* (see equation 9).[3] If the ultimate applied moment was larger than the moment capacity, the failure was considered to be potentially affected by a large longitudinal strain, and the specimen was excluded from the database.

Table 28 provides a summary of the number of tests for each concrete-mixture type relevant to each specimen type in the TFHRC database. The definitions of different types of LWC mixtures have been traditionally based on the use of lightweight or normal-weight constituent materials. The types of concrete mixtures used in the database included all-lightweight, sand-lightweight, specified density, and inverted mix. All-lightweight is defined as concrete with lightweight fine and coarse aggregate, while sand-lightweight is defined as concrete with lightweight coarse aggregate and either sand or a mixture of sand and lightweight fine aggregate. SDC is defined as concrete with a mixture of normal-weight and lightweight coarse aggregate and either sand or lightweight fine aggregate. An inverted mix has normal-weight coarse aggregate and lightweight fine aggregate. The tests indicated as "ACI-DafStb" are the selected tests from the ACI-DafStb database. These four databases, two for RC beams with and without shear reinforcement and two

for PC beams with and without shear reinforcement, are referred to in this report as the ACI-DafStb database. (For sources, see Bibliography section NWC Sources for ACI-DafStb Database.)

Table 28. Number of tests in the TFHRC shear database by specimen type and concrete mixture.

Specimen Type	Number of LWC Tests					Number of NWC ACI-DafStb Tests
	All-Lightweight	Sand-Lightweight	Specified Density	Inverted Mix	Total	
RC without A_v	151	156	0	0	307	648
RC with A_v	12	57	0	1	70	107
PC without A_v	14	9	7	0	30	100
PC with A_v	12	17	11	1	41	31
Total	189	239	18	2	448	886

A summary of the number of LWC tests in the TFHRC shear database is shown in table 29 by cross-sectional shape and presence of a cast-in-place (CIP) deck. The cross-sectional shapes in the database are rectangular, T-beams, and I-beams. The CIP decks were either LWC or NWC. A total of 81 percent of the RC specimens had a rectangular cross section, and none of the RC specimens had a CIP deck. Only 37 percent of the PC specimens had a rectangular cross section, and 35 percent had an LWC or NWC deck.

Table 29. Number of tests on LWC in the TFHRC shear database by specimen type, cross section, and CIP deck.

Specimen Type	Total LWC*	Cross-Section Shape			CIP Deck		
		Rectangular	T-Beam	I-Beam	No Deck	LWC Deck	NWC Deck
RC without A_v	307	255	43	9	307	0	0
RC with A_v	70	51	5	14	70	0	0
PC without A_v	30	22	0	8	28	0	2
PC with A_v	41	4	0	37	18	7	16
Total	448	332	48	68	423	7	18

*Total LWC specimens includes all-lightweight, sand-lightweight, specified density, and inverted mix.

The tests performed as part of the research program at TFHRC on LWC as described previously in this report are included in the TFHRC shear database. The tests were PC specimens with an area of the shear reinforcement within the spacing (A_v), using SDC with an I-shaped cross section and an LWC deck.

Distribution of Statistical Parameters for Specimens in the TFHRC Shear Database

A series of tables and figures were created to give statistical information for the parameters that influence shear resistance for the specimens in the TFHRC shear database. The statistical information is given by type of concrete mixture and then given again by type of specimen.

The information for RC specimens and PC specimens is shown by concrete mixture in table 30 and table 31, respectively. Table 32 provides the information for all RC and PC specimens.

The statistical information in the tables includes the mean value and range of values (i.e., maximum and minimum values) for concrete material properties, specimen geometry parameters, and maximum shear stress values. The concrete material properties include the compressive strength (f'_c), splitting tensile strength (f_{ct}), and unit weight (w_c). The specimen geometry parameters include the effective depth for shear (d_v), the ratio of the shear span (a) to effective shear depth (d_v), the nonprestressed longitudinal reinforcement ratio (ρ_ℓ or also referred to as A_s/bd_s) for RC specimens or the prestressed longitudinal reinforcement ratio (ρ_p or also referred to as $A_v/b_v s$) for PC specimens, and the stirrup strength ($\rho_v f_{yt}$). The average shear stress (v_u) and the ratio of v_u to f'_c are also given.

Table 30. Distribution of properties for RC specimens failing in the shear in TFHRC shear database.

Concrete-Mixture Type*	Property	Without Stirrups			With Stirrups		
		Mean	Maximum	Minimum	Mean	Maximum	Minimum
All-lightweight	f'_c (ksi)	4.53	8.16	1.79	4.35	9.54	2.93
All-lightweight	f_{ct} (ksi)	0.344	0.452	0.246	0.146	0.296	0.215
All-lightweight	w_c (kcf)	0.099	0.113	0.074	0.091	0.107	0.074
All-lightweight	d_v (inches)	8.73	17.15	4.15	13.82	29.14	5.75
All-lightweight	a/d_v	3.94	7.37	1.67	3.57	4.60	2.36
All-lightweight	v_u (ksi)	0.262	1.162	0.067	0.580	1.781	0.247
All-lightweight	v_u/f'_c	0.059	0.209	0.019	0.136	0.309	0.035
All-lightweight	ρ_ℓ (percent)	1.94	5.02	0.60	1.31	2.37	0.72
All-lightweight	$\rho_v f_{yt}$ (ksi)	—	—	—	0.415	1.470	0.066
Sand-lightweight	f'_c (ksi)	6.14	12.93	2.42	6.65	12.95	2.71
Sand-lightweight	f_{ct} (ksi)	0.203	0.571	0.239	0.245	0.571	0.234
Sand-lightweight	w_c (kcf)	0.095	0.133	0.086	0.117	0.131	0.086
Sand-lightweight	d_v (inches)	8.00	35.43	5.22	12.50	26.91	5.68
Sand-lightweight	a/d_v	3.41	7.46	1.11	2.88	4.64	1.15
Sand-lightweight	v_u (ksi)	0.367	1.492	0.083	0.645	1.953	0.098
Sand-lightweight	v_u/f'_c	0.064	0.257	0.013	0.114	0.298	0.009
Sand-lightweight	ρ_ℓ (percent)	1.96	4.18	0.29	2.09	4.52	0.65
Sand-lightweight	$\rho_v f_{yt}$ (ksi)	—	—	—	0.397	2.187	0.046
Inverted mix	f'_c (ksi)	—	—	—	9.06	9.06	9.06
Inverted mix	f_{ct} (ksi)	—	—	—	0.463	0.463	0.463
Inverted mix	w_c (kcf)	—	—	—	0.131	0.131	0.131
Inverted mix	d_v (inches)	—	—	—	19.16	19.16	19.16
Inverted mix	a/d_v	—	—	—	3.39	3.39	3.39
Inverted mix	v_u (ksi)	—	—	—	0.395	0.395	0.395
Inverted mix	v_u/f'_c	—	—	—	0.044	0.044	0.044
Inverted mix	ρ_ℓ (percent)	—	—	—	0.76	0.76	0.76
Inverted mix	$\rho_v f_{yt}$ (ksi)	—	—	—	0.066	0.066	0.066

1 inch = 25.4 mm.

1 ksi = 6.89 MPa.

1 kcf = 16,020 kg/m^3.

—There were no specimens for this concrete type or property.

*For all-lightweight concrete, there were 163 specimens total—151 without A_v and 12 with A_v. For sand-lightweight concrete, there were 213 specimens total—156 without A_v and 57 with A_v. For inverted mix, there was one specimen with A_v.

Table 31. Distribution of properties for PC specimens in the TFHRC shear database.

Concrete-Mixture Type	Property	Without Stirrups			With Stirrups		
		Mean	Maximum	Minimum	Mean	Maximum	Minimum
All-lightweight	f'_c (ksi)	5.58	6.68	4.80	7.64	9.43	5.99
All-lightweight	f_{ct} (ksi)	0.061	0.448	0.411	0.411	0.521	0.283
All-lightweight	w_c (kcf)	0.104	0.105	0.098	0.108	0.118	0.102
All-lightweight	d_v (inches)	4.72	9.87	2.78	16.83	19.09	16.23
All-lightweight	a/d_v	3.58	5.40	1.93	3.57	3.64	3.40
All-lightweight	v_u (ksi)	0.815	1.678	0.494	1.235	2.850	0.498
All-lightweight	v_u/f'_c	0.148	0.292	0.080	0.163	0.327	0.053
All-lightweight	ρ_p (percent)	1.41	1.95	1.00	0.29	0.76	0.19
All-lightweight	$\rho_v f_{yt}$ (ksi)	—	—	—	0.645	2.213	0.066
Sand-lightweight	f'_c (ksi)	8.78	10.09	4.74	10.07	13.10	6.50
Sand-lightweight	f_{ct} (ksi)	0.755	0.982	0.464	0.518	0.796	0.399
Sand-lightweight	w_c (kcf)	0.120	0.127	0.106	0.122	0.129	0.106
Sand-lightweight	d_v (inches)	9.93	23.28	5.67	31.27	52.54	16.37
Sand-lightweight	a/d_v	3.63	6.33	2.78	2.96	4.16	1.48
Sand-lightweight	v_u (ksi)	0.839	1.070	0.153	1.551	3.296	0.506
Sand-lightweight	v_u/f'_c	0.092	0.113	0.032	0.153	0.285	0.058
Sand-lightweight	ρ_p (percent)	0.33	0.42	0.14	0.23	0.76	0.10
Sand-lightweight	$\rho_v f_{yt}$ (ksi)	—	—	—	0.516	2.321	0.066
Specified density	f'_c (ksi)	9.72	12.06	7.96	10.71	11.90	9.20
Specified density	f_{ct} (ksi)	—	—	—	0.765	0.820	0.720
Specified density	w_c (kcf)	0.137	0.138	0.137	0.127	0.131	0.122
Specified density	d_v (inches)	9.00	9.00	9.00	40.83	48.60	31.75
Specified density	a/d_v	8.74	9.49	8.18	3.00	3.29	2.65
Specified density	v_u (ksi)	0.100	0.110	0.093	1.424	2.174	0.836
Specified density	v_u/f'_c	0.011	0.012	0.009	0.137	0.210	0.072
Specified density	ρ_p (percent)	0.23	0.27	0.21	0.16	0.21	0.12
Specified density	$\rho_v f_{yt}$ (ksi)	—	—	—	0.322	0.596	0.118
Inverted mix	f'_c (ksi)	—	—	—	8.88	8.88	8.88
Inverted mix	f_{ct} (ksi)	—	—	—	0.496	0.496	0.496

Concrete-Mixture Type	Property	Without Stirrups			With Stirrups		
		Mean	Maximum	Minimum	Mean	Maximum	Minimum
Inverted mix	w_c (kcf)	—	—	—	0.131	0.131	0.131
Inverted mix	d_v (inches)	—	—	—	18.95	18.95	18.95
Inverted mix	a/d_v	—	—	—	3.43	3.43	3.43
Inverted mix	v_u (ksi)	—	—	—	0.507	0.507	0.507
Inverted mix	v_u/f'_c	—	—	—	0.057	0.057	0.057
Inverted mix	ρ_p (percent)	—	—	—	0.76	0.76	0.76
Inverted mix	$\rho_v f_{yt}$ (ksi)	—	—	—	0.066	0.066	0.066

1 inch = 25.4 mm.
1 ksi = 6.89 MPa.
1 kcf = 16,020 kg/m^3.
—There were no specimens for this concrete type or property.
*For all-lightweight concrete, there were 26 specimens total—14 without A_v and 12 with A_v. For sand-lightweight concrete, there were 26 specimens total—9 without A_v and 17 with A_v. For specified density, there were 18 specimens total—7 without A_v and 11 with A_v. For inverted mix, there was one specimen with A_v.

Table 32. Distribution of properties for all specimens in the TFHRC shear database.

Reinforcement Type*	Property	Without Stirrups			With Stirrups		
		Mean	Maximum	Minimum	Mean	Maximum	Minimum
RC	f'_c (ksi)	5.35	12.93	1.79	6.29	12.95	2.71
RC	f_{ct} (ksi)	0.375	0.571	0.239	0.368	0.571	0.215
RC	w_c (kcf)	0.107	0.133	0.074	0.113	0.131	0.074
RC	d_v (inches)	8.36	35.43	4.15	12.82	29.14	5.68
RC	a/d_v	3.67	7.46	1.11	3.01	4.64	1.15
RC	v_u (ksi)	0.315	1.492	0.067	0.630	1.953	0.098
RC	v_u/f'_c	0.062	0.257	0.013	0.117	0.309	0.009
RC	ρ_ℓ (percent)	1.95	5.02	0.29	1.94	4.52	0.65
RC	$\rho_v f_{yt}$ (ksi)	—	—	—	0.395	2.187	0.046
PC	f'_c (ksi)	7.51	12.06	4.74	9.50	13.10	5.99
PC	f_{ct} (ksi)	0.765	0.982	0.411	0.596	0.820	0.283
PC	w_c (kcf)	0.117	0.138	0.098	0.119	0.131	0.102
PC	d_v (inches)	7.28	23.28	2.78	29.31	52.54	16.23
PC	a/d_v	4.80	9.49	1.93	3.16	4.16	1.48
PC	v_u (ksi)	0.655	1.678	0.093	1.399	3.296	0.498
PC	v_u/f'_c	0.099	0.292	0.009	0.149	0.327	0.053
PC	ρ_p (percent)	0.81	1.95	0.14	0.24	0.76	0.10
PC	$\rho_t f_{yt}$ (ksi)	—	—	—	0.491	2.321	0.066

1 inch = 25.4 mm.
1 ksi = 6.89 MPa.
1 kcf = 16,020 kg/m^3.
—There were no specimens for this property.
*For RC, there were 377 specimens total—307 without A_v and 70 with A_v. For PC, there were 71 specimens total—30 without A_v and 41 with A_v.

Figure 41 through figure 50 show the statistical information graphically. Figure 41 and figure 42 show v_u compared to f'_c by concrete-mixture type and specimen type, respectively. Figure 43 through figure 50 are in pairs to show the data by concrete-mixture type and specimen type and give v_u compared to w_c, f_{ct}, d_v, and a/d_v.

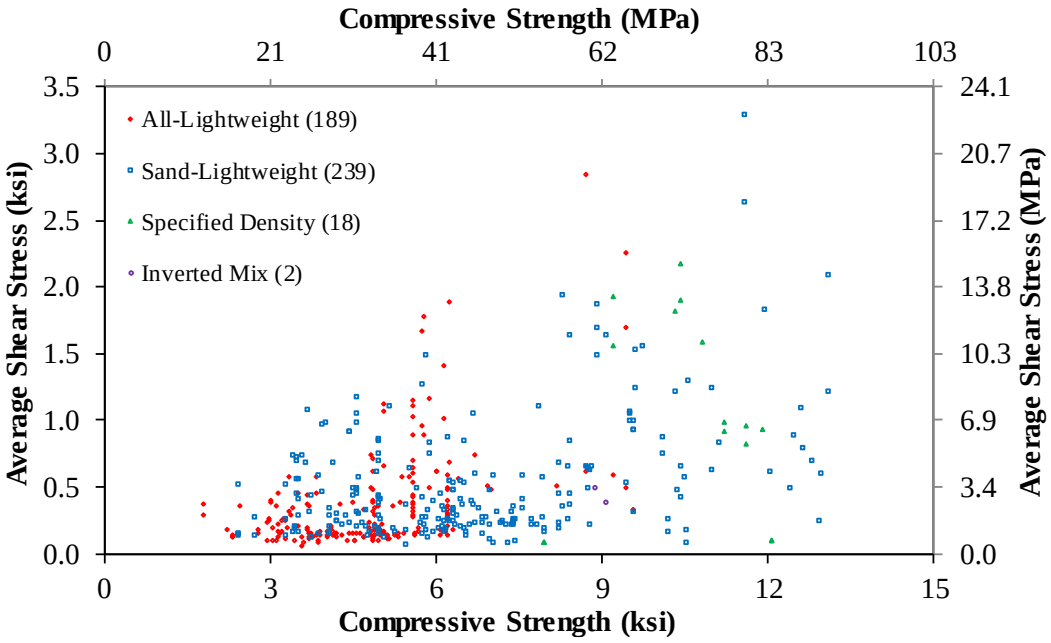

Source: FHWA.
1 ksi = 6.89 MPa.

Figure 41. Graph. Average shear stress compared to compressive strength by concrete-mixture type in the TFHRC shear database.

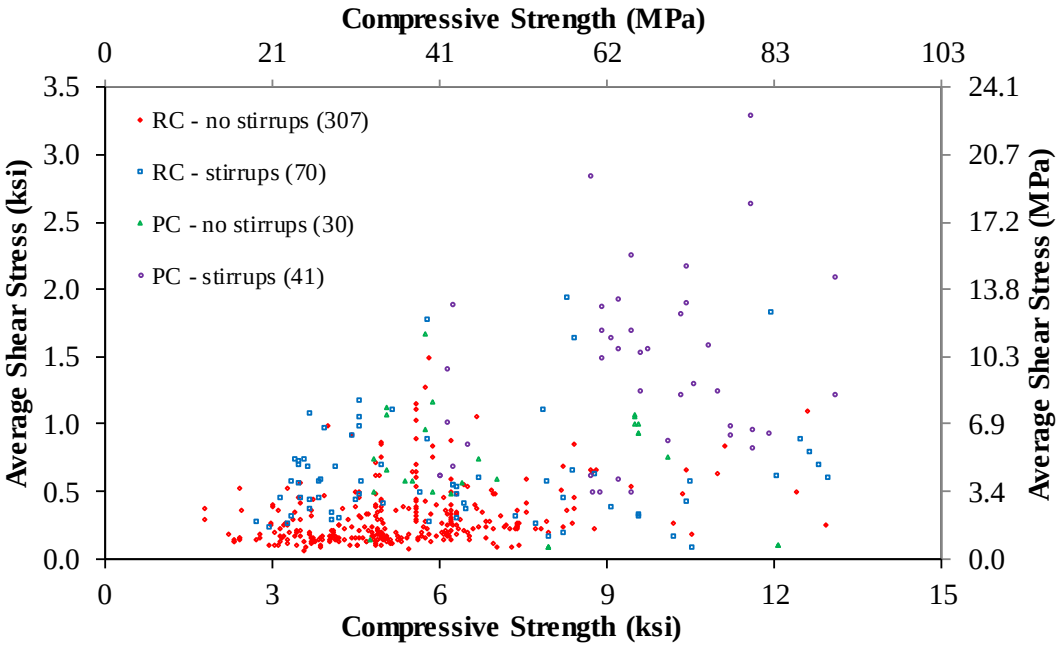

Source: FHWA.
1 ksi = 6.89 MPa.

Figure 42. Graph. Average shear stress compared to compressive strength by specimen type in the TFHRC shear database.

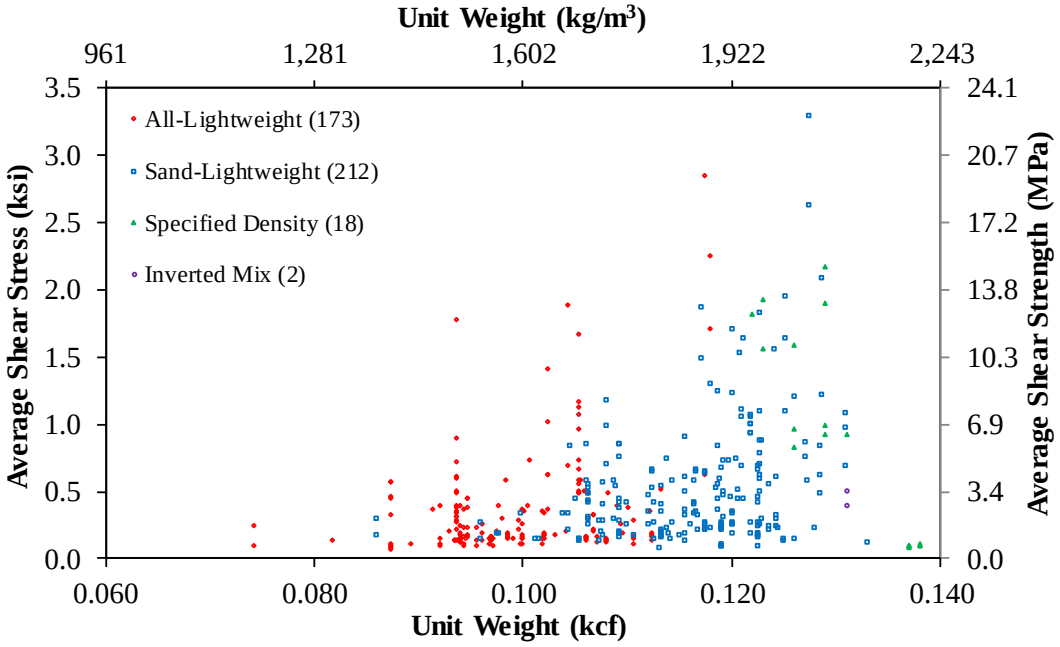

Source: FHWA.
1 ksi = 6.89 MPa.
1 kcf = 16,020 kg/m^3.

Figure 43. Graph. Average shear stress compared to unit weight by concrete-mixture type in the TFHRC shear database.

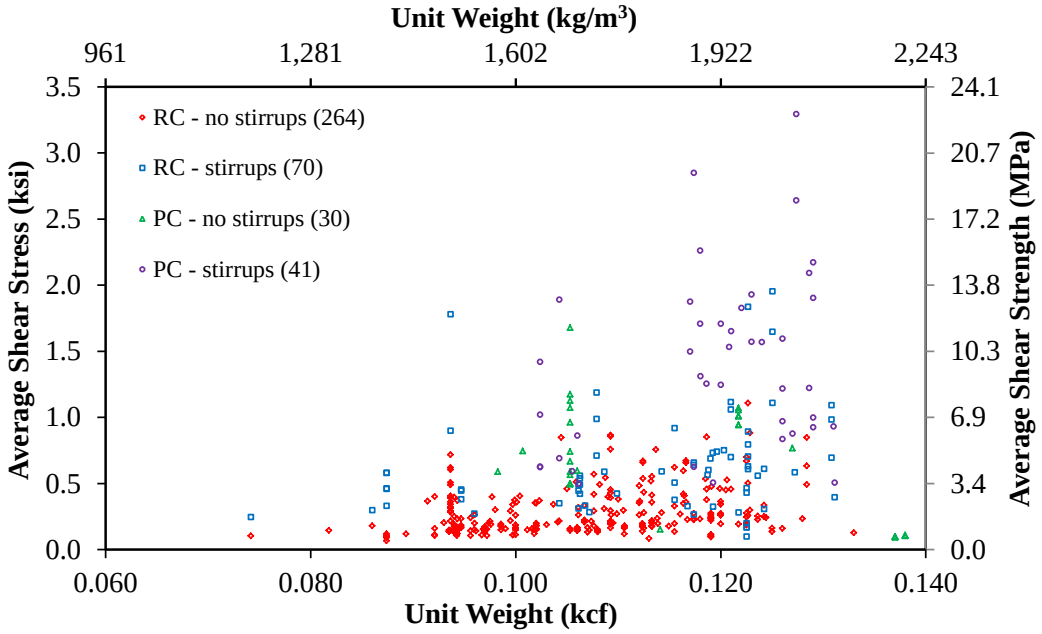

Source: FHWA.
1 ksi = 6.89 MPa.
1 kcf = 16,020 kg/m^3.

Figure 44. Graph. Average shear stress compared to unit weight by specimen type in the TFHRC shear database.

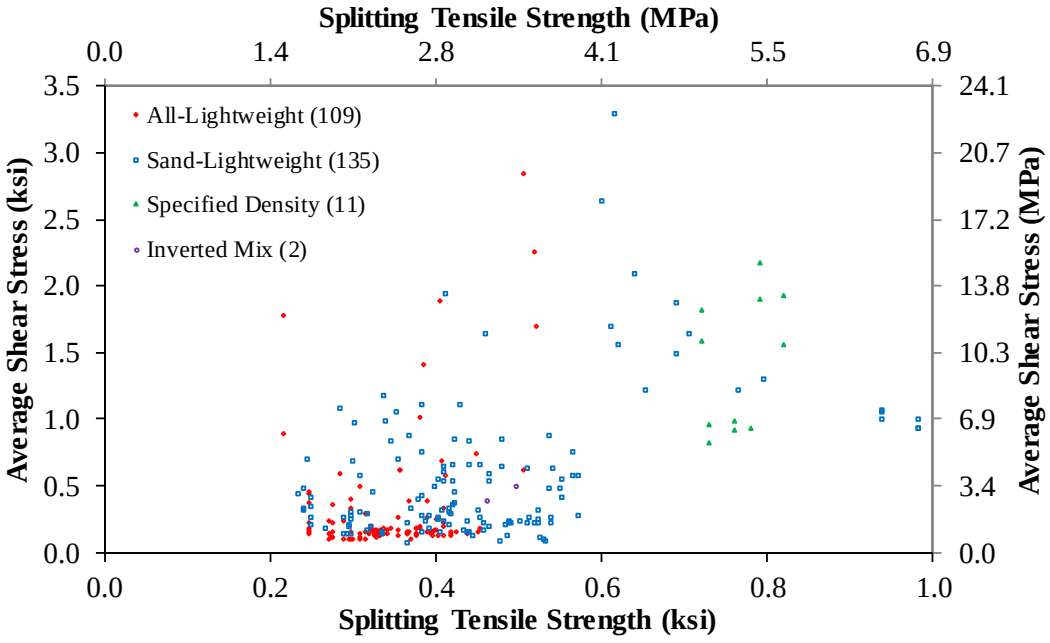

Source: FHWA.
1 ksi = 6.89 MPa.

Figure 45. Graph. Average shear stress compared to splitting tensile strength by concrete-mixture type in the TFHRC shear database.

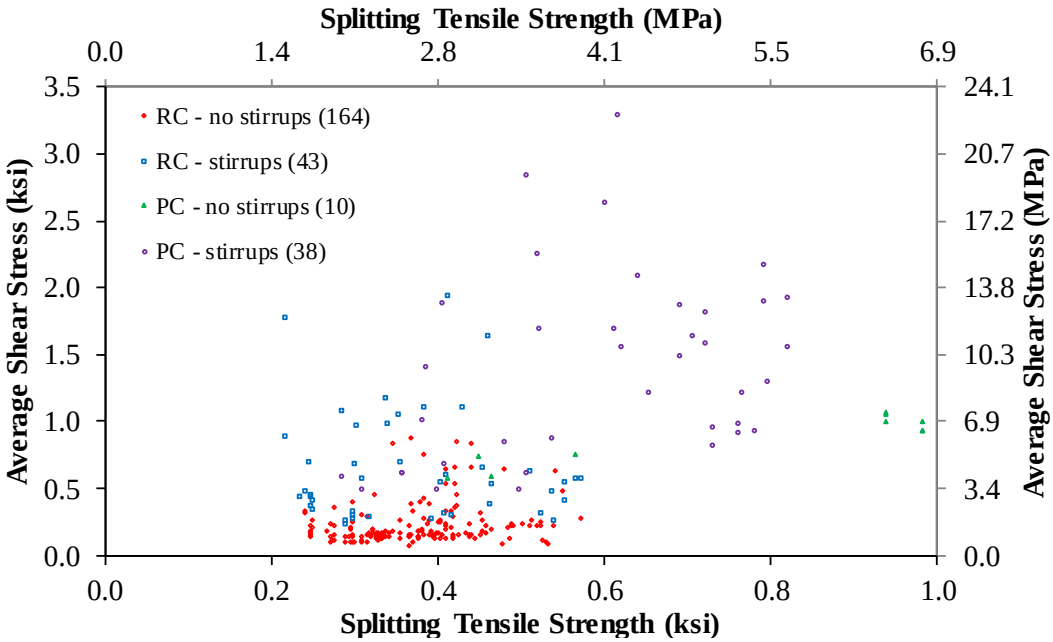

Source: FHWA.
1 ksi = 6.89 MPa.

Figure 46. Graph. Average shear stress compared to splitting tensile strength by specimen type in the TFHRC shear database.

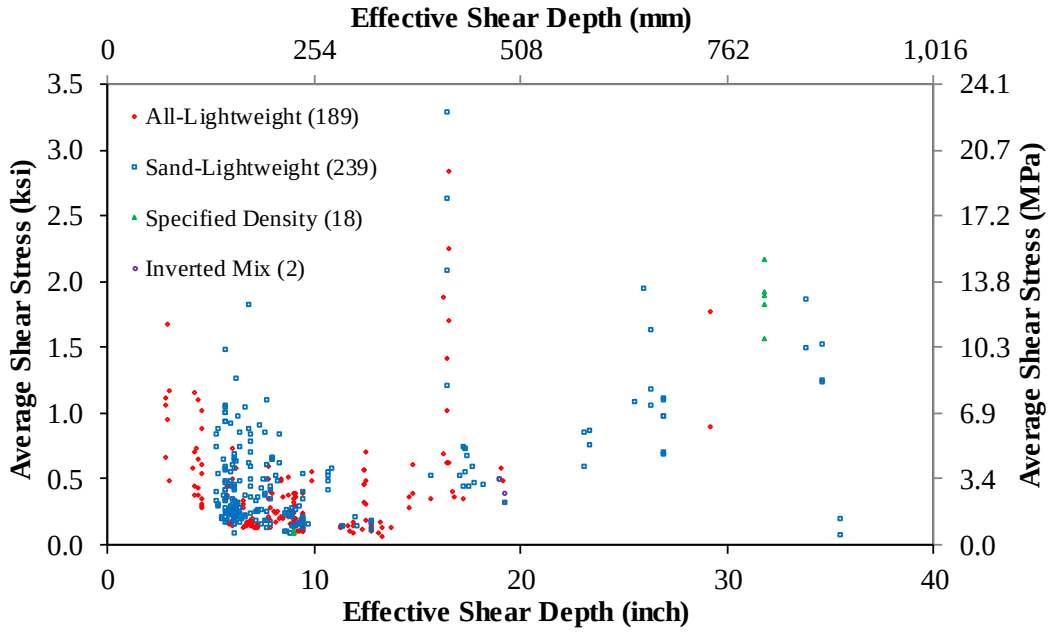

Source: FHWA.
1 ksi = 6.89 MPa.
1 inch = 25.4 mm.

Figure 47. Graph. Average shear stress compared to effective shear depth by concrete-mixture type in the TFHRC shear database.

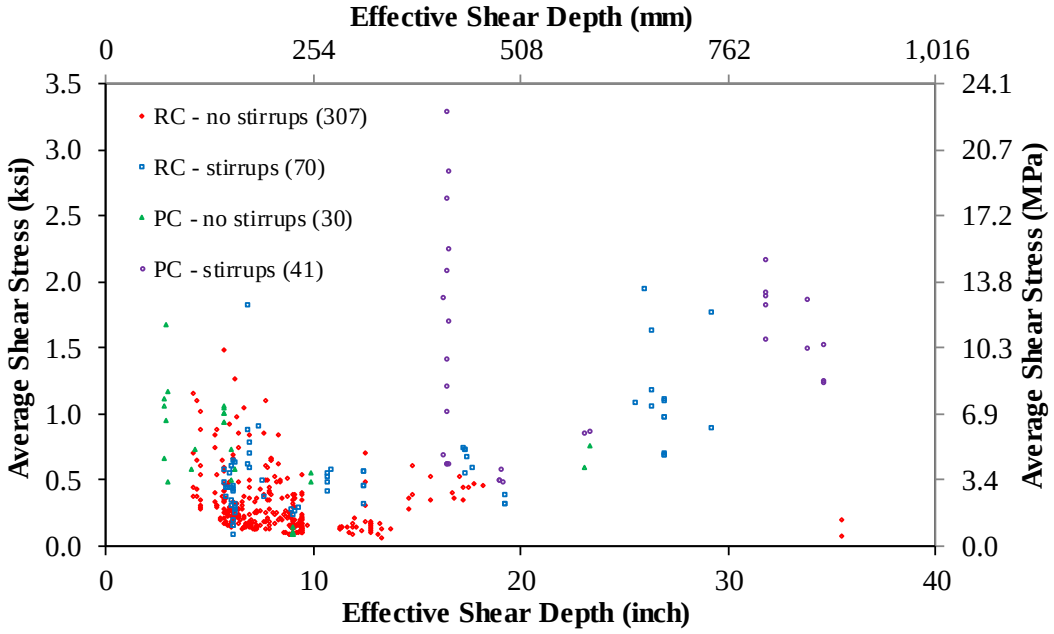

Source: FHWA.
1 ksi = 6.89 MPa.
1 inch = 25.4 mm.

Figure 48. Graph. Average shear stress compared to effective shear depth by specimen type in the TFHRC shear database.

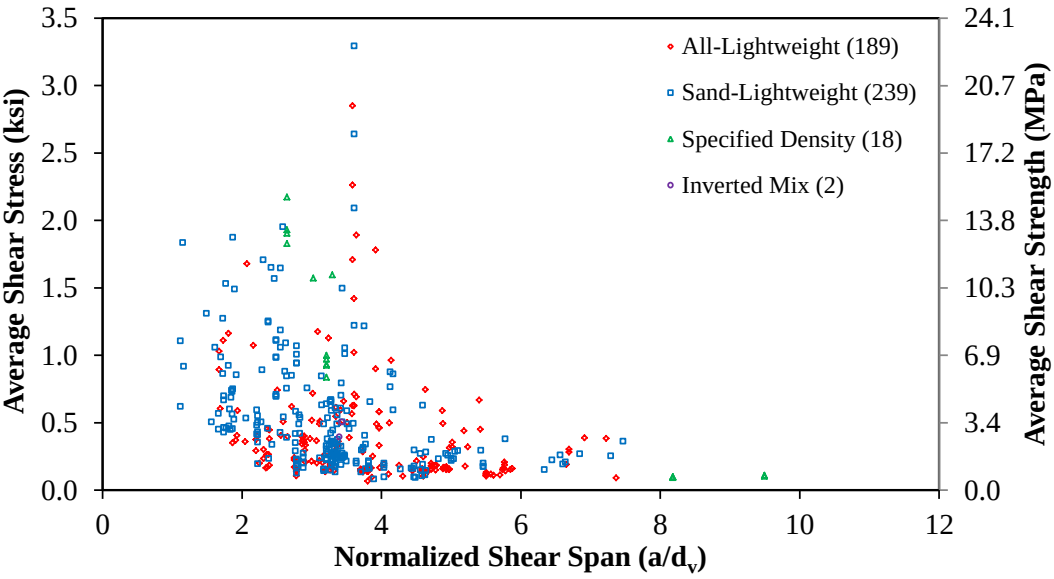

Source: FHWA.
1 ksi = 6.89 MPa.

Figure 49. Graph. Average shear stress compared to normalized shear span by concrete-mixture type in the TFHRC shear database.

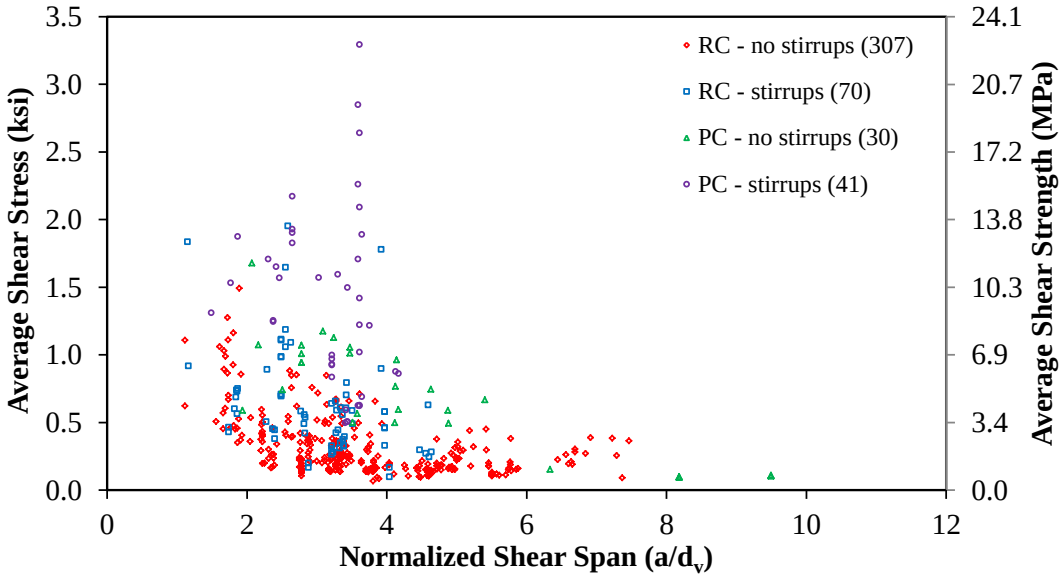

Source: FHWA.
1 ksi = 6.89 MPa.

Figure 50. Graph. Average shear stress compared to normalized shear span by specimen type in the TFHRC shear database.

Selection of Specimens for Comparison from the ACI-DafStb Database

The effect that lightweight aggregate has on shear resistance was evaluated by comparing LWC specimens to NWC specimens. ACI Committee 445 on shear and torsion and DafStb have collected a large number of NWC shear tests in four databases. (For sources, see Bibliography section NWC Sources for ACI-DafStb Database.) In order to determine the effect of LWC on shear resistance, the LWC specimens in the TFHRC shear database were compared to a subset of NWC specimens in the ACI-DafStb database that have similar parameters that are significant to shear resistance.

As shown in table 33, the 928 NWC specimens in the ACI-DafStb database had larger values for the two selected parameters of concrete compressive strength and specimen depth. The table gives the number of specimens in the ACI-DafStb database that exceed the maximum value for the parameter of the tests in the LWC database. The number of NWC prestressed specimens was limited to those that used pretensioning, and no post-tensioned specimens were included in the specimens selected from the ACI-DafStb database.

Table 33. Properties of shear specimens in the ACI-DafStb database and the number of specimens in the ACI-DafStb database within the property limits of the TFHRC shear database.

Dataset[a]	Specimen Type	Number Tests and Number within Limits	Limit	f'_c (ksi)	Member Height (h) (Inches)
ACI-DafStb	RC without A_v	684	Maximum	19.2	86.6
ACI-DafStb	RC with A_v	111	Maximum	17.3	49.2
ACI-DafStb	PC without A_v	100	Maximum	10.8	18.0
ACI-DafStb	PC with A_v	33	Maximum	14.1	54.0
TFHRC	RC without A_v	648	Maximum	13.0	42.0
TFHRC	RC without A_v	648	Number > Maximum[b]	21.0	15.0
TFHRC	RC with A_v	107	Maximum	13.0	42.0
TFHRC	RC with A_v	107	Number > Maximum[b]	3.0	1.0
TFHRC	PC without A_v	100	Maximum	13.0	62.0
TFHRC	PC without A_v	100	Number > Maximum[b]	0.0	0.0
TFHRC	PC with A_v	31	Maximum	13.0	62.0
TFHRC	PC with A_v	31	Number < Maximum[c]	2.0	0.0

1 inch = 25.4 mm.
1 ksi = 6.89 MPa.
[a]For ACI-DafStb, there were 928 specimens total that were all within the maximum limits of both parameters for the LWC datasets—784 without A_v and 144 with A_v. For TFHRC, there were 866 specimens total within limits—748 without A_v and 138 with A_v.
[b]The number of specimens in ACI-DafStb database were greater than the maximum parameter of the LWC dataset.
[c]The number of specimens in ACI-DafStb database were less than the number of specimens within limits of both parameters for the LWC datasets.

An NWC specimen in the ACI-DafStb database was assumed to be similar to the LWC specimens in the TFHRC shear database if both parameters (i.e., f'_c and h) were less than the maximum value of the parameters in the LWC database. One set of maximum values for the parameters were determined for the RC specimens, and another set of maximum values was determined for the PC specimens in the TFHRC shear database. There were 886 specimens from the ACI-DafStb database that were less than the maximum value of both parameters. In chapters 5–7 of this report, the specimens referred to as "NWC specimens" are the selected 886 NWC specimens from the ACI-DafStb database. (For sources, see Bibliography section NWC Sources for ACI-DafStb Database.)

Figures were created to show statistical information for three parameters that influence shear resistance for the selected NWC specimens from the ACI-DafStb database. Figure 51 through figure 53 show v_u compared to f'_c, d_v, and a/d_v, respectively.

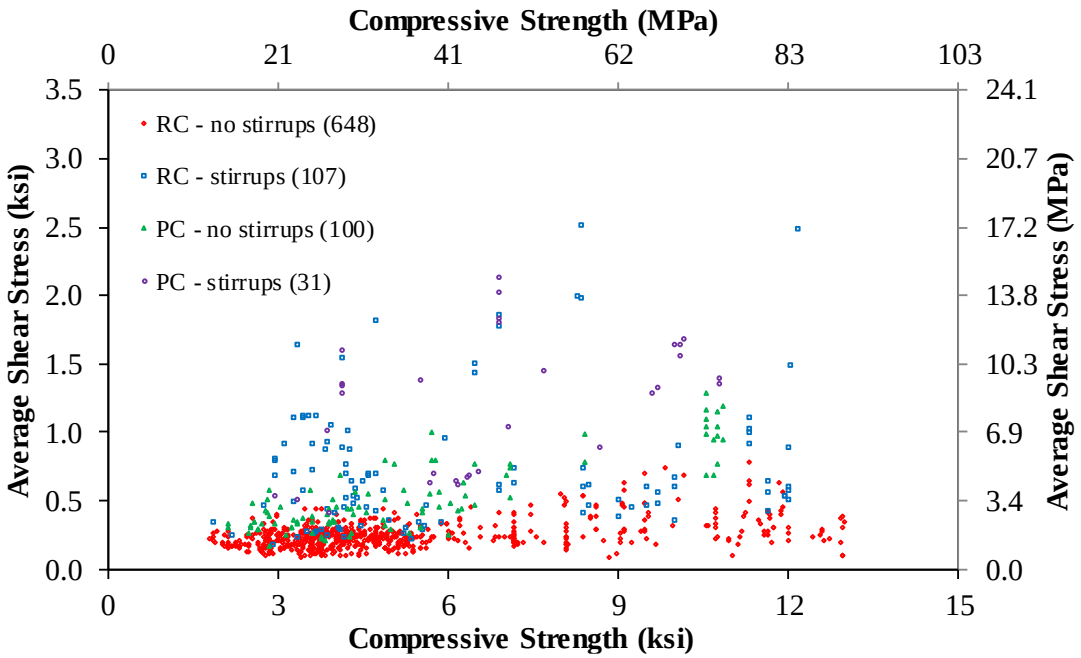

Source: FHWA.
1 ksi = 6.89 MPa.

Figure 51. Graph. Average shear stress compared to compressive strength by specimen type for the selected NWC specimens from the ACI-DafStb database.

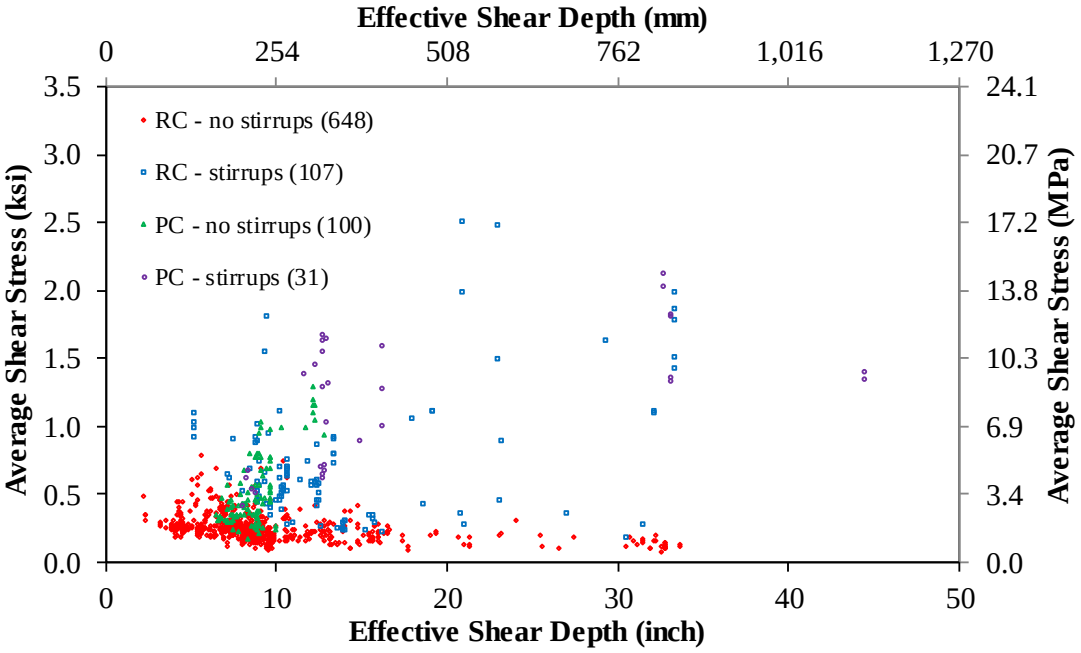

Source: FHWA.
1 ksi = 6.89 MPa.
1 inch = 25.4 mm.

Figure 52. Graph. Average shear stress compared to effective shear depth by specimen type for the selected NWC specimens from the ACI-DafStb database.

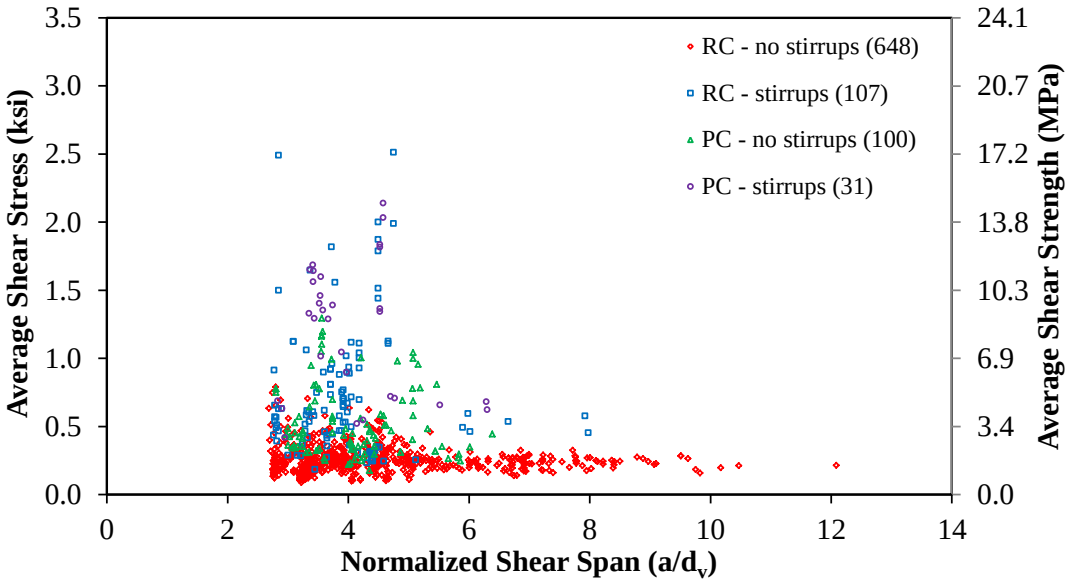

Source: FHWA.
1 ksi = 6.89 MPa.

Figure 53. Graph. Average shear stress compared to normalized shear span by specimen type for the selected NWC specimens from the ACI-DafStb database.

CHAPTER 5. SHEAR-STRESS ANALYSIS AND SHEAR-RESISTANCE ANALYSIS OF SPECIMENS IN THE TFHRC SHEAR DATABASE

INTRODUCTION

This chapter provides an analysis of the average shear stress at failure and the test-to-prediction ratios for LWC specimens in the TFHRC shear database. First, the average shear stress of LWC specimens is analyzed by specimen type and compared to NWC specimens. In this chapter, "specimen type" refers to the four combinations of RC and PC specimens with and without shear reinforcement. Next, the ratio of the maximum shear force (V_{test}) to the nominal shear resistance predicted using the four methods in the *AASHTO LRFD Bridge Design Specifications* is analyzed.[3] Different methods for accounting for LWC are compared, and new design expressions are proposed that include a proposed λ-factor based on unit weight to account for LWC. The effect that the proposed expression for the λ-factor has on the test-to-prediction ratios is evaluated. After, the ratios for LWC specimens to NWC specimens are compared. The last two sections evaluate the ratios near two limits specified by *AASHTO LRFD Bridge Design Specifications*—the lower limit on shear reinforcement and the upper limit on shear resistance.[3]

The quality of the prediction is given by its test-to-prediction ratio and COV describing the distribution of the ratios. A test-to-prediction ratio that is greater than unity indicates that the expression has underestimated the measured value, while a ratio that is less than unity indicates an overestimated value. COV indicates the amount of scatter in the test-to-prediction ratio, and a small COV is preferred.

The specimens included in this chapter were limited to those failing in shear and having an appropriate ratio of shear span to effective depth. As described previously in chapter 4 of this report, only LWC specimen failing in shear were included in the TFHRC shear database. A specimen was determined to have failed in shear if that was the mode of failure recorded in the literature and if the applied moment at failure was less than the calculated moment capacity given by equation 9. The NWC specimens in the ACI-DafStb database were also limited to those specimens failing in shear. A limit of 2.5 was placed on the a/d_v ratio for the LWC specimens. The NWC specimens in the ACI-DafStb database were already limited to a minimum a/d_v ratio of 2.5. (For sources, see Bibliography section NWC Sources for ACI-DafStb Database.)

The average shear stress and nominal shear resistance of each specimen were determined at the critical section for shear. The critical section for shear is taken as the effective shear depth (d_v) from the edge of the bearing plate. If the bearing plate width was not given, a value of 0.375 inch (9.5 mm) was assumed.

The shear resistance of the LWC and NWC specimens was determined following the procedure described in chapter 3 for the two methods of the general procedure and the Simplified-PC/RC method. The iterative process (also described in chapter 3) was followed to determine the shear resistance for the general procedures.

The term "proposed expression" in this report refers to a prediction expression that is being proposed to the AASHTO Subcommittee on Bridges and Structures (SCOBS) T-10 for

consideration as a design expression in the *AASHTO LRFD Bridge Design Specifications*.[3] Proposed expressions are also included in chapter 7 of this report.

ANALYSIS OF NORMALIZED SHEAR STRESS

This section includes a comparison of the normalized shear stress at failure for the LWC and NWC specimens from the ACI-DafStb database. The purpose of the comparison is to examine the effect of different parameters on shear resistance. The parameters were evaluated by comparing normalized shear to one of the parameters.

The normalized shear stress was compared to parameters that are known to affect shear resistance. The average shear stress given by equation 15 can be simplified by taking the resistance factor (ϕ) as 1.0 because v_u is determined using a test result. The resulting expression is shown in equation 41. For specimens without shear reinforcement, the shear stress was normalized by the concrete compressive strength (f'_c) and by two methods for determining β, which relates the effect of longitudinal strain to the shear resistance of the concrete. The normalized shear stress was compared to parameters that include the longitudinal reinforcement ratio (i.e., A_s/bd_s (referred to as ρ_ℓ previously) for RC and A_{ps}/bd_p (referred to as ρ_p previously) for PC), the net reinforcement strain (ε_s), the crack-spacing parameter (s_{xe}), the effective shear depth (d_v), and the shear span to effective shear depth ratio (a/d_v). For specimens with shear reinforcement, the shear stress was normalized by f'_c and by the amount of shear reinforcement ($b_v d_v/A_v f_y$). The normalized shear stress was compared to parameters that include the shear reinforcement ratio (ρ_v; also referred to as $A_v/b_v s$) multiplied by the stirrup yield strength (f_y), ρ_v multiplied by the ratio of f_y to $\sqrt{f'_c}$, and the ratio of the stirrup spacing (s) to d_v.

$$v_u = \frac{V_{test} - V_p}{b_v d_v} \tag{41}$$

The two methods for determining β from the shear tests are based on equation 21 and equation 22. The nominal shear resistance in equation 13 is taken as V_{test}. For tests of RC and PC members without shear reinforcement, V_s is zero. By combining equation 13, equation 16 for V_c, and equation 41, the resulting expression is given by equation 42, which can be simplified and solved for β to give equation 43. The expression for β in the *AASHTO LRFD Bridge Design Specifications* is given by equation 21 for members with shear reinforcement and by equation 22 for members without shear reinforcement.[3] The difference between equation 21 and equation 22 is a term that is a function of the crack-spacing parameter s_{xe}. The term with s_{xe} can be included with v_u in the determination of β, as given by equation 44. The net longitudinal strain at the centroid of the reinforcing (ε_s) can be determined using equation 18 and equation 19 with V_{test} substituted for V_u and the associated maximum moment at V_{test} substituted for M_u.

$$v_u = \frac{V_{test} - V_p}{b_v d_v} = 0.0316\beta\sqrt{f'_c} \tag{42}$$

$$\beta = \frac{v_u}{0.0316\sqrt{f'_c}} \tag{43}$$

$$\beta = \frac{v_u}{0.0316\sqrt{f'_c} \times 51/(39 + s_{xe})} \tag{44}$$

Three parameters were used to evaluate the normalized shear stress of RC and PC members with shear reinforcement. For the first parameter, V_s (see equation 17) is divided by the web area ($b_v d_v$) and cot θ is taken as 1.0. After simplification, the resulting expression is given by equation 45. The expression given by equation 45 is in terms of ρ_v (see equation 40) multiplied by f_y. The expression for minimum shear reinforcement given by equation 10 can be rearranged as an expression in terms of ρ_v and the ratio of f_y to $\sqrt{f'_c}$. This rearranged expression is shown in equation 46 and is the second parameter. The third parameter is the ratio of the stirrup spacing to d_v (i.e., normalized stirrup spacing).

$$\frac{V_s}{b_v d_v} = \left(\frac{A_v}{b_v s}\right) f_y \tag{45}$$

$$\left(\frac{A_v}{b_v s}\right) \frac{f_y}{\sqrt{f'_c}} = 0.0316 \tag{46}$$

The shear stress normalized by the amount of shear reinforcement ($b_v d_v / A_v f_y$) was also compared to the normalized stirrups spacing (s/d_v), which is the basis for equation 11 and equation 12, which are the expressions in the *AASHTO LRFD Bridge Design Specifications* for maximum stirrup spacing.[3] The nominal shear resistance given in equation 13 can be rearranged to isolate the terms that comprise v_u, which results in equation 47 after cot θ is taken as 1.0. Both sides are divided by $A_v f_y$, which gives the expression in equation 48. The application of equation 48 allows v_u normalized by the force in the shear reinforcement to be compared with s/d_v.

$$\left(\frac{V_{test} - V_p}{b_v d_v}\right) b_v d_v = V_c + A_v f_y \left(\frac{d_v}{s}\right) \tag{47}$$

$$v_u \left(\frac{b_v d_v}{A_v f_y}\right) = \frac{V_c}{A_v f_y} + \frac{d_v}{s} \tag{48}$$

Normalized shear stress is compared to each parameter in pairs of figures. The first figure in each pair provides the comparison for LWC specimens that are grouped by unit weight (w_c). The second figure in each pair gives the comparisons for the LWC specimens with a reported w_c, LWC specimens without a reported w_c, and NWC specimens. The first figure can be used to evaluate the effect of w_c on the parameter being compared, and the second figure can be used to evaluate the effect of the use of lightweight aggregate in general. The comparisons are grouped by specimen type: RC specimens without and with stirrups and PC specimens without and with stirrups. In the determination of the average shear stress, no modification for LWC was considered.

RC Specimens Without Shear Reinforcement

Figure 54 and figure 55 show a comparison of v_u normalized by f'_c to the longitudinal reinforcement ratio (A_s/bd_s) for RC specimens without shear reinforcement. Figure 54 gives the

data for specimens with a reported w_c. The data are given by ranges of w_c. Also shown in the figure is a least-squares linear-regression line for each range of w_c. All of the data in figure 54 are grouped together and shown in figure 55 as LWC data with a recorded w_c (i.e., LWC with w_c). Additional LWC specimens that did not have a recorded w_c (i.e., LWC without w_c) are also included in the figure. The large number of selected NWC specimens from the ACI-DafStb database is shown in figure 55. The number of data points in each group is shown in parentheses in the legend. The linear-regression lines in figure 54 show a trend of normalized shear stress increasing with longitudinal reinforcement ratio. There does not appear to be an obvious trend for the unit weight. The NWC data show a similar trend of normalized shear stress increasing with longitudinal reinforcement ratio. The linear-regression lines for the LWC with w_c regression line and the NWC data regression line intersect at a longitudinal reinforcement ratio of 0.034. If all of the LWC data are considered together, the regression lines for LWC and NWC intersect at a ratio of 0.030. This indicates that a small modification for LWC may be appropriate for most RC specimens without shear reinforcement.

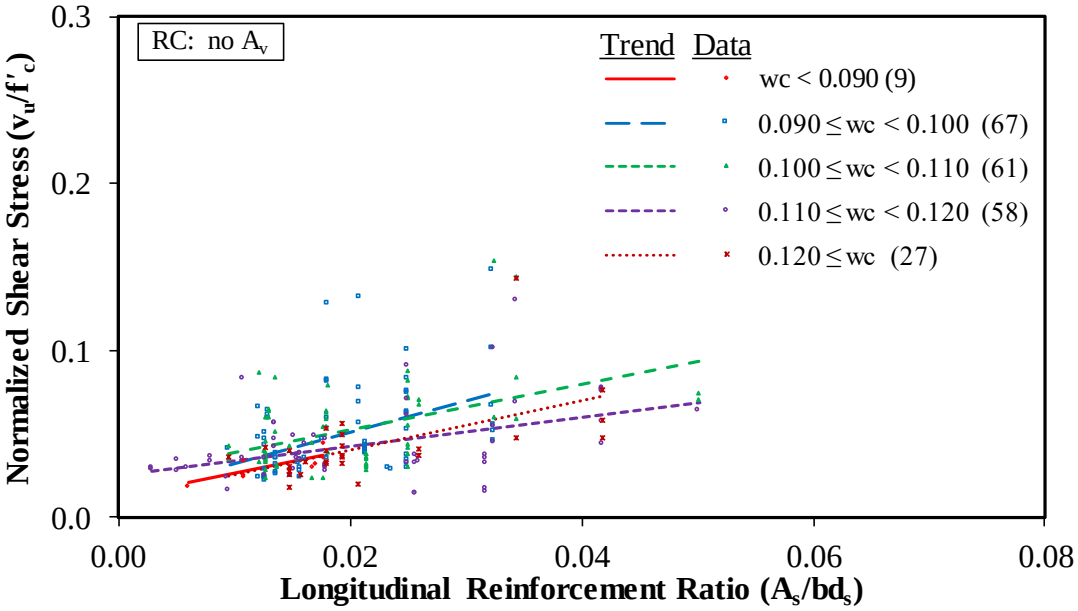

Source: FHWA.
Note: Unit weight (w_c) in the legend is measured in kcf where 1 kcf = 16,020 kg/m^3.

Figure 54. Graph. Normalized shear stress compared to longitudinal reinforcement ratio for LWC RC members without shear reinforcement in the TFHRC shear database.

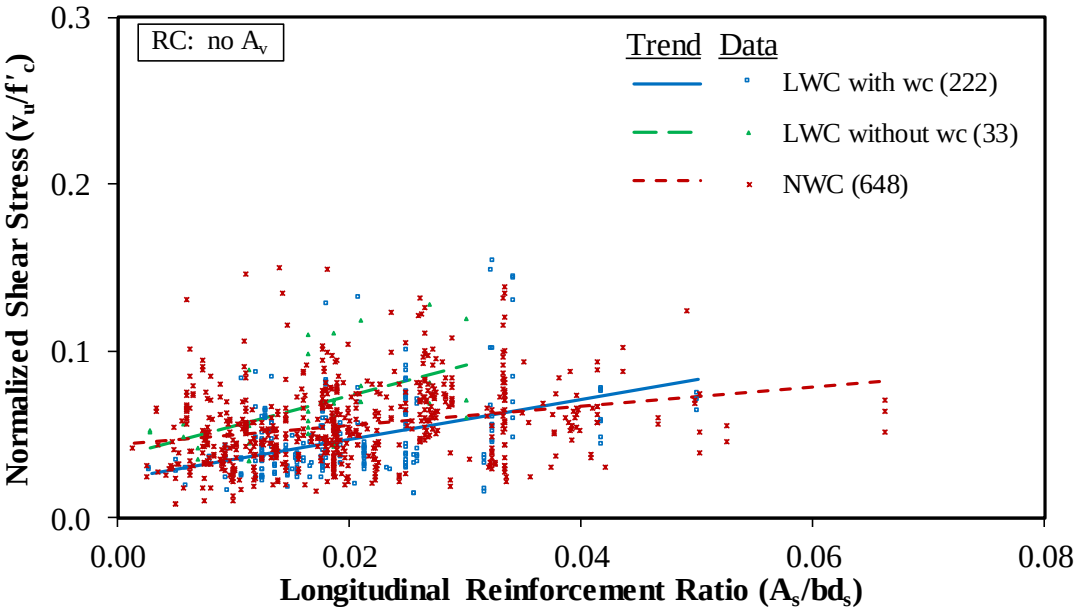

Source: FHWA.

Figure 55. Graph. Normalized shear stress compared to the longitudinal reinforcement ratio for LWC and NWC RC members without shear reinforcement in the TFHRC shear database.

Figure 56 and figure 57 show a comparison of v_u normalized by $0.316\sqrt{f'_c}$ (i.e., β given by equation 43) to the net reinforcement strain (ε_s). The shear specimen data are grouped in a similar manner as described previously for figure 54 and figure 55. Also shown in figure 56 and figure 57 is the prediction for β used by GP-equation in the *AASHTO LRFD Bridge Design Specifications*.[3] This expression for the prediction of β is given by equation 21.

A large number of LWC data points with an ε_s less than 0.001 inch/inch (0.001 mm/mm) in figure 56 are below the predicted value for β. In figure 57, a large number of NWC data points with an ε_s less than 0.0015 inch/inch (0.0015 mm/mm) are below the predicted value for β. In both figure 56 and figure 57, the regression lines for the LWC show an increase in the normalized shear stress with ε_s. As discussed chapter 4, section Shear Span to Effective Depth Ratio for RC Specimens Without Shear Reinforcement, most of the LWC data points with an ε_s greater than 0.001 inch/inch (0.001 mm/mm) and a high normalized shear stress have an a/d_v ratio between 2.5 and 3.0.

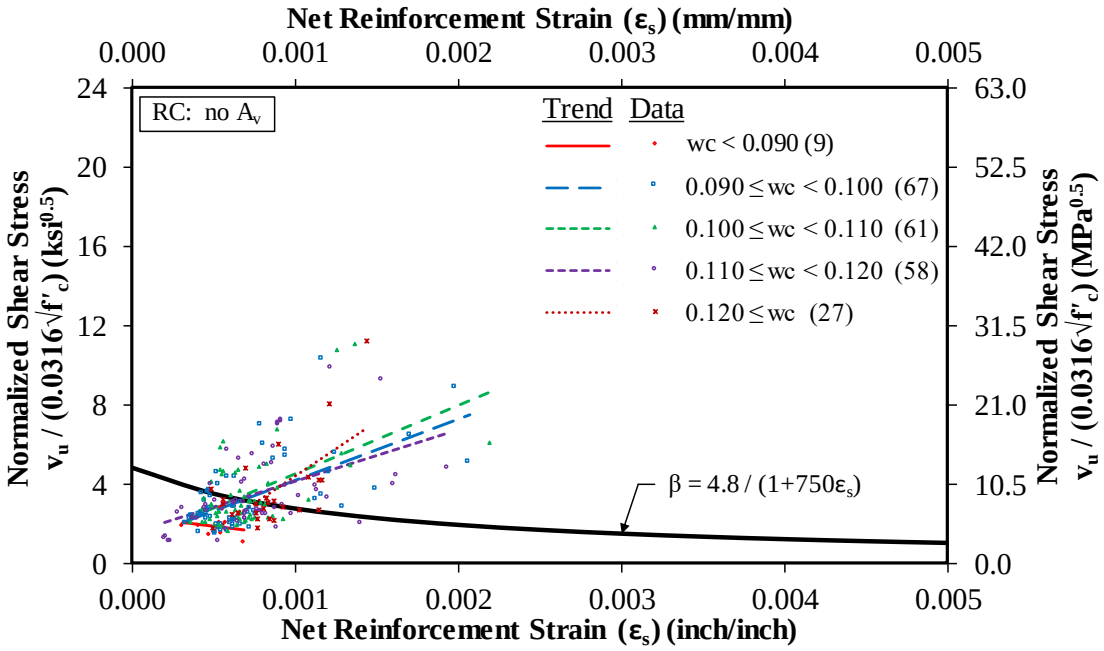

Source: FHWA.
1 ksi = 6.89 MPa.
1 inch/inch = 1 mm/mm.
Note: Unit weight (w_c) in the legend is measured in kcf where 1 kcf = 16,020 kg/m^3.

Figure 56. Graph. Normalized shear stress compared to net reinforcement strain for LWC RC members without shear reinforcement in the TFHRC shear database.

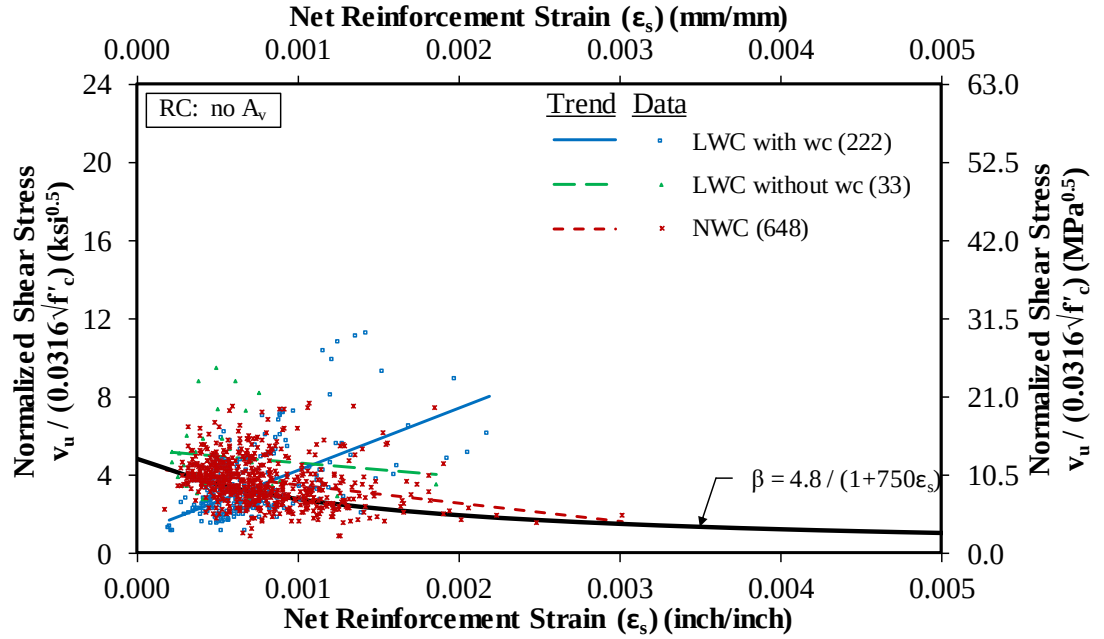

Source: FHWA.
1 ksi = 6.89 MPa.
1 inch/inch = 1 mm/mm.

Figure 57. Graph. Normalized shear stress compared to net reinforcement strain for LWC and NWC RC members without shear reinforcement in the TFHRC shear database.

Figure 58 and figure 59 show a comparison of v_u normalized by $0.316\sqrt{f'_c}$ and an additional term that is a function of the crack-spacing parameter s_{xe} (i.e., β given by equation 44) to the net reinforcement strain (ε_s). s_{xe} is shown in figure 60 and figure 61 for LWC and NWC specimens. For most of the specimens, s_{xe} is at the lower limit of 12 inches (305 mm). The specimens with an s_{xe} greater than the lower limit will have a larger normalized v_u. A comparison of figure 56 and figure 58 shows that there is very little noticeable difference in the position of the LWC data. This is likely due to the limited amount of data with s_{xe} greater than the lower limit of 12 inches (305 mm) and almost no data greater than 25 inches (635 mm). There are a significant number of NWC data points in figure 61 that are greater than 12 inches (305 mm) and some data points with s_{xe} greater than 40 inches (1016 mm). As a result, a comparison of figure 57 and figure 59 shows a slight increase in the normalized shear stresses (see figure 59), as indicated by the slight upward shift of the data.

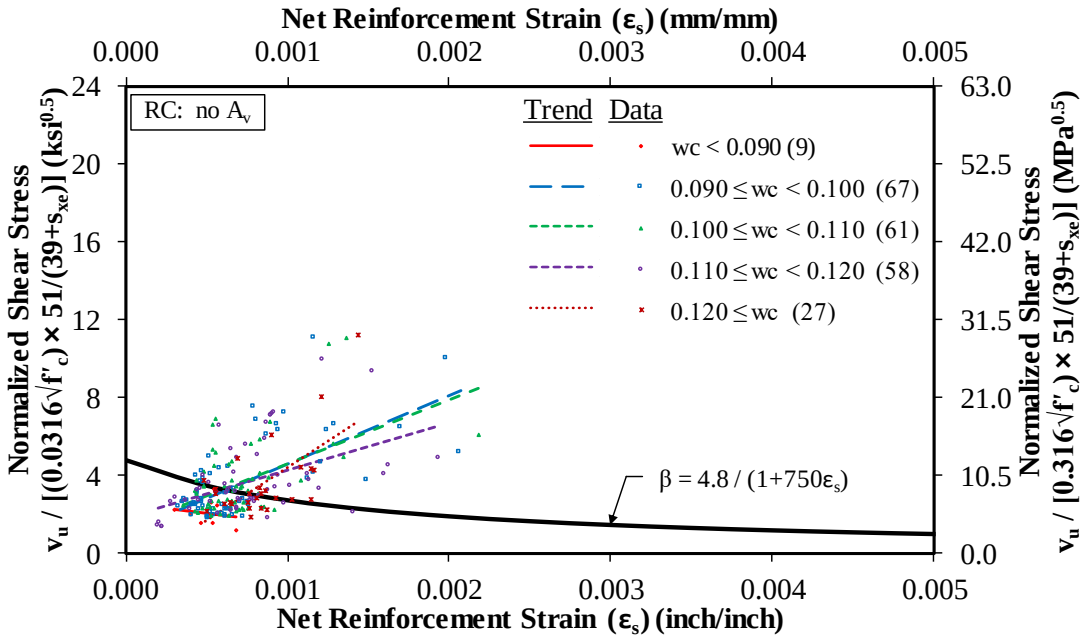

Source: FHWA.
1 ksi = 6.89 MPa.
1 inch/inch = 1 mm/mm.
Note: Unit weight (w_c) in the legend is measured in kcf where 1 kcf = 16,020 kg/m^3.

Figure 58. Graph. Shear stress normalized by a function accounting for crack spacing compared to net reinforcement strain for LWC RC members without shear reinforcement in the TFHRC shear database.

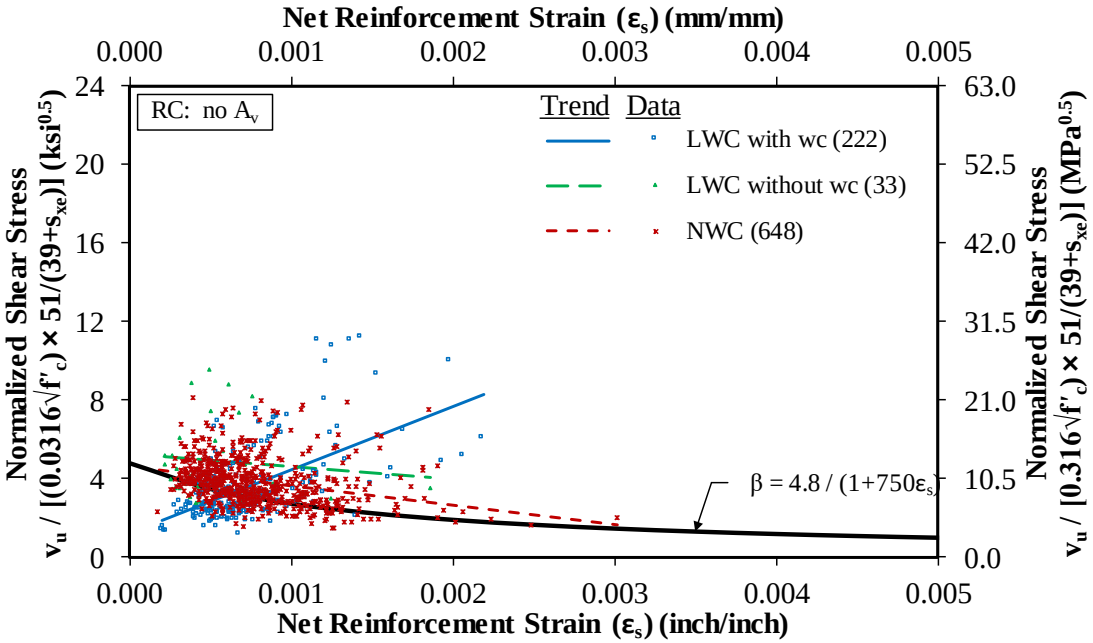

Source: FHWA.
1 ksi = 6.89 MPa.
1 inch/inch = 1 mm/mm.

Figure 59. Graph. Shear stress normalized by a function accounting for crack spacing compared to net reinforcement strain for LWC and NWC RC members without shear reinforcement in the TFHRC shear database.

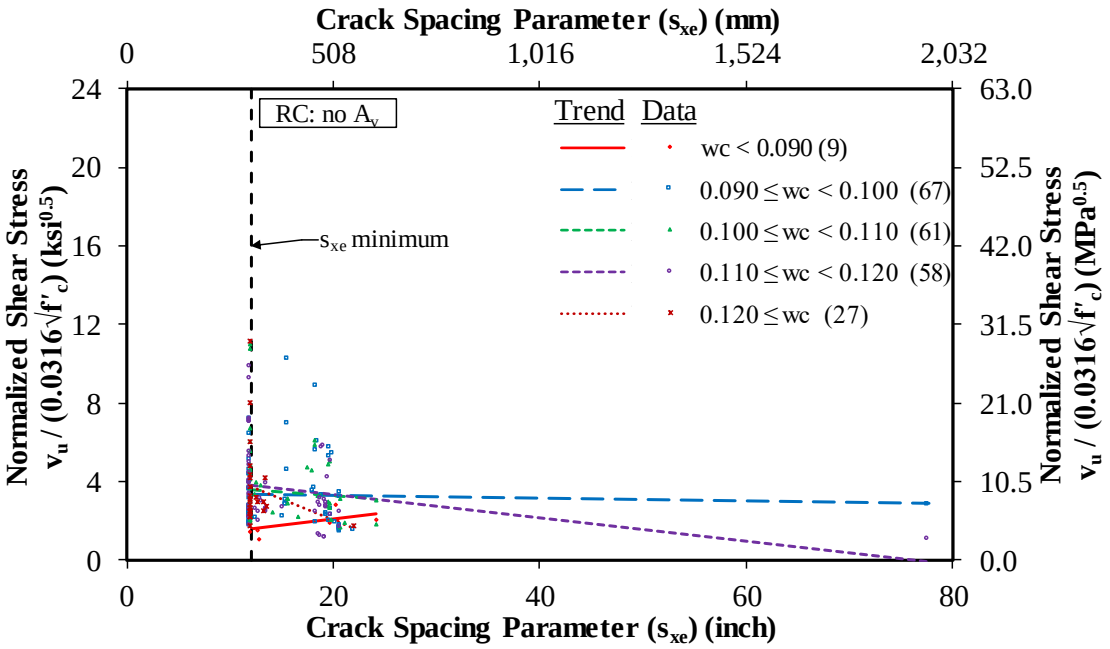

Source: FHWA.
1 ksi = 6.89 MPa.
1 inch = 25.4 mm.
Note: Unit weight (w_c) in the legend is measured in kcf where 1 kcf = 16,020 kg/m^3.

Figure 60. Graph. Normalized shear stress compared to crack-spacing parameter for LWC RC members without shear reinforcement in the TFHRC shear database.

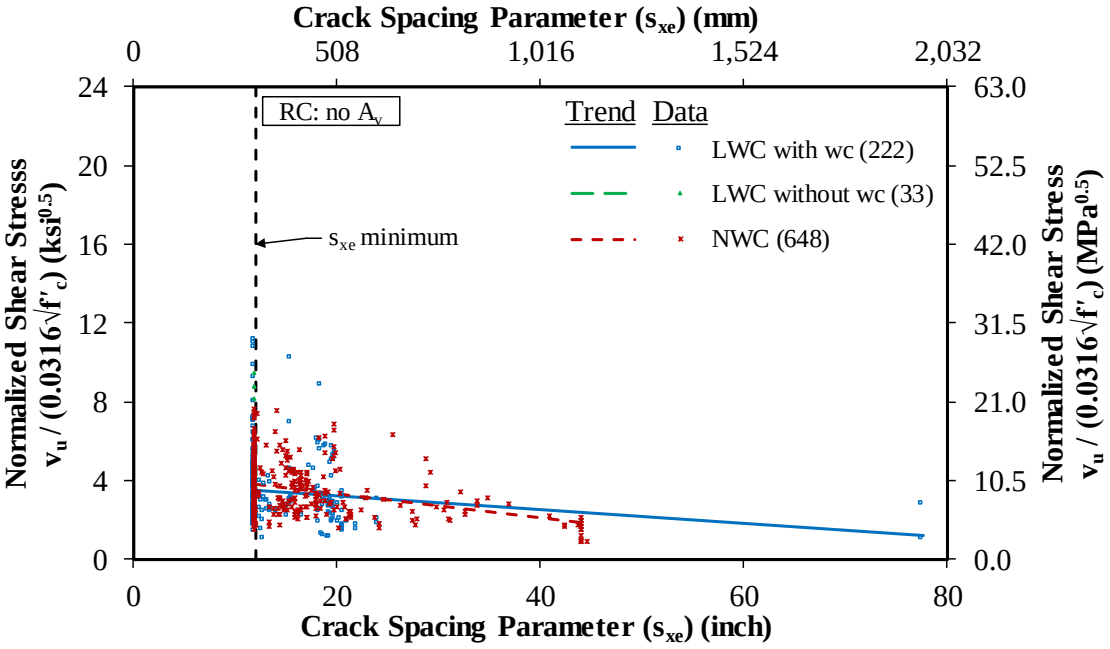

Source: FHWA.
1 ksi = 6.89 MPa.
1 inch = 25.4 mm.

Figure 61. Graph. Normalized shear stress compared to crack-spacing parameter for LWC and NWC RC members without shear reinforcement in the TFHRC shear database.

Figure 62 and figure 63 show a comparison of v_u normalized by $0.316\sqrt{f'_c}$ to the effective depth for shear. The purpose of these two figures is to investigate size effect for LWC specimens. Figure 62 does not indicate an obvious relationship between w_c and size effect. Both the regression lines for LWC and NWC indicate that normalized v_u decreases as the effective depth increases. The regression lines for LWC and NWC are nearly parallel with the LWC regression line slightly below the NWC line. There are only two LWC data points with d_v greater than 15 inches (381 mm), so it is difficult to come to a definitive conclusion on the size effect of LWC specimens.

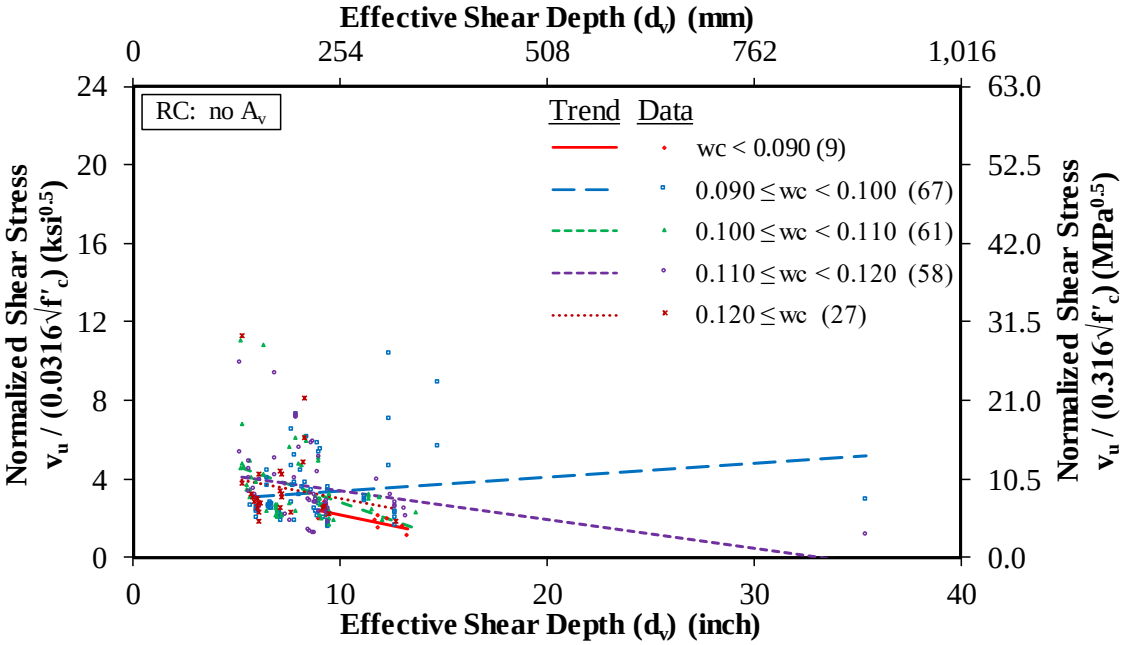

Source: FHWA.
1 ksi = 6.89 MPa.
Note: Unit weight (w_c) in the legend is measured in kcf where 1 kcf = 16,020 kg/m^3.

Figure 62. Graph. Normalized shear stress compared to effective shear depth for LWC RC members without shear reinforcement in the TFHRC shear database.

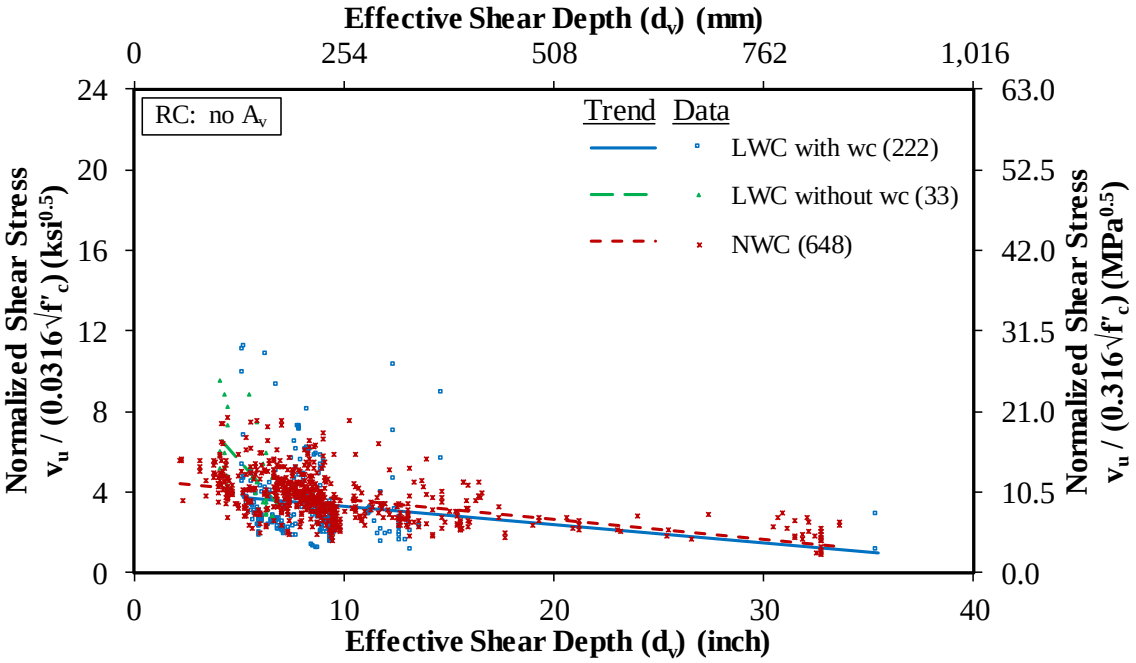

Source: FHWA.
1 ksi = 6.89 MPa.

Figure 63. Graph. Normalized shear stress compared to effective shear depth for LWC and NWC RC members without shear reinforcement in the TFHRC shear database.

RC Specimens With Shear Reinforcement

Figure 64 and figure 65 show a comparison of v_u normalized by f'_c to stirrup strength ($\rho_v f_{yt}$) for RC specimens with shear reinforcement. Figure 64 gives the data for specimens with a reported unit weight. Figure 65 shows the data from figure 64 and selected NWC specimens from the ACI-DafStb database.

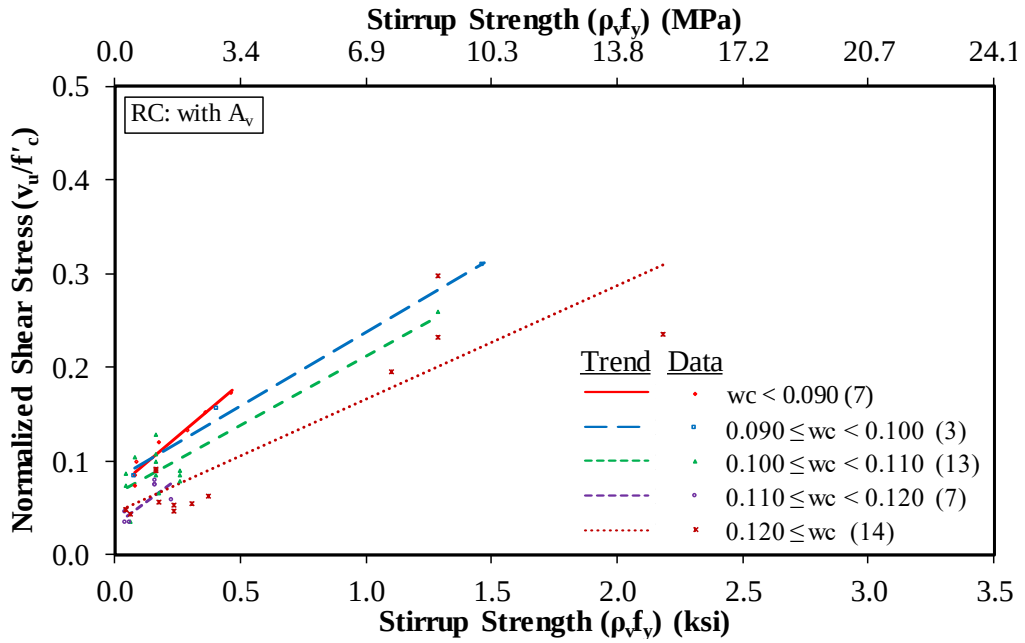

Source: FHWA.
1 ksi = 6.89 MPa.
Note: Unit weight (w_c) in the legend is measured in kcf where 1 kcf = 16,020 kg/m^3.

Figure 64. Graph. Normalized shear stress compared to stirrup strength for LWC RC members with shear reinforcement in the TFHRC shear database.

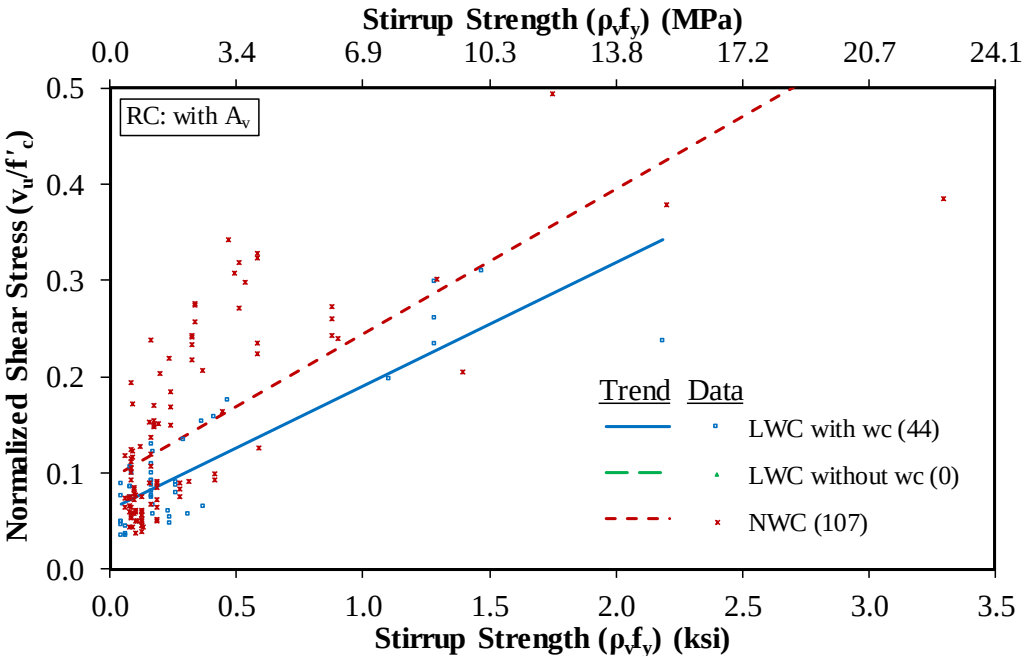

Source: FHWA.
1 ksi = 6.89 MPa.

Figure 65. Graph. Normalized shear stress compared to stirrup strength for LWC and NWC RC members with shear reinforcement in the TFHRC shear database.

Figure 64 appears to show a trend of normalized v_u decreasing as w_c increases. An additional comparison was made with the shear reinforcement ratio multiplied by the ratio of the stirrup yield strength to the square root of the concrete compressive strength ($f_y/\sqrt{f'_c}$). This additional comparison is in the form of an expression for the minimum amount of shear reinforcement given by equation 46 and is shown in figure 66 and figure 67. A vertical line at a value of 0.0316 in figure 66 and figure 67 indicates the minimum amount of shear reinforcement required by the *AASHTO LRFD Bridge Design Specifications*.[3] The LWC data shown in figure 66 do not show an obvious dependence of normalized v_u on w_c.

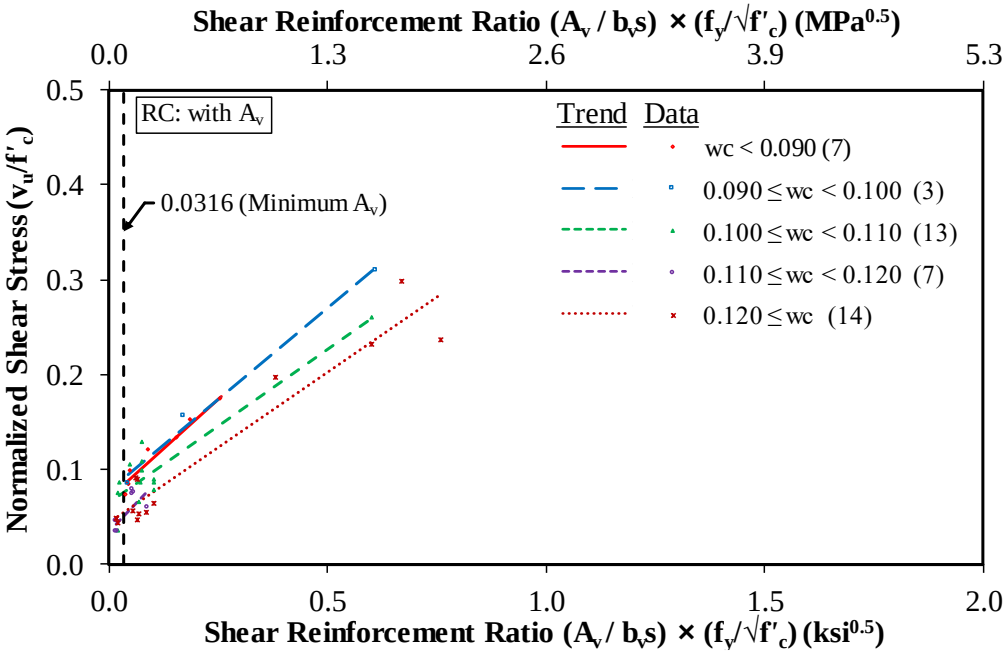

Source: FHWA.
1 ksi = 6.89 MPa.
Note: Unit weight (w_c) in the legend is measured in kcf where 1 kcf = 16,020 kg/m^3.

Figure 66. Graph. Normalized shear stress compared to shear reinforcement ratio multiplied by the ratio of stirrup yield strength to the square root of concrete compressive strength for LWC RC members with shear reinforcement in the TFHRC shear database.

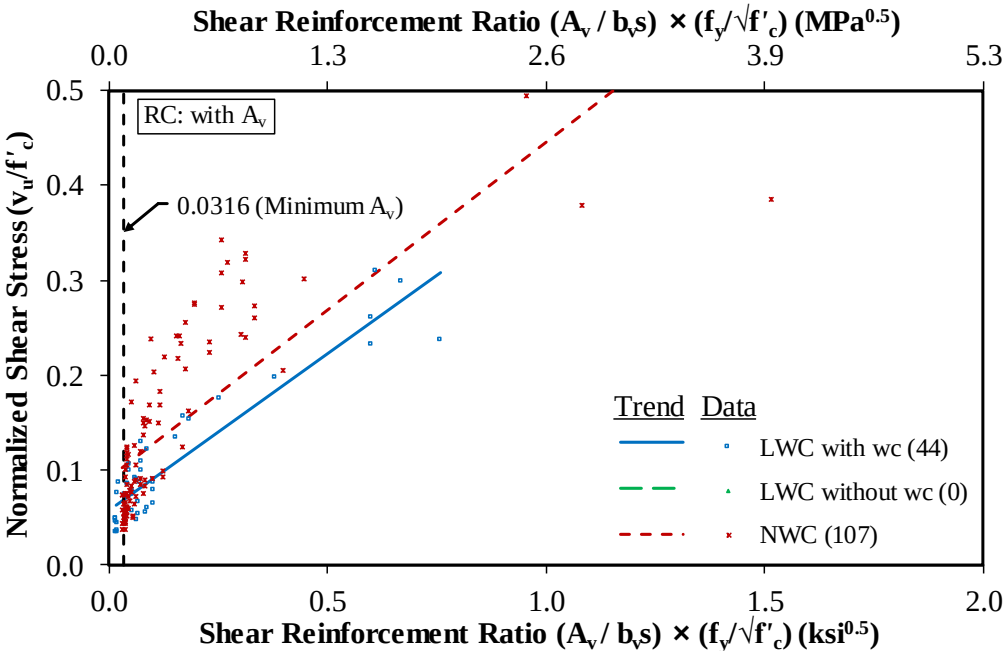

Source: FHWA.
1 ksi = 6.89 MPa.

Figure 67. Graph. Normalized shear stress compared to shear reinforcement ratio multiplied by the ratio of stirrup yield strength to the square root of concrete compressive strength for LWC and NWC RC members with shear reinforcement in the TFHRC shear database.

A comparison of the LWC and NWC in figure 65 and figure 67 shows that the regression lines for LWC and NWC are nearly parallel but that the line for the LWC data is much lower than the NWC line. It is interesting to observe that the difference between the LWC and NWC regression lines in figure 65 and figure 67 for RC specimens with shear reinforcement is much greater than the difference between the LWC and NWC regression lines in figure 55 for RC specimens without shear reinforcement. This suggests that the effect of lightweight aggregate on shear strength is more pronounced for members with shear reinforcement than for members without shear reinforcement.

Figure 68 and figure 69 show a comparison of v_u normalized by f'_c to the stirrup spacing (s) normalized by the effective shear depth (d_v) for RC specimens with shear reinforcement. These figures are intended to show the effect of stirrup spacing on v_u. A horizontal line is shown in the figures at 0.125 v_u/f'_c. A normalized v_u below this line has a maximum stirrup spacing (s_{max}) given by equation 11, and a normalized v_u above this line has an s_{max} given by equation 12. The vertical lines in the figures at $0.4d_v$ and $0.8d_v$ represent the limit on s_{max} given by equation 11 and equation 12. Data points that are below the horizontal line at 0.125 v_u/f'_c and to the right of the vertical line at $0.8d_v$ represent tests with stirrup spacings that exceed s_{max} given by equation 11. Similarly, stirrup spacing of the test with data points that are above the horizontal line at 0.125 v_u/f'_c and to the right of the vertical line at $0.4d_v$ exceed the s_{max} given by equation 12.

As shown in figure 68, most of the LWC tests satisfy the requirements in the *AASHTO LRFD Bridge Design Specifications* for maximum stirrup spacing.[3] There are only three data points

above the 0.125 v_u/f'_c line that have a stirrup spacing greater than s_{max}. There are several tests over a range of w_c that are below the 0.125 v_u/f'_c line and have a stirrup spacing greater than s_{max}. The stirrup spacing for all of these points is less than 0.9 s/d_v. A large number of the NWC data points shown in figure 69 have stirrup spacings that exceed s_{max}.

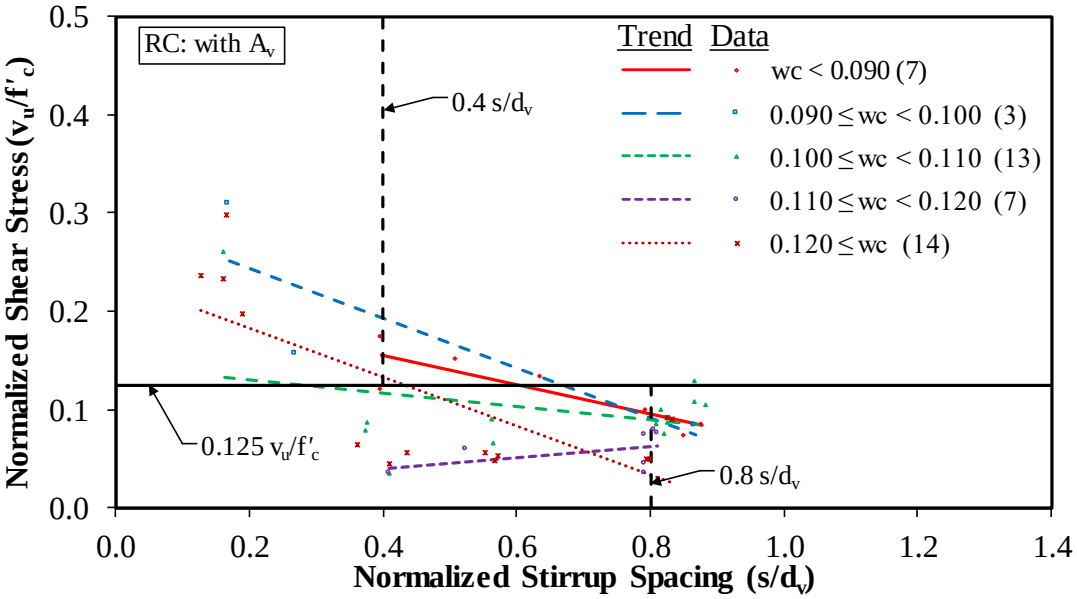

Source: FHWA.
Note: Unit weight (w_c) in the legend is measured in kcf where 1 kcf = 16,020 kg/m^3.

Figure 68. Graph. Normalized shear stress compared to normalized stirrup spacing for LWC RC members with shear reinforcement in the TFHRC shear database.

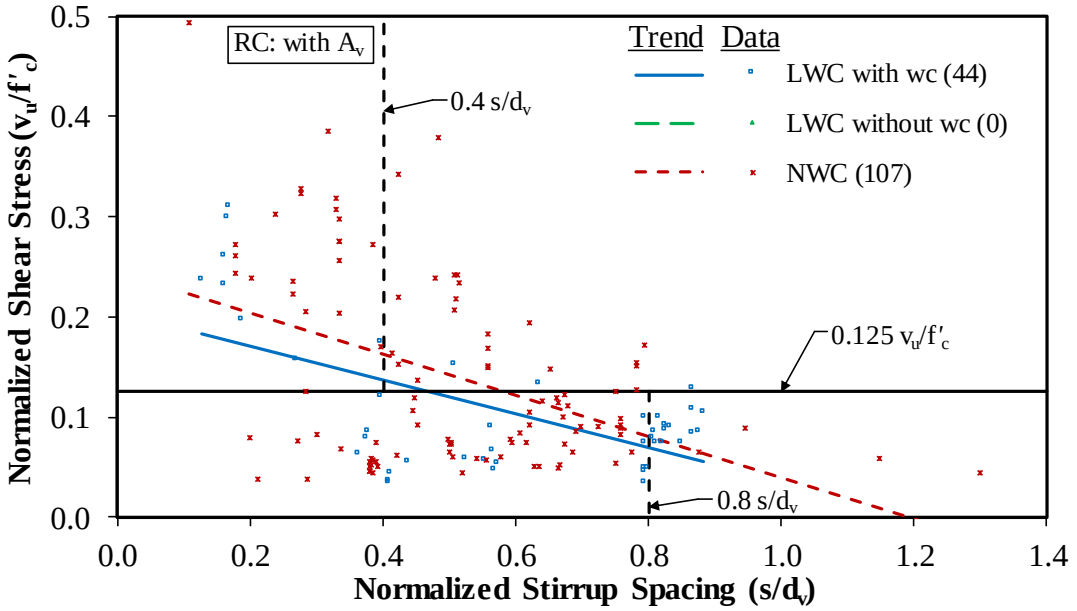

Source: FHWA.

Figure 69. Graph. Normalized shear stress compared to normalized stirrup spacing for LWC and NWC RC members with shear reinforcement in the TFHRC shear database.

The regression lines for the LWC and NWC data in figure 68 and figure 69 show a decrease in normalized v_u as the normalized stirrup spacing (s/d_v) increases. However, the data are not independent of the area of shear reinforcement, and the downward trend may be due to a decrease in the amount of shear reinforcement for the tests with large stirrup spacing. Alternatively, v_u can be normalized by the force in the shear reinforcement (see equation 48). The resulting data points are shown in figure 70 and figure 71. The trend line for the LWC data points in figure 71 shows a slight decrease in the normalized v_u as s/d_v increases. As shown in figure 70, there is not an obvious dependency of w_c on normalized v_u.

For s/d_v less than 0.8, the regression line for NWC data points is above the regression line for the LWC data points. However, the downward slope of the regression line for NWC data points in figure 71 is much greater than for the LWC regression line. At larger s/d_v, the shear reinforcement may be less effective at reducing the diagonal cracking.[14] Figure 71 indicates that, at larger s/d_v, the effectiveness of shear reinforcement in NWC behaves similarly to the effectiveness of shear reinforcement in LWC. The lower cracking strength of LWC appears to reduce the effectiveness of the shear reinforcement to reduce the propagation of the diagonal cracking.

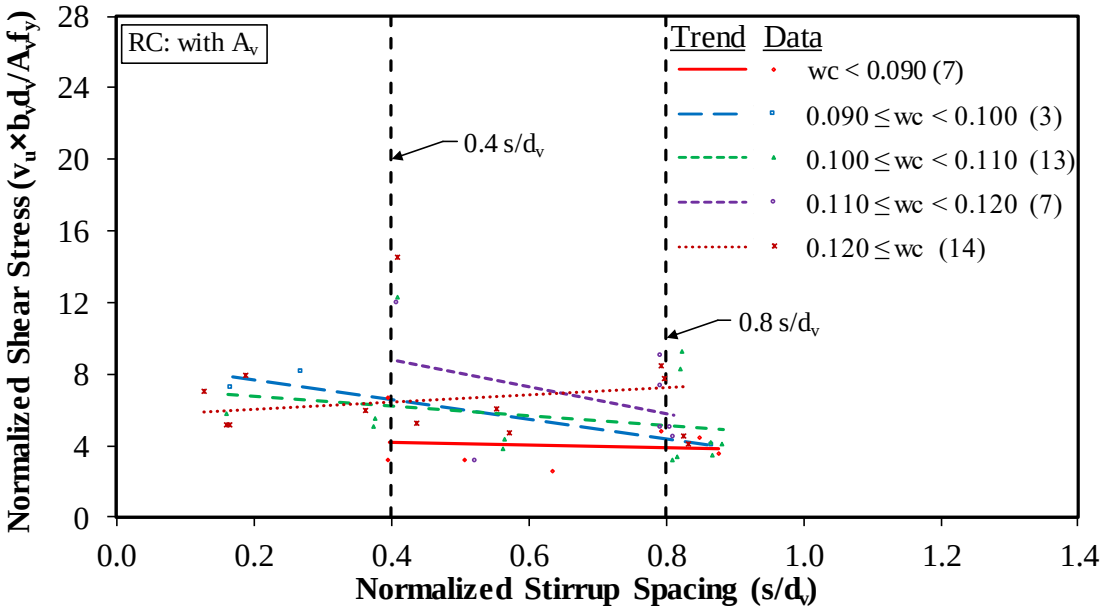

Source: FHWA.
Note: Unit weight (w_c) in the legend is measured in kcf where 1 kcf = 16,020 kg/m^3.

Figure 70. Graph. Shear stress normalized by a function accounting for the force in the shear reinforcement compared to normalized stirrup spacing for LWC RC members with shear reinforcement in the TFHRC shear database.

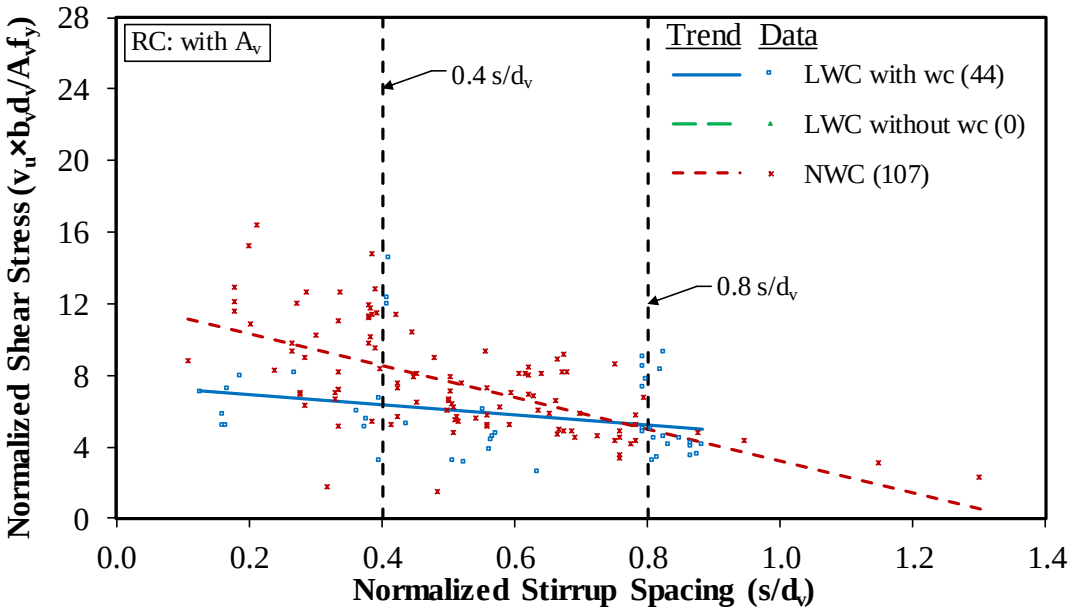

Source: FHWA.

Figure 71. Graph. Shear stress normalized by a function accounting for the force in the shear reinforcement compared to normalized stirrup spacing for LWC and NWC RC members with shear reinforcement in the TFHRC shear database.

PC Specimens Without Shear Reinforcement

Figure 72 and figure 73 show a comparison of v_u normalized by f'_c to the longitudinal reinforcement ratio (A_{ps}/bd_p) for PC specimens without shear reinforcement. The limited number of LWC data points in figure 72 does not give an obvious trend for the effect of w_c on normalized shear stress. The range of longitudinal reinforcement ratios for the test data is more limited for the NWC than for LWC. Over the range of ratios available for NWC, the trend line of the normalized shear stress for NWC is above the trend line for LWC, indicating a potential need for a reduction factor for LWC.

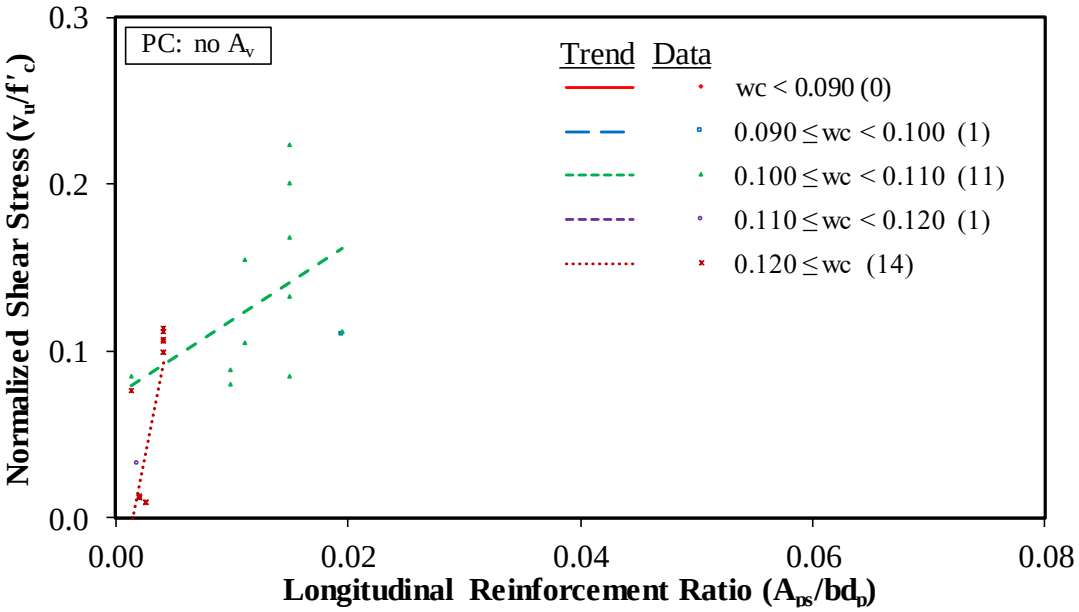

Source: FHWA.
Note: Unit weight (w_c) in the legend is measured in kcf where 1 kcf = 16,020 kg/m^3.

Figure 72. Graph. Normalized shear stress compared to longitudinal reinforcement ratio for LWC PC members without shear reinforcement in the TFHRC shear database.

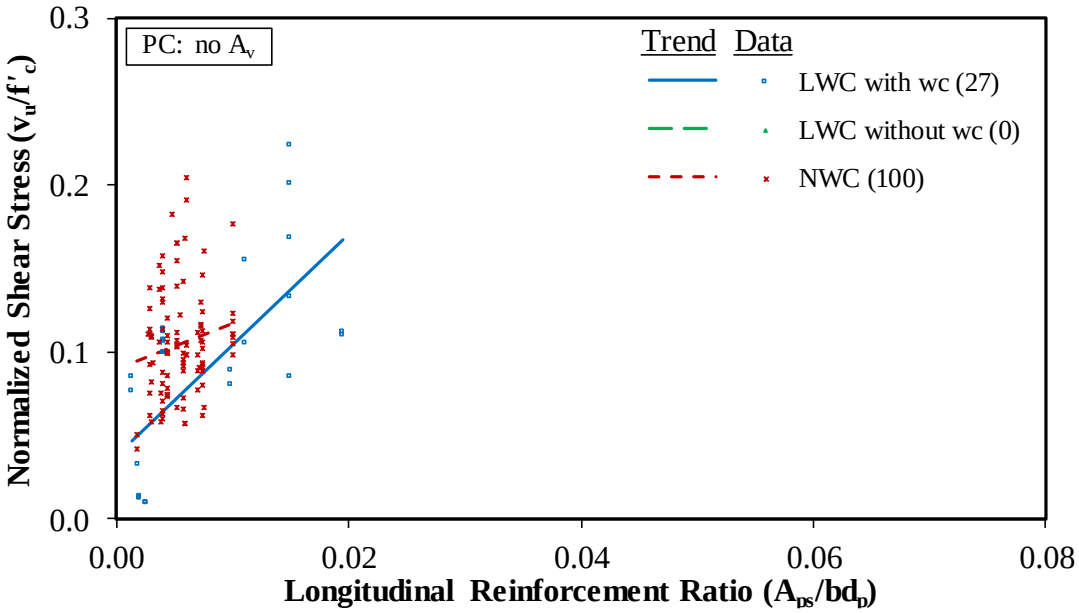

Source: FHWA.

Figure 73. Graph. Normalized shear stress compared to longitudinal reinforcement ratio for LWC and NWC PC members without shear reinforcement in the TFHRC shear database.

Figure 74 and figure 75 show a comparison of v_u normalized by $0.316\sqrt{f'_c}$ (i.e., β in equation 43) to the net reinforcement strain (ε_s). Except for the data from a single source, the rest of the LWC was above the prediction for β in equation 21. All of the NWC data with a tensile net

reinforcement strain (i.e., positive ε_s) were above the prediction for β, and most of the data with a compressive net reinforcement strain (i.e., negative ε_s) were above the prediction for β.

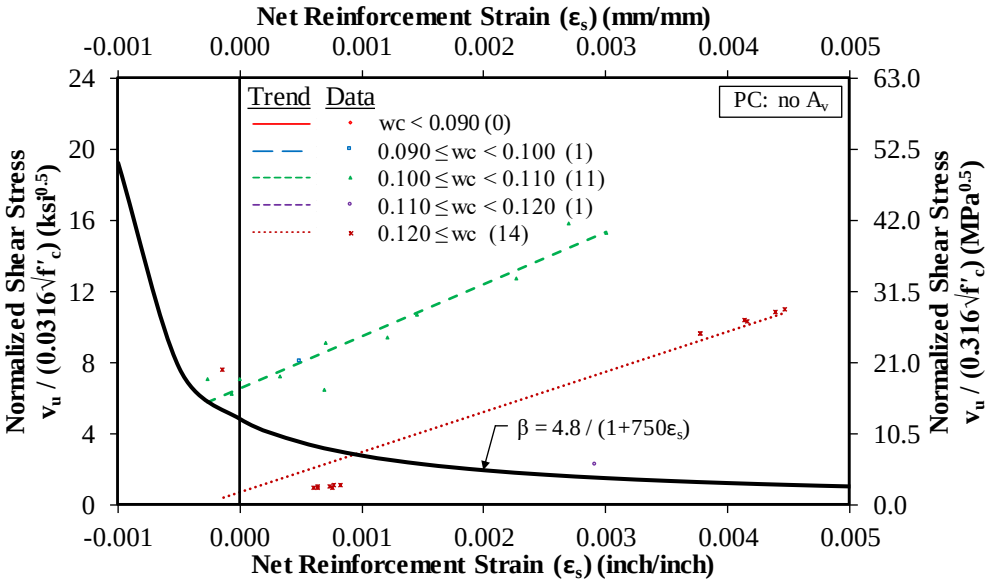

Source: FHWA.
1 ksi = 6.89 MPa.
1 inch/inch = 1 mm/mm.
Note: Unit weight (w_c) in the legend is measured in kcf where 1 kcf = 16,020 kg/m^3.

Figure 74. Graph. Normalized shear stress compared to net reinforcement strain for LWC PC members without shear reinforcement in the TFHRC shear database.

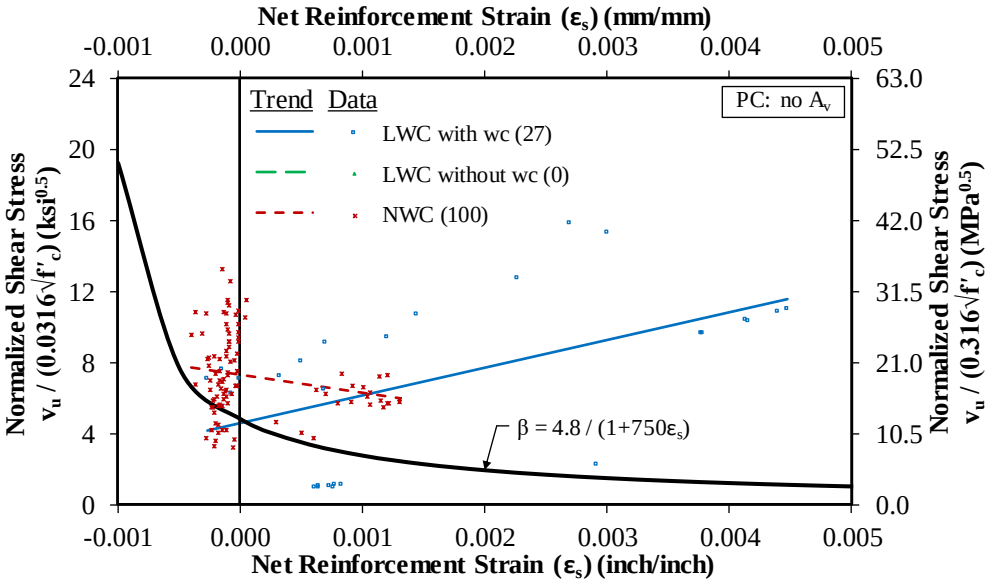

Source: FHWA.
1 ksi = 6.89 MPa.
1 inch/inch = 1 mm/mm.

Figure 75. Graph. Normalized shear stress compared to net reinforcement strain for LWC and NWC PC members without shear reinforcement in the TFHRC shear database.

Including the crack-spacing parameter (s_{xe}) in the normalized shear stress did not cause a noticeable difference in the position of the LWC data or NWC data in figure 76 and figure 77 when compared to their relative positions in figure 74 and figure 75. This is due to nearly all of the LWC data shown in figure 78 and most of the NWC data shown in figure 79 having an s_{xe} equal to the lower limit of 12 inches (305 mm).

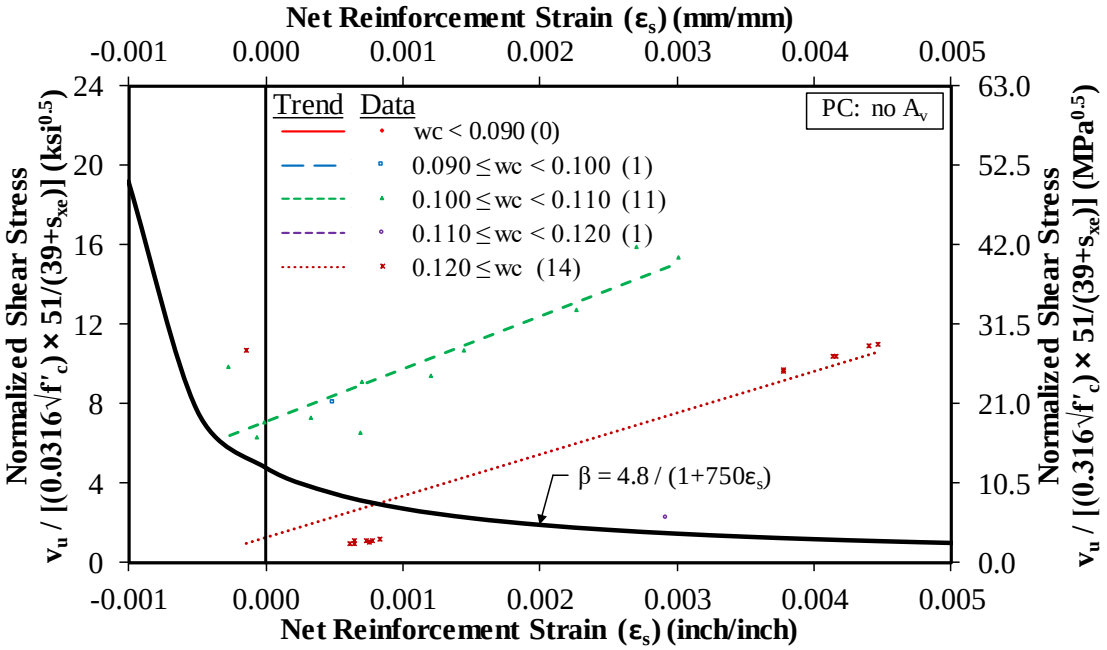

Source: FHWA.
1 ksi = 6.89 MPa.
1 inch/inch = 1 mm/mm.
Note: Unit weight (w_c) in the legend is measured in kcf where 1 kcf = 16,020 kg/m^3.

Figure 76. Graph. Shear stress normalized by a function accounting for the force in the shear reinforcement compared to net reinforcement strain for LWC PC members without shear reinforcement in the TFHRC shear database.

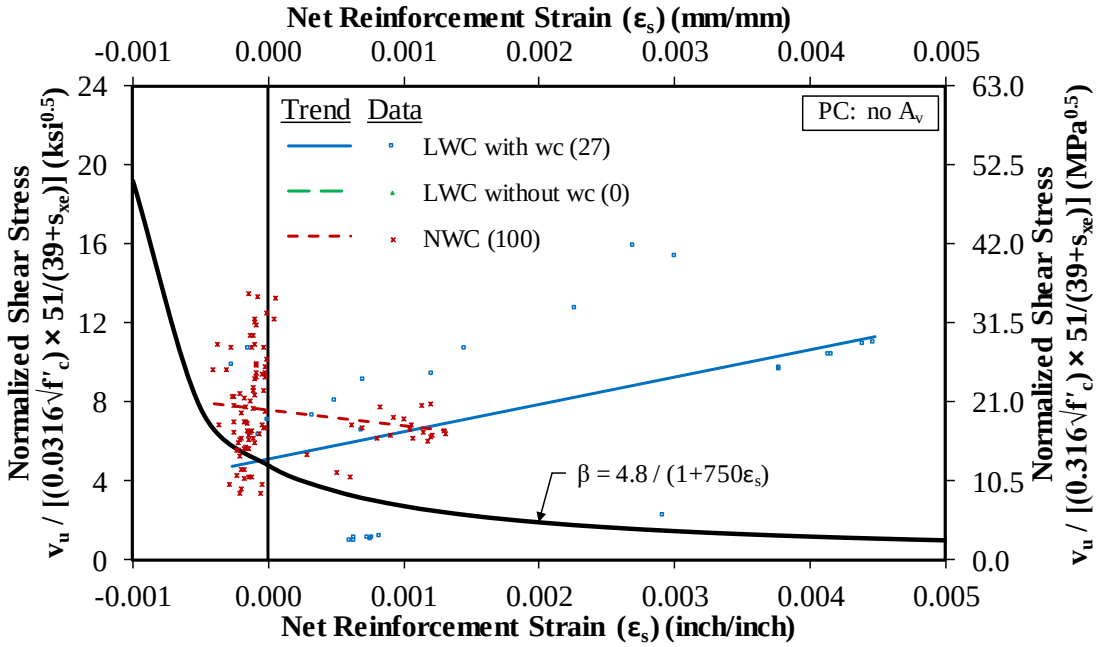

Source: FHWA.
1 ksi = 6.89 MPa.
1 inch/inch = 1 mm/mm.

Figure 77. Graph. Shear stress normalized by a function accounting for crack spacing compared to net reinforcement strain for LWC and NWC PC members without shear reinforcement in the TFHRC shear database.

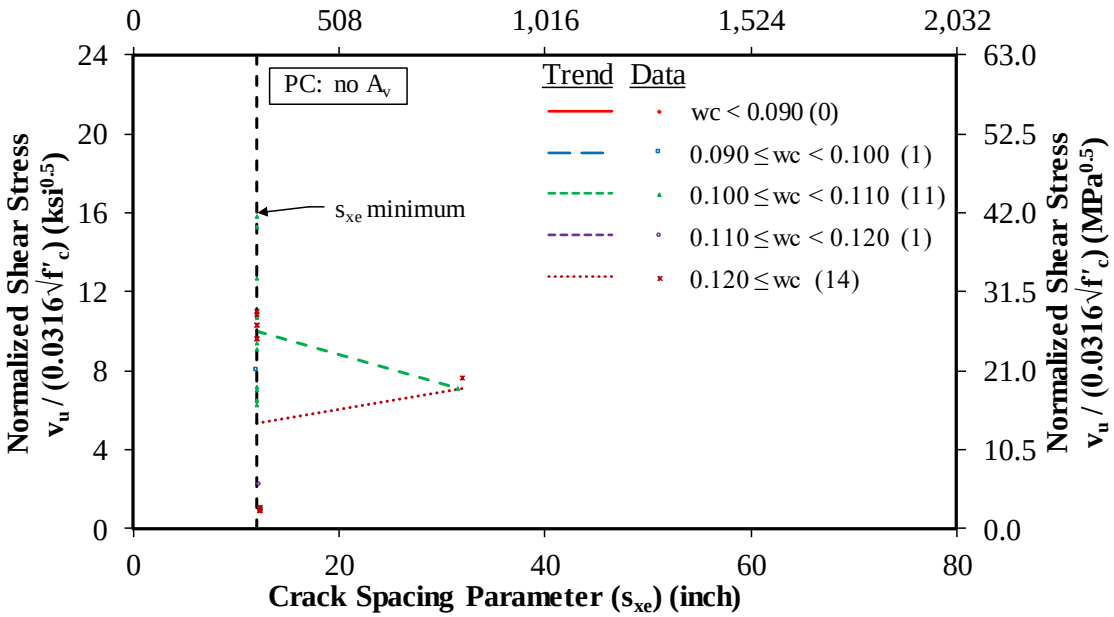

Source: FHWA.
1 ksi = 6.89 MPa.
1 inch = 25.4 mm.
Note: Unit weight (w_c) in the legend is measured in kcf where 1 kcf = 16,020 kg/m^3.

Figure 78. Graph. Normalized shear stress compared to crack-spacing parameter for LWC PC members without shear reinforcement in the TFHRC shear database.

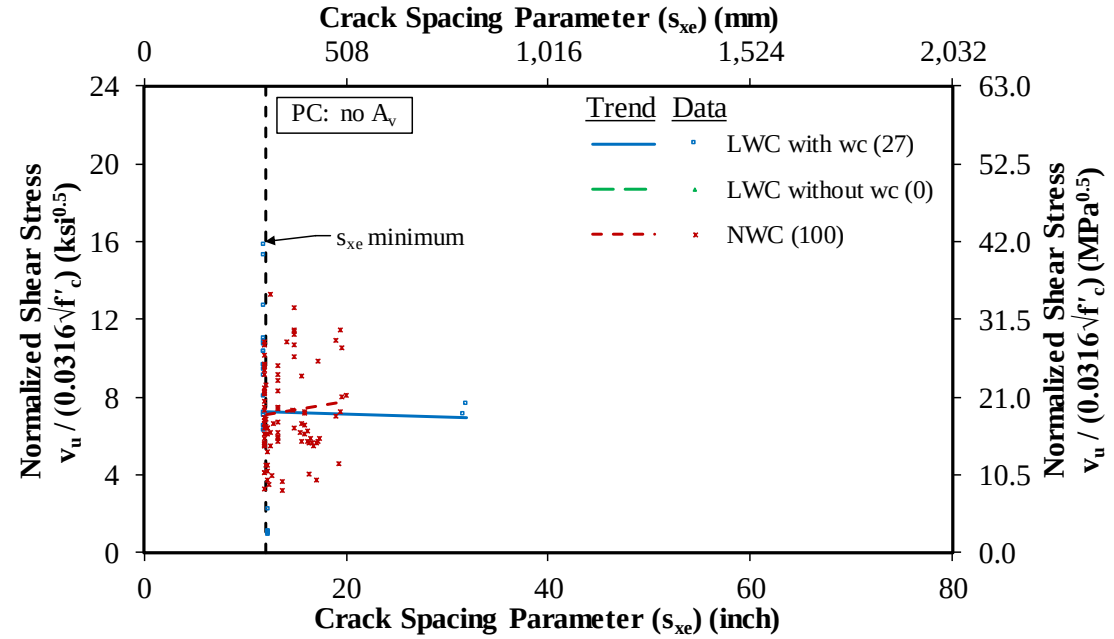

Source: FHWA.
1 ksi = 6.89 MPa.
1 inch = 25.4 mm.

Figure 79. Graph. Normalized shear stress compared to crack-spacing parameter for LWC and NWC PC members without shear reinforcement in the TFHRC shear database.

Normalized shear stress compared to effective depth for shear is shown in figure 80 and figure 81. There are only two LWC data points with a d_v greater than 10 inches (254 mm) and very few NWC data points with a d_v greater than or equal to 10 inches (254 mm). The effective depth for nearly all of the data was too small, and the number of data points available was too few to be used to determine the effect of d_v on normalized shear stress.

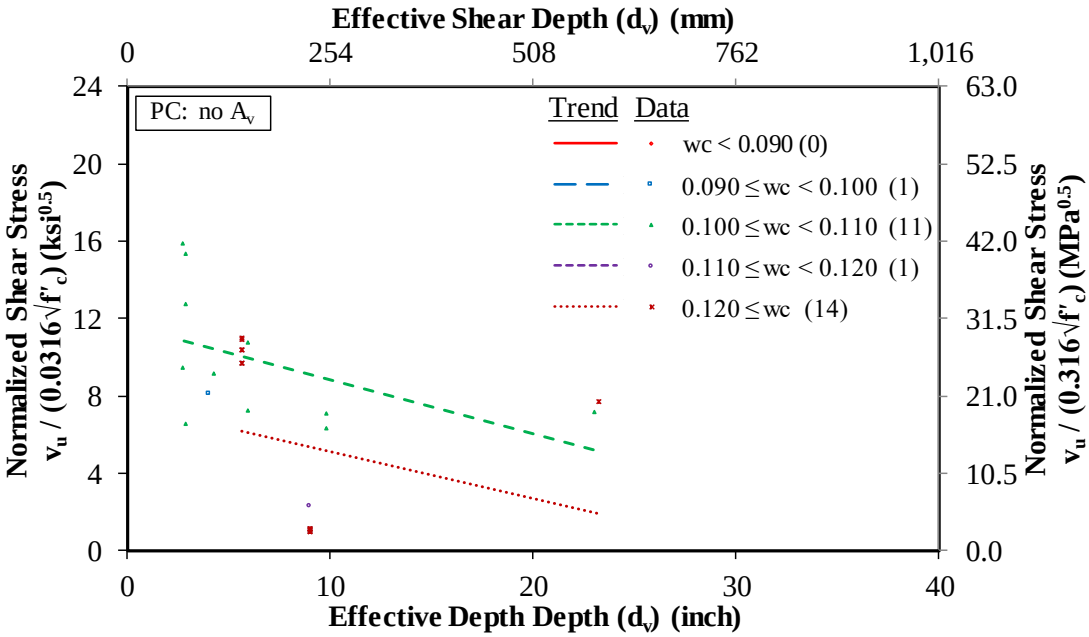

Source: FHWA.
1 ksi = 6.89 MPa.
1 inch = 25.4 mm.
Note: Unit weight (w_c) in the legend is measured in kcf where 1 kcf = 16,020 kg/m^3.

Figure 80. Graph. Normalized shear stress compared to effective shear depth for LWC PC members without shear reinforcement in the TFHRC shear database.

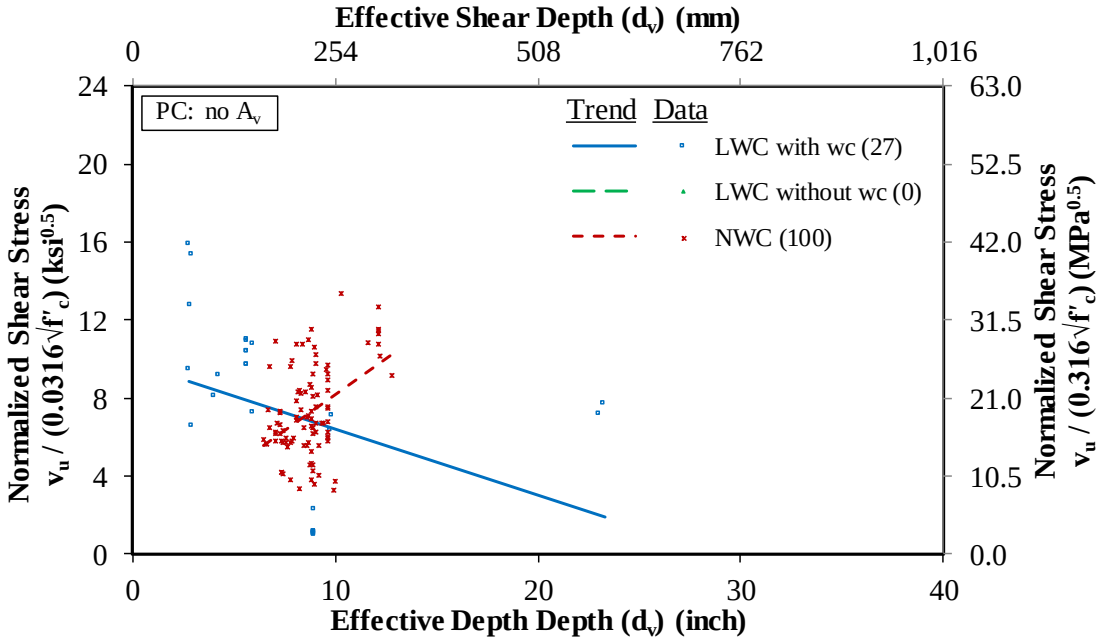

Source: FHWA.
1 ksi = 6.89 MPa.
1 inch = 25.4 mm.

Figure 81. Graph. Normalized shear stress compared to effective shear depth for LWC and NWC PC members without shear reinforcement in the TFHRC shear database.

PC Specimens With Shear Reinforcement

Figure 82 and figure 83 show a comparison of v_u normalized by f'_c to the shear reinforcement ratio ($A_v/b_v s$) multiplied by stirrup yield strength (f_y) for PC specimens with shear reinforcement. Figure 82 gives the data for specimens with a reported w_c. Figure 83 shows the data from figure 82 and selected NWC specimens from the ACI-DafStb database. Figure 82 for PC specimens with shear reinforcement appears to show a trend of normalized v_u decreasing as w_c increases, which was similar to the trend seen in figure 64 for RC specimens without shear reinforcement.

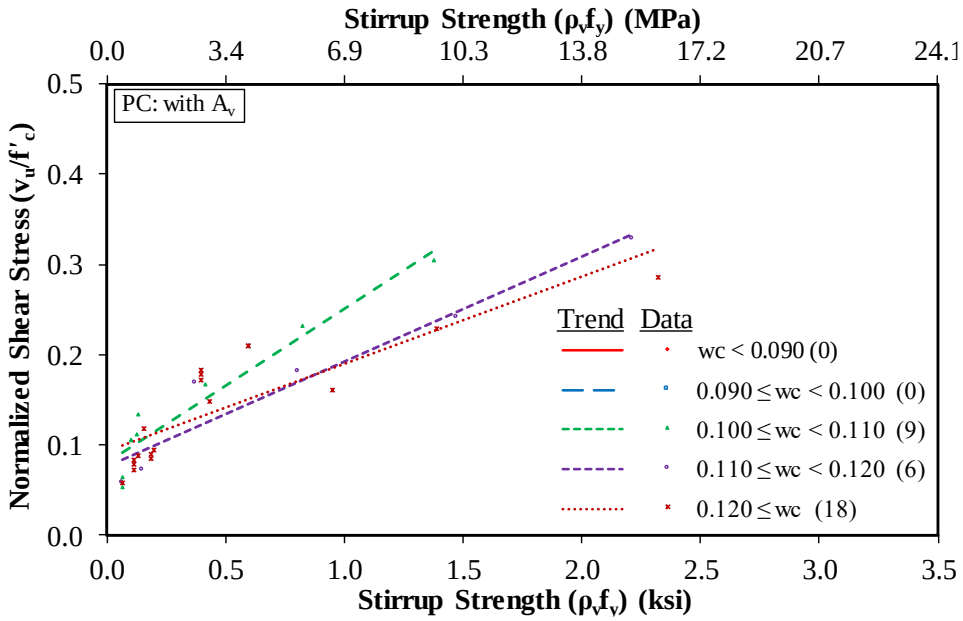

Source: FHWA.
1 ksi = 6.89 MPa.
Note: Unit weight (w_c) in the legend is measured in kcf where 1 kcf = 16,020 kg/m^3.

Figure 82. Graph. Normalized shear stress compared to stirrup strength for LWC PC members with shear reinforcement in the TFHRC shear database.

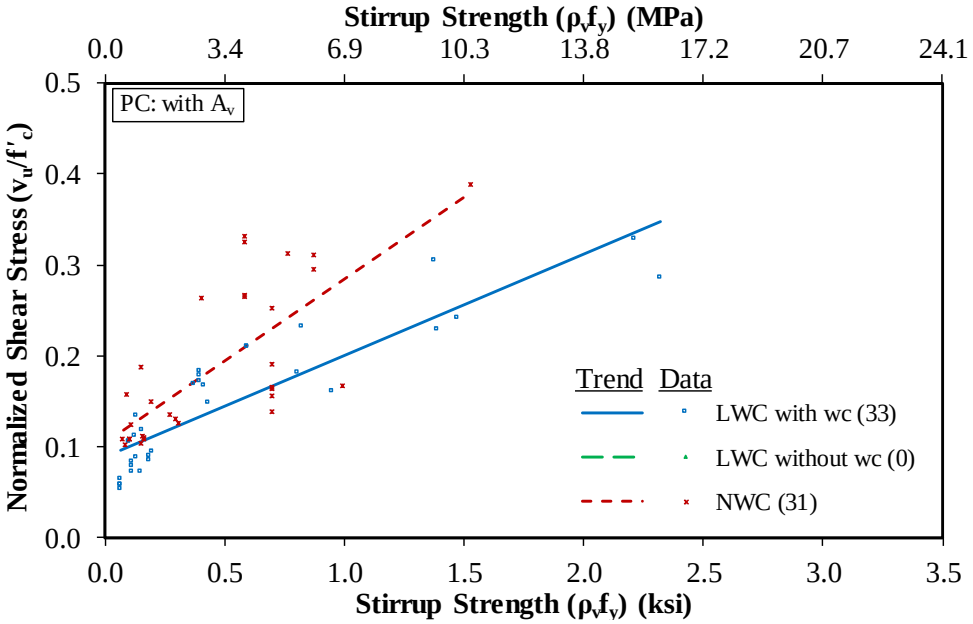

Source: FHWA.
1 ksi = 6.89 MPa.

Figure 83. Graph. Normalized shear stress compared to stirrup strength for LWC and NWC PC members with shear reinforcement in the TFHRC shear database.

Figure 84 and figure 85 show an additional comparison that was made with the shear reinforcement ratio multiplied by $f_y/\sqrt{f'_c}$. This additional comparison is in the form of an expression for the minimum amount of shear reinforcement given by equation 46, and the vertical line at a value of 0.0316 in figure 84 and figure 85 indicates the minimum amount of shear reinforcement required by the *AASHTO LRFD Bridge Design Specifications*.[3] The LWC data shown in figure 84 do not show an obvious dependence of normalized v_u on w_c. The LWC and NWC regression lines shown in figure 83 and figure 85 indicate that the line for the LWC data is lower than the NWC line. A similar trend was observed in figure 65 and figure 67 for RC specimens with shear reinforcement.

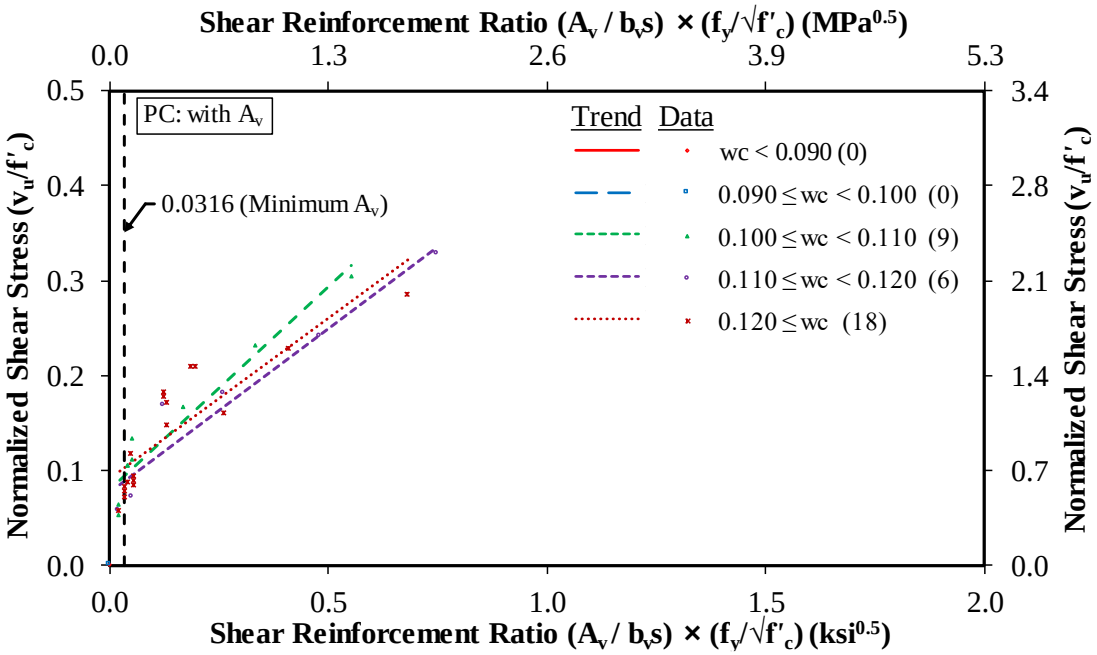

Source: FHWA.
Note: Unit weight (w_c) in the legend is measured in kcf where 1 kcf = 16,020 kg/m^3.

Figure 84. Graph. Normalized shear stress compared to shear reinforcement ratio multiplied by the ratio of stirrup yield strength to the square root of concrete compressive strength for LWC PC members with shear reinforcement in the TFHRC shear database.

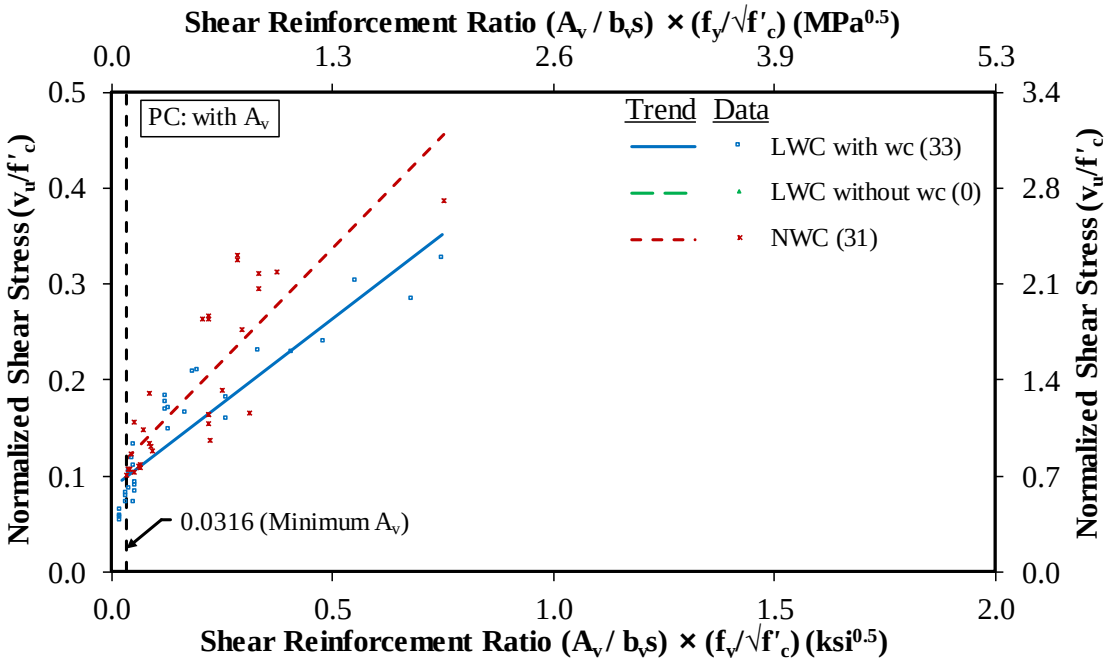

Source: FHWA.

Figure 85. Graph. Normalized shear stress compared to shear reinforcement ratio multiplied by the ratio of stirrup yield strength to the square root of concrete compressive strength for LWC and NWC PC members with shear reinforcement in the TFHRC shear database.

Figure 86 and figure 87 show a comparison of v_u normalized by f'_c to the s/d_v ratio for PC specimens with shear reinforcement. These figures are intended to show the effect of stirrup spacing on v_u. A horizontal line is shown at 0.125 v_u/f'_c. A normalized v_u below this line has a maximum stirrup spacing (s_{max}) given by equation 11, and a normalized v_u above this line has an s_{max} given by equation 12. The vertical lines in the figures at $0.4d_v$ and $0.8d_v$ represent the limit on s_{max} given by equation 11 and equation 12. Data points that are below the horizontal line at 0.125 v_u/f'_c and to the right of the vertical line at $0.8d_v$ represent tests with stirrup spacings that exceed the s_{max} given by equation 11. Similarly, stirrup spacing of the test with data points that are above the horizontal line at 0.125 v_u/f'_c and to the right of the vertical line at $0.4d_v$ exceed s_{max} given by equation 12.

As shown in figure 86, all but two LWC tests satisfy the requirements in the *AASHTO LRFD Bridge Design Specifications* for maximum stirrup spacing.[3] The stirrup spacing for both of these points is less than 0.9 s/d_v. Many of the NWC data points shown in figure 87 have stirrup spacings that exceed s_{max}.

The regression lines for the LWC and NWC data shown in figure 86 and figure 87 show a decrease in normalized v_u as the normalized stirrup spacing increases. However, as described previously for the RC data shown in figure 68 and figure 69, the data in figure 86 and figure 87 are not independent of the area of shear reinforcement, and the downward trend may be due to a decrease in the amount of shear reinforcement for the tests with large stirrup spacing.

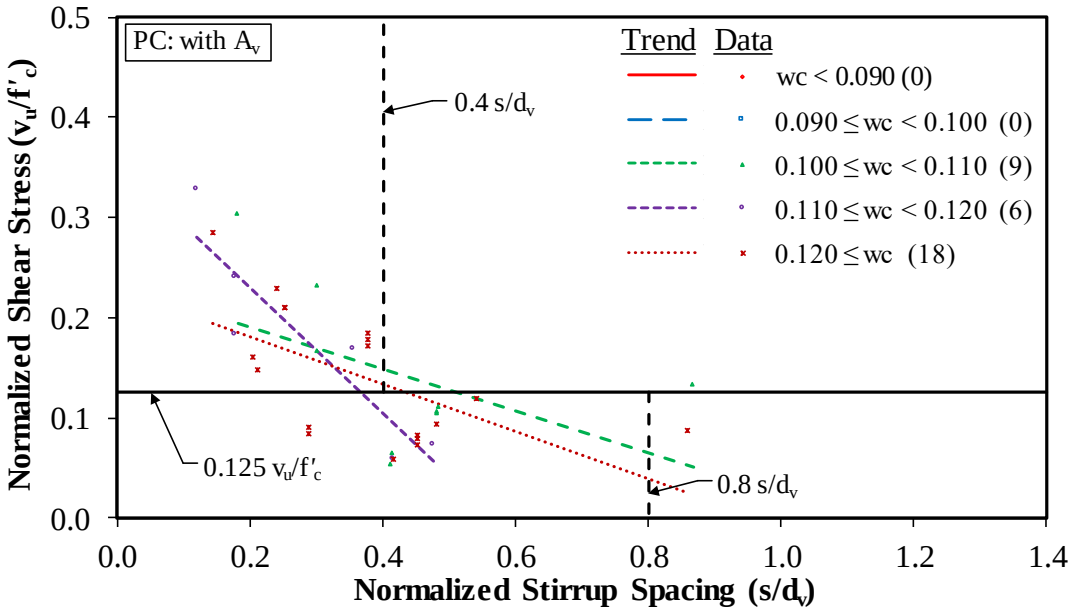

Source: FHWA.
Note: Unit weight (w_c) in the legend is measured in kcf where 1 kcf = 16,020 kg/m^3.

Figure 86. Graph. Normalized shear stress compared to normalized stirrup spacing for LWC PC members with shear reinforcement in the TFHRC shear database.

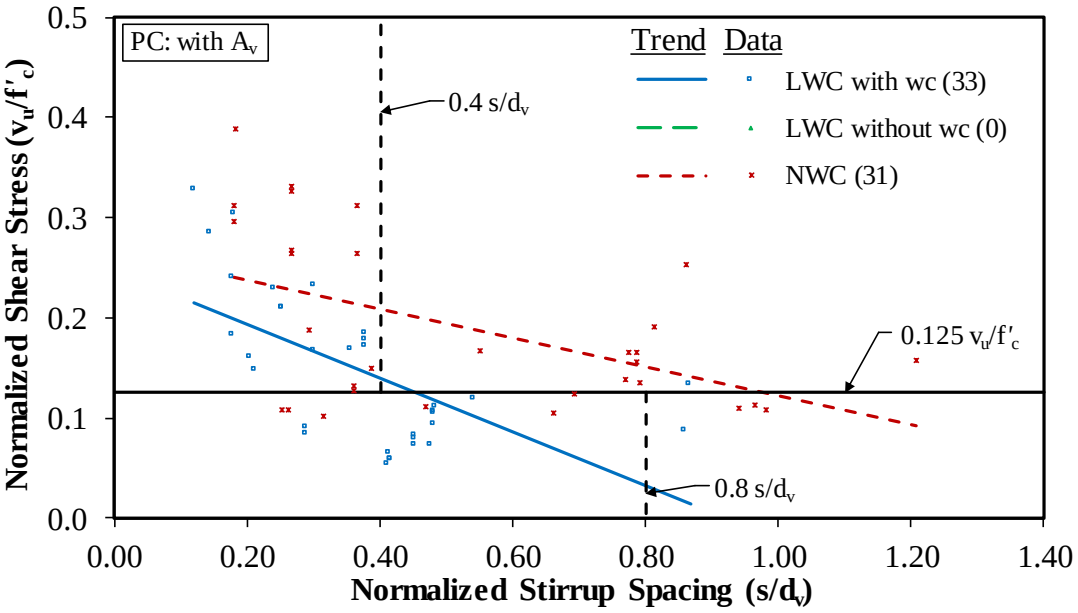

Source: FHWA.

Figure 87. Graph. Normalized shear stress compared to normalized stirrup spacing for LWC and NWC PC members with shear reinforcement in the TFHRC shear database.

Figure 88 and figure 89 show v_u normalized by the force in the shear reinforcement as given by equation 48. As shown in figure 88, there is not an obvious dependency of w_c on normalized v_u. The trend line for the LWC data points in figure 88 shows a slight decrease in the normalized v_u as s/d_v increases.

The location of the regression line for the NWC data in figure 89 for PC specimens is in a similar location to the regression line for the NWC data for RC specimens shown in figure 71. In both figures, the NWC regression line has a downward slope indicating a decrease in the normalized shear stress with increased normalized stirrup spacing. Interestingly, for LWC specimens with shear reinforcement, the regression line is above the NWC line for most of the data, while for RC specimens with shear reinforcement, the LWC regression line is below the NWC line for most of the data. The downward slope of the LWC regression line in both figure 71 and figure 89 is less than the slope of the regression line for NWC data, indicating a decreased dependence on the normalized stirrup spacing.

There are two explanations for why the LWC regression line is higher than the NWC regression line for PC specimens in figure 80 and why this trend was not observed in figure 71 for RC specimens. First, there are only two LWC data points in figure 89 with normalized stirrup spacing greater than 0.6, and in figure 71 for RC specimens, the data are more uniformly distributed across normalized stirrup spacings up to 0.9. Second, for the PC specimens, the mean compressive strength of the LWC specimens is 40 percent higher than the mean compressive strength of the NWC specimens, while for the RC specimens, the mean compressive strengths of the LWC and NWC specimens are nearly equal. The mean compressive strength of the LWC PC specimens is 9.5 ksi (65.5 MPa), while the mean compressive strength of the NWC PC specimens is 6.8 ksi (46.9 MPa). In contrast, the mean compressive strength of the LWC and NWC RC specimens is 6.3 ksi (43.4 MPa) and 6.2 ksi (42.7 MPa), respectively.

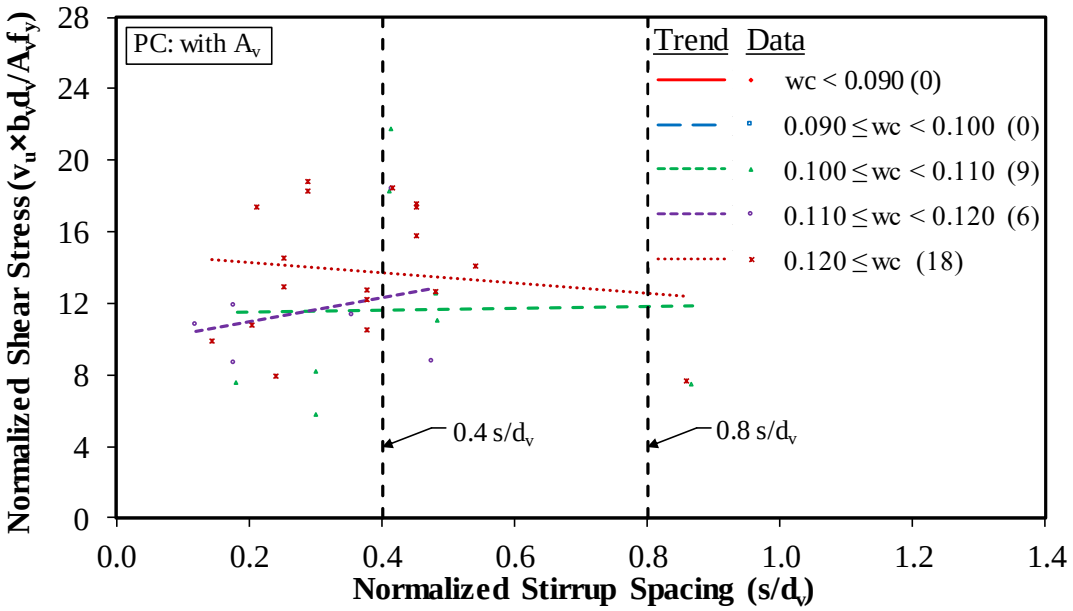

Source: FHWA.
Note: Unit weight (w_c) in the legend is measured in kcf where 1 kcf = 16,020 kg/m^3.

Figure 88. Graph. Shear stress normalized by a function accounting for the force in the shear reinforcement compared to normalized stirrup spacing for LWC PC members with shear reinforcement in the TFHRC shear database.

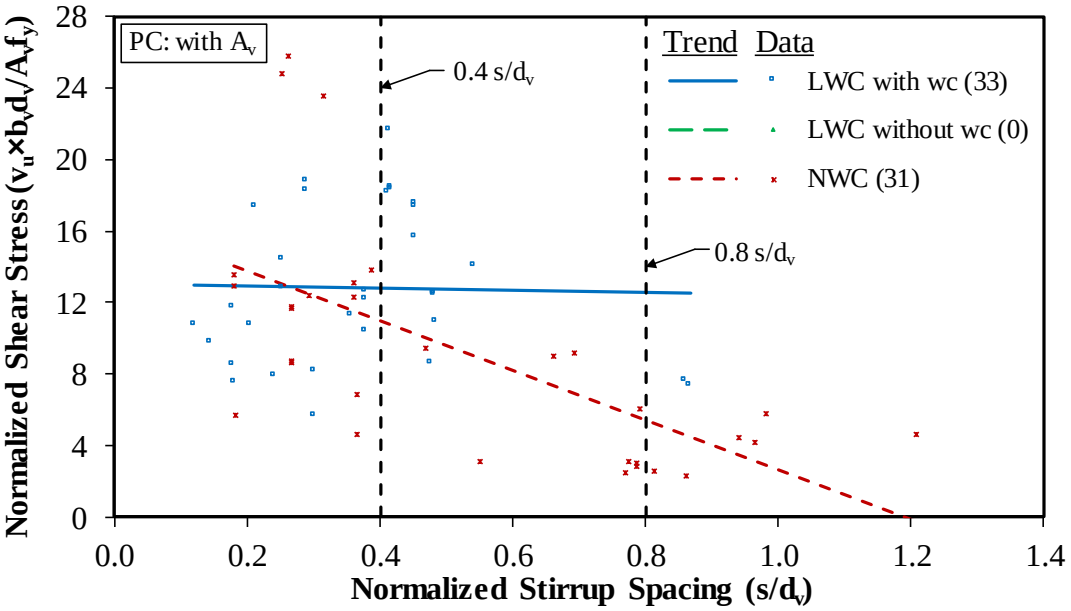

Source: FHWA.

Figure 89. Graph. Shear stress normalized by a function accounting for the force in the shear reinforcement compared to normalized stirrup spacing for LWC and NWC PC members with shear reinforcement in the TFHRC shear database.

Shear Span to Effective Depth Ratio for RC Specimens Without Shear Reinforcement

Figure 90 shows a comparison of v_u normalized $0.316\sqrt{f'_c}$ (i.e., β given by equation 43) to the net reinforcement strain (ε_s) for LWC RC specimens. The data are grouped by the shear span to effective depth ratio (a/d_v). Only specimens with an a/d_v ratio greater than or equal to 2.5 were included in the analysis described previously in this chapter. Most of the data from specimens with an a/d_v ratio greater than or equal to 4.0 were below the prediction for β given by equation 21. The normalized shear stress for some specimens with an ε_s greater than 0.001 inch/inch (0.001 mm/mm) and an a/d_v ratio between 2.5 and 3.0 were higher than specimens with a smaller a/d_v ratio. Overall, the regression lines show a clear trend of normalized shear stress increasing as the a/d_v ratio decreases.

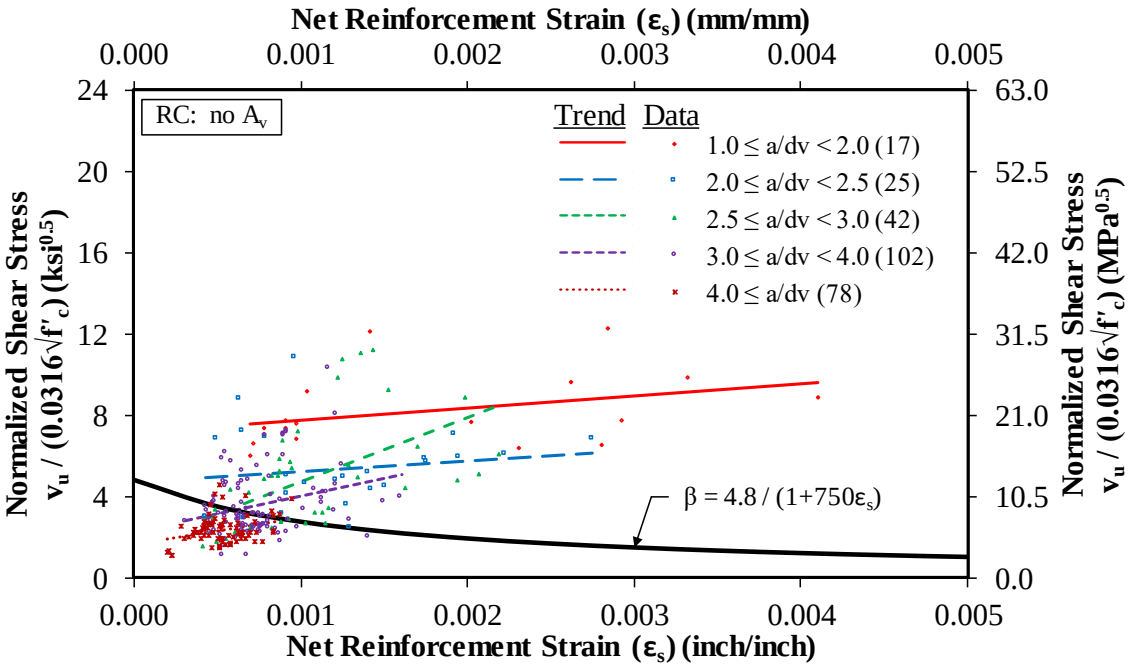

Source: FHWA.
1 ksi = 6.89 MPa.
1 inch/inch = 1 mm/mm.

Figure 90. Graph. Normalized shear stress compared to net reinforcement strain plotted by the ratio of shear span to the effective shear depth for LWC RC members without shear reinforcement in the TFHRC shear database.

Figure 91 shows a comparison of v_u normalized $0.316\sqrt{f'_c}$ (i.e., β given by equation 43) to the a/d_v ratio for LWC RC specimens. The data are grouped by unit weight (w_c). Nearly all of the regression lines for the different ranges of w_c are close to parallel and intersecting, indicating that the decrease in normalized v_u with increases in the a/d_v ratio is independent of w_c.

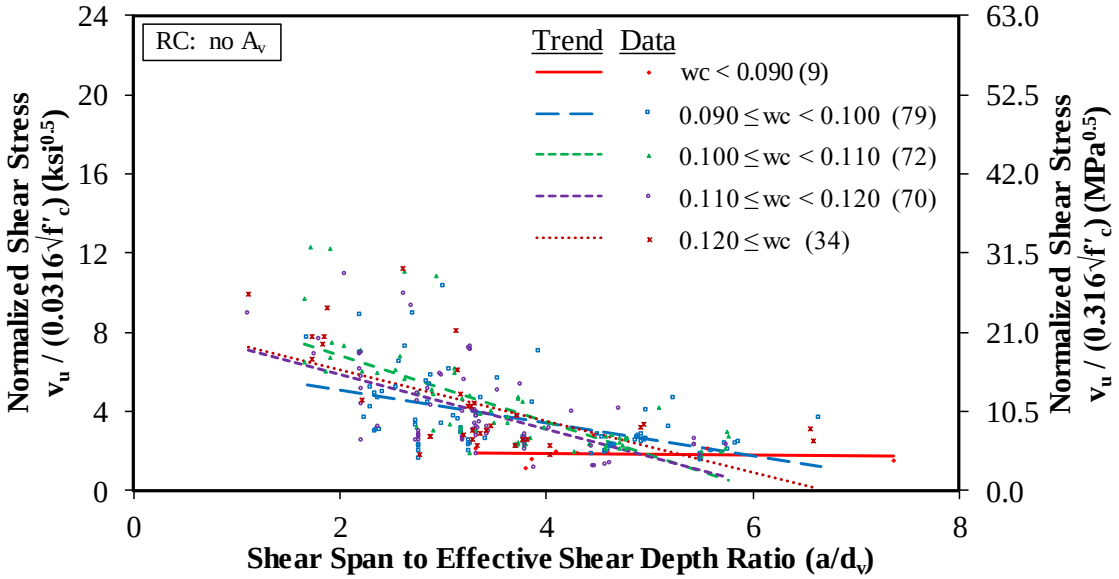

Source: FHWA.
1 ksi = 6.89 MPa.
Note: Unit weight (w_c) in the legend is measured in kcf where 1 kcf = 16,020 kg/m^3.

Figure 91. Graph. Normalized shear stress compared to the ratio of shear span to effective shear depth for LWC RC members without shear reinforcement in the TFHRC shear database.

COMPARISONS WITH PREDICTED SHEAR RESISTANCE

The following section discusses the test-to-prediction ratios for the specimens in the TFHRC shear database. The measured shear force at failure was compared to the predicted shear resistance determined using the GP-equation method, the GP-table method, and the Simplified-PC/RC method. Tests on RC specimens that satisfied the limits given in Article 5.8.3.4.1 of the *AASHTO LRFD Bridge Design Specifications* were also compared to the Simplified-RC method.[3]

The proposed expressions for shear resistance that include a λ-factor to account for LWC modification are presented. A proposed revision to the LWC modification of the expression for cot θ in the Simplified-PC/RC is described. The test-to-prediction ratios for the shear resistance of LWC specimens that included the proposed λ-factor based on w_c are discussed. Next, the test-to-prediction ratios determined using the proposed λ-factor based on w_c are compared to other methods for modification of shear resistance for LWC. Finally, the test-to-prediction ratios for LWC specimens are compared to the ratios for similar types of NWC specimens.

Proposed Expressions for Shear Resistance Including Modification Factor for LWC

Article 5.8.2.2 in the *AASHTO LRFD Bridge Design Specifications* states that all expressions in Article 5.8.2 and Article 5.8.3 shall be modified for the effects of LWC.[3] The modification consists of replacing $\sqrt{f'_c}$ with $4.7f_{ct}$ when the splitting tensile strength is specified. When f_{ct} is not specified, $\sqrt{f'_c}$ is replaced with $0.75\sqrt{f'_c}$ when all-lightweight concrete is used or $0.85\sqrt{f'_c}$ when sand-lightweight concrete is used.

A method to provide a more uniform treatment of LWC tensile strength has been proposed to section 5.4 of the *AASHTO LRFD Bridge Design Specifications* to add a definition of a modification factor for LWC, the λ-factor, which could then be referenced in other articles.[3,1] The λ-factor was previously developed from tests on LWC.[1] It is based on f_{ct} when available and w_c otherwise. The expression for the λ-factor based on w_c is given by equation 36 through equation 38, and equation 39 gives the expression for the λ-factor based on f_{ct}.

There are seven expressions in Article 5.8.2 and Article 5.8.3 with a $\sqrt{f'_c}$, and according to Article 5.8.2.2 of the *AASHTO LRFD Bridge Design Specifications*, each shall be modified for the effects of LWC.[3] A proposed expression that includes the λ-factor is described in this section for four of these current equations. The expression for the cracking torque given in Article 5.8.2.1 and the expression for the shear resistance provided by bent up bars given in Article 5.8.3.3 are beyond the scope of this report and will not be discussed. The expression for cot θ in the Simplified-PC/RC is intentionally not modified to include a λ-factor. The reason for the exclusion is described in the following section of this report.

The inclusion of the λ-factor is proposed for four expressions in Article 5.8.2 and Article 5.8.3 in the *AASHTO LRFD Bridge Design Specifications*.[3] The minimum amount of shear reinforcement in the *AASHTO LRFD Bridge Design Specifications* is given by equation 10.[3] The proposed expression is given by equation 49 and includes the λ-factor. The expression for the shear resistance provided by the concrete contribution in Article 5.8.3.3 is given by equation 16, and the proposed expression that includes the λ-factor is given by equation 50. The expressions for V_{cw} and V_{ci} that are part of the Simplified-PC/RC are given by equation 28 and equation 29, and the proposed expressions are given by equation 51 and equation 52.

$$A_v \geq 0.0316\lambda\sqrt{f'_c}\frac{b_v s}{f_y} \tag{49}$$

$$V_c = 0.0316\beta\lambda\sqrt{f'_c}b_v d_v \tag{50}$$

$$V_{cw} = \left(0.06\lambda\sqrt{f'_c} + 0.3f_{pc}\right)b_v d_v + V_p \tag{51}$$

$$V_{ci} = 0.02\lambda\sqrt{f'_c}b_v d_v + V_d + \frac{V_i M_{cre}}{M_{max}} \geq 0.06\lambda\sqrt{f'_c}b_v d_v \tag{52}$$

Removal of the Modification for LWC on Cot Theta of the Simplified-PC/RC Procedure

Article 5.8.2.2 of the *AASHTO LRFD Bridge Design Specifications* states that all expressions in Article 5.8.2 and Article 5.8.3 shall be modified for the effects of LWC.[3] This includes the expression for cot θ, given by equation 35, in the Simplified-PC/RC when V_{ci} is greater than V_{cw}. An expression for cot θ including the λ-factor is provided in equation 53.

$$cot\,\theta = 1.0 + 3\left(\frac{f_{pc}}{\lambda\sqrt{f'_c}}\right) \leq 1.8 \tag{53}$$

Cot θ determined using equation 35 or equation 53 will only affect the shear resistance determined for PC specimens with shear reinforcement. Cot θ is used in V_s given by equation 17 to determine the contribution of the shear reinforcement.

The test-to-prediction ratios for the Simplified-PC/RC procedure are shown in table 34 for PC specimens with shear reinforcement. They compare the modification based on unit weight (i.e., the proposed λ-factor based on w_c) (see equation 36 through equation 38), the modification based on concrete type (i.e., all-lightweight and sand-lightweight) currently used in the *AASHTO LRFD Bridge Design Specifications* (i.e., AASHTO modified), and modification based on f_{ct} (i.e., the proposed λ-factor based on f_{ct}) (see equation 39).[3] The test-to-prediction ratios in table 34 are also compared by the shear resistance determined without modification for LWC concrete (i.e., no modification for the λ-factor taken as 1) and the shear resistance determined with modification for LWC concrete included in the determination of V_c (lesser of equation 51 and equation 52). Two cases were considered when modification for LWC concrete was included in the determination of V_c: modification of cot θ (i.e., modification of V_c and cot θ using equation 53) and no modification of cot θ (i.e., modification of V_c only using equation 35).

Table 34. Test-to-prediction ratio of shear resistance for Simplified-PC/RC with and without LWC modification for LWC PC specimens with shear reinforcement in the TFHRC shear database.

LWC Modification and Specimen Group*	Simplified-PC/RC Modification for LWC	Mean	COV (Percent)	Maximum	Minimum	Percent Test-to-Prediction Ratio	
						<1.0	<0.8
Proposed λ-factor based on w_c, PC with A_v (33)	No modification	1.29	16.4	1.98	0.98	3.0	0.0
Proposed λ-factor based on w_c, PC with A_v (33)	Modification of V_c and cot θ	1.30	17.4	2.00	0.96	6.1	0.0
Proposed λ-factor based on w_c, PC with A_v (33)	Modification of V_c only	1.32	17.6	2.00	0.99	3.0	0.0
AASHTO modified PC with A_v (21)	No modification	1.28	19.1	1.98	0.98	4.8	0.0
AASHTO modified PC with A_v (21)	Modification of V_c and cot θ	1.31	21.3	2.05	0.95	9.5	0.0
AASHTO modified PC with A_v (21)	Modification of V_c only	1.35	21.2	2.09	1.00	0.0	0.0
Proposed λ-factor based on f_{ct}, PC with A_v (33)	No modification	1.29	16.4	1.98	0.98	3.0	0.0
Proposed λ-factor based on f_{ct}, PC with A_v (33)	Modification of V_c and cot θ	1.32	18.2	2.05	0.95	6.1	0.0
Proposed λ-factor based on f_{ct}, PC with A_v (33)	Modification of V_c only	1.35	18.6	2.09	1.00	3.0	0.0

*The number of specimens is shown in parentheses.

A comparison of the test-to-prediction ratios in table 34 shows that the mean ratios determined with modification for LWC were higher than the ratios determined without modification for LWC. However, the minimum test-to-prediction ratios determined by including the λ-factor in the expression for cot θ were less than the minimum ratios determined without modification for LWC. The minimum ratio determined using the modification for LWC in the *AASHTO LRFD Bridge Design Specifications* (AASHTO modified) and by including the LWC modification in the term for cot θ (modification of V_c and cot θ) was 0.95, which was less than the minimum ratio of 0.98 determined without modification for LWC. This indicates that V_n determined for an LWC PC girder using the Simplified-PC/RC procedure in the current *AASHTO LRFD Bridge Design Specifications* could be higher than the shear resistance determined for an identical NWC girder.[3] An identical girder would have the same cross section (b_v, d_v), design material properties (f'_c and f_y), reinforcement (A_v/s and f_{pc}), and internal forces (V_d and $V_i M_{cre}/M_{max}$).

The effect of including the modification for LWC in cot θ was evaluated by examining the ratio V_c, θ, V_s, and V_n determined by including the λ-factor in the expressions for V_c and the expression for cot θ to the same terms determined without modification for LWC. The ratio of these four terms are given in table 35 and were determined using the λ-factor based on w_c (see equation 36 through equation 38). All 33 PC specimens with shear reinforcement (PC with A_v) in the TFHRC shear database had a calculated V_{ci} greater than its calculated V_{cw}, and as a result, cot θ was determined using equation 35 or equation 53. The ratio of V_c was equal to the λ-factor itself and was slightly less than 1.0 for all values. The ratio of θ was less than or equal to 1.0, indicating that the predicted angle of compressive stresses was smaller if cot θ included the λ-factor (i.e., a predicted angle closer to horizontal). A smaller predicted angle results in an increase in the predicted contribution of the stirrups to the nominal shear resistance (i.e., larger V_s), as shown by the ratio of V_s in table 35. The ratio of V_s had a mean value of 1.03 and a maximum value of 1.09. V_s for nearly 70 percent of the LWC PC specimens with shear reinforcement in the TFHRC shear database determined by including the modification for LWC in the expression for cot θ were larger than if no modification for LWC had been included. The remaining LWC PC specimens with shear reinforcement had a ratio of V_s equal to 1.0 (i.e., the same V_s determined for both).

Table 35. Ratio of terms for shear resistance determined using Simplified-PC/RC with and without LWC modification included in the expression for cot θ for LWC PC specimens with shear reinforcement in the TFHRC shear database.

Specimen Group[a]	Simplified-PC/RC Ratio of Predictions	Term[b]	Mean	Maximum	Minimum	Percent Test-to-Prediction Ratio >1.0
Proposed λ-factor based on w_c, PC with A_v where $V_{ci} > V_{cw}$ (33)	Modification of V_c and cot θ/no modification	V_c (λ)	0.95	0.99	0.86	0.0
Proposed λ-factor based on w_c, PC with A_v where $V_{ci} > V_{cw}$ (33)	Modification of V_c and cot θ/no modification	θ	0.98	1.00	0.93	0.0
Proposed λ-factor based on w_c, PC with A_v where $V_{ci} > V_{cw}$ (33)	Modification of V_c and cot θ/no modification	V_s	1.03	1.09	1.00	69.7
Proposed λ-factor based on w_c, PC with A_v where $V_{ci} > V_{cw}$ (33)	Modification of V_c and cot θ/no modification	V_n	0.99	1.05	0.94	18.2
Proposed λ-factor based on w_c, PC with A_v where $V_{ci} > V_{cw}$ (33)	Modification of V_c only/no modification	V_n	0.98	1.00	0.91	0.0

[a]The number of specimens is shown in parentheses.
[b]The ratio for V_c is equal to the λ-factor.

Similar ratios for θ and V_s determined by including the λ-factor in the expressions for V_c but not in the expression for cot θ to the same θ and V_s determined without modification for LWC would all be 1.0 and are not given in table 35. The maximum ratio for shear resistance is 1.0, indicating that by using equation 35 to determine cot θ, V_n was always less than or equal to V_n determined without modification for LWC. The test-to-prediction ratios for the Simplified-PC/RC procedure in the remainder of this chapter all include cot θ determined using equation 35.

Test-to-Prediction Ratios for Shear Resistance Including Proposed LWC Modification Factor

This section includes several tables with the test-to-prediction ratios for the proposed λ-factor based on w_c given by equation 36 through equation 38. The ratios are given by the method used to determined shear resistance, specimen type, w_c, by concrete-mixture type.

The test-to-prediction ratios are shown in table 36 for all LWC specimens and by specimen type. For all of the specimens, the GP-equation and GP-table methods had similar ratios at 1.32 and 1.39, respectively. The Simplified-PC/RC procedure gave a more conservative prediction at 2.07. The COV for the three methods was high at nearly 50 percent for the general procedure methods and nearly 60 percent for the Simplified-PC/RC procedure. All three methods had more conservative predictions for the RC specimens without shear reinforcement (i.e., RC specimens without A_v) than for RC specimens with shear reinforcement (i.e., RC specimens with A_v). A similar trend was observed for PC specimens with and without shear reinforcement. All three methods gave more conservative predictions for PC specimens without shear reinforcement (i.e., PC specimens without A_v) than for RC specimens without shear reinforcement. The two general procedure methods also gave more conservative predictions for PC specimens with shear reinforcement (i.e., PC specimens with A_v) than for RC specimens with shear reinforcement. For the Simplified-PC/RC procedure, however, the prediction of RC specimens with shear reinforcement was more conservative than for PC specimens with shear reinforcement.

Table 36. Test-to-prediction ratio of shear resistance for design expressions with proposed expression for the λ-factor for LWC specimens in the TFHRC shear database.

Specimen Group*	Design Expression	Mean	COV (Percent)	Maximum	Minimum	Percent Test-to-Prediction Ratio	
						<1.0	<0.8
Proposed λ-factor based on w_c, all specimens (326)	GP-equation	1.33	48.9	4.13	0.43	34.0	9.2
Proposed λ-factor based on w_c, all specimens (326)	GP-table	1.40	47.5	4.19	0.46	24.8	6.1
Proposed λ-factor based on w_c, all specimens (326)	Simplified-PC/RC	2.09	58.3	7.43	0.43	5.2	3.7
Proposed λ-factor based on w_c, RC specimens without A_v (222)	GP-equation	1.30	47.5	3.85	0.43	39.2	9.5
Proposed λ-factor based on w_c, RC specimens without A_v (222)	GP-table	1.41	46.4	4.19	0.46	25.7	5.0
Proposed λ-factor based on w_c, RC specimens without A_v (222)	Simplified-PC/RC	2.21	54.0	7.43	0.67	3.2	2.3
Proposed λ-factor based on w_c, RC specimens with A_v (44)	GP-equation	1.12	18.9	1.62	0.75	36.4	4.5
Proposed λ-factor based on w_c, RC specimens with A_v (44)	GP-table	1.14	23.7	1.87	0.72	36.4	4.5
Proposed λ-factor based on w_c, RC specimens with A_v (44)	Simplified-PC/RC	1.57	22.4	2.50	0.93	4.5	0.0
Proposed λ-factor based on w_c, PC specimens without A_v (27)	GP-equation	2.08	54.9	4.13	0.56	25.9	25.9
Proposed λ-factor based on w_c, PC specimens without A_v (27)	GP-table	2.03	54.9	3.89	0.54	25.9	25.9
Proposed λ-factor based on w_c, PC specimens without A_v (27)	Simplified-PC/RC	2.92	70.3	6.80	0.43	25.9	25.9
Proposed λ-factor based on w_c, PC specimens with A_v (33)	GP-equation	1.24	10.0	1.52	0.97	3.0	0.0
Proposed λ-factor based on w_c, PC specimens with A_v (33)	GP-table	1.24	11.5	1.52	0.98	3.0	0.0
Proposed λ-factor based on w_c, PC specimens with A_v (33)	Simplified-PC/RC	1.32	17.6	2.00	0.99	3.0	0.0

*The number of specimens is shown in parentheses.

Table 37 through table 40 provide the test-to-prediction ratios for a particular specimen type. The ratios are given in groups by ranges of w_c and then by concrete-mixture type. Table 37 and table 38 shows ratios for RC specimens without and with shear reinforcement, respectively. The ratios for PC specimens without and with shear reinforcement are shown in table 39 and table 40. The test-to-prediction ratios in these tables give the same trend as for the specimens as a whole: the two general procedure methods give similar ratios, and the ratio for the Simplified-PC/RC procedure is higher. The most obvious exception is the ratios for the seven SDC PC specimens without shear reinforcement in table 39. All seven of these specimens were from the same study, and the low ratios for these specimens are observed throughout the tables and figures in this section.

Table 37. Test-to-prediction ratio of shear resistance for design expressions with proposed expression for the λ-factor for LWC RC specimens without stirrups in the TFHRC shear database.

Unit Weight Range or Concrete-Mixture Type*	Design Expression	Mean	COV (Percent)	Maximum	Minimum	Percent Test-to-Prediction Ratio	
						<1.0	<0.8
w_c < 0.090 kcf (9)	GP-equation	0.83	24.1	1.22	0.59	77.8	66.7
w_c < 0.090 kcf (9)	GP-table	0.91	22.2	1.31	0.65	66.7	33.3
w_c < 0.090 kcf (9)	Simplified-PC/RC	1.32	25.3	1.98	0.78	11.1	11.1
0.090 kcf ≤ w_c < 0.100 kcf (67)	GP-equation	1.36	51.5	3.85	0.74	46.3	7.5
0.090 kcf ≤ w_c < 0.100 kcf (67)	GP-table	1.48	51.4	4.19	0.79	28.4	1.5
0.90 kcf ≤ w_c < 0.100 kcf (67)	Simplified-PC/RC	2.31	54.1	7.24	1.05	0.0	0.0
0.100 kcf ≤ w_c < 0.110 kcf (61)	GP-equation	1.33	44.6	3.74	0.80	32.8	1.6
0.100 kcf ≤ w_c < 0.110 kcf (61)	GP-table	1.45	42.7	3.87	0.88	16.4	0.0
0.100 kcf ≤ w_c < 0.110 kcf (61)	Simplified-PC/RC	2.31	51.9	7.43	1.15	0.0	0.0
0.110 kcf ≤ w_c < 0.120 kcf (58)	GP-equation	1.30	45.0	3.13	0.43	31.0	12.1
0.110 kcf ≤ w_c < 0.120 kcf (58)	GP-table	1.40	43.5	3.23	0.46	25.9	8.6
0.110 kcf ≤ w_c < 0.120 kcf (58)	Simplified-PC/RC	2.18	53.9	6.11	0.67	8.6	6.9
0.120 kcf ≤ w_c (27)	GP-equation	1.22	45.9	3.35	0.69	40.7	7.4
0.120 kcf ≤ w_c (27)	GP-table	1.32	44.1	3.47	0.75	25.9	7.4
0.120 kcf ≤ w_c (27)	Simplified-PC/RC	2.03	56.2	6.41	0.94	3.7	0.0
All-lightweight (119)	GP-equation	1.26	47.5	3.85	0.59	47.9	10.9
All-lightweight (119)	GP-table	1.37	47.2	4.19	0.65	29.4	3.4
All-lightweight (119)	Simplified-PC/RC	2.13	51.5	7.24	0.78	0.8	0.8
Sand-lightweight (103)	GP-equation	1.35	47.4	3.74	0.43	29.1	7.8
Sand-lightweight (103)	GP-table	1.45	45.4	3.87	0.46	21.4	6.8
Sand-lightweight (103)	Simplified-PC/RC	2.29	56.3	7.43	0.67	5.8	3.9

1 kcf = 16,020 kg/m^3.

*The number of specimens is shown in parentheses.

Table 38. Test-to-prediction ratio of shear resistance for design expressions with proposed expression for the λ-factor for LWC RC specimens with stirrups in the TFHRC shear database.

Unit Weight Range or Concrete-Mixture Type*	Design Expression	Mean	COV (Percent)	Maximum	Minimum	Percent Test-to-Prediction Ratio	
						<1.0	<0.8
w_c < 0.090 kcf (7)	GP-equation	0.97	15.8	1.14	0.75	57.1	14.3
w_c < 0.090 kcf (7)	GP-table	0.96	15.3	1.14	0.75	57.1	14.3
w_c < 0.090 kcf (7)	Simplified-PC/RC	1.51	21.6	1.94	1.06	0.0	0.0
0.090 kcf ≤ w_c < 0.100 kcf (3)	GP-equation	1.13	8.7	1.24	1.05	0.0	0.0
0.090 kcf ≤ w_c < 0.100 kcf (3)	GP-table	1.12	9.5	1.24	1.04	0.0	0.0
0.090 kcf ≤ w_c < 0.100 kcf (3)	Simplified-PC/RC	1.55	17.7	1.73	1.24	0.0	0.0
0.100 kcf ≤ w_c < 0.110 kcf (13)	GP-equation	1.18	17.6	1.56	0.92	23.1	0.0
0.100 kcf ≤ w_c < 0.110 kcf (13)	GP-table	1.21	26.1	1.83	0.88	30.8	0.0
0.100 kcf ≤ w_c < 0.110 kcf (13)	Simplified-PC/RC	1.68	24.1	2.50	1.04	0.0	0.0
0.110 kcf ≤ w_c < 0.120 kcf (7)	GP-equation	1.21	22.4	1.50	0.75	28.6	14.3
0.110 kcf ≤ w_c < 0.120 kcf (7)	GP-table	1.25	22.5	1.59	0.72	14.3	14.3
0.110 kcf ≤ w_c < 0.120 kcf (7)	Simplified-PC/RC	1.65	23.6	2.08	1.04	0.0	0.0
0.120 kcf ≤ w_c (14)	GP-equation	1.09	18.8	1.62	0.90	50.0	0.0
0.120 kcf ≤ w_c (14)	GP-table	1.11	24.1	1.87	0.87	50.0	0.0
0.120 kcf ≤ w_c (14)	Simplified-PC/RC	1.45	20.7	1.98	0.93	14.3	0.0
All-lightweight (9)	GP-equation	1.05	21.3	1.48	0.75	44.4	11.1
All-lightweight (9)	GP-table	1.08	27.0	1.73	0.75	44.4	11.1
All-lightweight (9)	Simplified-PC/RC	1.48	19.9	1.94	1.06	0.0	0.0
Sand-lightweight (34)	GP-equation	1.12	17.3	1.56	0.75	35.3	2.9
Sand-lightweight (34)	GP-table	1.14	21.2	1.83	0.72	35.3	2.9
Sand-lightweight (34)	Simplified-PC/RC	1.59	23.3	2.50	0.93	5.9	0.0

1 kcf = 16,020 kg/m^3.

*The number of specimens is shown in parentheses.

Table 39. Test-to-prediction ratio of shear resistance for design expressions with proposed expression for the λ-factor for LWC PC specimens without stirrups in the TFHRC shear database.

Unit Weight Range or Concrete-Mixture Type*	Design Expression	Mean	COV (Percent)	Maximum	Minimum	Percent Test-to-Prediction Ratio	
						<1.0	<0.8
0.090 kcf ≤ w_c < 0.100 kcf (1)	GP-equation	2.44	—	2.44	2.44	0.0	0.0
0.090 kcf ≤ w_c < 0.100 kcf (1)	GP-table	2.41	—	2.41	2.41	0.0	0.0
0.090 kcf ≤ w_c < 0.100 kcf (1)	Simplified-PC/RC	4.55	—	4.55	4.55	0.0	0.0
0.100 kcf ≤ w_c < 0.110 kcf (11)	GP-equation	2.51	38.8	4.13	1.41	0.0	0.0
0.100 kcf ≤ w_c < 0.110 kcf (11)	GP-table	2.43	37.2	3.89	1.38	0.0	0.0
0.100 kcf ≤ w_c < 0.110 kcf (11)	Simplified-PC/RC	3.82	50.1	6.80	1.36	0.0	0.0
0.110 kcf ≤ w_c < 0.120 kcf (1)	GP-equation	1.28	—	1.28	1.28	0.0	0.0
0.110 kcf ≤ w_c < 0.120 kcf (1)	GP-table	1.24	—	1.24	1.24	0.0	0.0
0.110 kcf ≤ w_c < 0.120 kcf (1)	Simplified-PC/RC	1.10	—	1.10	1.10	0.0	0.0
0.120 kcf ≤ w_c (14)	GP-equation	1.77	70.5	3.30	0.56	50.0	50.0
0.120 kcf ≤ w_c (14)	GP-table	1.74	71.9	3.28	0.54	50.0	50.0
0.120 kcf ≤ w_c (14)	Simplified-PC/RC	2.22	89.1	4.69	0.43	50.0	50.0
All-lightweight (11)	GP-equation	2.57	36.9	4.13	1.41	0.0	0.0
All-lightweight (11)	GP-table	2.47	36.3	3.89	1.38	0.0	0.0
All-lightweight (11)	Simplified-PC/RC	4.11	42.3	6.80	1.82	0.0	0.0
Sand-lightweight (9)	GP-equation	2.62	28.8	3.30	1.28	0.0	0.0
Sand-lightweight (9)	GP-table	2.62	28.0	3.28	1.24	0.0	0.0
Sand-lightweight (9)	Simplified-PC/RC	3.37	46.1	4.69	1.10	0.0	0.0
Specified density (7)	GP-equation	0.61	5.7	0.65	0.56	100.0	100.0
Specified density (7)	GP-table	0.58	5.4	0.62	0.54	100.0	100.0
Specified density (7)	Simplified-PC/RC	0.46	5.7	0.49	0.43	100.0	100.0

1 kcf = 16,020 kg/m^3.
*The number of specimens is shown in parentheses.
—Calculation was not applicable for one data point.

Table 40. Test-to-prediction ratio of shear resistance for design expressions with proposed expression for the λ-factor for LWC PC specimens with stirrups in the TFHRC shear database.

Unit Weight Range or Concrete-Mixture Type*	Design Expression	Mean	COV (Percent)	Maximum	Minimum	Percent Test-to-Prediction Ratio	
						<1.0	<0.8
0.100 kcf ≤ w_c < 0.110 kcf (9)	GP-equation	1.25	9.7	1.39	1.03	0.0	0.0
0.100 kcf ≤ w_c < 0.110 kcf (9)	GP-table	1.24	11.4	1.42	1.02	0.0	0.0
0.100 kcf ≤ w_c < 0.110 kcf (9)	Simplified-PC/RC	1.41	20.3	1.80	1.03	0.0	0.0
0.110 kcf ≤ w_c < 0.120 kcf (6)	GP-equation	1.16	10.5	1.31	0.97	16.7	0.0
0.110 kcf ≤ w_c < 0.120 kcf (6)	GP-table	1.14	12.1	1.31	0.98	16.7	0.0
0.110 kcf ≤ w_c < 0.120 kcf (6)	Simplified-PC/RC	1.20	10.4	1.32	0.99	16.7	0.0
0.120 kcf ≤ w_c (18)	GP-equation	1.27	9.7	1.52	1.11	0.0	0.0
0.120 kcf ≤ w_c (18)	GP-table	1.28	10.6	1.52	1.01	0.0	0.0
0.120 kcf ≤ w_c (18)	Simplified-PC/RC	1.31	16.7	2.00	1.06	0.0	0.0
All-lightweight (12)	GP-equation	1.20	10.8	1.39	0.97	8.3	0.0
All-lightweight (12)	GP-table	1.19	11.6	1.36	0.98	8.3	0.0
All-lightweight (12)	Simplified-PC/RC	1.36	20.2	1.80	0.99	8.3	0.0
Sand-lightweight (9)	GP-equation	1.25	9.2	1.42	1.14	0.0	0.0
Sand-lightweight (9)	GP-table	1.25	11.8	1.45	1.04	0.0	0.0
Sand-lightweight (9)	Simplified-PC/RC	1.30	22.1	2.00	1.06	0.0	0.0
Specified density (11)	GP-equation	1.29	9.3	1.52	1.15	0.0	0.0
Specified density (11)	GP-table	1.31	8.4	1.52	1.19	0.0	0.0
Specified density (11)	Simplified-PC/RC	1.32	10.1	1.54	1.12	0.0	0.0
Inverted mix (1)	GP-equation	1.11	—	1.11	1.11	0.0	0.0
Inverted mix (1)	GP-table	1.01	—	1.01	1.01	0.0	0.0
Inverted mix (1)	Simplified-PC/RC	1.12	—	1.12	1.12	0.0	0.0

1 kcf = 16,020 kg/m^3.
*The number of specimens is shown in parentheses.
—Calculation was not applicable for one data point.

Comparison of the Basis for the LWC Modification Factor on Test-to-Prediction Ratio for Shear Resistance

This section includes figures and tables that provide comparisons of the method used to determine the LWC modification factor on the predicted shear resistance. Test-to-prediction ratios were determined for the specimens based on four different methods to account for LWC. These methods include no modification for LWC, the modification given in the current *AASHTO LRFD Bridge Design Specifications* based on mixture type, the proposed λ-factor based on w_c, and the proposed λ-factor based on splitting tensile strength.[3] The effect that the four methods of LWC modification have on the test-to-prediction ratios is given for each of the four design procedures in the *AASHTO LRFD Bridge Design Specifications*.[3]

The number of specimens given in each comparison depended on the information reported. The number of specimens in all of the figures and tables in this section was limited to the specimens with a w_c. The ratios determined using the method in the *AASHTO LRFD Bridge Design Specifications* were further limited to the specimens with all-lightweight or sand-lightweight concrete.[3] The ratios determined using the proposed λ-factor based on splitting tensile strength were limited to specimens with a reported splitting tensile strength.

Figure 92 and figure 93 show the ratios for the Simplified-RC procedure. In each figure, the ratios are compared to w_c, shown in groups by specimen type, and limited to RC specimens without and with shear reinforcement. Least squares regression lines are shown for the specimens in each group. Figure 92 shows the ratios determined without modification for LWC (i.e., no modification), and figure 93 shows the ratios determined using λ based on w_c. Note that the number of specimens is shown in parentheses in the legends for all remaining graphs found in this chapter (i.e., figure 92 through figure 165).

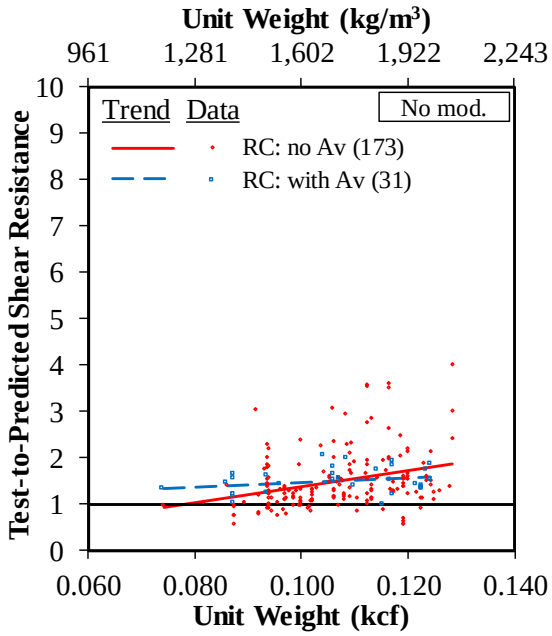

Source: FHWA.
1 kcf = 16,020 kg/m³.

Figure 92. Graph. Test-to-predicted shear resistance compared to unit weight for Simplified-RC with no LWC modification.

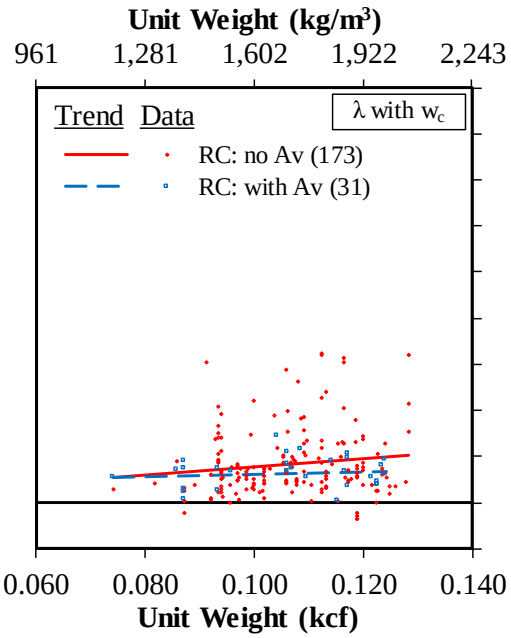

Source: FHWA.
1 kcf = 16,020 kg/m³.

Figure 93. Graph. Test-to-predicted shear resistance compared to unit weight for Simplified-RC with modification determined using proposed expression for the λ-factor based on w_c.

Figure 94 shows the ratios determined using the modification given in the *AASHTO LRFD Bridge Design Specifications* (i.e., AASHTO modified), and figure 95 shows the ratios determined using the λ-factor based on f_{ct}.[(3)] The ratios shown in figure 93 and figure 94 for the proposed λ-factor based on w_c and AASHTO modified appear similar and are shifted slightly higher than the ratios determined without modification. There were fewer specimens reported with a splitting tensile strength. The ratios shown for the proposed λ-factor based on f_{ct} appeared more scattered than the other methods for determining LWC modification, but most of the ratios were still greater than 1.0, indicating a conservative prediction. The trend line for the RC specimens with shear reinforcement was greater than 1.0 and nearly horizontal, indicating that there was no obvious trend in the test-to-prediction ratios with increasing unit weight. For the RC specimens without shear reinforcement, the trend line was greater than 1.0 and inclined slightly upward, indicating that the ratios increased as w_c increased. This increase is observed in the figures for all three methods of accounting for LWC and in the figure for no modification for LWC.

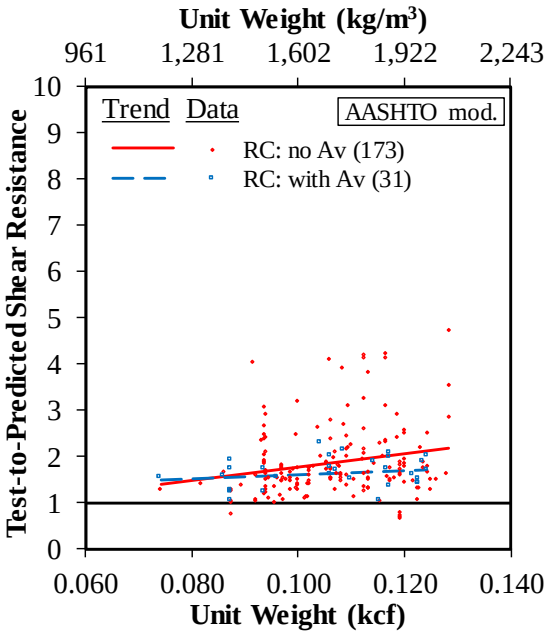

Source: FHWA.
1 kcf = 16,020 kg/m³.

Figure 94. Graph. Test-to-predicted shear resistance compared to unit weight for Simplified-RC with LWC modification determined using AASHTO modified.

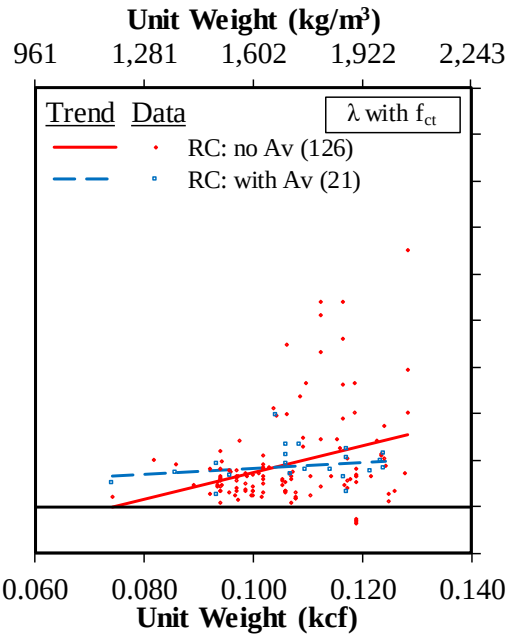

Source: FHWA.
1 kcf = 16,020 kg/m³.

Figure 95. Graph. Test-to-predicted shear resistance compared to unit weight for Simplified-RC with proposed expression for the λ-factor based on f_{ct}.

Figure 96 through figure 99 show the ratios for the GP-equation method in a similar format. The ratios are shown for all four groups of specimen type: RC specimens without and with shear reinforcement and PC specimens without and with shear reinforcement. Similar to figure 94 and figure 95, the ratios shown for the proposed λ-factor based on w_c and AASHTO modified appeared similar and were shifted slightly higher than the ratios determined without modification. The trend lines for all groups of specimens except for PC specimens without shear reinforcement were nearly horizontal and greater than 1.0. The trend line for the PC specimens without shear reinforcement had a downward trend both figure 96 and figure 97. Both figures include the seven SDC specimens with low test-to-prediction ratios. The ratios for these specimens were not included in either figure 98 or figure 99 because the specimens were not all-lightweight or sand-LWC, and splitting tensile strength values were not reported. In figure 98, the trend line for PC specimens without shear reinforcement did not include these seven points and was inclined slightly upward, indicating an increase in the test-to-prediction ratio as w_c increased.

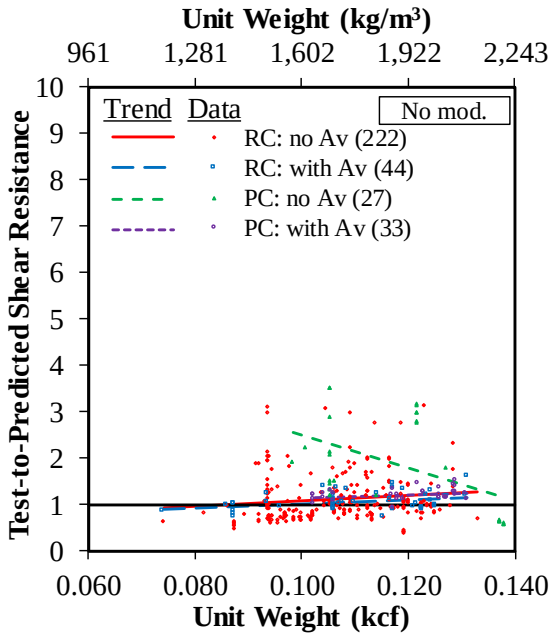

Source: FHWA.
1 kcf = 16,020 kg/m³.

Figure 96. Graph. Test-to-predicted shear resistance compared to unit weight for GP-equation method with no LWC modification.

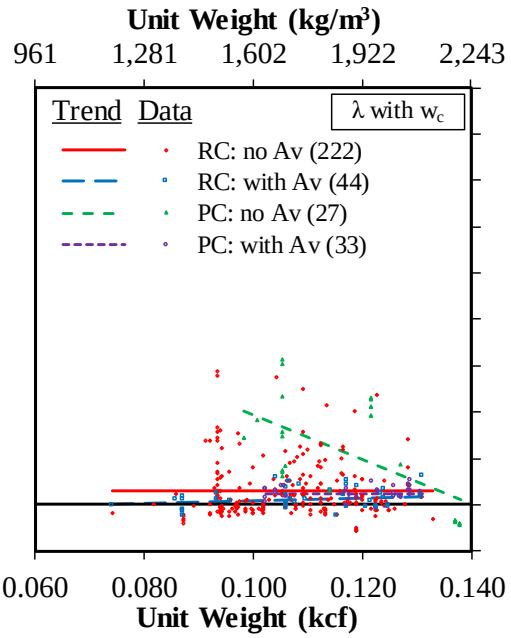

Source: FHWA.
1 kcf = 16,020 kg/m³.

Figure 97. Graph. Test-to-predicted shear resistance compared to unit weight for GP-equation method with modification determined using the proposed expression for the λ-factor based on w_c.

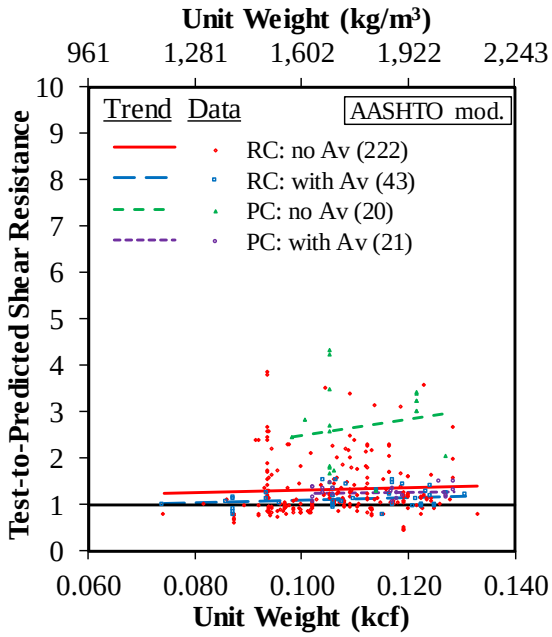

Source: FHWA.
1 kcf = 16,020 kg/m³.

Figure 98. Graph. Test-to-predicted shear resistance compared to unit weight for GP-equation method with LWC modification determined using AASHTO modified.

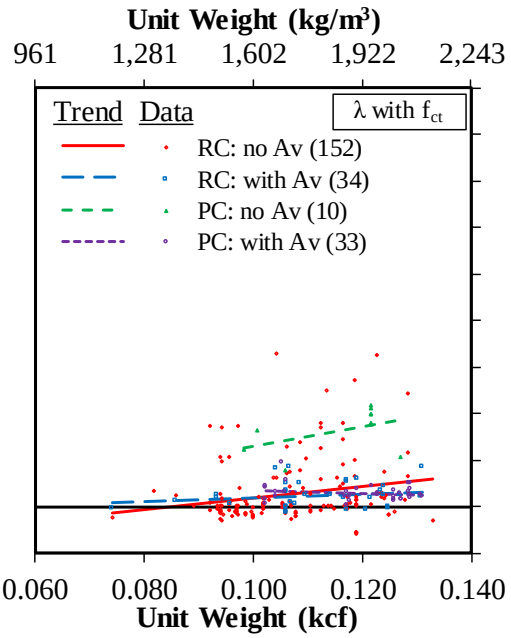

Source: FHWA.
1 kcf = 16,020 kg/m³.

Figure 99. Graph. Test-to-predicted shear resistance compared to unit weight for GP-equation method with LWC modification determined using proposed expression for the λ-factor based on f_{ct}.

Figure 100 through figure 103 show the ratios for the GP-table method. The method tends to produce similar test-to-prediction ratios, so although the ratios of individual specimens are in slightly different locations in figure 100 through figure 103 when compared to figure 96 through figure 99, the observed trends are similar.

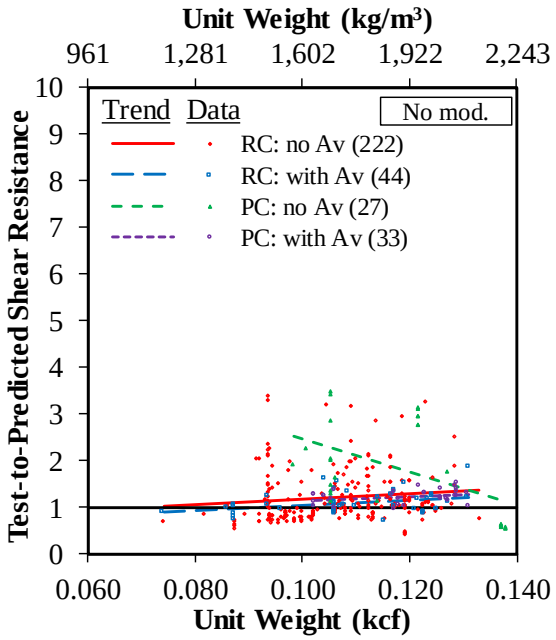

Source: FHWA.
1 kcf = 16,020 kg/m^3.

Figure 100. Graph. Test-to-predicted shear resistance compared to unit weight for GP-table method with no LWC modification.

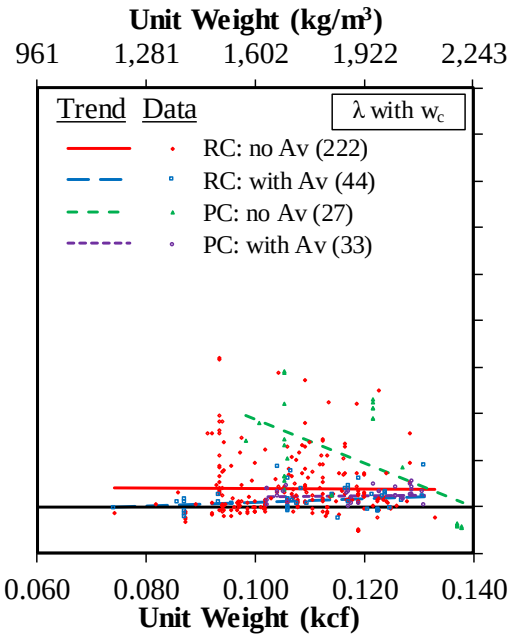

Source: FHWA.
1 kcf = 16,020 kg/m^3.

Figure 101. Graph. Test-to-predicted shear resistance compared to unit weight for GP-table method with LWC modification determined using proposed expression for the λ-factor based on w_c.

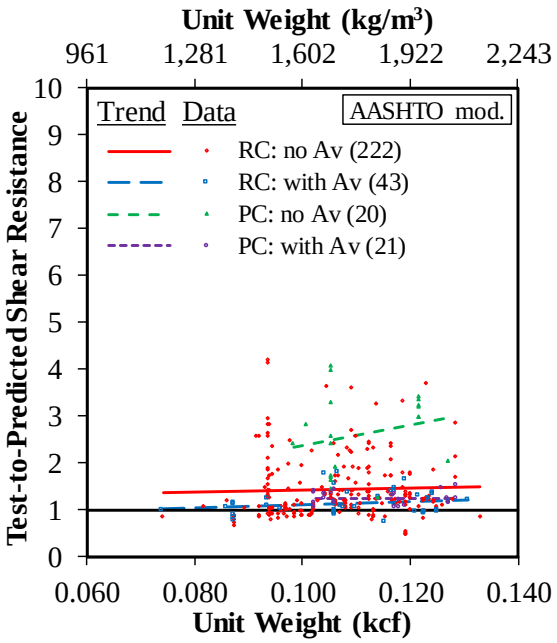

Source: FHWA.
1 kcf = 16,020 kg/m³.

Figure 102. Graph. Test-to-predicted shear resistance compared to unit weight for GP-table method with LWC modification determined using AASHTO modified.

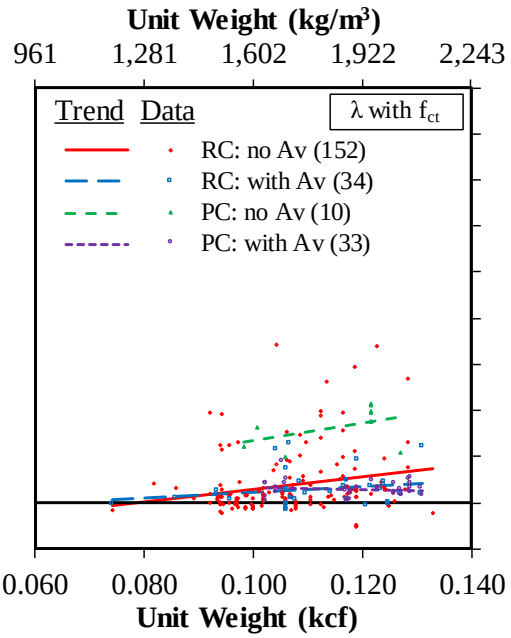

Source: FHWA.
1 kcf = 16,020 kg/m³.

Figure 103. Graph. Test-to-predicted shear resistance compared to unit weight for GP-table method with LWC modification determined using proposed expression for the λ-factor based on f_{ct}.

The ratios for the Simplified-PC/RC method are shown in figure 104 through figure 107. There is much more scatter observed in the ratios shown in these figures. The trend lines for RC and PC specimens with shear reinforcement are nearly horizontal and slightly greater than 1.0. The trend line for RC specimens without shear reinforcement is noticeably higher than the trend line for specimens with shear reinforcement, and the data points have much greater scatter. The trend line for the few PC specimens without shear reinforcement is much higher than the other three lines. The same seven SDC specimens caused a sharp downward trend in the regression lines shown in figure 104 and figure 105. Only a slight downward trend for the PC specimens without shear reinforcement is observed in figure 106 and figure 107 when the seven specimens are not included.

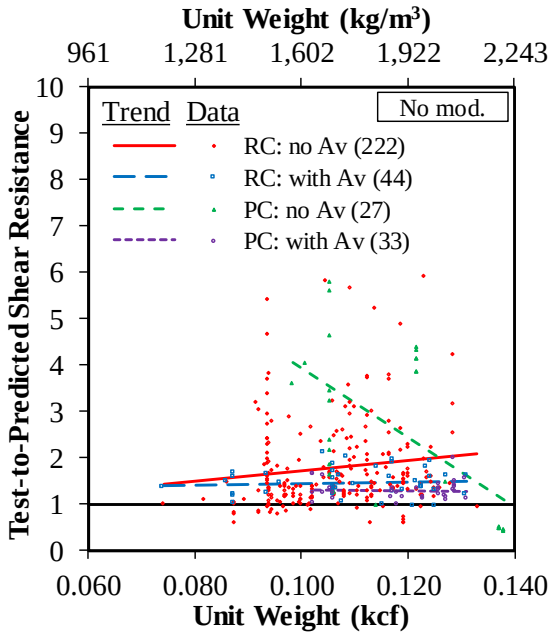

Source: FHWA.
1 kcf = 16,020 kg/m³.

Figure 104. Graph. Test-to-predicted shear resistance compared to unit weight for Simplified-PC/RC with no LWC modification.

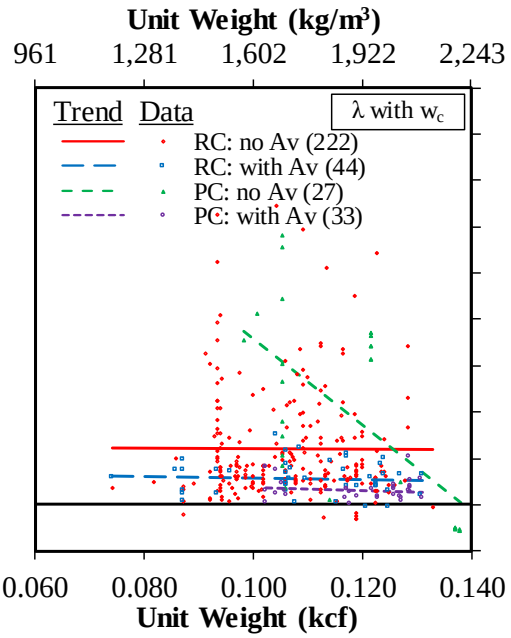

Source: FHWA.
1 kcf = 16,020 kg/m³.

Figure 105. Graph. Test-to-predicted shear resistance compared to unit weight for Simplified-PC/RC with LWC modification determined using proposed expression for the λ-factor based on w_c.

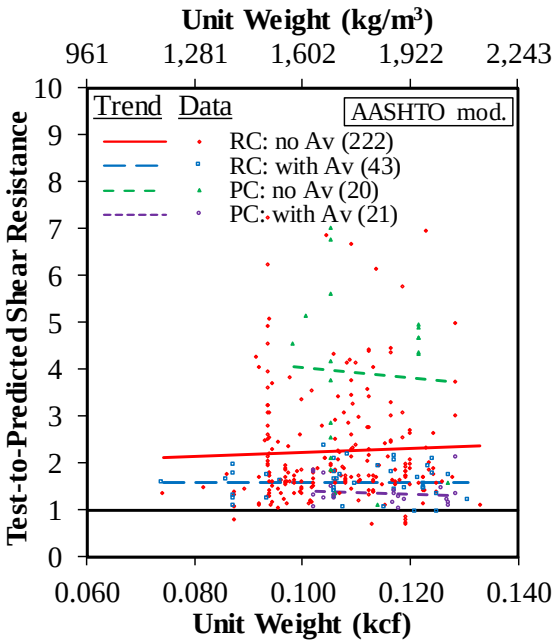

Source: FHWA.
1 kcf = 16,020 kg/m³.

Figure 106. Graph. Test-to-predicted shear resistance compared to unit weight for Simplified-PC/RC with LWC modification determined using AASHTO modified.

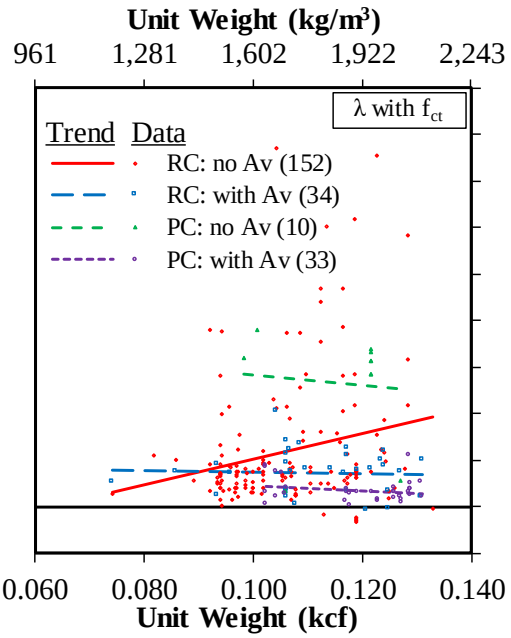

Source: FHWA.
1 kcf = 16,020 kg/m³.

Figure 107. Graph. Test-to-predicted shear resistance compared to unit weight for Simplified-PC/RC with LWC modification determined using proposed expression for the λ-factor based on f_{ct}.

The test-to-prediction ratios determined using the proposed λ-factor based on w_c were compared to the ratios determined without modification for LWC (see table 41), the ratios determined using AASHTO modified (see table), and the ratios determined using the proposed λ-factor based on f_{ct} (see table 43). The ratios in table 41 through table 43 were calculated for both methods of the general procedure and the Simplified-PC/RC procedure. The ratios for RC specimens determined using AASHTO modified and the proposed λ-factor based on w_c are provided in table 44 and also include calculations using the Simplified-RC procedure. The ratios in each table are given for all specimens. Additional ratios are given in groups to compare the ratios of specimens without and with shear reinforcement and to compare the ratios of RC and PC specimens.

The mean ratios in table 41 that were determined using the proposed λ-factor based on w_c were all greater than the mean ratios determined without modification for LWC. The ratios determined using the GP-equation and GP-table methods without modification for LWC were less than 1.0 for 48 and 41 percent of the specimens, respectively. Determining the shear resistance using the proposed λ-factor based on w_c reduced the number of specimens with ratios less than 1.0 to 35 and 26 percent for the two general procedure methods, respectively. By comparison, the number of specimens with a ratio less than 1.0 for shear resistance determined using the Simplified-PC/RC procedure was 12 percent with no modification for LWC and 6 percent with modification based on unit weight. The COV for a design method was similar regardless of the method of LWC modification.

Table 41. Test-to-predicted shear resistance for design expressions with no modification for LWC (λ-factor = 1) and modification determined using proposed expression for the λ-factor based on w_c.

LWC Modification and Specimen Group*	Design Expression	Mean	COV (Percent)	Maximum	Minimum	Percent Test-to-Prediction Ratio	
						<1.0	<0.8
No modification for LWC, all specimens (326)	GP-equation	1.17	48.1	3.51	0.39	47.2	24.2
No modification for LWC, all specimens (326)	GP-table	1.24	46.7	3.46	0.42	40.2	16.9
No modification for LWC, all specimens (326)	Simplified-PC/RC	1.76	57.0	5.91	0.43	11.0	4.6
No modification for LWC, specimens without A_v (249)	GP-equation	1.19	53.6	3.51	0.39	53.8	30.5
No modification for LWC, specimens without A_v (249)	GP-table	1.27	51.1	3.46	0.42	44.2	20.9
No modification for LWC, specimens without A_v (249)	Simplified-PC/RC	1.88	59.3	5.91	0.43	12.9	6.0
No modification for LWC, specimens with A_v (77)	GP-equation	1.12	16.3	1.61	0.73	26.0	3.9
No modification for LWC, specimens with A_v (77)	GP-table	1.14	19.0	1.85	0.69	27.3	3.9
No modification for LWC, specimens with A_v (77)	Simplified-PC/RC	1.38	19.6	2.11	0.93	5.2	0.0
No modification for LWC, RC specimens (266)	GP-equation	1.10	44.0	3.14	0.39	54.9	27.1
No modification for LWC, RC specimens (266)	GP-table	1.18	43.8	3.39	0.42	45.9	18.0
No modification for LWC, RC specimens (266)	Simplified-PC/RC	1.73	52.3	5.91	0.59	10.2	3.0
No modification for LWC, PC specimens (60)	GP-equation	1.50	50.4	3.51	0.56	13.3	11.7
No modification for LWC, PC specimens (60)	GP-table	1.49	50.1	3.46	0.54	15.0	11.7
No modification for LWC, PC specimens (60)	Simplified-PC/RC	1.87	72.1	5.80	0.43	15.0	11.7
Proposed λ-factor based on w_c, all specimens (326)	GP-equation	1.33	48.9	4.13	0.43	34.0	9.2
Proposed λ-factor based on w_c, all specimens (326)	GP-table	1.40	47.5	4.19	0.46	24.8	6.1
Proposed λ-factor based on w_c, all specimens (326)	Simplified-PC/RC	2.09	58.3	7.4	0.43	5.2	3.7

LWC Modification and Specimen Group*	Design Expression	Mean	COV (Percent)	Maximum	Minimum	Percent Test-to-Prediction Ratio	
						<1.0	<0.8
Proposed λ-factor based on w_c, specimens without A_v (249)	GP-equation	1.38	52.8	4.13	0.43	37.8	11.2
Proposed λ-factor based on w_c, specimens without A_v (249)	GP-table	1.47	50.2	4.19	0.46	25.7	7.2
Proposed λ-factor based on w_c, specimens without A_v (249)	Simplified-PC/RC	2.28	58.0	7.43	0.43	5.6	4.8
Proposed λ-factor based on w_c, specimens with A_v (77)	GP-equation	1.17	16.1	1.62	0.75	22.1	2.6
Proposed λ-factor based on w_c, specimens with A_v (77)	GP-table	1.18	19.4	1.87	0.72	22.1	2.6
Proposed λ-factor based on w_c, specimens with A_v (77)	Simplified-PC/RC	1.46	22.4	2.50	0.93	3.9	0.0
Proposed λ-factor based on w_c, RC specimens (266)	GP-equation	1.27	45.2	3.85	0.43	38.7	8.6
Proposed λ-factor based on w_c, RC specimens (266)	GP-table	1.36	45.0	4.19	0.46	27.4	4.9
Proposed λ-factor based on w_c, RC specimens (266)	Simplified-PC/RC	2.10	53.4	7.43	0.67	3.4	1.9
Proposed λ-factor based on w_c, PC specimens (60)	GP-equation	1.62	53.8	4.13	0.56	13.3	11.7
Proposed λ-factor based on w_c, PC specimens (60)	GP-table	1.60	53.0	3.89	0.54	13.3	11.7
Proposed λ-factor based on w_c, PC specimens (60)	Simplified-PC/RC	2.04	77.9	6.80	0.43	13.3	11.7

*The number of specimens is shown in parentheses.

Table 42 compares the ratios determined for specimens with all-lightweight and sand-lightweight concrete. The mean ratios determined using the modification for LWC in the AASHTO modified were 1 to 2 percent larger than the ratios determined using the proposed λ-factor based on w_c. The COV for a design method was similar regardless of the method of LWC modification.

Table 42. Test-to-predicted shear resistance for design expressions with LWC modification determined using AASHTO modified and proposed expression for the λ-factor based on w_c.

LWC Modification and Specimen Group*	Design Expression	Mean	COV (Percent)	Maximum	Minimum	Percent Test-to-Prediction Ratio	
						<1.0	< 0.8
AASHTO modified, all specimens (306)	GP-equation	1.37	49.4	4.32	0.44	32.7	6.9
AASHTO modified, all specimens (306)	GP-table	1.45	47.4	4.19	0.48	22.5	3.6
AASHTO modified, all specimens (306)	Simplified-PC/RC	2.20	56.6	7.24	0.70	2.6	1.6
AASHTO modified, specimens without A_v (242)	GP-equation	1.43	52.1	4.32	0.44	34.3	7.9
AASHTO modified, specimens without A_v (242)	GP-table	1.52	49.0	4.19	0.48	21.5	3.7
AASHTO modified, specimens without A_v (242)	Simplified-PC/RC	2.38	55.7	7.24	0.70	2.5	2.1
AASHTO modified, specimens with A_v (64)	GP-equation	1.15	16.5	1.52	0.75	26.6	3.1
AASHTO modified, specimens with A_v (64)	GP-table	1.16	19.5	1.79	0.72	26.6	3.1
AASHTO modified, specimens with A_v (64)	Simplified-PC/RC	1.50	22.8	2.36	0.93	3.1	0.0
AASHTO modified, RC specimens (265)	GP-equation	1.28	45.0	3.85	0.44	37.7	7.9
AASHTO modified, RC specimens (265)	GP-table	1.38	44.8	4.19	0.48	26.0	4.2
AASHTO modified, RC specimens (265)	Simplified-PC/RC	2.13	53.0	7.24	0.70	3.0	1.9
AASHTO modified, PC specimens (41)	GP-equation	1.95	49.0	4.32	1.03	0.0	0.0
AASHTO modified, PC specimens (41)	GP-table	1.91	47.9	4.06	1.02	0.0	0.0
AASHTO modified, PC specimens (41)	Simplified-PC/RC	2.60	68.1	7.02	1.00	0.0	0.0
Proposed λ-factor based on w_c, all specimens (306)	GP-equation	1.35	49.0	4.13	0.43	34.0	7.5
Proposed λ-factor based on w_c, all specimens (306)	GP-table	1.43	47.3	4.19	0.46	24.2	4.2
Proposed λ-factor based on w_c, all specimens (306)	Simplified-PC/RC	2.16	56.6	7.43	0.67	3.3	1.6

LWC Modification and Specimen Group*	Design Expression	Mean	COV (Percent)	Maximum	Minimum	Percent Test-to-Prediction Ratio	
						<1.0	< 0.8
Proposed λ-factor based on w_c, specimens without A_v (242)	GP-equation	1.41	51.9	4.13	0.43	36.0	8.7
Proposed λ-factor based on w_c, specimens without A_v (242)	GP-table	1.50	48.9	4.19	0.46	23.6	4.5
Proposed λ-factor based on w_c, specimens without A_v (242)	Simplified-PC/RC	2.33	55.9	7.43	0.67	2.9	2.1
Proposed λ-factor based on w_c, specimens with A_v (64)	GP-equation	1.15	16.2	1.56	0.75	26.6	3.1
Proposed λ-factor based on w_c, specimens with A_v (64)	GP-table	1.15	19.4	1.83	0.72	26.6	3.1
Proposed λ-factor based on w_c, specimens with A_v (64)	Simplified-PC/RC	1.49	23.3	2.50	0.93	4.7	0.0
Proposed λ-factor based on w_c, RC specimens (265)	GP-equation	1.27	45.3	3.85	0.43	38.9	8.7
Proposed λ-factor based on w_c, RC specimens (265)	GP-table	1.36	45.1	4.19	0.46	27.5	4.9
Proposed λ-factor based on w_c, RC specimens (265)	Simplified-PC/RC	2.10	53.5	7.43	0.67	3.4	1.9
Proposed λ-factor based on w_c, PC specimens (41)	GP-equation	1.89	48.0	4.13	0.97	2.4	0.0
Proposed λ-factor based on w_c, PC specimens (41)	GP-table	1.86	47.1	3.89	0.98	2.4	0.0
Proposed λ-factor based on w_c, PC specimens (41)	Simplified-PC/RC	2.52	67.1	6.80	0.99	2.4	0.0

*The number of specimens is shown in parentheses.

The ratios determined for specimens with a recorded splitting tensile test are provided in table 43. The mean ratios for all of the specimens were 5 to 7 percent larger for shear resistance determined using the proposed λ-factor based on f_{ct} than for the proposed λ-factor based on w_c. The COV for a design method was also larger for shear resistance determined using the proposed λ-factor based on f_{ct}.

Table 43. Test-to-predicted shear resistance for design expressions with LWC modification determined using proposed expression for the λ-factor based on f_{ct} and proposed expression for the λ-factor based on w_c.

LWC Modification and Specimen Group*	Design Expression	Mean	COV (Percent)	Maximum	Minimum	Percent Test-to-Prediction Ratio	
						<1.0	<0.8
Proposed λ-factor based on f_{ct}, all specimens (229)	GP-equation	1.33	48.3	4.27	0.42	31.9	5.7
Proposed λ-factor based on f_{ct}, all specimens (229)	GP-table	1.41	47.0	4.41	0.46	23.1	2.6
Proposed λ-factor based on f_{ct}, all specimens (229)	Simplified-PC/RC	2.08	62.0	8.70	0.65	3.9	1.7
Proposed λ-factor based on f_{ct}, specimens without A_v (162)	GP-equation	1.36	55.1	4.27	0.42	39.5	8.0
Proposed λ-factor based on f_{ct}, specimens without A_v (162)	GP-table	1.46	52.1	4.41	0.46	27.8	3.7
Proposed λ-factor based on f_{ct}, specimens without A_v (162)	Simplified-PC/RC	2.30	63.2	8.70	0.65	3.7	2.5
Proposed λ-factor based on f_{ct}, specimens with A_v (67)	GP-equation	1.26	18.1	1.92	0.87	13.4	0.0
Proposed λ-factor based on f_{ct}, specimens with A_v (67)	GP-table	1.29	22.7	2.28	0.83	11.9	0.0
Proposed λ-factor based on f_{ct}, specimens with A_v (67)	Simplified-PC/RC	1.54	27.3	3.03	0.93	4.5	0.0
Proposed λ-factor based on f_{ct}, RC specimens (186)	GP-equation	1.27	49.6	4.27	0.42	39.2	7.0
Proposed λ-factor based on f_{ct}, RC specimens (186)	GP-table	1.36	48.6	4.41	0.46	28.5	3.2
Proposed λ-factor based on f_{ct}, RC specimens (186)	Simplified-PC/RC	2.12	62.0	8.70	0.65	4.3	2.2
Proposed λ-factor based on f_{ct}, PC specimens (43)	GP-equation	1.60	40.1	3.16	1.01	0.0	0.0
Proposed λ-factor based on f_{ct}, PC specimens (43)	GP-table	1.60	39.5	3.13	1.01	0.0	0.0
Proposed λ-factor based on f_{ct}, PC specimens (43)	Simplified-PC/RC	1.88	61.0	4.79	1.00	2.3	0.0

LWC Modification and Specimen Group*	Design Expression	Mean	COV (Percent)	Maximum	Minimum	Percent Test-to-Prediction Ratio	
						<1.0	<0.8
Proposed λ-factor based on w_c, all specimens (229)	GP-equation	1.27	43.9	3.74	0.43	33.6	5.2
Proposed λ-factor based on w_c, all specimens (229)	GP-table	1.34	42.1	3.87	0.46	21.0	3.1
Proposed λ-factor based on w_c, all specimens (229)	Simplified-PC/RC	1.95	53.9	7.43	0.67	3.9	1.7
Proposed λ-factor based on w_c, specimens without A_v (162)	GP-equation	1.30	50.5	3.74	0.43	42.0	7.4
Proposed λ-factor based on w_c, specimens without A_v (162)	GP-table	1.39	47.0	3.87	0.46	24.1	4.3
Proposed λ-factor based on w_c, specimens without A_v (162)	Simplified-PC/RC	2.15	54.8	7.43	0.67	3.7	2.5
Proposed λ-factor based on w_c, specimens with A_v (67)	GP-equation	1.21	13.7	1.62	0.92	13.4	0.0
Proposed λ-factor based on w_c, specimens with A_v (67)	GP-table	1.23	17.1	1.87	0.88	13.4	0.0
Proposed λ-factor based on w_c, specimens with A_v (67)	Simplified-PC/RC	1.47	22.8	2.50	0.93	4.5	0.0
Proposed λ-factor based on w_c, RC specimens (186)	GP-equation	1.20	41.2	3.74	0.43	40.9	6.5
Proposed λ-factor based on w_c, RC specimens (186)	GP-table	1.28	40.1	3.87	0.46	25.3	3.8
Proposed λ-factor based on w_c, RC specimens (186)	Simplified-PC/RC	1.96	50.9	7.43	0.67	4.3	2.2
Proposed λ-factor based on w_c, PC specimens (43)	GP-equation	1.59	43.9	3.30	0.97	2.3	0.0
Proposed λ-factor based on w_c, PC specimens (43)	GP-table	1.59	43.8	3.28	0.98	2.3	0.0
Proposed λ-factor based on w_c, PC specimens (43)	Simplified-PC/RC	1.92	66.4	5.09	0.99	2.3	0.0

*The number of specimens is shown in parentheses.

The ratios determined for specimens with all-lightweight and sand-lightweight concrete that satisfied the limits for using the Simplified-RC procedure are included in table 44. The mean ratios for all of the specimens determined using the modification for LWC AASHTO modified method were 2 percent larger than the ratios determined using the proposed λ-factor based on w_c. The mean ratios determined using the Simplified-RC procedure were considerably larger than the ratios determined using either of the two general procedure methods, but the ratios were not quite as large as the ratios determined using the Simplified-PC/RC method. The COV for a design method was similar regardless of the method of LWC modification.

Table 44. Test-to-predicted shear resistance for design expressions for RC specimens with LWC modification determined using AASHTO modified and proposed expression for the λ-factor based on w_c.

LWC Modification and Specimen Group*	Design Expression	Mean	COV (Percent)	Maximum	Minimum	Percent Test-to-Prediction Ratio	
						<1.0	<0.8
AASHTO modified, all RC specimens (204)	Simplified-RC	1.83	38.9	4.73	0.67	2.9	2.5
AASHTO modified, all RC specimens (204)	GP-equation	1.14	32.4	2.65	0.44	42.6	9.3
AASHTO modified, all RC specimens (204)	GP-table	1.23	32.2	2.84	0.48	28.4	4.4
AASHTO modified, all RC specimens (204)	Simplified-PC/RC	1.92	39.1	4.98	0.71	2.5	2.0
AASHTO modified, RC specimens without A_v (173)	Simplified-RC	1.86	40.6	4.73	0.67	3.5	2.9
AASHTO modified, RC specimens without A_v (173)	GP-equation	1.14	34.3	2.65	0.44	43.9	9.8
AASHTO modified, RC specimens without A_v (173)	GP-table	1.24	33.4	2.84	0.48	27.7	4.0
AASHTO modified, RC specimens without A_v (173)	Simplified-PC/RC	1.96	40.6	4.98	0.71	2.9	2.3
AASHTO modified, RC specimens with A_v (31)	Simplified-RC	1.63	19.1	2.28	1.02	0.0	0.0
AASHTO modified, RC specimens with A_v (31)	GP-equation	1.12	18.3	1.51	0.75	35.5	6.5
AASHTO modified, RC specimens with A_v (31)	GP-table	1.13	20.9	1.74	0.72	32.3	6.5
AASHTO modified, RC specimens with A_v (31)	Simplified-PC/RC	1.67	19.5	2.36	1.04	0.0	0.0
Proposed λ based on w_c, all RC specimens (204)	Simplified-RC	1.79	38.1	4.23	0.64	3.4	2.5

LWC Modification and Specimen Group*	Design Expression	Mean	COV (Percent)	Maximum	Minimum	Percent Test-to-Prediction Ratio	
						<1.0	<0.8
Proposed λ based on w_c, all RC specimens (204)	Simplified-RC	1.79	38.1	4.23	0.64	3.4	2.5
Proposed λ-factor based on w_c, all RC specimens (204)	GP-equation	1.12	31.7	2.40	0.43	44.1	10.3
Proposed λ-factor based on w_c, all RC specimens (204)	GP-table	1.21	31.6	2.58	0.46	30.4	4.9
Proposed λ-factor based on w_c, all RC specimens (204)	Simplified-PC/RC	1.88	38.3	4.46	0.67	2.5	2.0
Proposed λ-factor with w_c, RC specimens without A_v (173)	Simplified-RC	1.82	39.8	4.23	0.64	4.0	2.9
Proposed λ-factor with w_c, RC specimens without A_v (173)	GP-equation	1.12	33.5	2.40	0.43	46.2	11.0
Proposed λ-factor with w_c, RC specimens without A_v (173)	GP-table	1.22	32.7	2.58	0.46	30.6	4.6
Proposed λ-factor with w_c, RC specimens without A_v (173)	Simplified-PC/RC	1.92	39.8	4.46	0.67	2.9	2.3
Proposed λ-factor with w_c, RC specimens with A_v (31)	Simplified-RC	1.63	20.0	2.41	1.02	0.0	0.0
Proposed λ-factor with w_c, RC specimens with A_v (31)	GP-equation	1.12	18.7	1.56	0.75	32.3	6.5
Proposed λ-factor with w_c, RC specimens with A_v (31)	GP-table	1.13	21.5	1.83	0.72	29.0	6.5
Proposed λ-factor with w_c, RC specimens with A_v (31)	Simplified-PC/RC	1.67	20.4	2.50	1.04	0.0	0.0

*The number of specimens is shown in parentheses.

COMPARISON OF LWC AND NWC ON TEST-TO-PREDICTION RATIO FOR SHEAR RESISTANCE

The following section compares the test-to-prediction ratios for the LWC specimens to the ratios for the selected NWC specimens from the ACI-DafStb database. (For sources, see Bibliography section NWC Sources for ACI-DafStb Database.) The ratios for the LWC specimens were determined using only the proposed λ-factor based on w_c to account for LWC. Shear resistance was determined for each of the four design procedures in the *AASHTO LRFD Bridge Design Specifications*.[3]

A comparison of test-to-prediction ratios for LWC and NWC specimens is provided. Specifically, the ratios are given in tables for the two methods of the general procedure and the Simplified-PC/RC procedure. Figures are presented for each specimen type that compare the ratios for the GP-equation method and the Simplified-PC/RC method. Additional figures for the GP-table method were not shown because of their similarity to the figures showing the GP-equation method. Figures showing the ratios for the Simplified-RC method are included for the RC specimens that satisfy the limitations of the method.

Table 45 provides the ratios for all LWC and NWC in the TFHRC shear database. The ratios are also given for all RC specimens and all PC specimens. The ratios are shown in table 46 by specimen type. The mean ratios for the LWC specimens were 9 to 10 percent larger than the ratios of the NWC specimens depending on the design procedure. The COV of the ratios for the LWC specimens was much larger than the COV of the NWC specimens. A similar trend was observed for all of the RC and PC specimens.

Table 45. Test-to-predicted shear resistance for design expressions with LWC modification determined using proposed expression for the λ-factor based on w_c for LWC and NWC specimens by reinforcement type.

Concrete Type and Specimen Group*	Design Expression	Mean	COV (Percent)	Maximum	Minimum	Percent Test-to-Prediction Ratio	
						<1.0	<0.8
NWC, all specimens (886)	GP-equation	1.21	24.4	2.44	0.58	21.7	2.8
NWC, all specimens (886)	GP-table	1.27	23.7	2.76	0.60	13.9	2.0
NWC, all specimens (886)	Simplified-PC/RC	1.89	31.9	4.06	0.48	4.1	0.8
LWC, λ-factor based on w_c, all specimens (326)	GP-equation	1.33	48.9	4.13	0.43	34.0	9.2
LWC, λ-factor based on w_c, all specimens (326)	GP-table	1.40	47.5	4.19	0.46	24.8	6.1
LWC, λ-factor based on w_c, all specimens (326)	Simplified-PC/RC	2.09	58.3	7.4	0.43	5.2	3.7
NWC, all RC specimens (755)	GP-equation	1.17	21.8	2.44	0.58	22.9	2.4
NWC, all RC specimens (755)	GP-table	1.24	21.8	2.76	0.60	13.5	1.2
NWC, all RC specimens (755)	Simplified-PC/RC	1.91	30.7	4.06	0.48	3.4	0.7
LWC, λ-factor based on w_c, all RC specimens (266)	GP-equation	1.27	45.2	3.85	0.43	38.7	8.6
LWC, λ-factor based on w_c, all RC specimens (266)	GP-table	1.36	45.0	4.19	0.46	27.4	4.9
LWC, λ-factor based on w_c, all RC specimens (266)	Simplified-PC/RC	2.10	53.4	7.43	0.67	3.4	1.9
NWC, all PC specimens (131)	GP-equation	1.40	29.3	2.43	0.63	14.5	5.3
NWC, all PC specimens (131)	GP-table	1.41	28.8	2.40	0.61	16.0	6.9
NWC, all PC specimens (131)	Simplified-PC/RC	1.77	38.5	3.73	0.71	7.6	1.5
LWC, λ-factor based on w_c, all PC specimens (60)	GP-equation	1.62	53.8	4.13	0.56	13.3	11.7
LWC, λ-factor based on w_c, all PC specimens (60)	GP-table	1.60	53.0	3.89	0.54	13.3	11.7
LWC, λ-factor based on w_c, all PC specimens (60)	Simplified-PC/RC	2.04	77.9	6.80	0.43	13.3	11.7

*The number of specimens is shown in parentheses.
Note: NWC specimens are from the ACI-DafStb database.

The same trend of the LWC specimens having a larger mean ratio was not observed for each specimen type, as shown in table 46. For RC and PC specimens without shear reinforcement, the LWC specimens had larger ratios than the NWC specimens. The ratios for RC specimens with shear reinforcement were 12 to 19 percent smaller than the ratios for the NWC specimens depending on the design procedure. For the PC specimens with shear reinforcement, the ratios for the LWC were similar to the ratios for the NWC specimens and ranged from 2 percent smaller to 6 percent larger than the ratios for the NWC specimens.

Table 46. Test-to-predicted shear resistance for design expressions with LWC modification determined using proposed expression for the λ-factor based on w_c for LWC and NWC specimens by specimen type.

Concrete Type and Specimen Group*	Design Expression	Mean	COV (Percent)	Maximum	Minimum	Percent Test-to-Prediction Ratio	
						<1.0	<0.8
NWC, RC specimens without A_v (648)	GP-equation	1.17	22.7	2.44	0.58	25.2	2.6
NWC, RC specimens without A_v (648)	GP-table	1.25	22.5	2.76	0.60	13.4	1.2
NWC, RC specimens without A_v (648)	Simplified-PC/RC	1.93	32.0	4.06	0.48	4.0	0.8
LWC, λ-factor based on w_c, RC specimens without A_v (222)	GP-equation	1.30	47.5	3.85	0.43	39.2	9.5
LWC, λ-factor based on w_c, RC specimens without A_v (222)	GP-table	1.41	46.4	4.19	0.46	25.7	5.0
LWC, λ-factor based on w_c, RC specimens without A_v (222)	Simplified-PC/RC	2.21	54.0	7.43	0.67	3.2	2.3
NWC, RC specimens with A_v (107)	GP-equation	1.22	15.0	1.97	0.70	9.3	0.9
NWC, RC specimens with A_v (107)	GP-table	1.21	16.2	1.97	0.70	14.0	0.9
NWC, RC specimens with A_v (107)	Simplified-PC/RC	1.81	18.6	2.62	1.07	0.0	0.0
LWC, λ-factor based on w_c, RC specimens with A_v (44)	GP-equation	1.12	18.9	1.62	0.75	36.4	4.5
LWC, λ-factor based on w_c, RC specimens with A_v (44)	GP-table	1.14	23.7	1.87	0.72	36.4	4.5
LWC, λ-factor based on w_c, RC specimens with A_v (44)	Simplified-PC/RC	1.57	22.4	2.50	0.93	4.5	0.0
NWC, PC specimens without A_v (100)	GP-equation	1.46	30.2	2.43	0.63	14.0	7.0
NWC, PC specimens without A_v (100)	GP-table	1.46	30.1	2.40	0.61	17.0	9.0
NWC, PC specimens without A_v (100)	Simplified-PC/RC	1.88	39.1	3.73	0.71	9.0	2.0
LWC, λ-factor with w_c, PC specimens without A_v (27)	GP-equation	2.08	54.9	4.13	0.56	25.9	25.9
LWC, λ-factor with w_c, PC specimens without A_v (27)	GP-table	2.03	54.9	3.89	0.54	25.9	25.9
LWC, λ-factor with w_c, PC specimens without A_v (27)	Simplified-PC/RC	2.92	70.3	6.80	0.43	25.9	25.9

Concrete Type and Specimen Group*	Design Expression	Mean	COV (Percent)	Maximum	Minimum	Percent Test-to-Prediction Ratio	
						<1.0	<0.8
NWC, PC specimens with A_v (31)	GP-equation	1.21	16.3	1.67	0.89	16.1	0.0
NWC, PC specimens with A_v (31)	GP-table	1.24	15.1	1.67	0.88	12.9	0.0
NWC, PC specimens with A_v (31)	Simplified-PC/RC	1.41	18.5	2.11	0.97	3.2	0.0
LWC, λ-factor based on w_c, PC specimens with A_v (33)	GP-equation	1.24	10.0	1.52	0.97	3.0	0.0
LWC, λ-factor based on w_c, PC specimens with A_v (33)	GP-table	1.24	11.5	1.52	0.98	3.0	0.0
LWC, λ-factor based on w_c, PC specimens with A_v (33)	Simplified-PC/RC	1.32	17.6	2.00	0.99	3.0	0.0

*The number of specimens is shown in parentheses.
Note: NWC specimens are from the ACI-DafStb database.

RC Specimens Without Shear Reinforcement

The test-to-prediction ratios determined for the Simplified-RC procedure for RC specimens without shear reinforcement are compared to concrete compressive strength (f'_c) and effective shear depth (d_v) in figure 108 through figure 111. The ratios in figure 108 and figure 109 for LWC specimens are grouped by ranges of w_c. The ratios in figure 110 and figure 111 are grouped by all of the LWC specimens and all of the NWC specimens. Least-squares linear-regression lines are shown for each group of specimens. Figure 108 and figure 110 compare the ratios to f'_c, while figure 109 and figure 111 compare the ratios to d_v.

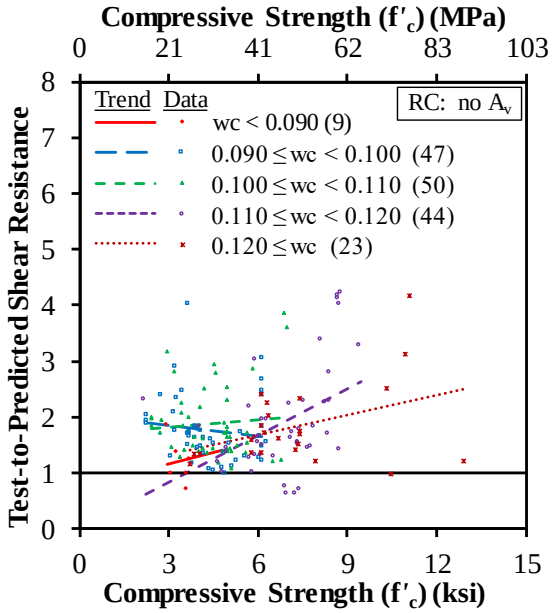

Source: FHWA.
1 ksi = 6.89 MPa.
Note: Unit weight (w_c) in the legend is measured in kcf where 1 kcf = 16,020 kg/m^3.

Figure 108. Graph. Test-to-predicted shear resistance compared to compressive strength for Simplified-RC for LWC RC members without shear reinforcement.

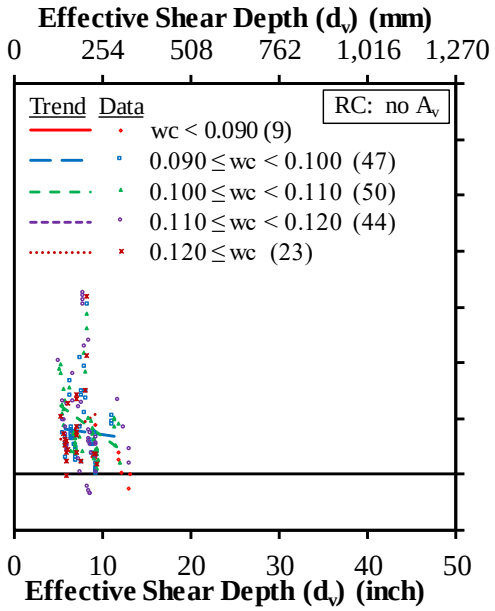

Source: FHWA.
1 inch = 25.4 mm.
Note: Unit weight (w_c) in the legend is measured in kcf where 1 kcf = 16,020 kg/m^3.

Figure 109. Graph. Test-to-predicted shear resistance compared to effective shear depth for Simplified-RC for LWC RC members without shear reinforcement.

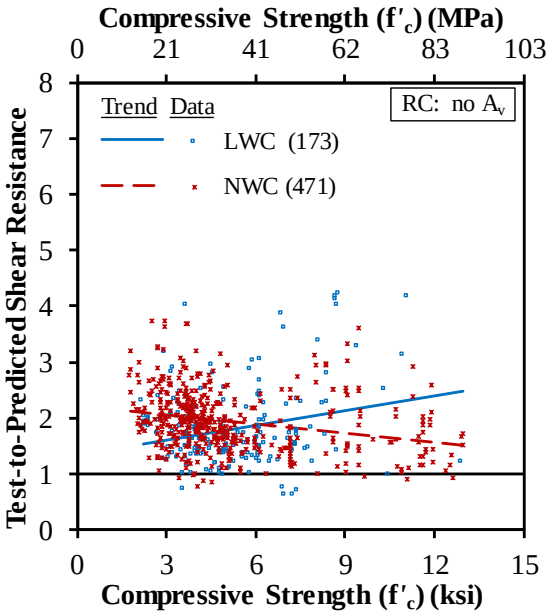

Source: FHWA.
1 ksi = 6.89 MPa.

Figure 110. Graph. Test-to-predicted shear resistance compared to compressive strength for Simplified-RC for LWC and NWC RC members without shear reinforcement.

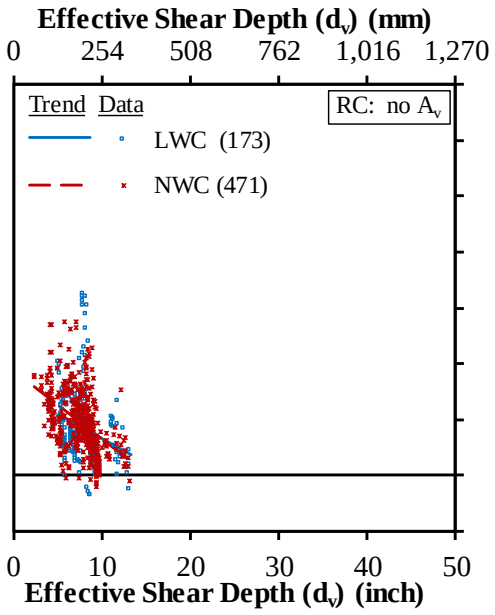

Source: FHWA.
1 inch = 25.4 mm.

Figure 111. Graph. Test-to-predicted shear resistance compared to effective shear depth for Simplified-RC for LWC and NWC RC members without shear reinforcement.

Figure 108 shows that most of the LWC specimens had a compressive strength of approximately 6 ksi (41 MPa) or less. In figure 110, the regression line for the LWC specimens with a compressive strength less than 6 ksi (41 MPa) was below the regression line for the NWC specimens, indicating a less-conservative prediction of shear resistance using the Simplified-RC procedure. For the smaller number of LWC specimens with an f'_c greater than 6 ksi (41 MPa), the trend line indicates that the prediction of shear resistance was more conservative than for the NWC specimens. There was no noticeable difference between LWC and NWC specimens with regard to effective shear depth over the limited range of d_v for the specimens that satisfied the limitations of the Simplified-RC procedure.

Figure 112 through figure 115 show similar information for the ratios determined using the GP-equation method. The trend line for the LWC specimens is above the NWC trend line in figure 114 over the entire range of compressive strengths for the specimens. The trend lines for the LWC and NWC specimens show a uniform ratio with increases in d_v, although the number of specimens with an effective depth greater than 15 inches (381 mm) is limited.

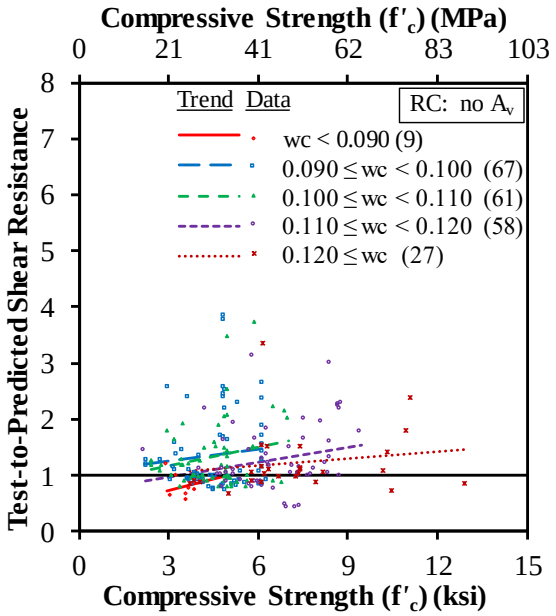

Source: FHWA.
1 ksi = 6.89 MPa.
Note: Unit weight (w_c) in the legend is measured in kcf where 1 kcf = 16,020 kg/m^3.

Figure 112. Graph. Test-to-predicted shear resistance compared to compressive strength for GP-equation method for LWC RC members without shear reinforcement.

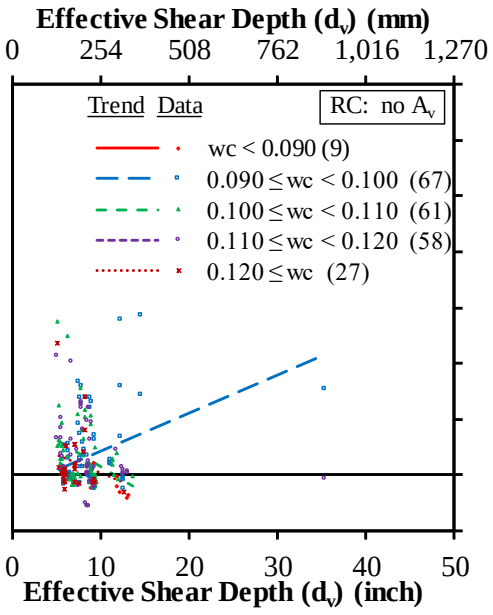

Source: FHWA.
1 inch = 25.4 mm.
Note: Unit weight (w_c) in the legend is measured in kcf where 1 kcf = 16,020 kg/m^3.

Figure 113. Graph. Test-to-predicted shear resistance compared to effective shear depth for GP-equation method for LWC RC members without shear reinforcement.

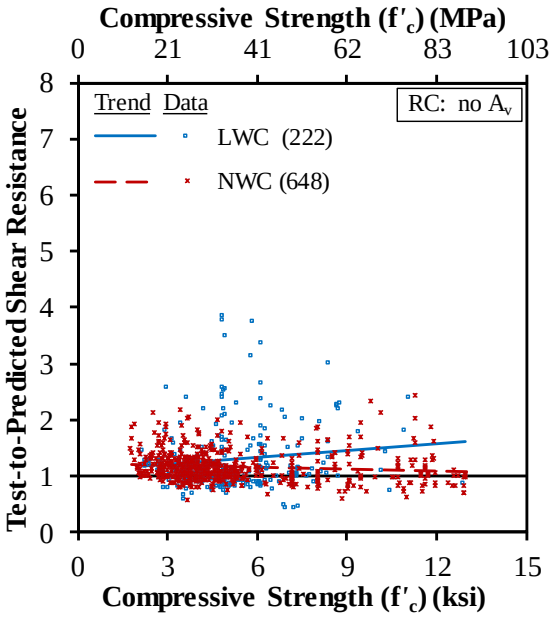

Source: FHWA.
1 ksi = 6.89 MPa.

Figure 114. Graph. Test-to-predicted shear resistance compared to compressive strength for GP-equation method for LWC and NWC RC members without shear reinforcement.

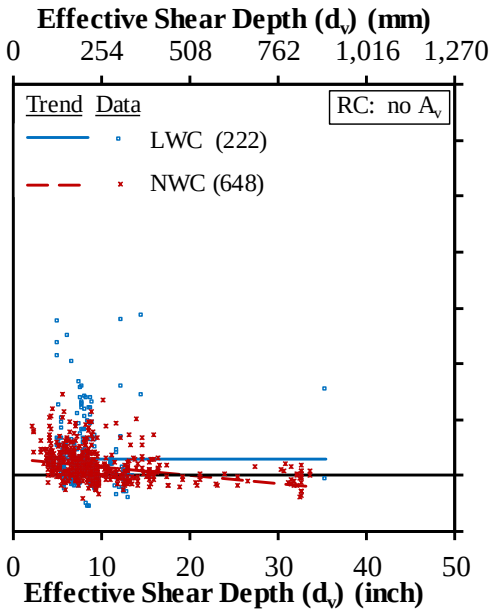

Source: FHWA.
1 inch = 25.4 mm.

Figure 115. Graph. Test-to-predicted shear resistance compared to effective shear depth for GP-equation method for LWC and NWC RC members without shear reinforcement.

The ratios determined using the Simplified-PC/RC method are shown in figure 116 through figure 119. The trend line for the LWC is inclined slightly upward, indicating that the predicted shear resistance became more conservative with increasing compressive strength. The opposite trend is observed for the NWC specimens, where the predicted shear resistance became slightly less conservative as compressive strength increased. The trend line for the ratios compared to d_v shows that, for the limited number of specimens with a d_v above 15 inches (381 mm), the shear resistance rapidly became less conservative as effective depth increased. The ratios were less than 1.0 for most of the NWC specimens with a d_v greater than 30 inches (762 mm).

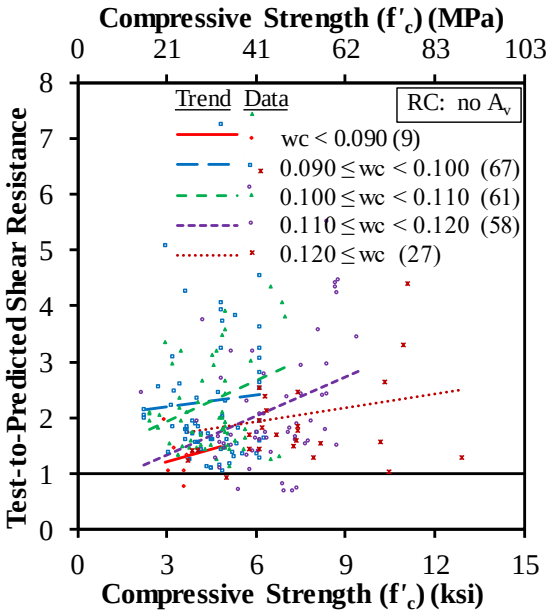

Source: FHWA.
1 ksi = 6.89 MPa.
Note: Unit weight (w_c) in the legend is measured in kcf where 1 kcf = 16,020 kg/m^3.

Figure 116. Graph. Test-to-predicted shear resistance compared to compressive strength for Simplified-PC/RC for LWC RC members without shear reinforcement.

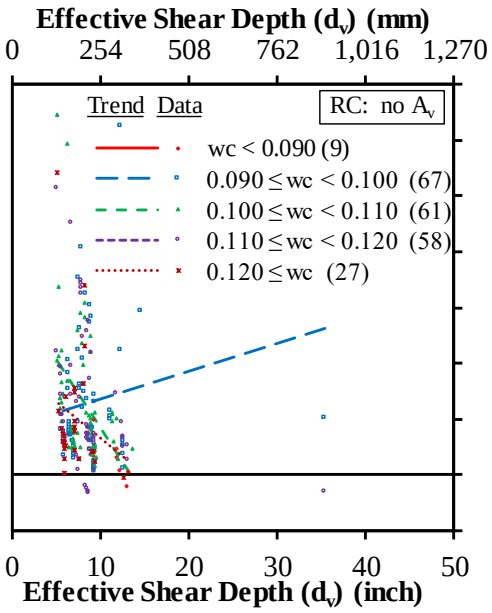

Source: FHWA.
1 inch = 25.4 mm.
Note: Unit weight (w_c) in the legend is measured in kcf where 1 kcf = 16,020 kg/m^3.

Figure 117. Graph. Test-to-predicted shear resistance compared to effective shear depth for Simplified-PC/RC for LWC RC members without shear reinforcement.

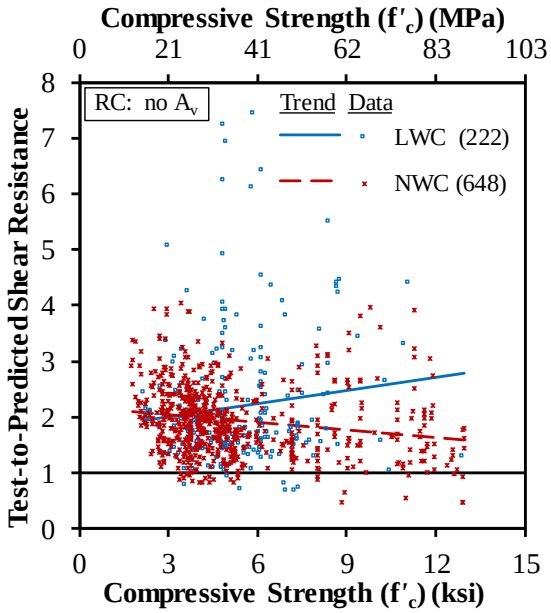

Source: FHWA.
1 ksi = 6.89 MPa.

Figure 118. Graph. Test-to-predicted shear resistance compared to compressive strength for Simplified-PC/RC for LWC and NWC RC members without shear reinforcement.

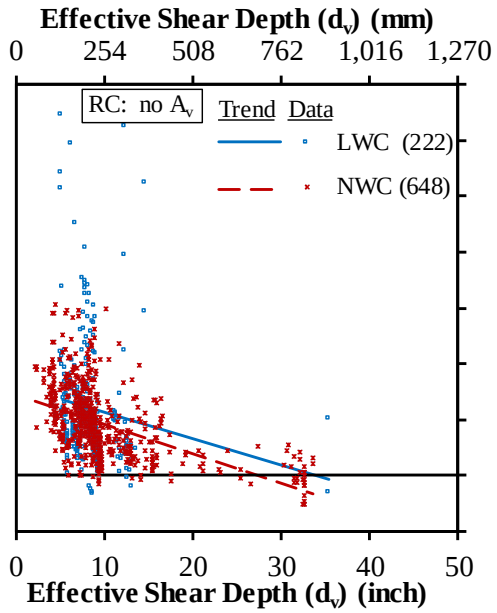

Source: FHWA.
1 inch = 25.4 mm.

Figure 119. Graph. Test-to-predicted shear resistance compared to effective shear depth for Simplified-PC/RC for LWC and NWC RC members without shear reinforcement.

RC Specimens With Shear Reinforcement

The test-to-prediction ratios are shown in figure 120 through figure 123 for RC specimens with shear reinforcement determined using the Simplified-RC method. The trend line for the LWC specimens is below the NWC trend line over the entire range of f'_c and d_v shown in figure 122.

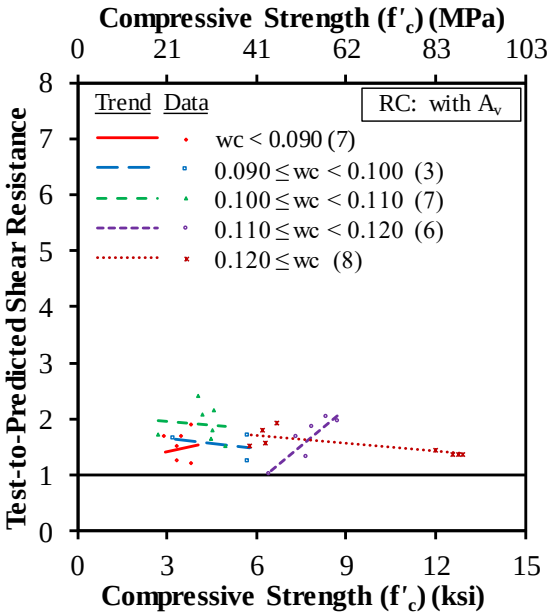

Source: FHWA.
1 ksi = 6.89 MPa.
Note: Unit weight (w_c) in the legend is measured in kcf where 1 kcf = 16,020 kg/m^3.

Figure 120. Graph. Test-to-predicted shear resistance compared to compressive strength for Simplified-RC for LWC RC members with shear reinforcement.

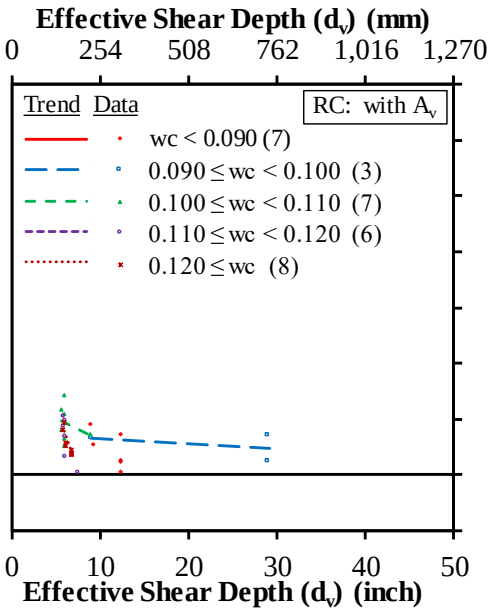

Source: FHWA.
1 inch = 25.4 mm.
Note: Unit weight (w_c) in the legend is measured in kcf where 1 kcf = 16,020 kg/m^3.

Figure 121. Graph. Test-to-predicted shear resistance compared to effective shear depth for Simplified-RC for LWC RC members with shear reinforcement.

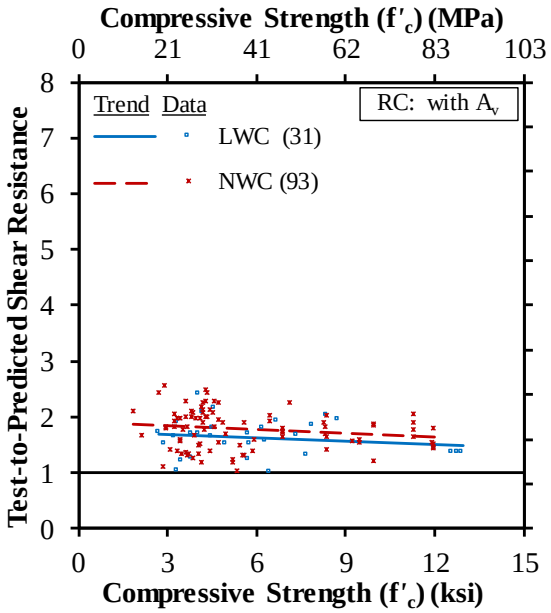

Source: FHWA.
1 ksi = 6.89 MPa.

Figure 122. Graph. Test-to-predicted shear resistance compared to compressive strength for Simplified-RC for LWC and NWC RC members with shear reinforcement.

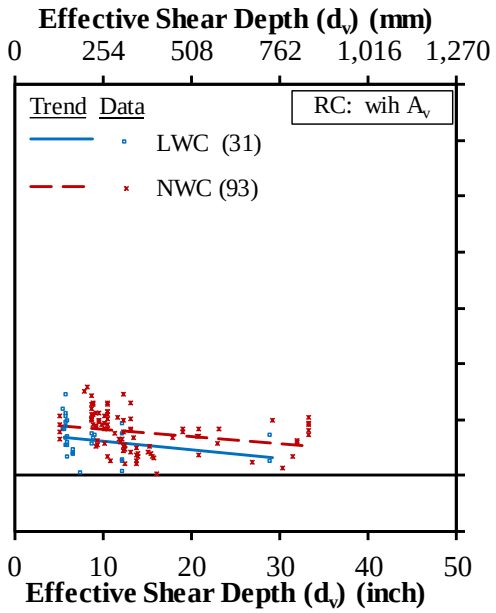

Source: FHWA.
1 inch = 25.4 mm.

Figure 123. Graph. Test-to-predicted shear resistance compared to effective shear depth for Simplified-RC for LWC and NWC RC members with shear reinforcement.

The ratios determined using the GP-equation method are shown in figure 124 through figure 127. The same trend is observed in regression lines for the LWC and NWC specimens. The main difference is that the trend lines appear parallel and are much closer to a ratio of 1.0.

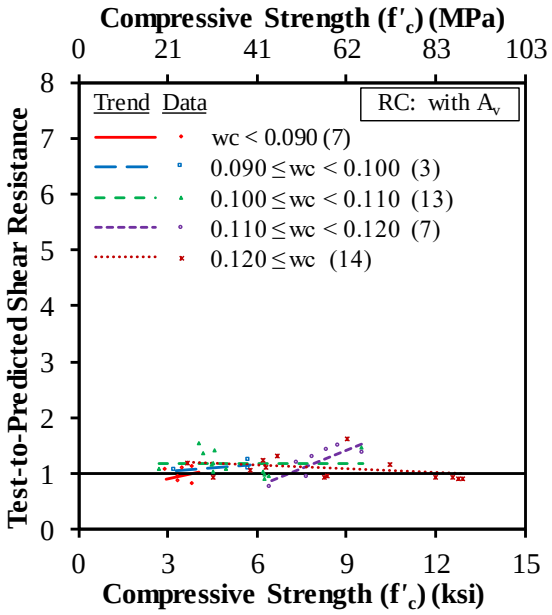

Source: FHWA.
1 ksi = 6.89 MPa.
Note: Unit weight (w_c) in the legend is measured in kcf where 1 kcf = 16,020 kg/m^3.

Figure 124. Graph. Test-to-predicted shear resistance compared to compressive strength for GP-equation method for LWC RC members with shear reinforcement.

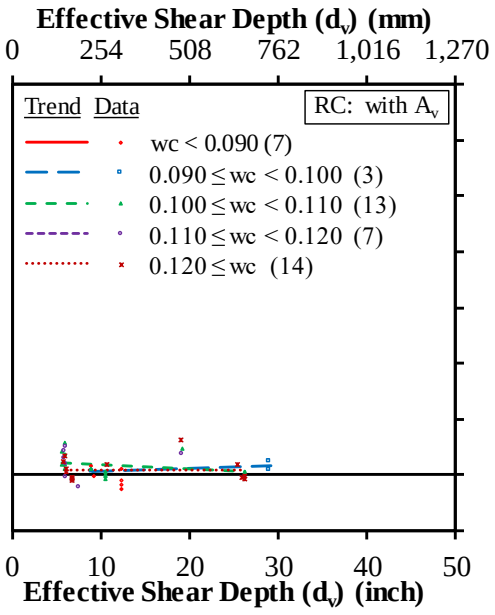

Source: FHWA.
1 inch = 25.4 mm.
Note: Unit weight (w_c) in the legend is measured in kcf where 1 kcf = 16,020 kg/m^3.

Figure 125. Graph. Test-to-predicted shear resistance compared to effective shear depth for GP-equation method for LWC RC members with shear reinforcement.

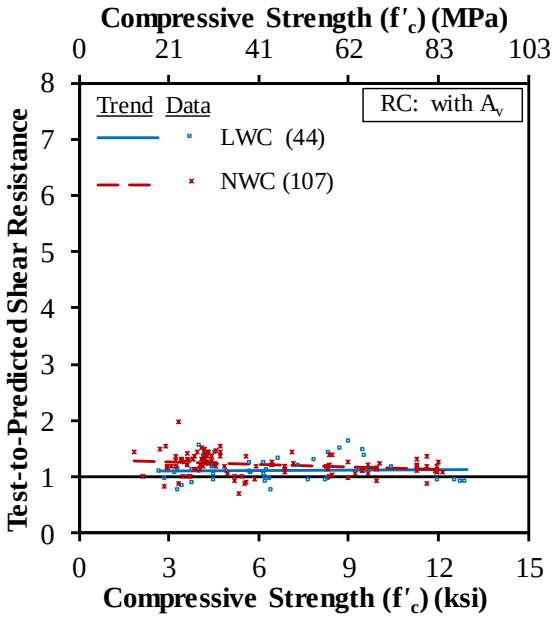

Source: FHWA.
1 ksi = 6.89 MPa.

Figure 126. Graph. Test-to-predicted shear resistance compared to compressive strength for GP-equation method for LWC and NWC RC members with shear reinforcement.

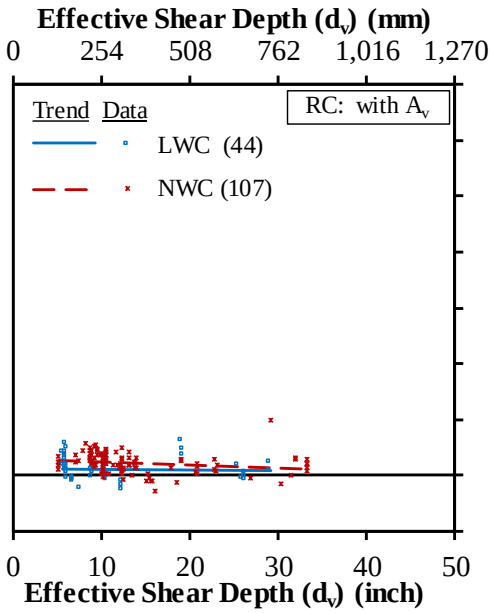

Source: FHWA.
1 ksi = 6.89 MPa.

Figure 127. Graph. Test-to-predicted shear resistance compared to effective shear depth for GP-equation method for LWC and NWC RC members with shear reinforcement.

Figure 128 through figure 131 show the ratios determined using the Simplified-PC/RC method. The trend line for the LWC specimens in figure 130 are below the trend line for the NWC specimens. The distance between the LWC and NWC trend lines is slightly larger than the difference shown in figure 122 and figure 123 and figure 126 and figure 127 for the Simplified-RC and GP-table method, respectively.

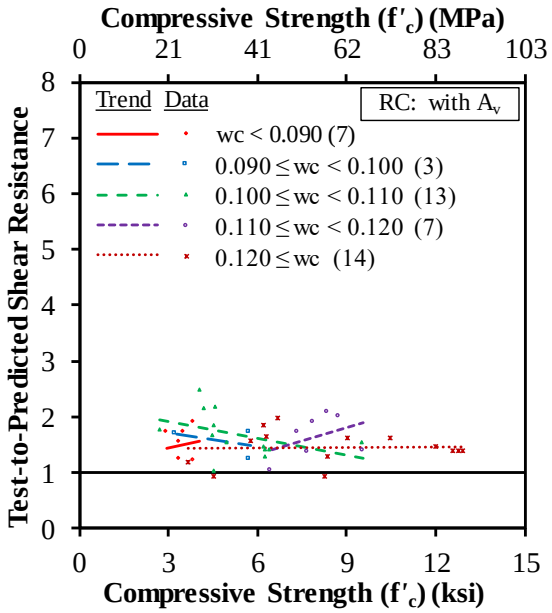

Source: FHWA.
1 ksi = 6.89 MPa.
Note: Unit weight (w_c) in the legend is measured in kcf where 1 kcf = 16,020 kg/m^3.

Figure 128. Graph. Test-to-predicted shear resistance compared to compressive strength for Simplified-PC/RC for LWC RC members with shear reinforcement.

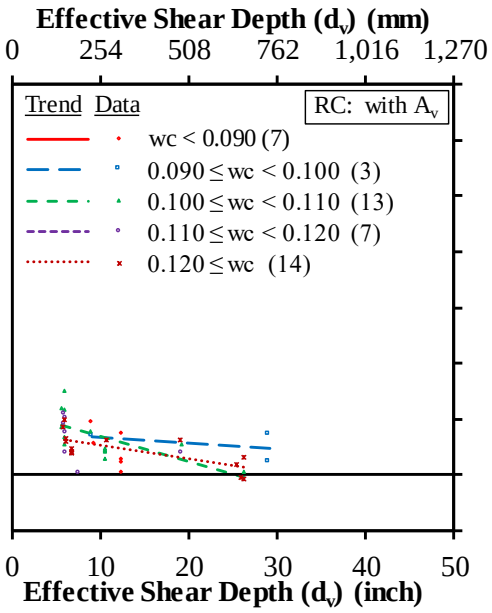

Source: FHWA.
1 inch = 25.4 mm.
Note: Unit weight (w_c) in the legend is measured in kcf where 1 kcf = 16,020 kg/m^3.

Figure 129. Graph. Test-to-predicted shear resistance compared to effective shear depth for Simplified-PC/RC for LWC RC members with shear reinforcement.

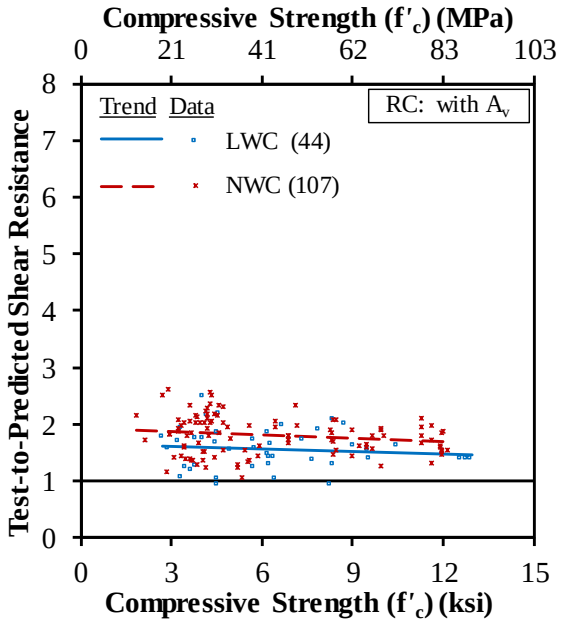

Source: FHWA.
1 ksi = 6.89 MPa.

Figure 130. Graph. Test-to-predicted shear resistance compared to compressive strength for Simplified-PC/RC for LWC and NWC RC members with shear reinforcement.

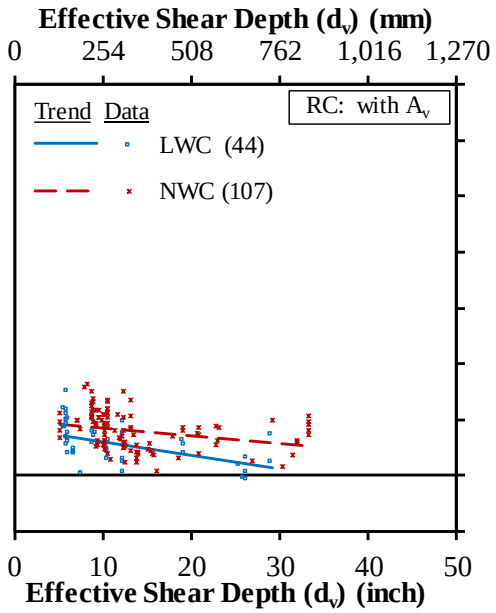

Source: FHWA.
1 inch = 25.4 mm.

Figure 131. Graph. Test-to-predicted shear resistance compared to effective shear depth for Simplified-PC/RC for LWC and NWC RC members with shear reinforcement.

PC Specimens Without Shear Reinforcement

The ratios for the limited number of LWC PC specimens without shear reinforcement are shown in figure 132 through figure 135 for shear resistance determined by the GP-equation procedure and in figure 136 through figure 139 for shear resistance determined by the Simplified-PC/RC procedure. The low V_{test} for the seven specimens described previously in this report has resulted in low test-to-prediction ratios for both procedures. The low ratios for these seven specimens, which have compressive strengths of approximately 8 and 12 ksi (55 and 83 MPa), had a large effect on the trend line for the LWC specimens. Excluding these seven tests, the trend line for the LWC specimens would be above the trend line for the NWC for both design procedures.

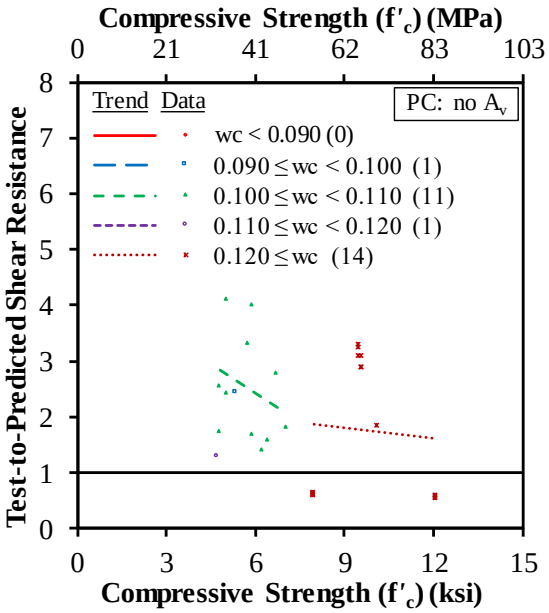

Source: FHWA.
1 ksi = 6.89 MPa.
Note: Unit weight (w_c) in the legend is measured in kcf where 1 kcf = 16,020 kg/m^3.

Figure 132. Graph. Test-to-predicted shear resistance compared to compressive strength for GP-equation method for LWC PC members without shear reinforcement.

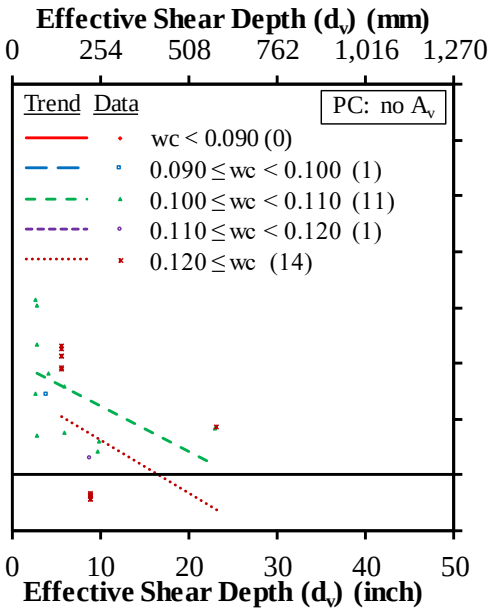

Source: FHWA.
1 inch = 25.4 mm.
Note: Unit weight (w_c) in the legend is measured in kcf where 1 kcf = 16,020 kg/m^3.

Figure 133. Graph. Test-to-predicted shear resistance compared to effective shear depth for GP-equation method for LWC PC members without shear reinforcement.

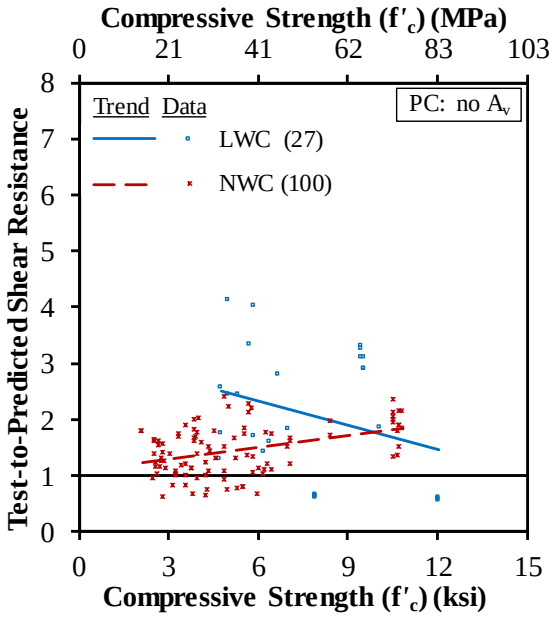

Source: FHWA.
1 ksi = 6.89 MPa.

Figure 134. Graph. Test-to-predicted shear resistance compared to compressive strength for GP-equation method for LWC and NWC PC members without shear reinforcement.

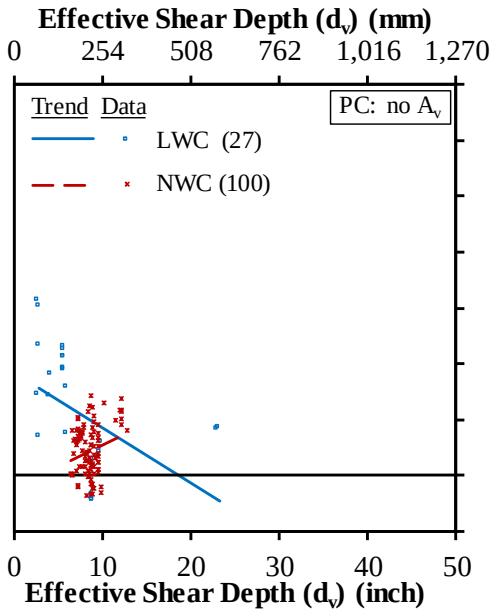

Source: FHWA.
1 inch = 25.4 mm.

Figure 135. Graph. Test-to-predicted shear resistance compared to effective shear depth for GP-equation method for LWC and NWC PC members without shear reinforcement.

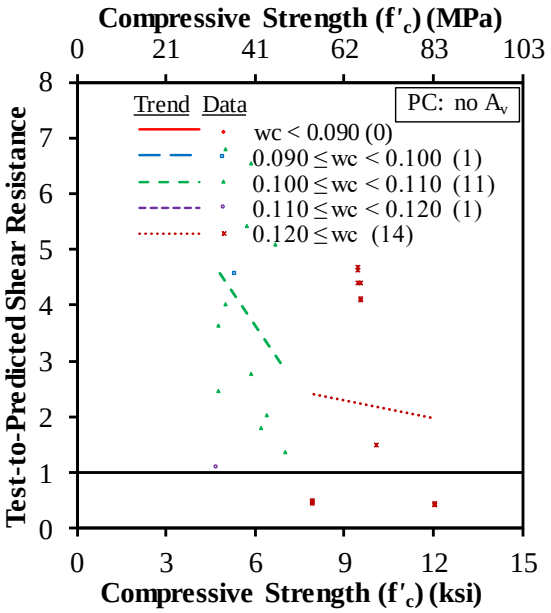

Source: FHWA.
1 ksi = 6.89 MPa.
Note: Unit weight (w_c) in the legend is measured in kcf where 1 kcf = 16,020 kg/m^3.

Figure 136. Graph. Test-to-predicted shear resistance compared to compressive strength for Simplified-PC/RC for LWC PC members without shear reinforcement.

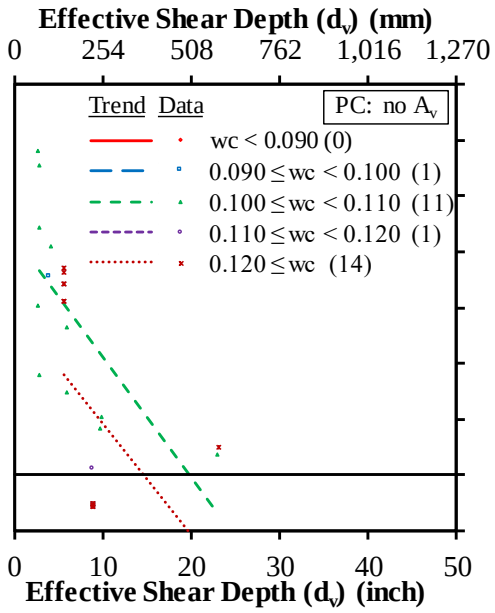

Source: FHWA.
1 inch = 25.4 mm.
Note: Unit weight (w_c) in the legend is measured in kcf where 1 kcf = 16,020 kg/m^3.

Figure 137. Graph. Test-to-predicted shear resistance compared to effective shear depth for Simplified-PC/RC for LWC PC members without shear reinforcement.

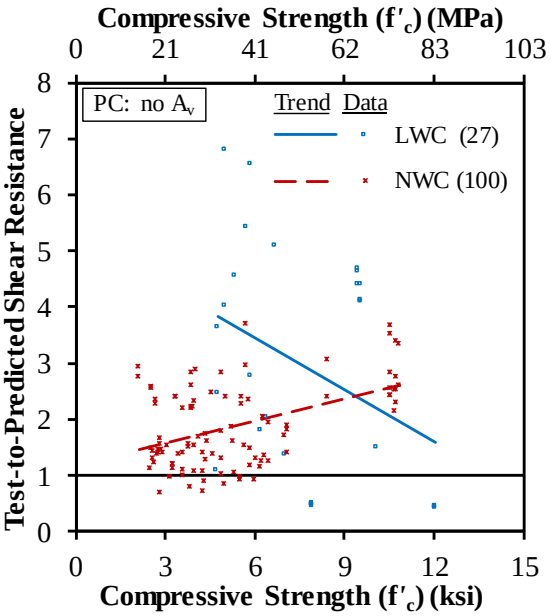

Source: FHWA.
1 ksi = 6.89 MPa.

Figure 138. Graph. Test-to-predicted shear resistance compared to compressive strength for Simplified-PC/RC for LWC and NWC PC members without shear reinforcement.

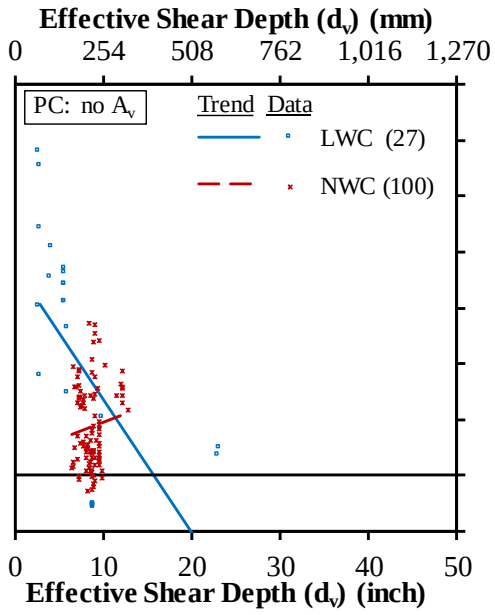

Source: FHWA.
1 inch = 25.4 mm.

Figure 139. Graph. Test-to-predicted shear resistance compared to effective shear depth for Simplified-PC/RC for LWC and NWC PC members without shear reinforcement.

PC Specimens With Shear Reinforcement

The ratios for the PC specimens with shear reinforcement are shown in figure 140 through figure 147. Figure 140 through figure 143 show the ratios for shear resistance determined using the GP-equation method, and figure 144 through figure 147 show the ratios for shear resistance determined using the Simplified-PC/RC procedure. The similar prediction of shear resistance for the LWC and NWC specimens is shown by their nearly overlapping trend lines in figure 142 and figure 143 as well as figure 146 and figure 147.

The 10 SDC specimens that are a part of the experimental research described in chapter 3 of this report can be seen in figure 140 through figure 147. The effective depth for these specimens was slightly greater than 30 inches (762 mm) and slightly less than 50 inches (1,270 mm). The trend lines for LWC that include these 10 specimens was parallel to the line, indicating a ratio of 1.0 in figure 142 and figure 143 as well as figure 146 and figure 147. This indicates that the ratios determined for both the GP-equation procedure and the Simplified-PC/RC procedure were independent of effective shear depth.

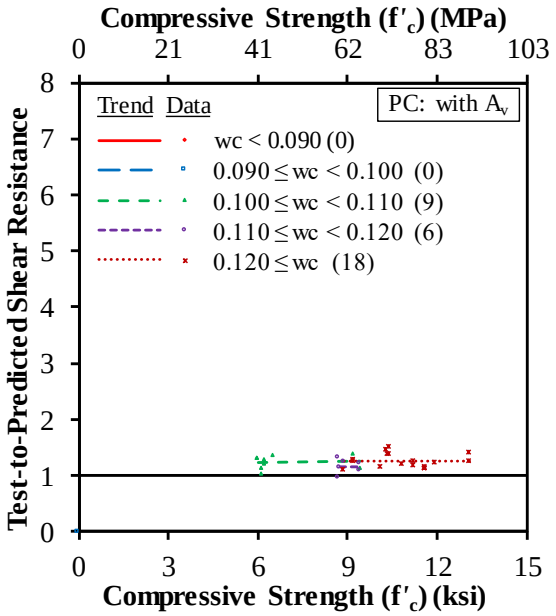

Source: FHWA.
1 ksi = 6.89 MPa.
Note: Unit weight (w_c) in the legend is measured in kcf where 1 kcf = 16,020 kg/m^3.

Figure 140. Graph. Test-to-predicted shear resistance compared to compressive strength for GP-equation method for LWC PC members with shear reinforcement.

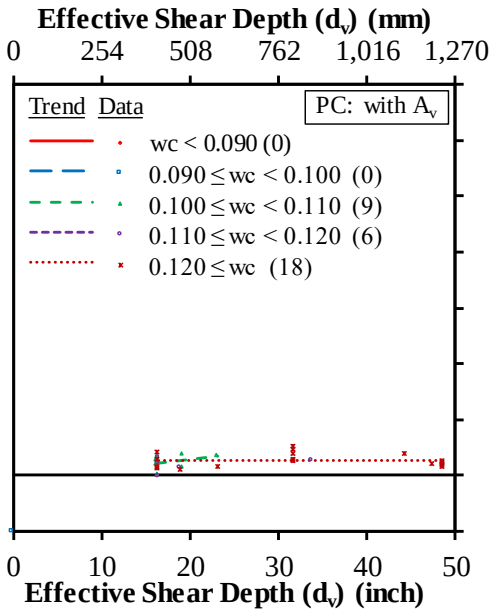

Source: FHWA.
1 inch = 25.4 mm.
Note: Unit weight (w_c) in the legend is measured in kcf where 1 kcf = 16,020 kg/m^3.

Figure 141. Graph. Test-to-predicted shear resistance compared to effective shear depth for GP-equation method for LWC PC members with shear reinforcement.

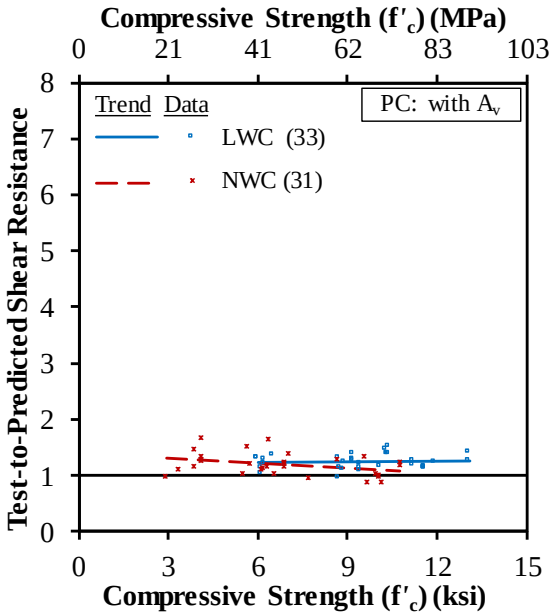

Source: FHWA.
1 ksi = 6.89 MPa.

Figure 142. Graph. Test-to-predicted shear resistance compared to compressive strength for GP-equation method for LWC and NWC PC members with shear reinforcement.

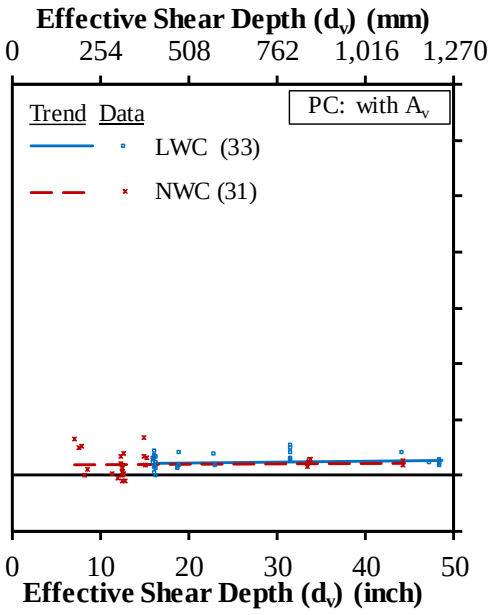

Source: FHWA.
1 inch = 25.4 mm.

Figure 143. Graph. Test-to-predicted shear resistance compared to effective shear depth for GP-equation method for LWC and NWC PC members with shear reinforcement.

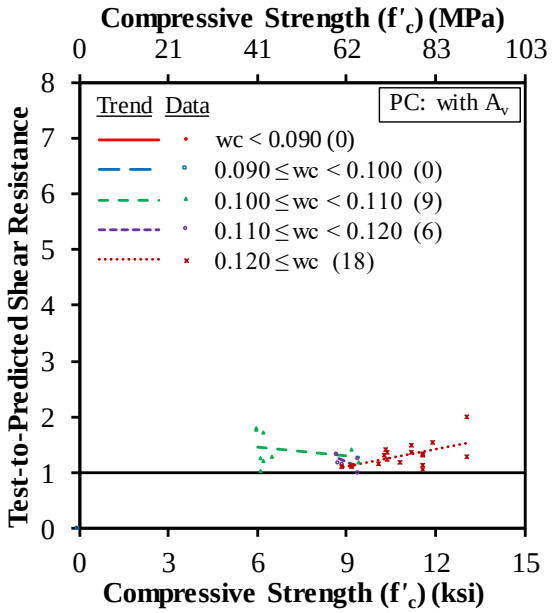

Source: FHWA.
1 ksi = 6.89 MPa.
Note: Unit weight (w_c) in the legend is measured in kcf where 1 kcf = 16,020 kg/m^3.

Figure 144. Graph. Test-to-predicted shear resistance compared to compressive strength for Simplified-PC/RC for LWC PC members with shear reinforcement.

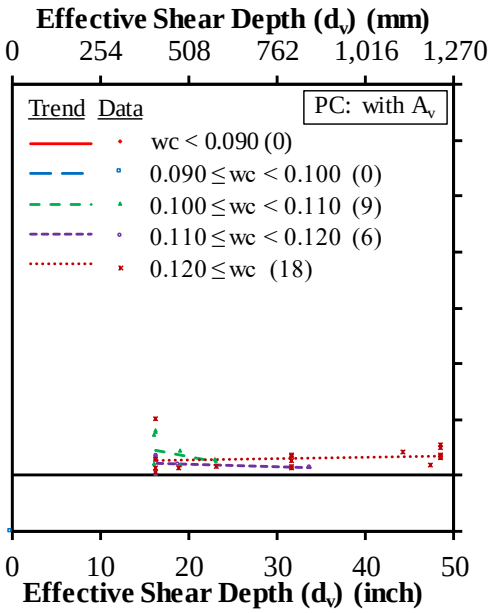

Source: FHWA.
1 inch = 25.4 mm.
Note: Unit weight (w_c) in the legend is measured in kcf where 1 kcf = 16,020 kg/m^3.

Figure 145. Graph. Test-to-predicted shear resistance compared to effective shear depth for Simplified-PC/RC for LWC PC members with shear reinforcement.

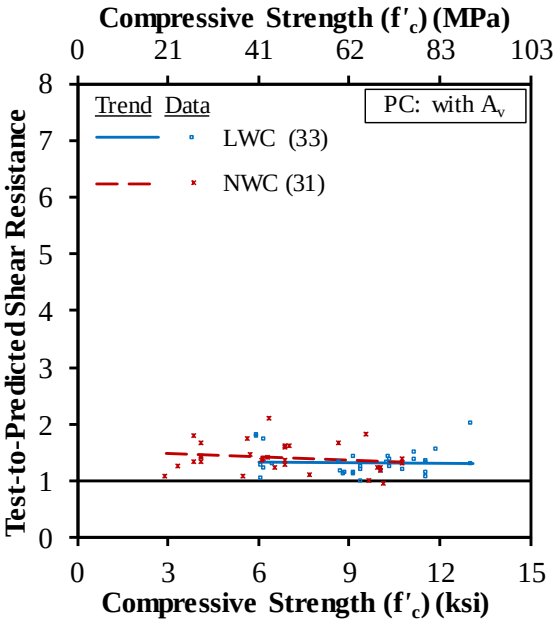

Source: FHWA.
1 ksi = 6.89 MPa.

Figure 146. Graph. Test-to-predicted shear resistance compared to compressive strength for Simplified-PC/RC for LWC and NWC PC members with shear reinforcement.

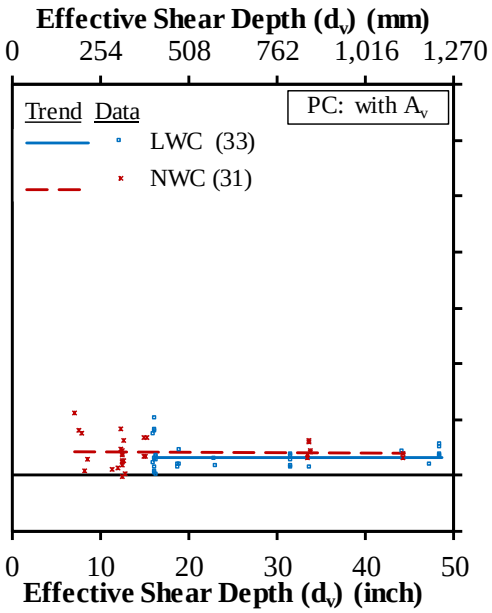

Source: FHWA.
1 inch = 25.4 mm.

Figure 147. Graph. Test-to-predicted shear resistance compared to effective shear depth for Simplified-PC/RC for LWC and NWC PC members with shear reinforcement.

Lower Limit on Shear Reinforcement in RC and PC Specimens

In this section, test-to-prediction ratios for shear resistance were used to evaluate the expression for minimum shear reinforcement. The expression for the minimum shear reinforcement in the *AASHTO LRFD Bridge Design Specifications* is provided in equation 10.[(3)] As specified in Article 5.8.2.2, this expression shall be modified for the effects of LWC. The proposed expression, including the λ-factor, is provided in equation 49. As a result of modifying the expression for LWC, the minimum amount of shear reinforcement determined for an LWC member was up to 25 percent less than the amount determined for a similar NWC member.

Figure 148 through figure 157 compare the test-to-prediction ratios to the amount of shear reinforcement. The ratios for the RC specimens were determined using the Simplified-RC procedure (see figure 148 and figure 149), the GP-equation method (see figure 150 and figure 151), and the Simplified-PC/RC procedure (see figure 152 and figure 153). Four figures give the ratios for PC members with shear reinforcement, which were determined using the GP-equation method (see figure 154 and figure 155) and the Simplified-PC/RC procedure (see figure 156 and figure 157). The amount of shear reinforcement is given as the reinforcement ratio ($A_v/b_v s$) multiplied by the ratio $f_y/\sqrt{f'_c}$. The amount of shear reinforcement expressed in this manner is based on the rearrangement of the equation for minimum shear reinforcement as shown in equation 46.

Figure 148 and figure 149 show the ratios determined using the Simplified-RC procedure for the RC specimens that satisfied the limits of the procedure. In figure 148, the ratios are shown in groups by w_c. The ratios for LWC and NWC specimens are shown in figure 149. The graph on the left in figure 148 and figure 149 shows the ratios over the full range of the horizontal axis, while the graph on the right shows the data for specimens over a range of shear reinforcement ratios closer to the minimum amount of shear reinforcement given by equation 10. The minimum amount of reinforcement is indicated by the vertical line at 0.0316.

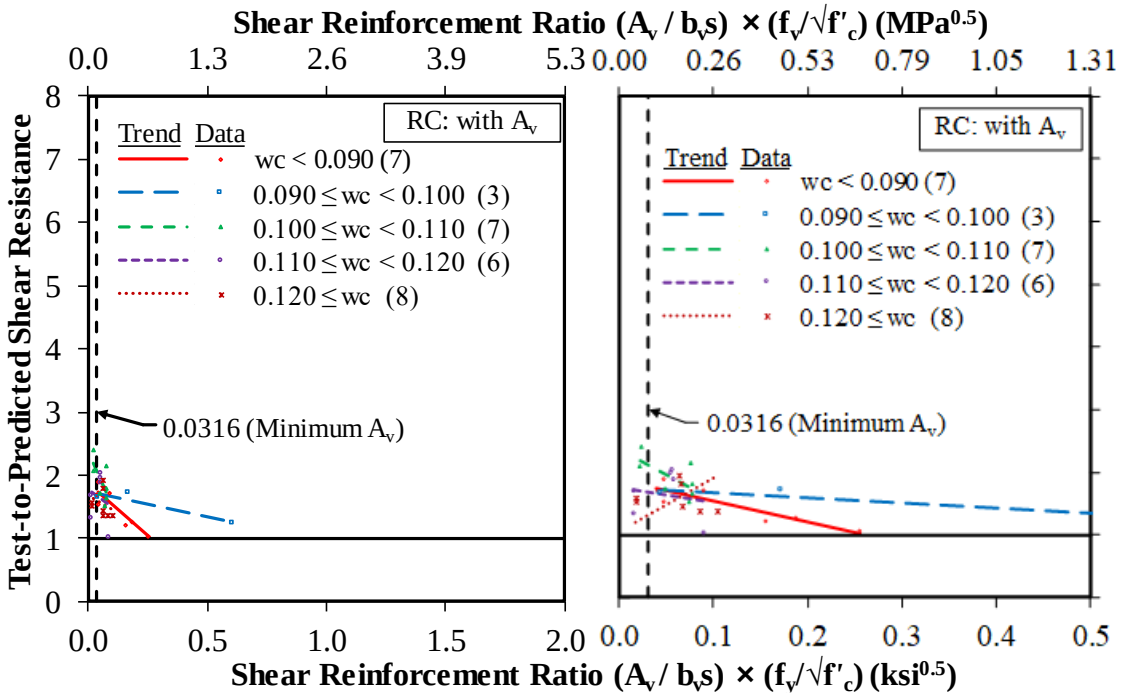

Source: FHWA.
1 ksi = 6.89 MPa.
Note: Unit weight (w_c) in the legend is measured in kcf where 1 kcf = 16,020 kg/m^3.

Figure 148. Graphs. Test-to-predicted shear resistance compared to shear reinforcement ratio multiplied by the ratio of stirrup yield strength to the square root of concrete compressive strength for Simplified-RC for LWC RC members with shear reinforcement.

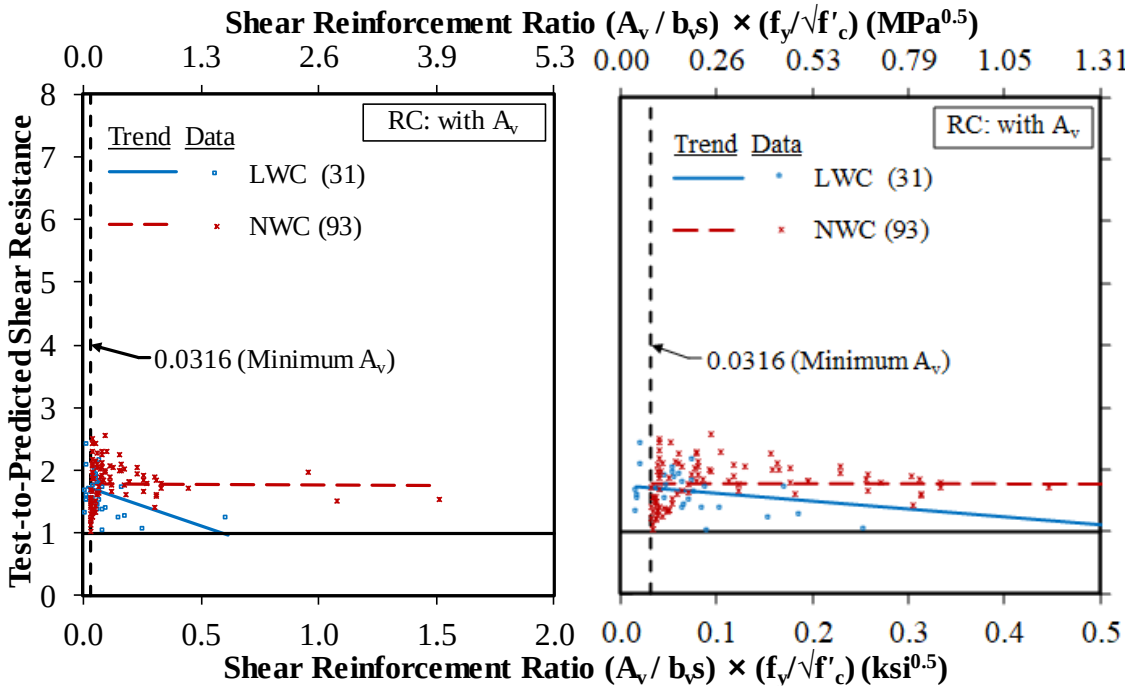

Source: FHWA.
1 ksi = 6.89 MPa.

Figure 149. Graphs. Test-to-predicted shear resistance compared to shear reinforcement ratio multiplied by the ratio of stirrup yield strength to the square root of concrete compressive strength for Simplified-RC for LWC and NWC RC members with shear reinforcement.

A λ-factor of 0.75 is the smallest modification factor possible for the proposed LWC modification factor using equation 36 through equation 38 and the smallest for all-lightweight concrete in the *AASHTO LRFD Bridge Design Specifications*.[3] Using the proposed equation 49 for the minimum amount of shear reinforcement with a λ-factor of 0.75 is shown by the vertical line at 0.0237 (i.e., a line slightly to the left of the one shown at 0.0316) in figure 148 and figure 149. There are six specimens with an amount of shear reinforcement less than the minimum given by equation 10 (i.e., shown on the left side of the vertical line at 0.0316). They have an amount of shear reinforcement that is also less than that given by equation 49 using a λ-factor of 0.75. As shown in figure 148, the test-to-prediction ratios for these six specimens appear to have similar values to the specimens with an amount of shear reinforcement slightly greater than the minimum amount given by equation 10. This is also indicated by the regression line for the LWC specimens in figure 149 that is slightly higher for the specimens with shear reinforcement less than the minimum amount.

The ratios determined using the GP-equation method are shown in figure 150 and figure 151, and the ratios determined using the Simplified-PC/RC procedure are shown in figure 152 and figure 153. Note that these four figures present the ratios in a similar manner as in figure 148 and figure 149. In each of these figures, the left-hand graph shows the ratios over the full range of the horizontal axis. The right-hand graph shows the data for specimens over a range of shear reinforcement ratios closer to the minimum amount of shear reinforcement given by equation 10.

There are nine specimens shown in figure 150 through figure 153 with an amount of shear reinforcement less than the minimum amount given by equation 10, as indicated by their position to the left of the vertical line at 0.0316. For all nine of these specimens, their amount of shear reinforcement is also less than that given by equation 49 using a λ-factor of 0.75. The test-to-prediction ratios for these nine specimens is similar to the ratios at slightly larger shear reinforcement values (i.e., slightly to the right of the line at 0.0316).

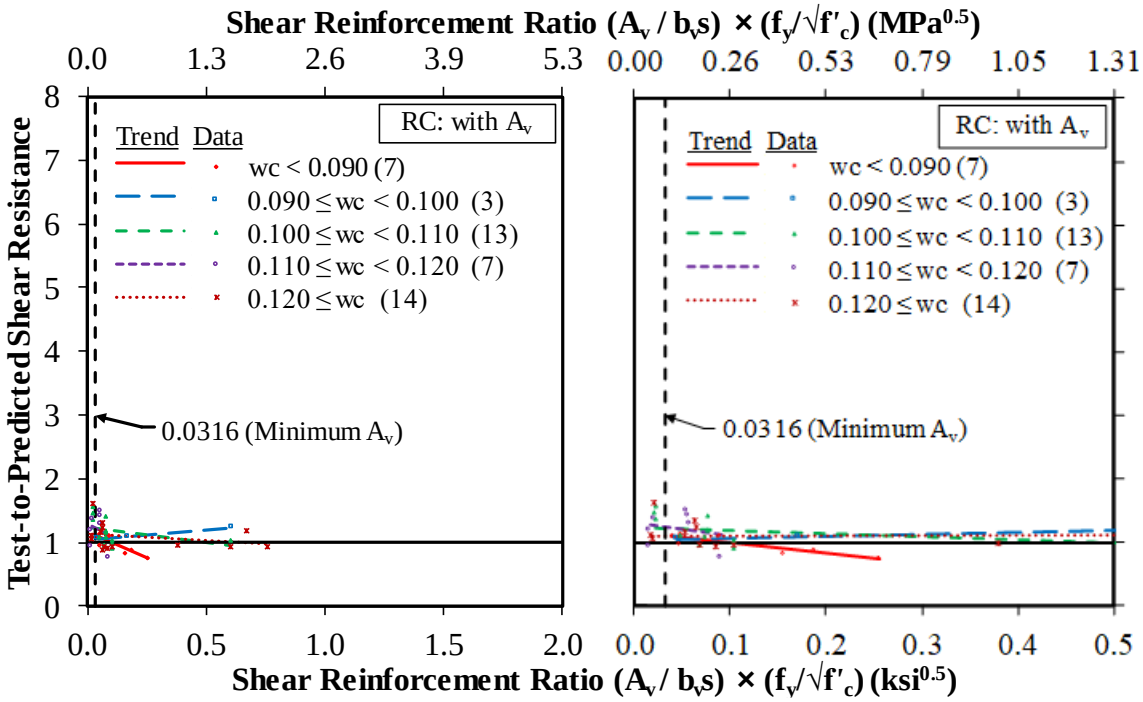

Source: FHWA.
1 ksi = 6.89 MPa.
Note: Unit weight (w_c) in the legend is measured in kcf where 1 kcf = 16,020 kg/m^3.

Figure 150. Graphs. Test-to-predicted shear resistance compared to the shear reinforcement ratio multiplied by the ratio of stirrup yield strength to the square root of concrete compressive strength for the GP-equation method for LWC RC members with shear reinforcement.

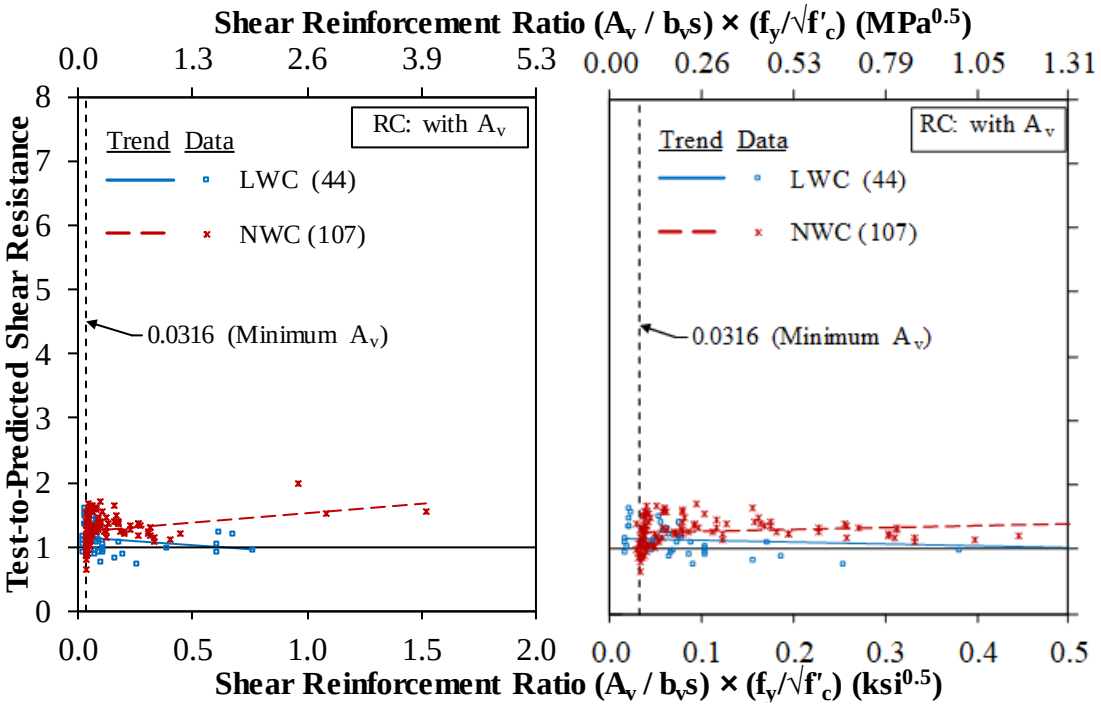

Source: FHWA.
1 ksi = 6.89 MPa.

Figure 151. Graphs. Test-to-predicted shear resistance compared to the shear reinforcement ratio multiplied by the ratio of stirrup yield strength to the square root of concrete compressive strength for the GP-equation method for LWC and NWC RC members with shear reinforcement.

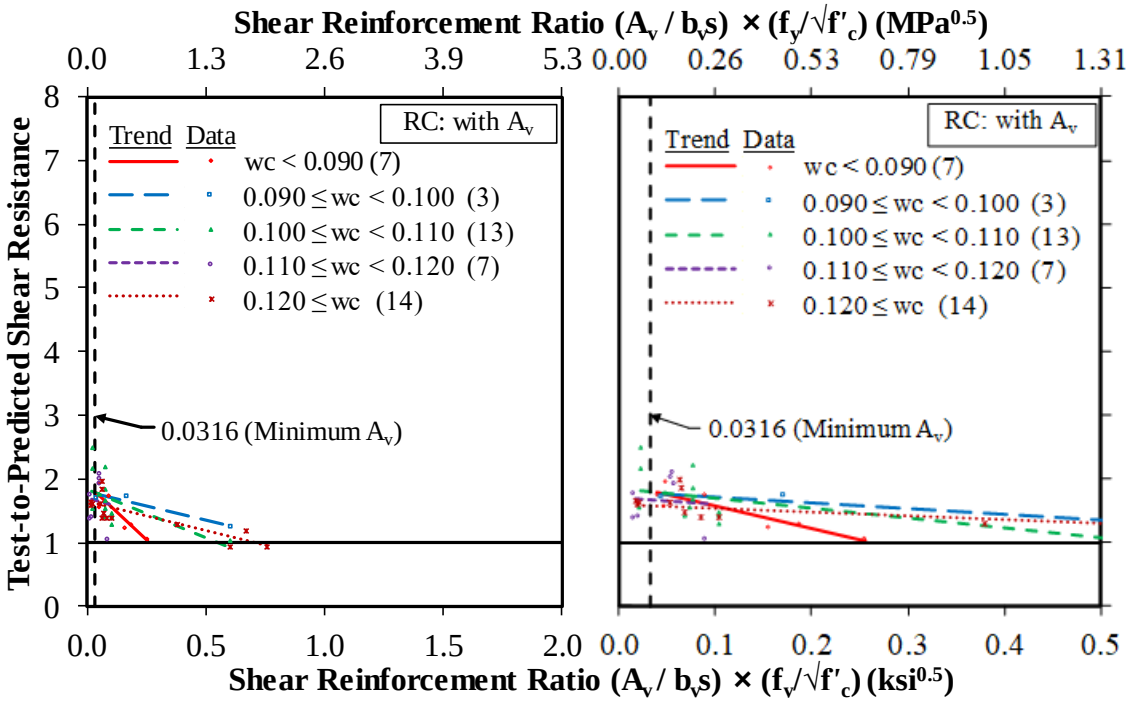

Source: FHWA.
1 ksi = 6.89 MPa.
Note: Unit weight (w_c) in the legend is measured in kcf where 1 kcf = 16,020 kg/m^3.

Figure 152. Graphs. Test-to-predicted shear resistance compared to the shear reinforcement ratio multiplied by the ratio of stirrup yield strength to the square root of concrete compressive strength for Simplified-PC/RC for LWC RC members with shear reinforcement.

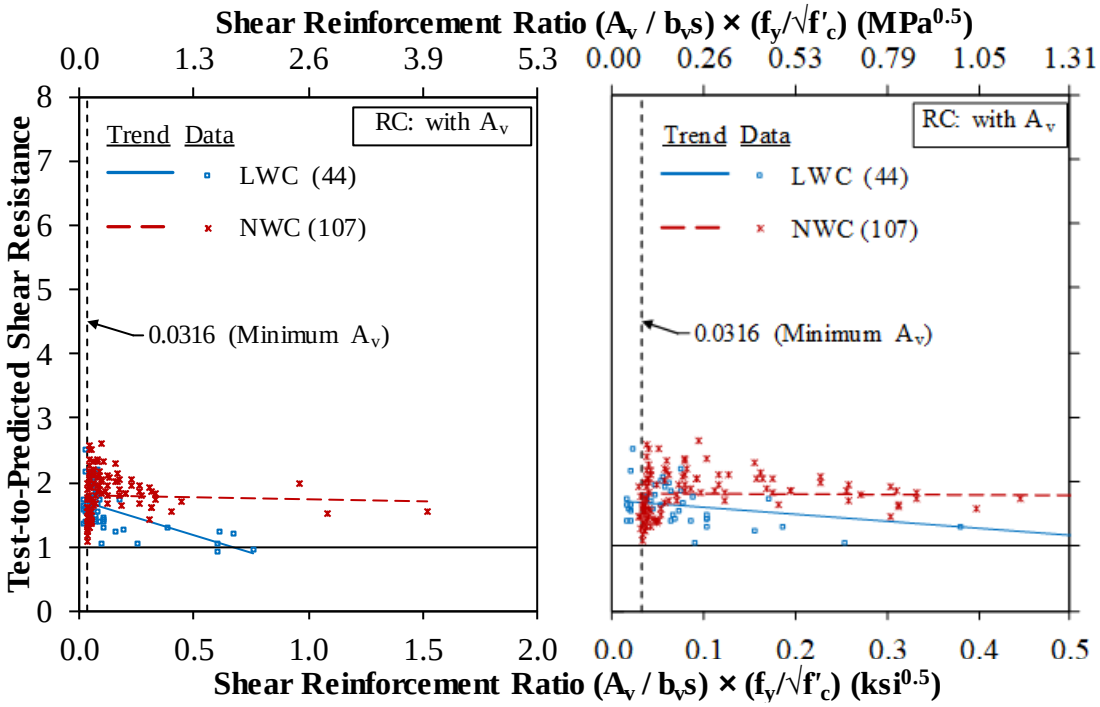

Source: FHWA.
1 ksi = 6.89 MPa.

Figure 153. Graphs. Test-to-predicted shear resistance compared to the shear reinforcement ratio multiplied by the ratio of stirrup yield strength to the square root of concrete compressive strength for Simplified-PC/RC for LWC and NWC RC members with shear reinforcement.

Similar trends were observed in the figures for PC specimens with shear reinforcement. Figure 154 and figure 155 show the ratios determined using the GP-equation method, and figure 156 and figure 157 show the ratios determined using the Simplified-PC/RC procedure. The four specimens with less shear reinforcement than the minimum given by equation 10 were also less than the minimum given by equation 49 using a λ-factor of 0.75. Similar to the RC specimens, these four PC specimens had similar test-to-prediction ratios as the specimens with slightly more shear reinforcement. Note that the four figures also present the ratios in a similar manner as in figure 148 and figure 149. In each of these figures, the left-hand graph shows the ratios over the full range of the horizontal axis, and the right-hand graph shows the data for specimens over a range of shear reinforcement ratios closer to the minimum amount of shear reinforcement given by equation 10.

For both RC and PC specimens in the TFHRC shear database, the test-to-prediction ratios for LWC specimens with less shear reinforcement than the minimums given by equation 10 and equation 49 are similar to the ratios for specimens with slightly more shear reinforcement. Also, nearly all of the LWC specimens with an amount of shear reinforcement near the minimum had ratios that were greater than 1.0 regardless of the method used to determine shear resistance.

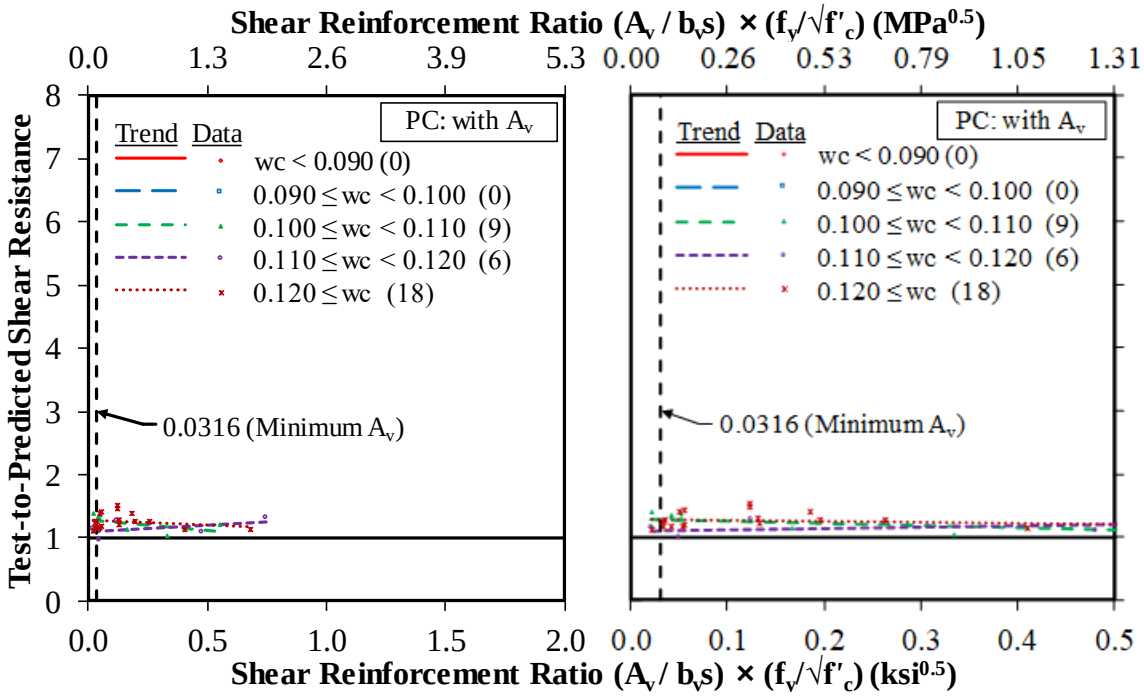

Source: FHWA.
1 ksi = 6.89 MPa.
Note: Unit weight (w_c) in the legend is measured in kcf where 1 kcf = 16,020 kg/m^3.

Figure 154. Graphs. Test-to-predicted shear resistance compared to the shear reinforcement ratio multiplied by the ratio of stirrup yield strength to the square root of concrete compressive strength for the GP-equation method for LWC PC members with shear reinforcement.

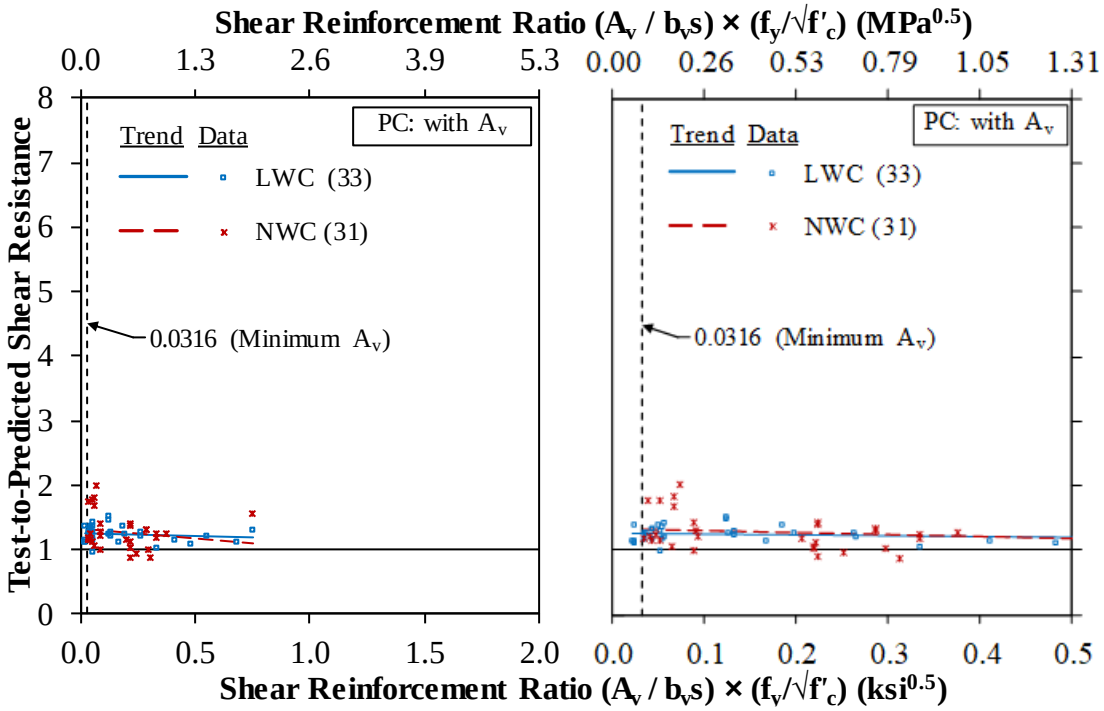

Source: FHWA.
1 ksi = 6.89 MPa.

Figure 155. Graphs. Test-to-predicted shear resistance compared to the shear reinforcement ratio multiplied by the ratio of stirrup yield strength to the square root of concrete compressive strength for the GP-equation method for LWC and NWC PC members with shear reinforcement.

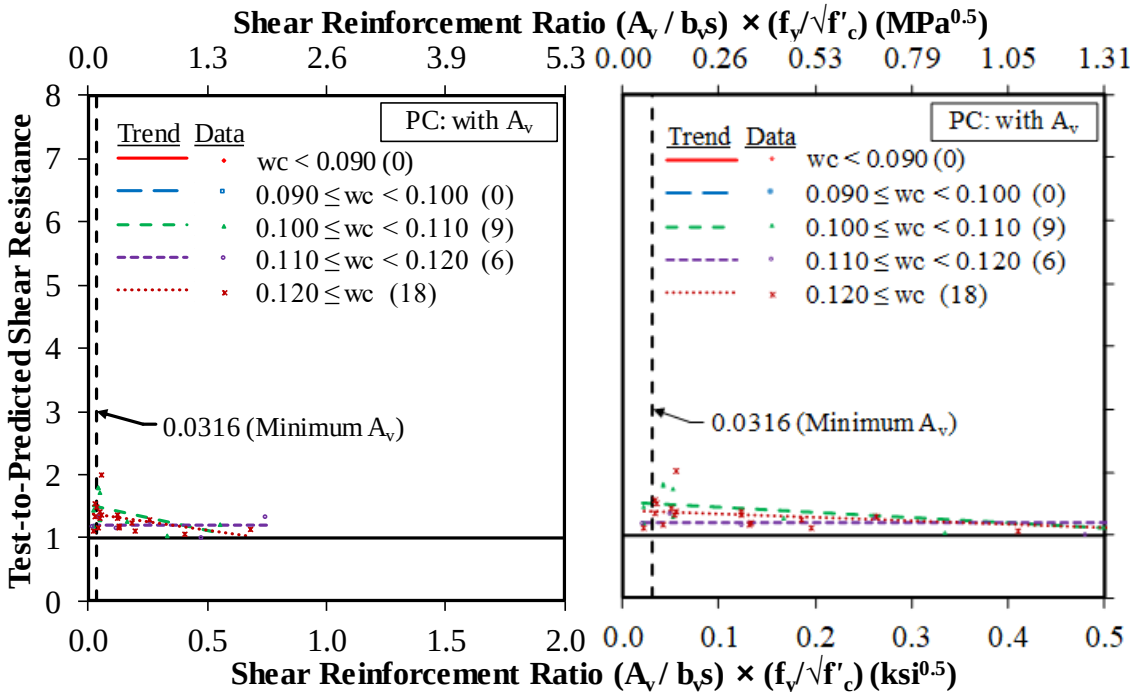

Source: FHWA.
1 ksi = 6.89 MPa.
Note: Unit weight (w_c) in the legend is measured in kcf where 1 kcf = 16,020 kg/m^3.

Figure 156. Graphs. Test-to-predicted shear resistance compared to the shear reinforcement ratio multiplied by the ratio of stirrup yield strength to the square root of concrete compressive strength for Simplified-PC/RC for LWC PC members with shear reinforcement.

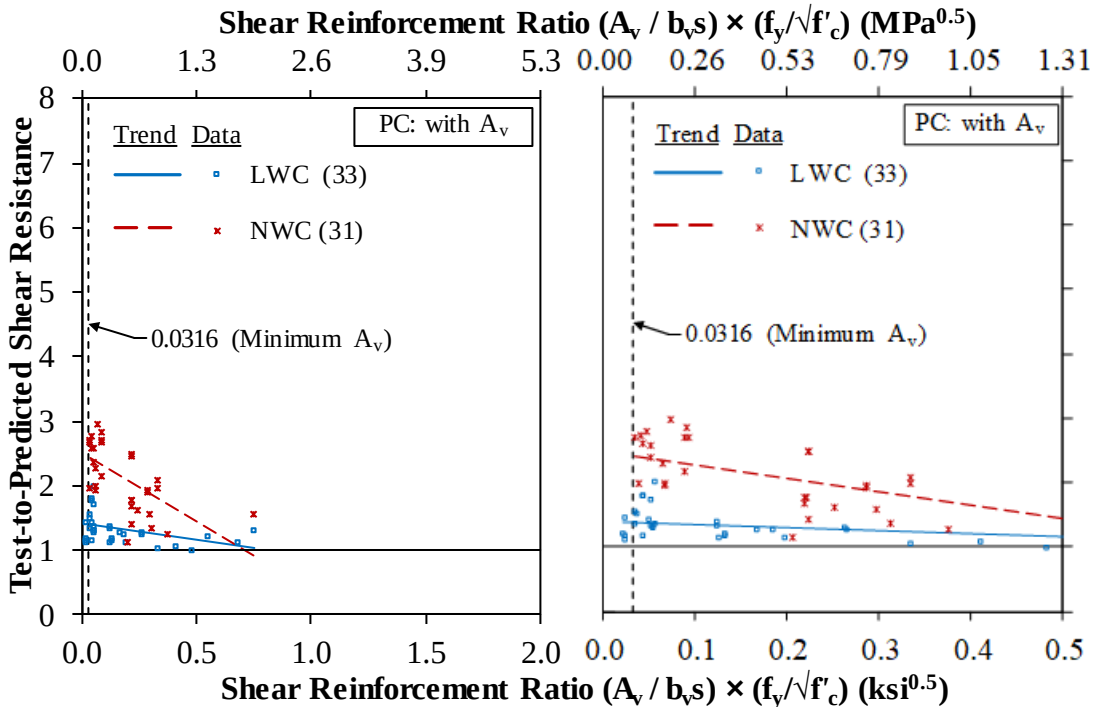

Source: FHWA.
1 ksi = 6.89 MPa.

Figure 157. Graphs. Test-to-predicted shear resistance compared to the shear reinforcement ratio multiplied by the ratio of stirrup yield strength to the square root of concrete compressive strength for Simplified-PC/RC for LWC and NWC PC members with shear reinforcement.

Upper Limit on Shear Resistance for RC and PC Specimens

In this section, test-to-prediction ratios for shear resistance were used to evaluate the upper limit on the average shear stress given by Article 5.8.3.3 in the *AASHTO LRFD Bridge Design Specifications*.[3] The expression for the upper limit is given by equation 14, which limits average stress equal to 25 percent of the concrete compressive strength.

Figure 158 through figure 165 compare the test-to-prediction ratios to the normalized average shear stress. Normalized shear stress is given as the ratio of average shear stress to f'_c. Average shear stress was determined using equation 39. Note that in each set of the following eight figures (see figure 158 through figure 165), the graph on the left shows the full range of shear stress on the horizontal axis, while the graph on the right shows the same graph over a limited range of shear stress near the upper limit of 0.25 f'_c on the horizontal axis. In each figure, a vertical line at 0.25 is shown to indicate the upper limit on shear stress. Two sets of figures are shown for RC specimens, and two more sets of figures are shown for PC specimens with shear reinforcement. The ratios were determined using the GP-equation and Simplified-PC/RC procedure for the both RC and PC specimens. Figures are not shown for the Simplified-RC procedure because only one specimen satisfied the limitations of the procedure that had a v_u greater than 0.25 f'_c.

The ratios for RC specimens determined using the GP-equation method are shown in figure 158 and figure 159, while figure 160 and figure 161 show the ratios determined using the Simplified-PC/RC procedure. These figures show that, for specimens with a normalized stress greater than the limit, there were no ratios less than 1.0. Also, the trend lines are nearly horizontal, indicating that ratios above and below the limit were similar. A similar trend is observed for the ratios of PC specimens. Figure 160 and figure 163 show the ratios determined using the GP-equation method. The ratios determined using the Simplified-PC/RC procedure are shown in figure 164 and figure 165.

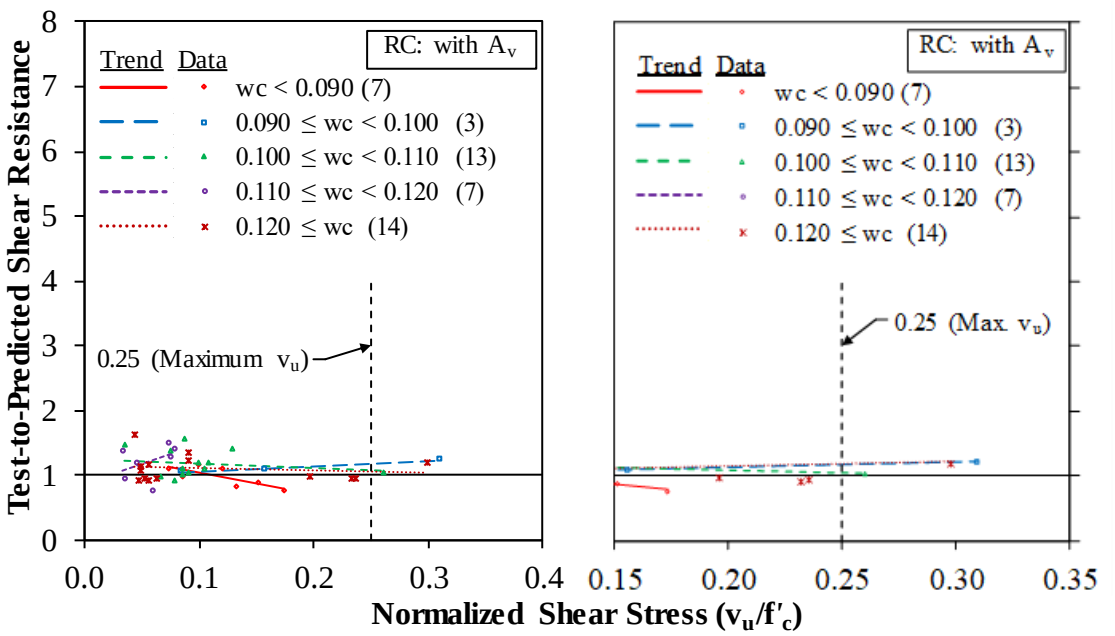

Source: FHWA.
Note: Unit weight (w_c) in the legend is measured in kcf where 1 kcf = 16,020 kg/m^3.

Figure 158. Graphs. Test-to-predicted shear resistance compared to normalized shear stress for the GP-equation method for LWC RC members with shear reinforcement.

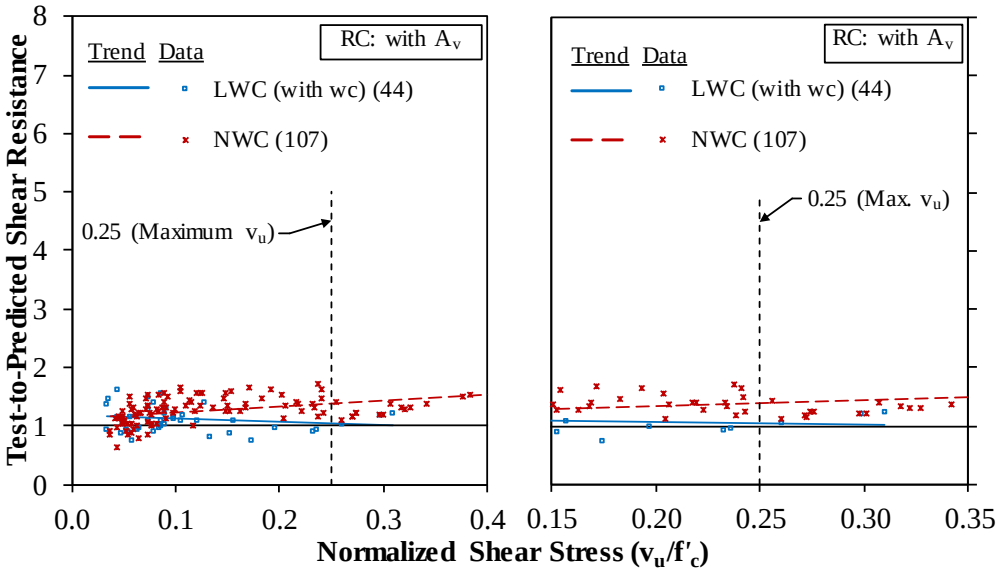

Source: FHWA.

Figure 159. Graphs. Test-to-predicted shear resistance compared to normalized shear stress for the GP-equation method for LWC and NWC RC members with shear reinforcement.

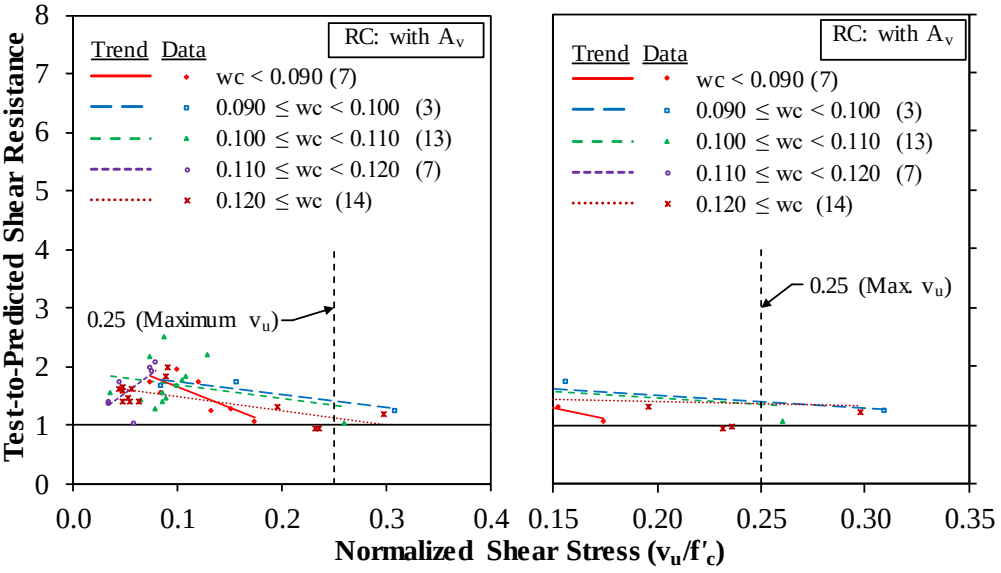

Source: FHWA.
Note: Unit weight (w_c) in the legend is measured in kcf where 1 kcf = 16,020 kg/m^3.

Figure 160. Graphs. Test-to-predicted shear resistance compared to normalized shear stress for Simplified-PC/RC for LWC RC members with shear reinforcement.

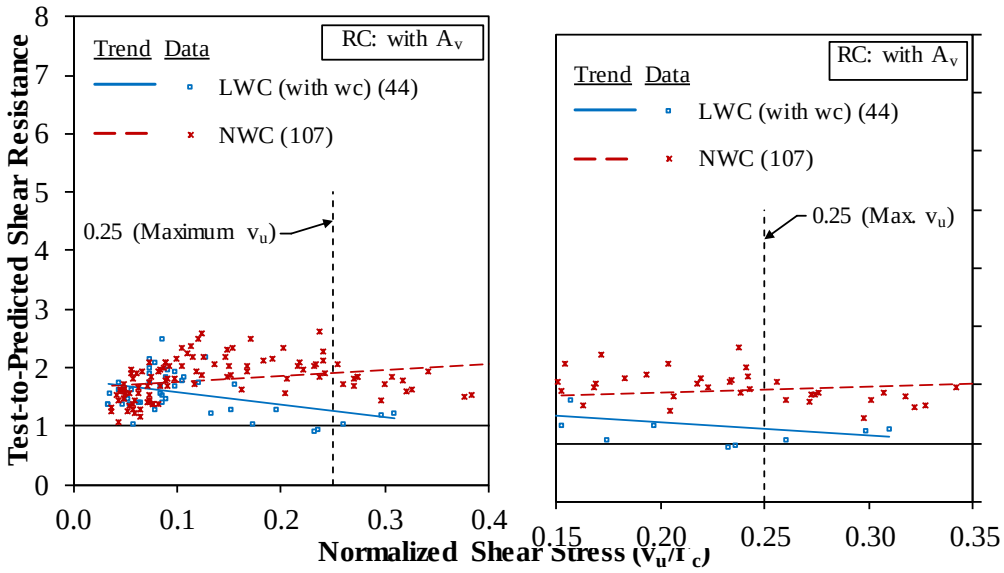

Source: FHWA.

Figure 161. Graphs. Test-to-predicted shear resistance compared to normalized shear stress for Simplified-PC/RC for LWC and NWC RC members with shear reinforcement.

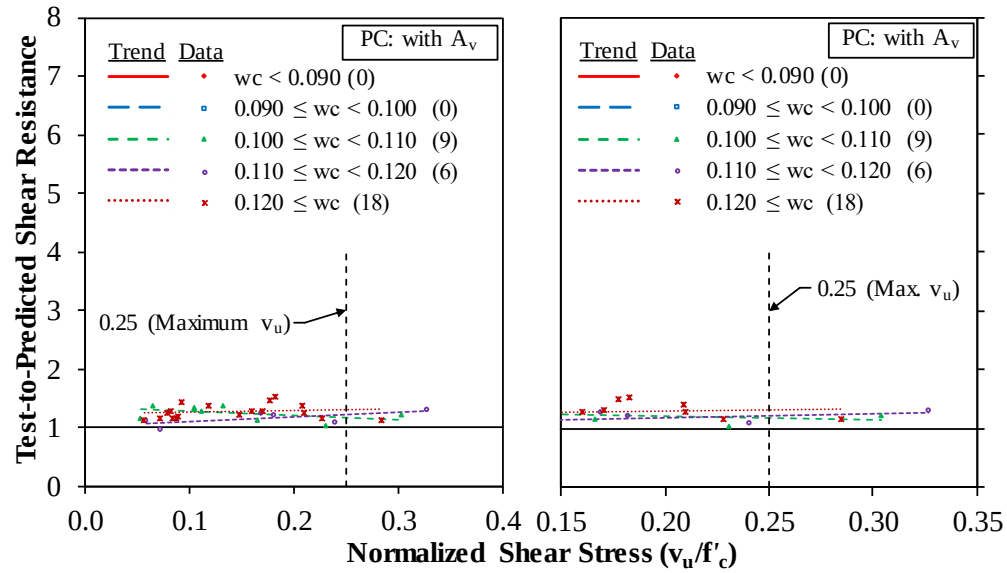

Source: FHWA.
Note: Unit weight (w_c) in the legend is measured in kcf where 1 kcf = 16,020 kg/m^3.

Figure 162. Graphs. Test-to-predicted shear resistance compared to normalized shear stress for the GP-equation method for LWC PC members with shear reinforcement.

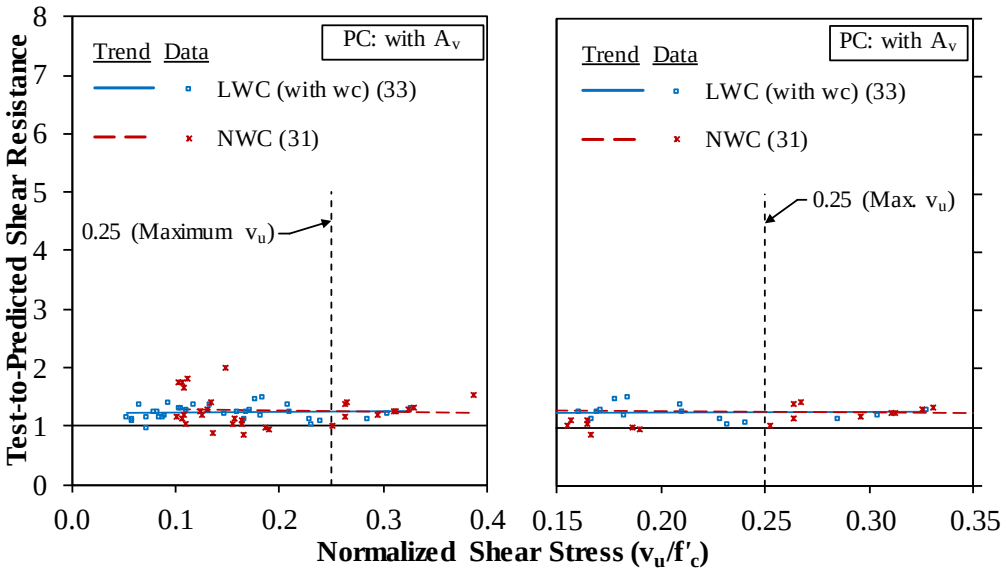

Source: FHWA.

Figure 163. Graphs. Test-to-predicted shear resistance compared to normalized shear stress for the GP-equation method for LWC and NWC PC members with shear reinforcement.

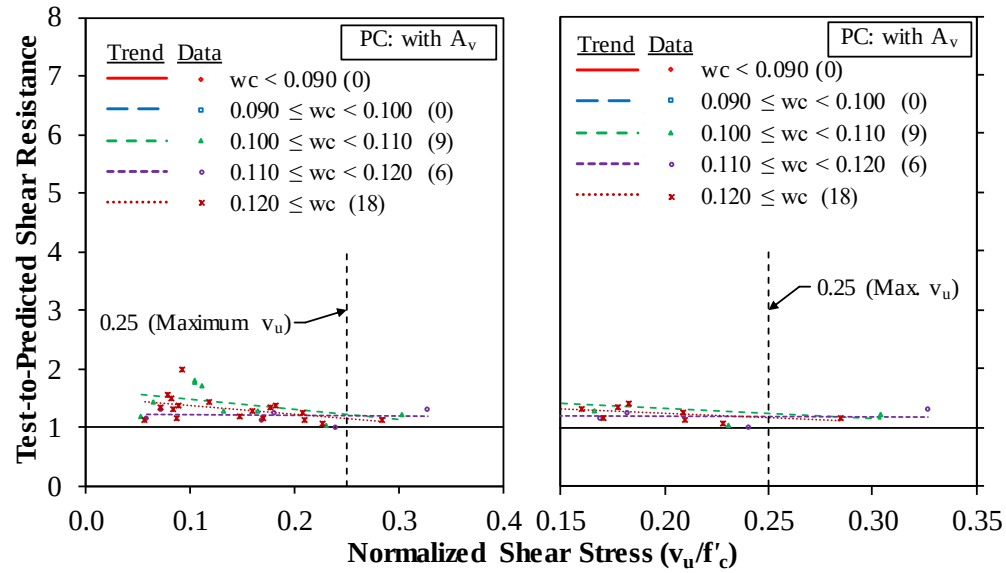

Source: FHWA.
Note: Unit weight (w_c) in the legend is measured in kcf where 1 kcf = 16,020 kg/m^3.

Figure 164. Graphs. Test-to-predicted shear resistance compared to normalized shear stress for Simplified-PC/RC for LWC PC members with shear reinforcement.

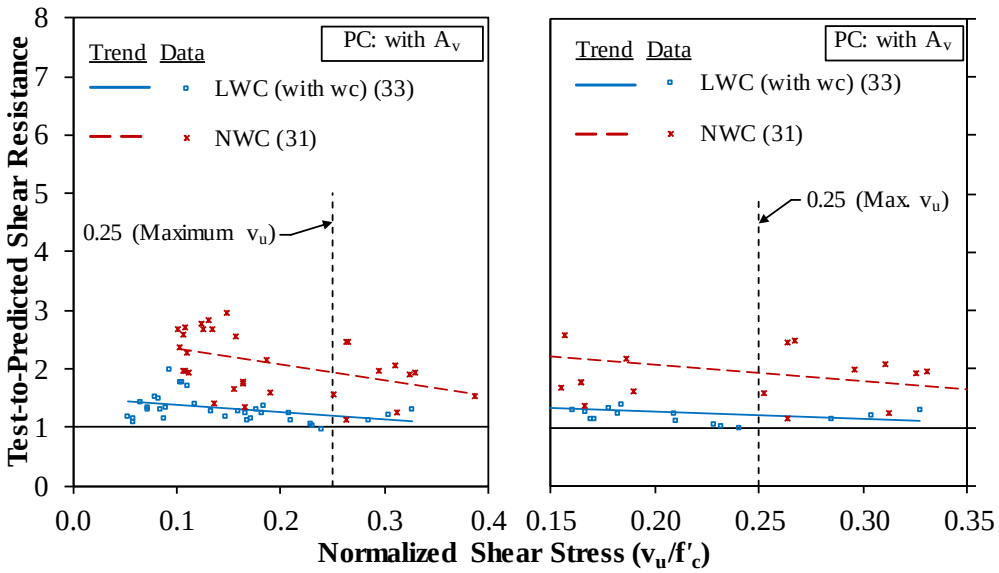

Source: FHWA.

Figure 165. Graphs. Test-to-predicted shear resistance compared to normalized shear stress for Simplified-PC/RC for LWC and NWC PC members with shear reinforcement.

SUMMARY OF SHEAR STRESS AND SHEAR RESISTANCE ANALYSES

The average shear stress at failure and predicted shear resistance was evaluated on tests of LWC beams. The results of LWC beam tests were compared to NWC beam tests to determine the effect of using lightweight aggregate.

Normalized Shear Stress

The regression line for the normalized shear stress of LWC specimens without shear reinforcement was slightly less than the normalized stress of NWC specimens, indicating a modification for LWC may be appropriate. A dependence of normalized shear strength on w_c was not observed for RC specimens without shear reinforcement. Although the data on LWC specimens with an effective depth greater than 15 inches (381 mm) was limited, the regression lines for both LWC and NWC showed a decrease in normalized stress as the effective depth increased. This indicates that there was some dependence of shear strength on the effective depth of RC beams without shear reinforcement.

The difference between the LWC and NWC regression lines indicating normalized shear stress was greater for specimens with shear reinforcement than for specimens without shear reinforcement. This suggests that the effect of lightweight aggregate on shear strength was more pronounced for members with shear reinforcement than for members without shear reinforcement. A dependence of normalized shear strength on w_c was not observed for RC specimens with shear reinforcement. The regression lines for both LWC and NWC showed a slight decrease in normalized shear stress as the normalized spacing of shear reinforcement increased.

There were a limited number of tests on PC specimens without shear reinforcement. The regression line for the normalized shear stress of the LWC data was below the regression line of the NWC data, indicating a potential need for a reduction factor for LWC. The limited LWC data did not allow a comparison of normalized shear strength with concrete unit weight for PC specimens without shear reinforcement.

Similar to the trend observed for RC specimens, the regression line for the normalized shear stress of LWC PC specimens with shear reinforcement was below the NWC regression line. A dependence of normalized shear strength on concrete unit weight was not observed for PC specimens with shear reinforcement. The regression lines for both LWC and NWC showed a decrease in normalized shear stress as the normalized spacing of shear reinforcement increased, although the slope of the LWC line was much less (i.e., closer to horizontal) than the NWC line.

A clear trend was shown of the normalized shear stress increasing for LWC specimens as the ratio of shear span-to-effective a/d_v decreased. This trend did not appear to be dependent on w_c.

Predicted Shear Resistance—Comparisons of Design Methodologies and LWC Modification Factor

In the *AASHTO LRFD Bridge Design Specifications*, the modification factor for LWC is applied to cot θ in the Simplified-PC/RC procedure.[3] For PC members with shear reinforcement, this can result in the predicted shear resistance of an LWC member being greater than the predicted resistance of a NWC member with similar dimensions and material strengths.

Test-to-prediction ratios were determined for the design methodologies in the *AASHTO LRFD Bridge Design Specifications* using the proposed expression for the λ-factor.[3] The mean test-to-prediction ratios for all specimens determined using the GP-equation and GP-table methods were similar with values of 1.32 and 1.39, respectively, and had a COV of nearly 50 percent. The mean ratio determined using the Simplified-PC/RC procedure was larger with a value of 2.07 and a COV of nearly 60 percent.

Test-to-prediction ratios were determined to compare the proposed λ-factor based on w_c and the modification for LWC in the *AASHTO LRFD Bridge Design Specifications* based on concrete constituents (i.e., all-lightweight and sand-lightweight).[3] The ratios were determined for specimens with either all-lightweight or sand-lightweight concrete. The mean ratios determined using the modification for LWC in the AASHTO modified method were 1 to 2 percent larger than the ratios determined using the proposed λ-factor based on w_c. The COV for a design method was nearly the same regardless of the method of LWC modification.

The test-to-prediction ratios for LWC specimens with less shear reinforcement than the minimum amount given by the *AASHTO LRFD Bridge Design Specifications* were similar to the ratios for specimens with slightly more shear reinforcement.[3] This trend was observed for both RC and PC specimens. Nearly all of the LWC specimens with an amount of shear reinforcement near the minimum had ratios that were greater than 1.0. This trend was observed regardless of the method used to determine shear resistance.

The mean test-to-prediction ratios for both RC and PC LWC specimens with a normalized stress greater than the upper limit given in the *AASHTO LRFD Bridge Design Specifications* were all

greater than 1.0.[3] The ratios for specimens slightly above and slightly below the limit were similar.

Predicted Shear Resistance—Comparison of LWC and NWC

The mean ratios determined for all of the LWC specimens in the TFHRC shear database were compared to the ratios determined for all of the NWC specimens in the ACI-DafStb database. (For sources, see both Bibliography sections.) The ratios of the LWC specimens were determined using the proposed λ-factor. The mean ratios for the LWC specimens were 9 to 10 percent larger than the ratios of the NWC specimens depending on the design procedure; however, the COVs determined for the LWC specimens were much larger than the COVs of the NWC specimens.

A comparison of the mean ratios for LWC specimens and the NWC specimens was also made by specimen type. The mean ratios for RC and PC LWC specimens without shear reinforcement were greater than the mean ratios for the NWC specimens. For the RC specimens with shear reinforcement, the mean ratios for the LWC specimens were less than for the NWC specimens but still greater than 1.0. The LWC and NWC PC specimens with shear reinforcement had similar mean test-to-prediction ratios and COVs. The COVs for the other three types of LWC specimens were nearly twice the COVs of the NWC specimens.

CHAPTER 6. REDUCTION FACTOR FOR LWC IN SHEAR

INTRODUCTION

The resistance factor (ϕ) for LWC in shear was determined by calculating the reliability index for LWC (β_{LWC}) and comparing the calculated β_{LWC} to a target reliability index of 3.5 and the reliability index for NWC (β_{NWC}) in shear.

The nominal unfactored load effects (i.e., dead loads and vehicular loads) used for design are given in Articles 3.5.1 and 3.6.1 of the *AASHTO LRFD Bridge Design Specifications*.[3] The total sum of these nominal unfactored loads (ΣQ_i) is given by equation 54. The dead load effects in the equation include the dead load of structural components (Q_{DC}) and the dead load of the wearing surface (Q_{DW}). The vehicular live load (Q_{LL}) and vehicular dynamic load allowance (Q_{IM}) are also included. The effect of the vehicular live load and dynamic load allowance are given together as the term Q_{LL+IM}. For design by LFRD, the nominal loads are factored. The total factored loads (Q) used for design are given by equation 55, where the nominal design loads are given by the unfactored load effects (Q_i), and the load factors are given by γ_i. In this chapter, the subscript i is used to denote the individual unfactored design loads (i.e., Q_{DC}, Q_{DW}, Q_{LL}, and Q_{IM}).

$$\Sigma Q_i = Q_{DC} + Q_{DW} + Q_{LL+IM} \tag{54}$$

$$Q = \Sigma \gamma_i Q_i \tag{55}$$

The load effects can be assumed to be normally distributed, as shown in figure 166. ΣQ_i and Q are shown in the figure as is the most frequent actual load effect, which is the mean load effect (m_Q). The ratio of a mean value to the nominal value used for design is known as the bias factor. The bias factor for the load effects (λ_{Qi}) is the ratio of the mean load effects to the unfactored load effects (see equation 56). The total mean load effect can then be determined as a sum of the individual mean load effects (see equation 57).

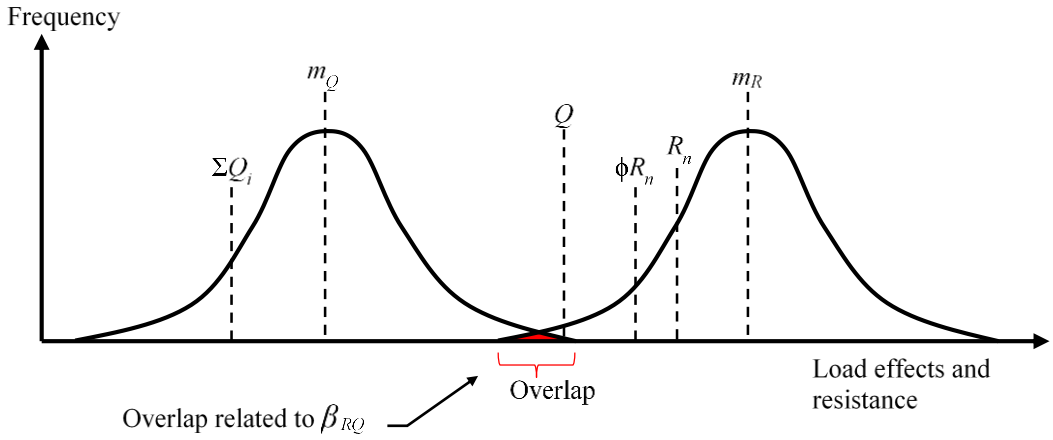

Source: FHWA.

Figure 166. Graph. Nominal, mean, and factored load effects and resistance.

Where:

ϕR_n = factored nominal resistance.
R_n = nominal resistance.
m_R = mean resistance.
β_{RQ} = reliability index.

$$\lambda_{Qi} = \frac{m_i}{Q_i} \tag{56}$$

Where m_i is the mean load effect of an individual load.

$$m_Q = \Sigma\left(Q_i \lambda_{Qi}\right) \tag{57}$$

Member resistance can also be assumed to be normally distributed, as shown in figure 166. The nominal resistance (R_n) is the calculated strength of a member. The mean resistance (m_R) is given by equation 58, where λ_R is the bias factor for resistance. Mean resistance is commonly assumed to be the product of the nominal resistance and three parameters that account for uncertainty in the actual member resistance. The product of ϕ and R_n is the factored nominal resistance (ϕR_n). R_n, m_R, and ϕR_n are all shown in figure 166. The determination of ϕ for LWC in shear is described in this chapter.

$$m_R = R_n \lambda_R \tag{58}$$

The three parameters that account for uncertainty in the actual member resistance are fabrication, material, and analysis.[48,49] The uncertainty in fabrication is due to differences between the nominal and actual overall cross-section dimensions. Material uncertainty is due to differences between the nominal and actual material properties of the concrete and reinforcement. The analysis uncertainty is a result of the approximate methods used to predict resistance. λ_R is assumed to be the product of the bias factors for uncertainty in the fabrication (λ_F), uncertainty in the material (λ_M), and uncertainty in the analysis (λ_P) (also referred to as the professional factor) (see equation 59). The COV for resistance (V_R) is given by equation 60, where V_F, V_M, and V_P are the COV of the uncertainty of the fabrication, material, and analysis parameters, respectively.

$$\lambda_R = \lambda_F \lambda_M \lambda_P \tag{59}$$

$$V_R = \sqrt{{V_F}^2 + {V_M}^2 + {V_P}^2} \tag{60}$$

The LRFD method of design is based on Q being less than ϕR_n, as given by equation 61. A failure is assumed in the event that Q exceeds ϕR_n. The probability of failure is then the area under the overlap of the distributions for load effects and resistance, as illustrated by the red shaded area in figure 166 labeled “overlap.”

$$Q \leq \phi R_n \tag{61}$$

The probability of failure (i.e., when $\phi R_n - Q < 0$) is related to β_{RQ}. The expression for β_{RQ} in equation 62 has been recently used to evaluate ϕ for structural concrete buildings.[48,50,51] In equation 62, σ_R and σ_Q are the standard deviation of the resistance and total load effect, respectively. In the evaluation, a resistance factor was selected, and then β_{RQ} was determined using equation 62 over a range of dead-to-total load ratios. The resulting β_{RQ} for LWC in shear was then compared to a target reliability index (β_{target}) and the β_{NWC} in shear to determine whether the selected resistance factor was adequate.

$$\beta_{RQ} = \frac{m_R - m_Q}{\sqrt{{\sigma_R}^2 + {\sigma_Q}^2}} \tag{62}$$

Where:

${\sigma_R}^2$ = variance of the resistance.
${\sigma_Q}^2$ = variance of the mean unfactored load effects.

METHOD TO DETERMINE THE RELIABILITY INDEX

The introduction to this chapter gave definitions for the important terms that are used to perform a reliability analysis to evaluate a selected ϕ. This section describes the method used to determine the mean and standard deviation of resistance and load effect that are needed to determine β_{RQ} using equation 62.

The three basic steps to determine β_{RQ} are described. The first step is to determine a relationship between R_n and the total nominal unfactored load effects (ΣQ_i). The next step is to determine the mean and standard deviation of the load effects (i.e., m_Q and σ_Q). The third step is to determine the mean of resistance (m_R) and the standard deviation of resistance (σ_R). Then, equation 62 can be used to determine β_{RQ}.

Relationship Between Nominal Resistance and Unfactored Loads

The nominal resistance and unfactored loads are related by considering the largest factored loads that can be used for design. The largest loads for design occur for the case of the factored loads equaling the factored nominal resistance as given by equation 63. An expression that relates the sum of ΣQ_i to the total factored load effects (Q) is needed.

$$Q = \phi R_n \tag{63}$$

The individual load effects due to dead load and vehicle live loads are given by the load combinations in Article 3.4.1 of the *AASHTO LRFD Bridge Design Specifications*.[3] The individual loads are multiplied by load factors (γ_i) in each load combination. Considering the effects of dead load and vehicular live load, the total factored loads are shown in equation 64. According to the *AASHTO LRFD Bridge Design Specifications*, the strength I load combination is used for the normal operational use of a bridge.[3] It has also been previously used to evaluate the structural reliability of bridges.[52] The load factors for the strength I load combination are load factor for load effects due to dead load of structural components (γ_{DC}) = 1.25, load factor for

load effects due to dead load of the wearing surface (γ_{DW}) = 1.50, and load factor for load effects due to combined vehicular live load and dynamic load allowance (γ_{LL+IM}) = 1.75.

$$Q = \gamma_{DC}Q_{DC} + \gamma_{DW}Q_{DW} + \gamma_{LL+IM}Q_{LL+IM} \tag{64}$$

r_Q is the ratio of the unfactored permanent loads (i.e., Q_{DC} and Q_{DW}) to the total unfactored force effect (ΣQ_i) (see equation 65). This is analogous to the ratio of dead load to the sum of dead and live loads previously used in the reliability analysis of buildings.[51,53]

$$r_Q = \frac{Q_{DC} + Q_{DW}}{\Sigma Q_i} \tag{65}$$

r_{DW} is the ratio of the dead load of the wearing surface (Q_{DW}) to the dead load of structural components (Q_{DC}) (see equation 66).

$$r_{DW} = \frac{Q_{DW}}{Q_{DC}} \tag{66}$$

The unfactored load effects can be expressed in terms ΣQ_i and the ratios r_Q and r_{DW}. Q_{DC} and Q_{DW} are provided in equation 67 and equation 68, respectively. The expression for the combined vehicular live load and dynamic load allowance (Q_{LL+IM}) is solved using equation 69. A more detailed explanation of the derivation of equation 67 through equation 69 is given in appendix D.

$$Q_{DC} = \left(\frac{r_Q}{1 + r_{DW}}\right)\Sigma Q_i \tag{67}$$

$$Q_{DW} = \left(\frac{r_{DW}r_Q}{1 + r_{DW}}\right)\Sigma Q_i \tag{68}$$

$$Q_{LL+IM} = \left(1 - r_Q\right)\Sigma Q_i \tag{69}$$

The nominal dynamic load allowance (*IM*) in the *AASHTO LRFD Bridge Design Specifications* is 0.33.[3] Q_{LL} can be separated from Q_{LL+IM} using *IM*, as shown in equation 70.

$$Q_{LL} = \frac{Q_{LL+IM}}{1 + IM} \tag{70}$$

The expressions for the individual load effects in equation 67 through equation 69 are then substituted into equation 64. After simplification, the resulting expression is in equation 71. The right-hand term of equation 71 is only a function of the load factors (γ_i) and the ratios r_Q and r_{DW}. Q can be expressed as ΣQ_i multiplied by the function of γ_i, r_Q, and r_{DW} (see equation 72).

$$Q = \Sigma Q_i\left[\left(\frac{r_Q}{1 + r_{DW}}\right)\left(\gamma_{DC} + \gamma_{DW}r_{DW}\right) + \gamma_{LL+IM}\left(1 - r_Q\right)\right] \tag{71}$$

$$Q = \Sigma Q_i f\left(\gamma_i, r_Q, r_{DW}\right) \tag{72}$$

After substituting equation 72 into equation 63 and rearranging, an expression for the relationship between ΣQ_i and R_n is created (see equation 73). A more detailed explanation of the derivation of equation 67 through equation 73 is provided in appendix D.

$$\Sigma Q_i = \frac{\phi R_n}{f(\gamma_i, r_Q, r_{DW})} \tag{73}$$

Mean and Standard Deviation of Unfactored Load Effects

The general expression for m_Q was previously provided in equation 57. For the case of load effects due to dead loads and vehicular live loads, m_Q is solved for using equation 74. The effects of Q_{LL} and Q_{IM} are considered separately in equation 74. This implies that Q_{LL} and Q_{IM} are uncorrelated, which is the assumption made in previous reliability analyses of bridges.[49,52] *IM* in equation 74 is a factor multiplied by Q_{LL}. The individual load effects in equation 74 are multiplied by bias factors.

$$m_Q = Q_{DC}\lambda_{DC} + Q_{DW}\lambda_{DW} + Q_{LL}\lambda_{LL} + (Q_{LL}IM)\lambda_{IM} \tag{74}$$

Where:

λ_{DC} = bias factor for the load effects due to dead load of structural components.
λ_{DW} = bias factor for the load effects due to dead load of the wearing surface.
λ_{LL} = bias factor for the load effects due to vehicular live load.
λ_{IM} = bias factor for the load effects due to vehicular dynamic load allowance.

Variation of the mean unfactored load effects ($\sigma_Q{}^2$) is the sum of the variation of the individual loads.[49,54] The definition of standard deviation is the square root of variance. The COV is the ratio of the standard deviation to the mean. The definition of the bias factor is the ratio of the mean to the nominal value. The general expression for $\sigma_Q{}^2$ is found in equation 75 and includes the progressive derivation by substituting the definitions of COV and bias factor. The expression for variance that includes the dead load and vehicular live load effects is solved for in equation 76. A more detailed explanation of the derivation of equation 74 and equation 76 is provided in appendix D.

$$\sigma_Q{}^2 = \Sigma(\sigma_{Qi})^2 = \Sigma(V_{Qi}m_{Qi})^2 = \Sigma[V_{Qi}(Q_i\lambda_{Qi})]^2 \tag{75}$$

Where:

σ_{Qi} = standard deviation of the individual load effects.
V_{Qi} = COV of the unfactored load effect.
m_{Qi} = mean of the individual load effects.

$$\sigma_Q{}^2 = (V_{DC}Q_{DC}\lambda_{DC})^2 + (V_{DW}Q_{DW}\lambda_{DW})^2 + (V_{LL}Q_{LL}\lambda_{LL})^2 + (V_{IM}Q_{IM}IM\lambda_{IM})^2 \tag{76}$$

Where:

V_{DC} = COV for the dead load of structural components.
V_{DW} = COV for the dead load of the wearing surface.
V_{LL} = COV for the vehicular live load.
V_{IM} = COV for the vehicular dynamic load allowance.

Mean and Standard Deviation of Resistance

The general expression for the mean of the resistance (m_R) was solved for in equation 58. The uncertainties due to fabrication and materials were determined together using a numerical technique known as Monte Carlo simulation.[55] The bias factor and COV for the combined uncertainty of the fabrication and materials are λ_{FM} and V_{FM}, respectively.[49,52] The expression for mean resistance that includes λ_{FM} is given by equation 77. The general expression given by equation 60 for the COV of the resistance (V_R) was modified to include V_{FM} (see equation 78). The expression for ${\sigma_R}^2$ (see equation 79) was determined by substituting equation 78 into the definition of standard deviation. A more detailed explanation of the derivation of equation 79 is provided in appendix D.

$$m_R = R_n \lambda_{FM} \lambda_P \tag{77}$$

$$V_R = \sqrt{{V_{FM}}^2 + {V_P}^2} \tag{78}$$

$${\sigma_R}^2 = {m_R}^2 \left({V_{FM}}^2 + {V_P}^2 \right) \tag{79}$$

Summary of the Solution Procedure

The following section summarizes the solution procedure used to determine β_{RQ}. A value of 1.0 was selected for R_n. The magnitude of R_n is not important because the nominal loads are determined as a fraction of R_n in the analysis. A trial value for ϕ was selected, and values for r_Q and r_{DW} were selected. ΣQ_i is determined using equation 73. The individual unfactored dead loads (i.e., Q_{DC} and Q_{DW}) are determined using equation 67 and equation 68. Q_{LL+IM} is determined using equation 69, and Q_{LL} is separated from Q_{LL+IM} using equation 70.

The mean unfactored load and the variance of the loads are determined using the statistical parameters λ_{Qi} and V_{Qi}. The bias factor (λ_{Qi}) and COV (V_{Qi}) for the individual loads were found in the literature and are described in the following section.[50,52] m_Q was determined using equation 74, and ${\sigma_Q}^2$ was determined using equation 76.

The mean resistance (m_R) and the variance of the resistance (${\sigma_R}^2$) were determined using the bias factors and COV for the uncertainty in the fabrication, materials, and analysis. The bias factors and COVs for the fabrication and material parameters (i.e., λ_{FM} and V_{FM}) were determined using Monte Carlo simulations that are described in the following section. The bias factor and COV for the analysis factor (i.e., λ_P and V_P) were determined using the specimens in the TFHRC shear database for shear described previously in this report. The statistical parameters for the analysis factor (i.e., professional factor) are also summarized in the following section and depend on the

type of specimen and analysis method for determining R_n. m_R and σ_R^2 were determined using equation 77 and equation 79, respectively.

β_{RQ} was determined using equation 62 for given values for r_Q and r_{DW}, a specific specimen type, and a specific analysis method for determining R_n. The values of r_Q were varied between 0 and 1.0 to produce a set of β_{RQ} values. Values for r_{DW} were determined as described in the following section. Separate calculations were made for three of the analysis methods used to determine R_n in the *AASHTO LRFD Bridge Design Specifications*.[3] Separate calculations were also made for an RC cross section and two different PC cross sections. A flowchart showing the method for determining β_{RQ} is given in figure 167. Figures showing the β_{RQ} values determined using this procedure and an analysis of results are included later in this chapter in the Reliability Index for RC and PC LWC Members in Shear section.

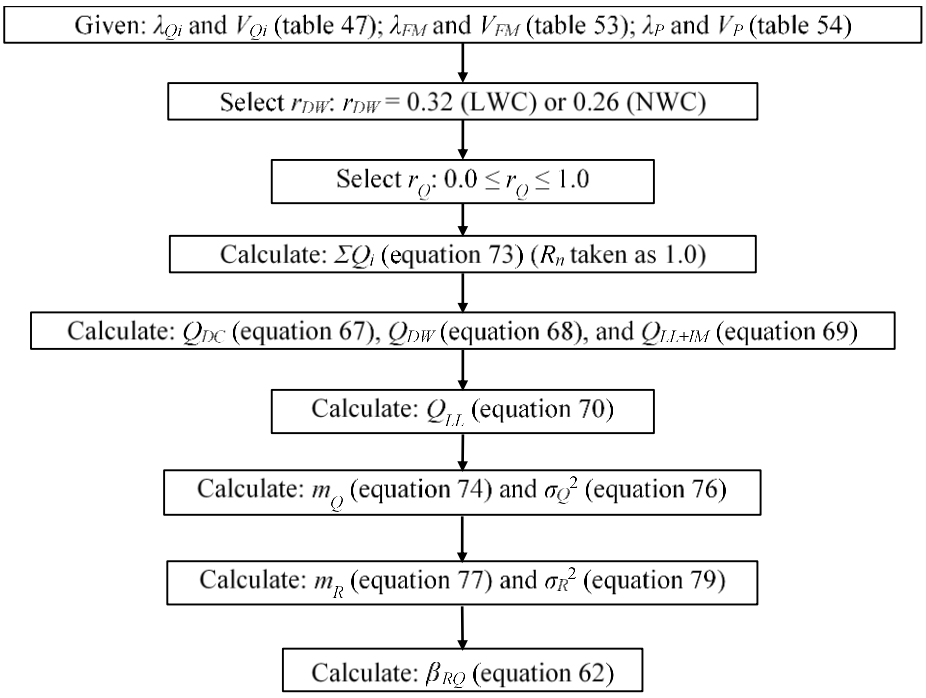

Source: FHWA.

Figure 167. Flowchart. Solution method for determining reliability index.

STATISTICAL PARAMETERS FOR LOAD EFFECTS AND RESISTANCE

This section describes the statistical parameters for load effects and resistance that are used in the reliability analysis described in this report. The mean, bias, and COV of the load effects are described as well as the numerical method used to determine the statistical parameters for the uncertainty in fabrication and materials. This section also provides the method used to determine the uncertainty in the analysis by analyzing databases of shear tests on LWC and NWC.

Load Effect Factors

The load factors for the dead load of structural components (Q_{DC}), dead load of the wearing surface (Q_{DW}), vehicular live load (Q_{LL}), and vehicular dynamic load allowance (Q_{IM}) specified for load combination strength I in the *AASHTO Bridge Design Specifications* are provided in table 47.[3] The bias factors and COV for the load effects that were determined in previous studies are also given in table 47.

Table 47. Statistical parameters for load effects.

Force Effect	γ_i	λ_{Qi}	V_{Qi} (Percent)	Reference
Q_{DC}	1.25	1.05	8.0	52
Q_{DW}	1.50	1.00	25.0	52
Q_{LL}	1.75	1.28	12.0	50 and 52
Q_{IM}	1.75	0.303	80.0	50 and 52

The term r_{DW} is used to define the ratio of Q_{DW} to Q_{DC} in this report. The ratio was estimated using four sets of assumed girder spacings and girder sizes. It was then determined for each case using equation 80. r_{DW} was determined for a bridge with LWC girders and deck and also for a bridge with NWC girders and deck. The assumed girder spacing, girder sizes, and calculated values of r_{DW} for an LWC bridge and an NWC bridge are provided in table 48. Based on the range values determined for the four cases, a value of 0.32 was selected for the r_{DW} for LWC bridges, and a value of 0.26 was selected for the value of r_{DW} for NWC bridges.

$$r_{DW} = \frac{Q_{DW}}{Q_{DC}} = \frac{\left[\left(\frac{t_{ws}}{12}\right)\left(\frac{s_{beam}}{12}\right)\right] w_{ws}}{\left[\left(\frac{t_{slab}}{12}\right)\left(\frac{s_{beam}}{12}\right)\right] w_{slab} + \left(\frac{A_{beam}}{144}\right) w_{beam}} \quad (80)$$

Where:

t_{ws} = wearing surface thickness.
s_{beam} = beam spacing.
w_{ws} = wearing surface unit weight.
t_{slab} = concrete slab thickness.
w_{slab} = slab unit weight.
A_{beam} = beam cross-sectional area.
w_{beam} = beam unit weight.

Table 48. Ratio of structural component dead load to wearing surface dead load (r_{DW}) determined using equation 80 for modeled bridge geometries.

Parameter	Case 1: Type I Girder With 4-ft Spacing	Case 2: Type VI Girder With 12-ft Spacing	Case 3: Type IV Girder With 12-ft Spacing	Case 4: Type IV Girder With 14-ft Spacing
Beam spacing, s_{beam} (inches)	48	144	144	168
Wearing surface thickness, t_{ws} (inches)	3.5	3.5	3.5	3.5
Wearing surface unit weight, w_{ws} (kcf)	0.140	0.140	0.140	0.140
Concrete slab thickness, t_{slab} (inches)	8.0	8.0	8.0	8.0
Slab unit weight, w_{slab} (kcf)	0.120	0.120	0.120	0.120
Beam cross-sectional area, A_{beam} (inches^2)	276	1085	789	789
Beam unit weight (LWC), w_{beam} (kcf)	0.120	0.120	0.120	0.120
Beam unit weight (NWC), w_{beam} (kcf)	0.150	0.150	0.150	0.150
Q_{DC}/Q_{DW} (LWC r_{DW})	0.297	0.263	0.303	0.322
Q_{DC}/Q_{DW} (NWC r_{DW})	0.238	0.210	0.242	0.257

1 ft = 0.305 m.
1 inch = 25.4 mm.
1 kcf = 16,020 kg/m^3.
1 inch^2 = 645.2 mm^2.

Fabrication and Material Factors for Resistance

The bias and COV due to the uncertainty in fabrication and materials (i.e., λ_{FM} and V_{FM}) were determined using the Monte Carlo simulation of statistical sampling.[49,50,55] Three different LWC and NWC cross sections were simulated to determine λ_{FM} and V_{FM}. Separate simulations were made of each cross section without and with shear reinforcement. Nominal geometric and material parameters for each simulated cross section are assumed to be normally distributed. The bias and COV were determined using 100,000 simulations for each cross section.

The uncertainty in fabrication and materials was evaluated by determining the nominal resistance for simulated cross sections. The cross sections had geometric and material properties that were assumed to be normally distributed. An RC cross section was simulated with the nominal parameters given in table 49. The geometric parameters are illustrated in figure 168. AASHTO type II and type IV prestressed girder cross sections were also simulated with the nominal parameters (see table 50 and table 51, respectively). Figure 169 illustrates the geometric parameters for the prestressed cross sections. The thickness of the flanges was taken as the thickness of the actual flange plus one-third the thickness of the chamfer. The nominal resistance was determined for two versions of each cross section: one without shear reinforcement and the other with shear reinforcement.

Table 49. Statistical parameters for simulated RC rectangular section.

Parameter Category	Parameter	Nominal Value	Bias	COV (Percent)	Reference
Geometry	$t_{flange,top}$ (inches)	7.25	0.92	12.0	49, 56, 57
Geometry	b (inches)	84	1.01	4.0	49, 56, 57
Geometry	h_{web} (inches)	28.75	0.99	4.0	49, 56, 57
Geometry	b_v (inches)	15	1.01	4.0	49, 56, 57
LWC properties	f'_c (ksi)	4	1.34	12.0	58
NWC properties	f'_c (ksi)	4	1.21	15.5	57
Reinforcement	A_s (inches^2)	15.94	1.13	3.0	49, 56, 59
Reinforcement	d_s (inches)	36	0.99	4.0	49, 56, 59
Reinforcement	A_v (inches^2)*	0.62	1.13	3.0	49, 56, 59
Reinforcement	s (inches)*	4.375	1.00	1.0	49, 56, 59
Reinforcement properties	f_y (A_s) (ksi)	60	1.13	3.0	59
Reinforcement properties	f_y (A_v) (ksi)*	60	1.13	3.0	59

1 inch = 25.4 mm.
1 ksi = 6.89 MPa.
1 inch^2 = 645.2 mm^2.
*Simulated LWC and NWC specimens with stirrups only.

Where:

$t_{flange,top}$ = beam top flange thickness of the simulated cross section.
h_{web} = height of the beam below the top flange of the simulated RC section and height of the beam below the deck of the simulated PC section.

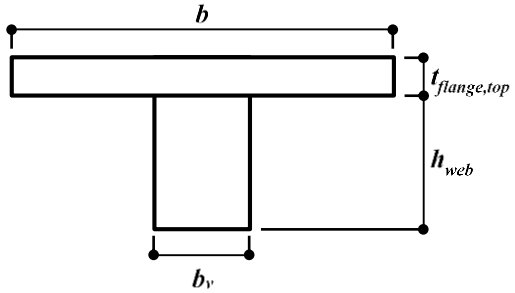

Source: FHWA.

Figure 168. Illustration. Geometric parameters for RC section.

Table 50. Statistical parameters for simulated type II girder.

Parameter Category	Parameter	Nominal Value	Bias	COV (Percent)	Reference
Geometry	t_{deck} (inches)	8	0.92	12.0	49, 56, and 57
Geometry	b_{deck} (inches)	81	1.01	4.0	49, 56, and 57
Geometry	h_{web} (inches)	36	1.00	2.5	57
Geometry	b_v (inches)	6	1.00	2.5	57
Geometry	$t_{flange,top}$ (inches)	12	1.00	2.5	57
Geometry	$b_{flange,top}$ (inches)	7	1.00	2.5	57
Geometry	$t_{flange,btm}$ (inches)	18	1.00	2.5	57
Geometry	$b_{flange,btm}$ (inches)	8	1.00	2.5	57
LWC properties	deck f'_c (ksi)	4	1.34	12	5758
LWC properties	beam f'_c (ksi)	6	1.34	14	58
LWC properties	beam f'_{ci} (ksi)	6	1.34	14	58
NWC properties	deck f'_c (ksi)	4	1.21	15.5	57
NWC properties	beam f'_c (ksi)	6	1.22	7.5	57
NWC properties	beam f'_{ci} (ksi)	4.2	1.22	7.5	57
Reinforcement	A_{ps} (inches^2)	1.84	1.045	2.5	49, 53, and 56
Reinforcement	d_p (inches)	40.7	1.00	6.0	49, 56, and 59
Reinforcement	A_v (inches^2)*	0.62	1.13	3.0	59
Reinforcement	s (inches)*	11.4	1.00	1.0	59
Reinforcement properties	f_{pu} (A_s) (ksi)	270	1.045	2.5	53
Reinforcement properties	f_y (A_v) (ksi)*	60	1.13	3	57, 59

1 inch = 25.4 mm.
1 ksi = 6.89 MPa.
1 inch^2 = 645.2 mm^2.
*Simulated LWC and NWC specimens with stirrups only.

Where:

t_{deck} = deck thickness of the simulated cross section.
b_{deck} = deck width of the simulated cross section.
$b_{flange,top}$ = beam top flange width of the simulated cross section.
$t_{flange,btm}$ = beam bottom flange thickness of the simulated cross section.
$b_{flange,btm}$ = beam bottom flange width of the simulated cross section.
f'_{ci} = concrete compressive strength at time of prestressing in reference to material test values and specified compressive strength at time of prestressing.

Table 51. Statistical parameters for simulated type IV girder.

Parameter Category	Parameter	Nominal Value	Bias	COV (Percent)	Reference
Geometry	t_{deck} (inches)	8	0.92	12.0	49, 56, and 57
Geometry	b_{deck} (inches)	81	1.01	4.0	49, 56, and 57
Geometry	h_{web} (inches)	54	1.00	2.5	57
Geometry	b_v (inches)	8	1.00	2.5	57
Geometry	$t_{flange,top}$ (inches)	20	1.00	2.5	57
Geometry	$b_{flange,top}$ (inches)	10	1.00	2.5	57
Geometry	$t_{flange,btm}$ (inches)	26	1.00	2.5	57
Geometry	$b_{flange,btm}$ (inches)	11	1.00	2.5	57
LWC properties	deck f'_c (ksi)	4	1.34	12	5958
LWC properties	beam f'_c (ksi)	6	1.34	14	58
LWC properties	beam f'_{ci} (ksi)	6	1.34	14	58
NWC properties	deck f'_c (ksi)	4	1.21	15.5	57
NWC properties	beam f'_c (ksi)	6	1.22	7.5	57
NWC properties	beam f'_{ci} (ksi)	4.2	1.22	7.5	57
Reinforcement	A_{ps} (inches^2)	4.59	1.045	2.5	49, 53, and 56
Reinforcement	d_p (inches)	55.6	1.00	6.0	49, 56, and 59
Reinforcement	A_v (inches^2)*	0.62	1.13	3.0	59
Reinforcement	s (inches)*	16.0	1.00	1.0	59
Reinforcement properties	f_{pu} (A_s) (ksi)	270	1.045	2.5	53
Reinforcement properties	f_y (A_v) (ksi)*	60	1.13	3	57 and 59

1 inch = 25.4 mm.
1 ksi = 6.89 MPa.
1 inch^2 = 645.2 mm^2.
*Simulated LWC and NWC specimens with stirrups only.

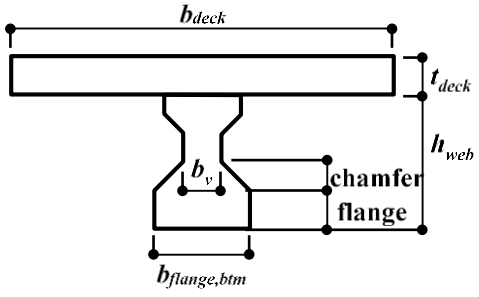

Source: FHWA.

A. Cross section.

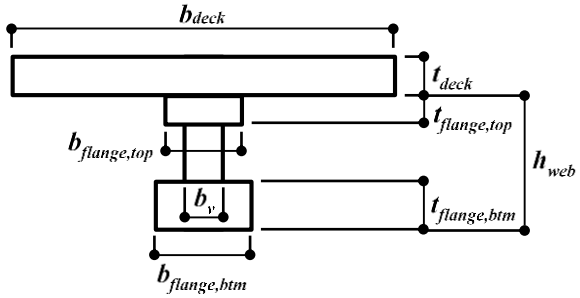

Source: FHWA.

B. Idealized PC cross section.

Figure 169. Illustrations. Geometric parameters for cross section and idealized PC sections.

For each simulation, a uniformly distributed random number was generated for each geometric and material parameter. The random number was used as the probability of a value in the normal cumulative distribution and was used to determine a simulated sample value of the parameter

with a given mean and standard deviation. After the geometric and material parameters were simulated, the nominal resistance was determined using the Simplified-RC procedure, the GP-equation method, and the Simplified-PC/RC procedure. The bias for each simulation was determined as the ratio of the nominal resistance using the simulated parameters to the nominal resistance determined using nominal values for the parameters. The mean and COV of the bias factors for all of simulations on a cross section is taken as λ_{FM} and V_{FM}, respectively.

The effect that the number of simulations has on the bias and COV of the RC section is given in table 52. The bias of the load effects was reported to three significant figures, as given in table 47. The COV of the load effects was reported to only two significant figures. The statistical parameters for geometry and materials were reported to a similar level of precision. As shown in table 52, λ_{FM} and V_{FM} obtained this level of precision for the RC cross section after 100,000 simulations. Fewer numbers of simulations were needed to obtain a similar level of accuracy for the type II and type IV cross sections.

Table 52. Effect of the number of simulations on the statistical parameters for the RC cross section determined using the Monte Carlo simulation for LWC.

Concrete Type and Specimen Group	Design Expression	Statistical Parameter	Number of Simulations			
			1,000	10,000	100,000	1 Million
RC cross section without A_v	Simplified-RC	λ_{FM}	1.1570	1.1540	1.1555	1.1554
	Simplified-RC	V_{FM} (percent)	9.750	9.454	9.523	9.568
RC cross section without A_v	GP-equation	λ_{FM}	1.1549	1.1531	1.1541	1.1540
	GP-equation	V_{FM} (percent)	7.284	7.081	7.140	7.178
RC cross section without A_v	Simplified-PC/RC	λ_{FM}	1.1570	1.1540	1.1555	1.1554
	Simplified-PC/RC	V_{FM} (percent)	9.750	9.454	9.523	9.568
RC cross section with A_v	Simplified-RC	λ_{FM}	1.2466	1.2455	1.2442	1.2442
	Simplified-RC	V_{FM} (percent)	6.728	6.934	6.900	6.904
RC cross section with A_v	GP-equation	λ_{FM}	1.2156	1.2150	1.2139	1.2139
	GP-equation	V_{FM} (percent)	5.775	5.888	5.874	5.858
RC cross section with A_v	Simplified-PC/RC	λ_{FM}	1.2475	1.2463	1.2451	1.2450
	Simplified-PC/RC	V_{FM} (percent)	6.741	6.948	6.915	6.919

In table 52, the bias and COV for the Simplified-RC and Simplified-PC/RC procedures are the same values for the RC cross section without shear reinforcement. V_{cw} (see equation 30) controlled the shear resistance for this cross section, so both design expressions for V_c are a function of $\sqrt{f'_c}b_v d_v$. The mean V_c values determined using the two procedures are different, but the simulated normal distributions of f'_c, b_v, and d_v will cause proportional changes in V_c, resulting in the same bias and COV for the two methods.

The bias and COV (i.e., λ_{FM} and V_{FM}) for the three LWC and NWC cross sections after 100,000 simulations are given in table 53. The statistical parameters in the table are the result of 1.2 million simulations. The calculation of nominal resistance by the GP-equation method required iterations, so the total time required for each simulation ranged from between 2 to 3 s. Simulations on the LWC RC cross sections were increased to 1 million simulations for a total of 3 million simulations completed for this research effort.

Table 53. Statistical parameters for fabrication and material factor determined using Monte Carlo simulation for LWC and NWC cross sections.

Concrete Type and Specimen Group	Design Expression	LWC (100,000 Simulations)		NWC (100,000 Simulations)	
		λ_{FM}	V_{FM} (Percent)	λ_{FM}	V_{FM} (Percent)
RC cross section without A_v	Simplified-RC	1.156	9.52	1.097	10.66
RC cross section without A_v	GP-equation	1.154	7.14	1.106	8.35
RC cross section without A_v	Simplified-PC/RC	1.156	9.52	1.097	10.66
RC cross section with A_v	Simplified-RC	1.244	6.90	1.231	7.31
RC cross section with A_v	GP-equation	1.214	5.87	1.184	9.19
RC cross section with A_v	Simplified-PC/RC	1.245	6.91	1.233	7.29
Type II without A_v	GP-equation	1.164	12.09	1.126	11.39
Type II without A_v	Simplified-PC/RC	1.138	9.77	1.113	9.38
Type II with A_v	GP-equation	1.153	4.88	1.151	4.87
Type II with A_v	Simplified-PC/RC	1.224	9.53	1.218	8.61
Type IV without A_v	GP-equation	1.147	15.35	1.136	15.83
Type IV without A_v	Simplified-PC/RC	1.142	10.81	1.117	10.51
Type IV with A_v	GP-equation	1.179	5.89	1.174	6.11
Type IV with A_v	Simplified-PC/RC	1.216	8.33	1.204	8.30

Note: NWC specimens were from the ACI-DafStb database.

Professional Factors for Resistance

The bias and COV due to uncertainty in the analysis (i.e., λ_P and V_P) were determined by analyzing the LWC and NWC shear test databases described and analyzed in a previous chapter of this report. The ratio of test-to-predicted shear resistance for each specimen type was analyzed separately. The test-to-prediction ratios were plotted on normal probability paper, and the bias and COV were determined from the tail of the data.

The bias and COV were determined by plotting the test-to-prediction ratios on normal probability paper. The ratios from a database were arranged in increasing order. The ratios were assigned a cumulative probability (p_n) determined using equation 81, where n was the smallest ratio of test-to-predicted shear resistance, and N was the total number of ratios of test-to-predicted shear resistance. The smallest ratio was assigned $n = 1$, and the largest ratio was assigned $n = N$. For each test-to-prediction ratio, the value of the ratio was plotted on the x-axis, and the standard normal variable was plotted on the y-axis. The standard normal variable was equal to the inverse of the cumulative probability. The mean value had a standard normal variable equal to zero, and the distance from the mean value was given in terms of the number of standard deviations. Data that followed a "perfect" normal distribution were arranged along a straight line on normal probability paper.[50]

$$p_n = \frac{n}{N+1} \tag{81}$$

The bias and COV were determined from the lower tail of the data. The mean test-to-prediction ratio was the bias factor (λ_P). The test-to-prediction ratios with a standard normal variable less than or equal to zero were defined as the "lower tail." A least-squares linear regression was determined for the data in the lower tail. The slope of the regression line was the reciprocal of the standard deviation. By definition, the COV (V_P) is the standard deviation divided by the mean test-to-prediction ratio. The data in the lower tail were used to determine the standard deviation because, in the event of a failure, they were due to the resistance being lower than the associated load effects. This is shown in figure 166 as the distribution representing load effects exceeding the lower tail of the distribution representing resistance.

The bias and COV were determined for each specimen type, concrete type, and method of determining nominal resistance. The four specimen types included RC specimens without and with shear reinforcement and PC specimens without and with shear reinforcement. The concrete types included LWC and NWC. The nominal resistance was determined using the Simplified-RC procedure, the GP-equation method, and the Simplified-PC/RC procedure. The bias and COV (i.e., λ_P and V_P) determined for each specimen type, concrete type, and calculation method is given in table 54.

Table 54. Statistical parameters for professional factor determined using the linear regression of the tail of the cumulative distribution function (CDF) for test-to-predicted resistance of LWC and NWC specimens.

Concrete Type and Specimen Group	Design Expression	Number of Specimens	λ_P	V_P (Percent)
LWC, RC specimens without A_v	Simplified-RC	169	1.61	20.3
LWC, RC specimens without A_v	GP-equation	218	1.05	16.6
LWC, RC specimens without A_v	Simplified-PC/RC	218	1.77	22.1
LWC, RC specimens with A_v	Simplified-RC	31	1.63	21.7
LWC, RC specimens with A_v	GP-equation	44	1.08	16.2
LWC, RC specimens with A_v	Simplified-PC/RC	44	1.55	22.3
LWC, PC specimens without A_v	GP-equation	20	2.56	36.6
LWC, PC specimens without A_v	Simplified-PC/RC	20	4.14	55.7
LWC, PC specimens with A_v	GP-equation	33	1.24	10.3
LWC, PC specimens with A_v	Simplified-PC/RC	33	1.27	11.8
NWC, RC specimens with A_v	Simplified-RC	471	1.87	23.3
NWC, RC specimens with A_v	GP-equation	648	1.14	19.3
NWC, RC specimens with A_v	Simplified-PC/RC	648	1.84	26.9
NWC, RC specimens with A_v	Simplified-RC	93	1.76	19.5
NWC, RC specimens with A_v	GP-equation	107	1.30	19.3
NWC, RC specimens with A_v	Simplified-PC/RC	107	1.78	18.0
NWC, PC specimens without A_v	GP-equation	100	1.46	30.6
NWC, PC specimens without A_v	Simplified-PC/RC	100	3.41	25.7
NWC, PC specimens with A_v	GP-equation	100	1.21	16.7
NWC, PC specimens with A_v	Simplified-PC/RC	100	2.05	25.4

Figure 170 through figure 175 show the CDF for the test-to-prediction ratios. Figure 170 and figure 171 show the CDF for LWC and NWC specimens determined using the Simplified-RC procedure. The CDF for LWC and NWC specimens determined using the GP-equation method is shown in figure 172 and figure 173. The CDF determined using the Simplified-PC/RC procedure is shown in figure 174 and figure 175 for LWC and NWC specimens, respectively. The data in each figure are grouped by specimen type with the number of specimens shown in parentheses. In each figure, the linear regression of lower tail is shown. A vertical line at a ratio of 1.0 is shown. Also shown in each figure are horizontal lines at standard normal variables of 0 and −1. The standard deviation is the horizontal distance from the intersection of the regression line with the standard normal variable at 0 and at −1.

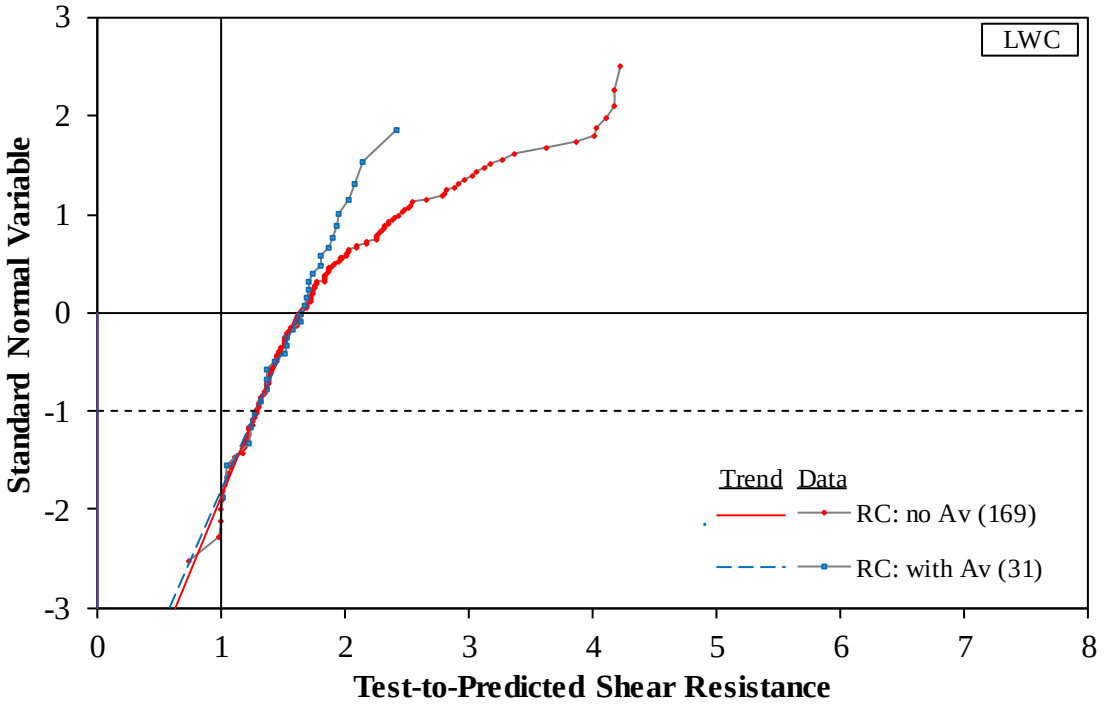

Source: FHWA.

Figure 170. Graph. CDFs for test-to-predicted shear resistance for Simplified-RC for LWC specimens.

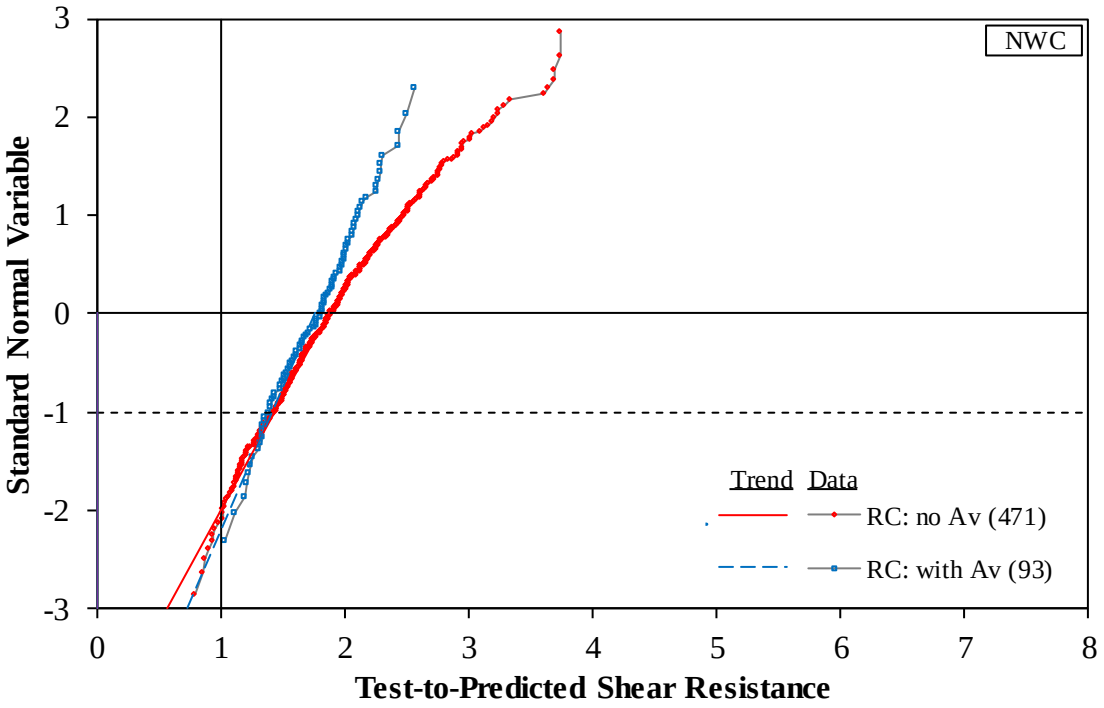

Source: FHWA.

Figure 171. Graph. CDFs for test-to-predicted shear resistance for Simplified-RC for NWC specimens.

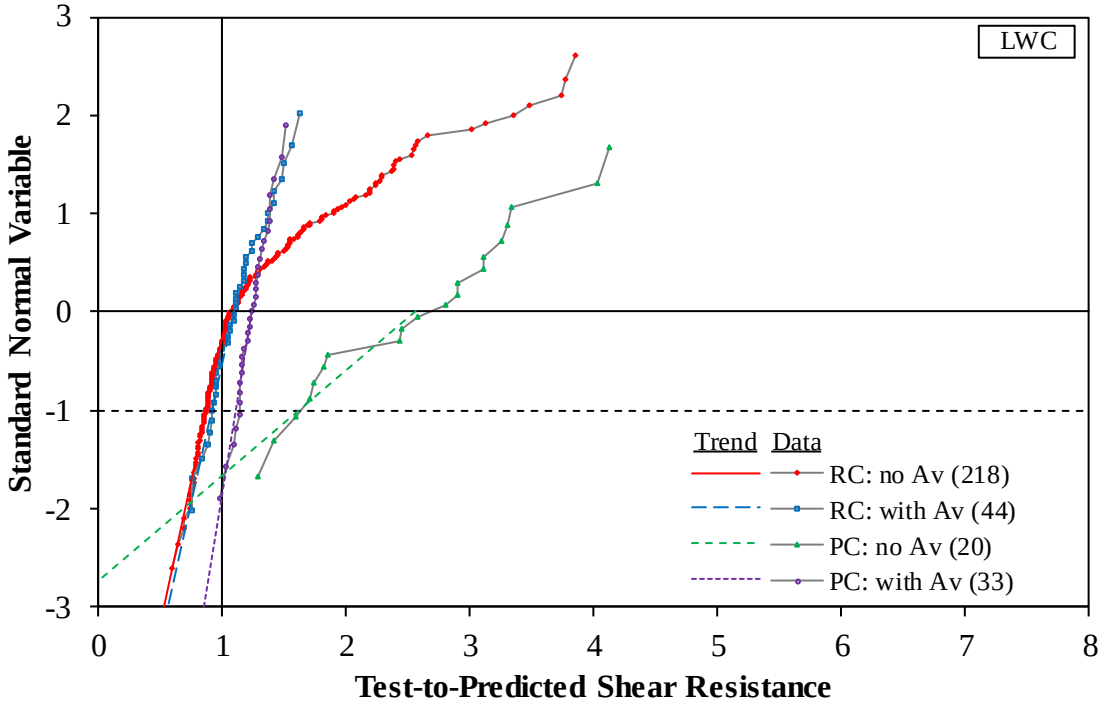

Source: FHWA.

Figure 172. Graph. CDFs for test-to-predicted shear resistance for the GP-equation method for LWC specimens.

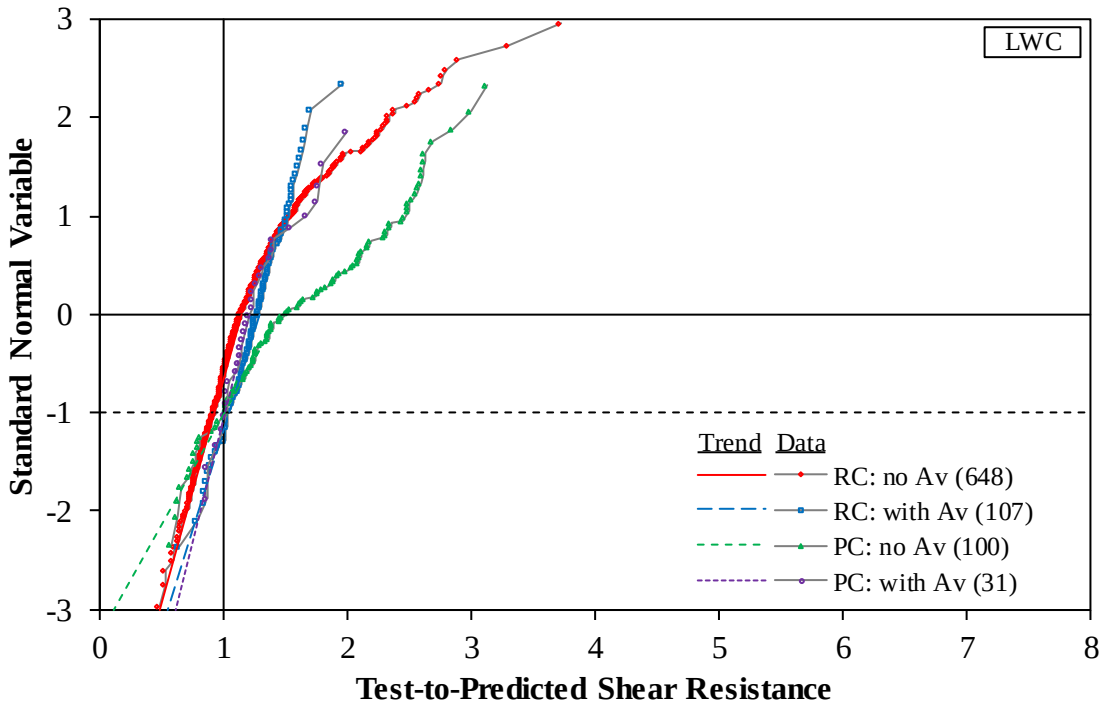

Source: FHWA.

Figure 173. Graph. CDFs for test-to-predicted shear resistance for GP-equation method for NWC specimens.

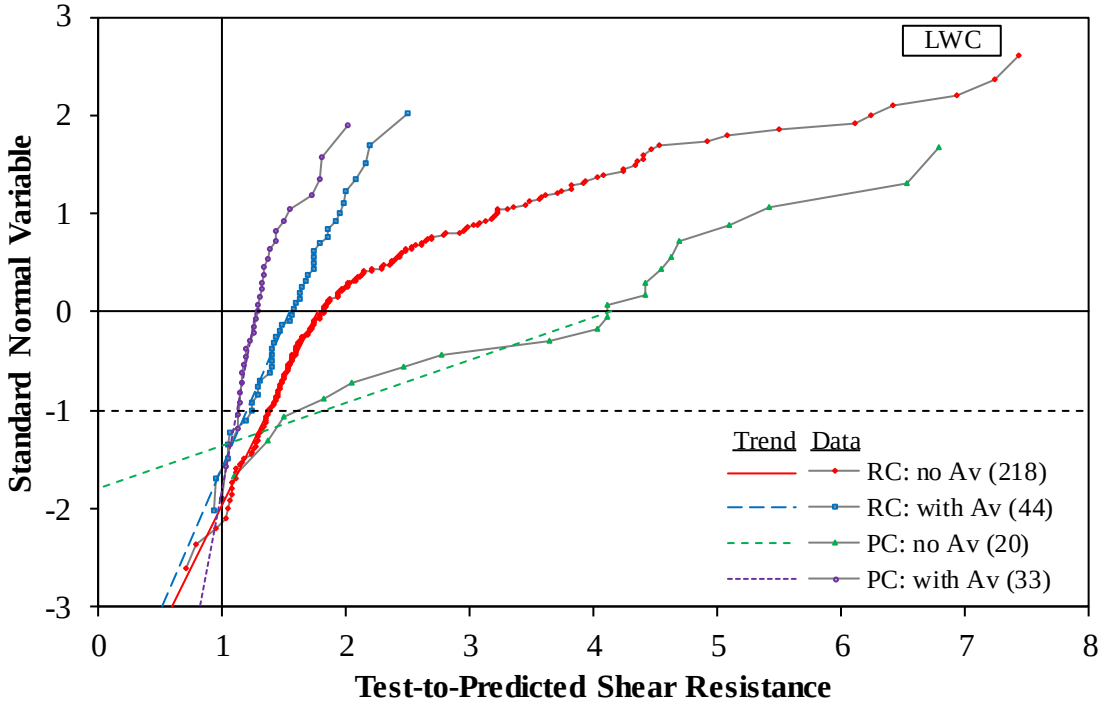

Source: FHWA.

Figure 174. Graph. CDFs for test-to-predicted shear resistance for Simplified-PC/RC for LWC specimens.

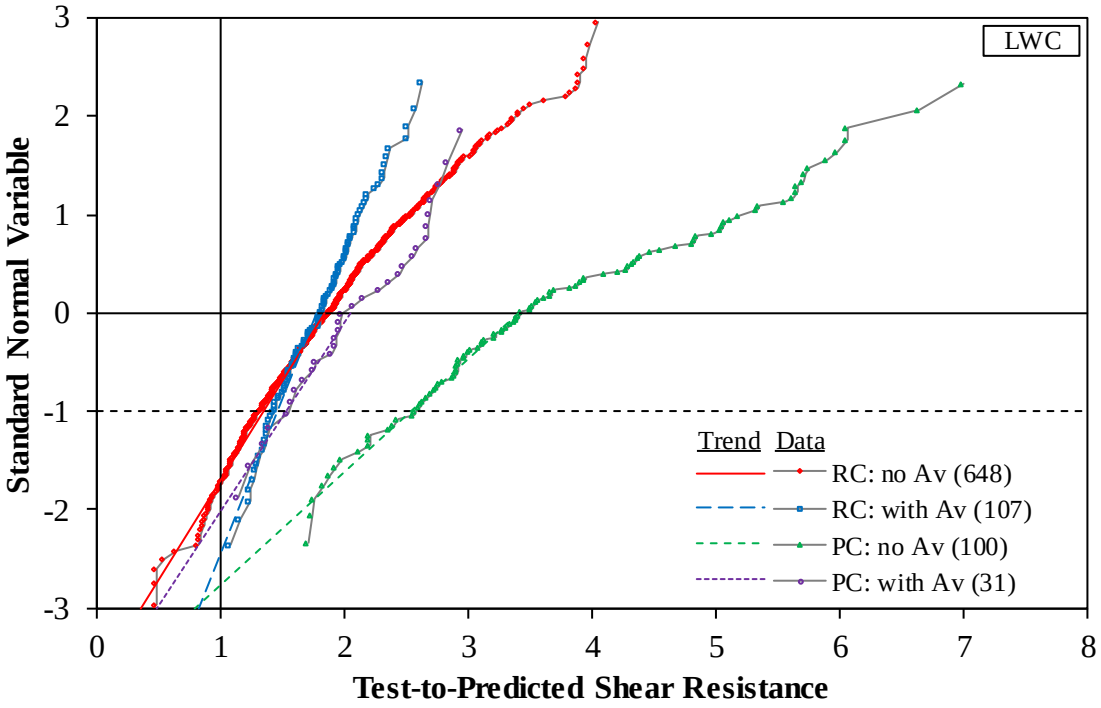

Source: FHWA.

Figure 175. Graph. CDFs for test-to-predicted shear resistance for Simplified-PC/RC for NWC specimens.

The test-to-prediction ratios for a limited number of LWC specimens were not included in the CDF to determine λ_P and V_P. A total of 11 tests were removed from the databases of RC specimens without stirrups (4 tests) and PC without stirrups (7 tests). For each specimen type, all the tests from only one reference were removed because they had a tested shear strength that was considerably lower than the shear strength of specimens with a similar size and material strengths. Including the test-to-prediction ratios from these few tests resulted in considerably higher values of V_p. More information about the excluded tests, including figures showing the CDFs, λ_P, and V_P of the data with the tests included, is given in appendix E.

RELIABILITY INDEX FOR RC AND PC LWC MEMBERS IN SHEAR

The mean β_{RQ} was determined for the shear resistance of LWC cross sections and compared to β_{target} and the mean reliability index for NWC cross sections. The uncertainty due to the loads was evaluated using data from previous studies to determine the mean and variation of the load.[50,52] The uncertainties due to fabrication, material, and analysis were evaluated using numerical simulation and evaluation of shear test results to determine the mean and variance of resistance. β_{RQ} for LWC and NWC in shear was then determined over a range of dead-to-total load ratios. β_{RQ} for LWC was compared to β_{target} and β_{RQ} for NWC.

Method of Determining Reliability Index

The *AASHTO LRFD Bridge Design Specifications* gives ϕ for LWC in shear as 0.80 and for NWC as 0.90.[3] β_{RQ} was evaluated at a resistance factor for LWC 0.75, 0.80, 0.85, and 0.90. These resistance factors were used to determine the mean and variation of the load (i.e., m_Q and σ_Q^2) using equation 74 and equation 76.

The uncertainties due to fabrication, material, and analysis were evaluated using numerical simulation and evaluation of shear test results. The bias and COV due to the uncertainty in the fabrication and materials (i.e., λ_{FM} and V_{FM}) were determined using Monte Carlo simulations on one RC and two PC cross sections. Each cross section was evaluated without and with shear reinforcement. The uncertainty in the analysis was evaluated using the LWC and NWC shear test databases to determine the bias and COV for the professional factor (i.e., λ_P and V_P). The mean and variance of resistance were determined using equation 77 and equation 79, which combine the bias and COV from the fabrication, material, and analysis uncertainty.

β_{RQ} was then determined using equation 62 for a range of r_Q values between 0 and 1.0 in increments of 0.05. The most probable values of r_Q are assumed to be between 0.3 and 0.7. This is the assumption used by a previous evaluation that determined β_{RQ} for beams over a range of dead-to-total load ratios.[51] The mean β_{RQ} was taken as the mean of β_{RQ} determined for $0.3 \leq r_Q \leq 0.7$.

A similar method was used to determine β_{RQ} for NWC beams in shear. The resistance factor of 0.9 that is given in the *AASHTO LRFD Bridge Design Specifications* was used to determine the mean and variation of the load.[3] Monte Carlo simulations were used on similar cross sections, and the shear test database for NWC described in a previous chapter was used to determine the mean and variation of the resistance. The mean β_{RQ} was determined for r_Q between 0.3 and 0.7.

Analysis of Reliability Index for LWC in Shear

β_{RQ} determined for each cross section, design expression, resistance factor, and concrete type is given in table 55. The purpose of this table is to compare β_{RQ} for LWC (β_{LWC}) determined using different resistance factors to the β_{RQ} for NWC (β_{NWC}). As shown in table 55, for the resistance factors evaluated (0.75, 0.80, 0.85, and 0.90), β_{LWC} was either less than or greater than β_{NWC} regardless of resistance factor or the design expression. The resistance factor of 0.75 is 0.05 less than the value for LWC used in the *AASHTO LRFD Bridge Design Specifications*, while resistance factors of 0.85 and 0.90 are 0.05 and 0.10 more, respectively.[3]

Table 55. Mean reliability index for LWC and NWC with varying resistance factor.

Specimen Group	Design Expression	Mean Reliability Index (β_{RQ})				
		LWC Resistance Factor				NWC Resistance Factor of 0.90
		0.75 (AASHTO – 0.05)	0.80 (AASHTO)	0.85 (AASHTO + 0.05)	0.90 (AASHTO + 0.10)	
RC beam without A_v	Simplified-RC	3.24	3.16	3.07	2.99	2.73
RC beam without A_v	GP-equation	3.16	3.00	2.84	2.69	2.43
RC beam without A_v	Simplified-PC/RC	3.12	3.05	2.98	2.91	2.41
RC beam with A_v	Simplified-RC	3.29	3.22	3.14	3.07	3.43
RC beam with A_v	GP-equation	3.53	3.38	3.22	3.07	2.79
RC beam with A_v	Simplified-PC/RC	3.15	3.07	3.00	2.92	3.70
Type II without A_v	GP-equation	2.15	2.12	2.09	2.06	1.92
Type II without A_v	Simplified-PC/RC	1.58	1.57	1.55	1.54	3.07
Type II with A_v	GP-equation	5.51	5.29	5.07	4.85	3.18
Type II with A_v	Simplified-PC/RC	4.38	4.23	4.08	3.93	2.81
Type IV without A_v	GP-equation	2.08	2.05	2.02	2.00	1.83
Type IV without A_v	Simplified-PC/RC	1.57	1.56	1.55	1.54	3.02
Type IV with A_v	GP-equation	5.38	5.17	4.96	4.75	3.16
Type IV with A_v	Simplified-PC/RC	4.58	4.42	4.26	4.10	2.81

Table 55 provides a comparison of the reliability index for the RC cross section. For RC beams without shear reinforcement, β_{LWC} was greater than the β_{NWC} regardless of the design expression. For RC beams with shear reinforcement, β_{LWC} determined using the GP-equation method was greater than the β_{NWC}. For the Simplified-RC and Simplified-PC/RC procedures, β_{NWC} was greater than β_{LWC}.

The reliability indexes determined for the type II cross section are also shown in table 55. β_{LWC} determined using the GP-equation method was greater than β_{NWC} for the cross section without and with shear reinforcement. For the Simplified-PC/RC procedure, β_{LWC} was considerably lower than β_{NWC} for the cross section without shear reinforcement and considerably higher than β_{NWC} for the cross section with shear reinforcement. The same trends were observed for the type IV cross section. The reason for the low β_{LWC} for the PC cross section without stirrups is the low COV (V_P) determined from the analysis of the shear database. This is observed as the much lower slope (i.e., PC no A_v) data plotted in figure 172 and figure 174.

The reliability index determined for LWC using a resistance factor of 0.90 ($\beta_{LWC,\,\phi\,=\,0.90}$) was compared to β_{NWC} and the target reliability index (β_{target}) in table 56. The purpose of this table is to compare β_{LWC} and β_{NWC} to β_{target}. It provides the ratio of $\beta_{LWC,\,\phi\,=\,0.90}$ to β_{NWC}, $\beta_{LWC,\,\phi\,=\,0.90}$ to β_{target}, and β_{NWC} to β_{target}. The ratios for the two PC cross sections are combined by taking the lower reliability index ratios. β_{LWC} was less than the β_{target} of 3.5 for all RC specimens, regardless of design expression. β_{NWC} was also less than β_{target} for all RC specimens except for specimens with shear reinforcement determined using the Simplified-PC/RC procedure. For PC specimens without shear reinforcement, both β_{LWC} and β_{NWC} were less than β_{target}. β_{LWC} was greater than β_{target} for PC specimens with shear reinforcement, regardless of the design expression, but β_{NWC} was less than β_{target}. The mean of reliability index was determined between r_Q values of 0.3 to 0.7, with a target reliability index of 3.5.

Table 56. Ratio of mean reliability index for LWC to NWC and both LWC and NWC to target reliability index.

Specimen Group	Design Expression	Ratio of $\beta_{LWC,\,\phi\,=\,0.90}$ to β_{NWC}	Ratio of $\beta_{LWC,\,\phi\,=\,0.90}$ to β_{target}	Ratio of β_{NWC} to β_{target}
RC beam without A_v	Simplified-RC	1.09	0.85	0.78
RC beam without A_v	GP-equation	1.11	0.77	0.69
RC beam without A_v	Simplified-PC/RC	1.21	0.83	0.69
RC beam with A_v	Simplified-RC	0.89	0.88	0.98
RC beam with A_v	GP-equation	1.10	0.88	0.80
RC beam with A_v	Simplified-PC/RC	0.79	0.83	1.06
Minimum PC without A_v	GP-equation	1.08	0.57	0.52
Minimum PC without A_v	Simplified-PC/RC	0.50	0.44	0.86
Minimum PC with A_v	GP-equation	1.50	1.36	0.90
Minimum PC with A_v	Simplified-PC/RC	1.40	1.12	0.80

β_{LWC} and β_{NWC} are shown graphically in figure 176 through figure 189. The resistance factors were compared to a range of r_Q between 0 and 1.0. Each figure shows β_{NWC} and the β_{LWC} for resistance factors of 0.75, 0.80, 0.85, and 0.90. A horizontal line is shown at 3.5 to indicate β_{target}. Vertical lines are shown at r_Q values of 0.3 and 0.7 to indicate the range over which the mean β_{RQ} was determined. The reliability indexes for RC cross sections without shear reinforcement are shown in figure 176 through figure 178 for the Simplified-RC procedure, the GP-equation method, and the Simplified-PC/RC procedure, respectively. The reliability indexes determined using the same three design expressions are shown in figure 179 through figure 181 for RC cross sections with shear reinforcement. The reliability indexes for PC cross sections were determined using the GP-equation method and the Simplified-PC/RC procedure. The reliability indexes for the type II cross section are shown in figure 182 through figure 185. Figure 186 through figure 189 show the reliability indexes for the type IV cross section.

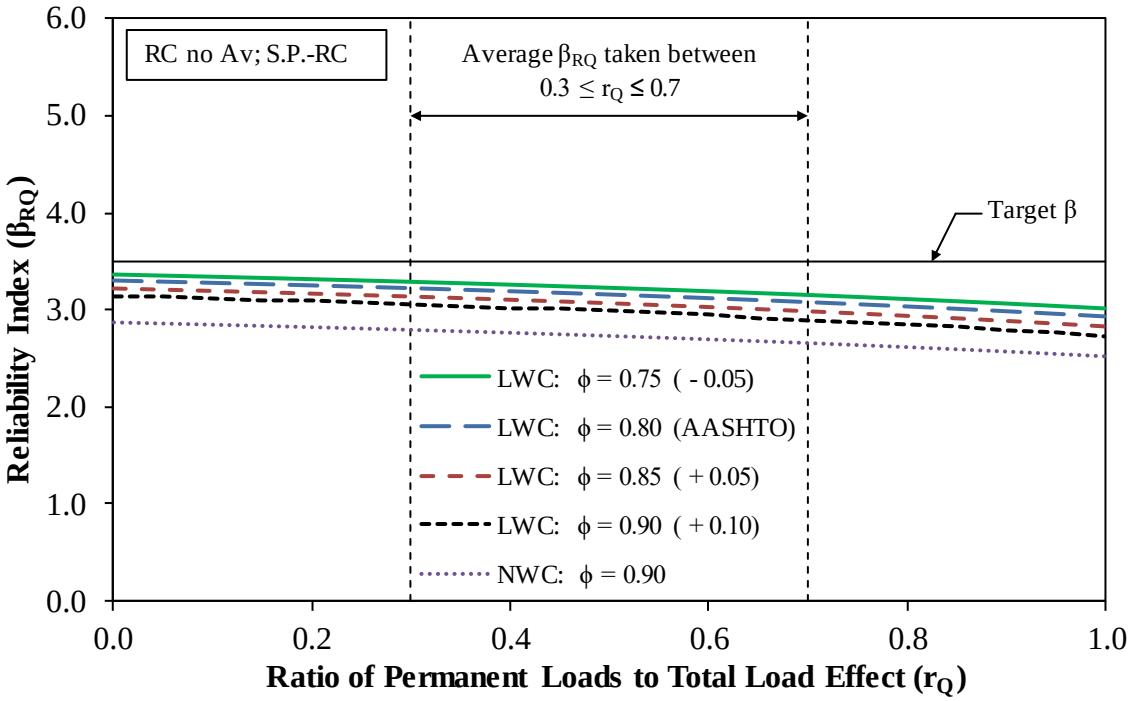

Source: FHWA.

Figure 176. Graph. Reliability index for LWC and NWC determined using Simplified-PC/RC compared to the ratio of permanent loads to total load effect for RC specimens without shear reinforcement.

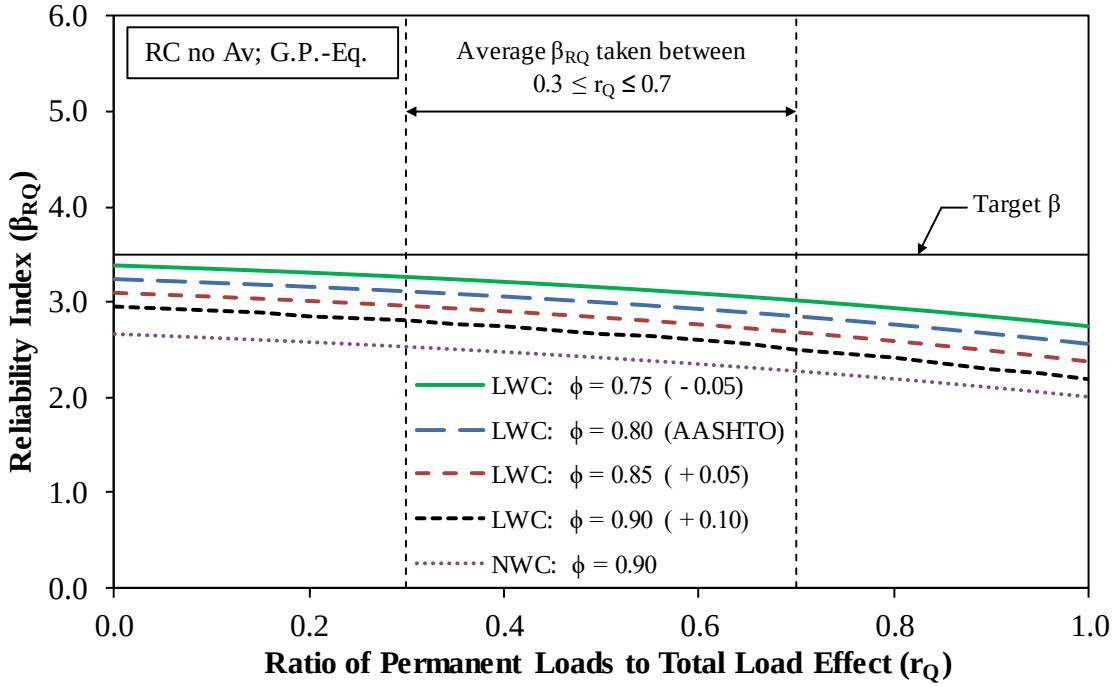

Source: FHWA.

Figure 177. Graph. Reliability index for LWC and NWC determined using the GP-equation method compared to the ratio of permanent loads to total load effect for RC specimens without shear reinforcement.

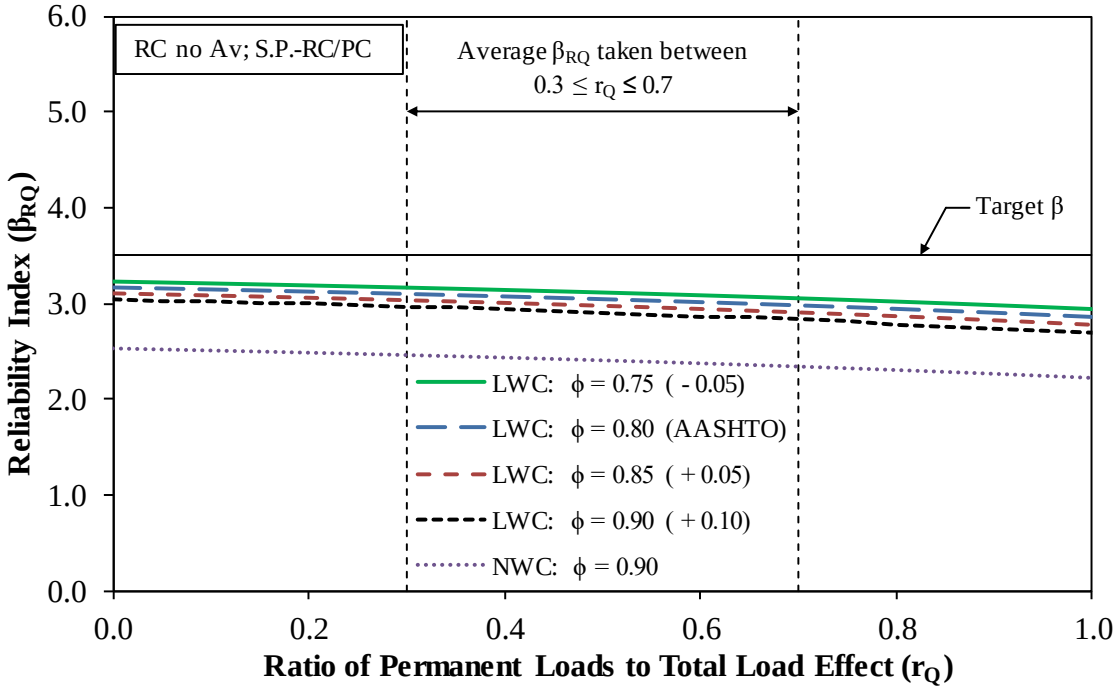

Source: FHWA.

Figure 178. Graph. Reliability index for LWC and NWC determined using Simplified-PC/RC compared to the ratio of permanent loads to total load effect for RC specimens without shear reinforcement.

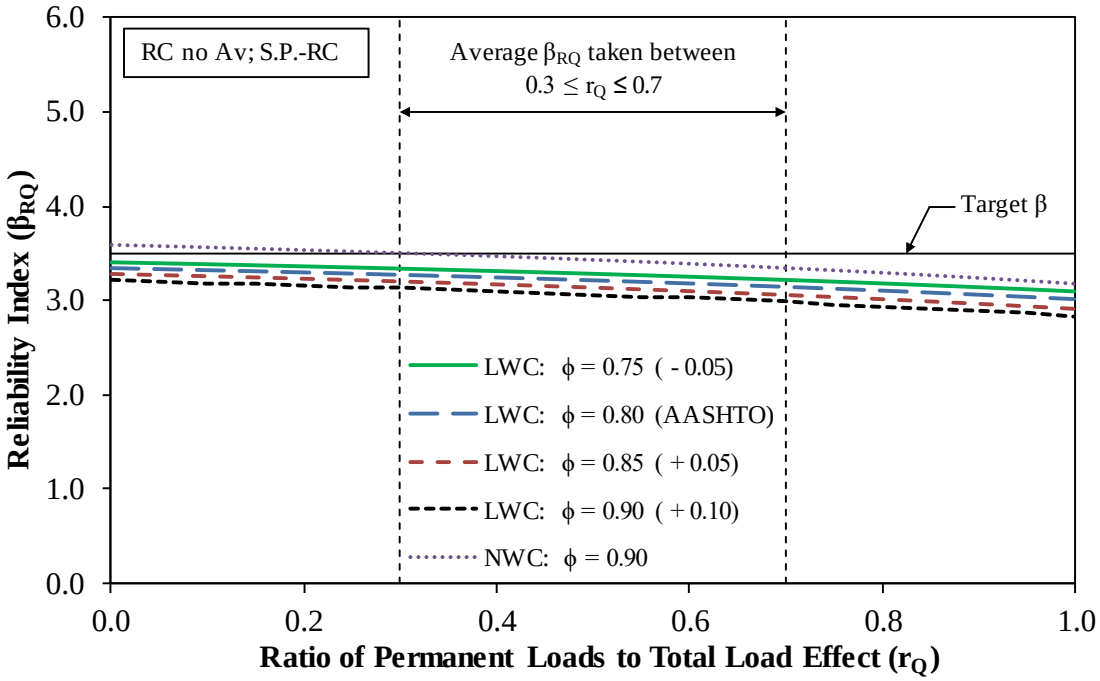

Source: FHWA.

Figure 179. Graph. Reliability index for LWC and NWC determined using Simplified-PC/RC compared to the ratio of permanent loads to total load effect for RC specimens with shear reinforcement.

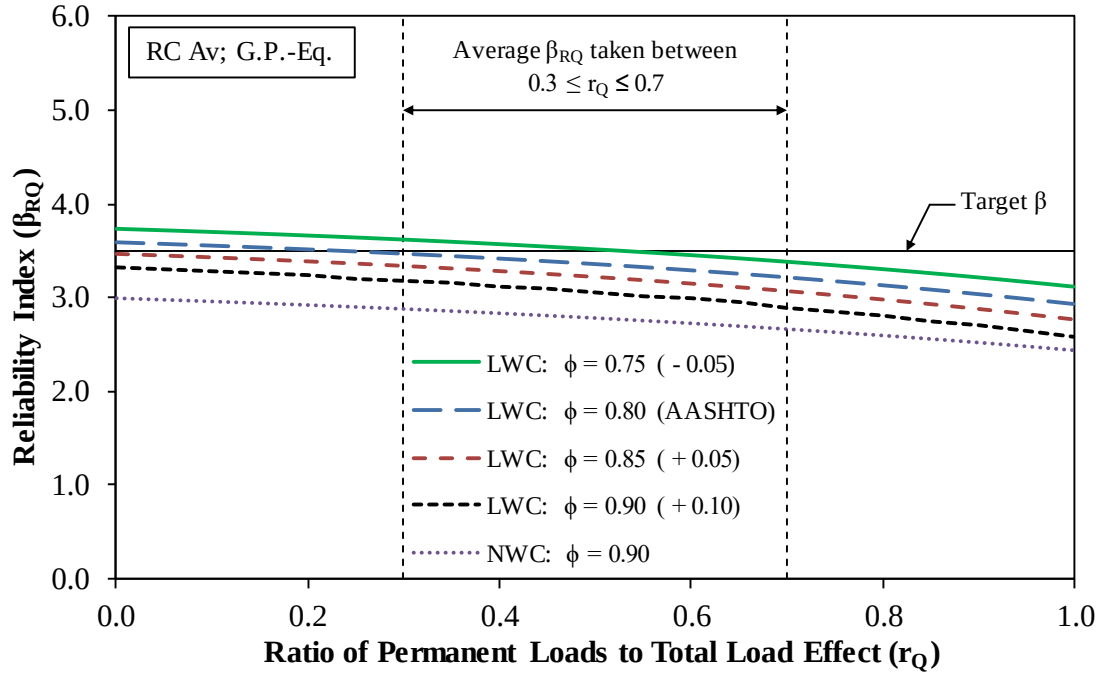

Source: FHWA.

Figure 180. Graph. Reliability index for LWC and NWC determined using the GP-equation method compared to the ratio of permanent loads to total load effect for RC specimens with shear reinforcement.

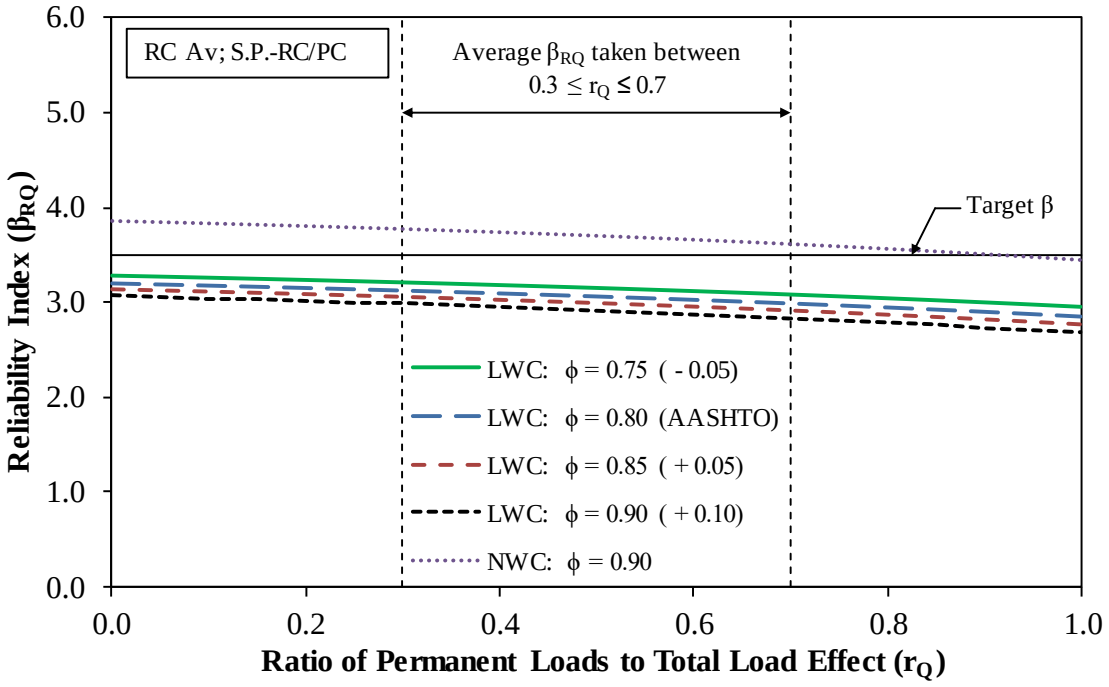

Source: FHWA.

Figure 181. Graph. Reliability index for LWC and NWC determined using Simplified-PC/RC compared to the ratio of permanent loads to the total load effect for RC specimens with shear reinforcement.

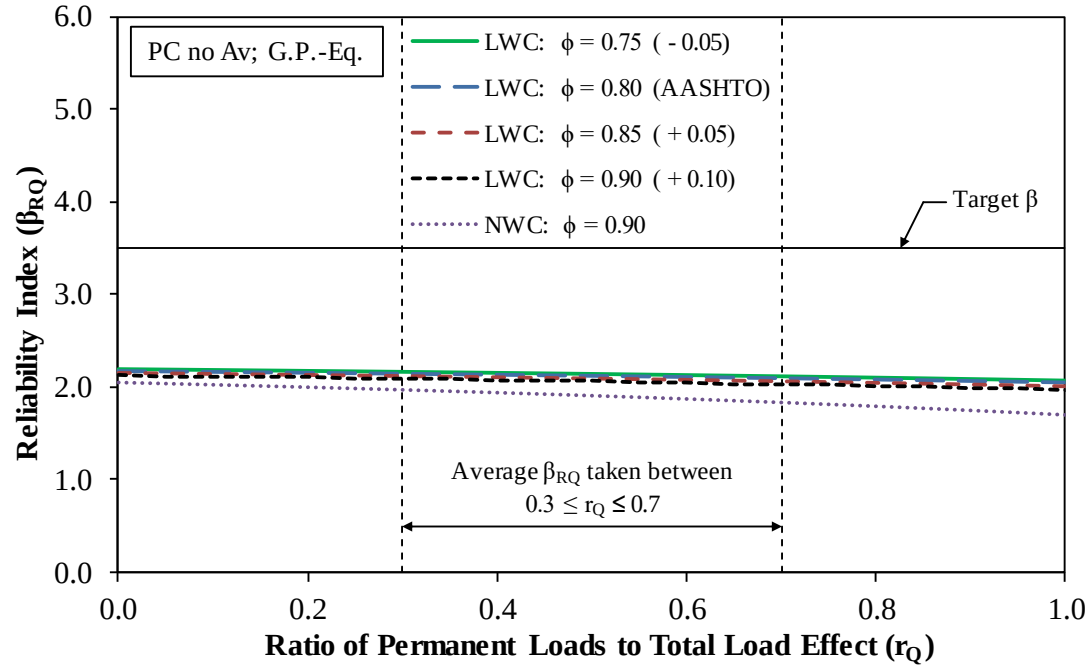

Source: FHWA.

Figure 182. Graph. Reliability index for LWC and NWC determined using the GP-equation method compared to the ratio of permanent loads to the total load effect for PC specimens without shear reinforcement (type II).

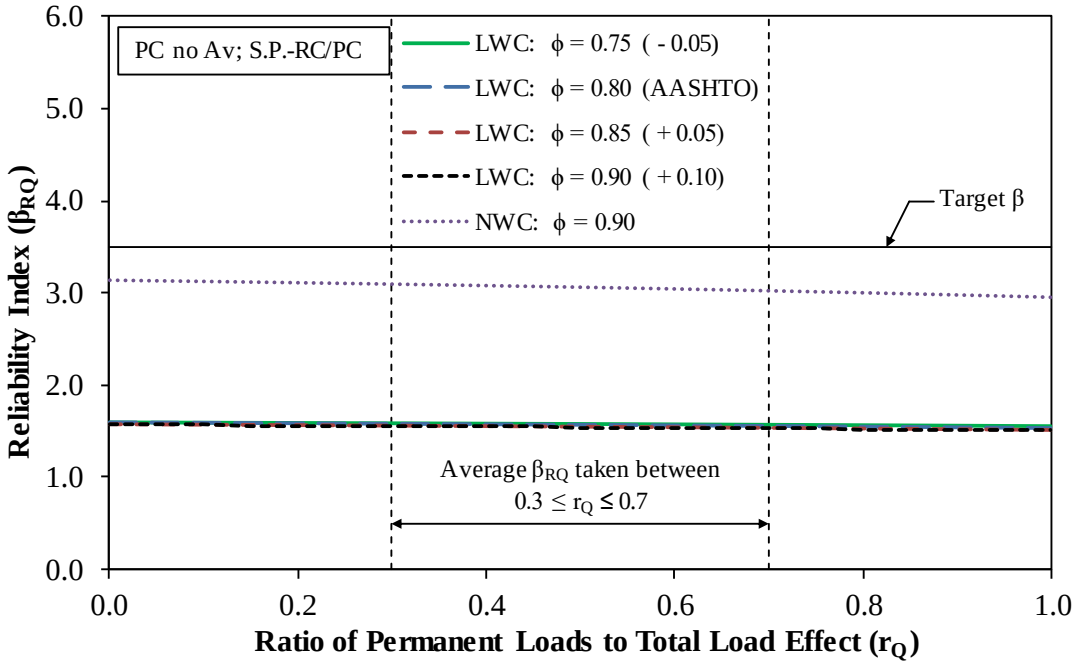

Source: FHWA.

Figure 183. Graph. Reliability index for LWC and NWC determined using Simplified-PC/RC compared to the ratio of permanent loads to the total load effect for PC specimens without shear reinforcement (type II).

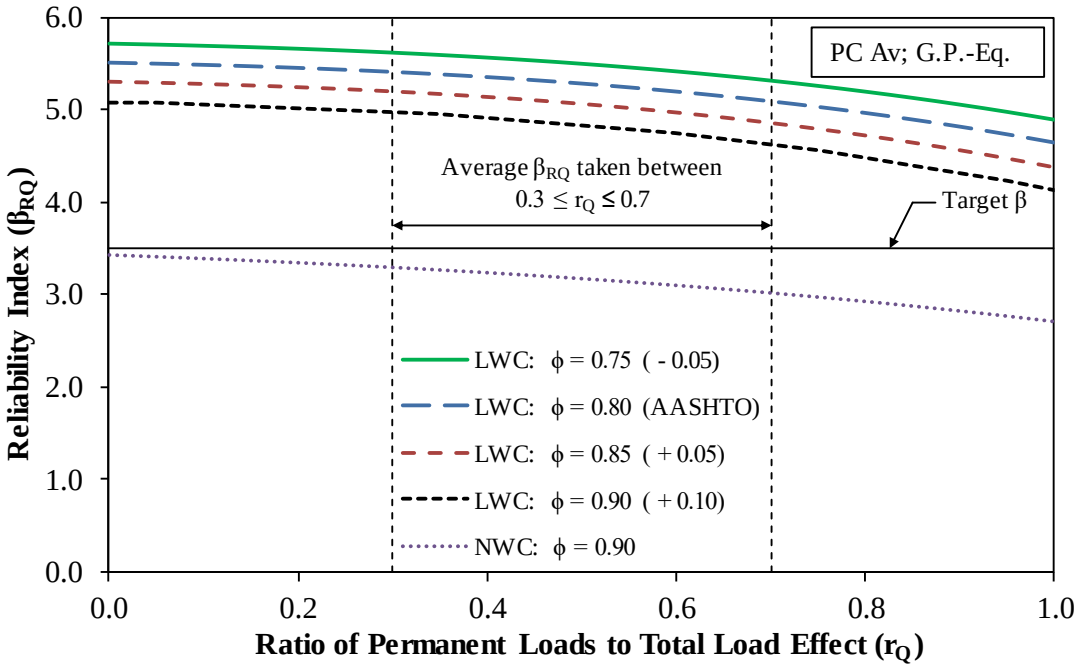

Source: FHWA.

Figure 184. Graph. Reliability index for LWC and NWC determined using the GP-equation method compared to the ratio of permanent loads to the total load effect for PC specimens with shear reinforcement (type II).

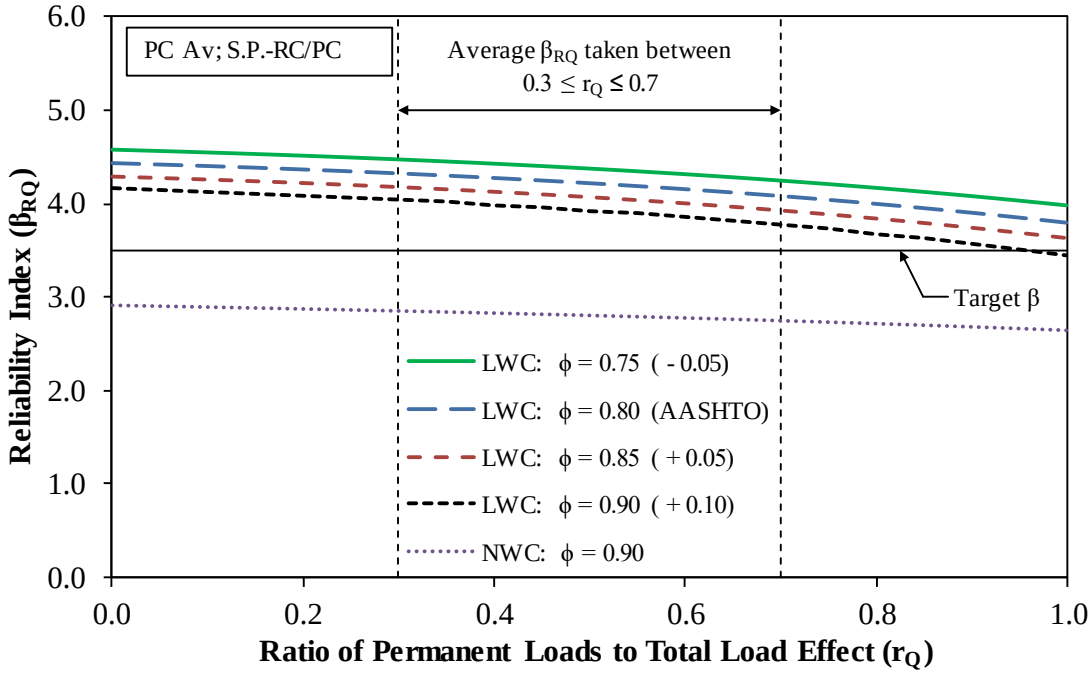

Source: FHWA.

Figure 185. Graph. Reliability index for LWC and NWC determined using Simplified-PC/RC compared to the ratio of permanent loads to the total load effect for PC specimens with shear reinforcement (type II).

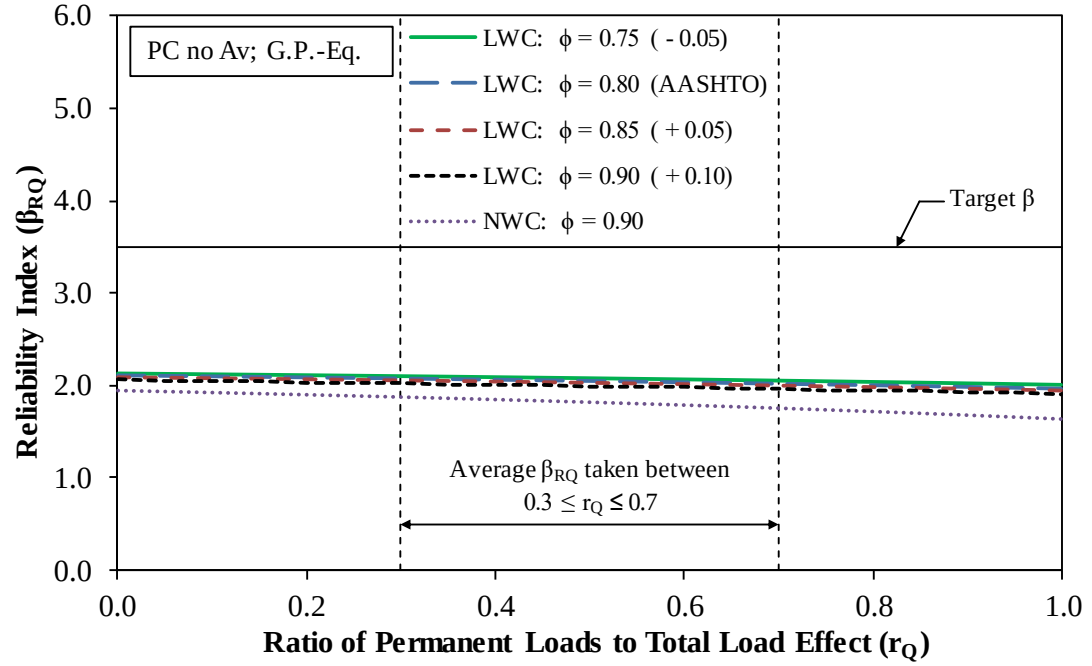

Source: FHWA.

Figure 186. Graph. Reliability index for LWC and NWC determined using the GP-equation method compared to the ratio of permanent loads to the total load effect for PC specimens without shear reinforcement (type IV).

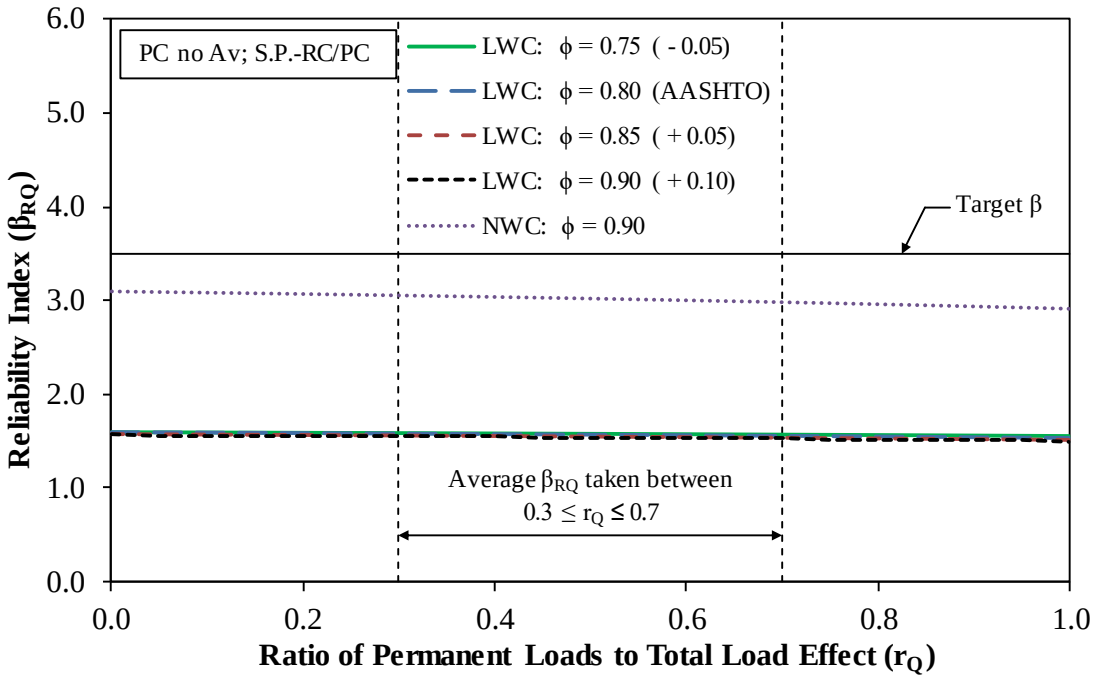

Source: FHWA.

Figure 187. Graph. Reliability index for LWC and NWC determined using Simplified-PC/RC compared to the ratio of permanent loads to the total load effect for PC specimens without shear reinforcement (type IV).

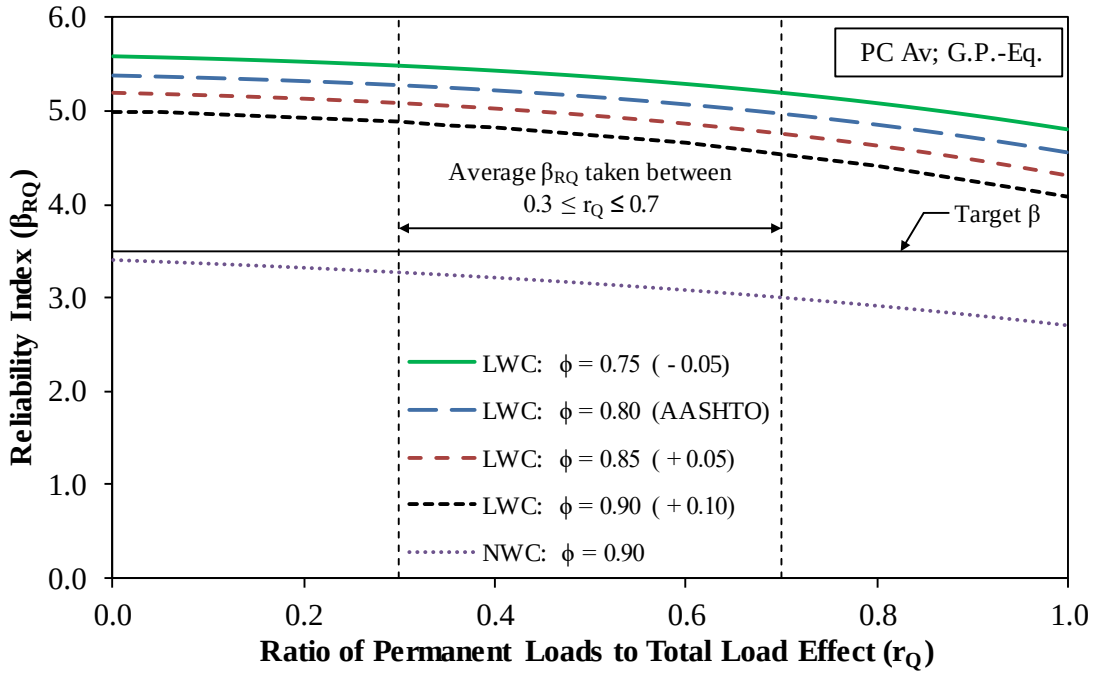

Source: FHWA.

Figure 188. Graph. Reliability index for LWC and NWC determined using the GP-equation method compared to the ratio of permanent loads to the total load effect for PC specimens with shear reinforcement (type IV).

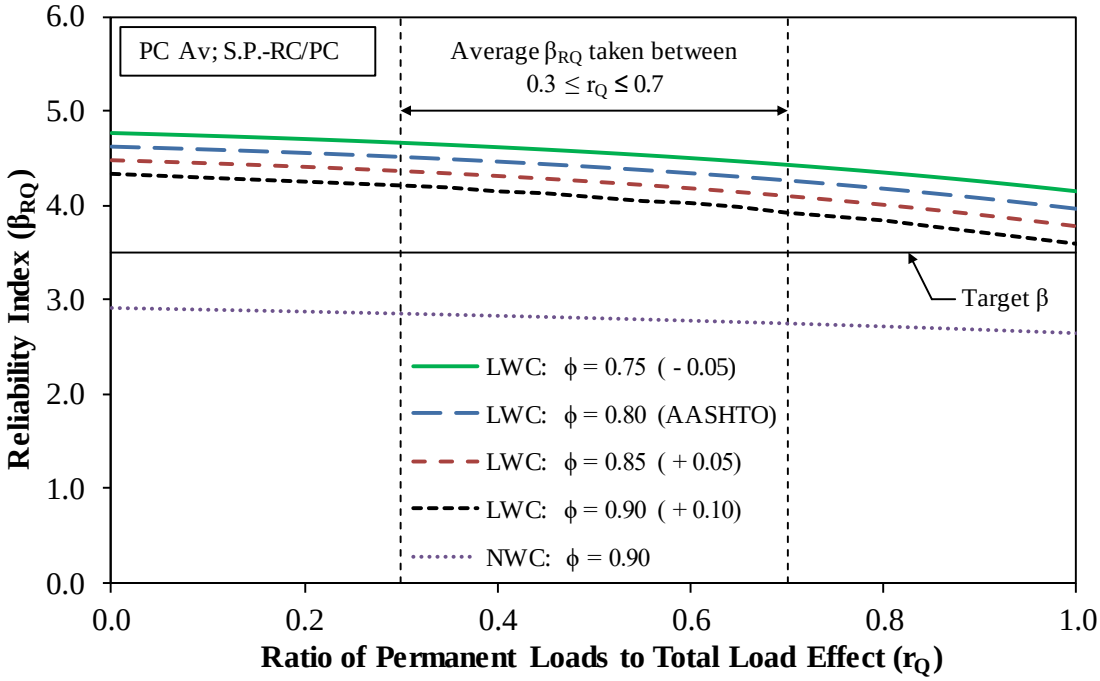

Source: FHWA.

Figure 189. Graph. Reliability index for LWC and NWC determined using Simplified-PC/RC compared to the ratio of permanent loads to the total load effect for PC specimens with shear reinforcement (type IV).

RELIABILITY INDEX FOR SHEAR FROM THE LITERATURE

The reliability index for LWC and NWC in shear has been determined in previous studies. (See references 49, 50, 52, 11, and 60.) The following summarizes the results from these previous studies and describes the differences in the methods of calculating the reliability index.

Studies on LWC

The reliability index for RC cross sections in shear was studied by Paczkowski and Nowak.[52] Shear test data from three previous studies that performed shear tests on both LWC and NWC were evaluated.[52] A total of 13 LWC and 13 NWC specimens were compared. The GP-equation method was used to determine nominal shear resistance. The study found that the mean test-to-predicted nominal shear resistance was 15 percent less for LWC specimens. Assumed values of λ_P and V_P of 1.075 and 10 percent, respectively, were used in the study for NWC. For the determination of the reliability index, λ_P for LWC was assumed to be 15 percent less than for NWC, and the same COV (V_P) was used. The reliability index was evaluated over a range of span lengths. The study concluded that a resistance factor of 0.80 for LWC gave a reliability index that was greater than the reliability index for NWC and the target reliability index of 3.5.

NCHRP Report 733 describes the testing and evaluation of high-strength LWC prestressed girders in shear.[11] The report also describes the evaluation of a database of LWC shear tests on prestressed girders that included tests from three previous studies. The report includes an evaluation of test-to-predicted shear resistance for LWC specimens using a resistance factor

of 0.85 to test-to-predicted shear resistance for NWC specimens using a resistance factor of 0.90. The recommended resistance factor in NCHRP Report 733 is 0.85 for LWC in shear.

After NCHRP Report 733 was submitted for publication, additional evaluation of the LWC database was performed that included a reliability analysis.[60] The LWC database used in the study included 154 RC beams and 22 PC beams. The average shear span to effective depth ratio of the RC specimens in the study was 2.81, and the average ratio for the PC specimens in the study was 2.32. The Rackwitz-Fiessler procedure was used to determine reliability index.[50,60] The study evaluated the reliability index for PC girders with shear reinforcement. The study found that a resistance factor of 1.0 for LWC in shear determined using the two methods of the general procedure would have a reliability index greater than the target reliability index of 3.5. For the Simplified-PC/RC procedure, a resistance factor of 0.95 was needed to have a reliability index greater than the target reliability index of 3.5.

The present research effort described in this report also found that the reliability index of prestressed cross sections with shear reinforcement was greater than the target reliability index of 3.5. The present research effort also found that the reliability index determined using the GP-equation method was greater than the reliability index determined using the Simplified-PC/RC procedure for prestressed cross sections with shear reinforcement.

Studies on NWC

NCHRP Report 368 describes the calibration of the LRFD bridge design code.[49] The reliability index was determined using the bias and COV of the professional factor (λ_P and V_P) for NWC in shear for RC and PC cross sections from another study.[56] λ_P and V_P used in the study for sections with shear reinforcement were 1.075 and 10 percent, respectively, and were assumptions. The bias and COV due to materials and fabrication were determined using MCFT, which is the basis for the general procedure in the *AASHTO LRFD Bridge Design Specifications*.[3] The expression for the reliability index was also different. It included a two-standard deviation offset for the mean and variance of the resistance. The resistance factor for shear recommended in the study was 0.90. The report showed a reliability index for RC and PC sections that was less than 3.5 for nearly all span lengths and girder spacings.

NCHRP Report 549 describes the development and evaluation of the Simplified-PC/RC procedure.[32] A reliability index was not determined as part of the study. Instead, a fractile level was calculated as the percentage of the test data less than a test-to-predicted shear resistance of 1.0. The result reported in NCHRP Report 549 for fractile level was 20.5 percent.[32]

SUMMARY OF THE ANALYSIS OF RELIABILITY INDEX FOR LWC IN SHEAR

The mean β_{RQ} was determined for the shear resistance of LWC cross sections. β_{RQ} for LWC was compared to the target reliability index and the mean reliability index for NWC cross sections. The uncertainty due to the loads was evaluated using data from previous studies to determine the mean and variation of the load. The uncertainty due to fabrication and materials was evaluated using the Monte Carlo simulation. One RC cross section and two PC cross sections were simulated. The uncertainty due to analysis was evaluated using LWC specimens and NWC specimens. The combined uncertainty was used to determine the mean and variance of

resistance. The reliability index was evaluated at a resistance factor for LWC of 0.75, 0.80, 0.85, and 0.90. β_{RQ} for LWC and NWC in shear was then determined over a range of dead-to-total load ratios. The reliability index for LWC was compared to the target reliability index and the reliability index for NWC.

β_{RQ} for LWC and NWC was compared to β_{target}. The reliability indexes determined for LWC were less than β_{target} for all cross sections except PC specimens with shear reinforcement, regardless of the resistance factor (up to $\phi = 0.90$) or the design expression used to determine nominal shear resistance. The reliability indexes determined for NWC were less than β_{target} for all cross sections except RC specimens with shear reinforcement determined using the Simplified-PC/RC procedure.

β_{LWC} was also compared to β_{NWC}. β_{LWC} determined using the GP-equation method was greater than the β_{NWC} for all cross sections. The Simplified-RC and Simplified-PC/RC procedures had β_{LWC} greater than β_{NWC} for RC specimens without shear reinforcement and had β_{NWC} greater than β_{LWC} for RC specimens with shear reinforcement. For PC specimens without shear reinforcement, the Simplified-PC/RC procedure had β_{NWC} greater than β_{LWC}. For PC specimens with shear reinforcement, β_{LWC} determined using the Simplified-PC/RC procedure was greater than β_{NWC}.

CHAPTER 7. PRELIMINARY RECOMMENDATIONS FOR *AASHTO LRFD BRIDGE DESIGN SPECIFICATIONS*[3]

INTRODUCTION

This chapter summarizes several preliminary recommended changes to the *AASHTO LRFD Bridge Design Specifications*.[3] The existing and recommended language is presented as it would appear in these specifications. The first two recommended changes regarding the definition of LWC and the introduction of an LWC modification factor (λ-factor) were previously described in a related document concerning the mechanical properties of LWC and are presented again for clarity.[1] Additional recommended changes are presented in this chapter that are based on the analysis described in this report. These additional recommendations are built on the two previous recommendations.

The recommended changes described in this chapter include the recommended new expression for the λ-factor. The λ-factor is not based on the proportions of constituent materials and includes tests from types of mix designs that are not explicitly permitted by the current edition of the *AASHTO LRFD Bridge Design Specifications*.[3] These mix types include specified density LWC (typically a blend of lightweight and normal-weight coarse aggregate) and inverted mixes (normal-weight coarse and lightweight fine aggregate). The recommended new expression for the λ-factor is instead based on unit weight (w_c) and splitting tensile strength (f_{ct}), and as a result, the definitions of sand-lightweight concrete and all-lightweight concrete would no longer be needed.

The changes to the *AASHTO LRFD Bridge Design Specifications* recommended in this chapter are in regard to the performance of LWC in shear. The first three recommended changes involve adding the new expression for the λ-factor to design expressions for nominal shear resistance. Another change involves adding the λ-factor to the design expression for minimum shear reinforcement. The final recommended change involves the reduction factor for LWC in shear and torsion.

This report previously described the shear performance of 15 LWC prestress girders tested at TFHRC. Additional shear tests on LWC specimens were found in the literature. (For sources, see Bibliography section LWC Sources for TFHRC Shear Database.) These tests on LWC were added to selected tests on NWC specimens found in the ACI-DafStb database. (For sources, see Bibliography section NWC Sources for ACI-DafStb Database.) The NWC specimens that were selected had parameters that are important to shear resistance that were similar to the LWC specimens. The recommended changes to the *AASHTO LRFD Bridge Design Specifications* were validated using the specimens from the TFHRC shear database and the ACI-DafStb database.

PROPOSED DEFINITION FOR LWC

The definition for LWC in the *AASHTO LRFD Bridge Design Specifications* is in Article 5.2 and states the following:

> *Lightweight Concrete* – Concrete containing lightweight aggregate and having an air-dry unit weight not exceeding 0.120 kcf, as determined by ASTM C567. Lightweight Concrete without natural sand is termed "all-lightweight concrete" and lightweight concrete in which all of the fine aggregate consists of normal weight sand is termed "sand-lightweight concrete." (p. 5-3)[3]

This definition limits the unit weight for LWC to 0.120 kcf (1,920 kg/m^3) and includes definitions for sand-lightweight and all-lightweight concretes. The proposed definition for LWC expands the range of w_c and eliminates the definitions for terms relating to the constituent materials in LWC. The proposed definition for LWC is as follows:

> *Lightweight Concrete* – Concrete containing lightweight aggregate and having an equilibrium density not exceeding 0.135 kcf, as determined by ASTM C567.

The term "air-dry unit weight" is used in the existing definition; however, this term is not found in ASTM C567.[61] The term is interpreted to be equivalent to the ASTM C567 term "equilibrium density." A statement could be added to the commentary to clarify the term "air-dry unit weight," or the term "equilibrium density" could be used in the definition for LWC.

PROPOSED EXPRESSION FOR LWC MODIFICATION FACTOR

The concept of including a modification factor for LWC in expressions for predicting nominal resistance is included in many articles of the *AASHTO LRFD Bridge Design Specifications*.[3] However, a single unified expression or LWC modification factor is not specified. This section proposes a new term, the λ-factor, to quantify the reduction in nominal resistance that could be included in any expression for nominal resistance. The language for the λ-factor could be based on the existing language for the modification factor for shear in Article 5.8.2.2 that states the following:

> Where lightweight aggregate concretes are used, the following modifications shall apply in determining resistance to torsion and shear:
>
> Where the average splitting tensile strength of lightweight concrete, f_{ct}, is specified, the term, $\sqrt{f'_c}$ in the expressions given in Articles 5.8.2 and 5.8.3 shall be replaced by: $4.7 f_{ct} < \sqrt{f'_c}$.
>
> Where f_{ct} is not specified, the term $0.75\sqrt{f'_c}$ for all lightweight concrete, and $0.85\sqrt{f'_c}$ for sand-lightweight concrete shall be substituted for $\sqrt{f'_c}$ in the expressions given in Articles 5.8.2 and 5.8.3.
>
> Linear interpolation may be employed when partial sand replacement is used. (p. 5-59)[3]

Article 5.8.2.2 specifically relates to torsion and shear, so a general λ-factor would not specifically reference those actions in its definition. The terms "sand-lightweight concrete" and "all-lightweight concrete" would not be used because the proposed new definition for LWC does not include them. The λ-factor relates to the material properties of structural LWC, so the new

article for the definition for the λ-factor could be located in Article 5.4.2. The λ-factor is referred to as Article 5.4.2.8 in this report. The proposed text for the λ-factor is as follows:

> Where lightweight aggregate concretes are used, the lightweight concrete modification factor, λ, shall be determined as:
>
> Where the average splitting tensile strength of lightweight concrete, f_{ct}, is specified, λ may be taken as: $4.7 f_{ct} / \sqrt{f'_c} \leq 1.0$.
>
> Where f_{ct} is not specified, λ may be taken as:
>
> $$0.75 \leq \lambda = 7.5 w_c \leq 1.0 \qquad (5.4.2.8\text{-}1)$$

The language for the λ-factor expression when f_{ct} is not specified follows the format of the ϕ-factor for flexure for prestressed and nonprestressed members in Article 5.5.4.2.1.

The effect of using the λ-factor in expressions for the development length of mild steel is evaluated in this report. The effect of using the λ-factor, in additional expressions for nominal resistance, still needs to be evaluated. The proposed λ-factor could then be included in additional expressions for nominal resistance in the *ASHTO LRFD Bridge Design Specifications*.[3] For example, the λ-factor could be added directly to design expressions for nominal shear resistance in Articles 5.8.2 and 5.8.3 and would replace the existing modification factor for LWC.

PROPOSED DESIGN EXPRESSIONS FOR NOMINAL SHEAR RESISTANCE

Three recommended changes to the *AASHTO LRFD Bridge Design Specifications* involve adding the λ-factor to the three terms for the nominal shear resistance provided by the concrete (i.e., V_c, V_{ci}, and V_{cw}). The change to the V_c term is described first and includes language for the nominal shear resistance (V_n). The changes to V_{ci} and V_{cw} are presented after the expression for V_c.

The proposed design expression for nominal shear resistance provided by tensile stresses in the concrete (V_c) is as follows:

> The nominal shear resistance, V_n, shall be determined as the lesser of:
>
> $V_n = V_c + V_s + V_p$
>
> $V_n = 0.25 f'_c b_v d_v + V_p$
>
> In which:
>
> $V_c = 0.0316 \beta \lambda \sqrt{f'_c} b_v d_v$, if the procedures of Articles 5.8.3.4.1 or 5.8.3.4.2 are used.
>
> V_c = The lesser of V_{ci} and V_{cw}, if the procedures of Article 5.8.3.4.3 are used.

The proposed design expression for nominal shear resistance provided by concrete when inclined cracking results from combined shear and moment (V_{ci}) is as follows:

V_{ci} shall be determined as:

$$V_{ci} = 0.02 \lambda \sqrt{f'_c}\, b_v\, d_v + V_d + V_i\, M_{cre} / M_{max} \geq 0.06 \lambda \sqrt{f'_c}\, b_v\, d_v$$

Where:

V_i = factored shear force at the section due to externally applied loads occurring simultaneously with the maximum factored moment at the section due to externally applied loads (M_{max}).
M_{cre} = moment causing flexural cracking at the section due to externally applied loads.

The proposed design expression for nominal shear resistance provided by concrete when inclined cracking results from excessive principal tensions in the web (V_{cw}) is as follows:

V_{cw} shall be determined as:

$$V_{cw} = (0.02 \lambda \sqrt{f'_c} + 0.30\, f_{pc})\, b_v d_v + V_p$$

The ratio of test-to-predicted shear resistance for LWC specimens in the TFHRC shear database was compared to compressive strength in figure 190 and figure 191. Figure 190 shows the ratios for RC specimens without shear reinforcement, and figure 191 shows the ratios for PC specimens with shear reinforcement. For comparison, the ratios for NWC specimens in the ACI-DafStb database are also shown in each figure. The nominal shear resistance was determined using the GP-equations method for β and θ given in Article 5.8.3.4.2 and the new expression λ-factor.[3)] Regression lines are shown for the LWC specimens and NWC specimens. The regression line for the LWC specimens is slightly greater than the regression line for NWC specimens for nearly all values of compressive strength. For both figures, the number of specimens is in parentheses in the legends.

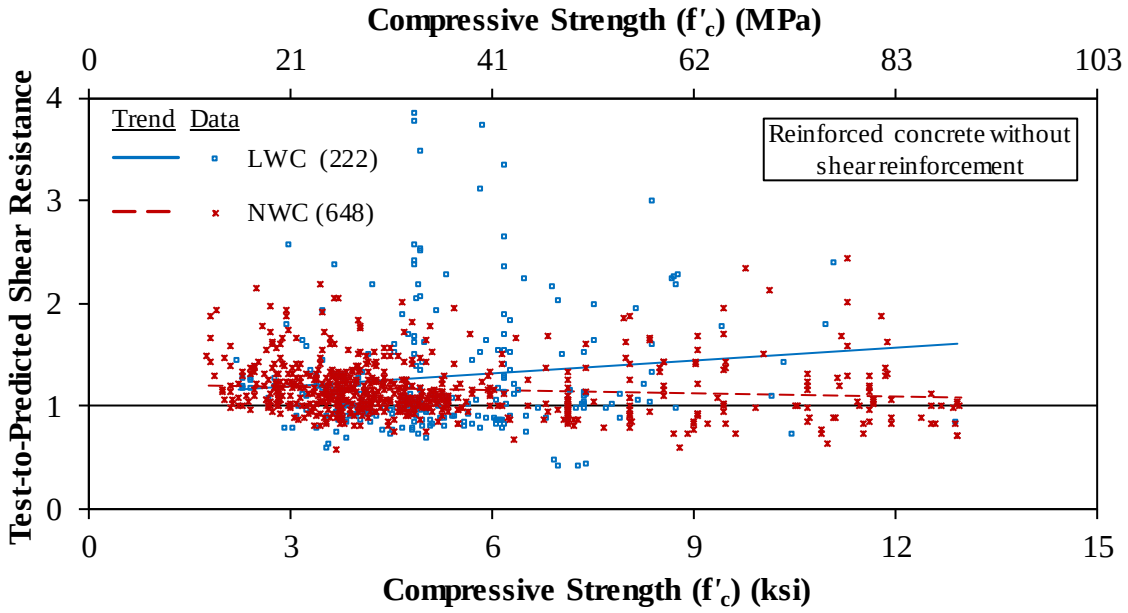

Source: FHWA.
1 ksi = 6.89 MPa.

Figure 190. Graph. Test-to-predicted shear resistance using GP-equation method for RC members without shear reinforcement.

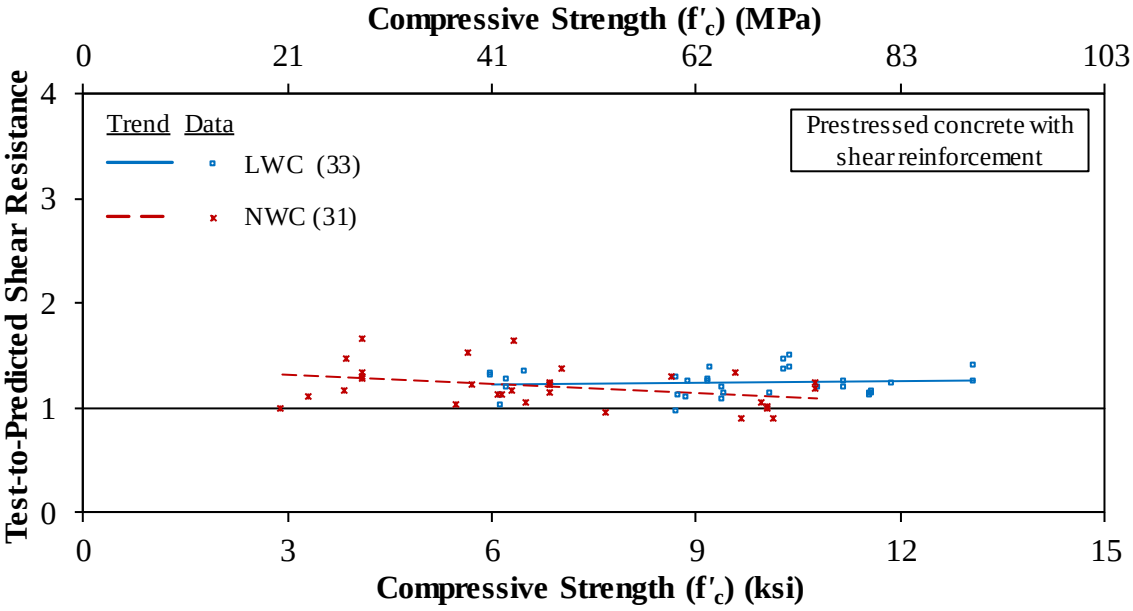

Source: FHWA.
1 ksi = 6.89 MPa.

Figure 191. Graph. Test-to-predicted shear resistance using GP-equation method for PC members with shear reinforcement.

PROPOSED DESIGN EXPRESSION FOR MINIMUM SHEAR REINFORCEMENT

A recommended change to the *AASHTO LRFD Bridge Design Specifications* involves adding the new expression for the λ-factor to the design expression for minimum shear reinforcement (i.e., transverse reinforcement). The proposed design expression for the minimum shear reinforcement is as follows:

> Except for segmental post-tensioned concrete box girder bridges, where transverse reinforcement is required, as specified in Article 5.8.2.4, the area of steel shall satisfy:
>
> $A_v \geq 0.0316\,\lambda\sqrt{f'_c}\,b_v s/f_y$

The ratio of test-to-predicted shear resistance for LWC specimens in the TFHRC shear database is compared to the shear reinforcement ratio in figure 192 for RC specimens and figure 193 for PC specimens. The nominal shear resistance was determined using the GP-equation method for β and θ given in Article 5.8.3.4.2 and the new expression for the λ-factor. A vertical line indicates the minimum amount of shear reinforcement specified by Article 5.8.2.5. The ratios of test-to-predicted shear resistance for the few specimens with less shear reinforcement than the required amount was similar to the ratios for specimens with slightly greater than the required amount. For comparison, NWC specimens in the ACI-DafStb database are also shown in the figure. For both figures, the number of specimens is in parentheses in the legends.

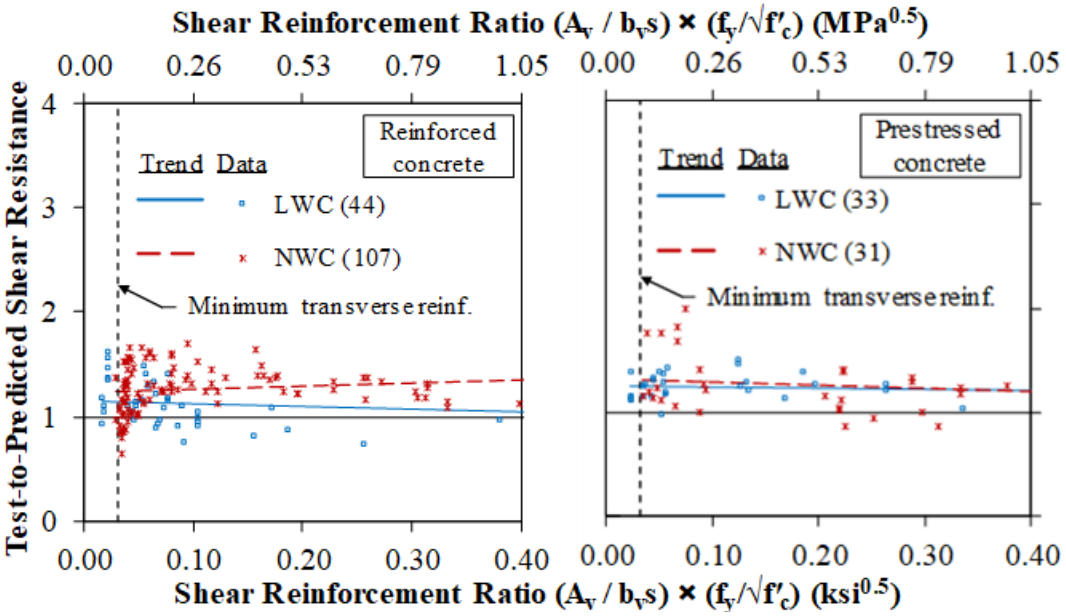

Source: FHWA.
1 ksi = 6.89 MPa.

Figure 192. Graph. Test-to-predicted shear resistance compared to shear reinforcement ratio multiplied by the ratio of stirrup yield strength to the square root of concrete compressive strength using GP-equation method for RC.

Source: FHWA.
1 ksi = 6.89 MPa.

Figure 193. Graph. Test-to-predicted shear resistance compared to shear reinforcement ratio multiplied by the ratio of stirrup yield strength to the square root of concrete compressive strength using GP-equation method for PC.

PROPOSED RESISTANCE FACTOR FOR SHEAR AND TORSION OF LWC

A reliability analysis was performed to evaluate the resistance factor for LWC in shear. Based on the analysis, a change to the reduction factor for LWC in shear and torsion is recommended. The proposed resistance factor for LWC in shear and torsion is as follows:

Resistance factor ϕ shall be taken as:

For shear and torsion:

Normal weight concrete……..0.90

Lightweight concrete……..0.90

Table 57 shows a comparison of the reliability index (β_{RQ}) for LWC using a resistance factor of 0.90 to β_{RQ} for NWC using a resistance factor of 0.90, as specified in Article 5.5.4.2.1. β_{RQ} were determined using the three different methods for calculating shear resistance in Article 5.8.3 and the new expression for the λ-factor. Table 57 shows that, for nominal resistance determined using

the GP-equation procedure, β_{RQ} for LWC with a resistance factor of 0.90 was greater than β_{RQ} for NWC.

Table 57. Reliability index for LWC and NWC in shear.

Specimen Group	Design Expression	β_{RQ}	
		LWC (ϕ = 0.90)	**NWC (ϕ = 0.90)**
RC beam without shear reinforcement	Simplified-RC	2.99	2.73
RC beam without shear reinforcement	GP-equation	2.69	2.43
RC beam without shear reinforcement	Simplified-PC/RC	2.91	2.41
RC beam with shear reinforcement	Simplified-RC	3.07	3.43
RC beam with shear reinforcement	GP-equation	3.07	2.79
RC beam with shear reinforcement	Simplified-PC/RC	2.92	3.70
PC girder without shear reinforcement	GP-equation	2.00	1.83
PC girder without shear reinforcement	Simplified-PC/RC	1.54	3.02
PC girder with shear reinforcement	GP-equation	4.75	3.16
PC girder with shear reinforcement	Simplified-PC/RC	4.10	2.81

CHAPTER 8. CONCLUSION

This report presented and described 30 shear tests on 15 LWC prestressed girders, a shear strength database, a reliability analysis, and potential revisions to the *AASHTO LRFD Bridge Design Specifications* relating to the shear resistance of LWC.[3] The proposed design expressions for shear resistance were compared to tested values in a database including over 400 tests on LWC that was collected as part of this research effort. A description of the database and the development and evaluation of prediction expressions was included in this report.

Future phases of this research compilation and analysis effort will include a synthesis of past work on structural performance of LWC. The test results will be compared to the prediction expressions for nominal resistance in the *AASHTO LRFD Bridge Design Specifications*, incorporating appropriate proposed revisions for LWC mechanical properties.[3]

APPENDIX A. REINFORCING BAR MATERIAL PROPERTIES

This appendix contains a table (see table 58) and figures (see figure 194 through figure 207) with material test data from the reinforcing bars used in the shear tests of LWC girders tested at TFHRC. The tensile data include yield strength (calculated using 0.2 percent offset method), ultimate strength, and stress–strain relationships of the mechanical tests.

Table 58. Reinforcing bar mechanical properties.

Tensile Test	Girder Design No.	Coupon	Bar Type	Bar Size	Yield Strength (ksi)	Ultimate Strength (ksi)
3-5A	5	1	Stirrup	3	69.1	112.1
3-5B	5	2	Stirrup	3	72.4	112.3
3-8A	8	1	Stirrup	3	70.5	109.3
3-8B	8	2	Stirrup	3	59.7	94.5
4-6A	6 and 7	1	Stirrup	4	64.6	95.1
4-7A	6 and 7	2	Stirrup	4	71.5	100.4
4-9A	9	1	Stirrup	4	66.0	105.7
4-9B	9	2	Stirrup	4	64.7	103.9
5-end	5–7	1	End longitudinal reinforcement	6	65.2	105.6
6-end	5–7	2	End longitudinal reinforcement	6	66.3	106.8
89-end-1	8 and 9	1	End longitudinal reinforcement	6	65.2	107.7
89-end-2	8 and 9	2	End longitudinal reinforcement	6	66.3	110.1
4-conf-1	5–9	1	Confinement reinforcement	4	65.5	106.5
4-conf-2	5–9	2	Confinement reinforcement	4	66.1	107.7

1 ksi = 6.89 MPa.

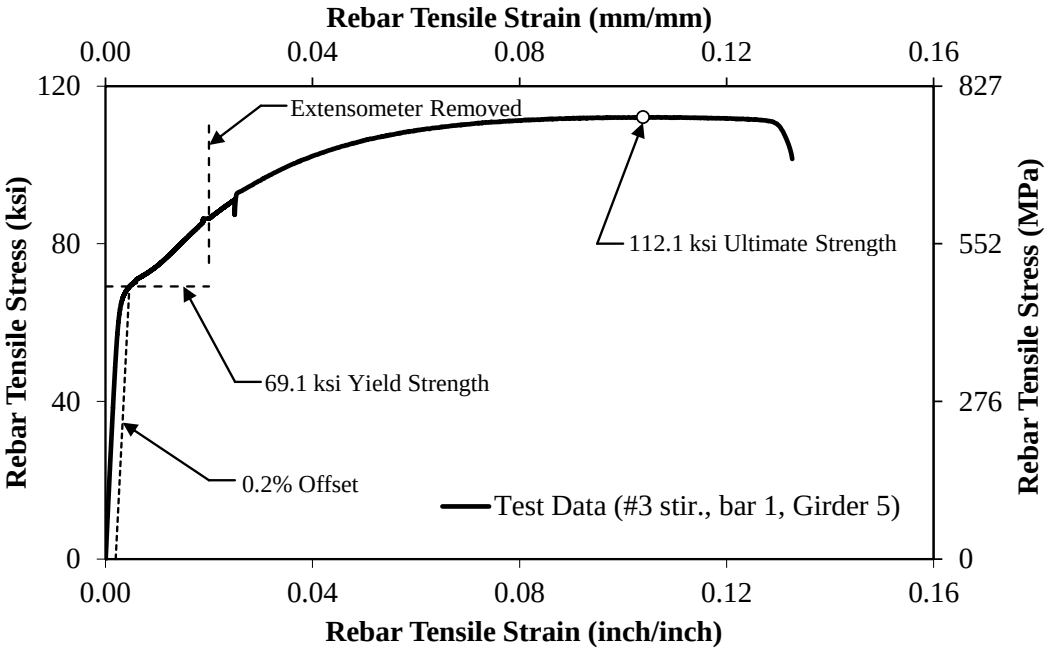

Source: FHWA.
1 ksi = 6.89 MPa.
1 inch/inch = 1 mm/mm.

Figure 194. Graph. Measured stress–strain relationship for #3 stirrup reinforcing bar for girder design 5—coupon 1.

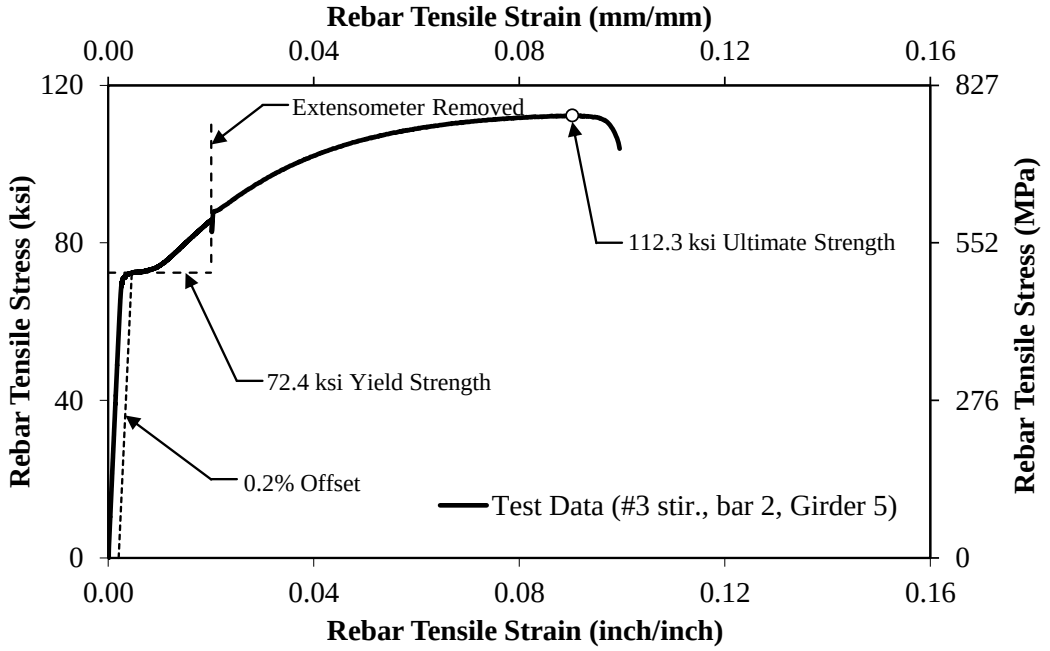

Source: FHWA.
1 ksi = 6.89 MPa.
1 inch/inch = 1 mm/mm.

Figure 195. Graph. Measured stress–strain relationship for #3 stirrup reinforcing bar for girder design 5—coupon 2.

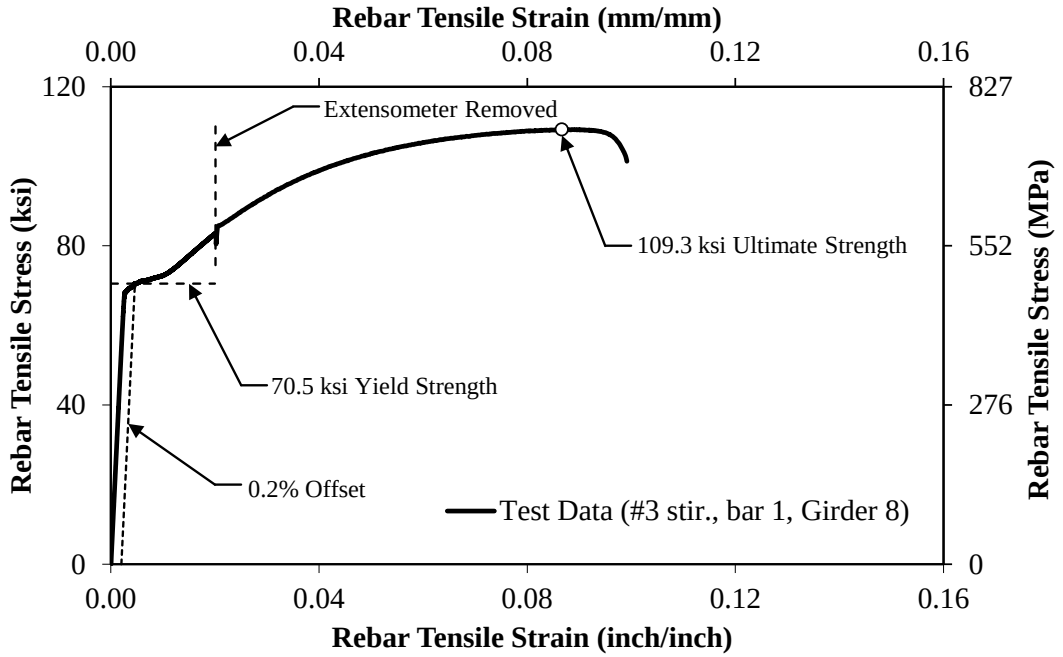

Source: FHWA.
1 ksi = 6.89 MPa.
1 inch/inch = 1 mm/mm.

Figure 196. Graph. Measured stress–strain relationship for #3 stirrup reinforcing bar for girder design 8—coupon 1.

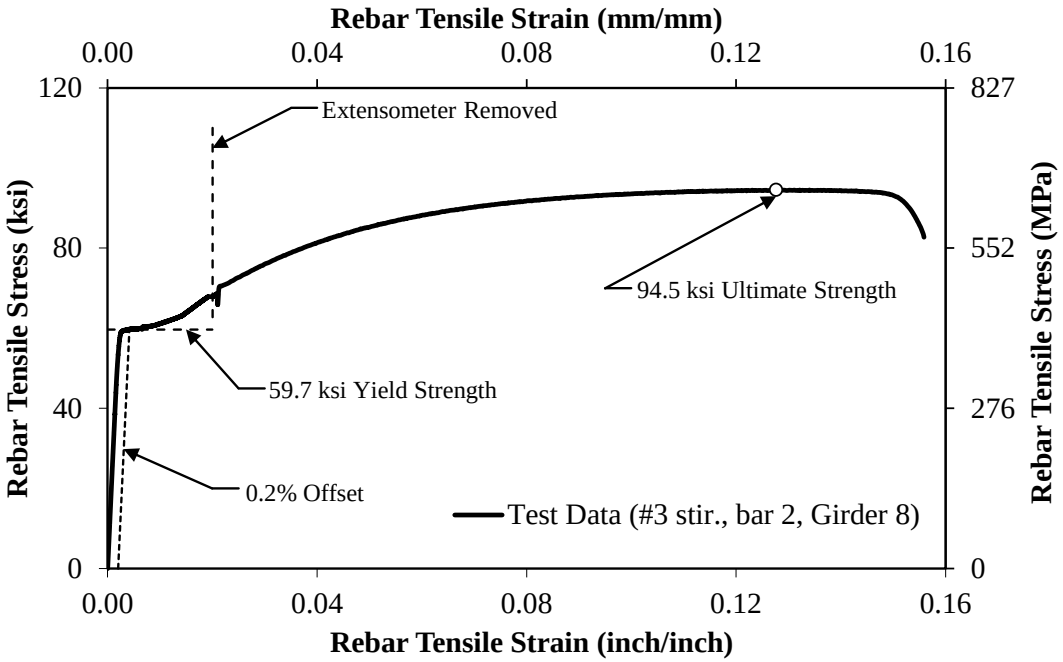

Source: FHWA.
1 ksi = 6.89 MPa.
1 inch/inch = 1 mm/mm.

Figure 197. Graph. Measured stress–strain relationship for #3 stirrup reinforcing bar for girder design 8—coupon 2.

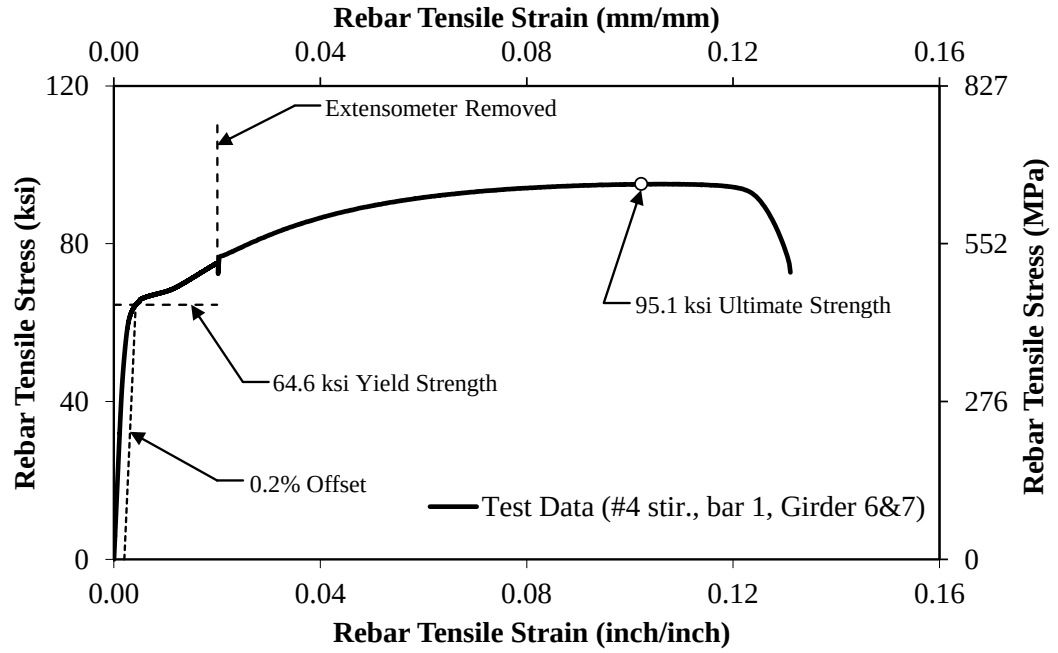

Source: FHWA.
1 ksi = 6.89 MPa.
1 inch/inch = 1 mm/mm.

Figure 198. Graph. Measured stress–strain relationship for #4 stirrup reinforcing bar for girder designs 6 and 7—coupon 1.

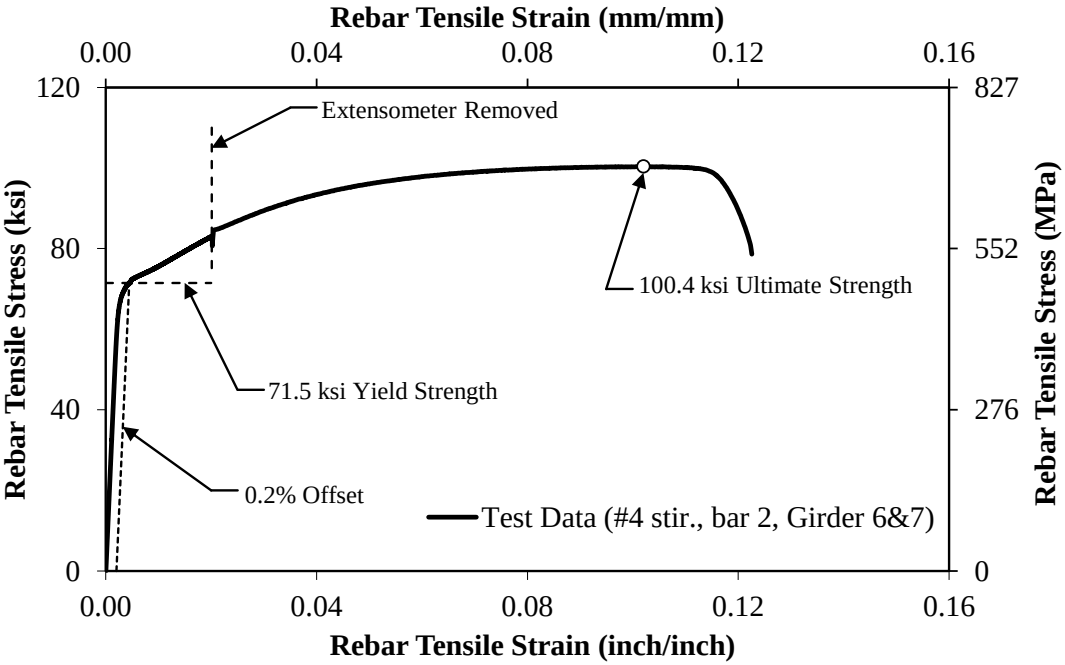

Source: FHWA.
1 ksi = 6.89 MPa.
1 inch/inch = 1 mm/mm.

Figure 199. Graph. Measured stress–strain relationship for #4 stirrup reinforcing bar for girder designs 6 and 7—coupon 2.

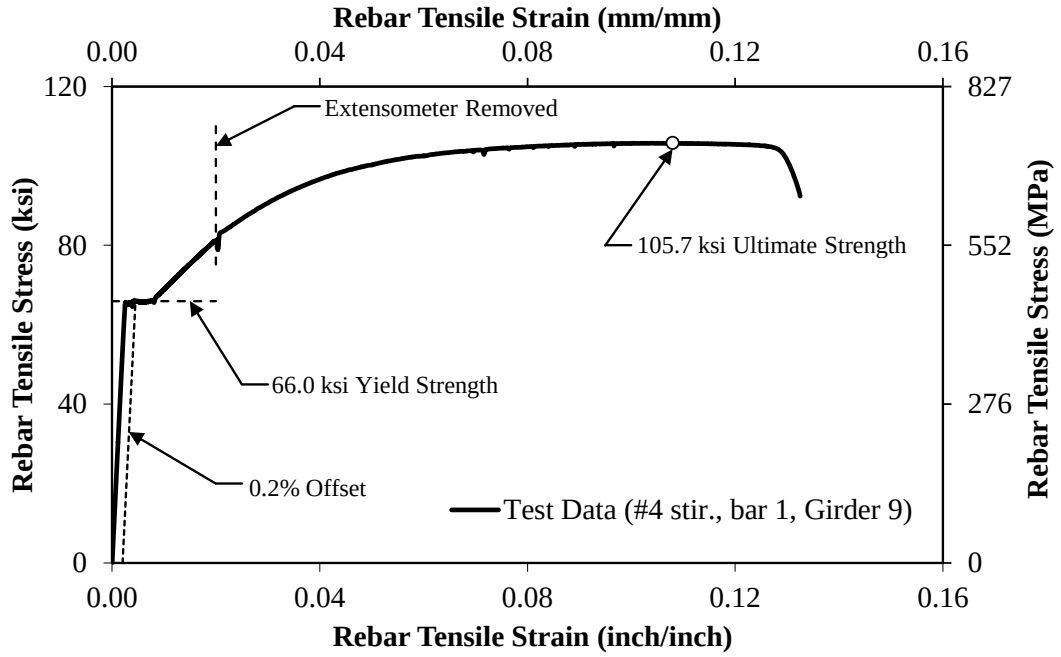

Source: FHWA.
1 ksi = 6.89 MPa.
1 inch/inch = 1 mm/mm.

Figure 200. Graph. Measured stress–strain relationship for #4 stirrup reinforcing bar for girder design 9—coupon 1.

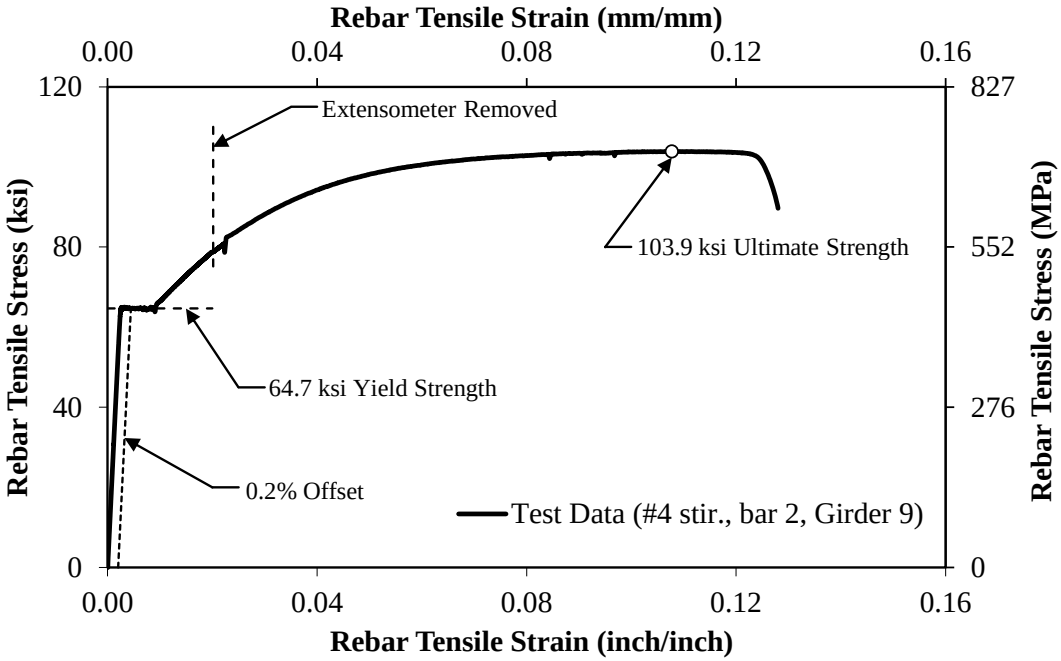

Source: FHWA.
1 ksi = 6.89 MPa.
1 inch/inch = 1 mm/mm.

Figure 201. Graph. Measured stress–strain relationship for #4 stirrup reinforcing bar for girder design 9—coupon 2.

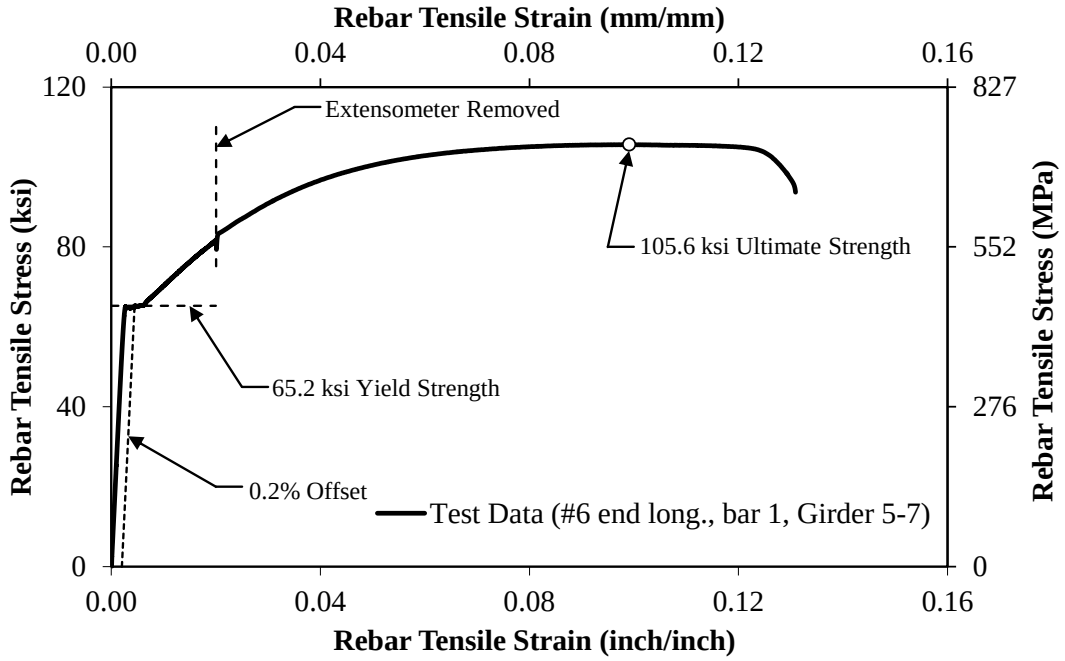

Source: FHWA.
1 ksi = 6.89 MPa.
1 inch/inch = 1 mm/mm.

Figure 202. Graph. Measured stress–strain relationship for #6 end longitudinal reinforcing bar for girder designs 5–7—coupon 1.

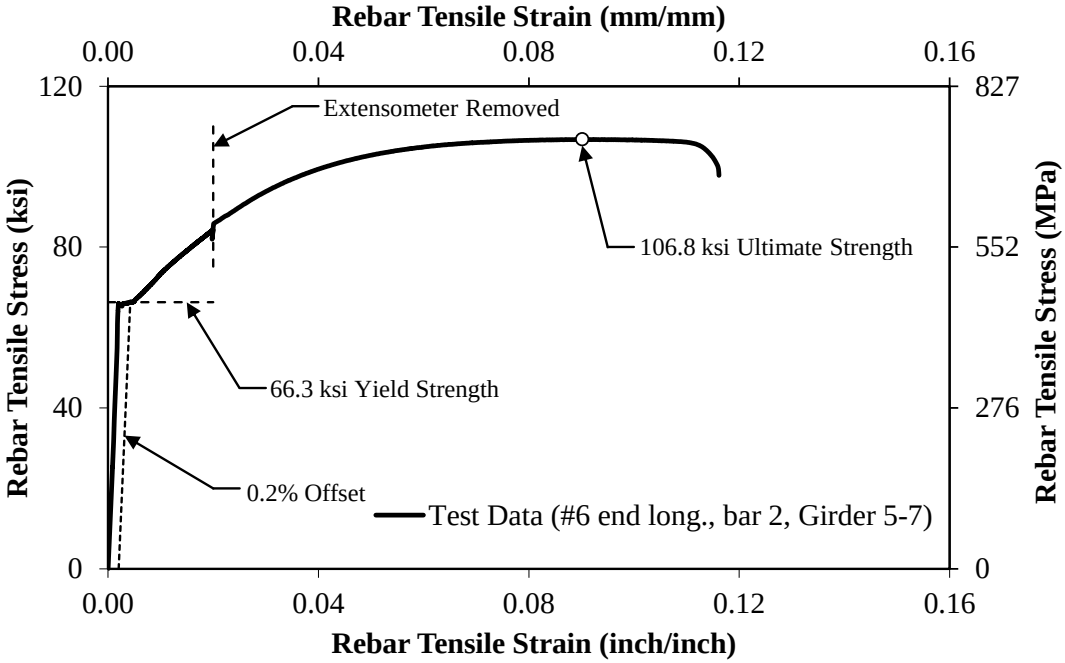

Source: FHWA.
1 ksi = 6.89 MPa.
1 inch/inch = 1 mm/mm.

Figure 203. Graph. Measured stress–strain relationship for #6 end longitudinal reinforcing bar for girder designs 5–7—coupon 2.

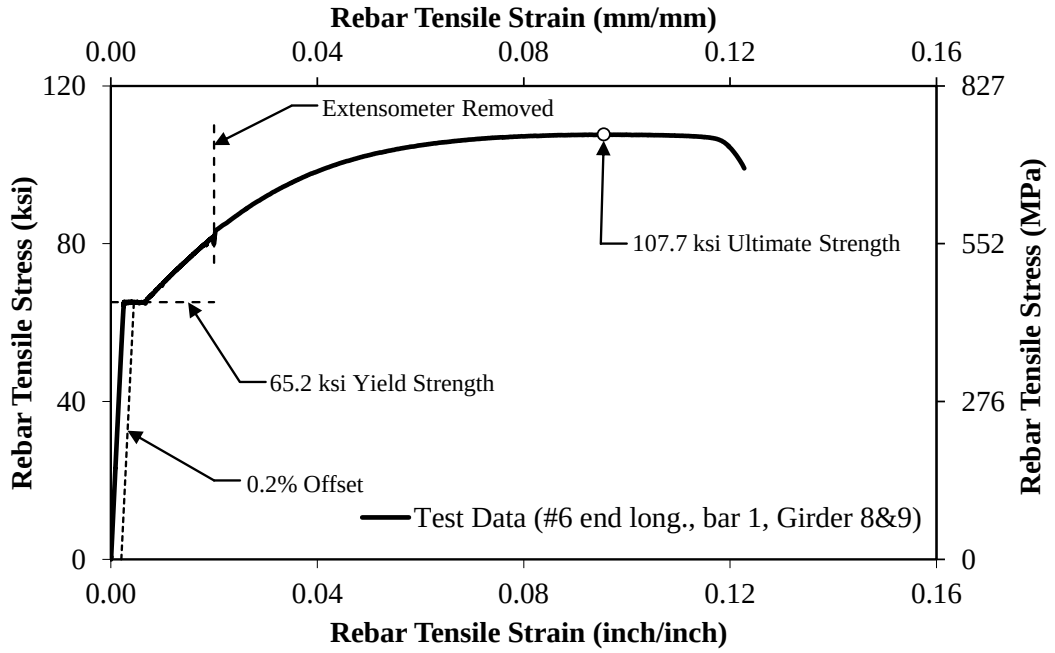

Source: FHWA.
1 ksi = 6.89 MPa.
1 inch/inch = 1 mm/mm.

Figure 204. Graph. Measured stress–strain relationship for #6 end longitudinal reinforcing bar for girder designs 8 and 9—coupon 1.

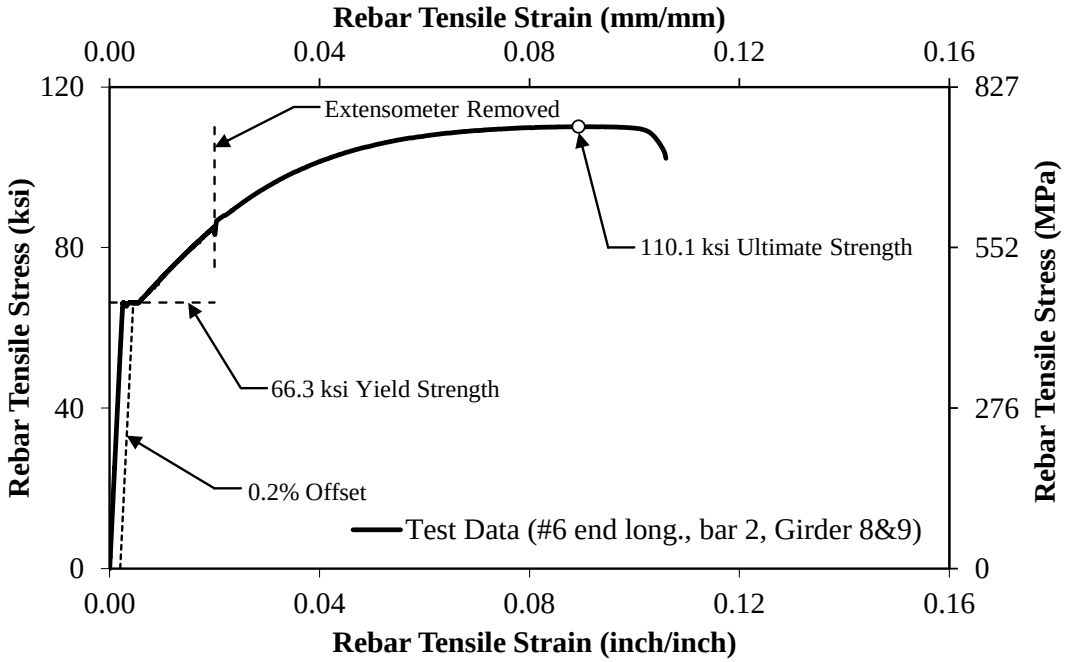

Source: FHWA.
1 ksi = 6.89 MPa.
1 inch/inch = 1 mm/mm.

Figure 205. Graph. Measured stress–strain relationship for #6 end longitudinal reinforcing bar for girder designs 8 and 9—coupon 2.

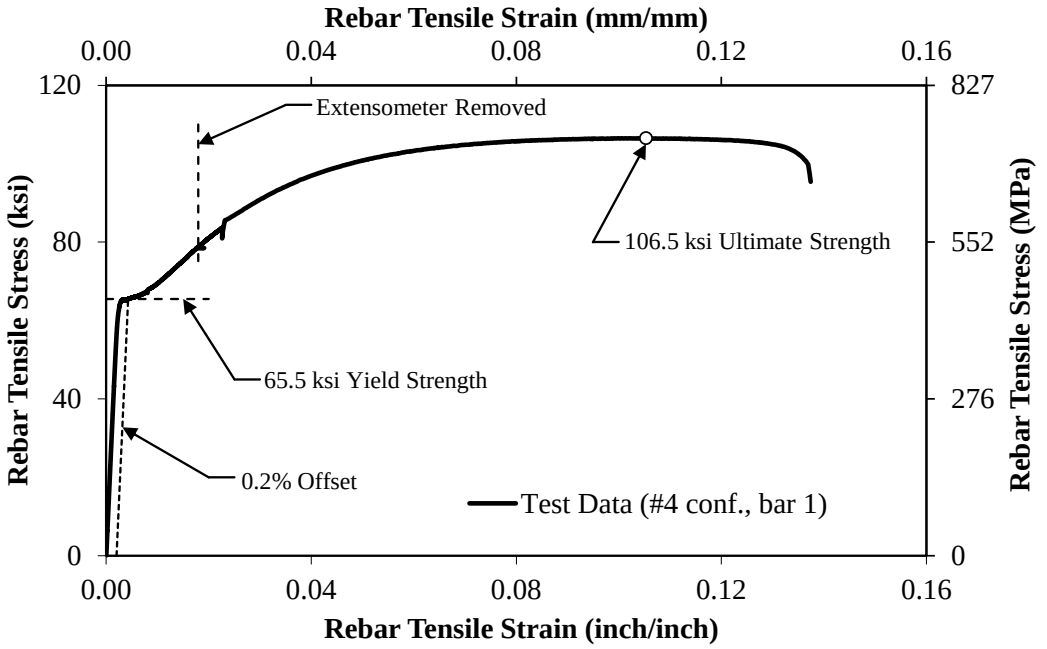

Source: FHWA.
1 ksi = 6.89 MPa.
1 inch/inch = 1 mm/mm.

Figure 206. Graph. Measured stress–strain relationship for #6 end confinement reinforcing bar for all girder designs—coupon 1.

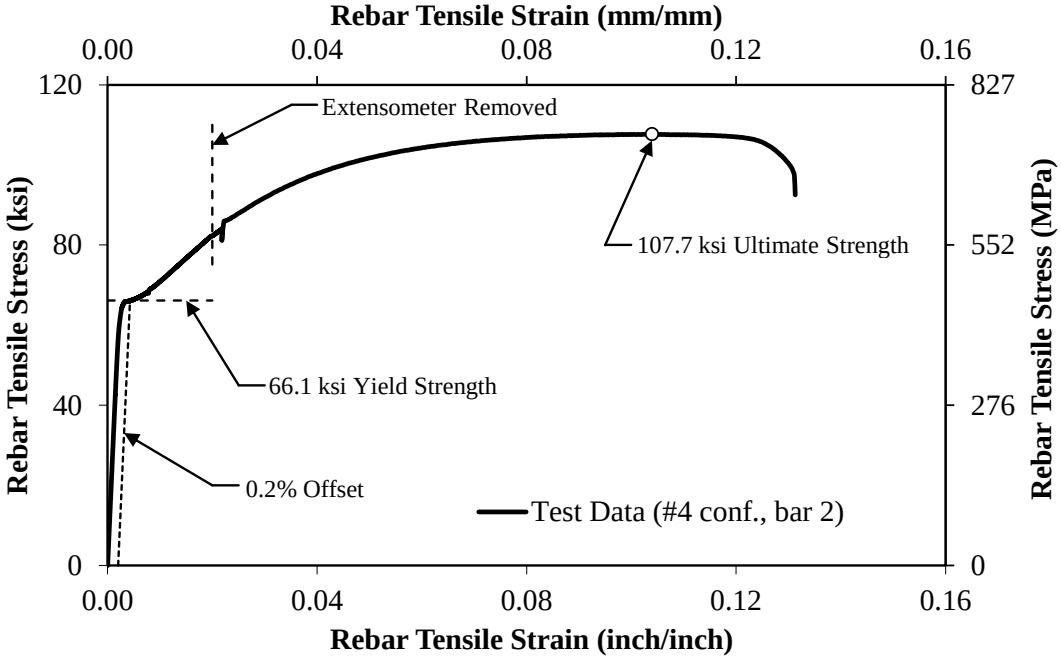

Source: FHWA.
1 ksi = 6.89 MPa.
1 inch/inch = 1 mm/mm.

Figure 207. Graph. Measured stress–strain relationship for #6 end confinement reinforcing bar for all girder designs—coupon 2.

APPENDIX B. LWC SPECIMENS IN TFHRC SHEAR DATABASE

This appendix contains a list of the LWC specimens in the TFHRC shear database (see table 59). These specimens include tests that failed in shear and tests that did not fail in shear.

Table 59. List of LWC shear test specimens in the TFHRC shear database.

Source*	Specimen Names
Ahmad, Xie, and Yu (1994)	LNN-1, LNN-2, LNN-3, LNW-1, LNW-2, LNW-3, LHN-1, LHN-2, LHN-3, LHW-1, LHW-2, LHW-3, LHW-3a, LHW-3b, LHW-4
Alrousan et al. (2011)	BL2.3C7.4, BL2.3C6.12, BL3.4C7.4, BL3.4C6.12, BL4.5C7.4, BL4.5C6.12
Brettle (1962)	MS5, MS6, MS6A, MS8, MS8A, MS15, MS16, MS9, MS9A, MS10, MS10A, MS10B, MS11, MS11A, MS11B, MS12, MS13, MS14, MS17, MS18
Clarke (1987)	1A, 1B, 2A, 2B, 3A, 3B, 4A, 4B, 5A, 5B, 6A, 6B, 9A, 9B, 10A, 10B, P1A, P1B, P2A, P2B, P5A, P5B, P6A, P6B, P7A, P7B, P8A, P8B, PUM 1A, PUM 1B, PUM 2A, PUM 2B, PUM 3A, PUM 3B, PUM 4A, PUM 4B, PUM 5A, PUM 6A, PUM 6B
Dymond, Roberts-Wollmann, and Cousins (2009)	Shear - Test 2, Flexure-Shear
EuroLightCon (2000)	VA05LWAC-active, VA05LWAC-passive, VA06LWAC-active, VA06LWAC-passive, VA07LWAC-active, VA07LWAC-passive, VA08LWAC-active, VA08LWAC-passive
Funahashi et al. (2002)	V1.8, V1.5, V1.2, V1.8d100, V1.5d100
Greene and Graybeal (2015)	A7L, B7L, C7L, A7D, C7D, B7D, A5D, B5D, C5D, A5L, B5L, C5L, A6D, B6D, C6D, A6L, B6L, C6L, C8D, A9L, C8L, A9D, B8D, A8D, B8L, A8L, B9L, C9L, B9D
Hamadi and Regan (1980a, 1980b)	LT-1, LT-2, LT-3, LT-4, LT-5, L1, L2, L3, L4, L5, S1, S2a, S2b, S3
Hanson (1958)	9C, 2A, 2B, 3A, 3B, 4A, 4B, 4C, 4D, 5A, 5B, 6A, 6B, 7A-x, 7A, 7B
Hanson (1961)	3A4, 4A4, 10A4, 2B4, 3B4, 4B4, 5B4, 6B4, 7B4, 10B4, 13B4, 10BW4, 2B2, 3B2, 4B2, 5B2, 6B2, 7B2, 10B2, 13B2, 2B3, 3B3, 4B3, 5B3, 6B3, 7B3, 10B3, 13B3, 7B1X, 10B1, 13B1
Hegger et al. (2005)	LWAC 1L, LWAC 1R, LWAC 2L, LWAC 2R, LWAC 3L, LWAC 3R, LWAC 4L, LWAC 4R, LWAC 5L, LWAC 5R, LWAC 6L, LWAC 6R, LWAC 7L, LWAC 7R
Hoff (1993)	LWC1-1, LWC1-2, LWC1-3, LWC2-1, LWC2-2, LWC2-3, HSLWC-1, HSLWC-2, HSLWC-3
Holste, Peterman, and Esmaeily (2011)	SCC #1
Ivey and Buth (1967)	1-1, 1-2, 1-3, 23-1, 23-2, 23-3, 23-1S, 23-2S, 23-3S, 27-1, 27-2, 27-3, 23-4, 23-5, 23-6, 23-7, 23-8, 23-9, 23-10, 23-11, 23-12, 23-13, 23-14, 23-15, 23-16, 23-17
Jindal (1966)	ALL-LW, ALL-LW, ALL-LW, SAND-LW, SAND-LW, SAND-LW
Kang et al. (2011)	LB-2, LB-3, LB-4
Kassner (2012)	T2.8.Typ.1, T2.8.Typ.2, T2.8.Min.1, T2.8.Min.2, BT.8.Typ.1, BT.8.Typ.2, BT.10.Typ.1, BT.10.Typ.2, BT.10.Min.1, BT.10.Min.2
Kawaguchi et al. (2000)	A1, A2, B1, B2, C1, C2, D1, D2, E
Meyer et al. (2002)	G1A-E, G1A-W, G1A-C, G1B-E, G1B-W, G1B-C, G1C-E, G1C-W, G1C-C, G2A-E, G2A-W, G2A-C, G2B-E, G2B-W, G2B-C, G2C-E, G2C-W, G2C-C
Murayama and Iwabuchi (1986)	B1, M1, BS1, BS2, BS3, BS4, BS5, BL1, BL2, BL3, BL4

Source*	Specimen Names
Nishibayashi, Kobayashi, and Yoshioka (1968)	L-3-16-10, L-3-D16-5, L-3-D16-10, L-3-13-0, L-3-D13-0, L-3-16-0, L-3-D16-0, L-4-13-0, L-4-D13-0, L-4-16-0, L-4-D16-0, P-3.5-D16-A, P-3.5-D16-B, P-3.5-D16-C, P-3.5-D13-A, P-3.5-D13-B, P-3.5-D13-C, P-4.5-D16-A, P-4.5-D16-B, P-4.5-D16-C, P-3.5-0-A, P-4.5-0-A
Peterman, Ramirez, and Okel (1999)	7k,SLW-FWC - 1S, 7k,SLW-FWC - 1L, 7k,SLW-FWC - 2S, 7k, SLW-FWC - 2L, 7k,SLW-FWC - 3S, 7k,SLW-FWC - 3L, 7k,SLW-IST - 1S, 7k,SLW-IST - 1L, 7k,SLW-IST - 2S, 7k,SLW-IST - 2L, 7k,SLW-IST - 3S, 7k,SLW-IST - 3L, 10k,SLW-IST - 1S, 10k,SLW-IST - 1L, 10k, SLW-IST - 2S, 10k,SLW-IST - 2L, 10k,SLW-IST - 3S, 10k,SLW-IST - 3L
Ramirez et al. (2000)	LWLA, LWLB, LWLC, LWLD, LWLHD, PC6N, PC6S, PC10N, PC10S
Richart and Jensen (1930)	1-1.75-2.25-A, 1-1.75-2.25-B, 1-2.25-2.75-A, 1-2.25-2.75-B, 1-2.25-2.75-A, 1-2.25-2.75-B, 1-2.25-2.75-A, 1-2.25-2.75-B, 1-2.25-2.75-A, 1-2.25-2.75-B, 1-2.75-3.25-A, 1-2.75-3.25-B, 1-2.25-2.75-A, 1-2.25-2.75-B, 1-2.25-2.75-A, 1-2.25-2.75-B, 1-2.75-3.25-A, 1-2.75-3.25-B
Ritthichauy et al. (2001)	ASL1, ASL2, ASL3, ASL4, SML1, SML2, ML1, ML2, ML3, ML4, TL1, TL2, TL3, TL4
Salandra and Ahmad (1989)	HR-NS-2.59, HR-NS-3.63, LR-NS-2.59, LR-NS-3.63
Swamy, Jones, and Chiam (1993)	1TL-2, 1TL-3, 2TL-2, 2TL-3, 3TL-2, 3TL-3
Tang, Yen, and Chen (2009)	LH3, LH4, LM3, LM4, LN3, LN4
Taylor and Brewer (1963)	B1, B10, B11, B12, B2, B3, B4, B5, B6, B7, B8, B9, C1, C10, C11, C12, C2, C3, C4, C5, C6, C7, C8, C9
Thorenfeldt and Drangsholt (1990)	B33, B34, B35
Thorenfeldt and Stemland (1995)	S1-B1, S1-B10, S1-B11, S1-B2, S1-B3, S1-B4, S1-B5, S1-B7, S1-B9, S2-B1, S2-B2, S2-B3, S2-B4, S2-B5
Thorenfeldt and Stemland (2000)	B2, B3, B5, B6, B8, B9
Thorenfeldt, Stemland, and Tomaszewicz (1995)	S3-B1, S3-B2
Walraven and Al-Zubi (1995)	Ae30H, Lg30h, Lg60h, Lg60m, Lr30h
Watanabe et al. (2003)	L1-0, L1-8, L2-0, L2-8, L3-0, L3-8, L3-16
Yang et al. (2011)	A-13, A-19, A-4, A-8, S-13, S-19, S-4, S-8

*Refer to the LWC Sources for TFHRC Shear Database section in the Bibliography for source information.

APPENDIX C. NWC SPECIMENS IN ACI-DAFSTB DATABASE

To determine the effect of LWC on shear resistance, the LWC specimens in the TFHRC shear database were compared to a subset of NWC specimens in the ACI-DafStb database that had similar parameters that were significant to shear resistance. This appendix contains a list of those selected specimens from the ACI-DafStb database that were compared to the TFHRC shear database (see table 60 through table 63).

Table 60. Selected NWC shear test specimens from the ACI-DafStb database—RC members without shear reinforcement.

Source*	Specimen Name
Adebar (1989)	ST1, ST2, ST3, ST8, ST16, ST23
Ahmad, Khaloo, and Poveda (1986)	A1, A2, A3, A7, A8, B1, B2, B3, B7, B8, B9, C1, C2, C3, C7, C8, C9
Ahmad, Park, and El-Dash (1995)	B7N, B7H, B8H
Al-Alusi (1957)	12, 11, 2, 21, 15, 10, 4, 13, 18, 7, 24, 16, 17, 8, 19, 25, 9, 20, 14, 23
Angelakos, Bentz, and Collins (2001)	DB0530, DB120, DB130, DB140, DB165, DB180, DB230
Aster and Koch (1974)	2, 3, 11, 12, 16
Bentz and Buckley (2005)	AT-2 (250A), AT-2 (250B), AT-2 (1000A), AT-2 (1000B), AT-2 (3000), AT-3 (A), AT-3 (C), AT-3 (B), AT-3 (D)
Bernander (1957)	A1, A2, A3, A4, A5, A6
Bernhardt and Fynboe (1986)	S6A, S6C, S9A, S9B
Bhal (1968)	B1, B2, B3, B5, B6, B7, B8
Bresler and Scordelis (1963)	0A-1, 0A-2, 0A-3
Cederwall, Hedman, and Losberg (1970, 1974)	734-34
Chana (1981)	2.1, 2.2, 2.3, 3.1, 3.2, 3.3, D1, D2, D3, 4.1, 4.2, 4.3, 4.4
Chang and Kesler (1958)	IA1, IB1, IC1, IC2, IIB1, IIC1, IIIA1, 4-21a, 4-22a, 4-23a, 4-23b, 5-21a, 5-21b, 5-22a, 5-22b, 5-23a, 5-23b
Cladera and Marí (2002)	H 50/1, H 50/5, H 60/1, H 75/1, H 100/1, H 100/5
Collins and Kuchma (1999)	B100, B100B, B100L, B100-R, B100L-R, BRL100
Diaz de Cossio and Siess (1960)	A-2, A-3, A-12, A-13, A-14
Drangsholt and Thorenfeldt (1992)	B11, B13, B14, B21, B23, B24, B43, B44, B61, B63, B64
Elzanaty et al. (1986)	F11, F12, F8, F13, F14, F1, F2, F10, F9, F15, F6
Feldman and Siess (1955)	L-2, L-2A, L-3, L-4, L-5, L-6, L2R, L2aR, L3R
Ferguson and Thompson (1953)	A1, A2, A3, A4, A5, A6, D1, D2, N1, N2, N3, G4, G5, G6, B1, B2, B3, B4, B5, C1, C2, L1, L2, L3
Ferguson (1956)	F2
Ghannoum (1998)	N155 (N), N155 (S), N220 (N), N220 (S), N350 (N), N350 (S), N485 (N), N485 (S), N960 (N), N960 (S), H90 (N), H90 (S), H155 (N), H155 (S), H220 (N), H220 (S), H350 (N), H350 (S), H485 (N), H485 (S), H960 (N), H960 (S)
Grimm (1996/1997)	S 1.1, S 1.2, S 1.3, S 2.2, S 2.4, S 3.2, S 3.4
Haddadin, Hong, and Mattock (1971)	A1, C1, E1, J1
Hallgren (1994)	B90SB5-2-33, B90SB6-2-33, B90SB9-2-31, B90SB10-2-31, B90SB13-2-86, B90SB14-2-86, B90SB17-2-45, B90SB18-2-45, B90SB21-2-85, B90SB22-2-85, B91SC1-2-62, B91SC2-2-62, B91SC3-2-69, B91SC4-2-69,

Source*	Specimen Name
	B91SD1-4-61, B91SD2-4-61, B91SD3-4-66, B91SD4-4-66, B91SD5-4-58, B91SD6-4-58
Hallgren (1996)	B3, B4, B5, B7
Hamadi (1976)	G1, G2, G4a, G4b
Hanson (1958)	8A-X, 8A, 8B, 8C, 8D
Hanson (1961)	8A4, 8B4, 8BW4, 8B2, 8B3
Hanson (1958)	M100-S0, M80-S0, M60-S0, M40-S0, M25-S0
Johnson and Ramirez (1989)	6
Kani (1967)	40, 41, 43, 44, 47, 48, 52, 55, 56, 57, 58, 59, 60, 81, 82, 83, 84, 91, 92, 93, 95, 96, 97, 98, 99, 63, 64, 65, 66, 68, 71, 74, 75, 76, 79, 271, 272, 273, 274
Kani, Huggins, and Wittkopp (1979)	266, 268, 179, 143, 149, 150, 151, 152, 153, 103, 105, 106, 111, 112, 115, 116, 163, 163', 166, 166', 121, 122, 123, 124, 126, 128, 130, 131, 132, 133, 27, 28, 29, 30, 31, 32, 33, 34, 35, 36, 182, 186, 187, 191, 193, 194, 195, 196, 197, 202, 206, 207, 208, 209, 210, 211, 212, 213, 214, 215, 216, 709, 666, 675, 718, 742, 744, 746, 502, 504
Kawano and Watanabe (1998)	A-1a, A-1b, A-2a, A-2b, A-3a, A-3b
Kim and Park (1994)	CTL-1, CTL-2, P1.0-1, P1.0-2, P3.4-1, P3.4-2, P4.6-1, P4.6-2, A4.5-1, A4.5-2, A6.0-1, A6.0-2, D142-1, D142-2, D550-1, D550-2, D915-1, D915-2
Krefeld and Thurston (1966)	11A2, 12A2, 18A2, 18B2, 18C2, 18D2, 13A2, 14A2, 15A2, 15B2, 16A2, 17A2, 18E2, 19A2, 20A2, 21A2, 1AC, 2AC, 3AC, 4AC, 5AC, 6AC, 2CC, 3CC, 4CC, 5CC, 6CC, 3GC, 6C, 3AAC, 4AAC, 5AAC, 6AAC, 3AC, 4AC, 5AC, 6AC, 4CC, 5CC, 6CC, 4EC, 5EC, 6EC, 4AAC, 5AAC, 3AC, 5AC, 4CC, 5CC, C, PCA, PCB, OCA, OCB, OCA, OCB
Krefeld and Thurston (1966)	B, C, D, E, F, D-1, E-1
Kuhlmann and Ehmann (2001)	A6-L, A6-R
Kuhlmann et al. (2002)	B1/l, B1/r, C3, C6
Kulkarni and Shah (1998)	B4JL25-S, B3OC25-S, B4JL20-S, B3SE03-S, B3DE03-S, B3NO15-S, B3NO30-S, B3NO30-H
Lambotte and Taerwe (1990)	NS-0.48, NS-0.97, NS-1.45, HS-0.97, HS-1.45
Laupa, Siess, and Newmark (1953)	S2, S3, S4, S5, S11, S13
Leonhardt and Walther (1962a, 1962b, 1962c, 1962d, 1962e)	P4, P6, P7, P9, 4l, 4r, 5l, 5r, 6l, 6r, 7-1, 7-2, 8-1, 8-2, EA1, EA2, D1/1, D1/2, D2/1, D2/2, D3/1, D3/2l, D3/2r, D4/1, D4/2l, D4/2r, C1, C2, C3, C4, E6
Leonhardt and Walther (1962a)	AT-1
Marti, Pralong, and Thürlimann (1977)	PS6, PS11
Maruyama and Rizkalla (1988)	RS1-0
Mathey and Watstein (1963)	IIIa-17, IIIa-18, Va-19, Va-20, VIb-21, VIb-22, VIb-23, VIa-24, VIa-25
Moayer and Regan (1974)	P41
Moayer and Regan (1974), Moody, et al. (1954, 1955a, 1955b)	A1, A2, A3, A4, B1, B2, B3, B4, 1, 2, 3, 4, 5, 6, 7, 9, 10, 11, 12, 13, 14, 15, 16
Morrow and Viest (1957)	B40 B4, B56 B2, B56 A4, B56 B4, B56 E4, B56 A6, B56 B6, B70 B2, B70 A4, B70 A6, B84 B4, B113 B4
Mphonde and Frantz (1984)	AO-3-3b, AO-3-3c, AO-7-3a, AO-7-3b, AO-11-3a, AO-11-3b, AO-15-3a, AO-15-3c, AO-3-2, AO-7-2, AO-11-2, AO-15-2a, AO-15-2b
Podgorniak-Stanik (1998)	BRL100, BN100, BN50, BN25
Rajagopalan and Ferguson (1968)	S-13, S-1, S-2, S-3, S-4, S-5, S-9, S-6, S-7, S-12
Regan (1971a, 1971b, 1971c)	R1, R2, R3, R7, R29, K3, N1, N2

Source*	Specimen Name
Reineck, Koch, and Schlaich (1978)	N6, N7, N8
Regan (1971a)	2, 3, 5, 6
Rosenbusch and Teutsch (2002)	1.2 / 1, 2.3 / 1, 2.4 / 1, 2.6 / 1
Rüsch, Haugli, and Mayer (1962)	X, Y, Z
Salandra and Ahmad (1989)	LR-2.59-NS, LR-3.63-NS, HR-2.59-NS, HR-3.63-NS
Scholz (1994)	A-2, B-2, B-3, C-2, C-3
Shin et al. (1999)	MHB 2.5-0, HB 2.5-0
Shin et al. (1999)	1A, 2A, 5A, 1B, 2B, 3B, 5B
Taylor (1972)	A1, A2, B1, B2, B3
Walraven (1978)	A1, A2, A3
Xie et al. (1994)	NNN-3
Yoon, Cook, and Mitchell (1996)	N1-S, M1-S, H1-S

*Refer to the NWC Sources for ACI-DafStb Database section in the Bibliography for source information.

Table 61. Selected NWC shear test specimens from the ACI-DafStb database—RC members with shear reinforcement.

Source*	Specimen Name
Angelakos (1999)	DB120M
Bernhardt and Fynboe (1986)	S7 A, S7 B, S8 A, S8 B
Bhal (1968)	B1S, B2S, B3S
Caflisch and Thürlimann (1970a, 1970b)	A0L
Cederwall, Hedman, and Losberg (1970)	H 50/3, H 50/4, H 60/2, H 60/3, H 60/4, H 75/2, H 75/4, H 100/2, H 100/3, H 100/4
Hamadi (1976)	GT-1, GT-2, GT-4
Kong and Rangan (1997)	S1-3, S1-4, S2-3, S2-4, S3-3, S3-4, S4-1, S4-4, S4-6, S5-1, S5-3, S7-3, S7-4
Krefeld and Thurston (1966)	26-1, 29c-2, 29g-2, 318-1, 321-1, 313.5-2, 39-3
Leonhardt and Walther (1962a, 1962b, 1962c, 1962d, 1962e)	ET2, ET3, ET4, T1 (r)
Leonhardt and Walther (1963)	TA11, TA12, TA14, TA15, TA16
Levi and Marro (1989, 1993)	RC 30 A1, RC 30 A2, RC 60 A1, RC 60 A2, RC 60 B1, RC 60 B2, RC 70 B1
Lyngberg (1974)	5A-0, 5B-0
Moayer and Regan (1974)	P20
Özden (1967)	T6, T7, T9, T10, T15
Palaskas, Attiogbe, and Darwin (1981)	A50, A50A, A75, B50, C50, C75
Özden (1967)	V1, VL1
Quast (1999)	1/1
Regan (1971a, 1971b, 1971c)	T3, T4, T6, T7, T8, T9, T13, T15, T17, T19, T20, T26, T32, T34, T35, T37, T38, W1, W5
Reineck (1991)	Stb III, Stb I
Roller and Russel (1990)	7
Shin et al. (1999)	MHB 2.5-25, HB 2.5-50
Soerensen (1974)	T-21, T-22, T-23
Stroband (1997)	2, 3
Yoon, Cook, and Mitchell (1996)	N2-N, M2-N, H2-N

*Refer to the NWC Sources for ACI-DafStb Database section in the Bibliography for source information.

Table 62. Selected NWC shear test specimens from the ACI-DafStb database—PC members without shear reinforcement.

Source*	Specimen Name
Arthur (1965)	A2, B1, B2, B3, B5, B8, B9, B11, D1, D2, E1, E2
Cederwall, Hedman, and Losberg (1970)	6, 7, 8, 9, 10, 11, 12, 13
Cederwall, Hedman, and Losberg (1974)	734-35, 734-36, 734-41, 734-42, 824-1A, 824-2A, 803-1, 803-2, 842-2, 842-3, 842-4, 842-5
Elzanaty, Nilson, and Slate (1985)	CW4, CI4, CW1, CW3, CW2, CW5, CW7, CW6, CW9, CW8, CI1, CI3, CI2, CI5, CI7, CI6, CI9, CI8
MacGregor (1958)	M15, M16
Mahgoub (1975)	A1, A6, A12, C4, C11, E1, E4, E6, G6
Olesen, Sozen, and Siess (1967)	AD1437, B1023, B1024, B1434, B1441, BD1418, BD1419, BD1423, BD1426, BD1427, BD1428, BD1434, BD1435, BD1442, BD2432
Sozen, Zwoyer, and Siess (1959)	A1231, A1253, A1256, B1120, B1129, B1140, B1210, B1226, B1229, B1234, B1235, B1250, B1261, B1316, B1326, B1341, B2126, B2209, B2223, B2230, B2241, B2268
Zwoyer (1953)	S-33, S-34

*Refer to the NWC Sources for ACI-DafStb Database section in the Bibliography for source information.

Table 63. Selected NWC shear test specimens from the ACI-DafStb database—PC members with shear reinforcement.

Source*	Specimen Name
Cederwall, Hedman, and Losberg (1970)	15, 18
Cederwall, Hedman, and Losberg (1974)	842-6
Cumming, Shield, and French (1998)	IA, IB
Elzanaty, Nilson, and Slate (1985)	CW10, CW11, CW12, CW13, CW14, CW15, CW16, CW17
Hanson and Hulsbos (1964)	F8A, F9A, F11A, F12A, F13A, F19A
Hegger et al. (2003)	NSC 1R, NSC 2L, NSC 2R
Hegger et al. (2001)	SVB 4a
Levi and Marro (1989)	PC 30A1, PC 30A2, PC 60A1, PC 60A2, PC 60B1, PC 60B2
Olesen, Sozen, and Siess (1967)	BW1434, BW1439

*Refer to the NWC Sources for ACI-DafStb Database section in the Bibliography for source information.

APPENDIX D. EQUATION DERIVATIONS FOR RELIABILITY ANALYSIS

This appendix contains derivations of the equations used in the reliability analysis. The first section contains the derivations of expressions for the unfactored load effects and the mean load effects. The second section contains the derivations of expressions for the variation of the unfactored load effects and resistance.

UNFACTORED LOAD EFFECTS AND MEAN LOAD EFFECTS

The load effects due to dead load and vehicular live load are considered in the reliability analysis in this report. The load effects include the dead load of structural components (Q_{DC}), the dead load of the wearing surface (Q_{DW}), the vehicular live load (Q_{LL}), and the dynamic load allowance (Q_{IM}). The *AASHTO LRFD Bridge Design Specifications* applies different load factors to these load effects.[3] Also, the statistical parameters are different for these load affects, so an expression is needed to determine the individual unfactored load effects given the total factored load effects (Q).

The term r_Q is defined as the ratio of the unfactored permanent loads (i.e., Q_{DC} and Q_{DW}) to the total unfactored force effect (ΣQ_i) (see equation 65). The term r_{DW} is defined as the ratio of Q_{DW} to Q_{DC} (see equation 66). Equation 64 relates ΣQ_i to Q. This section shows the derivations of expressions for the unfactored load effects that are functions of only the load factors (γ_i), the r_Q term, the r_{DW} term, and ΣQ_i.

Q_{DW} for the load effects due to dead load of the wearing surface is removed from the definition of r_Q (see equation 82). The definition of r_{DW} given by equation 66 is substituted for Q_{DW} in the definition for r_Q in equation 65. The expression is then simplified.

$$r_Q = \frac{Q_{DC} + Q_{DW}}{\Sigma Q_i} = \frac{Q_{DC} + r_{DW} Q_{DC}}{\Sigma Q_i} = \frac{Q_{DC}(1 + r_{DW})}{\Sigma Q_i} \tag{82}$$

The expression for Q_{DC} given by equation 83 is obtained by rearranging equation 82 as follows:

$$Q_{DC} = \frac{r_Q \Sigma Q_i}{(1 + r_{DW})} \tag{83}$$

The expression for Q_{DC} given by equation 83 is then substituted into the definition of r_{DW} given by equation 66 to obtain the expression for Q_{DW} given by equation 84 as follows:

$$Q_{DW} = r_{DW} Q_{DC} = \frac{r_{DW} r_Q \Sigma Q_i}{(1 + r_{DW})} \tag{84}$$

The derivation of the expression for Q_{LL+IM} requires several steps. In the expression for r_Q given by equation 65, ΣQ_i is multiplied by both sides to obtain equation 85. ΣQ_i is subtracted from both sides of equation 85 to obtain equation 86. In equation 87, ΣQ_i on the right-hand side is replaced by the expression for ΣQ_i given by equation 54. The expression is then simplified to give equation 88 and simplified further to give equation 89.

$$r_Q \Sigma Q_i = Q_{DC} + Q_{DW} \tag{85}$$

$$r_Q \Sigma Q_i - \Sigma Q_i = Q_{DC} + Q_{DW} - \Sigma Q_i \tag{86}$$

$$r_Q \Sigma Q_i - \Sigma Q_i = Q_{DC} + Q_{DW} - \left(Q_{DC} + Q_{DW} + Q_{LL+IM}\right) \tag{87}$$

$$r_Q \Sigma Q_i - \Sigma Q_i = -Q_{LL+IM} \tag{88}$$

$$Q_{LL+IM} = \Sigma Q_i - r_Q \Sigma Q_i = \left(1 - r_Q\right) \Sigma Q_i \tag{89}$$

The expressions for Q_{DC}, Q_{DW}, and Q_{LL+IM} in equation 83, equation 84, and equation 89, respectively, are substituted into the expression for total factored loads given by equation 64 to obtain equation 90. The expression is simplified to obtain equation 91 and further simplified to obtain equation 92. The term in brackets is restated as equation 93 and is a function of only the load factors (γ_i), r_Q, and r_{DW}.

$$Q = \gamma_{DC} \left(\frac{r_Q}{1 + r_{DW}}\right) \Sigma Q_i + \gamma_{DW} \left(\frac{r_{DW} r_Q}{1 + r_{DW}}\right) \Sigma Q_i + \gamma_{LL+IM} \left(1 - r_Q\right) \Sigma Q_i \tag{90}$$

$$Q = \Sigma Q_i \left[\gamma_{DC} \left(\frac{r_Q}{1 + r_{DW}}\right) + \gamma_{DW} \left(\frac{r_{DW} r_Q}{1 + r_{DW}}\right) + \gamma_{LL+IM} \left(1 - r_Q\right)\right] \tag{91}$$

$$Q = \Sigma Q_i \left[\left(\frac{r_Q}{1 + r_{DW}}\right) \left(\gamma_{DC} + \gamma_{DW} r_{DW}\right) + \gamma_{LL+IM} \left(1 - r_Q\right)\right] \tag{92}$$

$$f\left(\gamma_i, r_Q, r_{DW}\right) = \left[\left(\frac{r_Q}{1 + r_{DW}}\right) \left(\gamma_{DC} + \gamma_{DW} r_Q\right) + \gamma_{LL+IM} \left(1 - r_Q\right)\right] \tag{93}$$

The expression for vehicular live load effects given by equation 70 can be simplified as shown in equation 94. The expression for unfactored load effects given by equation 54 is substituted into the definition of mean load effects given by equation 56. The separation of the vehicular live load effects and the dynamic load allowance (*IM*) given by equation 94 are included to obtain equation 95 for the mean load effects.

$$Q_{LL+IM} = Q_{LL} \left(1 + IM\right) = Q_{LL} + Q_{LL} IM \tag{94}$$

$$m_Q = \Sigma \left(Q_i \lambda_i\right) = Q_{DC} \lambda_{DC} + Q_{DW} \lambda_{DW} + Q_{LL} \lambda_{LL} + \left(Q_{LL} IM\right) \lambda_{IM} \tag{95}$$

VARIATION OF UNFACTORED LOAD EFFECTS AND RESISTANCES

COV is defined as the ratio of the standard deviation to the mean value. The variation is the COV squared. The standard deviation of an unfactored load effect (σ_{Qi}) is then equal to the COV of the unfactored load effect (V_{Qi}) multiplied by the mean of the load effect (m_{Qi}), as given by equation 96. The definition of the bias factor for the load effects (λ_{Qi}) given by equation 56 is also included in equation 96. The variation of the total load effects is then the sum of the squares

of the standard deviation of the unfactored load effects, as given by equation 97. The individual load effects are substituted into equation 97 to obtain equation 98.

$$\sigma_{Qi} = V_{Qi} m_{Qi} = V_{Qi}\left(Q_i \lambda_{Qi}\right) \tag{96}$$

$$\sigma_Q{}^2 = \Sigma\left(\sigma_{Qi}{}^2\right) = \Sigma\left[V_{Qi}\left(Q_i \lambda_{Qi}\right)\right]^2 \tag{97}$$

$$\sigma_Q{}^2 = \left(V_{DC} Q_{DC} \lambda_{DC}\right)^2 + \left(V_{DW} Q_{DW} \lambda_{DW}\right)^2 + \left(V_{LL} Q_{LL} \lambda_{LL}\right)^2 + \left(V_{IM} Q_{IM} IM \lambda_{IM}\right)^2 \tag{98}$$

The variation in the resistance ($\sigma_R{}^2$) is due to the combined uncertainty in the fabrication and materials and the uncertainty in the analysis. The expression for $\sigma_R{}^2$ is given by equation 99 and COV of the combined fabrication and materials uncertainty (V_{FM}).

$$\sigma_R{}^2 = m_R{}^2 V_R{}^2 = m_R{}^2\left(V_{FM}{}^2 + V_P{}^2\right) \tag{99}$$

APPENDIX E. STATISTICAL PARAMETERS FOR EXCLUDED TESTS

The reliability analysis performed as part of the analysis described in this report excluded 15 shear tests from the TFHRC shear database. The tests were removed for the determination of the statistical parameters for the uncertainty in the analysis (i.e., λ_P and V_P). This appendix provides the bias, COV, and CDF with the 11 shear tests included.

A total of 11 tests were removed from the databases of RC specimens without stirrups (4 tests) and PC without stirrups (7 tests). For each specimen type, all the tests from only one reference were removed because they had a tested shear strength that was considerably lower than the shear strength of specimens with a similar size and material strengths.

The bias and COV (i.e., λ_P and V_P) determined for each specimen type, concrete type, and calculation method is shown in table 64 for the 11 shear tests included. The bias and COV in table 64 can be compared to those in table 54 with the 11 tests excluded.

Table 64. Statistical parameters for professional factor determined using linear regression of the tail of the CDF for test-to-predicted resistance of all LWC specimens.

Concrete Type and Specimen Group	Design Expression	Number of Specimens	Bias	COV (Percent)
LWC RC specimens without A_v	Simplified-RC	173	1.63	24.5
LWC RC specimens without A_v	GP-equation	222	1.07	21.3
LWC RC specimens without A_v	Simplified-PC/RC	222	1.78	25.1
LWC RC specimens with A_v	Simplified-RC	31	1.63	21.7
LWC RC specimens with A_v	GP-equation	44	1.08	16.2
LWC RC specimens with A_v	Simplified-PC/RC	44	1.55	22.3
LWC PC specimens without A_v	GP-equation	27	1.96	59.9
LWC PC specimens without A_v	Simplified-PC/RC	27	2.31	72.2
LWC PC specimens with A_v	GP-equation	33	1.24	10.3
LWC PC specimens with A_v	Simplified-PC/RC	33	1.27	11.8

For the RC specimens without shear reinforcement, the addition of the four tests resulted in a slightly higher bias and COV. These tests are shown in figure 208 through figure 210 and are shifted to the left (i.e., lower test-to-prediction ratio) of the line formed by the rest of the data in the tail of the CDF.

For the RC specimens with shear reinforcements, the four additional tests caused a bias factor reduction of 0.20 and the COV to more than double. Figure 208 through figure 210 show that these four tests were also shifted significantly to the left of the line formed by the rest of the data in the tail.

The COV of the PC specimens without shear reinforcement is high, even after excluding the seven tests. The bias factor with the seven tests included caused a small reduction in the bias for the test-to-prediction ratios determined using the GP-equation method. The inclusion of the seven points caused a 44 percent reduction of the bias factor determined using the Simplified-PC/RC procedure. An increase in the COV of more that 20 percent was observed by including

the seven points. The seven tests are shown in figure 209 and figure 210 and are also shifted to the left of the rest of the data. For each figure, the number of specimens is in parentheses in the legends.

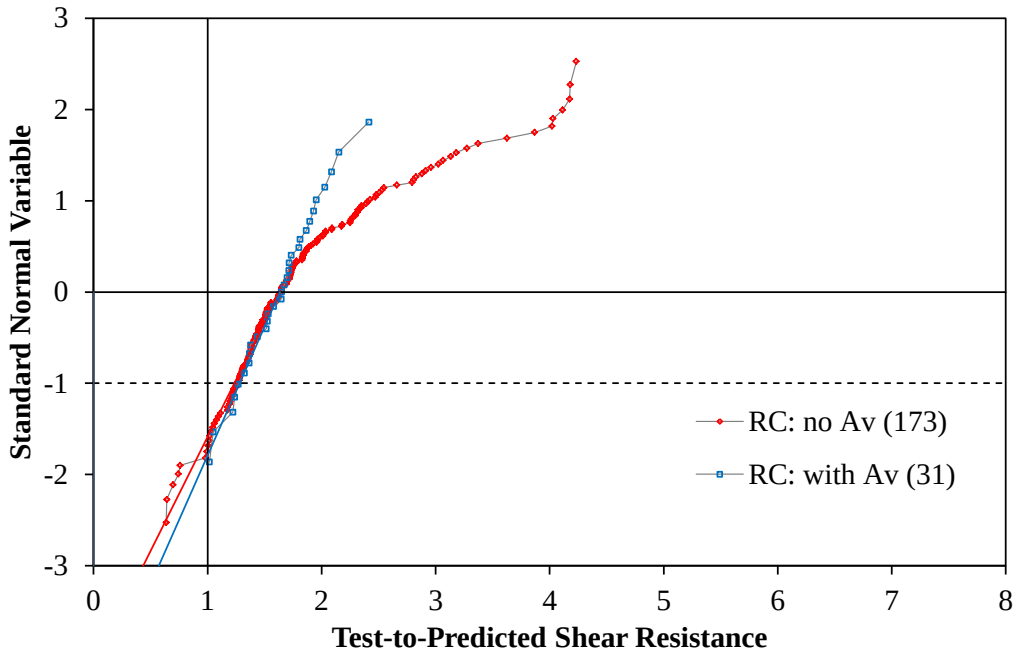

Source: FHWA.

Figure 208. Graph. CDFs for test-to-predicted shear resistance for Simplified-RC for all LWC specimens.

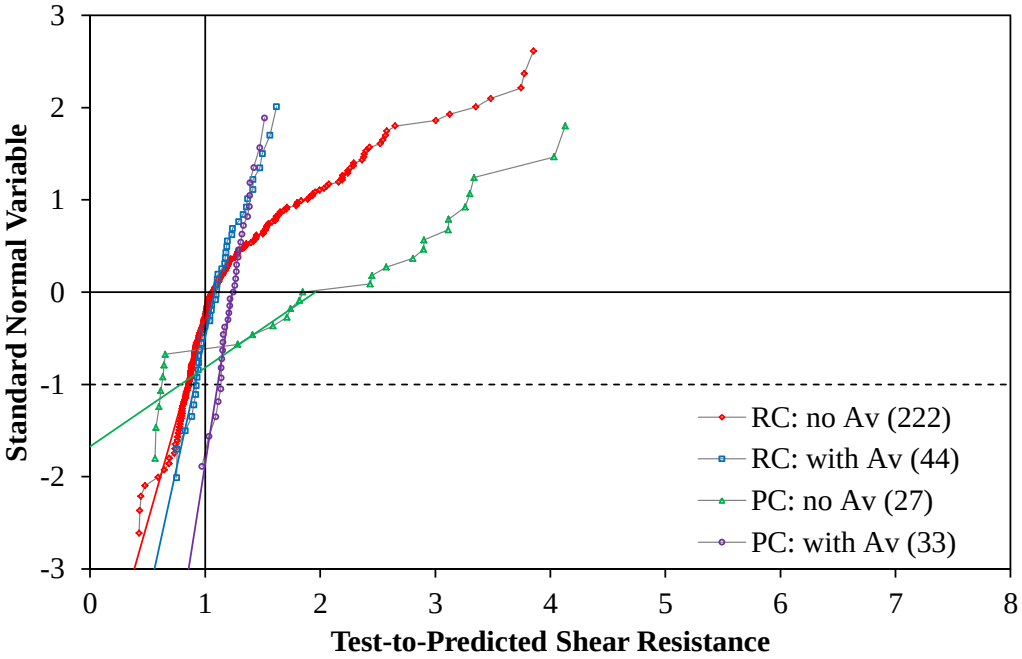

Source: FHWA.

Figure 209. Graph. CDFs for test-to-predicted shear resistance for the GP-equation method for all LWC specimens.

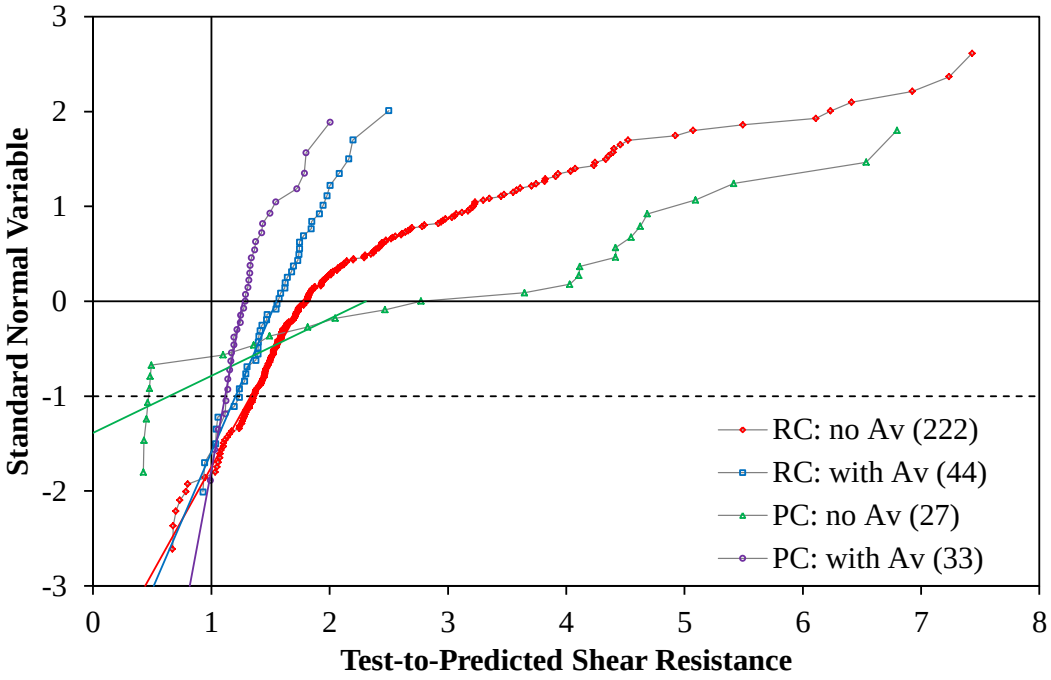

Source: FHWA.

Figure 210. Graph. CDFs for test-to-predicted shear resistance for Simplified-PC/RC for sections for all LWC specimens.

APPENDIX F. TFHRC PC GIRDER DRAWINGS

This appendix contains the drawings (see figure 211 through figure 215) of the TFHRC PC girders that were given to the beam fabricator.

Source: FHWA.

Figure 211. Illustration. Drawing of girder design 5.

Source: FHWA.

Figure 212. Illustration. Drawing of girder design 6.

Source: FHWA.

Figure 213. Illustration. Drawing of girder design 7.

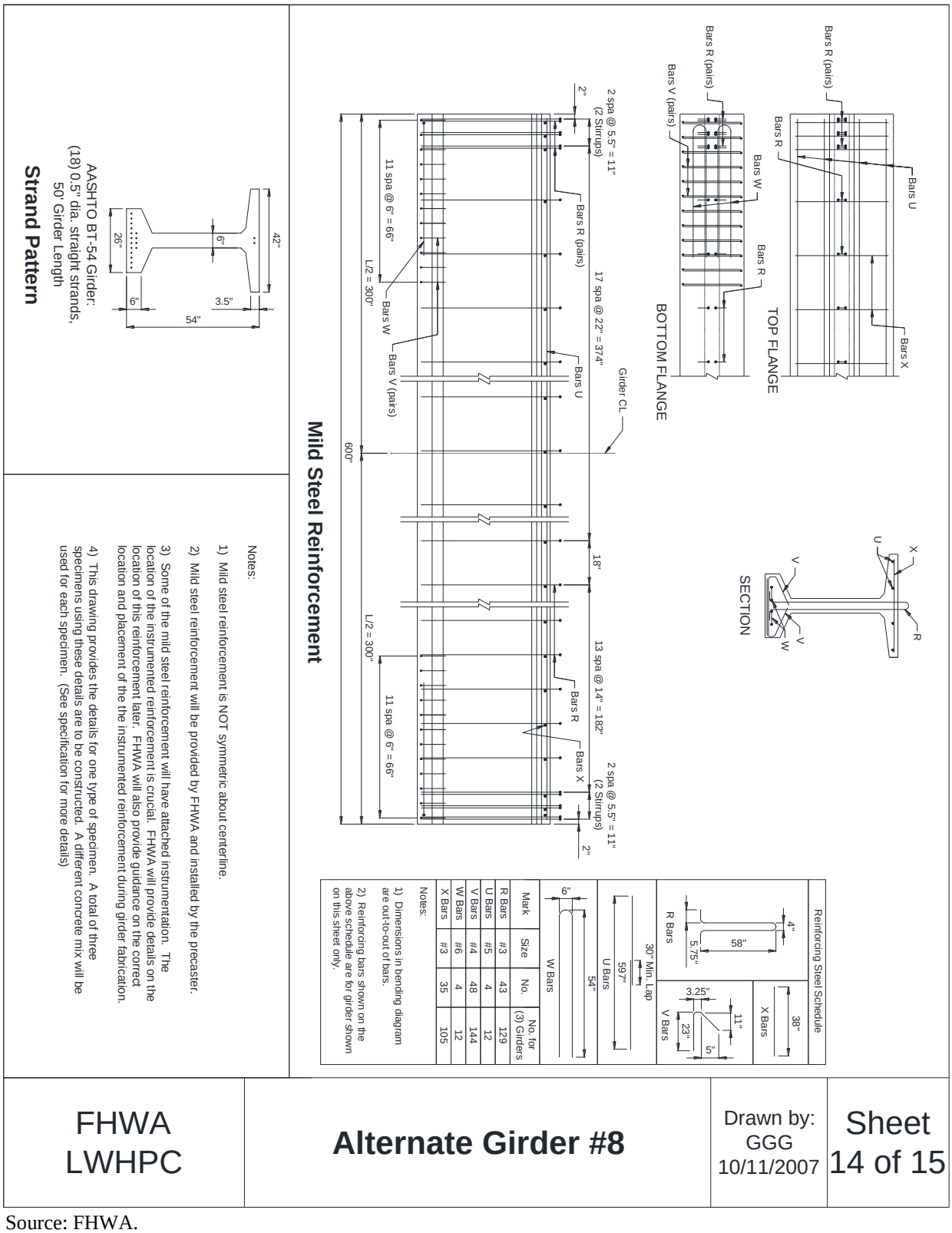

Source: FHWA.

Figure 214. Illustration. Drawing of girder design 8.

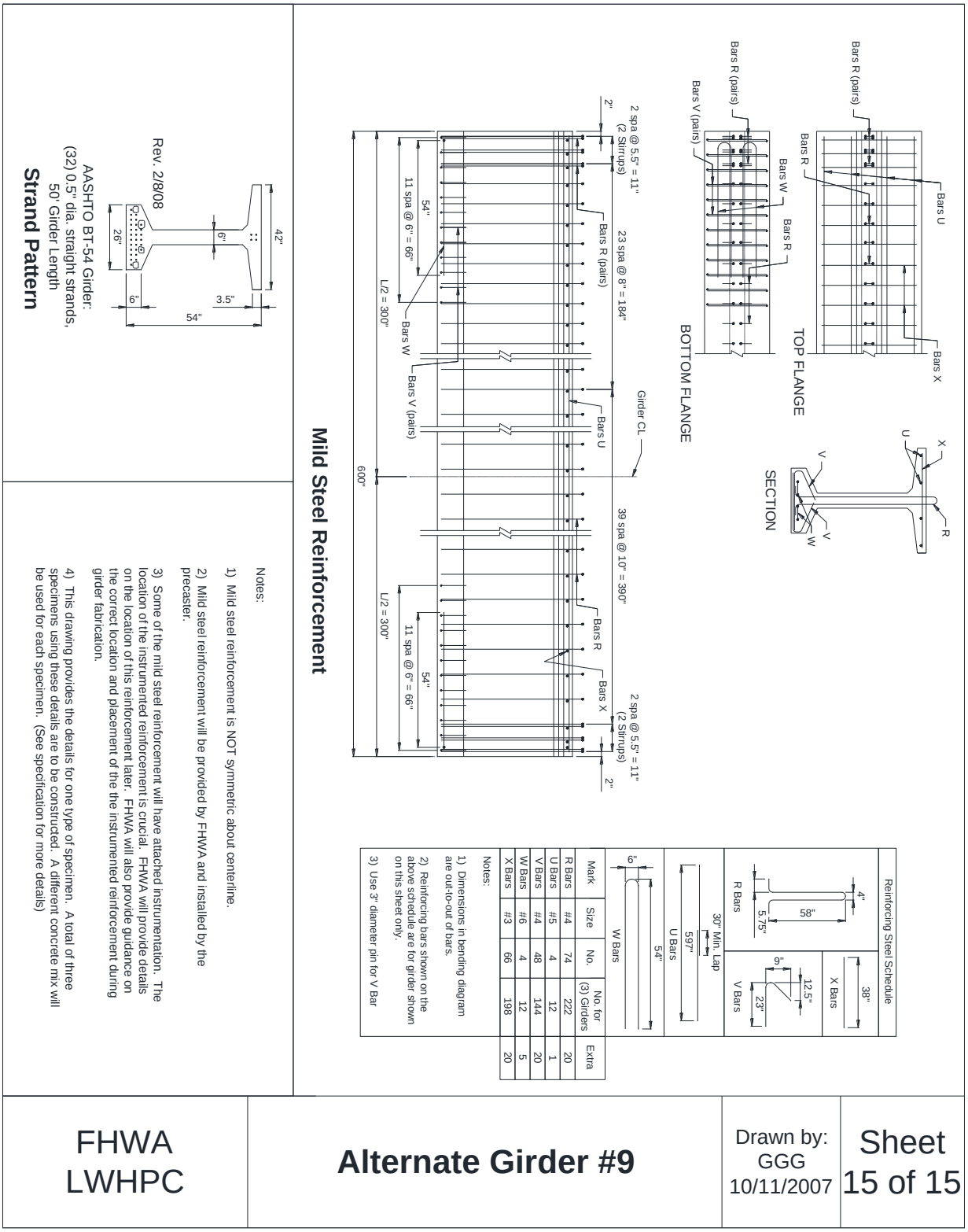

Source: FHWA.

Figure 215. Illustration. Drawing of girder design 9.

APPENDIX G. OBTAINING A DRAFT OF THE RESEARCH DATA

A hardcopy draft of the research data is available from Benjamin Graybeal, who can be contacted at Benjamin.Graybeal@dot.gov. The draft contains the detailed results of the 30 shear tests on high-strength LWC prestressed girders that were tested at TFHRC. Tables for each test give information about the girder geometry and reinforcement, material properties, and test setup. The tables also give the applied load, internal shear force, measured deflection, and measured reinforcement strain, strand slip, deck strain, and FRP strain. Figures show the applied load versus measured deflection and applied average shear stress versus measured average shear strain. Additional figures show the measured strain in the girder end reinforcement, measured longitudinal strain, measured transverse strain, and measured crack angles. Photographs show the girder before ultimate and after ultimate as well as the failure mode.

ACKNOWLEDGEMENTS

This report presents results from the FHWA LWC research program and is intended to both facilitate a broader understanding of the performance of LWC and to assist AASHTO SCOBS T-10 as it considers relevant revisions to section 5 of the *AASHTO LRFD Bridge Design Specifications*.[3] It does not constitute a policy statement or a recommendation from FHWA. Additionally, the publication of this report does not necessarily indicate approval or endorsement of the findings, opinions, conclusions, or recommendations either inferred or specifically expressed herein by FHWA or the U.S. Government. This report was created on behalf of FHWA as part of contract DTFH61-10-D-00017.

The authors would like to acknowledge the work of the T-10 Ad-hoc Group on LWC revisions to *AASHTO LRFD Bridge Design Specifications* for their assistance, helpful comments, and suggestions during the analysis and compilation of these results.[3] The work of Matthew Swenty, who assisted with the reliability analysis, is gratefully acknowledged by the authors. The authors would also like to gratefully acknowledge the work of the FHWA Research Library staff, who have been assisting in the collection of hundreds of articles relating to LWC, as well as the contribution of Dr. Karl-Heinz Reineck of the University of Stuttgart, Germany, who supplied the digital files of the ACI-DafStb database.

REFERENCES

1. Greene, G.G. and Graybeal, B.A. (2013). *Lightweight Concrete: Mechanical Properties*, Report No. FHWA-HRT-13-062, Federal Highway Administration, Washington, DC.

2. Greene, G.G. and Graybeal, B.A. (2014). *Lightweight Concrete: Development of Mild Steel in Tension*, Report No. FHWA-HRT-14-029, Federal Highway Administration, Washington, DC.

3. American Association of State Highway and Transportation Officials. (2012). *AASHTO LRFD Bridge Design Specifications*, Sixth Edition, American Association of State Highway and Transportation Officials, Washington, DC.

4. Greene, G.G. and Graybeal, B.A. (2015). *Lightweight Concrete: Shear Performance*, Report No. FHWA-HRT-15-021, Federal Highway Administration, Washington, DC.

5. ACI Committee 213. (1967). "Guide for Structural Lightweight Aggregate Concrete," *ACI Journal Proceedings*, *64*(8), pp. 433–469, American Concrete Institute, Farmington Hills, MI.

6. Hanson, J.A. (1961). "Tensile Strength and Diagonal Tension Resistance of Structural Lightweight Concrete," *ACI Journal Proceedings*, *58*(1), pp. 1–40, American Concrete Institute, Farmington Hills, MI.

7. Ivey, D.L. and Buth, E. (1966). "Splitting Tension Test of Structural Lightweight Concrete," *ASTM Journal of Materials*, *1*(4), pp. 859–871, ASTM International, West Conshohocken, PA.

8. Pauw, A. (1960). "Static Modulus of Elasticity of Concrete as Affected by Density," *ACI Journal Proceedings*, *57*(6), pp. 679–687, American Concrete, Institute, Farmington Hills, MI.

9. Rizkalla, S., Mirmiran, A., Zia, P., Russell, H., and Mast, R. (2007). *NCHRP Report 595: Application of the LRFD Bridge Design Specifications to High-Strength Structural Concrete: Flexure and Compression Provisions*, NCHRP Project 12-64, National Cooperative Highway Research Program, Washington, DC.

10. Ramirez, J.A. and Russell, B.W. (2008). *NCHRP Report 603: Transfer, Development, and Splice Length for Strand/Reinforcement in High-Strength Concrete*, NCHRP Project 12-60, National Cooperative Highway Research Program, Washington, DC.

11. Cousins, T., Roberts-Wollmann, C., and Brown, M.C. (2013). *NCHRP Report 733: High-Performance/High-Strength Lightweight Concrete for Bridge Girders and Decks*, NCHRP Project 18-15, National Cooperative Highway Research Program, Washington, DC.

12. Russell, H. (2007). *Synthesis of Research and Provisions Regarding the Use of Lightweight Concrete in Highway Bridges*, Report No. FHWA-HRT-07-053, Federal Highway Administration, Washington, DC.

13. ACI Committee 213. (2003). *Guide for Structural Lightweight Aggregate Concrete*, ACI 213R-03, American Concrete Institute, Farmington Hills, MI.

14. ACI-ASCE Committee 426. (1973). "The Shear Strength of Reinforced Concrete Members," *Journal of Structural Division, 99*(ST6), pp. 1,091–1,187, American Society of Civil Engineers, Reston, VA.

15. Walraven, J.C. (1981). "Fundamental Analysis of Aggregate Interlock," *Journal of Structural Division, 108*(ST11), pp. 2,245–2,270, American Society of Civil Engineers, Reston, VA.

16. ACI-ASCE Committee 326. (1962). "Shear and Diagonal Tension," *ACI Journal Proceedings, 59*(1), pp. 1–30, American Society of Civil Engineers, Reston, VA.

17. Bresler, B. and MacGregor, J.G. (1967). "Review of Concrete Beams Failing in Shear," *Journal of Structural Division, 93*(ST1), pp. 343–372, American Society of Civil Engineers, Reston, VA.

18. ACI Committee 318. (1963). *Building Code Requirements for Reinforced Concrete (ACI 318-63),* American Concrete Institute, Farmington Hills, MI.

19. Viest, I.M. (1959). Discussion of "Shear Strength of Lightweight Reinforced Concrete Beams," *ACI Journal Proceedings, 30*(9), American Concrete Institute, Farmington Hills, MI.

20. ACI-ASCE Committee 326. (1962). "Shear and Diagonal Tension," *ACI Journal Proceedings, 59*(1), pp. 277–344, American Society of Civil Engineers, Reston, VA.

21. Bresler, B. and Scordelis, A.C. (1963). "Shear Strength of Reinforced Concrete Beams," *ACI Journal Proceedings, 60*(1), pp. 51–74, American Concrete Institute, Farmington Hills, MI.

22. MacGregor, J.G. (1960). *Strength and Behavior of Prestressed Concrete Beams with Web Reinforcement*, Ph.D. Dissertation, University of Illinois, Urbana, IL.

23. ACI Committee 318. (2011). *Building Code Requirements for Reinforced Concrete (ACI 318-11) and Commentary,* American Concrete Institute, Farmington Hills, MI.

24. Ivey, D.L. and Buth, E. (1967). "Shear Capacity of Lightweight Concrete Beams," *ACI Journal Proceedings, 64*(10), pp. 634–643, American Concrete Institute, Farmington Hills, MI.

25. Hamadi, Y.D. and Regan, P.E. (1980). "Behaviour of Normal and Lightweight Aggregate Beams with Shear Cracks," *The Structural Engineer, 58B*(4), pp. 71–79, The Institution of Structural Engineers, London, United Kingdom.

26. Walraven, J. and Al-Zubi, N. (1995). "Shear Capacity of Lightweight Concrete Beams with Shear Reinforcement," *International Symposium on Structural Lightweight Aggregate Concrete*, pp. 91–104, Sandefjord, Norway.

27. ACI-ASCE Committee 445. (1999). *Recent Approaches to Shear Design of Structural Concrete*, American Concrete Institute, Farmington Hills, MI.

28. ACI Committee 318. (1995). *Building Code Requirements for Structural Concrete (ACI 318-95) and Commentary (ACI 318R-95)*, American Concrete Institute, Farmington Hills, MI.

29. Vecchio, F.J. and Collins, M.P. (1986). "The Modified Compression Field Theory for Reinforced Concrete Elements Subjected to Shear," *ACI Journal Proceedings, 83*(2), pp. 219–231, American Concrete Institute, Farmington Hills, MI.

30. Bentz, E.C., Vecchio, F.J., and Collins, M.P. (2006). "Simplified Modified Compression Field Theory for Calculating Shear Strength of Reinforced Concrete Elements," *ACI Structural Journal, 103*(4), pp. 614–624, American Concrete Institute, Farmington Hills, MI.

31. Collins, M.P. and Mitchell, D. (1991). *Prestressed Concrete Structures*, Prentice-Hall, Englewood Cliffs, NJ.

32. Hawkins, N.M., Kuchma, D.A., Mast, R.F., Marsh, M.L., and Reineck, K.-H. (2005). *Simplified Shear Design of Structural Concrete Members*, NCHRP Project 12-61, NCHRP Report 549, National Cooperative Highway Research Program, Washington, DC.

33. American Association of State Highway and Transportation Officials. (1996). *Standard Specifications for Highway Bridges*, 16th Edition, American Association of State Highway and Transportation Officials, Washington, DC.

34. ACI Committee 318. (2002). *Building Code Requirements for Structural Concrete (ACI 318-02) and Commentary (ACI 318R-02)*, American Concrete Institute, Farmington Hills, MI.

35. ACI Committee 408. (2003). *Bond and Development of Straight Reinforcing Bars in Tension*, ACI 408R-03, American Concrete Institute, Farmington Hills, MI.

36. Burge, T.A. (1983). "High-Strength Lightweight Concrete with Silica Fume," *ACI Special Publication, 79*, pp. 731–745, American Concrete Institute, Farmington Hills, MI.

37. Seabrook, P.I. and Wilson, H.S. (1988). "High Strength Lightweight Concrete for Use in Offshore Structures: Utilization of Fly Ash and Silica Fume," *International Journal of*

Cement Composites and Lightweight Concrete, *10*(3), pp. 183–192, Elsevier, Amsterdam, The Netherlands.

38. Yeginobali, A., Sobolev, K.G., Soboleva, S.V., and Tokyay, M. (1998). "High Strength Natural Lightweight Aggregate Concrete with Silica Fume," *ACI Special Publication*, *178*, pp. 739–758, American Concrete Institute, Farmington Hills, MI.

39. ASTM C31. (2006). "Standard Practice for Making and Curing Concrete Test Specimens in the Field," *Book of Standards Volume 4.02*, ASTM International, West Conshohocken, PA.

40. ASTM C39. (2001). "Standard Test Method for Compressive Strength of Cylindrical Concrete Specimens," *Book of Standards Volume 4.02*, ASTM International, West Conshohocken, PA.

41. ASTM C496. (2002). "Standard Test Method for Splitting Tensile Strength of Cylindrical Concrete Specimens," *Book of Standards Volume 4.02*, ASTM International, West Conshohocken, PA.

42. ASTM C469. (2002). "Standard Test Method for Static Modulus of Elasticity and Poisson's Ratio of Concrete in Compression," *Book of Standards Volume 4.02*, ASTM International, West Conshohocken, PA.

43. ASTM C615. (2008). "Standard Specification for Deformed and Plain Carbon-Steel Bars for Concrete Reinforcement," *Book of Standards Volume 1.04*, ASTM International, West Conshohocken, PA.

44. Reineck, K.-H., Kuchma, D.A., and Fitik, B. (2012). *Erweiterte Datenbanken zur Überprüfung der Querkraftbemessung von Konstruktionsbetonbauteilen ohne und mit Bügel* (*Extended Databases with Shear Tests on Structural Concrete Beams without and with Stirrups for the Assessment of Shear Design Procedures*), Deutscher Ausschuss für Stahlbeton (DafStb), H. 597, Beuth Verlag, Berlin, Germany.

45. Reineck, K.-H., Kuchma, D.A., and Fitik, B. (2010). *Extended Databases with Shear Tests on Structural Concrete Beams without and with Stirrups for the Assessment of Shear Design Procedures*, Research Report, Institut für Leichtbau Entwerfen und Konstruieren (ILEK) (Institute for Lightweight Structures and Conceptual Design), University of Stuttgart and University of Illinois, Champaign, Stuttgart, Germany, and Urbana, IL.

46. Reineck, K.-H., Bentz, E., Fitik, B., Kuchma, D.A., and Bayrak, O. (2013). "The ACI-DAfStb Database with Shear Tests on Slender Reinforced Concrete Beams without Stirrups," *ACI Structural Journal*, *110*(5), pp. 867–875, American Concrete Institute, Farmington Hills, MI.

47. Reineck, K.-H., Bentz, E., Fitik, B., Kuchma, D.A., and Bayrak, O. (2014). "The ACI-DAfStb Database with Shear Tests on Slender Reinforced Concrete Beams with Stirrups," *ACI Structural Journal*, *111*(5), pp. 1,147–1,156, American Concrete Institute, Farmington Hills, MI.

48. Ellingwood, B., Galambos, T.V., MacGregor, J.G., and Cornell, C.A. (1980). *Development of a Probability Based Load Criterion for American National Standard A58*, NBS Special Publication 577, National Bureau of Standards, Washington, DC.

49. Nowak, A.S. (1999). *NCHRP Report 368: Calibration of LRFD Bridge Design Code*, NCHRP Project C12-33, National Cooperative Highway Research Program, Washington, DC.

50. Nowak, A.S. and Collins, K. (2000). *Reliability of Structures*, Second Edition, McGraw-Hill Higher Education, New York, NY.

51. Szerszen, M.M. and Nowak, A.S. (2003). "Calibration of Design Code for Buildings (ACI 318): Part 2—Reliability Analysis and Resistance Factors," *ACI Structural Journal, 100*(3), pp. 383–391, American Concrete Institute, Farmington Hills, MI.

52. Paczkowski, P. and Nowak, A.S. (2010). *Reliability Models for Shear in Lightweight Reinforced Concrete Bridges*, Concrete Bridge Conference, Phoenix, AZ.

53. Szerszen, M.M. and Nowak, A.S. (2003). "Calibration of Design Code for Buildings (ACI 318): Part 1—Statistical Models for Resistance," *ACI Structural Journal, 100*(3), pp. 377–382, American Concrete Institute, Farmington Hills, MI.

54. Haldar, A. and Mahadevan, S. (2000). *Probability, Reliability and Statistical Methods in Engineering Design*, John Wiley and Sons, Inc., New York, NY.

55. Metropolis, N. and Ulam, S. (1949). "The Monte Carlo Method," *Journal of the American Statistical Association, 44*(247), pp. 335–341, Taylor and Francis, Oxfordshire, United Kingdom.

56. Yamani, A.S. (1992). *Reliability Evaluation of Shear Strength in Highway Girder Bridges*, Ph.D. Dissertation, Department of Civil Engineering, University of Michigan, Ann Arbor, MI.

57. Nowak, A.S., Rakoczy, A.M., and Szeliga, E.K. (2012). "Revised Statistical Resistance Models for R/C Structural Components," *ACI Special Publication, 284*, pp. 1–16, American Concrete Institute, Farmington Hills, MI.

58. Nowak, A.S. and Rakoczy, A.M. (2010). *Statistical Parameters for Compressive Strength of Lightweight Concrete*, Concrete Bridge Conference, Phoenix, AZ.

59. Rakoczy, A.M. and Nowak, A.S. (2013). "Resistance Model of Lightweight Concrete Members," *ACI Materials Journal, 110*(1), pp. 99–107, American Concrete Association, Farmington Hills, MI.

60. Kassner, B.L. (2012). *Shear Strength of Full-Scale Prestressed Lightweight Concrete Girders with Composite Decks*, Ph.D. Dissertation, Department of Civil Engineering, Virginia Polytechnic Institute and State University, Blacksburg, VA.

61. ASTM C567. (2005). “Standard Test Method for Determining Density of Structural Lightweight Concrete,” *Book of Standards Volume 4.02*, ASTM International, West Conshohocken, PA.

BIBLIOGRAPHY

INTRODUCTION

The bibliography for this report has been organized in two parts. The first part consists of source information for shear tests on LWC specimens included in the TFHRC shear database. The second part consists of source information for shear tests on NWC specimens in the ACI-DafStb database.

LWC SOURCES FOR TFHRC SHEAR DATABASE

Ahmad, S.H., Xie, Y., and Yu, T. (1994). "Shear Strength of Reinforced Lightweight Concrete Beams of Normal and High Strength Concrete," *Magazine of Concrete Research, 46*(166), pp. 57–66, ICE Publishing, Fitchburg, MA.

Alrousan, R., Issa, M.A., Ovitigala, T., and Issa, M.A. (2011). "Shear Strength of Lightweight Reinforced Concrete Beams Strengthened with CRFP Strips," *ACI Special Publication, 275*, pp. 571–590, American Concrete Institute, Farmington Hills, MI.

Brettle, H.J. (1962). "Structural Aspects of Prestressed Lightweight Aggregate Concrete," *Constructional Review, 35*(5), pp. 31–40, Nth Sydney, Sydney, Australia.

Clarke, J.L. (1987). "Shear Strength of Lightweight Aggregate Concrete Beams: Design to BS 8110," *Magazine of Concrete Research*, *39*(141), pp. 205–213, ICE Publishing, Fitchburg, MA.

Dymond, B.Z., Roberts-Wollmann, C.L., and Cousins, T.E. (2009). *Shear Strength of a PCBT-53 Girder Fabricated with Lightweight Self-Consolidating Concrete*, Report No. FHWA/VTRC 09-CR11, Virginia Transportation Research Council, Charlottesville, VA.

EuroLightCon. (2000). *Mechanical Properties of LWAC Compared with Both NWC and HSC*, Document BE96-3942/R27, European Union - Brite EuRam III, Luxembourg City, Luxembourg.

Funahashi, M., Hara, N., Yokota, H., and Niwa, J. (2002). "Shear Capacity of Reinforced Concrete Beams Using Super Lightweight Concrete," *Transactions of the Japan Concrete Institute*, *23*, pp. 377–384, Japan Concrete Institute, Tokyo, Japan.

Greene, G.G. and Graybeal, B.A. (2015). *Lightweight Concrete: Shear Performance*, Report No. FHWA-HRT-15-021, Federal Highway Administration, Washington, DC.

Hamadi, Y.D. and Regan, P.E. (1980a). "Behaviour in Shear of Beams with Flexural Cracks," *Magazine of Concrete Research*, *32*(111), pp. 67–78, ICE Publishing, Fitchburg, MA.

Hamadi, Y.D. and Regan, P.E. (1980b). "Behaviour of Normal and Lightweight Aggregate Beams with Shear Cracks," *The Structural Engineer, 58B*(4), pp. 71–79, The Institution of Structural Engineers, London, United Kingdom.

Hanson, J.A. (1958). "Shear Strength of Lightweight Reinforced Concrete Beams," *ACI Journal Proceedings*, *30*(3), pp. 387–403, American Concrete Association, Farmington Hills, MI.

Hanson, J.A. (1961). "Tensile Strength and Diagonal Tension Resistance of Structural Lightweight Concrete," *ACI Journal Proceedings*, *58*(1), pp. 1–40, American Concrete Association, Farmington Hills, MI.

Hegger, J., Will, N., Görtz, S., and Kommer, B. (2005). "Load Bearing Capacity of Prestressed Concrete Beams Made of High-Strength Lightweight Concrete," *BFT International*, *71*(3), pp. 34–45, BFT International, Gütersloh, Germany.

Hoff, G.C. (1993). "High Strength Lightweight Aggregate Concrete for Arctic Applications," *ACI Special Publication*, *136*, pp. 1–246, American Concrete Institute, Farmington Hills, MI.

Holste, J.R., Peterman, R.J., and Esmaeily, A.E. (2011). *Evaluating the Time-Dependent and Bond Characteristics of Lightweight Concrete Mixes for Kansas Prestressed Concrete Bridges*, Final Report, K-tran: KSU-08-02, Kansas State University Transportation Center, Manhattan, KS.

Ivey, D.L. and Buth, E. (1967). "Shear Capacity of Lightweight Concrete Beams," *ACI Journal Proceedings*, 64(10), pp. 634–643, American Concrete Institute, Farmington Hills, MI.

Jindal, B.K. (1966). "Behaviour of Reinforced Lightweight Concrete Beams in Flexure and Shear," *Indian Concrete Journal*, *40*(1), pp. 26–33, Indian Concrete Journal, Maharashtra, India.

Kang, T.H.K., Kim, W., Kwak, Y.K., and Hong, S.G. (2011). "Shear Testing of Steel Fiber-Reinforced Lightweight Concrete Beams without Web Reinforcement," *ACI Structural Journal*, *108*(5), pp. 553–561, American Concrete Institute, Farmington Hills, MI.

Kassner, B.L. (2012). *Shear Strength of Full-Scale Prestressed Lightweight Concrete Girders with Composite Decks*, Ph.D. Dissertation, Department of Civil Engineering, Virginia Polytechnic Institute and State University, Blacksburg, VA.

Kawaguchi, T., Niwa, J., Moon, J.H., and Maehori, S. (2000). "Shear Capacity of Normal Strength Super Lightweight RC Beams," *Transactions of the Japan Concrete Institute*, *22*, pp. 385–392, Japan Concrete Institute, Tokyo, Japan.

Meyer, K.F., Kahn, L.F., Lai, J.S., and Kurtis, K.E. (2002). *Transfer and Development Length of High Strength Lightweight Concrete Precast Prestressed Bridge Girders*, GDOT Research Project No. 2004, Task 5 Report, Georgia Department of Transportation, Atlanta, GA.

Murayama, Y. and Iwabuchi, A. (1986). "Flexural and Shear Strength of Reinforced High-Strength Lightweight Concrete Beams," *Transactions of the Japan Concrete Institute, 8*, pp. 267–274, Japan Concrete Institute, Tokyo, Japan.

Nishibayashi, S., Kobayashi, K., and Yoshioka, Y. (1968). "The Fundamental Studies on the Flexural and Shearing Properties of Concrete Beams with Artificial Lightweight Aggregate," *Transactions of the Japan Society of Civil Engineers, 155*, pp. 53–63, Japan Concrete Institute, Tokyo, Japan.

Peterman, R., Ramirez, J., and Okel, J. (1999). *Evaluation of Strand Transfer and Development Lengths in Pretensioned Girders with Semi-Lightweight Concrete*, Report No. FHWA-IN-JTRP-99/3, Federal Highway Administration, Washington, DC.

Ramirez, J., Olek, J., Rolle, E., and Malone, B. (2000). *Performance of Bridge Decks and Girders with Lightweight Aggregate Concrete, Final Report*, Report FHWA/IN/JTRP-98/17, Purdue University, West Lafayette, IN.

Richart, F.E. and Jensen, V.P. (1930). "Construction and Design Features of Haydite Concrete," *ACI Journal Proceedings*, *27*(10), pp. 151–182, American Concrete Institute, Farmington Hills, MI.

Ritthichauy, W., Siguyama, T., Okamoto, T., and Tsuji, Y. (2001). "Shear Tests on Reinforced Lightweight Aggregate Concrete Beams without Shear Reinforcement," *Concrete*, *23*(3), pp. 937–942 Japan Concrete Institute, Tokyo, Japan.

Salandra, M.A. and Ahmad, S.H. (1989). "Shear Capacity of Reinforced Lightweight High-Strength Concrete Beams," *ACI Structural Journal*, *86*(6), pp. 697–704, American Concrete Institute, Farmington Hills, MI.

Swamy, R.N. and Bandyopadhyay, A.K. (1979). "Shear Behaviour of Structural Lightweight Concrete T-Beams without Web Reinforcement," *Proceedings of the Institution of Civil Engineers (London)*, Part 2, *67*, pp. 341–354, Institute of Civil Engineers, London, United Kingdom.

Swamy, R.N. and Lambert, G.H. (1983). "Shear Strength of Lightweight Concrete T-Beams without Web Reinforcement," *The Structural Engineer, Part B—Quarterly*, *61B*(4), pp. 69–78, The Institution of Structural Engineers, London, United Kingdom.

Swamy, R.N., Jones, R., and Chiam, A.T.P. (1993). "Influence of Steel Fibers on the Shear Resistance of Lightweight Concrete I-Beams," *ACI Structural Journal*, *90*(1), pp. 103–114, American Concrete Institute, Farmington Hills, MI.

Tang, C.W., Yen, T., and Chen, H.J. (2009). "Shear Behavior of Reinforced Concrete Beams Made with Sedimentary Lightweight Aggregate without Shear Reinforcement," *Journal of Materials in Civil Engineering*, *21*(12), pp. 730–739, American Society of Civil Engineers, Reston, VA.

Taylor, R. and Brewer, R.S. (1963). "The Effect of Type of Aggregate on the Diagonal Cracking of Reinforced Concrete Beams," *Magazine of Concrete Research*, *15*(44), p. 87, ICE Publishing, Fitchburg, MA.

Thorenfeldt, E. and Drangsholt, G. (1990). "Shear Capacity of Reinforced High-Strength Concrete Beams," *ACI Special Publication*, *121*, pp. 29–154, American Concrete Institute, Farmington Hills, MI.

Thorenfeldt, E. and Stemland, H. (1995). "Shear Capacity of Lightweight Concrete Beams without Shear Reinforcement," *International Symposium on Structural Lightweight Aggregate Concrete*, pp. 244–255, Sandefjord, Norway.

Thorenfeldt, E. and Stemland, H. (2000). "Shear Capacity of Lightweight Concrete Beams without Shear Reinforcement," *Second International Symposium on Structural Lightweight Aggregate Concrete*, pp. 330–340, Kristiansand, Norway.

Thorenfeldt, E., Stemland, H., and Tomaszewicz, A. (1995). "Shear Capacity of Large I-Beams," *International Symposium on Structural Lightweight Aggregate Concrete*, pp. 733–744, Sandefjord, Norway.

Walraven, J. and Al-Zubi, N. (1995). "Shear Capacity of Lightweight Concrete Beams with Shear Reinforcement," *International Symposium on Structural Lightweight Aggregate Concrete*, pp. 91–104, Sandefjord, Norway.

Watanabe, H., Kawano, H., Suzuki, M., and Sato, S. (2003). "Shear Strength of PC Beams with High Strength Lightweight Aggregate Concrete," *Concrete Research and Technology*, *14*(1), pp. 41–54, Japan Concrete Institute, Tokyo, Japan.

Yang, K.H., Sim, J.I., Choi, B.J., and Lee, E.T. (2011). "Effect of Aggregate Size on Shear Behavior of Lightweight Concrete Continuous Slender Beams," *ACI Materials Journal*, *108*(5), pp. 501–509, American Concrete Institute, Farmington Hills, MI.

NWC SOURCES FOR ACI-DAFSTB DATABASE

Adebar, P.E. (1989). *Shear Design of Concrete Offshore Structures*, Master's Thesis, University of Toronto, Toronto, Canada.

Ahmad, S.H., Khaloo, A.R., and Poveda, A. (1986). "Shear Capacity of Reinforced High-Strength Concrete Beams," *ACI Journal Proceedings*, *83*(2), pp. 297–305, American Concrete Institute, Farmington Hills, MI.

Ahmad, S.H., Park, F., and El-Dash, K. (1995). "Web Reinforcement Effects on Shear Capacity of Reinforced High-Strength Concrete Beams," *Magazine of Concrete Research*, *47*(172), pp. 227–233, ICE Publishing, Fitchburg, MA.

Al-Alusi, A.F. (1957). "Diagonal Tension Strength of Reinforced Concrete T-beams with Varying Shear Span," *ACI Journal Proceedings*, *53*(5), pp. 1,067–1,077, American Concrete Institute, Farmington Hills, MI.

Angelakos, D. (1999). "The Influence of Concrete Strength and Longitudinal Reinforcement Ratio on the Shear Strength of Large-Size Reinforced Concrete Beams with and without

Transverse Reinforcement," Master's Thesis, Department of Civil Engineering, University of Toronto, Toronto, Canada.

Angelakos, D., Bentz, E.C., and Collins, M.P. (2001). "The Effect of Concrete Strength and Minimum Stirrups on the Shear Strength of Large Members," *ACI Structural Journal*, *98*(3), pp. 291–300, American Concrete Institute, Farmington Hills, MI.

Arthur, P.D. (1965). "The Shear Strength of Pre-Tensioned I-Beams with Unreinforced Webs," *Magazine of Concrete Research*, *17*(53), pp, 199–210, ICE Publishing, Fitchburg, MA.

Aster, H. and Koch, R. (1974). *Schubtragfähigkeit dicker Stahlbetonplatten*, BuStb 69, H.11, pp. 266–270, Ernst & Sohn, Berlin, Germany.

Bentz, E.C. and Buckley, S. (2005). "Repeating a Classic Set of Experiments on Size Effect in Shear of Members without Stirrups," *ACI Structural Journal*, *102*(6), pp. 832–838, American Concrete Institute, Farmington Hills, MI.

Bernander, K. (1957). "An Investigation of the Shear Strength of Concrete Beams without Stirrups or Diagonal Bars," *RILEM Symposium 1*, Stockholm, Sweden.

Bernhardt, C.J. and Fynboe, C.C. (1986). *High Strength Concrete Beams*, Nordic Concrete Research, Norske Betongforening, Oslo, Sweden.

Bhal, N.S. (1968). *Über den Einfluß der Balkenhöhe auf die SchuBTragfähigkeit von einfeldrigen Stahlbetonbalken mit und ohne Schubbewehrung*, Otto-Graf-Institut, H.35, Stuttgart, Germany.

Bresler, B. and Scordelis, A.C. (1963). "Shear Strength of Reinforced Concrete Beams," *ACI Journal Proceedings*, *60*(1), pp. 51–74, American Concrete Institute, Farmington Hills, MI.

Caflisch, R. and Thürlimann, B. (1970a). *Biegeversuche an teilweise vorgespannten Betonbalken*, IBK-Bericht Nr. 6504-1, ETH Zürich, März, Germany.

Caflisch, R. and Thürlimann, B. (1970b). *Schubversuche an teilweise vorgespannten Betonbalken*, IBK-Bericht Nr. 6504-2, ETH Zürich, Okt, Germany.

Cederwall, K., Hedman, O., and Losberg, A. (1970). *Shear Strength of Partially Prestressed Beams with Pretensioned Reinforcement of High Grade Deformed Bars*, Publication 70/6, Division of Concrete Structures, Chalmers University of Technology, Gothenburg, Sweden.

Cederwall, K., Hedman, O., and Losberg, A. (1974). "Shear Strength of Partially Prestressed Beams with Pretensioned Reinforcement of High Grade Deformed Bars," *ACI Special Publication*, *42*, American Concrete Institute, Farmington Hills, MI.

Chana, P.S. (1981). *Some Aspects of Modelling the Behaviour of Reinforced Concrete Under Shear Loading*, Technical Report 543, Cement and Concrete Association, Wexham Springs, United Kingdom.

Chang, T.S. and Kesler, C.E. (1958). "Static and Fatigue Strength in Shear of Beams with Tensile Reinforcement," *ACI Journal Proceedings*, *54*(6), pp. 1,033–1,057, American Concrete Institute, Farmington Hills, MI.

Cladera, A. and Marí, A.R. (2002). *Shear Strength of Reinforced High-Strength and Normal-Strength Concrete Beams: A New Simplified Shear Design Method*, Universitat Politécnica de Catalunya, Barcelona, Spain.

Collins, M.P. and Kuchma, D. (1999). "How Safe are our Large, Lightly Reinforced Concrete Beams, Slabs, and Footings?" *ACI Structural Journal*, *96*(4), pp. 482–490, American Concrete Institute, Farmington Hills, MI.

Cumming, D.A., Shield, C.K., and French, C.E. (1998). *Shear Capacity of High-Strength Concrete Prestressed Girders, Final Report*, Report No. MN/RC-1998/12, Department of Civil Engineering, University of Minnesota, Minneapolis, MN.

Diaz de Cossio, R. and Siess, C.P. (1960). "Behavior and Strength in Shear of Beams and Frames without Web Reinforcement," *ACI Journal Proceedings, 31*(8), pp. 695–735, American Concrete Institute, Farmington Hills, MI.

Drangsholt, G. and Thorenfeldt, E. (1992). *Shear Capacity of High Strength Concrete Beams*, Research Report No. 2.1, Structural Engineering–FCB, SINTEF, Trondheim, Norway.

Elzanaty, A.H., Nilson, A.H., and Slate, F.O. (1985). *Shear Critical High-Strength Concrete Beams*, Research Report No. 85-1, Department of Structural Engineering, Cornell University, Ithaca, NY.

Elzanaty, A.H., Nilson, A.H., and Slate, F.O. (1986). "Shear Capacity of Reinforced Concrete Beams Using High-Strength Concrete," *ACI Journal Proceedings*, *83*(2), pp. 290–296, American Concrete Institute, Farmington Hills, MI.

Feldman, A. and Siess, C.P. (1955). *Effect of Moment Shear Ratio on Diagonal Tension Cracking and Strength in Shear of Reinforced Concrete Beams*, Structural Research Series No. 107, University of Illinois Civil Engineering, Champaign, IL.

Ferguson, P.M. and Thompson, J.N. (1953). "Diagonal Tension in T-Beams without Stirrups," *ACI Journal Proceedings*, *49*(3), pp. 665–675, American Concrete Institute, Farmington Hills, MI.

Ferguson, P.M. (1956). "Some Implications of Recent Diagonal Tension Tests," *ACI Journal Proceedings*, *28*(2), pp. 157–172, American Concrete Institute, Farmington Hills, MI.

Ghannoum, W.M. (1998). *Size Effect on Shear Strength of Reinforced Concrete Beams*, Department of Civil Engineering and Applied Mechanics, McGill University Montréal, Canada.

Grimm, R. (1996/1997). *Einfluß bruchmechanischer Kenngrößen auf das Biege- und Schubtragverhaltenhochfester Betone*, Diss., Fachb. Konstr. Ingenieurbau der TH Darmstadt, 1996 und DafStb H.477, Beuth Verlag GmbH, Berlin, Germany.

Haddadin, M.J., Hong, S., and Mattock, A.H. (1971). "Stirrup Effectiveness in Reinforced Concrete Beams with Axial Force," *Journal of the Structural Division*, *97*(ST9), pp. 2,277–2,297, American Society of Civil Engineers, Reston, VA.

Hallgren, M. (1994). *Flexural and Shear Capacity of Reinforced High Strength Concrete Beams without Stirrups*, KTH Stockholm and TRITA-BKN, Stockholm, Sweden.

Hallgren, M. (1996). *Punching Shear Capacity of Reinforced High Strength Concrete Slabs*, Doctoral Thesis, KTH Stockholm and TRITA-BKN, Stockholm, Sweden.

Hamadi, Y.D. (1976). *Force Transfer Across Cracks in Concrete Structures*, Ph.D. Thesis, Polytechnic of Central London, London, United Kingdom.

Hanson, J.A. (1958). "Shear Strength of Lightweight Reinforced Concrete Beams," *ACI Journal Proceedings*, *30*(3), 387–403, American Concrete Association, Farmington Hills, MI.

Hanson, J.A. (1961). "Tensile Strength and Diagonal Tension Resistance of Structural Lightweight Concrete," *ACI Journal Proceedings*, *58*(1), pp. 1–40, American Concrete Association, Farmington Hills, MI.

Hanson, J.M. and Hulsbos, C.L. (1964). "Ultimate Shear Tests of Prestressed Concrete I-Beams under Concentrated and Uniform Loadings," *PCI Journal*, *9*(3), pp. 15–28, Precast/Prestressed Concrete Institute, Chicago, IL.

Hegger, J., Sherif, A., and Roeser, W. (2003). "Nonseismic Design of Beam-Column Joints," *ACI Structural Journal*, *100*(5), pp. 654–664, American Concrete Institute, Farmington Hills, MI.

Hegger, J., Görtz, S., Kommer, B., Will, N., Tigges, C., and Drössler, C. (2001). "Spannbeton-Fertigteilträger aus selbstverdichtendem Beton," *BFT International*, *67*(8), pp. 40–46, BFT International, Gütersloh, Germany.

Islam, M.S., Pam, H.J., and Kwan, A.K.H. (1998). "Shear Capacity of High-Strength Concrete Beams with their Point of Inflection within the Shear Span," *Proceedings of the Institution of Civil Engineers Structures and Buildings*, *128*(1), pp. 91–99, London, United Kingdom.

Johnson, M.K. and Ramirez, J.A. (1989). "Minimum Shear Reinforcement in Beams with Higher Strength Concrete," *ACI Structural Journal*, *86*(4), pp. 376–382, American Concrete Institute, Farmington Hills, MI.

Kani, G.N.J. (1967). "How Safe are our Large Reinforced Concrete Beams?" *ACI Journal Proceedings*, *64*(3), pp. 128–141, American Concrete Institute, Farmington Hills, MI.

Kani, M.W., Huggins, M.W., and Wittkopp, R.R. (1979). *Kani on Shear in Reinforced Concrete*, Department of Civil Engineering, University of Toronto, Toronto, Canada.

Kawano, H. and Watanabe, H. (1998). "Shear Strength of Reinforced Concrete Columns—Effect of Specimen Size and Load Reversal," *Proceedings of the Second International Conference on Concrete Under Severe Conditions (CONSEC)*, Tromsø, Norway.

Kim, J.-K. and Park, Y.-D. (1994). "Shear Strength of Reinforcement High Strength Concrete Beams without Web Reinforcement," *Magazine of Concrete Research*, *46*(166), pp. 7–16, ICE Publishing, Fitchburg, MA.

Kong, P. and Rangan, V. (1997). *Studies on Shear Strength of High Performance Concrete Beams*, Research Report No.2/97, Curtin University of Technology, Perth, Western Australia.

Krefeld, W.J. and Thurston, C.W. (1966). "Studies of the Shear and Diagonal Tension Strength of Simply Supported R.C.-Beams," *ACI Journal Proceedings*, *63*(4), pp. 451–476, American Concrete Institute, Farmington Hills, MI.

Küng, R. (1985). *Ein Beitrag zur Schubsicherung im Stahlbetonbau.Betonstahl in Entwicklung*, H.33, TOR-ISTEG Steel Corporation, Luxemburg City, Luxemburg.

Kuhlmann, U. and Ehmann, J. (2001). *Versuche zur Ermittlung der Querkrafttragfähigkeit von Verbundplatten unter Längszug ohne Schubbewehrung-Versuchsbericht*, Institut für Konstruktion und Entwurf Stahl-, Holz-, und Verbundbau, Universität Stuttgart, No. 2001-6X, University of Stuttgart, Stuttgart, Germany.

Kuhlmann, U., Zilch, K., Ehmann, J., Jähring, A., and Spitra, F. (2002). *Querkraftabtragung in Verbundträgern mit schlaff bewehrter und aus Zugbeanspruchung gerissener Stahlbetonplatte ohne Schubbewehrung-Mitteilungen*, Institut für Konstruktion und Entwurf Stahl-, Holz-, und Verbundbau, Universität Stuttgart, No. 2002-2, University of Stuttgart, Stuttgart, Germany.

Kulkarni, S.M. and Shah, S.P. (1998). "Response of Reinforced Concrete Beams at High Strain Rates," *ACI Structural Journal*, *95*(6), pp. 705–714, American Concrete Institute, Farmington Hills, MI.

Lambotte, H. and Taerwe, L.R. (1990). "Deflection and Cracking of High-Strength Concrete Beams and Slabs," *ACI Special Publication*, *121*, pp. 109–128, American Concrete Institute, Farmington Hills, MI.

Laupa, A., Siess, C.P., and Newmark, N.M. (1953). *The Shear Strength of Simple-Span Reinforced Concrete Beams without Web Reinforcement*, Structural Research Series No. 52, University of Illinois, Champaign, IL.

Leonhardt, F. and Walther, R. (1962a). *Schubversuche an einfeldrigen Stahlbetonbalken mit und ohne Schubbewehrung*, Deutscher Ausschuss für Stahlbeton (DafStb), H.151, Berlin, Germany.

Leonhardt, F. and Walther, R. (1962b). *Versuche an Plattenbalken mit hoher Schubbeanspruchung*, Deutscher Ausschuss für Stahlbeton (DafStb), H.152, Beuth Verlag, Berlin, Germany.

Leonhardt, F. and Walther, R. (1962c). *Versuche an schlaff bewehrten Rechteck- und Plattenbalken mit Schubbewehrung, 1*, Teil, Forschungsreihe über die Tragfähigkeit auf Schub von Stahl- und Spannbetonbalken, FMPA (Otto-Graf-Institut), Stuttgart, März, Germany.

Leonhardt, F. and Walther, R. (1962d). *Versuche an schlaff bewehrten Rechteckbalken und Platten ohne Schubbewehrung, 2*, Teil, Forschungsreihe über die Tragfähigkeit auf Schub von Stahl- und Spannbetonbalken, FMPA (Otto-Graf-Institut), Stuttgart, März, Germany.

Leonhardt, F. and Walther, R. (1962e). *Versuche an schlaff bewehrten Rechteckbalken und Platten ohne Schubbewehrung; Zusammenfassung und vorläufige Schlußfolgerungen*, Forschungsreihe über die Tragfähigkeit auf Schub von Stahl- und Spannbetonbalken, FMPA (Otto-Graf-Institut), Stuttgart, Germany.

Leonhardt, F. and Walther, R. (1963). *Schubversuche an Plattenbalken mit unterschiedlicher Schubbewehrung*, Deutscher Ausschuss für Stahlbeton (DafStb), H.156, Beuth Verlag, Berlin, Germany.

Levi, F. and Marro, P. (1993). "Shear Tests on HSC Prestressed Beams—Proposals of New Interpretative Models," *Proceedings of International Symposium on Utilization of High-Strength Concrete*, pp. 293–305, Lillehammer, Norway.

Levi, F. and Marro, P. (1989). "Shear Tests Up to Failure of Beams Made with Normal and High Strength Concrete," *CEB-Bulletin No. 193*, pp. 11–24, International Federation for Structural Concrete (fib), Lausanne, Switzerland.

Lyngberg, B.S. (1974). *Ultimate Shear Resistance of Partially Prestressed Reinforced Concrete I-Beams*, Structural Research Laboratory, Technical University of Denmark, Lyngby, Denmark.

Lubell, A., Sherwood, T., Bentz, E., and Collins, M. (2004). "Safe Shear Design of Large Wide Beams," *Concrete International*, *26*(1), pp, 62–78, American Concrete Institute, Farmington Hills, MI.

MacGregor, J.G. (1958). *Effect of Draped Reinforcement on Behavior of Prestressed Concrete Beams*, Civil Engineering Studies, Structural Research Series No. 154, University of Illinois, Champaign, IL.

Mahgoub, M.O. (1975). “Shear Strength of Prestressed Concrete Beams without Web Reinforcement,” *Magazine of Concrete Research*, *27*(93), pp. 219–228, ICE Publishing, Fitchburg, MA.

Marti, P., Pralong, J., and Thürlimann, B. (1977). *Schubversuche an Stahlbeton-Platten*, IBK-Bericht Nr. 7305-2, ETH, Zürich, Germany.

Maruyama, K. and Rizkalla, S.H. (1988). “Shear Design Consideration for Pretensioned Prestressed Beams,” *ACI Journal Proceedings*, *85*(5), pp. 492–498, American Concrete Institute, Farmington Hills, MI.

Mathey, R.G. and Watstein, D. (1963). “Shear Strength of Beams without Web Reinforcement Containing Deformed Bars of Different Yield Strengths,” *ACI Journal Proceedings*, *60*(2),
pp. 183–207, American Concrete Institute, Farmington Hills, MI.

Moayer, M. and Regan, P.E. (1974). “Shear Strength of Prestressed and Reinforced Concrete T-beams,” *ACI Special Publication*, *42*, pp. 183–214, American Concrete Institute, Farmington Hills, MI.

Moody, K.G., Viest, I.M., Elstner, R.C., and Hognestad, E. (1954). “Shear Strength of RC Beams Part 1—Tests of Simple Beams,” *ACI Journal Proceedings*, *26*(4), pp. 317–332, American Concrete Institute, Farmington Hills, MI.

Moody, K.G., Viest, I.M., Elstner, R.C., and Hognestad, E. (1955a). “Shear Strength of RC Beams Part 2—Tests of Restrained Beams without Web Reinforcement,” *ACI Journal Proceedings*, 26(5), pp. 417–434, American Concrete Institute, Farmington Hills, MI

Moody, K.G., Viest, I.M., Elstner, R.C., and Hognestad, E. (1955b). “Shear Strength of RC Beams Part 3—Tests of Restrained Beams with Web Reinforcement,” *ACI Journal Proceedings*, *26*(6), pp. 525–539, American Concrete Institute, Farmington Hills, MI.

Morrow, J.D. and Viest, F.M. (1957). “Shear Strength of RC Frame Members without Web Reinforcement,” *ACI Journal Proceedings*, *28*(9), pp. 833–869, American Concrete Institute, Farmington Hills, MI.

Mphonde, A.G. and Frantz, G.C. (1984). “Shear Tests of High- and Low-Strength Concrete Beams without Stirrups,” *ACI Journal Proceedings*, *81*(4), pp. 350–357, American Concrete Institute, Farmington Hills, MI.

Olesen, S.O., Sozen, M.A., and Siess, C.P. (1967). *Investigation of Prestressed Reinforced Concrete for Highway Bridges, Part IV: Strength in Shear of Beams with Web Reinforcement*, Bulletin No. 493, University of Illinois, Urbana-Champaign, IL.

Özden, K. (1967). *An Experimental Investigation on the Shear Strength of Reinforced Concrete Beams*, Structural Research Laboratory, Technical University of Denmark, Lyngby, Denmark.

Palaskas, M.N., Attiogbe, E.K., and Darwin, D. (1981). "Shear Strength of Lightly Reinforced T-Beams," *ACI Journal*, *78*(6), pp. 447–455, American Concrete Institute, Farmington Hills, MI

Petersson, T. (1972). *Shear and Torsion in Reinforced Concrete Beams*, Document D10, National Swedish Institute for Building Research, Gävle, Sweden.

Podgorniak-Stanik, B.A. (1998). *The Influence of Concrete Strength, Distribution of Longitudinal Reinforcement, Amount of Transverse Reinforcement and Member Size on Shear Strength of Reinforced Concrete Members*, University of Toronto, Toronto, Canada.

Quast, U. (1999). *Einfluß von Langzeitwirkungen auf den Neigungswinkel von Schubrissen*, Schlußberichtzum Forschungsvorhaben QU 48/5-1, Technische Universität Hamburg-Harburg, Hamburg, Germany.

Rajagopalan, K.S. and Ferguson, P.M. (1968). "Exploratory Shear Tests Emphasizing Percentage of Longitudinal Reinforcement," *ACI Journal Proceedings*, *65*(8), pp. 634–638, American Concrete Institute, Farmington Hills, MI.

Regan, P.E. (1971a). *Shear in Reinforced Concrete—An Analytical Study*, Report TN46, CIRIA, London, United Kingdom.

Regan, P.E. (1971b). *Shear in Reinforced Concrete—An Experimental Study*, Report TN45, CIRIA, London, United Kingdom.

Regan, P.E. (1971c). "Behaviour of Reinforced and Prestressed Concrete Subjected to Shear Forces," *Proceedings of the Institution of Civil Engineers*, Paper 7441S, Institution of Civil Engineers, London, United Kingdom.

Reineck, K.-H. (1991). "Ultimate Shear Force of Structural Concrete Members without Transverse Reinforcement Derived from a Mechanical Model," *ACI Structural Journal*, *88*(5), pp. 592–602, American Concrete Institute, Farmington Hills, MI.

Reineck, K.-H., Koch, R., and Schlaich, J. (1978). *Shear Tests on Reinforced Concrete Beams with Axial Compression for Offshore Structures—Final Test Report*, Institut für Massivbau, University of Stuttgart, Stuttgart, Germany.

Remmel, G. (1991). *Zum Zugtragverhalten hochfester Betone und seinem Einfluß auf die Querkrafttragfähigkeit von schlanken Bauteilen ohne Schubbewehrung*, Ph.D. Dissertation, Technische Universität Darmstadt, Darmstadt, Germany.

Roller, J.J. and Russel, H.G. (1990). "Shear Strength of High-Strength Concrete Beams with Web Reinforcement," *ACI Structural Journal*, *87*(2), pp. 191–198, American Concrete Institute, Farmington Hills, MI.

Rosenbusch, J. and Teutsch, M. (2002). *Trial Beams in Shear*, Brite/Euram project 97-4163, Final Report Sub Task 4.2, Institut für Baustoffe, Massivbau und Brandschutz, Technische Universität Braunschweig, Braunschweig, Germany.

Rüsch, H., Haugli, F.R., and Mayer, H. (1962). *Schubversuche an Stahlbeton-Rechteckbalken mit gleichmäßig verteilter Belastung*, Deutscher Ausschuss für Stahlbeton (DafStb), H.145, W, Ernst & Sohn, Berlin, Germany.

Salandra, M.A. and Ahmad, S.H. (1989). "Shear Capacity of Reinforced Lightweight High-Strength Concrete Beams," *ACI Structural Journal*, *86*(6), pp. 697–704, American Concrete Institute, Farmington Hills, MI.

Scholz, H. (1994). *Ein Querkrafttragmodell für Bauteile ohne Schubbewehrung im Bruchzustand aus normalfestem und hochfestem Beton*, Berichte aus dem Konstruktiven Ingenieurbau Heft 21, Technische Universität, Berlin, Germany.

Shin, S.-W., Lee, K.-S., Moon, J.-I., and Ghosh, S.K. (1999). "Shear Strength of Reinforced High-Strength Concrete Beams with Shear Span-to-Depth Ratios Between 1.5 and 2.5," *ACI Structural Journal*, *96*(4), pp. 549–556, American Concrete Institute, Farmington Hills, MI.

Soerensen, H.C. (1974). *Shear Test on 12 Reinforced Concrete T-Beams*, Structural Research Laboratory, Report No. R 60, Technical University of Denmark, Lyngby, Denmark.

Sozen, M.A., Zwoyer, E.M., and Siess, C.P. (1959). *Strength in Shear of Beams without Web Reinforcement*, Bulletin No. 452, University of Illinois, Urbana-Champaign, IL.

Stroband, J. (1997). "Shear Capacity of High-Strength Concrete Beams with Shear Reinforcement," *Progress in Concrete*, *5*, 87–96, Delft University of Technology, Delft, Netherlands.

Taylor, H.P.J. (1968). *Shear Stress in Reinforced Concrete Beams without Shear Reinforcement*, Technical Report No. 407, Cement and Concrete Association, Newcastle upon Tyne, United Kingdom.

Taylor, H.P.J. (1972). "Shear Strength of Large Beams," *Journal of the Structural Division*, *98*(ST11), pp. 2,473–2,490, American Society of Civil Engineers, Reston, VA.

Walraven, J.C. (1978). *The Influence of Depth on the Shear Strength of Lightweight Concrete Beams without Shear Reinforcement*, Report S-78-4, Stevin Laboratory, Delft University of Technology, Delft, Netherlands.

Xie, Y., Ahmad, S.H., Yu, T., Hino, S., and Chung, W. (1994). "Shear Ductility of Reinforced Concrete Beams of Normal and High-Strength Concrete," *ACI Structural Journal*, *91*(2), pp. 140–149, American Concrete Institute, Farmington Hills, MI.

Yoon, Y.-S., Cook, W.D., and Mitchell, D. (1996). "Minimum Shear Reinforcement in Normal, Medium and High-Strength Concrete Beams," *ACI Journal Proceedings*, *93*(5), pp. 576–584, American Concrete Institute, Farmington Hills, MI.

Zwoyer, E.M. (1953). *Shear Strength of Simply Supported Prestressed Concrete Beams*, Ph.D. Dissertation, University of Illinois, Champaign, IL.

HRDI-40/03-19(WEB)E